Author:
Edmunds, Grace L

Title:
Targeting Adenosine and TIM3 to Improve Anti-Tumour Immunity

Targeting Adenosine and TIM3 to Improve Anti-Tumour Immunity

Grace. L. Edmunds

A dissertation submitted to the University of Bristol in accordance with the requirements for award of the degree of Doctor of Philosophy in the faculty of Life Sciences

School of Cellular and Molecular Medicine

April 2019

Word Count: 84,819

Abstract

Signalling through co-inhibitory receptors is required to dampen inflammation at the end of an immune response. Suppression of CD8+ cytotoxic T lymphocyte responses is one mechanism by which inhibitory receptors downregulate inflammation. Within the tumour microenvironment, inhibitory receptor engagement occurs chronically and at high levels, such that CD8+ Tumour Infiltrating Lymphocytes (TILs) are suppressed within tumours.

In a murine renal carcinoma model (Renca), adoptive T cell transfer of tumour-specific CD8+ T cells, together with antagonists of two co-inhibitory receptors, were delivered as combination immunotherapy. Systemic blockade of both TIM3 and A2a-Adenosine Receptors resulted in complete tumour regression amongst RencaHA tumour-bearing mice; which was associated with an increase in the number of CD8+ TILs, reduced numbers of tumour-infiltrating FOXP3+ T-regulatory cells, and improved *ex vivo* cytotoxic function of CD8+ TILs. Moreover, blockade of TIM3 and A2aRs also led to the development of anti-tumour immune memory T cells, which enabled mice to resist rechallenge.

These data demonstrate that TIM3 and A2aR signalling synergise to inhibit the infiltration and cytotoxic effector function of anti-tumour CD8+ TILs, and that blockade of TIM3 and A2aRs may provide a novel immunotherapeutic strategy for the treatment of various human cancers.

I declare that the work in this dissertation was carried out in accordance with the requirements of the University's Regulations and Code of Practice for Research Degree Programmes and that it has not been submitted for any other academic award. Except where indicated by specific reference in the text, the work is the candidate's own work. Work done in collaboration with, or with the assistance of, others, is indicated as such. Any views expressed in the dissertation are those of the author.

Signed:

Date:

Acknowledgements

My thanks goes to my supervisors David Morgan and Christoph Wuelfing, for firing up my enthusiasm for science and for letting me pursue the work which truly interested me. I have learnt a great deal from you both and I am extremely grateful. You have also become great friends. Thanks also to Lindsay Nicholson, Mick Bailey, Linda Wooldridge, Ann Pullen and all of the staff at CMM, who have helped and advised me as I went from being a vet to being a scientist. Your assistance has been invaluable.

Thanks to Andy Herman for hours of help with FACS and Flow Cytometry. This work would not exist without your assistance. Also, to Lorena Sueiro-Ballasteros, not just for her endeavours in the flow facility but also for starting with me on my first day in the lab and being my friend and confidante ever since. I couldn't have got through the last few years without you, and I still owe you that coffee. I am grateful to Katy Jepson, Alan Leard, Dom Alibhai, Stephen Cross and all of the staff at the Wolfson Bioimaging Facility for being cheerful in the face of microscopes, and for making sure that I produced images which were adequately scientific as well as beautiful.

Thanks to Deniz, Rachel, Dhino, Carissa, Jiahe, Timse, Clara and Silvia who have all directly assisted me in the lab and in proofing this manuscript. I am also grateful to Sin Lih and Jorge for showing me how to use Matlab, and to Tom Dunning for helping me with 'R'. Thanks to Danielle, Fatemah, Anya, Ore, Cath, Rhiannon, Ella, Brownen, Yikui, Jiahe, Laura, Lea, Gaia, Harry, Hon, Emily, Fernando, Drinalda and everyone in the lab for being such great scientific advisors and friends. Thanks also to Awen Gallimore at Cardiff for your input during joint lab meetings and for the hybridoma cell lines. Thank you to the Acuto lab in Oxford for your assistance with Phosflow Lck staining.

I am deeply indebted to John Iredale and Jeremy Tavare, and to Jane, Tracey and everyone at GW4-CAT for adopting me as an honorary trainee and for giving me your time and mentorship. It has made an enormous difference to be part of a cohort and I can't thank you enough for the career advice. Thanks to the Wellcome Trust for awarding this fellowship and to the EBI for the primer funding which allowed me to apply for my PhD in the first place.

To Hannah, Vicky, Katie, Charlotte, Stu, Natalie, Kate, Tim, Gini, Harry, Delphine, Fred, Matt, Cal, Lauren and all at 182, thanks for always being there to look after me, for all of the packages through the post and for your support; you mean the world to me. Thanks to Will and Garv for sharing your incredible talents as producer and animator, bringing to life my vision of an immunology film. To Lally and Pete, thanks for believing in me, it really meant a lot. To City of Bristol Choir, thanks for delighting me, and sorry I missed so many rehearsals. To Grandma, Grandad and Katy, and to Granny and Grandpa, you inspire me every day.

Finally, this thesis is dedicated to Halbal, who has been unfailingly present and patient; somehow managing to make me smile through three degrees and many late evenings. It is also for Mum, Dad and John, who have always given unconditional support to everything I do. I cannot possibly express my gratitude to all four of you, thank you for your love.

Table of Contents

Table of Figures

Abbreviations

A2aR	A2a Adenosine Receptor
ADAP	Adhesion and Degranulation Adaptor Protein
ADP	Adenosine Diphosphate
AF	Alexafluor
AIRE	Autoimmune Regulator
AMP	Adenosine Monophosphate
ANOVA	Analysis of Variance
AP1	Activator Protein 1
APC	Antigen Presenting Cell
APECD	Autoimmune Polyendocrinopathy Candidiasis and Ectodermal Dystrophy
AR	Adenosine Receptor (A1, A2, A3 Rs)
ATP	Adenosine Triphosphate
ATT	Adoptive T cell transfer
B2M	Beta-2-Microglobulin
BALB/c	Bag and Albino
BCR	B Cell Receptor
BTLA	B- and T-Lymphocyte Attenuator
CaMKII	calcium-calmodulin-dependent Kinase II
cAMP	cyclic AMP
CAR	Chimeric Antigen Receptor
CCL	C-C motif chemokine ligand
CD	Cluster of Differentiation
CIR	Co-Inhibitory Receptor
CLP	Common Lymphoid Progenitor
CLR	C-type Lectin Receptor
Csk	C-terminal Src Kinase
cSMAC	central Supramolecular Activation Cluster
CSR	Class Switch Recombination
cTEC	Cortical Thymic Epithelial Cell
CTL	Cytotoxic T Lymphocyte
CTLA-4	Cytotoxic-T-Lymphocyte associated protein-4
CTV	Celltrace Violet
CXCR	C-X-C motif chemokine receptor
DAG	Diacylglycerol
DAMP	Damage-associated Molecular Pattern
DC	Dendritic Cell
DMSO	Dimethylsulphoxide
DN	Double Negative
DNA	Deoxyribonucleic acid
DP	Double Positive
DRiPs	Defective Ribosomal Products
EDTA	Ethylenediaminetetraacetic acid
EGF	Epidermal Growth Factor
EMT	Epithelial-Mesenchymal Transition
ER	Endoplasmic Reticulum
FAC	Final Assay Concentration
FACS	Fluorescence Activated cell Sorting
FAK	Focal Adhesion Kinase
FBS	Fetal Bovine Serum
FMO	Fluorescence Minus One
FOXP3	Forkhead-Box-P3
GF	Growth Factor
GFP	Green Fluorescent Protein
GM-CSF	Granulocyte Macrophage- Colony Stimulating Factor
HA	Haemagglutinin
HBV	Hepatitis B Virus
hCD2	human CD2
hCD58	human CD58
HCV	Hepatitis C Virus
HIV	Human Immunodeficiency Virus
HLA	Human Leukocyte Antigen
HR	Hazard ratio
HVEM	Herpesvirus Entry Mediator
iDC	immature Dendritic Cell
IDO	Indolamine Dioxygenase
IFN	Interferon
IFNy	Interferon Gamma
Ig	Immunoglobulin
IGF-1	Insulin-derived Growth Factor 1
IL	Interleukin
ILC	Innate Lymphoid Cells
IP3	Inositol-triphosphate
ITAM/ITIM	Immunoreceptor tyrosine-based activating /inhibitory motif
ITT	Immunoglobulin Tail Tyrosine
LAG3	Lymphocyte-activation Gene 3
LAT	Linker of Activated T cells
LCMV	Lymphocytic Choriomeningitis Virus
mAb	monoclonal Antibody
MAC	Membrane Attack Complex
MACS	Magnetic Activated cell Sorting
MANOVA	Multivariate Analysis of Variance
MAPK	Mitogen- activated protein kinase
MATS	Maximum Allowable Tumour Size
MBL	Mannose Binding Lectin
mDC	mature Dendritic Cell
MDSC	Myeloid Derived Suppressor Cell
MFI	Median Fluorescence Intensity
MHC	Major Histocompatibility Complex
MRD	Minimal Residual Disease
mTEC	Medullary Thymic Epithelial Cell
NECA	5'-N-Ethylcarboxamidoadenosine
NF- κB	Nuclear factor- κB
NFAT	Nuclear Factor of Activated T cells
NFIL3	Nuclear Factor, Interleukin 3 Regulated

NK	Natural Killer
NKT	Natural Killer T (cell)
NLR	Nod-like Receptor
NR	Non-responder
ns	not significant
NSCLC	Non-small cell Lung Cancer
Off-L	Off Interface Lamellae
PAG	Phosphoprotein associated with glycosphyngolipid
PAMP	Pathogen-associated Molecular Pattern
PBS	Phosphate Buffered Saline
PBMC	Peripheral Blood Mononuclear Cell
PC	Principal Component
PCA	Principal Component Analysis
PD-1	Programmed-cell Death protein -1
PD-L1	Programmed-cell Death protein -1 ligand
PFS	Progression Free Survival
PGE2	Prostaglandin-E2
PI3K	Phosphoinositol-3-kinase
PKA	Protein Kinase A
PKC	Protein Kinase C
PLC	Phospholipase C
PMA	Phorbol 12-myristate 13-acetate
pMHC	peptide-MHC
PRR	Pattern Recognition Receptor
pSMAC	Peripheral Supramolecular Activation Cluster
R	Responder
RAG	Recombinase Activating Gene
RLR	Rig-1 like Receptor
RNA	Ribonucleic acid
ROS	Reactive Oxygen Species
SCID	Severe Combined Immunodeficiency
SD	Standard Deviation
SEM	Standard Error of the Mean
SHM	Somatic Hypermutation
SIGLEC9	Sialic Acid Binding Ig Like Lectin 9
SIL	Spheroid Infiltrating Lymphocyte
SLT	Secondary Lymphoid Tissues
SME	Spheroid Microenvironment
SOS	Son of Sevenless
STING	Stimulator of Interferon Genes
T1/T2	Type 1/2 (macrophage)
TAM	Tumour-Associated Macrophage
TAP	Transporter associated with antigen processing
TCM	T Central Memory
TCR	T Cell Receptor
TDLN	Tumour Draining Lymph Node
Tdt	Terminal Deoxyribonucleotidyl Transferase
TEM	T Effector Memory
TGFB	Transforming Growth Factor Beta
Th1/2	T helper 1/2
TIGIT	T cell immunoreceptor with Ig and ITIM domains
TIL	Tumour Infiltrating Lymphocyte
TIRF	Total Internal Reflection (Microscopy)
TLR	Toll-like Receptor
TME	Tumour Microenvironment
TNFα	Tumour Necrosis Factor Alpha
Treg	T regulatory cell
TRM	T Resident Memory
Tx	Treatment
V,D,J	Variable, Diversity and Joining (regions)
VEGF	Vascular Endothelial Growth Factor
VISTA	V-domain Ig suppressor of T cell activation
Y	Tyrosine
ZM	ZM241385 (Specific A2aR Antagonist)

Chapter 1 Introduction

1.1 The Immune System

The immune system has evolved to defend the body from infection with micro-organisms such as viruses, bacteria, fungi, protozoa and parasites (1, 2). Those microorganisms which cause harm to the body are known as pathogens. In addition, the immune system can detect and respond to tissue damage by non-organic material, and to malignantly transformed cancer cells (2). Immune cells are capable of producing damage to living cells, therefore inbuilt into the immune system's design is its ability to ignore and preserve healthy self-tissue during pathogen destruction (1-3). Since pathogens have evolved in tandem with mammals, the immune system has also developed specialised adaptations, to tolerate non-harmful micro-organisms. The energy expended and the collateral self-damage incurred in eradicating non-pathogenic species could prove deleterious to the host (1-3). In addition, tolerance of some microbes such as gut microbiota is directly advantageous, because these microbes live in symbiosis with mammals, utilising the host's resources, but also providing important factors which sustain host survival and health (1, 3). Thus, when functioning optimally, the immune system will eradicate dangerous non-self threats, whilst ignoring benign or self-tissues. Immune cells discriminate between self and foreign material by detecting differences in the structural components or functional hallmarks of pathogens when compared to healthy body cells (2, 4).

1.2 Innate Immunity

The immune response is divided into two categories, 'Innate' and 'Adaptive' immunity (2, 5). The 'Innate' immune response comprises a range of cellular and non-cellular components. Whereas adaptive immune cell populations are pathogen specific, and clones of adaptive immune cells take time to expand in response to infection, innate effectors can respond to pathogens more generally and more rapidly (2, 4, 6). Innate immunity therefore functions to limit pathogen replication whilst the more efficient killing function of the adaptive immune system is recruited. Innate cells then support adaptive immune cell functions once they arrive (2, 5, 7). Examples of innate defences include: physical barriers, soluble small molecules, membrane bound receptors and specialised immune cells.

1.2.1 Physical Barriers

Physical innate defences include: Epithelia, meaning cells joined by tight junctions to prevent entry of noxious substances or pathogens; Mucous, which overlies some of these layers to trap harmful particles; and Cilia, which move contaminated mucous away, allowing it to be constantly replenished (2, 5).

1.2.2 Innate Immune Cells

Cells of the innate immune system include non-haematopoietic cells, however leukocytes are the most important cells for innate defence (2, 5). Important categories of innate immune cells include:

- Phagocytes such as macrophages and neutrophils, which physically engulf and digest pathogens;
- Granulocytes such as eosinophils, basophils and mast cells, whose primary role is the release of granules containing anti-microbial substances and inflammatory mediators such as histamine;
- Professional Antigen Presenting cells (APC) such as Dendritic Cells (DC) which efficiently take up and present antigen to prime adaptive immune cells;
- Innate Lymphoid Cells (ILCs), a more recently identified category of innate immune cell, which descend from the common lymphoid progenitor, but which do not possess T cell or B cell receptors. Innate helper cells and some types of intraepithelial lymphocyte are now included in this classification. Different classes of ILCs exert various functions including cytokine production and cytotoxicity (8).
- Natural Killer (NK) cells, which destroy damaged self-cells and are sometimes included in the ILC classification because they descend from lymphoid progenitors.

It is important to note that there is some overlap in the functions of innate cells, and most play a role in releasing anti-microbial substances, small molecules and cytokines which augment the general immune response, alongside their more specific functions (2, 5).

Innate leukocytes utilise germline encoded Pattern Recognition Receptors (PRRs), to recognise pathogens. PRRs developed during human-microbe co-evolution and respond to conserved structural features of microorganisms, known as Pathogen Associated Molecular Patterns

(PAMPs). Examples of PAMPs include bacterial cell wall components, or viral nucleic acids. Functional products of pathogenic infection such as virulence factors or toxins can also act as PAMPs (1, 2, 5). PAMPs are often evolutionarily conserved and essential for pathogen viability, such that the patterns detected by innate immune cells are those least likely to be lost from the pathogen genome (2, 4, 5).

PAMPs are confined to pathogen rather than host expression, however innate immune cells can detect self-tissue if cell damage or death produces conserved molecular signatures known as Damage Associated Molecular Patterns (DAMPs)(2, 5). Both innate immune responses and tissue repair are initiated by DAMPs. Families of PRRs which detect PAMPs and DAMPs include Toll-like Receptors (TLRs), Nucleotide-binding oligomerization domain-like receptors (NLRs), C-type lectin receptors (CLR), and RIG-1 like receptors (RLR). Each family of PRR is found at a different subcellular location, utilises different signal transduction mechanisms, and recognises different ligands (2, 5).

1.2.3 Small Molecules

The Complement Cascade represents a prominent small molecular mechanism of innate immune defence. Over 20 complement proteins circulate in the blood, mediating no effect until activated by one of three mechanisms, the Classical, Alternative and Mannose Binding Lectin (MBL) pathways (1, 2, 5). All of these pathways culminate in cleavage of Complement protein C3, into C3a and C3b.

The classical complement pathway is initiated when an antigen-antibody complex binds to C1, this results in generation of C4b2a, an enzyme capable of converting C3 into C3a, and C3b. After classical activation, C3a activates mast cells, whereas C3b binds to pathogen surfaces, opsonising them, meaning that they are marked out for destruction by immune cells such as phagocytes (1, 2, 5). The alternative complement pathway occurs when C3b along with other complement proteins known as Factor B, D, H and I bind to an activating surface such as a fungal cell wall. The presence of a normal mammalian cell surface inhibits this cascade. Alternative complement activation culminates in the formation of C3bBb, another enzyme capable of converting C3. In this manner, the presence of C3b initiates a positive feedback loop to amplify its own production (2, 5). The MBL pathway occurs when MBL binds to mannose residues on

the pathogen surface, activating its associated proteases MASP-1 and MASP-2. The activity of these enzymes results in the formation of C4b2a, and C3 is cleaved in a similar manner to classical complement activation (2, 5).

The consequence of any of the above initiating pathways is C3b production. C3b aids in the cleavage of C5 into C5a and C5b. C5a is an inflammatory mediator and a chemokine. Whereas C5b unites with C6,7,8 and 9 to form a Membrane Attack Complex (MAC), generating a pore in target surfaces such as bacterial cell membranes, and causing lysis of pathogens (1, 2, 5).

In summary, innate immunity makes use of a wide range of cell types, which are often resident at mucosal surfaces, where pathogens are likely to enter the body. Along with other small molecular and physical defences, innate immune cells generate a rapid response which represents a first line of defence (1, 2, 5).

1.3 Adaptive Immune Responses

The second division of the immune system is the 'Adaptive' response. The cells of the adaptive immune system are T and B Lymphocytes, which descend from a common lymphoid progenitor (CLP)(2, 4, 5). Mammalian cells present proteins on their surface to activate lymphocytes and to ensure that the body can defend against pathogens. Such proteins are known as antigens. The specific peptide sequence within the antigen which allows it to be recognised by the immune system, is known as an epitope (9). The differentiation between self and foreign antigens is a key mechanism by which the immune system recognises threats and ignores host tissues (1, 10).

Lymphocytes depend upon somatic rearrangement of genes to generate receptors that are capable of binding with great specificity to epitope sequences of antigens expressed by pathogens. Tolerance mechanisms ensure that lymphocytes with receptors that respond to self-antigen are deleted or suppressed (11). Immature T cells are identified by their expression of a T cell receptor (TCR), whereas committed B cells express membrane bound immunoglobulin, which acts as their antigen-detecting B cell receptor (BCR)(4). At baseline levels, an enormous range of TCR and BCR specificities are present in the body, but only a very small number of cells possess each receptor sequence (4). When a pathogen is encountered, innate antigen

presenting cells display peptides from the pathogen, inducing T cells or B cells with a receptor specific to that antigen to divide rapidly and form large clones (4). This process is slow, therefore, the innate immune system protects the body during the lag phase of adaptive immune expansion (2, 5).

Days later, the adaptive immune response becomes predominant, but innate cells are continually recruited and aid lymphocytes in fully eradicating the pathogen (2, 5). As well as antigen specificity, an important characteristic of adaptive immunity is that memory cell populations are produced as part of the proliferative phase. Memory cells are programmed to divide rapidly should the specific pathogen be encountered subsequently, meaning that the lag time for adaptive immune function is shorter during the second encounter with any given pathogen (12).

1.3.1 B Lymphocytes

B lymphocytes are a key immune cell subset, whose principal function is the production of Immunoglobulin (Ig). Mature B cells are characterised by cell surface markers including CD79a, CD79b, CD19, and CD20 (13). Most mature B cells reside within spleen, lymph node or gut associated lymphoid tissue. During B cell differentiation in the bone marrow, their B Cell Receptor (BCR), the Ig, is assembled by somatic recombination and expressed on their surface (Figure 1)(13).

Igs are composed of heavy and light chains. The heavy chain has a constant portion, forming the structural body of the Ig. The constant portion also determines the antibody class: IgM, IgD, IgE, IgA or IgG (13). Antibodies of different classes have subtly different properties making them more useful against different types of pathogen (1). The variable portion of the Ig heavy chain forms part of the antigen binding site, along with the variable region of the light chain. Ig light chains also have a smaller Constant region (1, 13).

Figure 1 - Gene Rearrangement during B cell development to produce diverse Immunoglobulin Structures

Antibodies are composed of heavy (H) and Light (L) chains, each of which contains constant (C) and variable (V) regions (13-15). Constant regions determine the class of the antibody. The variable portions of heavy and light chains combine to form a binding site of unique specificity (13-15). Each Heavy chain V region is composed of joining, variable and diversity segments (J_H, V_H, D_H). The final V region sequence is generated by somatic recombination in which deletion of nucleotides brings J_H, V_H, and D_H genes into contact (14, 15). The Light chain can be formed from either the Ig kappa or the Ig lambda locus (16). Somatic recombination brings variable (Vκ) and joining (Jκ) genes into contact to make the Light chain V region (14, 15). If the Light chain generated from the kappa locus is non-functional, re-arrangement at the lambda locus is attempted, however if neither locus produces a functional Light chain, the B cell undergoes apoptosis (13).

(Figure taken from "High-Throughput DNA Sequencing Analysis of Antibody Repertoires. Boyd and Joshi.2014 (16)).

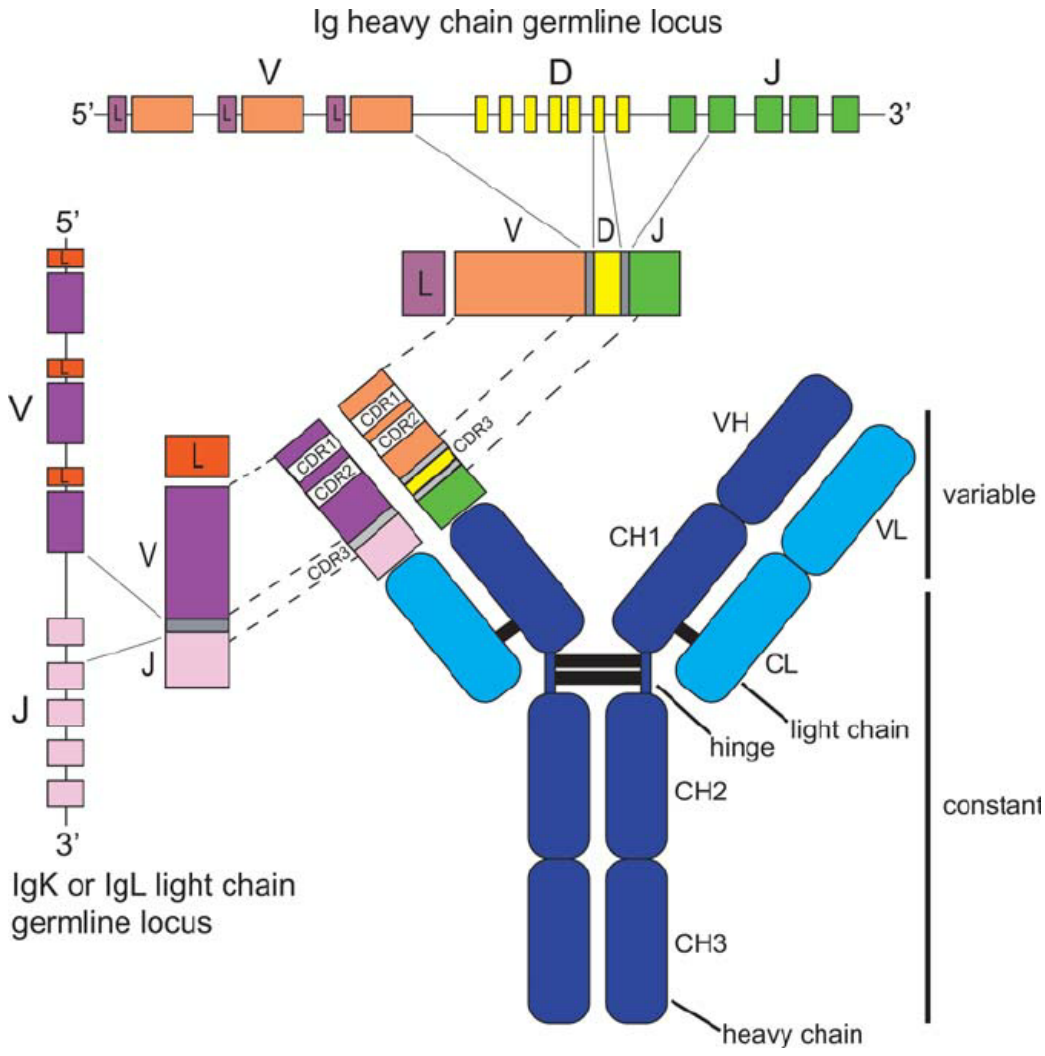

Antibody assembly within the immature B cell begins with connection of genes encoding the Ig heavy chain variable region. The joining, variable and diversity genes for the heavy chains (J_H, V_H, D_H), are connected by deletion of nucleotides between these regions in a process known as VDJ recombination (2). The enzyme terminal deoxyribonucleotidyl transferase (Tdt), which is active in developmental B cells, adds random nucleotides into the sites of VDJ joining. Therefore, Tdt introduces additional, non-gene-encoded variability to the hypervariable region of the antibody (2, 4). Joining of VDJ regions generates the amino terminal heavy chain regions. Alternative splicing of M and D constant regions onto the variable region causes Ig class M and D to be expressed at this stage of development (2).

The Ig heavy chain is tested for functionality and cells possessing a none functional heavy chain will apoptose. Those with functional heavy chains encounter the heterodimeric proteins VpreB and λ5 which interact with the heavy chains to act as surrogate light chains in the immature B cell until light chain rearrangement completes. The resultant receptor generated from rearranged heavy chains and surrogate light chains is called the pre-BCR (2, 4, 13). The surrogate light chain proteins ensure that although DJ recombination occurs on both chromosomes within the immature B cell, the V region is only added on one chromosome, thus conferring single antigenic specificity on the cell in a process called 'allelic exclusion' (1, 2).

Next, the light chain amino terminus is assembled by joining of genes coding for variable (Vκ) and joining constant (Jκ) kappa light chain regions on one chromosome. If a functional light chain is generated, it joins with a heavy chain producing functional Ig (4). If not, rearrangement occurs on the subsequent kappa chromosome. If the light chain is still none functional, lambda light chain gene rearrangement is tried (2). Together, the juxtaposition of different Ig gene segments therefore generates a huge repertoire of B cells, waiting to expand in number if their specific antigen is encountered during the host lifetime (13, 17).

The second stage of B cell development begins when antigen is encountered (Figure 2). Immature B cells, otherwise known as follicular B cells, are important for the first phase of the primary B cell response. Without receiving T cell help, these cells respond to antigen to produce IgM or IgD (4, 13). Activated B cells can persist within the periphery, producing IgM and IgD in a T cell-independent manner. The first week of the immune response is characterised by T cell

independent antibody production (13). Other B cells proceed to the secondary lymphoid tissues (SLT), where they become follicular B cells and undergo further maturation (13).

T cell-dependent B cell activation occurs in the Germinal Centres of SLT and is therefore termed the Germinal Centre (GC) reaction (13). The combination of signals received during this antigen-dependent development directs mature B cells down one of two lineages; the short lived effector B cell, known as the plasma cell, or the memory B cell (4). There are two key events which occur during B cell activation in Germinal centres, Somatic Hypermutation (SHM) and Class Switch Recombination (CSR)(2, 4, 13). B lymphocytes require two signals for T cell dependent activation at the lymph node. Signal one is crosslinking of antibody on the B cell surface by specific antigen. The mechanism by which B cells encounter antigen to crosslink antibody and produce Signal 1 is not well understood (4). Currently it is thought that antigen could enter B cell follicles, displayed on professional APC such as dendritic cells, phagocytes such as macrophages or other B cells. These various cells might utilise surface Ig or complement to bind antigens and display them within B cell follicles (4). Signal 2 is usually provided by T cells in the form of co-stimulatory interactions between CD40 or CD80/86 expressed on B cells with CD40-L and CD28 expressed on T cells (2, 18).

When B cells receive Signal 1, transduction occurs through the B cell receptor (the surface bound Ig) as well as its associate proteins Igα and Igβ (2, 13). Signalling downstream of the B cell receptor is similar to T cell Receptor signal transduction, which will be discussed in detail later. Briefly, B cell signalling involves phosphorylation of immunoreceptor tyrosine-based activation motifs (ITAMs) in the tails of B cell receptor proteins (13). Phosphorylation of ITAMs is mediated by Src kinase proteins and initiates recruitment of other proteins to the ITAMs, starting a cascade. BCR signalling culminates in Mitogen Activated Protein Kinase activation, Protein Kinase C activation, elevated intracellular calcium and the localisation of transcription factors to the nucleus where they initiate gene expression to promote B cell proliferation and development (13).

Figure 2 - The Stages and Anatomical Locations of B Cell Development

Pre-B cells develop when the rearranged Immunoglobulin heavy chain interacts with surrogate light chains to form the Pre-B cell receptor (13). Light chain rearrangement then proceeds and cells with a functional immunoglobulin variable region survive (14, 15). The constant regions expressed in B cells at this stage cause Ig class M to be expressed at the immature B cell surface. A subset of B cells proceed directly to the spleen and are activated immediately to become plasma cells which produce IgM and IgD in a T cell-independent manner. The first week of the immune response is characterised by T cell independent production of IgM (2, 5, 13). Other B cells exit the bone marrow and enter the lymph nodes to mature further, here they occupy the follicles and become known as follicular B cells. Follicular B cells which travel to the germinal centre encounter T cells and undergo the germinal centre reaction, which equips them for T cell-dependent antibody production and memory B cell formation (2, 5, 13). Here, class switch recombination (CSR) involves splicing of the heavy chain Variable regions to Constant heavy chains of the class IgG, IgE or IgA to allow production of antibodies besides IgD and IgM. Somatic Hypermutation (SHM) introduces point mutations into the variable region to widen the diversity of the antibody repertoire produced (14, 15). T cell dependent activation ensures that the antibody class produced is appropriate for the specific pathogen encountered, since different antibody classes perform different functions (2, 5).

(Figure adapted from "B Lymphocytes How They Develop and Function. LeBien and Tedder. 2008 "(13))

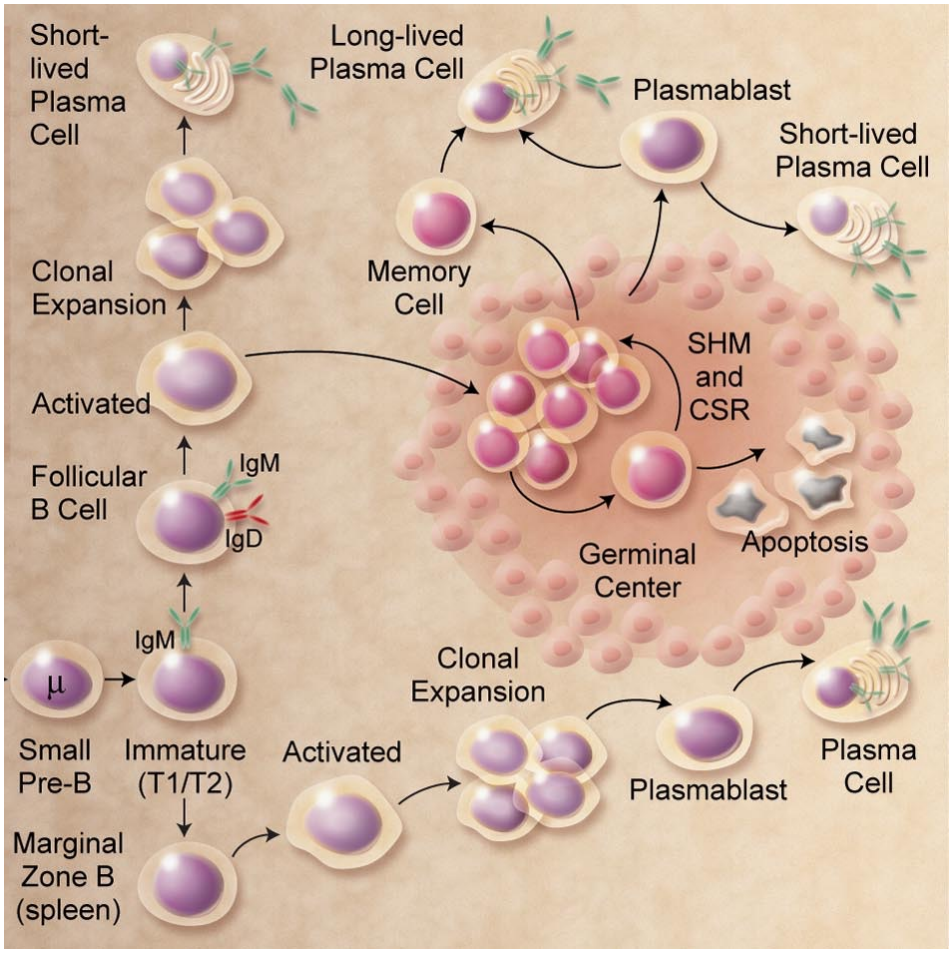

The presence of Signal 2 in the form of T cell co-stimulation, and Signal 3 in the form of T cell derived cytokines causes the B cell to undergo class switching, whereby the VDJ heavy chain region becomes spliced to exons encoding a new constant chain (13). This allows the B cell to transcribe different classes of antibody besides IgM and IgD. Because different antibody classes are more advantageous in the response to different pathogens, T cell help thus directs the B cell to produce the appropriate class of antibody (1, 13). The process of alternative splicing of the heavy chain VDJ regions to constant heavy chain regions of IgG, IgE and IgA is called Class switch recombination (CSR)(2, 13). Examples of T cell signals which induce CSR include IL-10 and TGFβ, which induce production of IgA; and IL-4 and IL-13 which induce production of IgE (13). The enzyme, Activation-Induced Cytidine Deaminase (AID) is important for CSR, although its exact mechanism of action remains to be defined (13, 14).

AID also contributes to Somatic Hypermutation (SHM) during the GC reaction, allowing point mutations to develop in the heavy and light chain variable regions of the BCR at around 10 million times the rate of background somatic mutations (15). SHM is thought to be crucial for the introduction of additional variety into the B cell antigen binding repertoire, and it results in the production of antibodies of higher antigen binding affinities, in a process known as Affinity Maturation (4, 13, 19, 20). Lack of AID leads to hyper-IgM immunodeficiency syndromes, since class switching is impaired (4). The timeline of B cell activation involves the primary immune response, whereby T-independent B cells produce predominantly IgM over the course of about a week (13). A T cell dependent phase of B cell activation typically follows after around two weeks in which affinity-matured IgE, IgG and IgA are produced. In the secondary response to antigen, memory B cells are able to produce class-switched and affinity-matured antibody within 7 days (4).

1.3.2 T Lymphocytes

1.3.2.1 T cells recognise Antigen presented on MHC Complexes

Different pathways allow presentation of antigen found in extracellular, intracellular and intravesicular sites to activate T lymphocytes (10, 21). Antigen presentation involves processing of proteins to generate small peptides which are displayed on the cell surface by apparatus known as Major Histocompatibility Molecules (MHC) (1, 10).

Presentation by Class I MHC molecules allows peptides from intracellular pathogens to be displayed on any normal self-cell which is infected by them (1). Therefore MHC-I presentation does not require professional APCs with specific antigen uptake abilities because antigens for class I presentation are found within the infected cell. The predominant cell type responding to antigen on MHC I molecules are CD8+ T cells which exert cytotoxicity, destroying both the infected self-cell and the pathogen it contains (1, 10). Malignant transformation of normal-cells also generates antigens which are different to the normal self-repertoire, thus cancer cells also present antigen on MHC I and are destroyed by CD8+ T cells (21).

MHC Class II presentation allows peptide epitopes from extracellular pathogens to be taken up by professional APCs and presented to immune cells (1, 10). The primary response to MHC Class II presentation is activation of CD4+ T cells which aid in directing B cells to secrete an Ig class appropriate for the pathogen detected (10). Intravesicular pathogens are also presented by MHC Class II molecules to CD4+ T cells (10).

An important additional pathway of antigen presentation is known as 'Cross Presentation', whereby antigens from inside infected self-cells are taken up by professional APCs such as DC (1). Because the DC itself is not usually infected, antigens from intracellular pathogens originate from another infected cell and are extracellular to the DC. Extracellular antigens usually enter the Class II pathway, however, these antigens must be able to enter the Class I pathway in DCs to allow DCs to present antigen to CD8+ T cells. Cross presentation of extracellular antigen on MHC I molecules allows DCs to prime naïve CD8+ T cells which then home to infected tissues and encounter the same antigen, this time presented by Class I presentation on infected somatic cells. CD8+ T cells then kill the infected cell. Cross presentation occurs only in professional APCs, and in some DCs it requires proteasomal activity, whereas in others it occurs in a proteasome independent manner (21-23).

1.3.2.1.1 MHC Class I and Cross-Presentation

The human HLA gene complex comprises three groups of genes, HLA-A, HLA-B and HLA-C, each of which encode different versions of the heterodimeric MHC I protein, formed of heavy and light chains. The MHC I light chain is called "β2-Microglobulin" (β2-M)(24). In the mouse, MHC-I genes are H2-K, H2-D and H2-L. Polymorphisms of HLA or H2 genes result in enormous

variation in the peptide binding sites of different MHC I molecules, as well as mediating slight differences in the speed and characteristics of peptide presentation by MHC I (1, 21). Polymorphisms amongst genes encoding MHC I are also linked to susceptibility to infection and autoimmune disease however, for many diseases the exact mutation associated with that syndrome has not yet been determined (10, 25).

MHC Class I molecules present peptides derived from the cytoplasm and nucleus of somatic cells (1). Cellular proteins are degraded by the proteasome at the end of their life and this process generates peptides for Class I presentation (10). Certain proteins enter the proteasome directly after translation, these proteins are termed defective ribosomal products (DRiPs) because their sequence or structure is usually erroneous (10, 21). Proteasomal peptide products arrive at Transporter associated with Antigen Presentation (TAP), which allows them to enter the Endoplasmic Reticulum (ER). Within the ER, MHC I molecules are present. To be fully stable, the MHC I heterodimer must bind to peptide (1, 10, 21). Therefore, in the ER, MHC I stability is maintained through formation of the protein loading complex, in which it binds to chaperone proteins such as Calreticulin, ERp57, PDI and Tapaisin, until peptide is encountered (1, 10, 21). Tapaisin interacts with TAP transporters, ensuring the proximity of chaperoned MHC I to peptide fragments entering the ER through TAP. Peptide binding triggers chaperone release and pMHC complexes are permitted to leave the ER, travelling to the cell surface via the Golgi (17, 21).

MHC Class I complexes are relatively stable at the cell surface, but may dissociate, producing free MHC I heavy chains. If free peptide and β2-M are available, the MHC I complex might reassemble and present a new peptide (21, 24). This is evidenced by the fact that murine splenocytes incubated in the presence of bovine β2-M generate new MHC I molecules composed of a murine heavy chain and a bovine β2-M light chain at the cell surface (24). In addition, MHC I heavy chains, or complexes, are internalised and degraded by the endosome. If they encounter epitopes to which they are able to bind during this process, then MHC I molecules can be immediately recycled to the cell surface, presenting new peptide (21).

Cross presentation of exogenous antigen on MHC I by DC also represents a unique mechanism by which peptide gains access to the MHC I molecule (23). Pathogen peptides are phagocytosed by DC and at this point they enter one of two pathways. In the cytosolic pathway, antigens exit

the phagosome for degradation in the cytoplasm. Peptides then either enter the ER and the classical MHC I presentation pathway, or re-enter a unique phagosomal/endosomal compartment and are presented by MHC I found there (22, 26). In the vacuolar pathway immature DCs utilise proteasome independent methods of cross presentation, whereby antigens are degraded directly within the phagosomal/endosomal compartment (23).

1.3.2.1.2 MHC Class II Presentation

The groups of genes encoding MHC Class II in man are HLA-DR, HLA-DQ and HLA-DP, and in mouse they are H2-A and H2-E (21). Specific polymorphisms found within MHC II genes have been associated with specific human autoimmune diseases. For example, coeliac disease occurs in individuals possessing the HLA-DQ2 or HLA-DQ8 alleles (25). In addition, although MHC II expression is usually restricted to professional APCs, MHC II can be upregulated in other cell types such as endothelia and fibroblasts by inflammatory molecules such as IFNγ (21). Atypical MHC Class II expression is observed in several disease states, including in mesenchymal stem cells during graft-versus-host-disease and in gut epithelia in Crohn's disease (25, 27, 28).

The peptides presented by MHC II originate outside the cell and are taken up into the endosomal compartment for degradation before being presented (1, 10, 21). MHC II is a heterodimeric protein made up of α and β chains which assemble in the ER and form a complex with an invariant chain protein (Ii) before being transported into a specific part of the endosome known as the MHC Class II Compartment (21, 29). Three MHC II heterodimers interact with one Ii trimer to form a complex which is stable in the endosome (29). The presence of Ii is thought to prevent peptide binding within the ER (30). In the endosome, part of the Ii chain is digested leaving a peptide known as CLIP occupying the peptide binding portion of the MHC II molecule. A chaperone, HLA-DM allows CLIP to exchange places with a peptide which has been degraded within the endosome (1, 21, 29). Although the main role of MHC II molecules is antigen presentation, they can also act to modulate immune responses by signalling from the membrane inwards, or from the intracellular compartment. It has been shown for example, that intracellular MHC II can feed into TLR signalling in innate immune cells, and that surface MHC II can influence apoptosis in primed APCs (21, 31).

In summary, antigen presentation by MHC molecules ensures that immune cells have access to antigen from different cellular compartments. The presence of MHC is required for signalling through T cell and B cell receptors, which cannot respond optimally to peptide unless it is presented in the context of MHC (1, 10). In addition, leukocytes such as NK cells respond to 'missing self' and detect foreign cells as much by their lack of self-MHC as by their expression of foreign antigen (32). For these reasons, it is not surprising that different alleles and polymorphisms in the HLA genes are found to associate strongly with immune-mediated disease (25).

1.3.2.2 T cell Development

T Lymphocytes are usually divided into four categories. Those expressing the αβ T Cell Receptor (TCR) are subdivided into CD4+ or CD8+ T cells, with different key functions (4). A third T cell subset express a γδTCR and a fourth T cell subset are CD4-CD8- and express the CD161 antigen more commonly found on NK-cells. This final subset have therefore been christened NKT cells (1, 2, 4). This section will focus on CD4+ and CD8+ αβ T Cell development in the thymus from the Common Lymphoid Progenitor (CLP), although other subsets will be mentioned where relevant.

The architecture of the thymic organ supports T cell development, and T cells migrate through the thymus, encountering different structures during their different stages of maturation (1, 33). Briefly, the stages of T cell development involve:

- Entry of thymic CLPs
- Formation of CD4+CD8+ (Double Positive, DP) thymocytes at the cortex
- Positive selection of functional DP thymocytes at the cortex
- Negative selection of strongly self-reactive DP thymocytes at the cortex
- Initiation of central tolerance at the thymic medulla and
- Thymocyte exit (4, 33).

Chemokine signalling is thought to be fundamental in the control of thymocyte trafficking and several immunodeficient phenotypes have been identified in chemokine knockout mice (33).

The first stage of thymocyte development involves colonisation of the thymus by thymic CLPs. In the fetus, CLP infiltration is regulated by CCL21 and CCL25 and can occur through vascular and non-vascular routes (33). Post-natally, CLP arrive from the bone marrow via the vasculature and enter the thymus at the cortico-medullary junction (4, 33). CLP are induced to proliferate under the influence of IL-7. Mutations in genes which encode the common γ chain of cytokine receptors limits IL-7 signalling during T cell development, thereby producing Severe Combined Immunodeficiency Syndrome (SCID), a disease characterised by low T cell numbers (4). Notch 1 and other transcription factors become active during thymocyte expansion and induce the expression of genes which commit cells to the T lymphocyte lineage (4, 33).

The thymocytes that result from committed CLPs do not express CD4 or CD8 co-receptors and are therefore known as double negative (DN) thymocytes. The first double negative development stage is termed DN1, and it is characterised by expression of CD44 and lack of expression of the IL-2 receptor α-chain, CD25 (CD44+CD25-). DN2 thymocytes maintain expression of the CD44 adhesion molecule but gain expression of CD25 (CD44+CD25+)(1, 34). DN thymocytes are induced to migrate towards the thymic subcapsule in a process regulated by CXCR4, CCR7 and CCR9 (33). During migration, the pool of DN2 T cell precursors undergoes a process of TCR gene rearrangement similar to that which occurs during B cell development, in order to endow thymocytes with a functional TCR comprising pairs of either α and β or γ and δ chains (4, 35).

All TCR gene loci contain Variable (V) and Joining (J) regions, however, only β and δ genes contain Diversity (D) segments. An enzyme, VDJ recombinase, which is encoded by the genes RAG1 and RAG2, mediates splicing of V, J and (for β and δ) D segments together, producing a sequence which encodes the β or γδ TCR chains (2, 4, 35, 36). α chain rearrangement occurs later (35). Thymocytes become dedicated to αβ or γδ lineages thanks to TCR gene recombination at this stage (35). Various cleavage and repair enzymes, such as Artemis, XRCC4 and DNA Ligase 4 are required to correctly arrange V, J and D genes. Mutations in the genes which encode the above enzymes, or in RAG1 and 2 genes are associated with SCID (4, 36). In a similar manner to that described in VDJ recombination within B cells, Tdt adds additional nucleotides into the VDJ junctions in order to introduce additional variation into the TCR repertoire (2). Inherent small differences in the nucleotide sequences at the ends of spliced VDJ segments also introduce variability (4).

After β chain rearrangement, thymocytes downregulate CD44. This stage of thymocyte development is known as DN3. CD44-CD25+ DN3 thymocytes undergo β-selection, which ensures that those cells without a correctly rearranged TCRβ chain are directed to apoptosis (34). Cells which pass β selection become CD44-CD25- DN4 thymocytes. The resultant β-chains assemble with pre-TCR α chains such that a pre-TCR is expressed on the thymocyte surface (2, 34). The pre-TCR complexes with CD3 so that DN4 thymocytes survive and proliferate, downregulating DNA recombinases and eventually upregulating CD4 and CD8 to become double positive (DP) thymocytes (1, 34, 35).

DP thymocytes migrate to the cortex of the thymus, where recombinase genes are re-expressed and α chain rearrangement occurs (35). The re-arranged αβ T cell receptor is tested, through interaction with self-peptide-MHC (pMHC) complexes on thymic cortical epithelial cells (cTECs) (33). The interaction between thymocytes and self- antigens presented by cTECs allows discrimination between thymocytes with functional and non-functional αβ TCRs. Those possessing a TCR which is unable to respond to self-pMHC with sufficient affinity are deemed to have a non-functional TCR and undergo apoptosis (2, 34, 35). This process is known as Positive Selection (4).

Negative Selection also occurs within the thymic cortex, meaning that DP thymocytes which respond to self pMHC with high affinity are also deleted. Negative Selection generates central tolerance to self, because T cells which respond to self-antigen with high-affinity could react to self-tissue and generate autoimmune damage if allowed to enter the adult repertoire (4, 33). DP thymocytes passing both positive and negative selection at the cortex then downregulate either the CD8 or CD4 co-receptor, becoming a single CD8+ or CD4+ thymocyte, and migrate to the thymic medulla (33). Here, they again encounter self-antigen presented as pMHC complexes, this time by medullary TECs (mTECs) and professional APCs (33).

Further negative selection occurs at the thymic medulla, making doubly certain that thymocytes possessing a TCR with high affinity for self-antigen are induced to die by apoptosis and do not leave the thymus (1, 33, 34). Presentation of self-peptides in the thymic medulla is regulated by the gene Autoimmune Regulator (AIRE), and AIRE-deficient individuals experience a syndrome known as Autoimmune Polyendocrinopathy Candidiasis Ectodermal

Dystrophy (APECD)(4). The thymic medulla also contributes to the development of peripheral tolerance mechanisms, since it appears to be the site of development for T regulatory cells which express the transcription factor Forkhead Box P3 (FOXP3)(33). Mature thymocytes, expressing either CD4 or CD8, and which pass negative selection, exit the thymus in a process thought to be regulated by sphingosine-1-phosphate expression (33).

1.3.2.3 γδ T cells

Although the work contained within this thesis is primarily concerned with αβ T cells, the existence of T cells with a γδ TCR is important and must be briefly acknowledged. γδ T cells and NK cells are sometimes defined as neither truly innate nor adaptive immune cells since they respond to both conserved microbial motifs, like innate immune cells, and to MHC-mediated antigen presentation, like lymphocytes (37). Furthermore, certain microbes such as Human Cytomegalovirus (HCMV) can induce γδ T cells to undergo clonal expansion like true adaptive cells (37, 38). However, some γδ T cells acquire full maturity pre-natally and these cells therefore represent truly innate lymphocytes (37). Antigen Recognition by γδ T cells depends upon only the variable portions of the γ and δ TCR genes, rather than the full rearranged TCR (39).

Various sub –groups of γδ T cells are defined by the variable segments they possess within their re-arranged γδ chain, or by their different anatomical locations (39). Often these two ideas align, since γδ T cells possessing the same TCR tend to localise together (37). For example, cells with the Vδ1 chain are likely to be found at mucosal surfaces, whereas those expressing Vγ9Vδ2 are found in peripheral blood (39). Although the γδ TCR is not MHC restricted, meaning that it can recognise peptide presented on either MHC I or MHC II, many γδ T cells express CD8. Thus, they often behave in a similar manner to CD8+ T cells, detecting antigen on the surface of infected or malignantly transformed self-cells (37). Indeed their lack of MHC restriction makes γδ T cells particularly advantageous in the host defence against tumours, since tumours may downregulate MHC I to evade CD8+ T cell attack (6). Additionally, γδ T cells express other receptors such as NKG2D which allow them to recognise tumours with great efficiency, even when tumour antigens are unprocessed (6, 39).

1.3.2.4 CD8+ T cells

1.3.2.4.1 CD8+ T cell Activation

CD8+ T cells are the killer cells within the adaptive immune system. CD8+ T cells recognise infected or malignantly transformed self-cells and kill them to protect the host. After exit from the thymus, naïve CD8+ T cells, which have not yet encountered antigen, reside in the secondary lymphoid tissues, especially the lymph nodes (33). The first encounter between a naïve CD8+ T cell and its specific antigen usually occurs in the lymph node. Dendritic cells take up antigens at infected tissues and travel to the lymph nodes where they process peptides and present them to naïve CD8+ T cells on MHC Class I molecules (40-42). During the initial priming encounter, three signals are required to produce activation of the CD8+ T cell, allowing it to expand and form a clone of antigen-specific effector cells. If a suboptimal combination of signals is encountered at priming, naïve CD8+ T cells may become tolerant to the antigen presented, rather than proliferating and acquiring cytotoxic function (42). The first signal required for CD8+ T cell activation is Signal 1, which is provided by the interaction of the peptide-MHC I complex with the TCR-CD3 complex. If the TCR exhibits very high affinity for peptide, a strong Signal 1 can prime CD8+ T cells without the need for any other stimuli (41, 42). Signal 2 occurs in the form of co-stimulatory interactions between DCs and CD8+ T cells. Important examples of co-stimulation occurring in CD8+ T cells include:

- Interaction between the CD8 co-receptor and the MHC I protein, which increases the stability of Signal 1;
- Binding of CD28 on T cells to CD80/86 on APCs such as DCs;
- Binding of Lymphocyte Function-associated Antigen-1 (LFA-1) on T cells to Intercellular Adhesion Molecule-1 (ICAM-1) on APCs.

Signal 3 is provided by external immune cells and comprises cytokine and chemokine signalling, which promotes T cell activation, differentiation and migration to infected sites (42-44). The combination of cytokines received at priming can influence activated CD8+ T cells to become cytotoxic effectors, quiescent tolerant cells or regulatory cells. The signalling received at priming can also affect CD8 + T cell memory potential (12, 42, 45). After priming, CD8+ T cells proliferate and leave the LN, homing to the site of infection. Primed effector CD8+ T cells, which are capable of killing target cells, are known as Cytotoxic T Lymphocytes (CTL)(41, 42).

1.3.2.4.2 T Cell Receptor Signalling

- ***Spatiotemporal Control of TCR Signalling and Immune Synapse Structure***

TCR signalling at priming proceeds in a similar manner in both CD4+ and CD8+ T cells. TCR engagement initiates a signalling cascade, which is amplified by the aggregation of signalling molecules around lipid rafts at a membrane-defined area known as the immune synapse (46, 47). There are subtle differences between the signalling that occurs within CD8+ T cell immune synapses during priming and during killing of target cells (48). Recent studies in our laboratory are concerned with the localisation of TCR intermediates in time and space, and the fact that this plays a crucial role in amplification and termination of the TCR signalling pathway (47).

The TCR and other signalling proteins aggregate in microclusters after the T cell membrane contacts the APC membrane. These clusters coalesce to form a larger island of signalling molecules known as the central supramolecular activation cluster (cSMAC). We have shown that the ability of cells to form a cSMAC is directly related to the efficiency of TCR signalling as measured by the phosphorylation of intermediates downstream (47). Some TCR signalling proteins show a predilection to accumulate in the region around the cSMAC, known as the peripheral SMAC (pSMAC). Thus, the complete immune synapse is often said to form a characteristic 'bullseye pattern' (Figure 3). Further subdomains of the immune synapse are continually being identified (46).

Figure 3 - Signalling Domains at the Immune Synapse

Confocal microscopy was used to image CD4+ T cells during formation of immune synapses (cell couples) between T cells and Antigen Presenting Cells (APCs). Genes encoding various components of the T cell receptor signalling apparatus were transduced into T cells before imaging. The localisation of GFP-tagged signalling intermediates was determined across >50 cell couples for each intermediate (47).
Different TCR signalling molecules localise to a range of distributions at the immune synapse. The front-on view shows the synapse from the point of view of an antigen presenting cell. The top-down view shows the view looking at a T cell-APC couple from above (47). The central distribution and peripheral distribution represent the pSMAC and cSMAC, however some molecules occupy other domains in the immune synapse, indicating diverse patterning of different signalling receptors during T cell immune synapse formation (47).

Figure taken from "Spatiotemporal Patterning During T Cell Activation is Highly Diverse. Singleton, Wuelfing et al. 2009"(47).

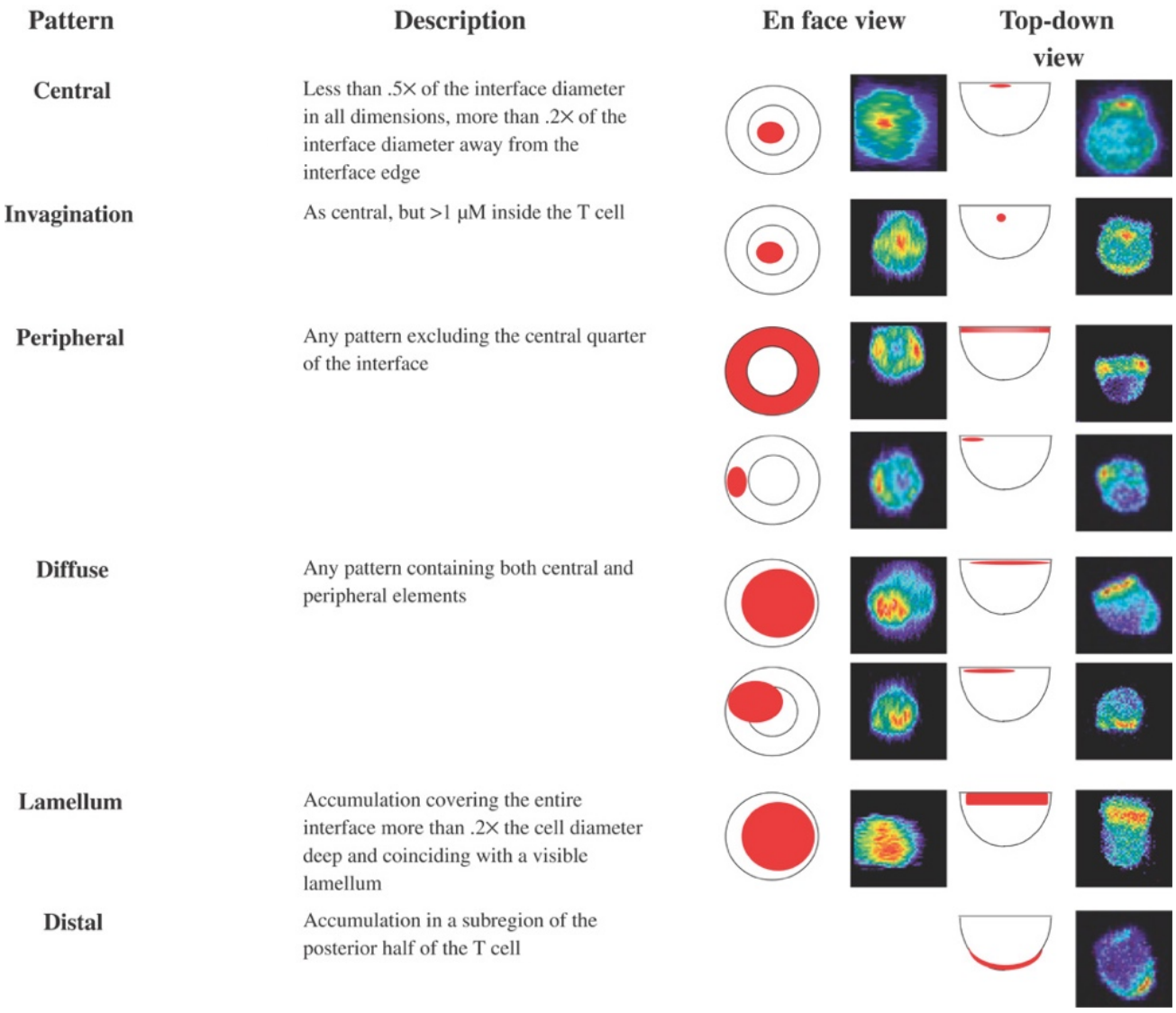

The net results of TCR signalling are: calcium influx into the T cell cytoplasm; the activation of transcription factors; and the translocation of these transcription factors into the nucleus, where they promote CD8+ T cell survival, production of IL-2 and expression of the IL-2 Receptor (47, 49). IL-2 is the cytokine which drives CD8+ T cell proliferation and the acquisition of effector function after priming. CD8+ T cells receive IL-2 signals in an autocrine and paracrine manner (50). Other main effects of TCR signalling are actin-reorganisation, cell-cell adhesion, and translocation of the Microtubule Organising Centre to the immune synapse (51, 52). During priming, MTOC translocation serves to allow the release of granules containing cytokines towards the APC, as well as allowing subsequent cell division and memory formation from the primed CD8+ T cell (46). During killing by CD8+ T cells the MTOC also functions to allow the delivery of cytotoxic granules to the immune synapse. These granules can then be released towards the target cell (48, 51).

- ***The Proximal TCR Signalling Cascade***

Upon TCR engagement, Src family kinases such as Lck are brought into contact with both the ζ-chains of the TCR and with CD3 molecules which are associated with the TCR (49, 53) (Figure 4). A pool of Lck remains near the T cell membrane in the steady state where it is required for TCR activation. Although Lck molecules are constitutively located at the plasma membrane because they are myristolated and palmitoylated, CD4 and CD8 co-receptors, as well as certain co-stimulatory or inhibitory receptors such as TIM3, are thought to control the proximity of the Lck pool to the immune synapse, determining the activation threshold of the T cell (54, 55). Lck can only signal in its open, activated state, which is produced after phosphorylation at Y394, added to Lck by its own autophosphorylation (49, 53). Active Lck phosphorylates ITAMs on CD3 and TCR ζ chains after the TCR is engaged.

How the Lck-TCR interaction is initiated remains unclear, and two models have been postulated to explain initiation of TCR signalling (49, 53). The conformational change or mechanosensor model proposes that the CD3ε tails are buried within the T cell membrane, and only become accessible to Lck upon TCR engagement (53, 56, 57). The kinetic segregation model is based on the idea that immune synapse formation forces the T cell and APC membranes into close proximity. The reduction in space at the immune synapse causes exclusion of the large phosphatase CD45 from the cSMAC, and also forces the TCR nearer to the pool of Lck (49, 58).

Active Lck mediates phosphorylation of ITAMs on CD3 chains and TCR ζ chains. This permits recruitment of ZAP70 by the TCR ζ chains, causing ZAP70 to become active and acquire kinase activity. ZAP70 in turn, phosphorylates ITAMs on Linker for Activation of T cells (LAT), a scaffolding protein which plays a key role in the recruitment of other proteins which amplify the TCR signal (49, 57, 59). The protein complex formed around LAT is known as the LAT signalosome, and members of this protein aggregation are seen to localise centrally at the cSMAC of the immune synapse. Components of the LAT signalosome include:

- Adhesion and Degranulation-promoting Adaptor Protein (ADAP)
- Growth-factor Receptor Bound protein 2 (GRB2)
- GRB2-related Kinase Adaptor Protein (GADS)
- SH2-domain-containing Leukocyte Protein of 76 kDa (SLP76)
- Phospholipase Cγ1 (PLCγ1)
- Interleukin-2-inducible T-cell Kinase (ITK)
- VAV1 (49, 60).

TCR chains, ZAP-70, LAT, PLC γ1, PKCθ, Rac and Rho are other proteins which have been shown by our lab to localise to the cSMAC (47). The correct aggregation of the TCR, the LAT signalosome and its associates appears to be crucial for the resultant arms of TCR signalling to proceed (47, 59). Indeed, loss of one component of the signalosome profoundly affects the ability of others to function (46). These data emphasise once again the importance of spatial control of TCR signalling (61).

Downstream of the LAT signalosome, the three main effects of TCR signalling are propagated. Firstly, the actin re-organisation pathway results from signalling through SLP-76, VAV1, another kinase NCK1, and Wiskott-Aldrich Syndrome family Proteins (WASP)(49). Secondly, cell-cell adhesion descends principally from ADAP (49).

Finally, there are three pathways leading to the transcription of genes for T cell function, the Calcium ($Ca2^{+}$) pathway, the Mitogen-activated Protein Kinase (MAPK) pathway and the Nuclear Factor-κB (NF-κB) pathway. These pathways originate from PLCγ1 activity, partially regulated by SLP-76. PLCγ1 catalyses the breakdown of Phosphatidylinositol-4,5-biphosphate

(PIP_2) into inositol-1,4,5-triphosphate (IP_3) and Diacylglycerol (DAG), and these two molecules initiate downstream signalling (50, 60). PLCγ2 may also play a role in T cells, however it is known to be more important in BCR signalling (62).

- ***The MAPK Pathway***

DAG associates with membrane lipids and acts as a scaffold to recruit further TCR signalling intermediates to the membrane, notably, PKCθ and RasGRP. RasGRP is a guanine nucleotide exchange factor (GEF) which activates Ras, a GTPase (46). Ras activation is one of the chief upstream controllers of MAPK activation. Son of Sevenless (SOS), another GEF, can also activate Ras after being recruited to the LAT signalosome by Grb2 (46, 50). A cascade of MAPK activation ensues downstream of Ras. MAP Kinase Kinase Kinase (Raf) phosphorylates MAP Kinase Kinase (Mek) which phosphorylates Erk, a MAPK, culminating in activation of the AP-1 transcription factor complex which promotes IL-2 and IL-2 receptor transcription (57). Other MAPK proteins which are activated after TCR signalling include Rac and CDC42. These proteins regulate actin polymerisation at the immune synapse as well as activating MEK signalling, leading to translocation of the transcription factors FOS and JUN to the nucleus (57). FOS and JUN co-ordinate AP-1 to promote genes required for T cell effector functions. The regulation of Ras by multiple components exemplifies the important fact that TCR signalling is not linear; at each stage it can be influenced by the availability and activity at the immune synapse of multiple concurrent factors (46, 47, 49).

- ***The NF-κB Pathway***

DAG also recruits PKCθ, which feeds into the second of the three main transcription factor pathways occurring after TCR stimulation, that of NF-κB. Inhibitor of-κB (IκB) is a sequestering protein which constitutively binds NF-κB to keep it in the cytoplasm. PKCθ activation causes a complex to form, containing the proteins CARMA-1, Bcl10 and MALT1. These proteins activate IKK, causing it to dissociate from NF-κB, which allows NF-κB to enter the nucleus (46, 50).

- ***The Calcium Pathway***

IP_3, also a product of PLCγ-mediated degradation of PIP_2, is a second messenger which causes intracellular calcium elevation through its binding to calcium channels on the endoplasmic reticulum (ER)(46). Escape of calcium from the ER to the cytoplasm down a concentration gradient causes a modest elevation in intracellular calcium, which leads to opening of calcium-

responsive calcium channels at the cell-surface membrane, causing further calcium influx from the extracellular fluid (46, 50). The transcription factor NFAT is also calcium responsive, and is caused to translocate to the nucleus and mediate its activity following this sustained calcium flux. Therefore, both NFAT and NF-κB activation proceed from PLCγ signalling (46). The presence of elevated intracellular calcium is an effective experimental indicator of successful TCR signal transduction and may be achieved using a variety of calcium sensors such as Fura and GcAMP6 (63, 64).

The MAPK pathway can also activate NFAT. Phosphatidylinositol 3-Kinase (PI3K) is another mediator which is activated downstream of Ras. It exerts its kinase function on PIP_2 to produce PIP_3 which recruits Akt to the cell membrane. Akt, as well as exerting pro-survival effects, phosphorylates GSK3. GSK3 would normally add phosphate groups to NFAT to prevent its nuclear translocation, but this is abrogated when Akt phosphorylates GSK3. Thus, as well as being promoted by calcium flux, NFAT's nuclear translocation and function is promoted by PI3K through Ras signalling (46)

Figure 4 – T Cell Receptor Signalling

Signalling through the T Cell receptor (TCR) alpha and beta chains occurs when the TCR encounters specific antigen presented on MHC molecules (2, 5, 49, 57). Binding of the CD4 or CD8 co-receptor increases the stability of the TCR interaction. CD4 or CD8 receptor tails provide a reservoir for active Lck, phosphorylated at Y394 (49, 53). Upon TCR engagement, Lck contacts the TCR ζ chains and the CD3 molecule, adding phosphate groups to Immunoreceptor Tyrosine Based Activation Motifs (ITAMs). ZAP70 is recruited to these ITAMs and phosphorylates ITAMs on LAT, allowing the recruitment of multiple proteins to form the LAT signalosome (47, 49, 57). Downstream of the signalosome, Adhesion and Degranulation-promoting Adaptor Protein (ADAP) initiates a cascade promoting cell-cell adhesion, which increases the stability of the T cell-APC interaction. SH2-domain-containing Leukocyte Protein of 76kDa (SLP76) and VAV1 initiate actin re-organisation and FOS/JUN activation through the Rho GTPases CDC42 and Rac. Phospholipase Cγ1 (PLCγ1) catalyses the breakdown of Phosphatidylinositol-4,5-biphosphate (PIP_2) into inositol-1,4,5-triphosphate ($InsP_3$) and Diacylglycerol (DAG)(49, 57). Together $InsP_3$ and DAG initiate three cascades leading to transcription of genes which promote T cell survival and proliferation. These cascades are the Calcium pathway, the Mitogen Activated Protein Kinase (MAPK) Pathway, and the NF-κB pathway (49, 57).

Figure taken from "Regulatory mechanisms in T Cell receptor Signalling. Guillaume Gaud, Renaud Lesourne and Paul. E. Love. 2018 " (57).

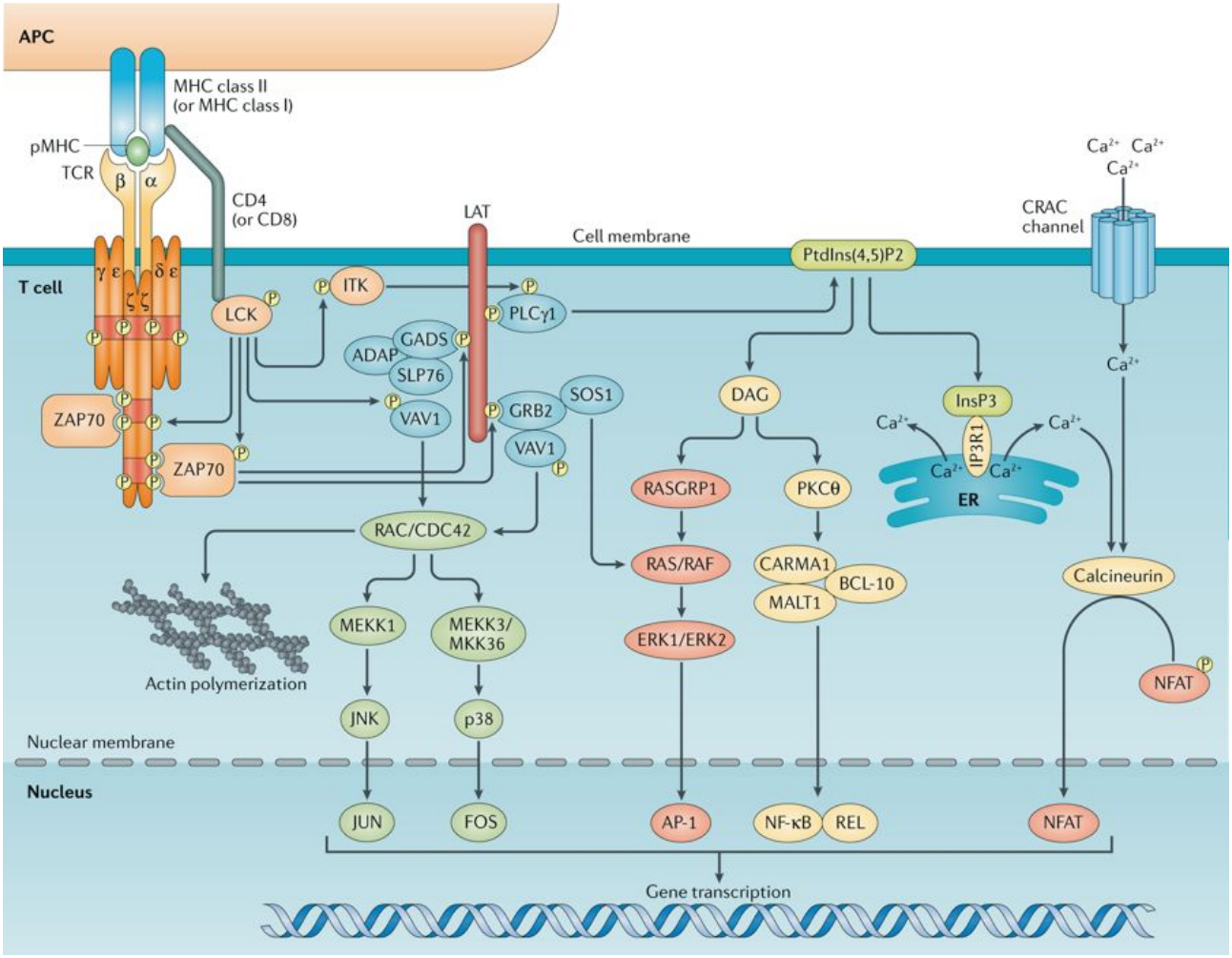

- ***Negative Regulation of TCR signalling***

As well as propagating signals for T cell activation, the TCR signalling apparatus must be equipped such that signalling can be downregulated when the T cell has completed its function, or when self-antigen is encountered, to prevent auto-immunity (49, 57). Negative regulation of proximal TCR signalling is co-ordinated by several factors. Phosphatases, such as SH2-domain-containing Phosphatase 1 (SHP1), remove activating phosphorylation marks from proximal proteins such as Lck and ZAP70 (57). The addition of phosphorylation marks can also be inhibitory. Diacylglycerol kinase (DGK) phosphorylates DAG to inactivate it (57).

Lck is controlled by both phosphorylation and dephosphorylation. Upon TCR engagement, Lck autophosphorylates its own Y394 residue to become active (49, 53). To antagonise this, C-terminal Src Kinase (CSK) phosphorylates Lck at its inhibitory site, Y505 to inactivate it. CD45 can remove both activating (Y394) and inhibitory (Y505) phosphorylation residues from Lck (49, 53). Recent data suggests that in any given cell, Lck can assume 4 states:

- Primed (no phosphorylation)
- Activated (Y394 only)
- Inhibited (Y505 only)
- Active double phosphorylated (DPho)(Y394 and Y505)

The proportion of these different Lck states determines whether TCR signalling proceeds, because active Lck is required for signal propagation (53). Therefore the balance between CD45 activity (removal of phosphates at Y394 and Y505), and that of Csk, (addition at Y505), determines the rate at which active Lck, and TCR signalling, is inhibited (53). After TCR stimulation, active Lck in the open conformation appears to preferentially localise to the immune synapse when compared to inactive Lck (53). Exclusion of CD45 during initial TCR signalling might also permit Lck activity to increase in the spatial confines of the immune synapse. Control of the activation state of Lck, and its subcellular location are believed to be important ways in which immunoinhibitory molecules and co-inhibitory receptors modulate TCR signal transduction (65, 66). Other mechanisms by which TCR signalling is controlled, besides phosphorylation, include internalisation of signalling molecules. As well as being required for signal amplification initially, the correct formation of the cSMAC in space and time is thought to permit TCR internalisation for signalling termination (46). Ubiquitination of signalling intermediates by ligases such as Cb1 also targets them for degradation in order to downregulate TCR signalling (46).

Figure 5 - Control of Lck Signalling downstream of the T Cell Receptor

Lck is present within CD8+ T cells in three main phosphorylated forms, and the balance of availability of these phosphotypes affects the potential for successful TCR signalling (53). Autophosphorylation of Lck p394 occurs in response to TCR agonism and causes Lck to assume an open, active confirmation. Phosphorylation of p505 is added by kinases such as Csk, to mediate a closed, inactive confirmation. Lck without phosphorylation is known as primed Lck, since it may change in confirmation to become either active or inactive. Double phosphorylated (dPho) Lck also exists and possesses similar kinase activity to Lck 394. CD45 can remove both phosphorylation marks, therefore dPho Lck can also remain active or become inactive depending on which site is dephosphorylated (53). Thus, both kinases and phosphatases control the function of Lck. The percentage of each Lck phosphotype in resting Jurkat T cells is indicated according to recent data (53). Human naïve T cells display similar percentages. The availability of active Lck is a crucial regulator of TCR signalling, and a pool of active Lck is maintained at the immune synapse by the action of proteins including the CD4/8 co-receptor. The TCR signalling threshold can therefore be modulated via Lck phosphorylation and by the size and location of the active Lck reservoir (49, 53).

Schematic based on the work of Nika et al. 2010 (53).

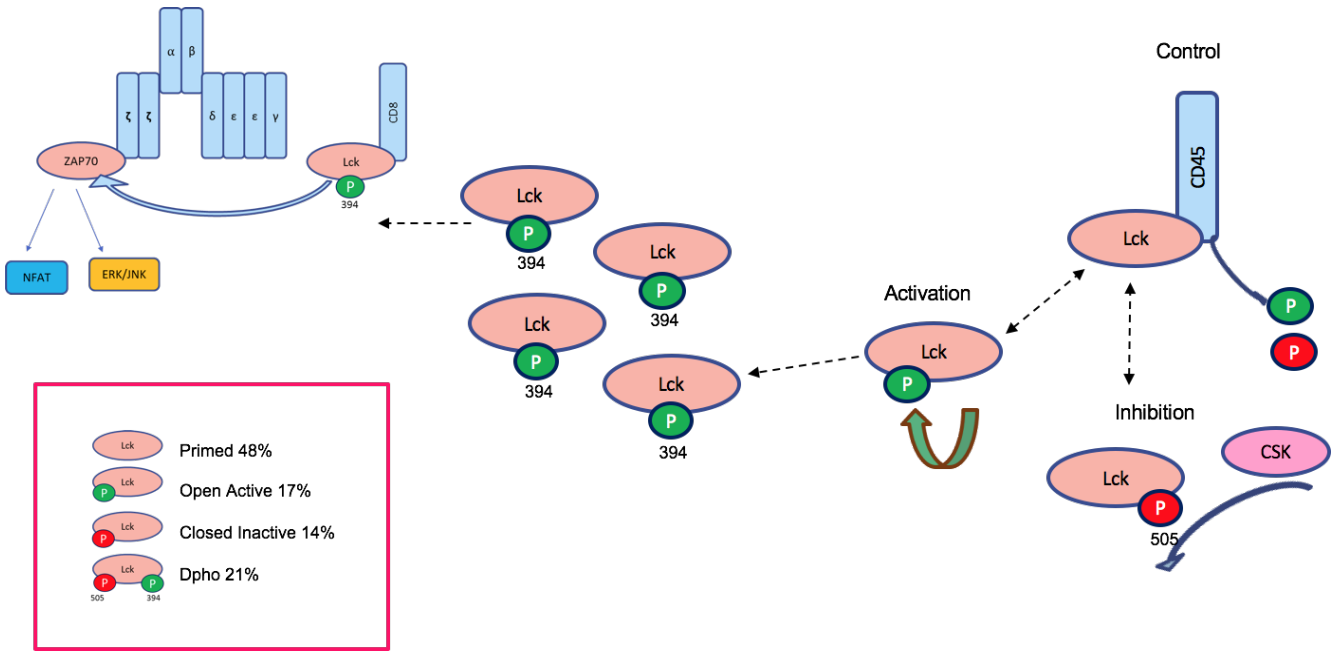

1.3.2.4.3 CD8+ T Cell-mediated Cytotoxicity

After priming, naïve CD8+ T cells differentiate into CTL, whose function is to kill virally infected or malignantly transformed self-cells which must be destroyed in order to protect the host (67). Primed CTL home to the tissues where they encounter antigen for the second time, this time presented at the target cell surface rather than on the surface of professional APCs. Correct immune synapse formation between the TCR of the CTL and peptide-MHC I on the target cell, permits exocytosis of cytotoxic granules containing perforin and Granzyme-B into a membrane defined region. This allows cytotoxic granules to act on the target cell and destroy it with minimal collateral damage to surrounding tissue (1, 48, 67). Perforin channels insert in the target cell membrane, allowing Granzyme B to enter the target cell and induce caspase activation to initiate apoptosis. Together the actions of membrane disruption and Granzyme-B induced apoptosis result in target cell destruction (67, 68). The peptides which are presented on target cells are derived from the infecting virus, or from components of the cancerous self-cell. Although some tumour-antigens are derived from self-tissue, their damaged or mutated nature means that the immune system responds to them as foreign and does not initiate peripheral tolerance upon encountering them (42). CD8+ T cells can also kill target cells in a calcium-independent manner through interactions between Fas-L on T cells and Fas on target cells, however, this method of killing is far less efficient than perforin and granzyme-B delivery via the immune synapse (67).

The pMHC interaction with the CTL TCR initiates broadly the same signalling cascade during both priming and at killing, however there are a few key differences (48, 69). At priming, the chief function of TCR signalling is to promote IL-2 gene transcription and proliferative signals to drive T cell expansion. However, during killing, the purpose of immune synapse formation is to allow the release of granules (48). In this second encounter with pMHC, the immune synapse forms more transiently, allowing CTL to deliver multiple lytic hits sequentially to the same cell. Furthermore, the threshold for CTL activation by TCR stimulation is lower at killing when compared to priming. This means that the TCR can signal effectively and promote killing without the need for high levels of Signal 2 or Signal 3 (49). CTL must be able to kill without Signal 2, because unlike professional APCs, target cells do not always express co-stimulatory molecules (44). Many proteins within the TCR signalling cascade, that localise to lipid rafts at the immune synapse and which are activated by phosphorylation at priming, will re-locate to the immune synapse in smaller amounts during killing. Therefore the overall amplification of

the TCR signalling cascade occurs to lower levels during killing when compared to priming (70). Nonetheless, TCR signalling still results in the formation of the cSMAC and pSMAC after interaction with target cells (48).

A crucial event occurring downstream of CTL TCR engagement, is the rearrangement of the actin cytoskeleton. One well-established function of actin-rearrangement is to enable MTOC translocation from its position behind the nucleus, to supply lytic granules at the immune synapse (1, 48, 71). The Golgi and the endosomal recycling compartment migrate with the MTOC and form the source of the cytotoxic granules to be secreted, as well as providing a source of recycling for signal intermediates (48, 72, 73). Actin must relocate from a patch below the cSMAC to a ring beyond the pSMAC in order to generate forces for MTOC translocation (48, 72-74). Rho GTPases such as CDC42, signalling molecules such as ADAP, and motor proteins including dynein, may all co-ordinate with actin to regulate MTOC translocation (48, 75).

Although the role of actin in MTOC translocation is undisputed, actin rearrangement could also be required for other aspects of cytotoxic granule release by CTL. Our lab are interested in two models which attempt to explain how actin regulates cytotoxic granule delivery. The first model, the 'Actin Maintenance' model, suggests that formation of an actin ring at the pSMAC, and maintenance of this ring for a period of several minutes, is required to maintain immune synapse stability within a T cell-target cell couple thereby allowing the delivery of a lytic hit (76). In this model, the peripheral ring appears to ensure that actin-mediated membrane projections generated by the CTL are always directed towards the immune synapse, to maintain the forces holding CTL and target cell together. In conditions where the peripheral actin ring is lost, functionless membrane projections known as Off-Interface Lamellae (Off-L) are seen to extend in random directions, and the CTL may move away from the site of the interface, translocating over the target cell membrane. Movement of the CTL away from the site of initial immune synapse formation could terminate or prevent lytic granule release (76, 77).

However, another model, the 'Actin Clearance' model, states that the formation of a peripheral actin ring is only important by virtue of the fact that in forming a ring structure, actin clears from the cSMAC. Such clearance is fundamental to the production of an actin-free region at the centre of the immune synapse through which cytotoxic granules are released (71). One piece of evidence which contradicts this model is that in NK cells, cytotoxic granules have been shown

to pass through an actin meshwork, so a requirement for actin clearance amongst CTL necessitates further investigation (71, 78).

Rather than just forming a central patch or a ring, actin can occur in many patterns at the immune synapse. Figure 6 illustrates actin patterns observed using live cell imaging of T cell-target-cell couples, in which the T cell expresses F-tractin (a GFP-conjugated form of F-actin)(71). Actin patterning at the immune synapse can characterised in the same way as other signalling intermediates described in Figure 3, with the most important distinction being between 'Peripheral' and 'Asymmetric' actin patterns, representing a full or partial actin ring respectively; and 'Central' 'Lamellal' or 'Diffuse' patterns, which involve actin covering the cSMAC (47). The Actin maintenance and Clearance models disagree about which patterns should be permissive to cytotoxic granule release. By correlating actin patterning at the immune synapse with the delivery of effective killing by CTL it may be possible to determine which model best explains the association between actin and granule release (Figure 6). This is the focus of current work within our laboratory.

Figure 6 – Two Models of Actin regulation to allow Granule Release at the CTL Immune Synapse

Confocal imaging can be used to assess the localisation of GFP-conjugated forms of F-actin (F-tractin) during immune synapse formation between cytotoxic T Lymphocytes (CTL) and target cells (76, 77). Soon after TCR engagement, a lamellal actin patch forms below the region of the entire immune synapse (Initial Coupling). Actin is then reorganised. Each pattern is shown as cross-section of T-cell-target-cell couple, and a front-on view (as if seen from the target cell)(71, 76, 77). There are two models which link reorganisation of actin at the CTL immune synapse to the delivery of cytotoxic granules. (A) The Actin Maintenance Model suggests that maintenance of a complete Peripheral actin ring over a period of minutes is required to maintain immune synapse stability, keeping the T cell at the same place on the target cell membrane for sufficient duration to allow delivery of lytic granules (76, 77). Other Actin patterns could also allow such stability (lamellal, diffuse, central) however this is not known. Asymmetric actin (a partial ring) does not maintain sufficient stability. (B) The Actin Clearance model suggests that actin clearance away from the cSMAC is required to permit granule release through the centre of the immune synapse (71). Even if the peripheral ring is incomplete (Asymmetric) or only maintained for a short duration, as long as the cSMAC is free of actin, cytotoxic granules can be delivered. Lamellal, diffuse and central patterns would obstruct the cSMAC and prevent granule release according to the Actin Clearance model.

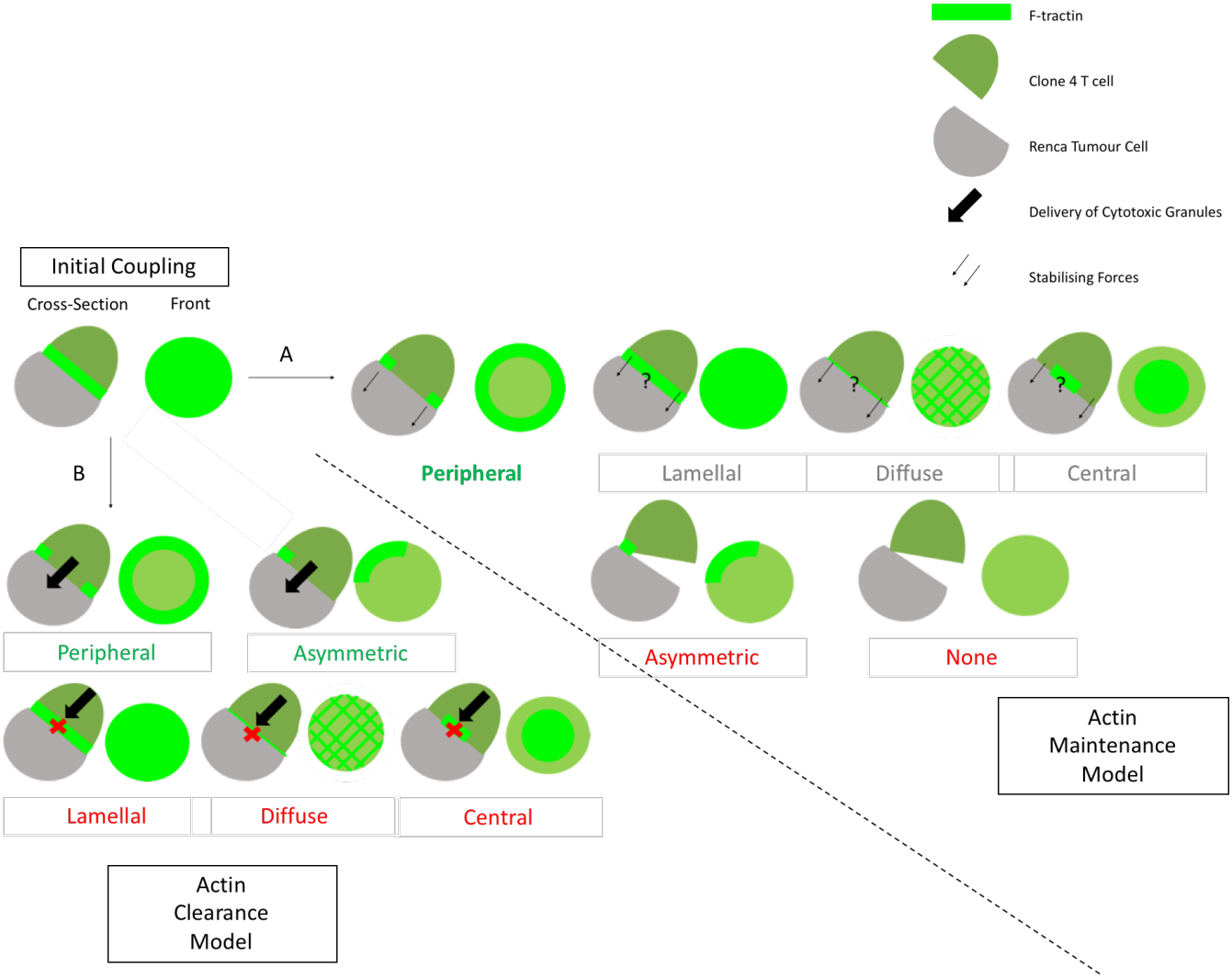

1.3.2.5 CD4+ T cells

CD4+ T cells modulate the CD8+ T cell, B cell and innate immune responses to pathogens, predominantly by releasing different cytokines. To date, many CD4+ T cell subsets have been defined, and these subcategories are subject to constant revision. CD4+ TCRs respond to antigen presented on MHC class II molecules, hence they are activated in response to antigens which originate extrinsic to the host's cells, usually deriving from extracellular pathogen.

1.3.2.5.1 CD4+ T cell Development

CD4+ T cells follow the same developmental path as CD8+ T cells. However, an important distinction occurs at the terminal stages of CD4+ Thymocyte development, allowing the formation of regulatory CD4+ T cells (79). Mature CD4+ Thymocytes undergo two possible fates. Either, CD4+ thymocytes become naïve CD4+CD25^{hi}FOXP3+ natural T regulatory cells (nTregs), which are capable of downmodulating the immune response immediately after leaving the thymus, or CD4+CD25^{lo}FOXP3- T cells leave the thymus and are induced to a particular CD4+ T cell function, either helper or regulatory, by signals in the periphery (1, 80). Whilst CD4+ T cells which respond to self-antigen with high affinity are usually deleted in the thymus, self-responders which express FOXP3 are protected from deletion. This is because the expression of FOXP3 programmes nTregs to exert regulatory, rather than self-reactive immune functions when self-antigen is encountered with high affinity (81). nTregs tend to suppress in a contact-dependent fashion, whereas Tregs which develop after thymic exit (peripheral or pTregs) tend to modulate other immune cells via cytokine release. The role of cytokines in nTreg-mediated suppression is not well understood, however, they are thought to require TGFβ, IL-2 and IL-15 signalling for their development (80). These cytokines seem to play a partially redundant role in nTreg generation, because deletion of at least 2 of them is required before defects in the number of nTregs are observed (82).

1.3.2.5.2 CD4+ T cell Activation

Conventional CD4+ T cells, which develop from CD4+ CD25^{lo} FOXP3- cells exiting the thymus, are divided into the following subsets: Th1, Th2 and Th17 helper cells, and induced Tregs (79). Other less-studied subsets also exist, such as Th9 cells and T follicular helper cells. CD4+ T cells are primed at the lymph node in response to antigen presentation on MHC Class II molecules expressed by DCs (79).

When a pathogen is encountered in the periphery, DCs produce different cytokines depending on which PAMPs and DAMPs are present to ligate receptors such as TLRs within the DC (79). DCs then prime CD4+ T cells, and the DC-derived cytokines provide Signal 3. The profile of cytokines generated by DCs at Signal 3 determines the transcription factor expression and epigenetic regulation which occurs within CD4+ T cells during activation (79, 83). Variation in transcription factor expression, as well as factors such as the strength of the TCR Signal 1 and co stimulatory Signal 2 result in CD4+ T cell differentiation to helper or regulatory subsets (79, 83). CD4+ T cell subsets are therefore induced by distinct cytokines, express different transcription factors and chemokine receptors and produce different effector cytokines (Table 1). The production of cytokines by DCs thus effectively acts as a messenger, relaying information from PAMPs and DAMPs to the adaptive immune system, to ensure that CD4+ T cells activated at the lymph node are equipped to deal with the pathogen which was encountered by DCs in the periphery (79, 83). However, after lineage acquisition in CD4+ T cells, the transcription factors associated with other lineages are not permanently downregulated, and they can be reprogrammed causing CD4+ T cells to acquire another lineage (79). CD4+ T cell plasticity has been best characterised amongst Th17 and pTreg populations (83).

Once activated, CD4+ T cells, can stimulate DCs via CD40/CD40-Ligand interactions, which make DCs more efficient at inducing further T cell responses (79). A subset of CD4+ T cells migrate to lymph node germinal centres where they become resident T follicular helper cells, whose role is to support B cells during somatic hypermutation and class switch recombination, generating high affinity antibody responses (13, 79). However, most CD4+ T cells leave the lymph node and circulate to the tissues after priming.

Table 1- CD4+ T cell Subsets

CD4+ T cell Subset	Cytokines/Molecules Produced	Transcription Factors Expressed
T Follicular Helper cells (Tfh)	IL-21	Bcl-6
Th1 cells	IFNγ	T-Bet
Th2 cells	IL-4, IL-5, IL-13	GATA-3
Th17 cells	IL-17A, IL-17F, IL-22	RORγt
Peripheral T regulatory cells	TGFβ	FOXP3
Tr1 cells	IL-10, Adenosine	FOXP3-
Th3 cells	TGFβ	FOXP3-

1.3.2.5.3 CD4+ T cell Effector function

During priming by DCs, signalling events downstream of the CD4+ TCR are largely the same as CD8+ T cell signalling events. However, during the subsequent interaction between primed T cells and pMHC, CD4+ and CD8+ T cells differ. The primary function of CD8+ T cells is to kill, whereas the function of CD4+ T cells is to direct the immune response to cope with specific types of pathogen. Effector CD4+ T cells, which have been diverted to a particular lineage by DCs at priming, encounter peptide for a second time when it is presented on MHC II by professional antigen presenting cells (APCs) such as B cells, other DCs or macrophages (84). During this second interaction, different CD4+ T cell subsets release characteristic cytokines to divert the immune response. Direct engagement of receptors on the APC with ligands on CD4+ T cells also provides co-stimulation to APCs, making their functions more efficient (5).

The Th1 subset of CD4+ T cells assists with cell mediated immunity directed at intracellular pathogens, by producing cytokines such as IFNγ. IFNγ causes macrophages to upregulate phagocytic activity and stimulates CD8+ T cells to kill infected or damaged self-cells (79). IFNγ also upregulates MHC I expression at the surface of infected or malignant cells, making CD8+ T cell recognition more likely (83). Th2 cells produce IL-4, IL-5 and IL-13, which promote degranulation of eosinophils, basophils and neutrophils in response to infection with fungal

cells or multicellular pathogens such as helminths (83). Dysregulation of Th2-mediated immunity occurs in allergy and in asthma. Th17 cells produce IL-17 and IL-22, which promote neutrophil responses and activate epithelia (79).

Regulatory subtypes of CD4+ T cells include nTreg which develop in the thymus (1.3.2.5.1), and peripheral Tregs (pTreg), which develop from CD4+CD25^{lo}FOXP3- precursors. Adoptive transfer experiments show that pTreg can develop in response to TCR stimulation with either self or foreign antigen *in vivo* (85, 86). pTreg modulate effector T cell priming and function, preventing autoimmunity. They produce TGFβ and IL-10, and express the transcription factor FOXP3. Co-inhibitory receptors, such as Cytotoxic T Lymphocyte Associated Antigen -4 (CTLA-4) and Programmed Cell Death Protein-1 (PD-1) are also characteristically upregulated amongst pTregs when compared to CD4+ T helper cells (83, 87).

The development of pTreg has been shown to require IL-2 and TGFβ, but it can occur *in vitro* in response to anti-CD3/28 mAb stimulation, hence pTregs can develop in the absence of APCs (82, 87). *In vitro* primed pTregs are known as inducible Tregs (iTregs). TGFβ induces the formation of pTreg in the periphery and *in vitro*, provided IL-2 is present. Without IL-2, expansion of CD4+CD25- T cell activation in the presence of TGFβ produces tolerant T cells which are unresponsive to re-stimulation (87). The addition of TGFβ to cultures of CD8+ T cells also produces CD8+CD103+ Treg cells with regulatory abilities such as IL-10 production (88). CD4+FOXP3+ pTreg have been shown to develop into inflammatory Th17 cells under inflammatory conditions in the presence of IL-6 (88). Therefore, the lineage commitment of pTreg is not finite and they can be re-directed to become T helper cells under certain conditions (89).

Other subsets of extrathymic Treg have also been characterised which, unlike pTreg, do not express FOXP3. The most well-studied subsets of CD4+FOXP3- Tregs are Tr1 cells and Th3 cells. Tr1 cells are formed when CD4+FOXP3- cells are subject to chronic antigenic stimulation, in the presence of the cytokine IL-10. Tr1 cells suppress in several characteristic ways, mostly through their inhibitory effects on DC-mediated antigen presentation to T cells, but also through the production of adenosine via the ectoenzymes CD39 and CD73 (90). Th3 cells are TGFβ secreting cells, which are mainly found at mucosal surfaces and have been studied in the context of oral tolerance induction. The precise mechanism governing Th3 cell development is

unknown, but it appears to involve unique events occurring at mucosal surfaces, especially in the gut. The signals which induce CD4+ T cells to become Th3 cells may involve a combination of Th2 cytokines such as IL-4, as well as the presence of TGFβ, IL-10 and IL-12. Th3 formation could also require the presence of mucosal APCs which are influenced by TGFβ (91).

1.3.2.6 T cell Fates – Memory, Exhaustion or Tolerance

Up to now, this review has covered the activation and effector functions of CD4+ and CD8+ T lymphocytes. This effector response typically takes place within 1-2 weeks of infection with a pathogen. When the antigen presented to naïve T cells is foreign, and displayed in an inflammatory environment, CD4+ and CD8+ T cells are primed by mature DCs causing them to proliferate and upregulate characteristic transcription factors, homing receptors and cytokines (12, 92, 93). During the immune response to acute infection, the acquisition of effector function amongst T cells occurs during clonal expansion and they eradicate pathogen (94). Besides acquiring effector function, it is now known that T cells can develop other fates between priming and death. For clarity, these fates are defined separately as Memory, Tolerance and Exhaustion, although they do share certain characteristics (94). A simplified model of fate acquisition is that naïve T cells proceed to Effector function, pathogen eradication and Memory T cell formation in the case of acute infection. However, T cell Exhaustion results if infection is not eradicated and becomes chronic. T cell Tolerance occurs if the antigens which prime T cells are self-antigens (Figure 7) (12, 45, 93).

Figure 7 - T Cell Fates, Memory, Exhaustion and Tolerance

Naïve T cells can acquire several fates depending on the conditions they experience during activation and during their functional lifetime (12, 93, 95). The first fate is activation and memory formation (top line)(12, 96). T cells are primed by dendritic cells (DCs), which take up antigen at the tissues and migrate to the lymph node to display antigen to T cells (42, 67). The T cell Receptor/Antigen interaction is termed 'Signal 1'. Strong signal 1 usually only occurs in response to foreign antigen, since strongly self-reactive T cells are deleted at the thymus before entering the peripheral repertoire (34). Foreign antigen is usually encountered by DCs in association with pathogenic and damage molecules which activate DCs, causing them to mature. Mature DCs (mDC) provide strong co-stimulation to T cells (Signal 2), alongside inflammatory cytokines such as interferon gamma (IFNγ)(Signal 3). Receipt of a combination of strong Signal 1,2, and 3 primes naïve T cells to become effectors (Teff) (2, 5, 42).

Effector T cells produce characteristic cytokines during the acute response, progressing from only IL-2 production, to polyfunctional release of IL-2, IFNγ and TNF-α. CD4+ T cells activate B cells, DCs and macrophages, and CD8+ T cells kill the pathogen during this effector phase (92, 95). After successful eradication of acute infection, Teff cells transiently produce IL-10 and upregulate co-inhibitory receptors to induce contraction of the immune response. Many Teff become senescent but a few cells possess the ability to form self-renewing memory populations (Tmem) which exhibit accelerated expansion and pathogen clearance if the infection is encountered again (12, 45, 95).

If the immune response cannot successfully eradicate pathogen, such as in chronic viral infections and cancer, the continued presence of antigen induces exhaustion amongst T cells (right downward arrow). Prolonged and high-level expression of IL-10 and co-inhibitory receptors causes Teff cells to acquire an exhausted phenotype (Tex). The release of cytokines including TGFβ, IL-10 and IL-27 by exhausted and regulatory immune cells supports the transition to Tex cells (93, 95). The acquisition of exhaustion is associated with the upregulation of transcription factors such as EOMES and T-bet, which regulate different genes in exhausted cells when compared to Teff or Tmem cells. Exhausted cells are not inert or senescent, and can be returned to effector function under certain conditions (93, 95).

Finally, if initial priming of T cells involves self-antigen, such antigens usually engage the TCR with weak affinity (left downward panel)(33). In addition, DCs rarely encounter such antigen in the context of inflammation or damage, so they are often displayed on immature DC (iDC). The combination of low Signal 1 and 2 encountered with self-antigen primes T cells to a state of abortive activation or tolerance (Ttol)(42, 97). The development of tolerance is further encouraged through signal 3, in the form of anti-inflammatory cytokines such as IL-10, TGFβ and IL-27, released by T regulatory (Treg) cells. Ttol cells exhibit diminished responses to antigen. Although they can recover and become effectors, epigenetic and genetic tolerance programming is remembered (97). Treg cells originate in the thymus or as an alternative to Ttol after priming with self-antigen. Treg can express the transcription factor FOXP3.

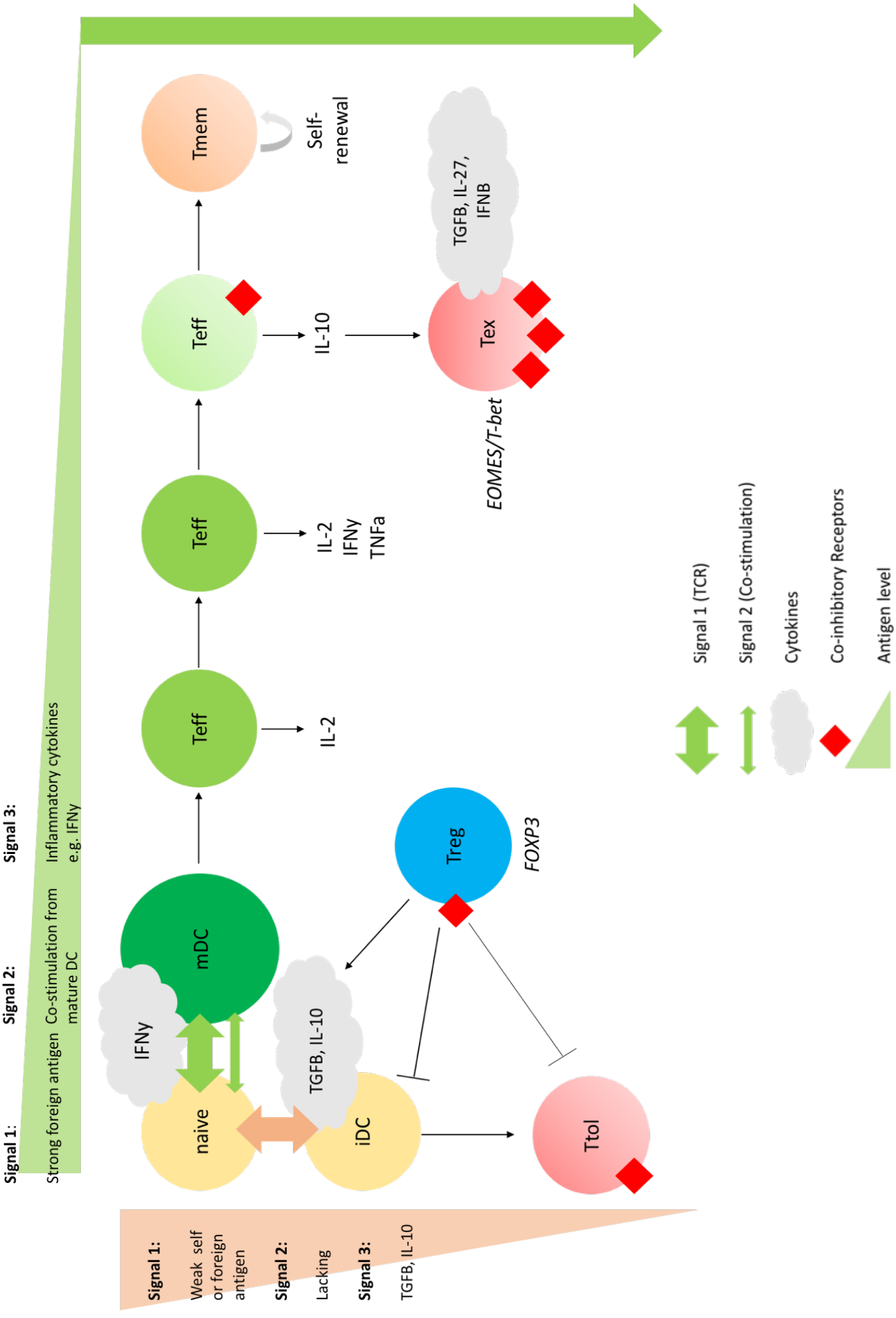
Signal 1:
Strong foreign antigen
Signal 2:
Co-stimulation from mature DC
Signal 3:
Inflammatory cytokines e.g. IFNy
naive
mDC
IFNy
iDC
TGFB, IL-10
Teff
Teff
Teff
Tmem
Self-renewal
IL-2
IL-2 IFNy TNFa
IL-10
Treg
FOXP3
Tex
TGFB, IL-27, IFNB
EOMES/T-bet
Ttol
Signal 1: Weak self or foreign antigen
Signal 2: Lacking
Signal 3: TGFB, IL-10
Signal 1 (TCR)
Signal 2 (Co-stimulation)
Cytokines
Co-inhibitory Receptors
Antigen level

1.3.2.6.1 Acute Infection leads to T cell memory

During the timeline of an acute immune response, cytokine production by effector CD4+ and CD8+ T cells involves first the production of IL-2, and then both IL-2 and IFNγ (92). Effector T cells often produce TNF-α as well, and are therefore known as polyfunctional effectors (92). T effector cells eradicate acute pathogen infection, at which point several events indicate the end of an acute immune response (12, 93, 98). As levels of infection wane, T cell activity must be dampened to prevent damage to host tissues, and a population of memory T cells must be generated (12, 45). The production of IL-10 by CD8+ T cells is usually associated with the end of acute immune effector function, and the onset of this transition (92).

Optimal priming causes many T cells to form rapidly expanding clones of effectors which contract and die. However, some T cells become longer lived memory cells which retain the ability to rapidly proliferate and exert effector functions. If antigen is encountered a second time by the host, the immune memory response is sufficiently rapid to eradicate pathogen before the host experiences disease symptoms (12, 45). Memory responses are therefore the physiological fate of some T cells at the end of infection (93, 95).

Several models have been proposed to explain when and how T cells are determined either to become short lived effectors, or to enter T cell memory development (12, 45, 99). No model fits perfectly with current observations, but common to all models is the idea that the environment encountered by a CTL during priming, migration and killing can have a profound effect on memory cell-fate decisions (12, 96, 100, 101). At the end of the immune response, CD8+ T cells which are destined for senescence or apoptosis, and those which form memory cells, differ in their surface marker, genetic and proteomic expression signatures, their ability to proliferate, their migratory and effector functions and their longevity. Memory T cells are conventionally further divided into 'Effector' and 'Central' memory phenotypes by these factors and by their typical anatomical location (12, 45, 96).

Murine T cells after acute activation are $CD62L^{low}$, CD44+, CD69+, CD103- and possess efficient migratory and cytolytic abilities. CD8+ T Effector Memory cells maintain some of the migratory and rapid killing functions of effector cells, but despite maintaining proliferative potential they are not actively dividing and produce little to no IL-2. They are identified by the signature

CD62L^{low}, CD44+, CD69-, CD103a-. Conversely, CD8+ T Central Memory cells are hugely effective at antigen-responsive proliferation and migration but less effective killers; they express CD62L^{low}, CD44+, CD69-, CD103a- (102). Memory T cell populations are maintained in the absence of antigen by slow cell renewal which resembles stem cell behaviour and is dependent on IL-7 and IL-15 (95).

Although the use of TEM and TCM subsets is convenient, there could be some plasticity between these fates. Furthermore, more than 30 subtypes of memory cells have now been identified, expressing different behaviours and different cell surface markers, These subsets have been better characterised amongst human lymphocytes when compared to murine populations (12, 45, 100). Overall, a fine balance of immunostimulatory and immunosuppressive factors, timed correctly over the course of the immune response is likely to be required to generate optimal T cell memory (12, 93). Besides memory formation, T cells can acquire two other fates after activation.

1.3.2.6.2 Chronic Infection leads to T cell Exhaustion

During chronic viral infection, the pathogen evades eradication and antigen is chronically present. In this scenario, the host protects itself from persistent immune activity by diverting T cells towards a fate known as Exhaustion, in which they lose effector function (93). Exhaustion is therefore a host-determined, protective response to chronic antigen in which the body sacrifices pathogen clearance, to prevent immune damage to tissues through persistent attempts at viral eradication (12, 95, 98, 103, 104). Notably, phenotypic characteristics of Exhausted T cells, such as the expression of co-inhibitory receptors and the production of IL-10, are observed transiently amongst T cells at the end of acute immune responses, however, it is chronic expression of this phenotype without progressing to senescence or memory, which defines Exhausted T cells (95). During chronic infection, Exhausted T cells therefore develop at the expense of memory populations (95, 98). Exhausted T cells have also been characterised in other disease settings in which chronic antigen persists, such as cancer and autoimmune disease. Such studies have identified a spectrum of exhausted T cell phenotypes (92, 93, 103-109).

- ***Characteristics of Exhausted T cells***

Exhausted T cells are distinct from Tolerant T cells because Tolerant cells are produced during priming if signal 1 and signal 2 are weak, and are less responsive to TCR stimulation. Exhausted T cells were activated to become effectors during priming, but the presence of chronic antigen along with other factors causes them to progressively lose effector function during their T cell lifetime. However, a state of exhaustion is sometimes reversible (95, 110).

The loss of effector functions by exhausted T cells occur in a stepwise fashion in peripheral tissues (111). Firstly, proliferative ability is lost, along with effector cytokine production. Amongst CD8+ T cells taken from acute infection, the progressive loss of IL-2, IFNγ and TNF-α which occurs at the end of inflammation is followed by a short period of IL-10 production, before memory formation. However, in exhaustion, cells produce IL-10 for prolonged periods, contributing to the suppression of other immune cells (92, 95).

After altered cytokine production, exhausted T cells exhibit alterations in migratory ability. Studies in Lymphocytic Choriomeningitis Virus (LCMV) infection have shown that CD8+ T cells in the secondary lymphoid tissues lose expression of CD44 and CD62L during chronic viral infection, when compared to acute stimulation. This results in an impaired ability of CD8+ T cells to leave the secondary lymphoid tissues, meaning that only T cells which left for the periphery during early infection are present at sites of viral replication. Chronically infected individuals therefore lack a source of freshly primed T cells specific to viral antigen, and cells in the periphery become exhausted, rather than memory populations (111).

After losing cytokine production and migratory function, exhausted CD8+ T cells also lose the ability to release cytotoxic granules (51, 77). Next, exhausted T cells upregulate the expression of co-inhibitory receptors (CIRs) on their surface, including CTLA-4, PD-1, Lymphocyte Activation Gene 3 Protein (LAG3), T-cell Immunoglobulin and Mucin-domain containing-3 (TIM3) and T cell Immunoreceptor with Immunoglobulin and ITIM domains (TIGIT)(95, 103, 112). These alterations are accompanied by upregulation of the expression of genes such as T-bet and EOMES (93, 95, 107).

- ***Factors which Promote T cell Exhaustion***

◊ *Chronic Antigenic Stimulus*

Although several influences are required to promote T cell exhaustion, the chronicity of antigenic stimulus is thought to be crucial as shown by studies in animal models and human patients infected with LCMV, Human Immunodeficiency Virus (HIV), Hepatitis B Virus (HBV), Hepatitis C Virus (HCV) and cancer. It has been identified that increased chronicity and avidity of antigenic stimulation correlates with more severe and irreversibly exhausted T cell phenotypes, and with deletion of exhausted T cells (95, 111, 113, 114). Early intervention in HCV and HBV treatment, which removes the chronic viral stimulus, appears to alter the progression of CD8+ T cells, preventing them from becoming exhausted (95, 113). Continuous antigen, as opposed to intermittent exposure appears to be required to achieve exhaustion amongst T cells (111, 114).

◊ *Co-inhibitory Receptor Signalling*

Crucial to the development of exhausted T cell phenotypes, is the upregulation of co-inhibitory receptors (CIRs) amongst CD8+ T cells. CIRs expressed on exhausted T cells include CTLA-4, PD-1, TIM3, TIGIT, LAG3, 2B4, CD160 and others (95). Some CIRs are upregulated as a functional consequence of normal activation, and effector T cells which function normally in terms of migration, killing and cytokine production do express CIRs. However, the presence of chronic antigen, along with other immunosuppressive cells and cytokines, induces aberrantly high and prolonged expression of CIRs during exhaustion (95, 115, 116). Additionally, a key marker of exhaustion is the expression of multiple CIRs in combination (95, 103).

Blockade of more than one inhibitory receptor is required to efficiently reverse T cell exhaustion in a variety of viral and tumour settings (103, 115, 117). Evidence from models of CMV suggest that in various diseases different CIRs could act as major and minor regulators of the immune response. In CMV, TIM3 and LAG3 are minor regulators, and blockade of these molecules alone produces only minor improvements in viral clearance unless blocked with a major regulator, such as PD-1 (118).

In cancer, a recent categorisation divided CD8+ tumour infiltrating lymphocytes (TILs) from a model of B16F10 melanoma into categories based on their CIR expression profile. Functional

TILs expressed PD-1 only and possessed a gene signature characteristic of effector T cells, whilst tumour-suppressed TILs expressed multiple CIRs and possessed an exhausted genotype (119). Similar divisions have also been identified in chronic viral infections such as LCMV and Hepatitis B and C (120). It has now been shown that single PD-1 expression, and expression of PD-1 with multiple other CIRs, is regulated by different genetic pathways. A gene module has been identified which is associated with co-expression of TIM3, LAG3, TIGIT, PD-1 and the cytokine IL-10 (121) (Figure 8). The transcription factors Prdm-1 and c-Maf were induced downstream of IL-27 signalling and promoted expression of this CIR module (121). Prdm-1 and c-Maf knockout CD8+ TILs did not develop an exhausted genotype within the tumour microenvironment, therefore upregulation of combinations of CIRs in controlled by the CIR gene module is required for the expression of genes related to exhaustion (121).

Two novel putative CIRs, Procr and Pdpn, were identified by studying IL-27 inducible genes. Deficiency in either of these molecules is associated with a reduction in tumour growth in murine models, supporting the finding that IL-27 induces multiple CIR expression and controls exhaustion amongst T cells (121).

Although the gene expression of multiple CIRs could be controlled by common transcription factors, the synergistic effect of blocking of multiple CIRs suggests that their engagement by ligands could produce T cell inhibition through disparate downstream mechanisms (95). It is now recognised that ligation of most inhibitory receptors exerts suppression on T cells by one of three mechanisms: spatial segregation of TCR signalling components to impair cSMAC formation; altered location or activation of TCR and cytokine signalling intermediates; or altered transcription of inflammatory genes and induction of anti-inflammatory gene targets (95). The interplay between CIR engagement and the downregulation of co-stimulatory signalling through pathways such as TRAF-1 and 4-1BB also influences the specific phenotype of exhausted T cells. Agonism of co-stimulatory pathways can reverse exhaustion in scenarios such as LCMV infection and cancer (119).

Figure 8 - IL-27 signalling induces expression of the Co-inhibitory Receptor Gene Module

Signalling initiated by interactions between interleukin -27 (IL-27) and the IL-27 Receptor (IL-27R) expressed on CD4+ and CD8+ T cells causes activation of the transcription factors Prdm-1 and c-Maf. Prdm-1 and c-Maf do not physically interact, but they exhibit overlapping binding sites. These binding sites were found to promote expression of a gene module which encodes concurrent expression of multiple co-inhibitory receptors, and the cytokine IL-10. Programmed Cell Death Protein-1 (PD-1), Lymphocyte Activation Gene 3 Protein (LAG3), T-cell Immunoglobulin and Mucin-domain containing-3 (TIM3), T cell Immunoreceptor with Immunoglobulin and ITIM domains (TIGIT), Protein-C receptor (Procr), Podoplanin (Pdpn)(121, 122).

Schematic based on the work of Chihara et al. 2018 (121).

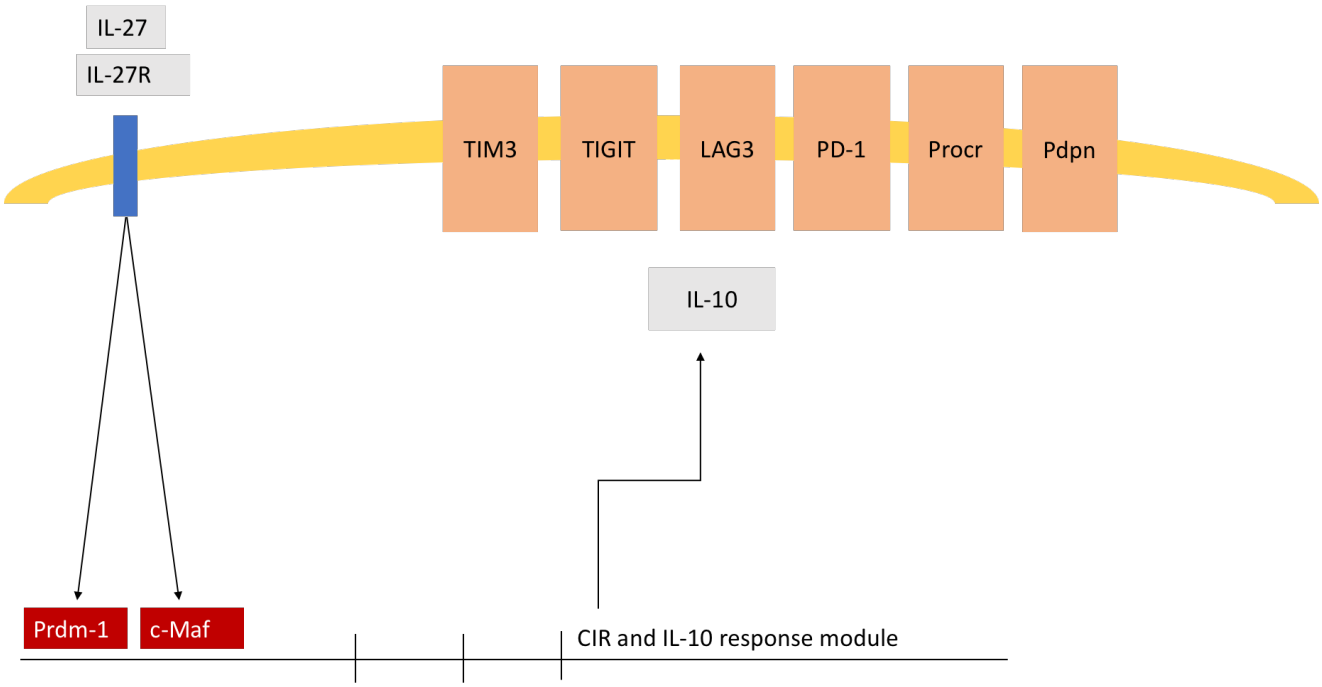

CTLA-4

CTLA-4 is expressed on effector T cells for a period of 24-48h after TCR engagement, during which time it performs a homeostatic role by limiting the magnitude of TCR signalling (123). It is expressed characteristically on Tregs for the duration of their lifetime, and on exhausted T cells for extended periods (123). Vesicular stores of CTLA-4 localise to the immune synapse after TCR ligation and TCR signal strength influences the levels of CTLA-4 which insert into the membrane. Endocytosis of CTLA-4 also regulates its action (123, 124). CTLA-4 exerts several effects on TCR signalling. It is ligated by CD80/86 expressed on APCs, and thus it competitively inhibits CD28 signalling, reducing the levels of co-stimulation received by the T cell. CD80/86 expressed on APCs may also be pulled in and internalised after interacting with CTLA-4, reducing the availability of co-stimulatory ligands for CD28 still further (124).

Ligation of CTLA-4 also results in signalling via its Immunoreceptor Tyrosine Inhibitory Motif (ITIM) domain, which recruits the inhibitory phosphatase PP2A to the immune synapse. Key targets of PP2A include Akt (123, 124). Formation of the LAT signalosome is also inhibited by phosphatases downstream of CTLA-4 ligation (123). Furthermore, CTLA-4 signals back to APCs, causing them to release indoleamine-2,3-dioxygenase (IDO), which inhibits T cell function (123). Therefore, CTLA-4 expression on effector T cells limits activation of the T cell itself, whereas CTLA-4 expressed on regulatory T cells reduces the efficiency of antigen presentation by professional APCs (124). Due to its effects on APC antigen-presentation and the receipt of co-stimulation by T cells, CTLA-4 disproportionally inhibits priming of naïve T cells, rather than the effector interaction between TCR and target cell. This means that CTLA-4 regulates the T cell response at an earlier stage than other CIRs (124).

PD-1

PD-1 expressed on T cells binds to its ligand, PD-L1 expressed on immune cells and tumour cells (76). An established mechanism of PD-1 signalling is the recruitment of the phosphatases SHP-1 and SHP-2 to its Immunoreceptor Tyrosine based Switch Motif (ITSM), thereby inhibiting TCR signalling through de-phosphorylation of key TCR signalling intermediates (123). PD-1 also possesses an ITIM motif, the role of which is imprecisely understood. Furthermore, a range of TCR intermediates appear to be directly modulated by PD-1, including

Ras, PI3K and AKT signalling (95). Some studies suggest that PD-1 also exerts its inhibitory effect by antagonising the effects of CD28 co-stimulation and thus, re-invigoration of the T cell immune response in the presence of PD-1 blockade could rely on CD28 signalling (119). For this reason, blockade of CTLA-4 and PD-1 has been shown to produce synergy in restoring exhausted T cells to effector function (119).

As discussed, there is now much evidence to suggest that the expression of PD-1 without concurrent expression of other CIRs is not associated with an exhausted genotype (76, 95, 103, 121). This new information has relevance because many studies of PD-1 signalling have been performed using *in vitro* primed cells which do not express other CIRs besides PD-1. Thus, *in vitro* models of exhaustion fail to produce many of the phenotypes seen *in vivo*, notably defective T cell migration, infiltration and altered transcription of effector genes such as BATF (95). Use of IL-27 to promote expression of multiple CIRs at once could allow us to generate better models of exhaustion, including PD-1 signalling, *in vitro*. In addition, the longevity of antigen signalling experienced during chronic viral infection and cancer is much greater when compared to short term *in vitro* cultures (76). Other work has also identified different roles of PD-1 signalling *in vitro* and *in vivo*. Administering anti-PD-1 mAb to tumour-bearing mice improved T cell polarisation and the formation of immune synapses by CD8+ T cells extracted from tumours, but blockade of PD-1 amongst *in vitro* primed CD8+ T cells inhibited immune synapse formation (76, 95).

TIGIT

TIGIT is expressed on T cells and NK cells. TIGIT expressed on T cells can bind to either CD155 or CD112 expressed on APCs, other T cells and tumour cells (120). The CD112-TIGIT interaction may not produce functional effects (120). CD226 is an alternative receptor for CD155 which produces costimulatory effects whereas TIGIT-CD155 binding produces inhibitory signalling. Therefore, the balance of expression of CD226 versus TIGIT determines whether CD155 produces stimulatory or inhibitory effects on T cells (120, 125). CD96 is another receptor for CD155, which is expressed primarily on NK cells and some T cells, and is thought to have immunoinhibitory effects.

In similarity with CTLA-4, TIGIT can also reverse signal to APCs, causing DCs to produce IL-10 and reducing their ability to prime T cells (120, 125). TIGIT contains an ITIM and an immunoglobulin tail tyrosine (ITT) motif in its cytoplasmic signalling portion, both of which have been shown to recruit phosphatases and inhibit NK cell signalling (125). Until recently, it appeared that TIGIT mainly influenced T cells indirectly, through its effects on DCs, but it has recently been shown to directly mediate downregulation of TCR, CD3 and PLCγ molecules, presumably through the action of its ITIM domain. TIGIT also actively downregulates pro-apoptotic signalling (120). Thus, TIGIT favours the survival of T cells, whilst rendering them exhausted.

LAG3

The CIR LAG-3 regulates the activity of CD4+ and CD8+ T cells and NK cells. Until recently, the only confirmed ligand for LAG3 was MHC II, and thus its proposed mechanism of action was competitive inhibition of CD4 co-receptor binding (120, 126). However, recently published work has shown that Fibrinogen-like Protein 1 (FLG-1), a hepatocyte metabolite, could have LAG3 binding capability (126). This work has implications for cancer immunotherapy, since molecules blocking LAG3-MHC II interactions have entered clinical trials but antibodies which block non-MHC binding sites of LAG3 have proved equally useful in mouse tumour models (126). Furthermore, LAG3-MHC II blocking mAbs have produced only partial control of tumour growth as a single agent, and since FLG-1 binding does not affect or exclude MHC II binding to LAG3, it is possible that these molecules form a complex, and that both the LAG3-MHC II and LAG3-FLG-1 interactions could require blockade in order to improve anti-tumour immune responses (126). The intracellular pathways which occur downstream of LAG3-FLG-1 interactions remain to be determined (121). Galectin-3 and LSECtin (Liver and lymph node sinusoidal endothelial cell C-type lectin) represent other ligands of LAG3 which may have immunosuppressive effects (126).

TIM3

TIM3 Discovery and Disease Associations

TIM3 is a co-inhibitory receptor expressed by CD8+ T cells, CD4+ T helper and T regulatory cells, DCs, macrophages, monocytes and NK cells (103, 116, 120, 127). The TIM3 protein is composed of an immunoglobulin variable domain, a mucin domain, a transmembrane region, and an intracellular signalling portion (127). The role of TIM3 in the downregulation of Th1 cells in the immune system is undisputed. The discovery of TIM3 was achieved during the search for regulators of Th1 immunity using a model of experimental autoimmune encephalitis (EAE), in which the authors noted that anti-TIM3mAb treatment accelerates disease progression and increases the number of inflammatory lesions (128). At this time, the expression of TIM3 was only identified amongst CD4+ T helper cells, and its proposed mechanism of action was engagement of an unknown ligand on macrophages to inhibit pro-inflammatory macrophage function (128). Since then, many studies have revealed that TIM3 is expressed on diverse immune cell types and that it is engaged by various ligands to produce a range of immunoinhibitory functions.

Aberrantly low TIM3 expression amongst peripheral blood cells is associated with autoimmune disease, and has been quantified in human patients with multiple sclerosis, psoriasis, Crohn's disease and rheumatoid arthritis (55, 116, 127, 129). Loss of function mutations in the TIM3 gene are associated with Subcutaneous panniculitis-like T cell lymphoma, a rare cancer associated with auto-immune syndromes which is treatable through immunosuppression (130). Conversely, TIM3 is expressed at aberrantly high levels amongst immune cells in chronic viral infections and cancers, where immune exhaustion contributes to pathology (116, 120, 129, 131, 132). TIM3+ cells are elevated in the blood of patients with chronic viral infections; including HIV, Hepatitis B and Hepatitis C viruses (HBV, HCV)(120). TIM3+ NK cells assist in the maintenance of maternal tolerance to fetal antigens (133). TIM3+PD-1+ cells have been identified as one of the most suppressed populations of CD8+ T cells within tumours, due to their inability to produce IL-2, IFNγ and TNF-α, hence TIM3 plays a key role in immune suppression by the tumour-microenvironment (116, 129, 131). However, the group which postulated that TIM3+PD-1+ cells are the most suppressed populations within tumours did not examine the other co-inhibitory receptors expressed by TIM3+PD-1+ cells. The recent discovery that TIM3, TIGIT, LAG3, PD-1 and IL-10 are co-regulated by the same module of genes

suggests that in fact TIM3+PD-1+ cells are simply cells in which the CIR gene module is active (121). TIM3 is also expressed on CD4+FOXP3+ Tregs and enhances their regulatory abilities (134).

Regulation of TIM3 expression

Several studies have identified a link between IL-27 signalling and TIM3 expression. Priming in the presence of IL-27 induces TIM3 mRNA and protein expression amongst CD4+ T cells (121). IL-27 has been shown to regulate the activity of the transcription factors ETS1 and NFIL3, which form a complex that regulates both TIM3, IL-2 and IL-10 expression. NFIL3 promotes tolerogenic downregulation of IL-2 and elevated IL-10 and TIM3 expression, whereas ETS1 has the opposite effect on these cytokines (135). Thus, TIM3 was shown to be co-regulated with the immunoinhibitory cytokine IL-10, in CD4+ T cells (135-137).

In work defining the CIR module of gene expression, the transcription factors Prdm-1 and c-Maf were determined to control TIM3 expression downstream of IL-27, rather than ETS-1 and NFIL3. Thus, several transcription factors have been identified as regulators of TIM3 expression, including ETS-1/NFIL3 and Prdm-1/c-Maf. However, IL-27 signalling appears to feed into both pathways, making IL-27 crucial for TIM3 expression (116, 120, 121, 135, 137). Co-induction of IL-10 transcription alongside TIM3 expression is also common to both proposed pathways (121).

IFNβ induces IL-27 expression and thus indirectly promotes TIM3 expression (121). Blockade of IFNβ controls chronic viral infection, and administration of IFNβ produces beneficial effects in the treatment of MS. Therefore, recent work supports the idea that certain cytokines such as IL-27, are master regulators causing expression of several co-inhibitory receptors concurrently with cytokines such as IL-10. Different transcription factors may orchestrate CIR expression downstream of the same cytokine and further studies are required to identify which transcription factors are active in different contexts (121).

TIM3 Ligands and Signalling

The TIM3 cytoplasmic domain contains 5 tyrosine residues. The kinases ITK, Lck and Fyn can all phosphorylate TIM3 at Tyrosine 265 and 263, however these residues are occupied in the resting state by a molecule called Bat3. If Bat3 is released after ligand engagement of TIM3, Src

kinases can bind to Y265 and Y263 in place of Bat3 (54, 120). Several ligands have been proposed for TIM3. In particular, binding of either of the molecules Galectin-9 or Ceacam-1 has been shown to be required for TIM3 to exert an inhibitory effect on T cells (138).

In the absence of ligands, the presence of TIM3 on the T cell surface could actually produce stimulatory effects (116, 138). Bat3, bound to the TIM3 cytoplasmic tail, acts as a reservoir for active Lck possessing the Y394 phosphorylation. Thus the availability of active Lck, a limiting factor for TCR signalling, is actually increased if TIM3 is present on the surface of T cells without being engaged (138). Although Ceacam-1 and Galectin-9 bind to the TIM3 molecule at different sites, binding of either ligand promotes release of Bat3, and Bat3 takes with it the pool of Lck required for TCR signalling. Bat3 release also vacates binding sites at the TIM3 tail (Figure 9) (54, 134).

Current evidence suggests that Fyn binds to the tails of TIM3 in place of Bat3, and activates PAG to recruit Csk, which downregulates TCR signalling (54). Bat3-/- cells demonstrate elevated phosphorylation of Lck at Y505 (the inactive form of Lck), suggesting that events following Bat3 release are associated with the addition of an inhibitory phosphate group at Y505 of Lck, as well as removal of Lck from the location of the TCR (54). The recruitment of other SH2 domain-containing proteins in the place of Bat3 could be responsible for this effect (120). Thus sequestration of Lck away from the immune synapse, and replacement of Bat3 by inhibitory kinases is one mechanism by which TIM3 engagement downmodulates TCR signalling, and TIM3-ligand binding is crucial for TIM3 to exert inhibitory effects (Figure 9)(138).

Figure 9 - TIM3 modulates Lck availability via BAT3

Schematic illustrating the proposed effects of TIM3 signalling on Lck localisation. (A) Shows the effect of TIM3 when it is not engaged by an inhibitory ligand. Unengaged TIM3 cytoplasmic tails are thought to bind to Bat3, which acts as a reservoir for primed Lck, phosphorylated at Y394. This increases the availability of Lck at the immune synapse to propagate TCR signalling (54, 55, 138). Hence, unless an inhibitory ligand is present, TIM3 lowers the threshold for TCR signalling. (B) Illustrates the proposed localisation of Lck when TIM3 is engaged by an inhibitory ligand. After TIM3 engagement by Ceacam-1 or Galectin-9, BAT 3 detaches from the TIM3 cytoplasmic tail, and with it removes a pool of Lck, reducing the potential for TCR signal amplification (54, 55, 121). Y256 and Y263 in the TIM3 tail, which were occupied by Bat3, become available to bind Src kinases such as Fyn.

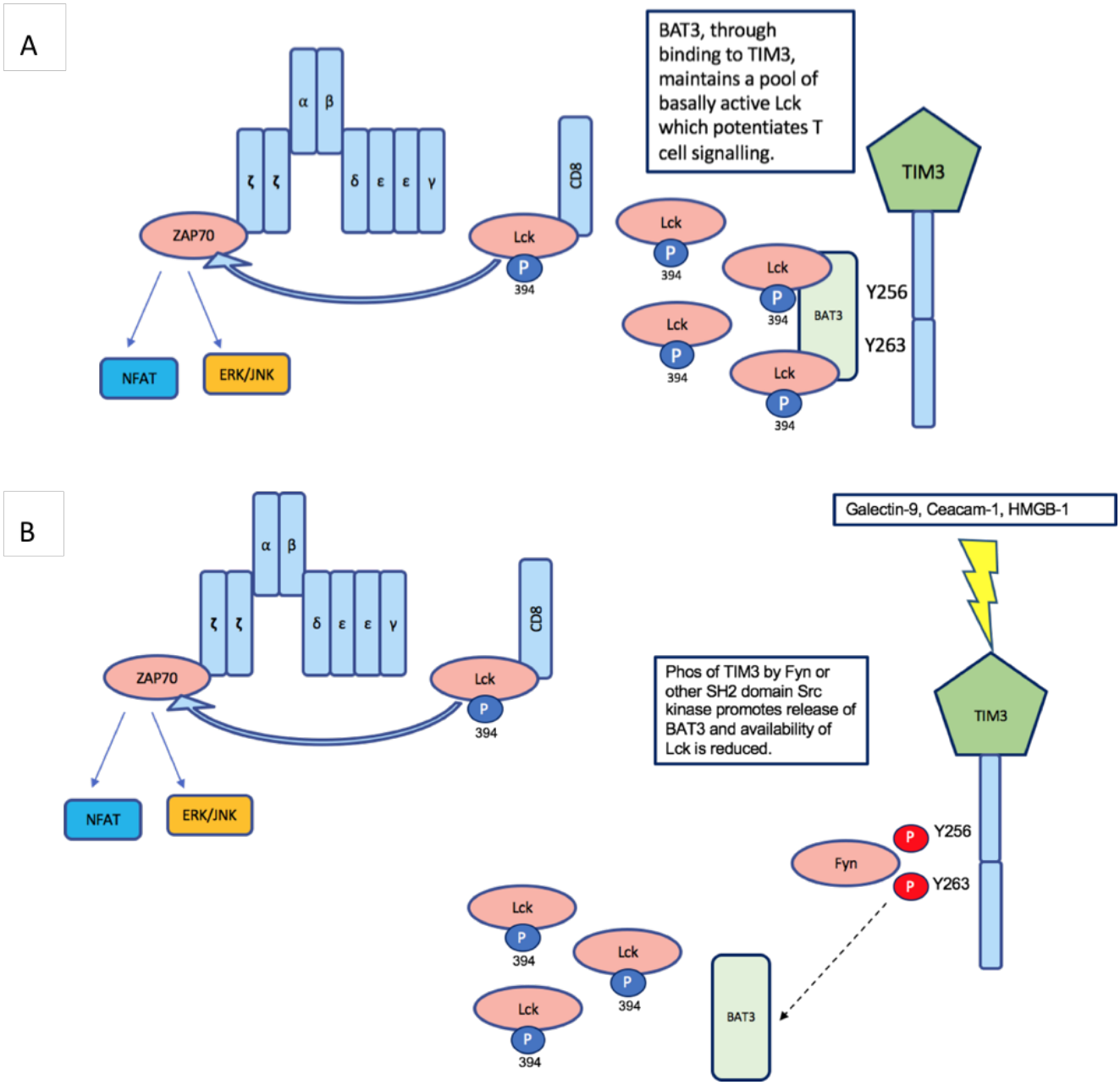

The interaction between the TIM3 ligands Galectin-9 and Ceacam-1 can occur in *cis*, on the same cell, or in *trans*, between two cells. It has been postulated that expression of Ceacam-1 with TIM3 in *cis* by T cells was required for the TIM-3 protein to be translated and expressed at the cell surface. However, these findings have since been challenged, due to the discovery that TIM3 and Ceacam-1 can be independently expressed (134, 138). As both Ceacam-1 and Galectin-9 interact with TIM3 in both *cis* and *trans*, the effects of ligand binding on TIM3 could also be spatially controlled. Amongst macrophages, binding of T cell-expressed TIM3 to macrophage-expressed Galectin-9 in *trans* inhibits TLR signalling, reducing IL-12 production. However, if macrophage-expressed TIM3 binds Galectin-9 on the same cell in *cis*, TLR signalling is promoted (127). Thus TIM3 appears to produce different signalling when expressed alone or when engaged by inhibitory ligands, and it could signal differently depending on whether it is ligated by binding partners expressed on the same cell in *cis*, or on other cells in *trans* (54, 138).

Another important ligand for TIM3 is phosphatidylserine (PSer) which is released by apoptotic cells. PSer appears to be particularly important for TIM3 signalling in innate immune cells, however it is unknown whether PSer binding to TIM3 expressed on lymphocytes, feeds back into lymphocyte function (127). It has been proposed that there is a link between PSer engagement of TIM3 and IL-10 production by lymphocytes, however the mechanism behind this association remains to be demonstrated (134, 135, 137). PSer engagement of TIM3 expressed on macrophages encourages phagocytosis of apoptotic bodies, however, engagement of TIM3 on lymphocytes does not lead them to acquire phagocytic abilities (127). If apoptotic bodies are not removed by the immune system their presence leads to the development of auto-reactive antibodies and autoimmune syndromes, thus PSer-TIM3 interactions play a key role in immune tolerance (127). Additionally, TIM3 may encourage uptake of apoptotic bodies, and presentation of antigen derived from them, by DC (127). CD8+ DC are more efficient at this process, and they express TIM3 at higher levels than CD8- DC (127).

High Mobility Group Protein B1 (HMGB1) is another ligand which strongly affects innate immunity when binding to TIM3 (120). Whereas binding of PSer to TIM3 expressed on DC appears to assist DC in their uptake of apoptotic bodies, binding of HMGB1 to TIM3 limits the other uptake ability of DCs, their ability to process DNA or RNA (120). HMGB1 normally facilitates binding of DNA to RAGE and TLR receptors within DC, however TIM3 limits this process (120). The uptake of tumour-derived DNA and its recognition as a damage signal is a

key step required for DC activation and maturation within tumours, therefore limitation of nucleic acid uptake by TIM3 signalling prevents DC maturation and effective presentation of tumour antigens to prime anti-tumour T cells (120, 134). Ceacam-1 and HMGB-1 demonstrate overlapping binding sites on the TIM3 molecule, however, at present it appears that the different ligands signal in different cell types, rather than competing for TIM3 binding (134).

The TIM3 ectodomain can be cleaved off by the action of A Disintegrin and Metalloprotease (ADAM). TIM3 cleavage could function to terminate signalling through TIM3, however, the cleaved domain may retain signalling capability and transfer it elsewhere, thus, further study is required to determine the functional impact of TIM3 cleavage (134).

In summary, TIM3 is considered to be an important CIR which controls the magnitude of the immune response. Reduced TIM3 expression is associated with exacerbation of autoinflammatory diseases and elevated TIM3 expression is associated with an ineffective and exhausted immune response in cancer and chronic viral infection. However, TIM3 can produce activating immune signals if expressed in the absence of inhibitory ligand binding.

◊ *Soluble Mediators*

IL-10

Soluble mediators are also important in the induction of T cell exhaustion (95, 139-141). IL-10 is a cytokine produced both CD4+ and CD8+ T effector cells towards the end of the acute immune response. However, it is produced chronically by exhausted or regulatory CD4+ and CD8+ T cells (92, 93, 107). B lymphocytes, NK cells, DCs and monocytes can also produce IL-10 (95). Induction of IL-10 production may be dependent upon IL-27 (121, 142).

IL-10 has been cited as a beneficial factor required for activated CD8+ T cell growth and maintenance, however many of the findings which support this idea are derived from *in vitro* data (143). Much like that of CIRs such as PD-1, IL-10 signalling behaves differently i*n vitro* and *in vivo*. The presence of single, short term IL-10 expression in *in vitro* culture is non-suppressive and might even be beneficial to T cell proliferation (143). However prolonged IL-10 expression alongside expression of multiple combinations of CIRs is associated with T cell exhaustion

during chronic infections such as LCMV, or in tumours, where IL-10 is encountered for long periods alongside other tolerogenic stimuli (95).

IL-10 is also known to inhibit the production of TNF-α and IL-1β by macrophages and monocytes, thus its influence affects innate immune cells and lymphocytes (142-144). IL-10 signalling also potentiates the development of regulatory cell populations including CD4+ Tregs and Myeloid Derived Suppressor Cells (MDSC) (145). Blockade of the IL-10 Receptor produces therapeutic benefit in a variety of chronic viral scenarios (142, 143). Observations in a murine model of CMV indicate that blocking the IL-10R in the early phase of the disease interferes with immune downregulation and can result in host pathology, equivalent to blocking the response to acute viral infection. However, once chronicity is established, blocking the IL-10R mediates viral clearance and reduced transmission rather than causing deleterious pathology to the host (142). These findings suggest that blocking IL-10 during its physiological function in managing acute immunity might not be beneficial, but in the context of T cell exhaustion due to chronic antigen, IL-10 blockade can produce therapeutic benefit (95, 142). The signalling which occurs downstream of the IL-10R is not well understood, and a more precise understanding of this pathway could allow us to manipulate IL-10 signalling for therapeutic benefit (95).

Type 1 and Type 2 Interferons

Type 1 IFNs such as IFNα and IFNβ are antiviral mediators which promote DC function and CD8+ T cell priming through Signal 3 (142). Type 2 IFNs such as IFNγ exert a pro-inflammatory effect on immune cells involved in Th1 mediated immunity, promoting killing by CD8+ T cells, cytokine release from Th1 CD4+ T helper cells, and the development of pro-inflammatory macrophages with efficient phagocytic abilities (2, 5). In cancer, both immune cells and tumour cells respond to IFNs to produce chemokines and cytokines which favour immune infiltration and activation early in tumour growth (141). However, chronic exposure to Type 1 and 2 IFN causes immune downregulation and is associated with disease severity in HIV and Hepatitis B Viruses (142). Type 1 IFN has been shown by several groups to induce IL-27 production and thus to indirectly influence the expression of IL-10 and CIRs (121, 142). Tumour cells also select for the upregulation of PD-L1 in the presence of chronic interferon stimulation (141).

TGFβ

TGFβ induces the development of regulatory T cell populations from naïve or effector cells and is crucially important for physiological control of the immune system (82, 146, 147). However it is also implicated in reversible T cell exhaustion during pathological states (118). TGFβ signals via SMAD proteins, and elevated SMAD2 phosphorylation occurs amongst CD8+ T cells in chronic viral infection, however blocking TGFβ did not improve viral elimination in mouse CMV models (118). Blocking TGFβ does produce clinical benefit in cancer, and knockdown of all three TGFβ isoforms improves viral clearance in LCMV. However, these effects appear to occur indirectly, because regulatory T cell development is impaired after TGFβ is lost, causing generalised immune activation. TGFβ also directly promotes invasion and metastasis amongst cancer cells, supporting the idea that the benefit of blocking TGFβ in cancer does not derive from a reversal of T cell exhaustion (95, 118).

◊ *Transcription factors*

There is significant evidence that exhausted CD4+ and CD8+ T cells represent a different genetic and phenotypic T cell fate when compared to either regulatory T cells or memory T cells. Transcriptional regulation of genes which regulate metabolism and inflammatory responses is markedly altered during exhaustion (95). Key transcription factors which are expressed in exhausted T cells include T-bet and EOMES. Factors such as the availability of pro-inflammatory cytokines from CD4+ T helper cells, and the strength and duration of chronic antigen engagement, produce heterogenous populations of exhausted cells with different gene expression profiles (95). Whereas FOXP3 is a canonical transcription factor of nTreg and pTreg cells, a genetic biomarker of exhausted cells has not yet been identified (82, 95). The identification of a specific biomarker of exhausted cells would be useful, to allow the accurate assessment of disease progression and the response to immunotherapy in many chronic diseases (95). Therefore, further characterisation of the transcriptome of exhausted cells is an area of research priority.

1.3.2.6.3 Recognition of Self-Antigen leads to T cell Tolerance

A third fate assumed by primed T cells is T cell tolerance. Although tolerance and exhaustion are similar because both involve a loss of T cell effector ability, tolerance is usually triggered by

self-antigen, whereas exhaustion results from chronic exposure to pathogenic antigen (67, 148). However, immune tolerance does not only involve T cells, and is really a term referring to all mechanisms by which the immune system ignores healthy self-tissues or matter which is non-threatening, such as food.

T cell tolerance occurs when self-antigen is presented on MHC molecules at priming or during effector function, to ensure that the T cell response to self-tissue is halted at an early stage, preventing autoimmunity. The T cells which experience tolerance are either deleted, primed to become tolerant, or diverted to form regulatory T cells (95). Some of the same cytokines and soluble mediators which lead to T cell exhaustion can also cause T cells to become tolerant or regulatory depending on the time and context in which they are encountered (94).

The inbuilt systems which maintain immune homeostasis are categorised into peripheral or central tolerance mechanisms. Central tolerance refers to the process of thymic selection of T cells, such that those with TCRs which respond to self-peptides with high affinity are deleted from the T cell repertoire before entering the periphery (Section 1.3.2.2) (94, 124). However, T cells which respond to self-peptide-MHC complexes with weak affinity are permitted to leave the thymus, because a weak reactivity to self-antigen indicates that their TCR is functional (1). These naïve T cells enter the circulation and make up the peripheral T cell repertoire. Their activity is controlled by processes of peripheral tolerance, as even weakly self-reactive T cells have the potential to activate in response to self-tissues (1). Peripheral tolerance mechanisms include tolerogenic priming, ignorance, and suppression by regulatory T cells.

- ***Tolerogenic Priming***

The T cell fate at priming depends partly on the effectiveness of antigen presentation by DCs (94). T cells require a combination of Signal 1, Signal 2 and Signal 3 to activate correctly. If one of these signals is weak, the presence of strong signals from the other pathways can compensate. For example, if weakly self-reactive T cells encounter self-peptide presented on MHC molecules by DCs, they will receive only weak Signal 1. However, if DCs were to provide lots of co-stimulation and inflammatory cytokines to boost Signal 2 and 3, activation against self-antigen could still proceed successfully. This rarely occurs, because DCs executing immunosurveillance for pathogens generally do not encounter self-antigen in the context of

PAMPs or DAMPs, so they rarely activate and mature when presenting self-antigen. When presenting weak Signal 1, immature DCs cannot provide sufficient signal 2 and 3 to compensate, so peripheral T cells do not activate to self-antigen (94). Priming of naïve T cells by weak signal 1, 2 and 3 usually produces either apoptosis, or a tolerant state (42).

After tolerogenic priming, T cells generally lack proliferative and cytokine production abilities. However, although tolerant T cells are less responsive than exhausted T cells to TCR stimulation, in some cases T cells may recover from either tolerance or exhaustion (42). *Ex vivo* expansion with IL-15 or *in vivo* expansion in response to lymphodepletion are two methods by which tolerant T cells have been re-programmed to effectors (94). However, tolerance is regulated by genetics and epigenetics, as well as by the environment (94). T cells can remember tolerance programming, and rescued tolerant T cells which have restored effector function, will often eventually return back to tolerance even in an inflammatory environment, as shown by adoptive transfer experiments (94).

Rarely, damage or infection within self-tissues releases DAMPs and PAMPs which activate DCs presenting self-antigen in a process called bystander activation. DCs then mature and provide Signal 2 and 3 to self-reactive T cells (149). In this manner, a traumatic event such as physical injury can initiate autoimmunity, and bystander activation could be involved in the pathogenesis of diseases such as multiple sclerosis (149). T cell tolerance is now recognised as a distinct phenotype from T cell anergy which is a state that develops from *in vitro* priming in the absence of co-stimulation (149).

- ***Immune Ignorance***

Immune ignorance is another tolerance mechanism whereby physical barriers such as the blood brain barrier create immunoprivileged sites in the body which cannot be accessed by effector immune cells. The central nervous system and the eye are the most well studied examples of immunoprivileged sites, and entry of effector T cells into the eye is important in the pathology of uveitis (149).

- ***Regulatory T cells***

Another important tolerance mechanism is the presence of Regulatory T cells. Regulatory T

cells represent a distinct fate from tolerised T cells. Priming with low signal 1 and 2 can lead to tolerance, or it can lead to regulatory T cell development if cytokines such as TGFβ, IL-10 and IL-27 make up Signal 3 (88, 95, 150). Similarly, exposure to chronic antigen can produce regulatory, rather than exhausted T cells, under certain conditions. There is some functional overlap between exhausted and regulatory T cells, since exhausted T cells produce IL-10 and express co-inhibitory receptors, therefore they are 'amateur' regulatory cells. However, professional regulatory T cells function possess a different genetic and epigenetic profile and perform more diverse mechanisms of suppression besides IL-10 and CIR engagement (151). The subsets of CD4+ T regulatory cells have already been described (Section 1.3.2.5).

CD8+ T regulatory cells also exist and can be either naturally occurring in the thymus (CD8+ nTreg) or adaptively generated in the periphery (CD8+ pTreg). In CD8+ T cells, there is no marker which differentiates naturally occurring and peripheral CD8+ Tregs. CD4+ and CD8+ nTregs express FOXP3 and CTLA-4 and suppress in a similar, contact dependent manner (151). It was thought that professional CD8+ pTregs did not exist, and that CD8+ T cells exerting regulatory functions were simply exhausted cells producing transient IL-10. However distinct populations of CD8+ pTregs have now been isolated from transplant patients, autoimmune disease, LCMV and cancer in humans and animal models (151). These cells have distinct genetic and epigenetic changes when compared to exhausted CD8+ T cells. Antigen presentation by immature DCs or in the presence of tumour cells are two methods which successfully produce CD8+ pTreg *in vitro (151).*

Both CD4+ and CD8+ pTregs suppress in multiple ways. Measuring the proliferation of effectors in the presence of an undefined T cell population is now a standard assay to determine whether this population represents Treg cells (152). Cell-cell contact between Tregs and DCs/T effectors reduces effector cell proliferation and IL-2 production. CTLA-4 and LFA1 expressed on Tregs engage ligands on DCs to limit their antigen-presenting abilities (152). Contact-independent mechanisms of Treg suppression include excessive binding to IL-2, sequestering it away from effectors, and production of the immunosuppressive cytokines IL-10, TGFβ and IL-35 (153). Both CD4+pTreg and CD4+ Tr1 cells can also produce adenosine since they express the adenosine producing enzymes CD39 and CD73, and previous data from our laboratory shows that CD4+ Tregs from tumours suppress T effector cells in an adenosine dependent manner (152, 154). CD8+ Treg expression of CD39 and CD73 has not previously been studied. Recent

evidence suggests that CD4+ Tregs can also directly interact with TCR signalling, by depleting calcium stores within T effector cells, however the mechanism for this finding remains unknown (152). Therefore, Tregs inhibit the efficacy of T cells at priming and proliferation in the presence of APCs, and can also directly inhibit the functions of primed, effector T cells. Together these effects allow Tregs to maintain peripheral tolerance. However, aberrant Treg activity occurs in cancer and in chronic infection, where Treg-derived signals can produce a disadvantageous state of exhaustion, rather than physiological tolerance (94).

1.4 Cancer

Cancer is a disease wherein the patient's somatic cells accrue genetic mutations and epigenetic alterations, resulting in the acquisition of traits which induce harm to normal tissues (155, 156). Six of these traits termed the 'Hallmarks of Cancer' were described by Hanahan and Weinberg (Figure 10)(155, 156). The six hallmarks which develop during the evolution of most cancers are: continuous proliferative signalling; evasion of growth suppression; acquisition of invasive and metastatic abilities; resistance to apoptosis; limitless replicative potential and the induction of angiogenesis in the TME (155, 156).

These hallmarks have since been expanded to include reprogrammed metabolism and evasion of immune attack because cancer pathogenesis does not only involve malignantly transformed cancer cells (155). Normal immune and stromal cells which are unmutated, but form part of the Tumour Microenvironment (TME) are induced by cancer cells to provide growth factors, nutrients and immunosuppressive molecules to support cancer growth and progression (155).

1.4.1 Sustained Proliferative Signalling and reduced Growth Inhibition

Sustained proliferative signalling is achieved primarily through Growth Factors (GF) which signal through receptor tyrosine kinases. In normal cell populations the magnitude of GF signalling, and therefore cell growth and entry into cell division is tightly regulated, however cancers either elevate GF signalling, or become able to signal independently of GFs. For example, somatic mutations in melanoma produce B-raf mutations in a subset of cancers, resulting in constitutively active MAPK signalling (155).

As well as sustaining pro-growth signals, cancer cells must evade anti-growth signals (155). Low availability of GF, oxygen and nutrients, as well as internal stress or damage signals, and excessive contact with other cells, are all signals which will halt cell division in non-malignant cells (155, 157). Cancers acquire mutations in the genes which regulate these processes so that they can continue to grow in the crowded and hypoxic conditions of the TME (157). For example, the tumour suppressor gene VHL limits cell growth in hypoxic conditions. VHL is mutated in Von Hippel Lindau (VHL) disease, which manifests as Renal Clear Cell Carcinomas, central nervous system tumours and pancreatic neuroendocrine malignancies (155, 158).

Figure 10 - The Hallmarks of Cancer

The hallmarks of cancer were described by Hanahan and Weinberg as the characteristics which are acquired in order for normal cells to become transformed cancer cells (156). These hallmarks represent adaptations which allow cancer cells to possess a survival advantage within the tumour microenvironment (TME). The 6 original hallmarks are sustained proliferative signalling; evasion of growth suppression; acquisition of invasive and metastatic abilities; resistance to apoptosis; replicative immortality, and the induction of angiogenesis in the TME (155, 156). Added to this list now are reprogrammed metabolism and evasion of immune attack, because the importance of the tumour microenvironment, and the non-cancer cell types which occupy it, must also be encapsulated within cancer hallmarks (155).

Figure taken from (159) adapted from 'Hallmarks of Cancer, the Next Generation' Hanahan and Weinberg 2011'(155).

1.4.2 Resistance to Apoptosis and Limitless Proliferative Potential

Cancer cells resist apoptosis in response to several triggers which would normally cause untransformed cells to die. For example, cancer cells possess an enhanced DNA mutation rate when compared to normal cell populations (155). DNA damage or mutations would normally lead to apoptosis, however, mutations in genes which initiate apoptosis after DNA damage, such as P53, is a key initiating event in several tumours. Loss of the DNA damage response allows subsequent high levels of mutation to occur without the induction of apoptosis or senescence (155, 160).

Cancers also evade apoptosis in response to metabolic derangements which occur within the TME and would ordinarily cause apoptosis (155). Apoptosis can be initiated by extracellular and intracellular signals, regulated by disparate machinery. However, both pathways converge on the activation of two pro-apoptotic proteins, Bax and Bak, which result in release of cytochrome-c from the mitochondria, initiating a cascade of caspase protein activation culminating in cell death (155, 161). An example of a key survival signal which is upregulated in many cancers including prostate, colon and lung carcinomas, glioblastoma, melanoma and rhabdomyosarcoma is Insulin like Growth Factor Receptor (IGF-1R)(161). Cixutumumab, a monoclonal antibody to the IGF-1R is being trialled in the clinic to treat several cancers (162).

As well as apoptosis, cancers also resist senescence. Under normal conditions, somatic cells are programmed to exit cell division after a set number of divisions. The finite number of cell divisions is indicated by progressive telomere shortening with each division. However, cancer cells, which are known as immortalised because of their capacity for limitless replication, express telomerase, an enzyme which adds telomeres back onto the end of DNA and thus extends the cell's replicative lifetime (155).

1.4.3 Neoangiogenesis and Metastasis

Previously, formation of novel blood vessels was thought to occur late in cancer development, to supply the centre of the enlarging mass with nutrients and oxygen. However, neoangiogenesis has now been identified in early tumours and in pre-malignancy (155). The acquisition of blood vessels supplies nutrients to cancer cells and supports metastasis (155). Important promotors of angiogenesis include Vascular Endothelial Growth Factor-A (VEGF-A).

In healthy individuals, angiogenesis is only initiated in unique and controlled scenarios such as wound healing. Physiological triggers for VEGF expression include hypoxia and GF signalling and healthy angiogenesis is time-limited (155). However, tumour neoangiogenesis occurs chronically and results in morphologically abnormal blood vessels (155).

Importantly, innate immune cells can promote angiogenesis as well as a range of tumorigenic processes, during inflammation in pre-cancerous tissues. Thus, although immune destruction represents a powerful mechanism by which tumours can be combatted, angiogenesis is a perfect example of a pro-tumorigenic process which is initiated by immune cells (155, 163).

As well as acquiring new vasculature, a key hallmark of cancer cells is the acquisition of metastatic potential (155). Cancer cells must invade surrounding blood and lymph vessels, traffic through them, and escape at distant body sites to form new tumours. Key regulators of this process include transcription factors involved in Epithelial-Mesenchymal transition (EMT), a process which normally occurs during wound healing and embryogenesis, but becomes dysregulated in cancer metastasis (155). For example, the transcription factor Snail represses the activity of E-cadherin, the most well studied anti-metastatic regulator. E-cadherin forms junctions with other epithelial cells in order to maintain organ structure, and dysregulation of this process allows cancer cells to spread. Snail function has been shown to be required for metastasis in a proportion of human breast cancers (164). After arrival at a new tumour site, metastatic clones of tumour cells which have undergone EMT may then undergo the reverse process, MET, allowing them to persist and form new tumour masses (155). Selection pressure from the new environment can induce migrating metastatic cancer cells to attain new qualities, distinct from that of the original tumour (155).

1.4.4 The Tumour Microenvironment

In addition to the six hallmarks of cancer cell populations, the existence of a TME is also key to cancer development, and the TME has its own hallmarks. An important implication of the concept of the TME is that the study of the molecular characteristics of cancer cells themselves is insufficient to fully characterise the likely aggressiveness and behaviour of an individual tumour (139, 155, 165).

The niche propagated by tumour cells contains blood vessel endothelia and pericytes, immune cells, cancer associated fibroblasts, and stromal cells as well as cancer cells themselves (155). The first hallmark of the TME is that non-cancer cell populations provide sustenance signals which maintain proliferation and immortality amongst cancer cells whilst promoting invasion and angiogenesis (155). In turn, cancer cells signal to the stroma to encourage this sustaining behaviour. For example, tumour associated mesenchymal stromal cells are induced by cancer cells to secrete CCL5, which confers invasive abilities upon tumour cell populations (155).

A second TME hallmark is the ability of tumour cells and their associated niche to subvert the anti-cancer immune response. Cancer immunosuppression is discussed in detail later (155). Finally, cancer cells exhibit deranged control of metabolism, which enables them to survive in the challenging conditions generated by a rapidly proliferating mass of cells with heterogenous spatial areas within the TME (155). Cancer cells upregulate glucose transporters and readily switch from oxidative phosphorylation to glycolysis as their chief use of glucose. This phenomenon is known as the Warburg effect and it allows cancer cells to survive in poorly vascularised tumours, where oxygen is scarce (155, 166).

1.4.5 Heterogenous Cancer Cell Populations

The hallmarks of cancer, however, are not accrued by all cells within the tumour. Usually, cancers arise from a heterogenous population of cells, of which only a few, termed cancer stem cells (CSCs) are able to actively generate new tumours by developing hallmarks (167). Cell surface markers have been developed which identify CSC populations in a variety of human tumours, and they activate characteristic signalling pathways which give CSCs stem-like abilities. Activation of the Wnt/β-catenin, Notch and PI3k pathways is characteristic of CSCs (167). These pathways represent three of the ten pathways cited by The Cancer Genome Atlas as being present in over 80% of cancers, indicating the importance of CSC populations in propagating tumour growth (168). The CSC concept challenged the previously accepted natural selection model of tumour development: that heterogenous populations of cancer cells with high genetic and epigenetic instability respond to selection pressures in a purely Darwinian manner. Thus, each population would have equal potential to form the final tumour, depending on the environmental pressures encountered (155, 167). Newer models combine both the CSC and evolution paradigms with novel understanding of the microenvironment. Current models

suggest that although cancers propagate from stem cells, and under selection pressure become increasingly homogenous over time, other small populations of cancer stem cells do persist, providing a source of new mutations (167). These CSCs can develop into new cancer cell clones if new selection pressures are encountered (167). Furthermore, cells without intrinsic stemness can be induced to acquire CSC properties due to signalling within the TME (167). For this reason, cancers rapidly acquire resistance to drugs targeted at them, because cell populations which lack the drug receptor, or possess a redundant pathway to the one being blocked, can survive treatment and proliferate to dominate the new tumour cell population (155, 167).

1.5 The Immune Response to Cancer

The concept that the immune system can detect and respond to cancer was first described by Burnet and Thomas, and termed cancer immunosurveillance (169). The interaction between the immune system and cancer is complex, because immune cells can both promote and inhibit cancer growth (155, 169). Whether the immune system exerts a positive or negative prognostic influence depends on several factors, but perhaps most importantly on the timing of immune infiltrate with respect to tumour growth (169). Chronic pro-inflammatory signalling can propagate tumour initiation in non-cancerous tissue, invoking wound healing responses which upregulate pathways involved in transformation, angiogenesis and metastasis (155, 169). However, in established cancers, immune cells can directly lyse cancer cells and mediate tumour regression. In particular, CD8+ T cells and NK cells have the ability to directly lyse tumour cells (155). CD8+ T cells have been proven to recognise tumour-derived antigens which are naturally expressed on MHC-1 molecules in tumours (170).

The interaction between the immune system and tumours is now described as cancer immunoediting, because the immune response to an individual tumour can shape the phenotype of that particular cancer (139, 169). Immunoediting occurs over three phases of tumour interaction with the immune system, termed Elimination, Equilibrium and Escape (169, 171, 172). Firstly, tumour cells are eliminated by competent immune cells which recognise them as different from healthy self-tissue. Only tumour cells which possess specific mutations, enabling them to resist immune attack, can survive. As these cells become more numerous, a point of equilibrium is reached, during which the immune system is able to destroy tumour

cells as fast as they proliferate, so their number remains constant. Finally, tumour cells escape immune control, leading to the development of a cancer mass, which possesses an immunosuppressive TME (173). In the case of haematological malignancies, although cancer cells are found diffusely within the body and they do not occupy a physical niche, their effect on the cells around them is also described as a microenvironment (171).

1.5.1 Requirements for successful Tumour Immunosurveillance

Chen and Mellman recently described a progression of events that are required for the immune system to effectively detect and attack tumours. Mostly these events involve the development of a successful CD8+ T cell response, supported by Th1 cells and cytokines. NK cells can kill tumours but play a less significant role (174). Subversion of any of these events forms the basis of cancer immunoediting and escape from immune destruction (Figure 11). The progression for steps to cancer immune destruction is described as a cycle, because killing of cancer cells by immune cells causes release of cancer antigens and upregulation of damage signalling within the tumour, thereby amplifying and perpetuating the cycle of immune attack (174). The ways that tumours inhibit steps in the cancer immunity cycle generate a complex phenotype of CD8+ T cells. T cell dysfunction within tumours can be related to exhaustion, because cancers represent a source of chronic antigen, and to tolerance, because many cancer antigens are self-antigens (175). However, cancers also select for cancer-specific immunosuppressive factors which synergise with exhaustion and tolerance signalling to produce a unique dysfunctional genotype and phenotype observed only in tumours (94). For clarity, this will be discussed as a distinct T cell fate termed “Tumour Suppression”.

1.5.1.1 Step 1,2 and 3- Presentation of Tumour- Antigens by DCs to prime T cells

The first event required for anti-tumour immunity is the expression of antigen by cancer cells in a context recognised by the immune system as foreign. The immune system will generally only break tolerance and respond to antigen if the peptide presented is non-self, or if it is a self-peptide associated with significant danger signals including DAMPs (42). Tumour antigens are divided into tumour-specific antigens (TSA) which are novel, non-self and uniquely expressed in tumour tissue, or tumour associated antigens (TAA) which can be expressed in both tumour and other tissues. Many TAA display tissue-specific expression, for example Melan-A is expressed uniquely in melanocytes, and is overexpressed in tumour versus normal skin.

Therefore targeting of Melan-A by the immune system will produce a largely tumour-specific response even though it is a TAA and not a TSA (176). It is now thought that most tumours express TSA or at least highly TAA at some stage in their development. Therefore there are antigens which can effectively be targeted by the immune system in most cancers (176). In addition, the expression of TSA is favoured in tumours with a high mutational burden such as melanoma or lung cancer, where genomic instability is caused by ultraviolet radiation and smoking respectively. Many mutations that enable tumours to be recognised by the immune system are random, generated by DNA damage or defects in DNA repair, and they usually differ from cancer driving mutations in that they do not confer growth advantages upon a cell population (177).

When cancer cells die and release antigen, it is taken up by DCs. DAMPs ligate receptors such as TLRs which activate these DCs to become mature DC (mDC) from immature DC (iDC). mDC present peptide on MHC I and MHC II to T cells at the tumour-draining lymph node (TDLN) whilst providing high levels of Signal 2 and 3. The levels of Signal 2 and 3 provided is sufficient to prime anti-tumour T cells even if the tumour expresses self-antigen, as long as damage signalling is present to induce DC maturation. However, if damage signalling within the tumour is lacking and DCs remain immature, the priming that occurs can cause T cells to assume regulatory or tolerant fates in response to tumour antigen.

Cancers limit antigen presentation by DCs by eliminating clones of cells which express non-self antigen, or by editing antigens so that they are no-longer recognised as foreign. Such antigenic drift is often seen within immunogenic tumours (174). Cancers also downregulate the production of danger signals required for DC maturation. The fact that cancer cells resist apoptosis during cellular stress means that low levels of cell death reduce the availability of both antigen and DAMPs for DCs (155). Inducing damage responses within the tumour using chemotherapy or radiation can therefore encourage DCs to take up and present antigen in an immunogenic fashion (155). Alternatively, engagement of co-inhibitory ligands and cytokine receptors on DC can inhibit their ability to mature, or to present antigen. For example, VEGF, lactic acid, TGF-β and IL-10 all prevent DC maturation within tumours (178). The interaction between DC and T cells at the TDLN can also be impaired if regulatory immune cell populations establish in the lymph node and produce cytokines which are associated with tolerogenic Signal 3. CD4+ Tregs at the TDLN can produce TGFβ and IL-10, for example (89).

Figure 11 - The Cancer Immunity Cycle

The cancer immunity cycle describes the events which are required for effective anti-tumour immunity. These events are known as a cycle, because Step7- tumour killing by immune cells releases antigen and damage signals to promote Step 1 in the cycle, amplifying the response further (174). Steps 1, 2 and 3 involve the expression and release of tumour antigens, uptake of these antigens by dendritic cells (DC), and DC maturation and presentation of antigen to prime anti-tumour CD8+ T cells at the tumour draining lymph node (TDLN). Steps 4 and 5 involve the traffic of CD8+ T cells to tumours, and tumour-infiltration. Step 6 is the recognition and killing of tumours by primed CD8+ T cells. Thus there are three key levels at which CD8+ T cell-mediated anti-cancer immunity is inhibited, priming, infiltration and killing (174). Depending on the tumour type, different stages of the cycle are inhibited, and therapy should aim to define and target the areas of weakness in the cancer immunity cycle for each individual tumour (119, 174).

Figure taken from 'The Cancer Immunity Cycle. Chen and Mellman. 2013'(174).

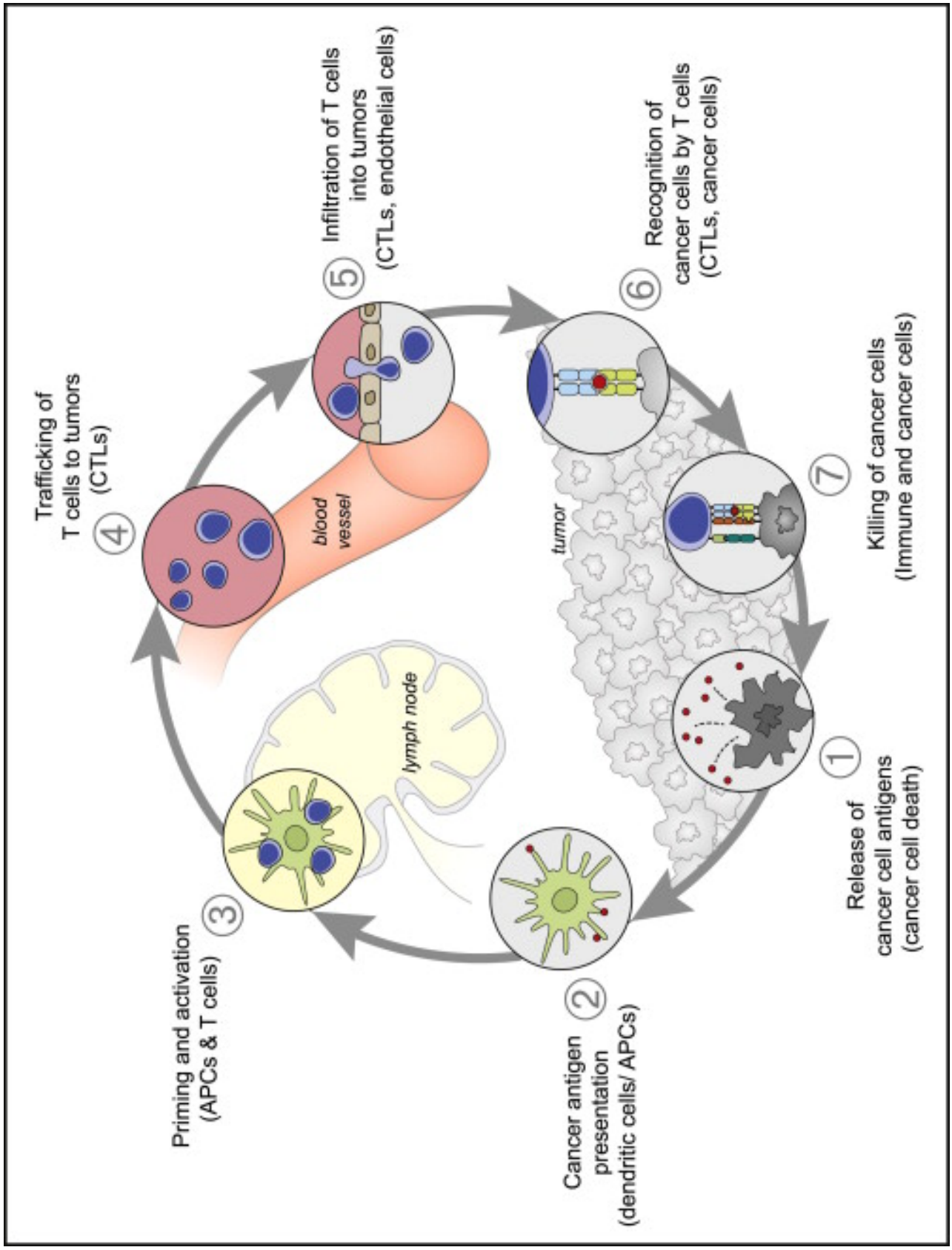
1
Release of
cancer cell antigens
(cancer cell death)
2
Cancer antigen
presentation
(dendritic cells/ APCs)
3
Priming and activation
(APCs & T cells)
4
Trafficking of
T cells to tumors
(CTLs)
5
Infiltration of T cells
into tumors
(CTLs, endothelial cells)
6
Recognition of
cancer cells by T cells
(CTLs, cancer cells)
7
Killing of cancer cells
(Immune and cancer cells)
blood
vessel
lymph node
tumor

1.5.1.2 Step 4 and 5 – Trafficking and Infiltration of T cells into tumours

Tumours can prevent T cell infiltration in several ways. Soluble mediators found in the TDLN can reduce the ability of CD8+ T cells to migrate to tumours. For example, Adenosine and PGE_2 signalling in the TDLN elevates PKA activity within T cells. PKA could reduce Rho-A activity, which is required for T cell transmigration through epithelia (Section 1.5.1.3.1) (179). Other factors which are encountered once T cells reach the TME can also prevent infiltration. For example, reactive oxygen species within the TME can nitrosylate chemokines such as CCL2 which are important for the recruitment of CD8+ T cells (178, 180). As well as disruption of chemokine signalling, tumours possess abnormal blood vessel morphology (178). The presence of factors such as VEGF which promote neoangiogenesis also inhibit T cell passage across endothelia (178). Furthermore, regulatory T cells can influence tumour vessel architecture, and depletion of CD4+ FOXP3+ Tregs has been associated with the development of high endothelial venules, which are specialised to allow T cell infiltration into tumours (180).

1.5.1.3 Steps 6 and 7 – Recognition and Killing of Cancer cells by T cells

In some tumours, a T cell infiltrate is present, CD8+ T cells are found to be unable to kill tumour tissue when assayed *ex vivo* (51). Multiple pathways known to mediate exhaustion or tolerance operate within the TME and suppress CD8+ TILs, however there are some immunosuppressive factors which are unique, or disproportionately upregulated in tumours when compared to other scenarios. These include: cell types such as myeloid derived suppressor cells (MDSC), tumour associated macrophages (TAM) and cancer associated fibroblasts (CAF); soluble molecules such as Adenosine and PGE_2 signalling, and expression of unique combinations of CIRs (181-184).

1.5.1.3.1 Tumours contain Unique Immunosuppressive Influences

- ***Myeloid Derived Suppressor Cells***

An important suppressive cell population identified in cancer are Myeloid Derived Suppressor Cells (MDSC). Although MDSC are observed in other diseases such as Multiple Sclerosis, they play a minor role in immunosuppression in non-cancer scenarios, and depletion of MDSC does not produce clinical benefit in mouse models of autoimmune disease (174). MDSC are immature cells of the myeloid lineage, which express CD11b and Gr-1. Their differentiation is induced by

IL-6, VEGF, PGE_2, and Granulocyte Macrophage -Colony Stimulating Factor (GM-CSF) (185). TIM3 engagement of Galectin-9 on cells of the monocytic lineage also induces MDSC development (134). MDSC are divided into a CD11b+LY6G+$LY6C^{low}$granulocytic subset, and a CD11b+LY6G−$LY6C^{hi}$ monocytic subset (185). MDSC can perform certain functions of both granulocytes and monocytes, but they also suppress T cells by several mechanisms. The activity of iNOS and arginase-1 within MDSC degrades arginine, an amino acid required for T cell proliferation. These enzymes also generate reactive oxygen species (ROS) and peroxynitrate, which inhibit T cells, and may also nitrosylate components of the T cell receptor, reducing TCR signalling efficiency (185).

- ***Tumour Associated Macrophages***

Macrophages are categorised as Type 1 or Type 2 depending on their phenotype. T1 are pro-inflammatory, they produce IFNγ, IL-12 and TNFα, and they efficiently phagocytose and present antigens (127). T1 macrophages are typically associated with a good prognosis amongst cancer patients, however their presence can be detrimental in tumour initiation, where inflammation can propagate malignant transformation (163). Macrophages found within the tumour are known as tumour associated macrophages (TAM)(127). Signalling derived from cancer cells, hypoxia and immune factors such as TGFβ, IL-4, IL-10, IL-13 and GM-CSF usually diverts TAM to acquire an anti-inflammatory T2 phenotype. T2 TAM express arginase and produce ROS in a similar manner to MDSC, causing suppression of T cells. However, TAM also produce potent oncogenic effects on cancer cells. For example, TAM can provide EGF signalling to encourage proliferation amongst breast cancer cells (186). Macrophages can also produce factors which promote EMT amongst cancer cells, and they can generate pro-angiogenic factors such as VEGF. Thus, TAM represent an important immunosuppressive and pro-oncogenic cell population in many cancers (186, 187).

- ***Co-Inhibitory Receptors and Cancer***

CIRs are receptors expressed on the surface of immune cells which, when engaged, downregulate inflammatory activity. Physiologically, they help to downregulate normal immune responses, however they become overexpressed, and expressed in unique combinations, during exhaustion, tolerance, and tumour suppression. Recent work identified a CIR gene expression module which regulates the expression of TIM3, TIGIT, LAG3, PD-1 and IL-

10 concurrently within tumours. Furthermore, this work categorised TILs extracted from B16F10 melanoma into two populations based on their expression of CIRs. Clustering analyses identified single PD-1 expressing TILs as having an effector genotype, whereas TILs which co-expressed combinations of TIM3, TIGIT, LAG3 and PD-1 exhibited an exhausted genotype (121, 134). Further work is required to elucidate whether TILs from other cancers can be divided into effector and suppressed populations using their CIR expression profiles. Additionally, the expression of other CIRs besides those listed above, such as Ceacam-1, has not yet been examined in this context (121).

One important CIR in the context of cancer is TIM3 (134). TIM3 expression in tumour patients has been shown to be elevated amongst TILs when compared to peripheral blood cells (129, 188, 189). Additionally, in a model of allograft tolerance, TIM3+ Tregs are found only in graft tissue and not in the blood, spleen or LN (190). These studies suggest that TIM3 expression is differentially regulated in the tumour and in peripheral sites, which may allow TIM3 to be targeted therapeutically in cancer without producing systemic autoimmunity (116, 188).
Mechanistically, TIM3 is known to be important in cancer-mediated immunosuppression. Polymorphisms in the TIM3 gene are associated with increased susceptibility to cancers such as NSCLC (134). Elevated TIM3 expression by DCs is invoked by VEFG-α and IL-10 in the TME and is associated with reduced DC maturity and poor antigen presentation (134). TIM3 is also upregulated amongst NK cells in cancer and TIM3 expression marks dysfunctional NK cell populations (120). TIM3+FOXP3+ Tregs from tumours produce more IL-10 and TGF-β and express greater levels of CD39 than those without TIM3. In CD8+ TILs, TIM3 expression is associated with a loss of IFNγ production and TIM3 expression by tumour cells themselves is associated with oncogenic characteristics including stem-cell like characteristics and the acquisition of metastatic abilities (134). The HeLa cancer cell line shows reduced metastatic potential *in vitro* when TIM3 is knocked down (127). Therefore, TIM3 represents an important CIR expressed on multiple cell populations within the TME, however its expression is largely tumour-specific (120, 134).

TIM3 expression can also be used as a prognostic biomarker in cancer patients (116). The presence of TIM3+ Tregs correlates with poor prognosis in Non-Small Cell Lung Cancer (NSCLC). TIM3 expression by NK cells correlates with poor prognosis in Metastatic melanoma, and elevated TIM3 RNA levels within tissue samples is associated with a negative prognosis in

prostate, renal, gastric and cervical cancers (120, 134). anti-TIM3mAb therapy improves the response to anti-PD-1 blockade in clinical trials of melanoma, NSCLC and non-Hodgkin's lymphoma, and TIM3 blockade rescues escape from anti-PD-1 mAb therapy in a mouse tumour model, therefore it could represent an effective new target for immunotherapy (115, 120).

- ***Soluble Mediators and Cancer***

Although soluble mediators such as chemokines and cytokines including IL-10 and TGFβ are important in mediating T cell exhaustion during chronic infection, there are some soluble mediators of immunosuppression which are predominantly seen within cancers. Adenosine and Prostaglandin- E_2 (PGE_2) are two mediators which, although they are transiently upregulated at the end of the immune response between acute infection and memory formation, do not become chronically elevated except in cancer (181-183, 191). Furthermore, the levels of adenosine identified in tumours is elevated 100 fold when compared to inflamed tissue, therefore adenosine is an example of a soluble mediator which plays a unique role in cancer when compared to other scenarios (181-183, 191).

◊ *Prostaglandin E_2*

PGE_2 is produced from arachidonic acid by the action of cyclooxygenase enzymes (98). PGE_2 plays a pro-inflammatory role in acute inflammation and cyclooxygenase inhibitors are potent anti-inflammatory medicines. However, chronic exposure to PGE_2 limits effector function amongst CD4+ T cells, CD8+ T cells, NK cells and DCs. PGE_2 also diverts T cells to produce tolerogenic cytokines such as IL-10, and induces monocyte precursors to form MDSC within tumours (98, 192). During chronic LCMV infection, CD8+ T cells were found to upregulate PGE_2 receptors due to chronic antigen exposure. Thus, elevated production of PGE_2 and an increased sensitivity of immune cells to respond to it both play a role in exhaustion. However, levels of PGE_2 become more elevated and more persistent within tumours when compared to chronic viral infection.

PGE_2 is particularly important in colorectal carcinomas. One mechanism by which PGE_2 accumulates in these cancers, is a tumour-associated mutation in the gene encoding 15-PDGH, one of the enzymes which degrades PGE_2, although other imbalances in the breakdown and production of PGE_2 have been identified in a variety of tumours (193). PGE_2 receptors are G-

protein coupled receptors which produce elevated cyclic AMP within cells, thus PGE_2 signalling could act through the same pathway as adenosine signalling, discussed below (98).

◊ *Adenosine*

Adenosine Production

Adenosine a metabolite that is produced by the sequential action of the enzymes CD39 and CD73 (181). CD39 is expressed primarily on immune cells and converts ATP to AMP through the removal of two phosphate groups, whereas CD73 is stromally expressed and catalyses the conversion of AMP to adenosine (182). ATP exerts pro-inflammatory effects on immune cells via purinergic PX2R receptors, whereas adenosine is predominantly immunosuppressive, therefore the conversion of ATP to adenosine represents a switch by which inflammation is downregulated (194). The production of adenosine is a protective response triggered by the presence of hypoxia or necrosis, which is indicative of inflammation-induced tissue damage (195). However, adenosine production becomes dysregulated in cancer, and it reaches up to 100 fold higher concentrations within the hypoxic tumour microenvironment when compared to inflamed tissue (191, 196-199).

HIF1α and HIF2 are the critical hypoxia-induced regulators of adenosine signalling. Signalling downstream of HIF induces CD39 and CD73 expression, increases expression of the immunoinhibitory A2a and A2b adenosine receptors, and reduces the expression of nucleotide transporters which allow adenosine uptake into cells to reduce extracellular concentrations (200). Thus, the high levels of HIF which are produced in hypoxic tumours result in elevated adenosine signalling amongst tumour-infiltrating immune cells (200).

Adenosine Receptors

Immune cells express 4 adenosine receptor subtypes, A1, A2a, A2b and A3. Whilst A1 and A3 receptors are predominantly pro-inflammatory, A2a and A2b receptors produce immunosuppressive effects (140, 182-184, 191, 200). Of these, A2a receptors (A2aRs) are the highest affinity receptor, and they are responsible for adenosine-mediated immunosuppression in cancers, as evidenced by the ability of single A2aR blockade to restrain tumour growth in several murine cancer models (181-184, 195). A2aRs are upregulated in an adenosine dependent manner following T cell activation (201).

Inhibition of TCR Signalling through Lck

Although the exact mechanism by which A2a Receptor engagement inhibits CD8+ T cells is unidentified, A2a receptors are G-protein coupled, and A2aR signalling induces the accumulation of cyclic AMP (194). Adenylyl cyclase activity has been demonstrated at lipid rafts containing TCRs, indicating that the presence of A2aRs or PGE_2 receptors can result in cAMP production locally at the immune synapse (202). Together these data suggest that engagement of A2aRs affects TCR signalling within T cells (194, 201). Other observations in T cells support this hypothesis. The accumulation of cyclic AMP in T cells is known to produce inhibition of TCR ζ chain phosphorylation and to be associated with reduced IL-2 production (65, 203, 204). Furthermore, the pre-clinical benefit of A2aR antagonism in models of murine cancer is lost if IFNγ is neutralised, suggesting that A2aRs directly affect cytokine production by CD4+ and CD8+ T cells. TNFα and IFNγ production by A2aR-/- Chimeric Antigen Receptor (CAR) CD8+ T cells is improved after extraction from the TME, when compared to WT CAR T cells (201). Adoptive transfer of A2aR -/- CAR T cells is associated with a greater proportion of endogenous CD8+CD44+ T cells in the spleen. This suggests that if adoptively transferred T cells, primed outside the host, are resistant to A2aR engagement, then priming of the host's endogenous T cell populations is facilitated.

cAMP has been shown to reduce the activity of Lck at the immune synapse, therefore immune modulators such as adenosine and PGE_2, which produce elevated cAMP, could exert their effects through Lck (65). Lck is negatively regulated by phosphorylation of its tyrosine residue Y505 (49, 53). The kinase Csk is a key mediator of Lck phosphorylation at this residue. It appears that Phosphoprotein Associated with Glycosphingolipid-enriched membrane domains (PAG) binds Csk and brings Csk into spatial contact with lipid rafts containing Lck, allowing it to add phosphorylation to Lck505 and produce the inactive Lck form (65, 203, 204). Protein Kinase A type I (PKA) which is constitutively associated with TCR microclusters, localises at elevated levels in response to increased cAMP accumulation, and further activates Csk in its location at the immune synapse (65, 202). Thus, a cAMP-PKA-Csk axis acting to reduce Lck activity represents one mechanism by which adenosine signalling could negatively regulate T cells (Figure 12). Blocking PKA produces an improvement in T cell production of IL-2 in cells taken from HIV patients (202). However, a direct link between adenosine receptors and the Lck pathway has only been established up to the level of PKA activation, and an A2aR dependent

effect on Lck signalling remains to be demonstrated (194). PKA activity can also influence other downstream mediators of TCR signalling, inhibiting NFAT nuclear translocation, Ras-Raf signalling, and calcium mobilisation by PLCγ, although the exact molecular interactions occurring to mediate these functions are not well understood (205) .

Inhibition of Actin Re-organisation for Migration and Immune Synapse Formation

As well as directly influencing TCR signalling, PKA regulates actin dynamics and cell morphology in several cell types. In lymphocytes, cAMP could influence cell morphology by elevating PKA-mediated phosphorylation of the Rho GTPase, RhoA (206, 207). PKA can be recruited to RhoA through the A-Kinase-Anchoring-Protein activity of Ezrin, where it phosphorylates Ser188 (208). This limits the activity of RhoA, by increasing its interaction with guanine nucleotide dissociation inhibitors, and removing it physically from the location of the plasma membrane (206).

The functions of Rho-A in lymphocytes are numerous and not fully elucidated. Rho A signals at the rear of T cells to orchestrate T cell migration and homing, (207). However, T cell polarity and migration has not been examined in Rho-A knockout mice to identify the exact migratory deficiencies that could result from a loss of RhoA (207). Rho-GTPases also play a role in correct spatiotemporal organisation of immune synapse signalling machinery after TCR/pMHC interactions, but again the way in which RhoA affects TCR signalling intermediates and actin dynamics at the immune synapse has not been defined (207). One proposed mechanism by which cAMP and PKA could inhibit immune synapse formation through RhoA is by reducing the interaction between RhoA and ROCK. This would lead to reduced myosin light chain phosphorylation, reduced actinomyosin contractility and suppressed MTOC translocation amongst CD8+ T cells. In this way, PKA would provide a direct link between engagement of A2aR and PGE_2 signalling in the TME, and the MTOC translocation defects identified by several groups in tumour-infiltrating T cells (48, 71, 73).

PKA can also mediate translocation of the Rho-GTPase CDC42 to the cytosol. CDC42 knockdown impairs microcluster formation and actin-polymerisation at the immune synapse, thus PKA could impair actin dynamics via CDC42. Overall, the regulation of actin dynamics by PKA in lymphocytes requires further investigation to determine how adenosine and PGE_2 feed into this

pathway, and whether PKA affects actin through CDC42, Rho-A or both pathways together (179, 208).

Upregulation of Co-Inhibitory Receptor Expression

Another mechanism by which adenosine signalling could produce T cell inhibition relates to production of the inhibitory cytokine IL-27. Autocrine and paracrine IL-27 signalling mediates upregulation of the gene module controlling CIR expression and IL-10 production in T cells (121, 144). A cAMP/PKA axis has been shown to increase IL-27 production by increasing binding of cyclic AMP response element binding protein (CREB) to the IL-27 promotor. Although CREB is produced with NF-κB, AP1 and other transcription factors contributing to T cell activation, CREB can bind to the IL-27/EB13 promotor region as well as promoting IL-2 production and proliferation (144). CREB is required for IL-27 production, whereas other transcription factors downstream of TCR stimulation are dispensable (208). Therefore CREB, produced in response to TCR stimulation and PKA signalling, has both stimulatory and inhibitory effects.

Although a direct link between adenosine receptor signalling and IL-27 production has not been explored, PGE_2, which also acts to elevate intracellular cAMP, has been shown to directly influence IL-27 production via CREB (144, 150). Furthermore, an association between elevated cAMP and IL-10 production has also been demonstrated. Blockade of PKA reduces IL-10 secretion in response to cAMP agonists, although whether this occurs via a reduction in IL-27 driven IL-10 production has not been shown. Therefore, upstream cyclic AMP signalling could be an important driver of an IL-27/IL-10 pathway, but this remains to be fully proven (150).

Figure 12 – Inhibition of T cell functions downstream of A2a Adenosine Receptor Engagement

The immunoinhibitory A2a Adenosine Receptor is a G-protein coupled receptor. Ligation of this receptor by adenosine induces elevation of cyclic AMP at the T cell membrane (191). cAMP has been associated with multiple signalling events in T cells.

Firstly, cAMP recruits and activates Protein kinase A (PKA), which activates Csk. Csk is known to add the inhibitory Y505 phosphorylation to Lck, inhibiting TCR signalling, however the effects of A2aR engagement on Lck phosphotype have not been conclusively demonstrated (204, 209, 210).

PKA also inhibits the actin regulators RhoA and CDC42, which could interfere with T cell migration, polarisation and MTOC translocation to the immune synapse (205).

Finally, elevated cAMP is associated with the activation of the CREB transcription factor, which promotes IL-27 expression (205). Autocrine and paracrine IL-27 signalling produces expression of the co-inhibitory receptor gene module within T cells, causing the expression of multiple co-inhibitory receptors and IL-10 o be upregulated concurrently. Again, a complete pathway from A2aR signalling to IL-27 production remains to be demonstrated (121).

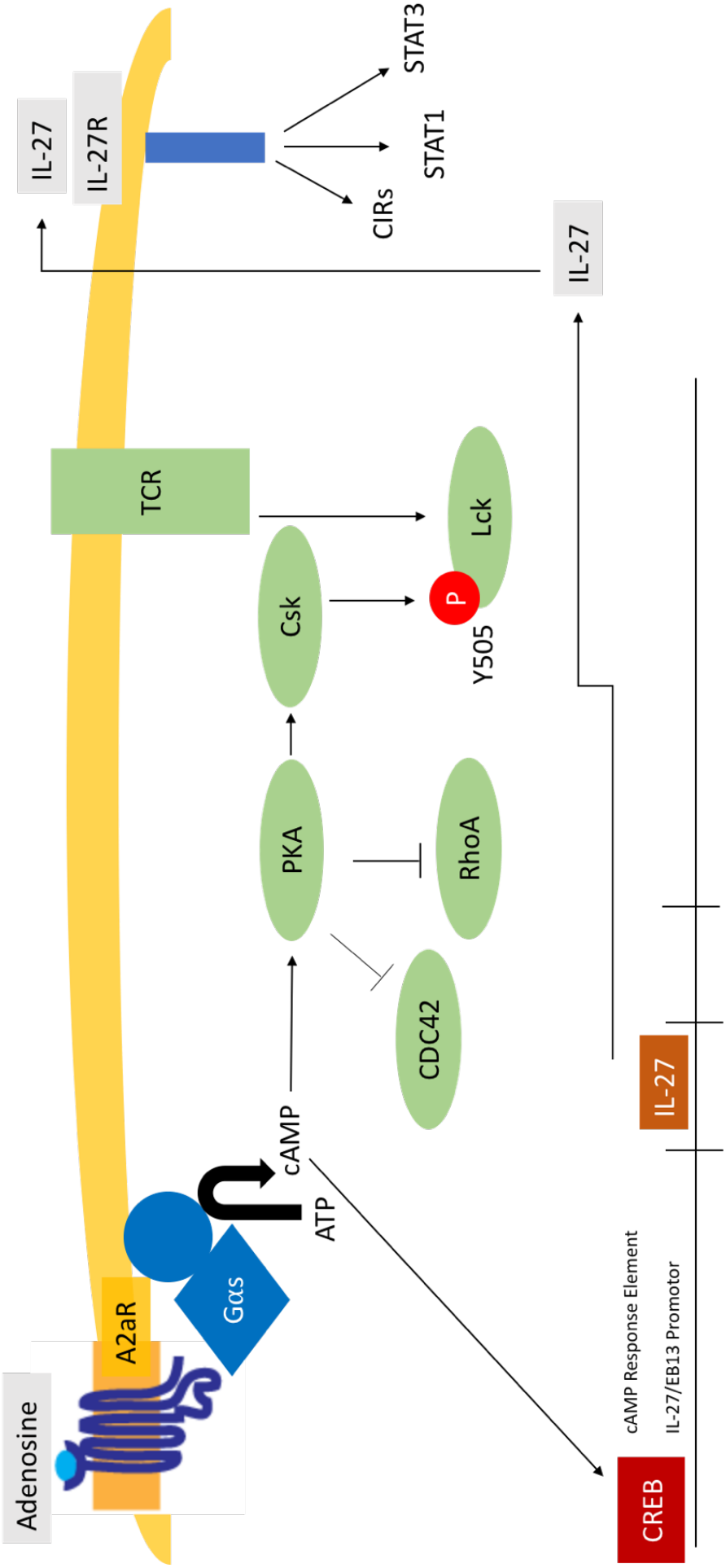
Adenosine
A2aR
Gαs
cAMP
ATP
PKA
CDC42
RhoA
Csk
TCR
Lck
P
Y505
IL-27
IL-27R
CIRs
STAT1
STAT3
IL-27
CREB
cAMP Response Element
IL-27/EB13 Promotor

Since IL-27 signalling promotes expression of a module of genes including IL-10 and CIR expression, either adenosine or PGE_2 signalling could feed into the expression of multiple inhibitory receptors and IL-10 concurrently (121). Further work should examine whether adenosine and PGE_2 mediate redundant effects via cyclic AMP, and whether a cAMP/IL-27/IL-10 and CIR pathway co-ordinates the effect of adenosine and PGE_2 amongst tumour-infiltrating T cells.

Taken together, these data suggest that Adenosine signalling through A2a receptors could inhibit T cells through multiple pathways, and further molecular studies are required to elucidate its exact effects. Furthermore, the effects of other adenosine receptors could antagonise or synergise with A2aR signalling, and the balance of adenosine receptor expression under different scenarios could be an important determinant of whether Adenosine is immunosuppressive to T cells.

Studying Adenosine Receptors In Vitro

The effects of A2aR agonists and antagonists on immune cells *in vitro* has not been well studied. In neuronal cells, A2aRs form complexes with dopaminergic D_2R receptors. A2aR agonists and antagonists bind with different conformation to the A2aR when administered singly or simultaneously to *in vitro* neuronal cultures, and they produce different effects on signalling through the A2aR-D_2R heteromer depending on the levels of starting intracellular calcium and the concentration administered. Antagonists have been shown to both inhibit and potentiate A2aR-D_2R signalling in different contexts (211, 212) . It remains to be determined whether adenosine receptor antagonists can both stimulate and inhibit A2aRs expressed on immune cells, in a similar manner when used i*n vitro*, however studies using these molecules appear to be difficult to execute and have produced conflicting results (211, 212).

Adenosine Signalling in Cancer Patients

Clinically, CD73 expression can be used as a biomarker for cancer prognosis, and elevated CD73 expression is associated with negative outcomes in HNSCC, NSCLC, ovarian, prostate, renal, gastric and breast carcinomas (195). Furthermore, many groups are investigating the usefulness of A2aR adenosine receptor antagonists and Anti-CD73 mAbs in the treatment of

cancer (1.6.3.3.3). Therefore, A2aR signalling is an important tumour-specific pathway that could be targeted for immunotherapy.

1.6 Current Approaches to Cancer Therapy

1.6.1 Traditional Cytotoxic Therapies

The mainstay of cancer therapy still consists of surgical excision or de-bulking, followed by treatment of residual disease with chemotherapy or radiotherapy, aimed at the non-specific destruction of rapidly dividing cells (213). Such therapies are successful in destroying cancer cells, but are associated with a high level of toxicity, since the body depends on rapid cell division for the maintenance of tissues such as the intestine and skin (213). More advanced methods for delivery of cytotoxic agents and radiation allows for more specific delivery to the tumour site, and ensures that these therapies are still important in the clinic. However, targeted therapies are often used alongside cytotoxic agents to reduce the dose required and limit adverse effects (214).

1.6.2 Targeted Therapies

The term targeted therapies refers to the use of agents which block pathways known to be genetically mutated within the cancer but not within the patient's body cells. For example, Epidermal Growth Factor (EGF) inhibitors, are used in lung cancer to combat cases in which the extracellular domain of the EGF receptor is mutated, resulting in aberrant pro-proliferative signalling (213).

However, the genetic instability of cancer cells and the presence of CSC clones in established tumours means that many cancers rapidly acquire resistance to targeted therapy. For example, in Chronic Myeloid Leukaemia, Bcr-Abl pathway inhibitors such as imatinib are effective drugs, however, clones of cancer cells emerge in the face of imatinib treatment, which have a mutated Bcr-Abl kinase that signals in the presence of the drug (213). Furthermore, several redundant pathways tend to contribute to each cancer hallmark and in the face of targeted therapy, other pathways can become mutated to allow that hallmark to persist. The idea of whole hallmark targeting is therefore under investigation as a therapeutic strategy with reduced potential for acquired resistance. However, the identification of key upstream regulators of many pathways is required to implement whole hallmark targeting (213).

1.6.3 Immunotherapies

Although targeted therapy offer great potential in the treatment of many types of cancer, a key criticism is that it only takes into account the cancer cells themselves and neglects to consider the importance of other cell types in the TME. Amongst therapies which target cells extrinsic to cancer cell populations is immunotherapy, the concept of pharmacologically encouraging cancer killing by immune cells (174). The use of immunotherapy to treat patients with cancer has seen a rapid increase in study over the last 15 years, and several single and dual therapy combinations are now licensed to treat a variety of cancers (174). One of the greatest breakthroughs in cancer immunotherapy was the improvement in overall response rate from 15% 2 year survival with chemotherapy to 54% 2 year survival when anti-CTLA-4 and anti-PD-1 monoclonal antibodies were used to treat advanced melanoma (117). However, the use of these monoclonal antibodies did not give rise to survival benefit in other cancers.

To determine why this occurred, the immune character of individual tumours must be characterised. Tumours are hugely complex in terms of their immune infiltrate, and the character and location of tumour immune cells has been shown to be a better indicator of prognosis than traditional tumour grading in several cancer types (119). In particular, studies of different cancers revealed that the presence of a CD8+ T cell infiltrate is more strongly associated than any other cell type, with prognosis and response to immunotherapy (119). These findings have led to a classification known as the immunoscore, which categorises tumours based on the number and location of CD8+ and CD3+ cells, and the other immunosuppressive factors found within the TME (Figure 13). Tumours are described as Hot, Cold, Altered-Excluded or Altered-Immunosuppressive, on the basis of their immune infiltrate (119). These categories reflect the steps of the cancer immunity cycle which are inhibited in each cancer type.

Hot tumours possess large numbers of CD8+ TILs, which characteristically express CIRs but no other forms of suppression. Altered-Immunosuppressed tumours express intermediate numbers of CD8+ TILs, and soluble mediators such as IL-10 and TGFβ, and suppressive cell populations such as CD4+ Tregs and MDSC also contribute to immunosuppression alongside CIR expression. Altered-Excluded tumours lack T cell infiltration except at the tumour periphery. They are often hypoxic with abnormal vasculature and are rich in adenosine. Cold tumours lack T cells at the centre and periphery, and T cell priming is frequently found to be

insufficient at the TDLN (119). Therefore in Cold tumours and some Excluded tumours, inhibition of priming and infiltration into the tumour is a key limiting step in anti-tumour immunity whereas in Altered-Immunosuppressed or Hot tumours, suppression within the microenvironment plays a more important role (174).

Immunotherapy for Excluded or Cold tumours must therefore target steps 4 and 5 in the cancer immunity cycle, involving a combination approach which increases the number of immune cells penetrating the tumour, and then potentiates their function once inside. Conversely, immunotherapy for hot tumours is based predominantly on modulation of TIL function through CIR blockade (119). Melanoma is a hot tumour which permits priming and infiltration of immune cells, and once in the tumour, blockade of CIRs is often sufficient to restore the tumour killing by CD8+ T cells. Therefore, the immunoscore of Melanoma indicates why CTLA-4 and PD-1 blockade is so effective in treating skin cancer. However, in other cancer immunotypes, we need to help immune cells to infiltrate, and target other immunosuppressive axes besides CIRs in order to generate anti-tumour immunity. Thus, current evidence suggests that effective immunotherapies can be designed to treat almost all tumours as long as the chosen intervention targets the necessary steps in the cancer-immunity cycle, accounting for tumour immunotype.

Figure 13 - Tumour Immunoscore Categories

Cancers are categorised by the quality and quantity of their immune infiltrate, and the immunosuppressive pathways that are present, in order to generate an immunoscore (119).

Hot tumours possess large numbers of CD8+ TILs, which are predominantly suppressed by Co-Inhibitory Receptor (CIR/checkpoint) expression. Hence these tumours respond well to CIR blockade for immunotherapy.

Cold tumours lack an immune infiltrate, and priming and trafficking of CD8+ Cytotoxic T cells into tumours must be promoted by immunotherapy.

Altered-Excluded and Altered-Immunosuppressed immunoscores are assigned to tumours which have CD8+TILs (here, labelled CT cells). However, in Excluded and Immunosuppressed tumours, a complex combination of immunosuppressive (IM) immune cells and soluble factors synergise with co-inhibitory receptor expression to suppress CD8+ TIL cytotoxic function. Hence improving the priming and infiltration of CD8+ TILs into Immunosuppressed or Excluded tumours is beneficial, to change the quality of the infiltrate towards an inflammatory, anti-tumour type (119). Excluded tumours are differentiated from immunosuppressed tumours, because they have fewer CD8+ TILs ,

Figures taken from ‘Approaches to treat immune hot, altered and cold tumours with combination immunotherapies. Galon and Bruni. 2019 (119).

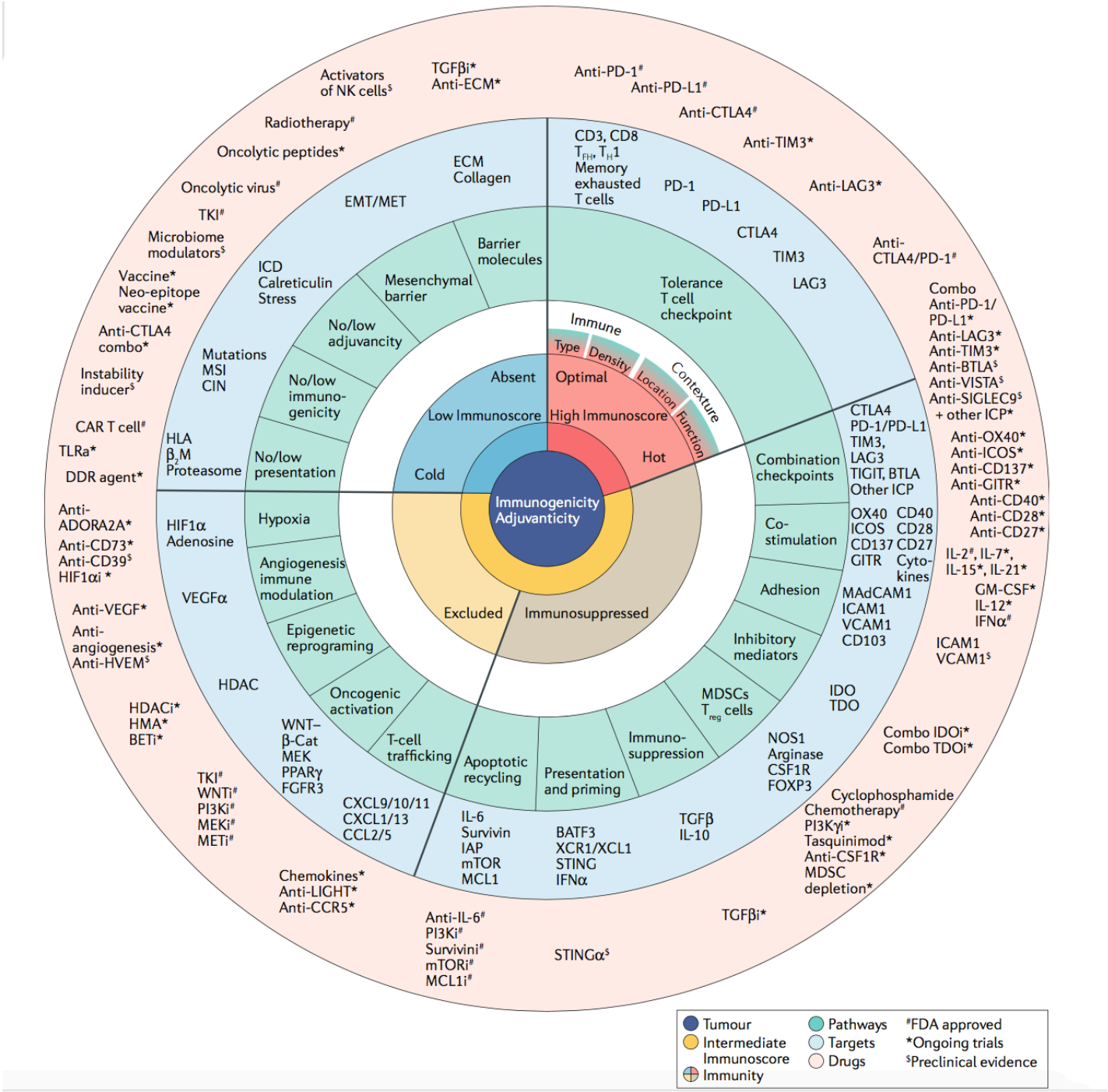
Activators of NK cells$
TGFβi* Anti-ECM*
Anti-PD-1# Anti-PD-L1#
Anti-CTLA4#
Anti-TIM3*
Anti-LAG3*
Anti-CTLA4/PD-1#
Radiotherapy#
Oncolytic peptides*
Oncolytic virus#
TKI#
Microbiome modulators$
Vaccine* Neo-epitope vaccine*
Anti-CTLA4 combo*
Instability inducer$
CAR T cell#
TLRa*
DDR agent*
Anti-ADORA2A* Anti-CD73* Anti-CD39$ HIF1αi *
Anti-VEGF* Anti-angiogenesis* Anti-HVEM$
HDACi* HMA* BETi*
TKI# WNTi# PI3Ki# MEKi# METi#
Chemokines* Anti-LIGHT* Anti-CCR5*
Anti-IL-6# PI3Ki# Survivini# mTORi# MCL1i#
STINGα$
TGFβi*
Combo Anti-PD-1/ PD-L1* Anti-LAG3* Anti-TIM3* Anti-BTLA$ Anti-VISTA$ Anti-SIGLEC9$ + other ICP*
Anti-OX40* Anti-ICOS* Anti-CD137* Anti-GITR* Anti-CD40* Anti-CD28* Anti-CD27*
IL-2#, IL-7*, IL-15*, IL-21*
GM-CSF* IL-12* IFNα#
ICAM1 VCAM1$
Combo IDOi* Combo TDOi*
Cyclophosphamide Chemotherapy# PI3Kγi* Tasquinimod* Anti-CSF1R* MDSC depletion*
ECM Collagen
EMT/MET
ICD Calreticulin Stress
Mutations MSI CIN
HLA β2M Proteasome
HIF1α Adenosine
VEGFα
HDAC
WNT– β-Cat MEK PPARγ FGFR3
CXCL9/10/11 CXCL1/13 CCL2/5
IL-6 Survivin IAP mTOR MCL1
BATF3 XCR1/XCL1 STING IFNα
TGFβ IL-10
NOS1 Arginase CSF1R FOXP3
IDO TDO
CD3, CD8 TFH, TH1 Memory exhausted T cells
PD-1
PD-L1
CTLA4
TIM3
LAG3
Tolerance T cell checkpoint
CTLA4 PD-1/PD-L1 TIM3, LAG3 TIGIT, BTLA Other ICP
OX40 CD40 ICOS CD28 CD137 CD27 GITR Cyto-kines
MAdCM1 ICAM1 VCAM1 CD103
Barrier molecules
Mesenchymal barrier
No/low adjuvancity
No/low immuno-genicity
No/low presentation
Hypoxia
Angiogenesis immune modulation
Epigenetic reprograming
Oncogenic activation
T-cell trafficking
Apoptotic recycling
Presentation and priming
Immuno-suppression
MDSCs Treg cells
Inhibitory mediators
Adhesion
Co-stimulation
Combination checkpoints
Immune
Type
Density
Location
Function
Contexture
Absent
Optimal
Low Immunoscore
High Immunoscore
Cold
Hot
Immunogenicity Adjuvanticity
Excluded
Immunosuppressed
Tumour
Intermediate Immunoscore
Immunity
Pathways
Targets
Drugs
#FDA approved
*Ongoing trials
$Preclinical evidence

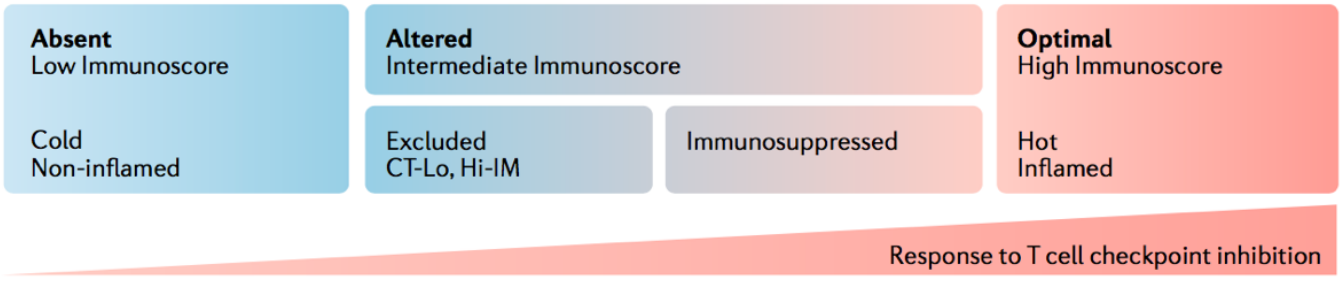
Absent
Low Immunoscore
Cold
Non-inflamed
Altered
Intermediate Immunoscore
Excluded
CT-Lo, Hi-IM
Immunosuppressed
Optimal
High Immunoscore
Hot
Inflamed
Response to T cell checkpoint inhibition

1.6.3.1 Therapies which ensure the Priming of Tumour Specific T cells

1.6.3.1.1 Tumour Vaccines and modulators of DC function

The first attempts at improving the CD8+ T cell response to cancer involved the generation of tumour vaccines. However, vaccines produced limited clinical benefit in cancer for several reasons. Firstly, it is difficult to identify Tumour Associated Antigen in many cancers, and therefore to determine which antigens to use in vaccines (176). Computational strategies are currently being utilised to determine which antigens are presented by tumours on MHC I, however it is likely that epitopes presented on MHC II to activate CD4+ T cell help would also need to be included in vaccines (215). Furthermore, tumours quickly downregulate the expression of antigens contained within tumour vaccines, and assume a TME lacking in damage signals and replete with immunoinhibitory signalling, which renders DCs unable to take up and present vaccine antigen in an immunogenic context at the TDLN (105). Therefore, tumour vaccines have key limitations.

Many new approaches focus on the selection of specific chemotherapy and radiotherapy designed to increase damage signalling within the tumour and render it more immunogenic, without destroying immune cells. In this respect the tumour itself acts as a source of antigen for the immune system, an intrinsic vaccine. Alternatively, adoptive transfer of competent, mature DCs already presenting peptide into tumour patients could bypass the need for vaccines (174). Another method to improve DC maturation and presentation of tumour antigen involves the stimulator of interferon genes (STING) agonists, molecules which stimulate the type-1 IFN pathway and increase cross presentation of tumour antigen by DCs (216). Therefore the combination of these therapies with subsequent modification of the TME can be sufficient to turn cold tumours into hot tumours and to render them immunotherapy-responsive (119).

1.6.3.1.2 Adoptive T Cell Transfer Therapies

Since the successful priming of naïve T cells is a rate limiting step in anti-tumour immunity, Adoptive T cell Transfer (ATT) therapies aim to circumventing the need for priming in the patient. ATT involves generating activated tumour specific CD8+ T cells *ex vivo*, which can then be infused into cancer patients and mediate tumour destruction (174, 217). ATT may consist of either naturally occurring CD8+ T cells or genetically engineered T cells. Some groups are also investigating the use of NKT cells and γδ T cell for adoptive transfer therapies (217). A key

challenge of using naturally occurring anti-tumour T cells from the patient's peripheral blood, is that it is difficult to identify those with a TCR specific to tumour antigen. Whilst reactivity of T cells to tumour tissue can be assayed, many tumour-specific T cell clones found within the blood are shown to cross-react with self-tissue, and thus severe toxicity can be associated with ATT (218). Key advances have occurred in the field of ATT when improved methods were developed to isolate CD8+ TILs from tumour tissue itself. Although these cells appeared exhausted on isolation, careful cell culture enabled them to recover cytotoxic function. In one trial, re-infusion into patients produced objective responses in 50-70% of melanoma patients with only one incidence of severe toxicity amongst 93 patients (219).

Alternatively, the use of genetically modified T cells has shown great promise in ATT therapy. Vectors encoding an engineered T cell receptor with specificity to a chosen tumour-specific antigen can be expressed in T cells before ATT. These cells recognise the desired antigen presented by tumours on MHC molecules, however tumours are adept at downregulating MHC to avoid expressing antigens to which the TCR is specific (217). Alternatively, Chimeric Antigen Receptors (CARs) can be generated. These receptors possess an antibody-like extracellular domain, which can bind to extracellular tumour antigens with great specificity and without MHC presentation (217). Engagement of this domain triggers signalling though an intracellular TCR signalling motif, effectively activating T cell killing without the need for endogenous TCR engagement. CAR-T cells have produced striking results in haematological malignancies, with 100% response rates reported by one trial in 2014, however their use in solid tumours has produced consistently disappointing results. The TME can suppress CAR-T cell signalling in a similar manner to endogenous T cell signalling, and trials which combine engineered T cells with co-inhibitory receptor blockade or other therapies which modulate the microenvironment are necessary (217). Both engineered TCRs and CARs have a place in ATT, because engineered T cells require MHC to respond to antigen presentation and can therefore respond to intracellular tumour antigens which are presented, whereas CARs are limited to detecting extracellular antigens (217).

Key obstacles to the use of the various ATT therapies available at present therefore include: off-target autoimmune activity leading to toxicity; antigenic drift or downregulation of MHC by the tumour to evade immune attack; and the effect of the TME, which suppresses ATT CD8+ T cells as it would any other population, preventing them from performing their killing function (217).

1.6.3.2 Therapies which Improve T cell Infiltration

There are several strategies designed to improve CD8+ T cell infiltration into solid tumours. Notably, few of these therapies have proved promising as single agents, and it is now accepted that when CD8+ T cell infiltration occurs into tumours, the suppressive TME inhibits their cytotoxic function. Therefore, future trials will combine the use of pro-infiltration drugs with blockade of CIRs and soluble mediators found in the TME (119). Examples of drugs which could modulate T cell trafficking include monoclonal antibodies blocking the lymphotoxin-β pathway, stimulating the production of chemokines which recruit T cells (220). In addition, although anti-angiogenic therapies have produced limited benefit as single agents, the use of drugs such as VEGF antagonists has been shown to produce morphologically more normal tumour vasculature, which could allow T cells to infiltrate the TME (119).

1.6.3.3 Therapies which improve T cell function within the Tumour

1.6.3.3.1 Co-Inhibitory Receptor Blockade

A major breakthrough in tumour immunotherapy came with the licensing of anti-CTLA-4 mAb. Blockade of the CIR CTLA-4 produced 30% 2-year survival rates in melanoma patients with disease refractory to chemotherapy (117, 221, 222). Since then, the major beneficial effect produced by anti-CTLA-4 mAb was found to be an improvement in T cell priming at the TDLN, however, blocking CTLA-4 can also improve CD8+ TIL effector function and reduce CD4+ Treg activity within the TME (119). Following anti-CTLA-4 mAb therapies, PD-1 and PD-L1 blocking mAb were also licensed (134). Blocking the PD-1/PD-L1 interaction improved the function of CD8+ T cells infiltrating the TME, thus the activity of anti-CTLA-4 at the TDLN synergises with anti-PD-1 mAb at the TME to produce both better priming and improved effector function of CD8+ TILs (119). Whereas the overall response rate with either agent alone varies across trials, it sits at around 30% in melanoma, when compared to 50% for both agents in combination (119).

Currently, CTLA-4 and PD-1 are the only co-inhibitory receptors for which there is a licensed blocking mAb. Although these mAb produce good results in hot tumours such as melanoma, where CIR expression is the main inhibitor of CD8+ T cells, they have failed to produce clinical other tumour types. We now know that in tumours with Immunosuppressed, Excluded or Cold

immunoscores, targeting other aspects of the cancer immunity cycle alongside CIRs within the tumour is likely to produce greater benefits (121, 134).

Furthermore, another key obstacle to the use of anti-CTLA-4 and anti-PD-1 immunotherapies is the significant incidence of Grade 3 or 4 toxicities in the recipients of this combination. Most incidences of toxicity involve immune mediated colitis, and cutaneous inflammation, are potentially fatal, and result in discontinuation of therapy (117, 221, 222). However, pre-clinical data suggests that blockade of other CIRs could provide clinical benefit in cancer and that other CIRs could be targeted with lower incidences of autoimmune side effects (119). TIM3 antagonists have shown great promise in rescuing tumours which acquired resistance to anti-PD-1 blockade in a murine model of lung adenocarcinoma (115). Since TIM3 is expressed at higher levels amongst TILs when compared with PBMC, current studies suggest that anti-TIM3mAb can be administered with minimal toxicity (134). LAG-3 is another CIR, which is important in CD4+ Treg function and anti-LAG3 mAb are in current clinical trials (223). Other potential CIRs which could be targeted either alone or in combination include TIGIT, BTLA, HVEM, VISTA and SIGLEC9 (119). Blockade of alternative CIRs in combination is a field of much interest, however there is limited clinical trial data about the use of such therapies as yet (119, 134).

1.6.3.3.2 Selective targeting of Inhibitory Cell Populations

Several pharmacological agents are available, which block the function of MDSCs. A recent trial blocking IDO signalling in combination with PD-1 blockade in melanoma did not produce improved results over anti-PD-1 monotherapy. However, this approach might not be appropriate for melanomas which, as hot tumours, are regulated primarily by immune checkpoints. Therefore, trials of these MDSC inhibitors in tumours with a more complex immune landscape could provide synergistic improvements in anti-tumour immunity (119). Indeed, depletion of MDSCs results in tumour shrinkage in head and neck cancers, a tumour rich in MDSC populations, when combined with checkpoint blockade (119). TIM3 blockade has been shown to reduce MDSC numbers at tumour sites, and could be another approach to reducing MDSC activity (134). Another approach to immunotherapy involves depletion of regulatory CD4+ T cells, although this is difficult to achieve in human patients without depleting all T regulatory cells and unleashing systemic autoimmunity. Identification of hallmarks of

cancer-specific T regulatory cell populations could enable selective Treg depletion therapies to be developed (180, 223). Administration of IL-21 as an anti-cancer agent has shown promise in reducing the expression of TGFβ and FOXP3 by CD4+ T cells (119).

1.6.3.3.3 Modulation of Adenosine Signalling

At present, there are two key approaches to pharmacologically block adenosine signalling within tumours: blockade of A2a adenosine receptors, and anti CD73 mAb therapy (184). Antibodies to CD39 are also available however off-target autoimmune side effects directed at the vasculature were noted in mouse studies therefore they have not currently entered human clinical trials (184, 224). The use of pre-clinical A2aR antagonists such as ZM241385 limited tumour growth in models of sarcoma and breast carcinoma, as well as reducing metastasis in the B16F10 melanoma model (183, 225). More recently, A2aR blockade has been shown to synergise with both anti-PD-1 blockade and the use of CAR T cells in murine models of immunotherapy (184, 201). This latter combination addresses the finding that CAR T cells have proven ineffective in solid tumours because of the immunosuppressive microenvironment, and demonstrates the promise of combining TME modulation with adoptive T cell transfer to treat cancers with more complex immunoscores (201). At present, only one human clinical trial utilising A2aR antagonists as a single agent or combined with anti-PD-L1 mAb, has released results, (195). Renal carcinoma, NSCLC and breast cancer patients are included in the same trial, and the current overall response rate reached 45%. Other immunotherapies such as anti-CTLA-4 and anti-PD-1 monotherapy produce comparable results in melanoma but not in other solid tumours (195, 226-228).

A major advantage of the use of A2aR antagonists in the clinic is that they are orally deliverable small molecules, and their use has not been associated with significant toxicity. A2aR antagonists also cross the blood brain barrier, making them applicable in neurological tumours. A2aR antagonists were previously utilised in Phase 1 trials for Parkinson's disease, in which no toxicity was observed. In the only current trial, mild fatigue was the sole side effect reported in 79/80 patients, with only one trial member experiencing immune-related adverse effects in the form of reversible haemolytic anaemia (224, 227, 228). Anti-CD73 mAb are currently in clinical trials as a single agent or in combination with anti-PD-L1 mAb, however no results have yet been disclosed (224). As a monoclonal antibody, anti-CD73 therapy is not orally deliverable,

and does not cross the blood brain barrier, thus it is associated with some disadvantages when compared to small-molecular A2aR antagonists.

1.6.4 Future Directions of Immunotherapy

Certain immunotherapies can block tolerance mechanisms which are necessary for normal immune homeostasis, but are subverted by cancer to avoid immune attack. Therefore, blocking these tolerance pathways and activating the immune system to treat cancer can be associated with significant toxicity which is difficult to manage clinically (117, 221, 222, 229). The identification of drug targets which are selectively upregulated in tumours, and which are less important in systemic immune regulation could allow us to produce immunotherapies with fewer side effects. Furthermore, generalised activation of the entire cancer immunity cycle is more likely to produce toxicity when compared with identifying and targeting the key limiting step in each cancer or patient individually (174).

Adenosine is an ideal candidate for tumour-specific immunotherapy, since its production is stimulated by hypoxia, and its concentration within tumours is found to be up to 100 times higher than in inflamed tissues. Similarly, the expression of the CIR TIM3 has been shown to be much lower amongst immune cells in the peripheral blood of cancer patients when compared with the tumour, meaning that blocking TIM3 will likely produce tumour specific effects (129, 190).

Another recent development in cancer immunotherapy is the identification of certain species of gut microbiota as prognostic markers for response to immunotherapy. Treatment with favourable bacteria could therefore be used as an adjunct to immunotherapy, however the efficacy of this approach has not yet been evaluated (119).

To-date, the development of reliable anti-tumour immune memory has not been achieved in human cancer patients (230). Together, current clinical and pre-clinical data suggest that there is a need to equip anti-cancer immune cells with the ability to function within the suppressive TME generated by solid tumours, such that they exert effective cytotoxic anti-tumour responses, whilst also generating a memory pool (139). Anti-cancer immune memory would theoretically equip patients with the ability to prevent cancer recurrence and eradicate

minimal residual disease, without further treatment (12, 45, 230). However, the effect of tumour-derived inhibitory signals on memory T cell development has not been well studied. In addition, we know more about the effect of chronic antigen on memory T cells in a viral scenario, when compared with a tumour burden. A focus on generating anti-tumour immune memory with immunotherapy is therefore an important future challenge (12).

1.7 Studying the Immune Response to Cancer

1.7.1 The RencaHA Model

The studies outlined in this thesis investigate the hypothesis that CD8+ T cells are suppressed after entry into the tumour microenvironment (TME). Tumour-suppression of CD8+ TILs' cytotoxic effector function means that they do not control tumour growth. Our laboratory utilises a model of murine renal carcinoma, the RencaHA tumour model, to identify mechanisms of suppression of CD8+ T cells within the TME (44, 68, 76, 231).

The RencaHA model utilises Adoptive T cell Transfer (ATT) in which CD8+ T cells are primed outside the host to acquire CTL effector function and are adoptively transferred into tumour-bearing mice, before being recovered from the TME and studied. This allows the characterisation of phenotypic and functional changes that occurred within CD8+ T cells whilst inside the RencaHA TME (68, 232) (Figure 14).

The RencaHA model, utilises murine renal carcinoma cells (Renca) which express the dominant K^d restricted epitope (518-526, IYSTVASSL) of the hemagglutinin (HA) protein from influenza A/PR/8/H1N1 (RencaHA cells). Therefore, HA from influenza is a model, tumour-specific neoantigen (40, 233). RencaHA tumour cells are injected subcutaneously into the dorsal neck region of BALB/c mice, where the tumour grows.

Figure 14 - The RencaHA Tumour Model

To study the suppressive effects of the tumour microenvironment, a model of Adoptive T cell transfer is used. Murine Renal Carcinoma (Renca) cell lines, express HA antigen from the influenza as a model, tumour-specific neoantigen (RencaHA cells)(233). RencaHA tumours grow after subcutaneous injection into BALB/c Thy1.2+/+ mice.

Left Panel:
For non-adoptive transfer experiments, mixed affinity, Thy1.2+/+ CD4+ and CD8+ Tumour Infiltrating Lymphocytes (TILs) derived from the endogenous repertoire of the BALB/c host mouse, are extracted from Renca HA tumours to assess their phenotype and function.

Right Panel:
For adoptive transfer experiments, TCR transgenic, HA-specific, CD8+ T cells (Clone 4 cells) taken from Thy1.1+/+ Clone 4 mice, are activated to form Cytotoxic T Lymphocytes (CTL)(68). This provides a population of *in vitro* primed, tumour-antigen specific CTL. Some primed Clone 4 CTL are adoptively transferred into RencaHA-bearing mice and become TILs, whilst another population are maintained in *in vitro* culture. Comparison of Clone 4 CTL and TILs allows the suppressive effects of the RencaHA Tumour Microenvironment on Clone 4 T cell effector function to be determined.

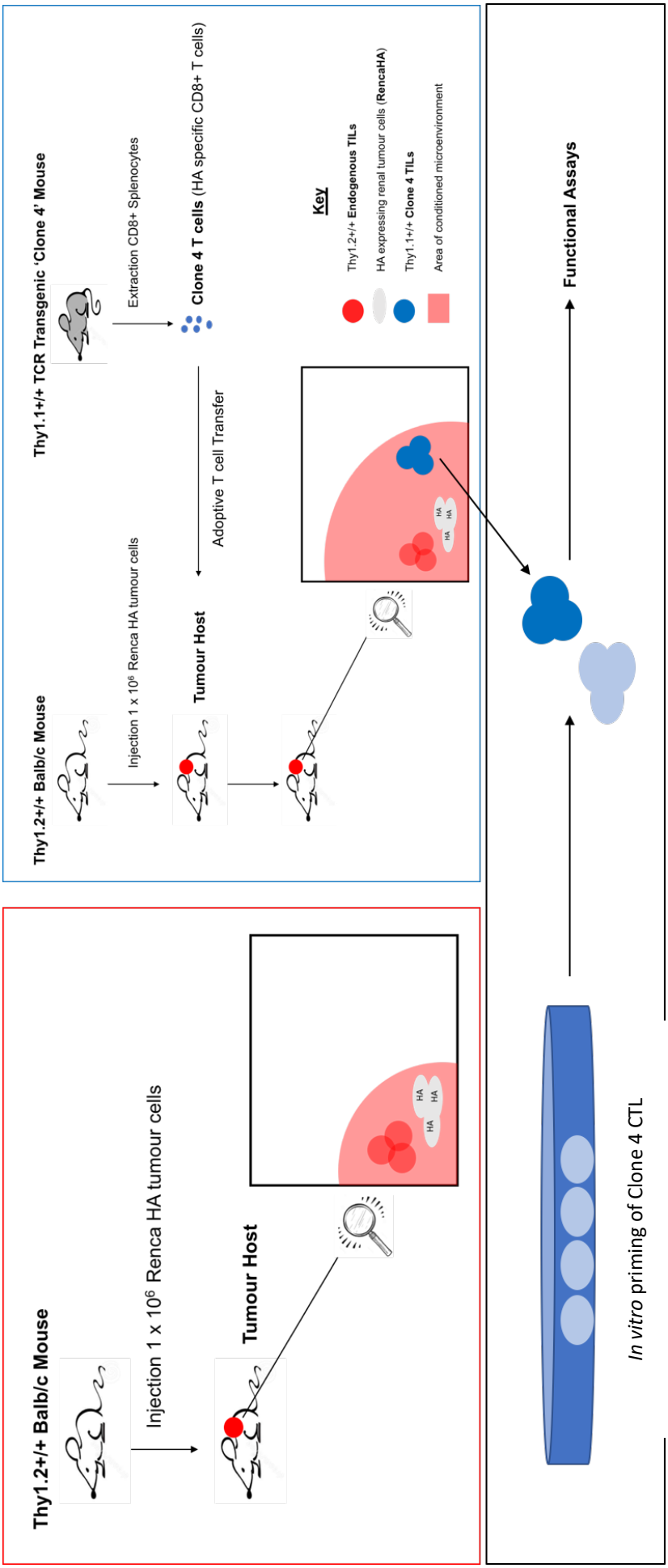
Thy1.2+/+ Balb/c Mouse
Injection 1 x 10⁶ Renca HA tumour cells
Tumour Host
HA
HA
HA
Thy1.2+/+ Balb/c Mouse
Injection 1 x 10⁶ Renca HA tumour cells
Tumour Host
Thy1.1+/+ TCR Transgenic 'Clone 4' Mouse
Extraction CD8+ Splenocytes
Clone 4 T cells (HA specific CD8+ T cells)
Adoptive T cell Transfer
Key
Thy1.2+/+ Endogenous TILs
HA expressing renal tumour cells (RencaHA)
Thy1.1+/+ Clone 4 TILs
Area of conditioned microenvironment
Functional Assays
In vitro priming of Clone 4 CTL

The endogenous immune cells of tumour bearing BALB/c mice in the RencaHA model express the Thy1.2+/+ lineage marker. Cells of the host's endogenous Thy1.2+ CD8+ T cell repertoire can be isolated from the tumour utilising Fluorescent Activated Cell Sorting (FACS) based on antibody staining for CD8+ T cells expressing Thy1.2 (68). These data indicate that even without ATT, RencaHA tumours possess CD8+ Tumour Infiltrating Lymphocytes (TILs) (Figure 14). There are a variety of TCR clones in the endogenous CD8+ T cell repertoire, hence endogenous Thy1.2+ CD8+ TILs are likely to respond to a variety of RencaHA tumour antigens with mixed affinities, rather than just responding to the model HA antigen (176).

For ATT experiments, Thy1.1+ 'Clone 4' CD8+ T cells are used, and their transgenic TCR responds with high-affinity to the HA antigen expressed by RencaHA tumours. Clone 4 T cells are primed *ex vivo* to generate Cytotoxic T Lymphocytes (CTL). After adoptive transfer, Clone 4 CTL infiltrate RencaHA tumours and become Clone 4 TILs. Clone 4 TILs can be subsequently harvested from the tumour using FACS sorting for the Thy1.1 lineage marker to distinguish them from endogenous Thy1.2+ CD8+ TILs derived from the BALB/c recipient mouse (Figure 14)(68). Thus, our model of adoptive T cell transfer allows the use of assays which compare cytokine production, *ex vivo* cytotoxicity, and TCR signalling between CTL and TILs from the same starting Clone 4 T cell population, allowing the identification of differences in T cell effector function which are induced by the TME (77).

1.7.3 Clone 4 T cells lose their cytotoxic function after transfer into RencaHA tumours

Previous work in the RencaHA model used microscopy to demonstrate that Clone 4 CTL primed *in vitro* are able to directly lyse a monolayer of tumour target cells. However, Clone 4 TILs exhibited reduced killing of tumour target cells *ex vivo* when compared with CTL. Therefore, Clone 4 T cell cytotoxicity is impaired after exposure to the Renca TME (Rachel Ambler)(76, 77). To determine the mechanism by which cytotoxicity was inhibited amongst Clone 4 TILs, the stability of immune synapses was compared between Clone 4 TILs and Clone 4 CTL using live cell imaging. Two parameters of immune synapse stability were assessed based on cell morphology, and Clone 4 TILs were shown to produce less stable immune synapses when compared with CTL (Rachel Ambler)(76, 77). Therefore, Clone 4 TILs lose their ability to lyse tumour cell targets after exposure to the TME, and this loss of cytotoxicity could be associated with immune synapse instability amongst TILs when compared with CTL (76, 77).

1.7.4 Immunosuppressive pathways within the RencaHA Tumour Microenvironment

1.7.4.1 Co-inhibitory Receptors

Further studies set out to identify the immunosuppressive pathways within RencaHA tumours, which could have resulted in suppression of the cytotoxic ability of adoptively transferred Clone 4 TILs. Expression of the co-inhibitory receptor PD-1 is elevated amongst Clone 4 TILs in the Renca HA model when compared with CTL primed *in vitro* (44, 154). Work performed in our lab suggests that engagement of the PD-1/PD-L1 axis is one mediator of Clone 4 TIL suppression.

Systemic blockade of PD-1 amongst RencaHA tumour bearing mice produced partial control of tumour growth and improved the killing ability of Clone 4 TILs in *ex vivo* cytotoxicity assays (76). Anti-PD1 mAb therapy also improved immune synapse stability amongst Clone 4 TILs during *ex vivo* imaging of immune synapse formation (76). However, treatment with blocking anti-PD-1 mAb does not produce complete regression of RencaHA tumours. Therefore, other immunosuppressive factors could also suppress Clone 4 TILs in the RencaHA TME, besides PD-1 engagement (119).

1.7.4.2 Regulatory Immune Cells

CD11b+Gr1+ MDSC have been isolated from RencaHA tumours and characterised using flow cytometry. However, the effect of MDSC depletion or anti-MDSC therapy in the Renca tumour model has not been examined. Thus, MDSC could play a role in the suppression of Clone 4 TILs in RencaHA tumours, but their impact has not been confirmed (Zane Al Yafei)(154, 234).

Both CD4+FOXP3+ pTreg and CD4+FOXP3- Tr1 cells have been isolated from RencaHA tumours (154). Co-culture of both subsets of CD4+ Treg from the RencaHA TME with *in vitro* primed Clone 4 CD8+ CTL suppresses CTL proliferation *ex vivo* (154). However, it was shown that CD4+ Tregs isolated from RencaHA tumours do not produce IL-10 or TGF-β, which are canonical methods by which Tregs suppress CD8+ T cells (Figure 15A & B) (154). Thus, it was hypothesised that CD4+ Tregs from RencaHA tumours must suppress Clone 4 CTL by another method.

1.7.4.3 Adenosine

Further study demonstrated that both CD4+FOXP3+ pTregs and CD4+FOXP3- Tr1 cells extracted from RencaHA tumours express the adenosine producing ectoenzymes CD39 and CD73, indicating that they are capable of producing adenosine (Figure 15C)(154). Renca HA tumour cells do not express CD39 or CD73, thus CD4+ Tregs are a key source of adenosine-producing enzymes in our model (235). Several groups have shown that CD39 and CD73 expression correlates with poor prognosis in animal tumour models and in cancer patients. Furthermore, knockdown or blockade of inhibitory A2a adenosine receptors improves control of tumour growth in a CD8+ T cell dependent manner (236-238). In our model*, the ex vivo* suppression of CTL proliferation that occurred in the presence of CD4+ Tregs extracted from RencaHA tumours was abolished in the presence of the specific A2aR antagonist ZM241385 (Figure 15D)(154). Together, these data indicate that adenosine production by regulatory CD4+ Tregs is an important mechanism by which they suppress Clone 4 TIL function *ex vivo*. However, it is not known whether engagement of A2a adenosine receptors on Clone 4 TILs *in vivo* suppresses their anti-tumour effector function within the RencaHA TME (154).

Figure 15 - CD4+ Tregs within Renca tumours do not produce IL-10 or TGFB, but they do express the adenosine producing enzymes CD39 and CD73

Tumours and Tumour Draining Lymph Nodes were harvested from RencaHA tumour-bearing BALB/c mice (A) Cells were FACS sorted according to their expression of CD4 and CD25 and then co-cultured with naïve CD8+ Clone 4 T cells in the presence of irradiated mature dendritic cells and K^dHA peptide. After 3 days of culture, the supernatant was collected and analysed by ELISA for TGFβ. N = 10 mice over two experiments. Mean +/- SEM shown. (B) Cells were incubated with PMA/Ionomycin and Golgi plug for 3 hours, fixed, permeabilised and stained using anti-IL-10 mAb. Representative flow cytometric data are shown. N = 15 mice over 3 experiments. (C) Cells were fixed, permeabilised and stained with anti-FOXP3, anti-CD39 and anti-CD73 antibodies. Representative flow cytometric data are shown. N = 15 mice over 3 experiments. (D) Cells were FACS sorted according to their expression of CD4 and CD25 before being co-cultured with naïve CD8+ Clone 4 T cells in the presence of irradiated mature dendritic cells and K^dHA peptide. The A2a adenosine receptor antagonist ZM241385 was added to a subset of cells. Cells were cultured for 3 days and ^3H-Thymidine was added for the last 8h of culture. ^3H-thymidine incorporation (cpm) is shown as Mean +/- SEM. N=10 mice over two experiments. P<0.001*** paired t-test.

Figures taken from PhD thesis 'Tumour-specific CTL, what does it take to wake them up? Zane Al Yafei. 2012'(154).

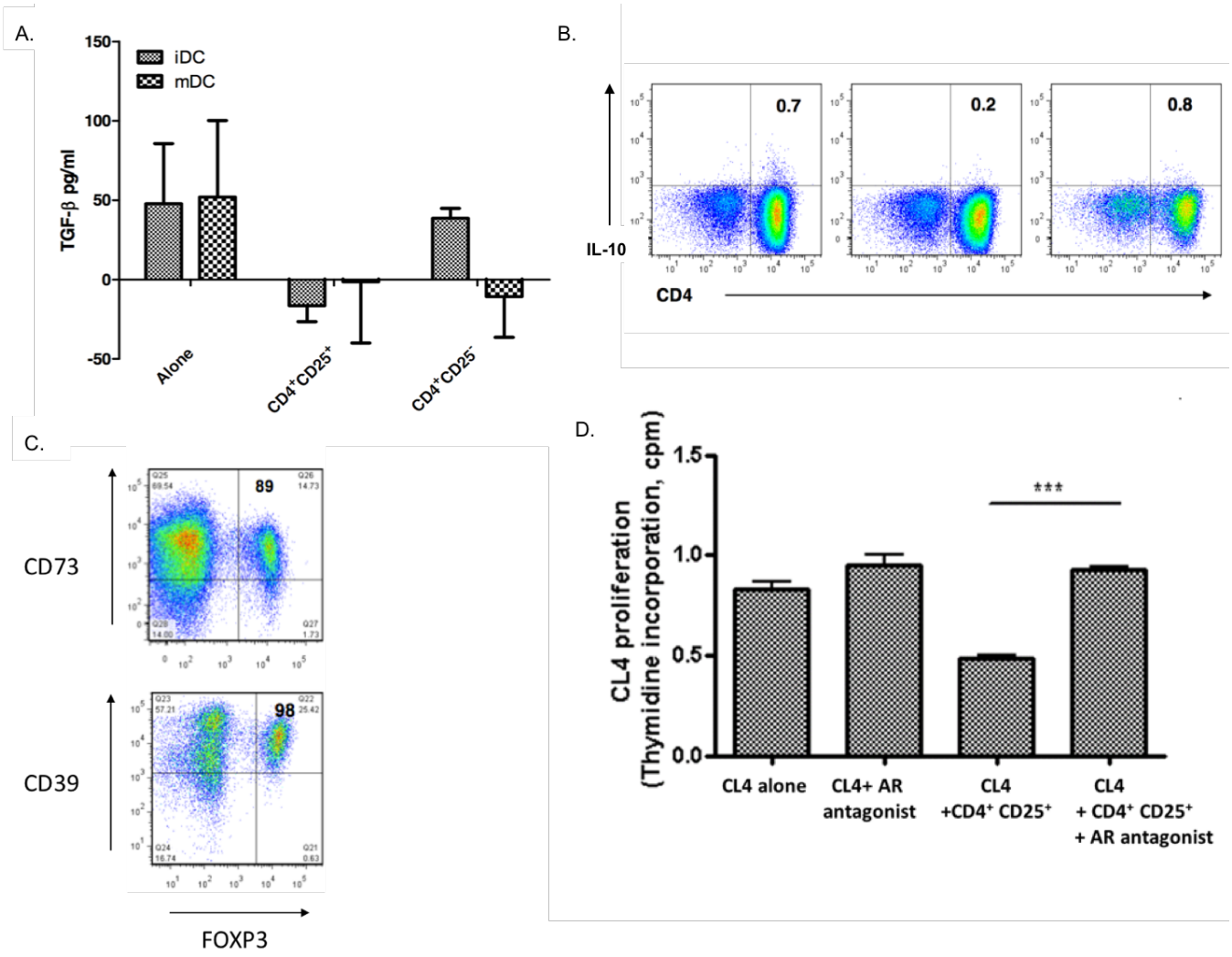

1.8 Aims and Structure of this Work

Based on previous work, this thesis will address the hypothesis that engagement of A2a Adenosine Receptors on ATT Thy1.1+ Clone 4 CD8+ TILs, and the host's endogenous Thy1.2+ CD8+ TILs, suppresses their CD8+ T cell effector functions within the RencaHA TME (Figure 16).

Although it has been shown that Clone 4 TILs lose their cytotoxic ability within the RencaHA TME, other aspects of effector function have not been compared between Clone 4 CTL and TILs. Therefore, in Chapter 3, effector cytokine production and co-inhibitory receptor expression were also compared between Clone 4 TILs and CTL, using flow cytometry. In addition, the host's endogenous Thy1.2+ CD8+ TIL population was characterised for the first time. We hypothesised that Thy1.2+ endogenous CD8+ TILs within RencaHA tumours could produce suppressive molecules such as IL-10 and adenosine thus, instead of acting as effectors which kill cancer cells, they could act as CD8+ Tregs which suppress adoptively transferred Thy1.1+ Clone 4 TILs. Suppression assays were used to address this question.

Chapter 4 aimed to demonstrate the importance of A2a Adenosine Receptor signalling in suppressing anti-tumour immunity within RencaHA tumours *in vivo*. To achieve this, specific A2aR-Antagonist was administered systemically to tumour bearing mice, and tumour growth assessed. Experiments in this chapter lead to the hypothesis that blocking TIM3 alongside A2aRs could produce synergistic benefit to anti-tumour immunity, enabling improved control of tumour growth when compared with blocking A2aRs alone.

In Chapter 5, *ex vivo* analyses were used to address the hypothesis that blockade of A2aRs and TIM3 directly improved the killing function of adoptively transferred Thy1.1+ Clone 4 TILs. Cytotoxic function and Immune Synapse Stability of Clone 4 TILs was compared between treated and control mice using live cell imaging, to address this question. To further quantify the direct effects of A2aR and TIM3 engagement on Clone 4 T cell function, an *in vitro* model of adenosine and TIM3 signalling was developed as described in Chapter 6.

As well as improving tumour killing by CD8+ T cells, we hypothesised that blockade of A2aRs and TIM3 amongst RencaHA tumour bearing mice improved their anti-tumour immune memory T cell responses. To address this hypothesis, in Chapter 7, the proportions of different

memory T cell subsets were compared between treated and untreated RencaHA tumour-bearing mice using flow cytometric analyses and depletion experiments.

Overall, this work sets out to determine the efficacy of blocking A2a Adenosine Receptors for immunotherapy in the RencaHA model. It identifies a combination immunotherapy strategy using both A2aR antagonism and TIM3 blockade, and determines some mechanisms by which these two signalling pathways could synergise to inhibit CD8+ T cell effector function and memory formation. This work lays the foundations for A2aR and TIM3 blockade to be translated into the clinic.

Figure 16- Flow Chart summarising Structure and Key Findings of Results Chapters

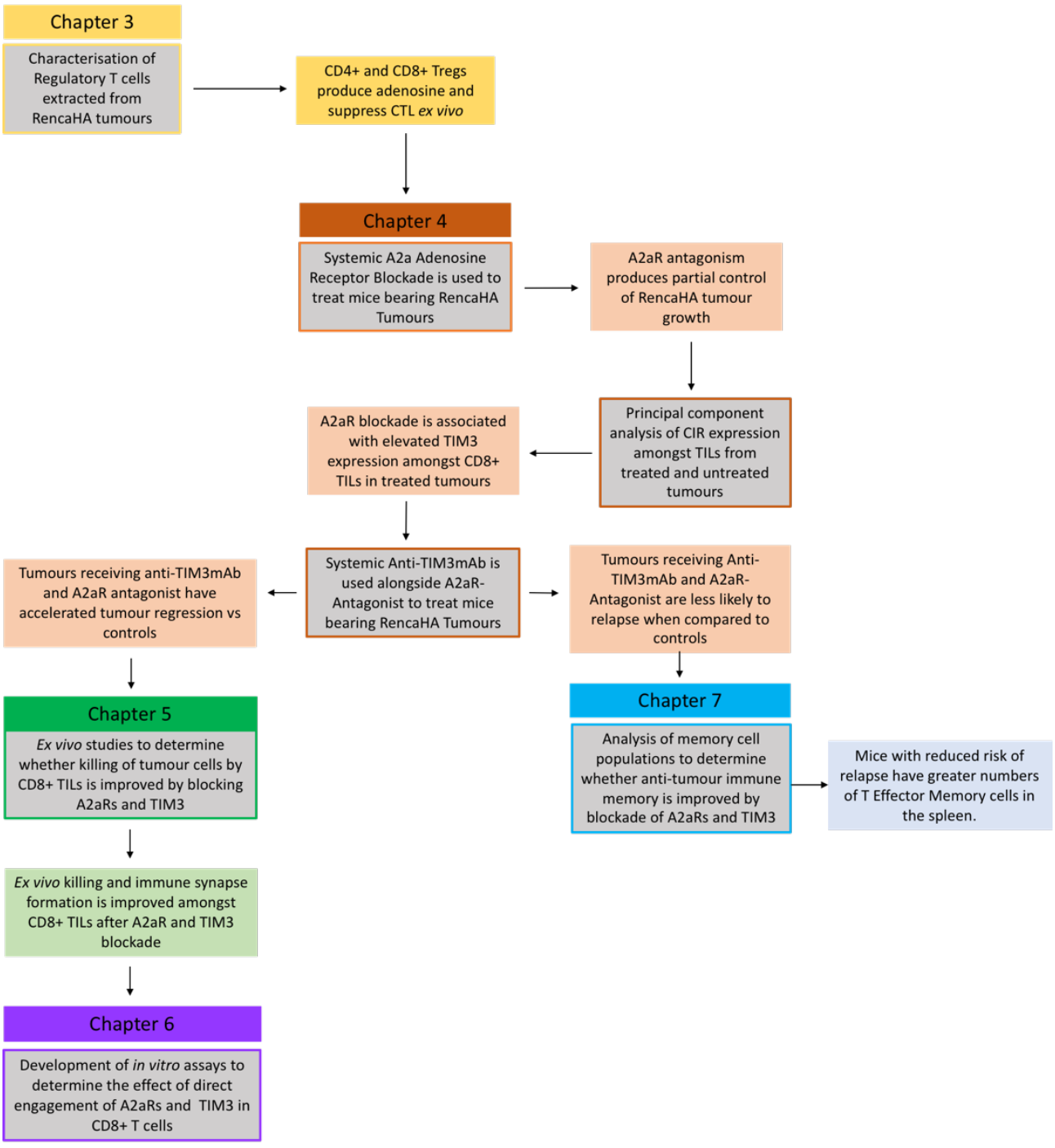

Chapter 2 Methods

2.1 Mice

2.1.1 Animals and Treatments

2.1.1.1 Clone 4 Mice

TCR-transgenic, BALB/c, Clone 4 +/-, Thy1.1+/+ mice were bred at the University of Bristol Animal Services Unit (239). Mice were genotyped using blood samples harvested in blood buffer from the tail vein. Blood samples were stained using anti-mouse Vβ8.1 (eBioscience, KJ16-133, FITC) and anti-mouse CD8α (Biolegend, 53-6.7, APC) and analysed using flow cytometry. At or over 6 weeks old Clone 4+ mice were humanely culled, and spleens harvested as a source of Thy1.1+/+ Clone 4 CD8+ T cells.

2.1.1.2 BALB/c Mice, Tumour Growth and Treatment Experiments

6-week-old Thy1.2 +/+ BALB/c mice were obtained from Charles River UK. On day 0, BALB/c mice were injected subcutaneously, in the dorsal neck region, with 1 x 10^6 RencaHA tumour cells in 100 µl PBS per 1 x 10^6 cells via a 25G needle. RencaHA cells were washed twice in an excess of PBS before injection. Tumour measurement and treatment began at day 12, when tumours reached 5 mm in either direction. Mice were grouped for treatment by randomly assigning a numeric identification to each mouse. For adoptive transfer experiments, mice received 3.5 to 5 x 10^6 Clone 4 CD8+ T cells, primed using k^dHA peptide (as detailed in 2.4.1) and transferred i.v. in PBS on day 5 after activation. For *in vivo* immunotherapy experiments, control mice received 100 µl vehicle (15% DMSO, 15% Cremophore EL, 70% PBS) +/- 100 µg/mouse isotype control (Rat IgG2a, 2A3, BioXcell InVivoMAb)(240). Additional batches of untreated mice were used to augment the numbers of control mice for sampling at later timepoints, because vehicle treated mice reached Maximum Allowable Tumour Size (MATS) and were culled at early timepoints. ANCOVA was used to confirm that there was no significant difference in co-inhibitory receptor expression between vehicle treated and untreated mice of equivalent volume ($p = 0.596$). Treated mice received combinations of 10 mg/kg ZM241385 (A2aR-Antagonist) injected intraperitoneally in 100 µl Vehicle (15% DMSO, 15% Cremophore EL, 70% PBS) and 100 µg/mouse anti-TIM3mAb (RMT-23, BioXcell InVivoMAb injected intraperitoneally in 100 µl PBS on alternate days throughout the experiment. Tumours were

measured on alternate days using calipers and the volume calculated using the modified elliptical formula:

Volume = 0.5 (length x (width$^{2)}$)

Influenza challenge was achieved by injecting 200 µl A/PR/8/H1N1 virus in allantoic fluid into each mouse intraperitoneally via a 25G needle. This volume has been calculated to achieve a titre of 1200 HA units (68). Rechallenge with tumour cells was achieved by injecting a further 1 x 10^6 RencaHA cells subcutaneously into the dorsal neck region in PBS after the initial tumour had regressed (remained <5 mm diameter for 8 days = stable remission). Depletion of CD8+ T cells or Thy1.1+ T cells was performed by injection of depleting mAb (Anti-CD8 Clone 53-5.8 InVivoMAb, 100 µg/mouse, Thy1.1 Clone 19E12 InVivoMAb, 250 µg/mouse). One experimental repeat for each treatment experiment was performed blinded, but this was not technically achievable for all repeats due to a limited number of operators. All experiments were compliant with UK Home Office Guidelines.

2.2 Media and Reagents

2.2.1 Complete Medium

Complete medium was comprised of 89% RPMI + L-Glutamine (Gibco), 10% FBS (Hyclone), 1% PenStrep (Gibco), 0.04% β-Mercapto Ethanol (Gibco). Selective antibiotics were added for tumour cell culture as indicated. Complete medium + IL-2 was generated by supplementing with 50 U/ml recombinant human IL-2 (National Institute of Health/NCI BRB Preclinical Repository). Additional reagents were prepared and added to achieve the stated final assay concentration (FAC) in the culture well as follows:

2.2.2 Additional Reagents added to Complete Medium

2.2.2.1 Adenosine

FAC 1.25 µM or 0.625 µM. For 0.2 mM stock 53.5 mg adenosine powder (Sigma) was added to 1 ml dH20 and used immediately. The solution cannot be stored.

2.2.2.2 TGFβ

FAC 10 ng/ml attained by adding 40 µl of frozen stock (12.5 µg/ml) (Biolegend) per 50 ml IL-2 medium.

2.2.2.3 PGE2

FAC 1 µM. Powder (Life Technologies) was reconstituted using 283.7 µl ethanol, to make 10 mM stock, stored at -20°C. From the stock vial, 2 µl was added to 198 µl PBS to make a 100x substock then 10 µl was added per 1 ml of complete medium.

2.2.2.4 TG4-155 (Antagonist of EP2 Receptor for PGE2)

FAC 1 µM. From the stock vial (Sigma) stored at 4 °C, 3.94 µl was added into 246 µl PBS to make a 200x substock, therefore add 5 µl was added per 1 ml complete medium.

2.2.2.5 NECA (Pan-Adenosine Receptor Agonist)

FAC 1 µM or 10 µM for most experiments. To make frozen stocks, 10 mg of a 50 mg vial of powder (Sigma) (stored at 4°C) was weighed into an Eppendorf. 1 ml DMSO was added and the solution briefly vortexed to dissolve solute. The 20 µl of solution was rapidly aliquoted into eppendorfs at room temperature and frozen immediately at -20°C. Frozen stocks were replaced after one month. On the day of use, a 10 mM substock was prepared by adding 10 µl frozen stock to 30 µl PBS. 1 µl per 1 ml complete medium was added for NECA 10 µM conditions, or a further 1 in 10 dilution of the 10 mM substock was performed, before 1 µl was added in 1 ml complete medium for NECA 1 µM conditions.

2.2.2.6 ZM241385 (A2a Adenosine Receptor Antagonist)

FAC 1.25 µM. To a 5 mg vial of powder (Santa Cruz, stored at room temperature), 296.4 µl of DMSO was added and the solution briefly vortexed. 20 µl aliquots were rapidly prepared at room temperature and frozen immediately at -20°C. Frozen stocks were used within 1 month. On the day of use, a 1.25 mM substock was generated by adding 2.5 µl of stock to 97.5 µl PBS and 1 µl was added per 1 ml of culture medium.

2.2.2.7 CGS21680 (Specific A2a Adenosine Receptor Agonist)

FAC 1 μM. 1 mg of a 5 mg vial of powder (Tocris, stored at -20°C) was added to 370 μl DMSO, 50 μl aliquots were prepared at room temperature and immediately frozen at -20°C. 20 μl was added to 80 μl PBS to make a 1 mM substock then 1 μl was added to 1 ml complete medium in the culture well.

2.2.3 Fluorobrite Complete Medium

Complete medium was prepared for cytotoxicity assays using 88% Fluorobrite DMEM (Thermofisher) 10% FBS (Hyclone), 1% L-glutamine (Gibco) (stored at -20°C and thawed on day of use), 1% PenStrep (Gibco), 0.04% β-Mercapto Ethanol (Gibco).

2.2.4 Phoenix Medium

Phoenix incomplete medium was prepared from 88% DMEM (Gibco), 10% FBS (Hyclone), 1% PenStrep (Gibco), 1% MEM None Essential Amino Acids (Gibco). For long term culture, 300 μg/ml hygromycin and 1 μg/ml diphtheria toxin was added to produce Phoenix Complete medium.

2.2.5 FACS Buffer, MACS buffer and Imaging Buffer

PBS (Gibco) without calcium or magnesium was supplemented with 2.5% w/v Bovine Serum Albumin (Sigma) to generate FACS buffer. MACS buffer was prepared in the same way but with the addition of 2 mM EDTA (Sigma). Imaging buffer was prepared from PBS with 1 mM $CaCl_2$ (Sigma) , 500 μM $MgCl_2$ (Sigma) and 10% FBS (Hyclone).

2.2.6 Chloroquine

Chloroquine was prepared in distilled water to a concentration of 4.1 mg/ml, protected from light and filter sterilized before addition to cell culture.

2.3 Maintenance and Culture of Cell Lines

2.3.1 Renca Tumour Cells

The murine Renal Carcinoma 'RencaWT' cell line was maintained in 5 ml or 10 ml complete medium in 25 ml or 75 ml vented flasks respectively. Cells were passaged every 48 hours, and maintained at <80% density. To passage cells, culture medium was removed, and the flask washed in 10 ml PBS to remove protein from the adherent cells. 2 ml of 0.05% Trypsin 0.02% EDTA (Sigma) was added and the flask incubated at 37°C for 2 minutes. The flask was agitated, and microscopy was used to confirm cell detachment. Cells were collected in 5 ml complete medium and centrifuged at 200 xg for 3 minutes. 10% of cells were placed in a new flask of the same size and the media replaced. Genticin (100 μg/ml) was added as selective antibiotic to RencaHA cultures expressing a plasmid coding for haemagglutinin (RencaHA) from the mouse-adapted influenza strain A/PR8. Hygromycin (250 μg/ml) was added to cultures containing the mCherry or hCD58 expressing plasmids (RencaWT^{mCherry}, RencaHA^{mCherry}, RencaWT^{mCherry}hCD58). Cell lines containing both mCherry and HA plasmids received both hygromycin and Genticin at the above concentrations.

2.3.1.1 Lipofectamine transfection of Renca Tumour cells

Renca^{mCherry}HA or Renca^{mCherry}WT tumour cells were transfected with plasmids (containing both a hygromycin resistance gene and the gene encoding GCAMP6s) using lipofectamine (Invitrogen) and following the manufacturer's protocol for adherent cells. Cells containing the GCAMP6s plasmid were identified by harvesting cells after the transfection period and resuspending in imaging buffer at 1 x 10^7 cells per 300 μl. Cells were incubated for 30s with 200 ng/ml ionomycin to induce calcium flux before FACS sorting of green fluorescent cells. Renca cells were then cultured in hygromycin-containing complete medium (Renca^{Mch}WTGCAMP6s) or hygromycin and G418 (Renca^{Mch}HAGCAMP6s).

2.3.2 Phoenix cells

The Phoenix cell line is derived from 293T transformed embryonic renal cells. Phoenix cells may be easily transfected with a vector containing a gene of interest using calcium phosphate precipitation, routinely generating transfection rates of >50% (76). Phoenix cells were maintained in complete medium in 60 x 15 mm Primaria coated cell culture dishes (Falcon).

Cells were passaged by removing media and directly adding 1 ml 0.02% EDTA (Sigma) to the plate before incubation for 1 minute at 37°C. Cells were collected by washing with DMEM using a P1000 pipette to aspirate medium before centrifugation at 200 xg for 3 minutes. 600,000 cells were re-plated in 6 ml phoenix complete medium. For production of retrovirus, phoenix cells were passaged into in antibiotic-free incomplete medium 72h before transfection to ensure the correct density. Alternatively, cells were passaged into incomplete medium, cultured for 72h, then split in half before being transfected the next day.

2.3.2.1 Production of Retrovirus

In our protocol, the required density of Phoenix cells is generated on Day 1 (Figure 17). Calcium phosphate precipitation is used to transfect phoenix cells with a vector, encoding a protein of interest conjugated to GFP or mCherry. Plasmids expressing GFP-conjugated proteins were generated using cloning (as detailed in 2.5). 25 µl chloroquine was added directly to the phoenix cell plate and the plate placed at 37°C until other solutions were prepared.

Then, the following solutions were generated from sterile filtered reagents to make enough volume for 1 phoenix plate Solution A: 2 µl 1M NaOH, 500 µl Hepes Buffered Saline (HBS). Solution B: 500 µl dH20, 5 µl of plasmid at >3000 ng/µl DNA. To solution B, 62 µL 2M $CaCl_2$ was added dropwise to produce a visible precipitate. Solution B is was then added to Solution A by running dropwise whilst rapidly mixing the solution using a stripette gun. The resultant mixture is added directly to the phoenix plate which has been incubating with chloroquine.

Phoenix cells produce gag-pol, and envelope protein for ecotropic retrovirus, releasing the packaged vector within a few days. After 24h, phoenix medium is aspirated, and fresh incomplete medium added. After a further 48h, the retrovirus containing medium is harvested. At this point, phoenix cell supernatant is used to resuspend primary murine T cells after 24h of priming using pulsed splenocyte reaction (see 2.4.1) (47, 241).

Cells were harvested and washed 5 times in RPMI (Gibco). Incomplete medium containing retrovirus was collected from phoenix cells after 48h of culture leaving the cell layer intact and centrifuged for 3 minutes at 200 xg to remove contaminating cells. Washed Clone 4 cells were resuspended in 1 ml retrovirus-containing Phoenix medium per 1 well of Clone 4 cells, and re-

plated into a fresh, flat bottomed 24 well plate (Corning). 8 µg/ml protamine sulphate was added to each well, the 24 well plate was sealed using parafilm and centrifuged at 200 xg for 2 hours at 32°C. After centrifugation, phoenix media was aspirated from each well without disturbing the cell layer, and 2 ml IL-2 medium was added to each well. Cells were pipetted up and down using a P1000 pipette to resuspend in the medium and culture continued until Day 8. At this point, fluorescent activated cell sorting of GFP+ or mCherry+ T cells allows selection of T cells transfected with the desired protein construct. Fluorescent protein levels correlate with expression of the desired protein, so selecting GFP low, medium or high cells allows the generation of T cells which express a protein at below, equal to or above endogenous levels.

Figure 17 - Use of the Phoenix Ecotropic Retroviral system to generate T cells expressing GFP-conjugated signalling proteins

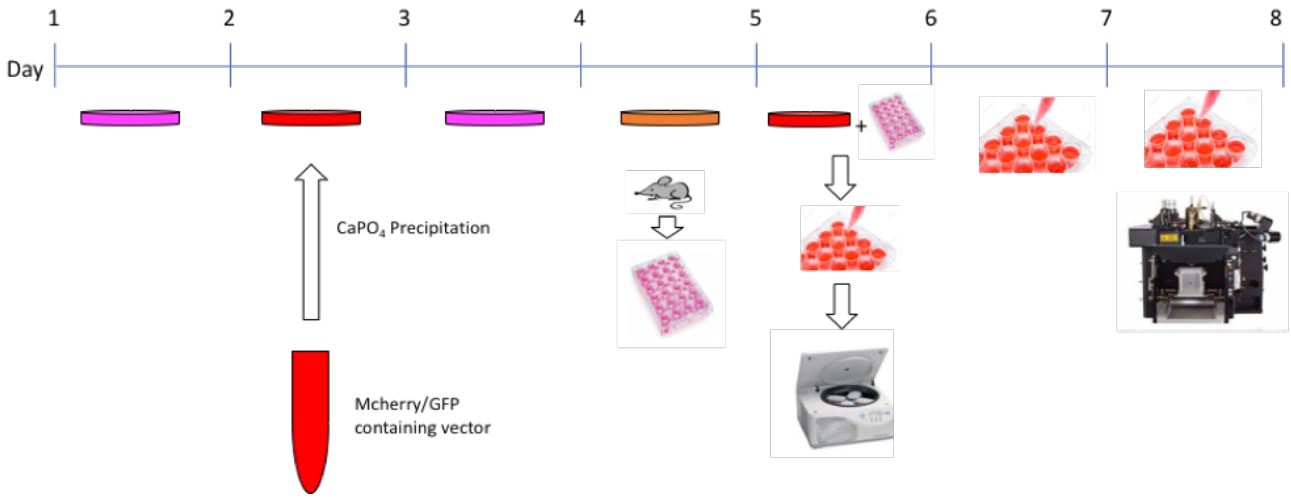

2.4 Culture of Primary Clone 4 CD8+ T cells

Clone 4 CD8+ T cells were harvested from the secondary tissues of Clone 4 mice and primed in 3 different ways:

2.4.1 Pulsed Splenocyte Reaction and Variations

Clone 4 cells were extracted from splenic tissue by maceration through a 40 µM cell strainer. Red blood cells were lysed using ACK Lysis buffer (Gibco). The remaining splenocytes were resuspended at 5 x 10^6 cells/ml of complete medium. 5 x 10^6 cells were then plated in each well

of a flat bottomed 24 well plate (Corning). Each well was treated with 1 µl of peptides 518-526 (IYSTVASSL) of the influenza hemagglutinin (A/PR/8/H1N1) protein (K^dHA peptide) (1 mg/ml) for 24 hours to initiate T cell activation. Culture was performed at 37°C and 5% CO_2. After 24h, cells were washed 5 times in RPMI (Gibco) and resuspended in 5 x 10^6/2 ml IL-2 medium. Transduction with retroviral constructs was performed at this point. Cells were then passaged every 12 hours using fresh IL-2 medium after attaining 90% density. All experiments were carried out between 5-8 days after priming, when cells possess optimal functionality (76, 77).

2.4.1.1 Retroviral Transduction

See section 2.3.2.1

2.4.1.2 Ex Vivo stimulation of TILs to identify the presence of Thy1.1+ memory cells

Spleen maceration and preparation was performed as above, but cells were not washed after 24h, and instead the media was exchanged for fresh IL-2 medium at this time. Cells were passaged every 12 hours in IL-2 medium and were analysed at 3d or 8d, as described in Chapter 7, Figure 55.

2.4.1.3 Non-IL-2 Containing cultures

For some killing assays, IL-2 was omitted from pulsed splenocyte culture conditions as indicated.

2.4.1.4 In vitro culture to engage hCD2TIM3 constructs using Mitomycin-C treated Renca cells

On day 0, 2 µg/ml mitomycin-C was added to a 75 ml flask of Renca tumour cells growing at 60-80% confluence in 10 ml complete medium. The flask was cultured overnight. Treated Renca cells were harvested (as described in section 2.3.1) and washed once in RMPI (Gibco) to remove mitomycin-C. One T75 flask of Renca cells harvested at 60-80% confluence was resuspended in 20 ml of complete medium to make “Renca-cell-medium”. From day 2 of culture of Clone 4 T cells, Renca-cell medium was used to make up half of the total well volume each time cells were passaged. Fresh Renca cell medium was prepared daily from flasks treated with mitomycin-C the night before. To engage hCD2TIM3 constructs, Renca$HA^{mCherry}$CD58 were added, to leave

constructs unengaged, RencaHA cells were added to Clone 4 T cell culture (Chapter 6, Figure 48).

2.4.2 CD3/28 mAb Activation

On day 0, a flat-bottomed 24 well plate (Corning) was coated with anti-CD3mAb (145-2C11 BioXcell) by adding 250 µl 10 µg/ml antibody to each well in PBS. The plate was incubated at 4°C overnight. On day 1, spleens and lymph nodes of Clone 4 mice were macerated by forcing mechanically through a 40 µM strainer, and red blood cells were lysed. The single cell suspension was centrifuged at 250 xg for 5 minutes and the pellet resuspended in 450 µl MACS buffer + 50 µl anti-CD8a microbeads (Miltenyi) per single mouse, for 15 minutes at 4°C. Cells were washed in an excess of MACS buffer and centrifuged at 250 xg for 5 minutes before being resuspended in 6 ml MACS buffer and passed over a pre-washed LS-column attached to a MACS magnet (Miltenyi). The flow-through was then passed over the magnet for a second time, before the magnet washed with 9 ml MACS buffer, and the CD8+ T cells selected by forcing 6 ml MACS buffer rapidly over the column after removal from the magnet. Cells were counted and resuspended at 2 x 10^6 CD8+ Clone 4 T cells per 1.5 ml complete medium. The pre-coated 24 well plate was flicked upside down to remove anti-CD3 mAb and 1.5 ml cells were immediately added to each well. 0.5 ml anti-CD28 mAb (37.51 BioXcell) was added to each well at 4 µg/ml in complete medium, to produce a FAC of 1 µg/ml anti-CD28 per well. Cells were cultured at 37°C 5% CO_2 for the indicated time period before being harvested and analysed. IL-2 was not supplemented in anti-CD3/28 cultures. When using 96 well flat-bottomed plates (Corning), 100 µl of anti-CD3 mAb was used to coat each well, and 1 x 10^5 cells were plated in a total of 100 µl complete medium containing 1 µg/ml anti-CD28.

2.4.2.1 ^{3}H Thymidine Proliferation Assays

Clone 4 T cells were primed using anti-CD3/28 mAb stimulation in a flat bottomed 96 well plate and cultured for the desired time at 37°C. ^{3}H-thymidine (Amersham Life Science, London, UK) was added for the final 8h of cell culture at 1.45 mBq/ml and culture was continued in a radiation-safe incubator under the same conditions. At the time of harvest, the entire plate was frozen at -20°C for at least 24 hours. The plate was then defrosted to produce cell lysis, and harvested using a 96 well Tomtec harvester. ^{3}H-Thymidine incorporation was measured using a Microbeta scintillation counter (PerkinElmer).

2.4.3 Activation using pulsed APCs and TIL Suppression Assays

2.4.3.1 Irradiation of Renca tumour cells

RencaWT tumour cells were incubated with 2 mg/ml (2 µl per 1 ml) K^dHA peptide for 1h and 10 minutes prior to irradiation. 1-5 x 10^6 cells were placed in 5 ml complete medium in a 50 ml falcon tube. The falcon tube was subjected to 2h13m of irradiation in a gamma irradiation facility at the University of Bristol. This achieved a total of 9600 Rads using Cs^{137} (Gravatom projects, Gosport, UK). Irradiated cells were washed in complete medium and used to prime naïve CD8+ T cells.

2.4.3.2 Activation of Clone 4 T cells with Irradiated Renca Tumour cells

Clone 4 T cells were stained with Celltrace Violet (Thermofisher) (as detailed in 2.9.1). K^dHA peptide-pulsed and irradiated Renca tumour cells were plated with 1 x 10^5 naïve Clone 4 T cells purified using MACS (as in section 2.4.2) at a ratio of 1:1. A round bottomed 96 well plate was used for pulsed APC cultures in a total of 200 µl volume. For suppression assays, 1 x 10^5 additional Clone 4 CTL (control) or 1 x 10^5 CD8+ TILs were also added to the culture well in a total volume of 200 µl. Proliferation was quantified after 72h of culture at 37°C, 5% CO_2, by quantifying loss of Celltrace Violet staining using flow cytometry.

2.5 Cloning

All plasmids used in this work were produced in-house. Cloning of GFP-containing plasmids was performed using the In-Fusion Cloning kit (Clontech). The manufacturer's protocol was followed. Vector NTI software was used to design PCR primers to amplify an insert encoding a signalling intermediate of interest. This insert was placed into a digested plasmid backbone containing pGC-eGFP. Concentrations of vector and insert were determined after each step by running 1 µl of product on an agarose gel containing EtBr. To generate hCD2TIM3 constructs, site directed mutagenesis was performed using QuickChange Lightening multi-site mutagenesis protocol and kit (Agilent technologies).

2.6 Extraction of CD8+ T cells from Tumour Tissue

RencaHA tumours were dissected from mice and macerated in 2.25 ml RPMI without protein. The resulting suspension was digested by addition of a murine tumour enzyme kit (Miltenyi)

according to the manufacturers' directions and incubated at 37°C for 40 minutes with gentle vortexing every 10 minutes. The suspension was then gently passed through a 70 μM cell strainer into a 50 ml falcon by washing in PBS, and pelleted. Any material left in the strainer was not forced through to prevent blocking of the LS column. The single cell suspension was centrifuged at 250 xg for 5 minutes. The supernatant was removed, and the pellet resuspended in 2 ml/tumour Ack lysis buffer (Gibco). Lysis buffer was quenched in 10 ml complete medium and 20 ml PBS before centrifuging. After red cell lysis, tumours were incubated for 30 minutes in 600 μl MACS buffer with 50 μl murine anti-CD8α or anti-CD45 magnetic microbeads (MACS, Miltenyi). Cells were washed in an excess of MACS buffer, pelleted and passed over a pre-washed magnetic column (Miltenyi-LS) in a MACS Magnet (Miltenyi) in 6 ml of MACS buffer. The flow through was not passed over the column. The column was washed in 8 ml MACS buffer, and T cells were then extracted by forcing 6 ml of MACS buffer rapidly over the column after removal from the magnet. If the column blocked, the material still to be passed over was aspirated from the top of the column and run over a new, pre-wet column. T cells are forced off the blocked column using 6 ml of MACS buffer after removal from the magnet. Flow cytometric staining of the suspension was performed as described in section 2.9. Alternatively, for FACS sorting, tumour cell suspension was incubated in FcBlock for 15 minutes at room temperature in 200 μl FACS buffer, then fluorescently conjugated antibodies were added without washing at the desired concentration. Cells were then resuspended in imaging buffer at
10 x 10^6 cells /300 μl and the desired populations were sorted using a BD influx cell sorter.

2.7 Extraction of CD8+ T cells from Skin

Skin was harvested from the dorsal neck region or the ear using a 4 mm biopsy punch after clipping as closely as possible to remove hair. Skin was harvested into HBSS without Calcium or Magnesium (Gibco). Subcutaneous fat was dissected away by blunt dissection until translucent skin was exposed from underneath. Skin was floated dermal side down on 20 mM EDTA (Sigma) for 3h at 37°C in a 6 mm petri dish. Under a dissecting microscope, the epidermis was then peeled off from the dermis. Cleaned skin was macerated using a scalpel blade and up to 4 punches per tube were placed into 8ml HBSS with Ca^{2+} and Mg^{2+}. 1 mg/ml Collagenase IV (Life technologies) and 0.5 mg/ml DNase I (Sigma) were added and the tube placed in a bacterial shaker for 1h, with tubes horizontal at 100 rotations per minute, 37^0C. After this time the tube was filtered through a 70 μm filter and FCS added to 10% of final volume. Cells were

spun at 400 xg for 8 minutes. Then, cells were centrifuged again in HBSS +1% FCS before flow cytometric staining.

2.8 Imaging and Image Analysis

2.8.1 Live Cell Imaging of Immune Synapse Formation and Localisation of Signaling Intermediates

1 x 10^6 Renca tumour target cells were pulsed with k^dHA peptide by adding 2 μl to 1 ml complete medium (2 μg/ml for 1 hour at 37°C). This ensured uniform expression of the HA peptide by various Renca cell lines. Cells were then resuspended at 1 x 10^6/400 μl Imaging Buffer. 40,000 *in vitro* primed Clone 4 CTL or TILs were FACS sorted into eppendorfs, centrifuged at 300xg for 4 minutes and the pellet resuspended in 5 μl imaging buffer. 5 μl of T cells was plated with 1-1.5 μl Renca target cells in 50 μl imaging buffer, in a 384-well, glass-bottomed imaging plate (Brooks). If imaging was performed in a 1536 well plate, 5 μl T cells and 1.5 μl Renca cells were plated with no additional volume, and imaging proceeded as described. If any reagents such as NECA were included in cell culture, they were added to imaging buffer at an equivalent final assay concentration for the duration of imaging. A spinning disc confocal microscope (SDCM) system was used to image the cells. This was comprised of a temperature-controlled Ultraview ERS 6FE confocal system (Perkin-Elmer), a fluorescent microscope (LeicaDM16000) and a CSU22 Spinning Disc (Yokogawa) and 'Volocity' Image Acquisition Programme. 40x magnification was used for all experiments with an oil immersion lens. Immune synapse formation was imaged every 20 seconds over 15 minutes. A z-stack of GFP fluorescent images and one DIC reference image were acquired for each 15 minute run of cells (76, 77). Images were analysed by two operators using Metamorph (Molecular Devices) software. DIC images were assessed to identify the point of initiation of tight cell coupling and to identify off-interface lamellae and translocation (Chapter 5, Figure 35). GFP images were visualized using a pseudocolour look up table at 12 time points after cell couple initiation, to assess the localization of GFP-conjugated signaling intermediates (Figure 3). Localisation was categorized into one of 7 patterns as described by the Wuelfing lab's previous studies (76, 77, 242).

2.8.2 Microscope-based Cytotoxicity Assays

The IncuCyte™ Live Cell analysis system and IncuCyte™ ZOOM software (Essen Bioscience) were used to quantify target cell killing by *in vitro* primed Clone 4 cells or TILs. 1 x 10^6 Renca^{mCherry}WT target cells were either untreated (control), or pulsed with 2 μl/1 ml (2 μg/ml)

k^dHA peptide for 1 hour. Cells were centrifuged and resuspended in 3.33 ml Fluorobrite complete medium (Thermo Fisher) to achieve a concentration of 15,000 cells in 50 µl. Cells were plated in each well of a 384 well Perkin Elmer plastic-bottomed view plate and incubated for 4 hours to adhere. Live Clone 4 CTL or TILs were FACS sorted to be added to the plate in 50 µl Fluorobrite medium 4 hours after target cells were plated.

For experiments using only *in vitro* primed CTL, an effector : target ratio of 2:3 was used for all conditions, i.e. 10,000 CTL were plated onto 15,000 Renca cell targets. For experiments involving TILs, a 1:1 E:T ratio was used for all conditions therefore 15,000 CTL or TILs were plated onto 15,000 Renca targets. If cells had been treated with reagents such as NECA during cell culture, the final assay concentrations of these treatments were maintained in Fluorobrite medium for the duration of the cytotoxicity assay by adding T cells in 50 µl of in Fluorobrite medium with 2x reagent.

Images were taken every 15 minutes for 14 hours at 1600 ms exposure using a 10x lens. The total red object (mCherry target cell) area (um/well) was quantified at each time point from the time at which Control Clone 4 CTL started killing, until they had eradicated the entire Renca cell monolayer as determined by visual image analysis and the gradient of red object area. Data was exported from IncuCyte™ ZOOM software and graphs were produced using Excel and Prism. A percentage reduction in red object area was calculated over the selected time period and normalised to the growth of RencaWT (control) cells which were not pulsed with cognate HA antigen and were therefore not killed by Clone 4 CTL or TILs.

2.8.3 TIRF Microscopy

Each well of a glass-bottomed 384 well Perkin Elmer View plate was washed using 50 µl 1% acetic acid, 70% ethanol for 15 mins at RT. For a 1536 well plate, 4 µl of washing solution was utilised. The solution was aspirated away, and the plate baked at 60°C for 30 minutes by placing on a heat block. The plate was cooled.

2.8.3.1 Coating Imaging plate with Poly-L Lysine (PLL)

0.01% PLL (Sigma) was diluted to 0.01% in dH20. 50 µl PLL was added to each well and incubated for 15 minutes at room temperature. The solution was removed, and the plate baked for 30 minutes at 60°C as before.

2.8.3.2 Temporal Coating of Imaging Plate with Anti-CD3mAb and ICAM-Fc

After cleaning, or after PLL coating (if using) the plate was cooled and PBS containing 10 µg/ml anti-CD3mAb and 2.5 µg/ml ICAM Fc was added at 50 µl per well. The plate was incubated overnight at 4°C, the solution was aspirated, and cells were added to the plate in imaging buffer just before imaging.

2.8.3.3 Coating of Imaging Plate with Biotin/Neutravidin and Anti-CD3 mAb

Alternatively, instead of temporal coating with both anti-CD3mAb and ICAM-Fc, rapid coating of the imaging plate with biotin/neutravidin anti-CD3mAb could be achieved. BSA solution (500 µl biotin BSA 2 mg/ml ThermoScientific + 10 µl Tris pH8.0 + 50 µl 1M NaCl + 440 µl dH20) was added at 50 µl per well and the plate incubated at 37°C for 15 minutes, The solution was removed and the plate washed once with TSO solution (940 µl dH20 + 10 µl Tris pH8.0 + 50 µl 1M NaCL). Then, 50 µl Neutravidin solution was added to the plate (20 µl 1 mg/ml neutravidin, 80 µl dH20) and the plate incubated for 1 minute at 37°C. The plate was washed 3 times in TSO and twice with PBS before 10 µg/ml anti-CD3 was added in PBS, 50 µl per well. The plate was incubated at 37°C for ten minutes, then washed twice in imaging buffer. Imaging buffer was left in the well until T cells were added for imaging.

2.8.3.4 TIRF Imaging

T cells were prepared for live cell imaging as in section 2.8.1. 40 µl of imaging buffer was added into the view plate and 5 µl of T cells was added on top just before imaging. 300 ms exposure was used to image T cells to a depth of 70 nm in the GFP channel. Images were obtained at 20s intervals for 7 minutes using a Leica AM TIRF MC system attached to a Leica DMI 6000 inverted epifluorescence microscope. A 63x TIRF oil immersion lens was used. Images were analysed using Image J (Fiji)™(243).

2.8.4 Staining and Imaging of fixed Clone 4 T cells on Coverslips

2.8.4.1 In situ staining of T cells on Coverslips using Phalloidin, Celltrace reagents and Antibodies

15 mm circular coverslips were washed in 10% Sodium Dodecyl Sulphate (SDS) for 10 minutes whilst shaking gently. Coverslips were then dipped up 10 times into dH20 before being immersed in 100% ethanol for 30 minutes. Coverslips were again dipped 10 times into dH20, placed on a foil covered tray on a 60°C heat block for 30 min. The perimeter of the coverslip was outlined using a hydrophobic pen and the coverslip was stored at room temperature until use. 1 x 10^6 Renca WT cells were pulsed with 2 µl K^dHA in 1 ml of complete medium (2 µg/ml). Cells were incubated for 1h 10 minutes at 37°C before being centrifuged and resuspended in 400 µl of imaging buffer. 40 µl of imaging buffer was added to the clean coverslip and 10 µl pulsed Renca cell suspension was placed onto this droplet. Coverslips were placed at 37°C for 4 hours to allow Renca cell adherence. Clone 4 CTL or TILs were harvested and resuspended at 400,000 cells per 200 µl imaging buffer. A subset of Clone 4 cells was treated with pervanadate before plating on the coverslip as described in section 2.9.2. In some experiments, Clone 4 cells were stained with Celltrace Violet or CFSE prior to use as described in section 2.9.1. For anti-LAT/PhosphoLAT or PKCθ staining, imaging buffer was aspirated gently off the Renca cell layer and Clone 4 CTL were added on top of Renca cells in 15 µl imaging buffer. After 2 minutes, 50 µl of 4% paraformaldehyde was added directly onto the T cells without aspirating imaging buffer. The coverslip was incubated for 20 minutes at 4°C. Paraformaldehyde was gently aspirated from the coverslip and one PBS wash was performed by adding 200 µl to the coverslip then gently aspirating from the bottom edge. NH_4Cl was added and the coverslip incubated for 10 minutes at 4°C. 3 PBS washes were performed and then cells were permeabilised by adding 50 µl 0,02% Triton X-100. Cells were incubated for 30 minutes at room temperature, Triton-X was aspirated and Fc Block (BD Biosciences) plus primary antibody was added at the desired concentration in 200 µl of PBS containing 1% w/v BSA. Coverslips were incubated at 4°C overnight. After incubation, primary antibody was aspirated, and the coverslip washed 3 times with PBS + 1% w/v BSA. Secondary antibody was added at the requisite concentration in PBS + 1% w/v BSA and the coverslip was incubated for 1 hour at 4°C. 3 PBS washes were performed and the coverslip mounted using ProLong Gold Antifade Mountant (Invitrogen). For phalloidin staining, AF488 Phalloidin (Thermofisher) was prepared according to manufacturer's instructions. 5 µl phalloidin was dissolved in 200 µl PBS and added per coverslip, after fixation

and permeabilization. The coverslip was incubated at room temperature for 20 minutes before being washed 3 times in PBS and mounted. For PhosphoLck staining, the protocol was performed as above except the fixation step was performed using 1x Phosflow cytofix buffer (BD), warmed to 37°C for at least half an hour before use. Fixation was carried out for 15 minutes at 4°C. Cells were washed as above and placed into 200 µl 1x BD Phosflow Perm Buffer 2, pre-chilled to -20°C. Coverslips were kept on ice for 30 minutes and then washed 3 times in PBS 1% w/v BSA. Antibodies were added in 1x BD Phosflow Perm Buffer 2 at the desired concentration and cells were incubated at room temperature for 60 minutes. Slides were washed in PBS 1% w/v BSA and fixed in 4% paraformaldehyde for 20 minutes at 4°C. The slide was washed in PBS and mounted as above.

2.8.4.2 Imaging of Fixed Clone 4 T cells on Coverslips using Confocal Microscopy

A 21-30 µM Z stack was acquired in 1 µM slices using a Confocal 8 tandem scanner confocal system comprising a Leica confocal laser scanning microscope attached to a Leica inverted epifluorescence microscope (243). A mark and find experiment was set to image 100 cells per slide over evenly distributed sections. Images were analysed using Image J (Fiji)™ (243).

2.9 Flow Cytometry

Full flow cytometric gating for all experiments is shown in Appendix 2.

2.9.1 Celltrace Violet and CFSE Staining

Celltrace (Thermofisher) reagents were resuspended in DMSO according to manufacturer protocols. Clone 4 T cells were washed in an excess of PBS before being resuspended in PBS at a concentration of 4 x 10^6 cells per 1 ml. 1 µl Celltrace reagent was added per 1 ml cell suspension, the solution was briefly vortexed and maintained at 37°C for 20 minutes. 3 times the volume of complete medium was then added, and cells were incubated for 15 minutes to quench Celltrace staining. Cells were then placed in culture. If celltrace reagents were used to identify cells under confocal or widefield microscopy, 10x the above concentration was added on the day of imaging (10 µl per 1 ml PBS), but the protocol was otherwise the same.

2.9.2 Pervanadate treatment of T cells

20 mM Sodium Orthovanadate ($NaVO_4$) was prepared and stored in aliquots at -20°C. Just before use, 3% H_20_2 solution was prepared by diluting 30% solution (Sigma) in dH20. 4 µl H_20_2 and 20 µl $NaVO_4$ were combined with 976 µl dH20 to make 1 ml of 2x pervanadate solution and incubated in the dark for ten minutes. Pervanadate was added to T cells in an equal volume of medium and cells were incubated in the resulting 1x Pervanadate solution for 5 minutes at 37°C before being used in assays.

2.9.3 Cell Surface Staining with Fluorescently-Conjugated Antibodies

In vitro primed Clone 4 CTL or TILs were counted and centrifuged at 250 xg for 5 minutes before being resuspended in PBS at a concentration of 1 x 10^6 cells/1 ml. 2.5 x 10^5-1 x 10^6 cells for each condition were placed into a polystyrene FACS tube (Corning). Cells were centrifuged and resuspended in 100 µl PBS per tube with 1 µl/100 µl Zombie Aqua or Zombie Near Infared Fixable Live Cell Detection reagent (Biolegend). Tubes were incubated for 15 minutes in the dark at room temperature. Cells were washed in 3 ml FACS buffer and resuspended in 100 µl per tube FcBlock (BDBiosciences) for 15 minutes at 4°C. Cells were washed in 3 ml FACS buffer, pelleted and resuspended in 100 µl FACS buffer per tube with antibody at the required concentration (Table 2). Cells were incubated for 30 minutes at 4°C. Antibody concentration was determined by titration using 5 concentrations centred around the manufacturer's recommended protocol. Cells were washed in 3 ml FACS buffer to remove excess antibody before being fixed in 1% paraformaldehyde and analysed within 5 days using a Fortessa Flow Cytometer and BD FACSDiva Software (BD Biosciences). Flow cytometric data were analysed using FlowJo (Treestar) software. Gating was performed using fluorescence minus one (FMO) samples for each antibody stain.

2.9.4 Intracellular Cytokine Staining

Cells were stained for extracellular markers as above. However instead of fixation in 1% paraformaldehyde for storage, cells were fixed in 4% paraformaldehyde for 20 minutes at room temperature, washed 2 times in 3 ml FACS buffer, resuspended in FACS buffer and stored overnight. Within 72 hours, cells were pelleted and transferred into a 96 well v bottomed plate in 100 µl perm/wash buffer from (BD Biosciences ICCS Kit). The plate was incubated for 15

minutes at room temperature in the dark before being centrifuged at 450 xg for 2 minutes. Antibodies for intracellular cytokines were added to each well at the correct concentration in 100 μl perm buffer, and cells were mixed using a multichannel pipette. The plate was incubated for 30 minutes at 4°C. Cells were washed twice in 200 μl FACS buffer per wash and then fixed in 4% paraformaldehyde for analysis within 1 week as described. In some cells, intracellular staining was performed directly after harvesting as indicated. A subset of cells was treated with 20 ng/ml Ionomycin (Calbiochem), 10 ng/ml PMA (Calbiochem) and 1 μl/1 ml Golgi Plug as per manufacturer's instructions for 4h at 37°C before extracellular or intracellular staining steps were performed. For ICCS using TILs, CD8+ TILs were purified further from the produced using MACS, by FACS sorting, so that tumour stroma was not present for PMA/Ionomycin stimulation.

2.9.5 Phosflow Staining for Lck Phosphotypes

Staining for extracellular markers was performed as described. However, before starting 100 μl per tube of 1 x phosflow cytofix buffer (BD Biosciences) was warmed to 37°C for at least half an hour and 1 ml per tube of 1 x Phos Perm Buffer 2 (BD Biosciences) was cooled until it reached -20°C. The exact perm buffer to be used depends on the chosen phosflow antibody panel. After staining for extracellular markers, instead of being fixed in 1% paraformaldehyde for analysis, cells were centrifuged at 250 xg for 5 minutes and all supernatant removed to <50 μl in each tube. Cells were fixed in 100 μl phosflow cytofix from the 37°C aliquot, vortexed briefly and incubated for 15 minutes at 4°C. Tubes were topped up with 1 ml FACS buffer, centrifuged and washed twice in 1 ml FACS buffer. After each centrifugation step, all supernatant was removed to <50 μl and the tube vortexed to resuspend well. Cells were resuspended in 1 ml perm buffer per tube at -20 degrees, vortexed and kept on ice for 30 minutes. Tubes were centrifuged and resuspended in antibodies made up in 50 μl per tube of room temperature perm buffer 2. Phosflow antibody solutions were prepared immediately prior to use. Tubes were incubated for 60 minutes at room temperature then topped up with 1 ml FACS buffer and centrifuged. Cells were washed once in 3 ml FACS and then fixed in 200-300 μl per tube of 1% paraformaldehyde before being analysed within 1 week.

2.10 Anti-CD8 depleting Antibody production from Hybridoma cell lines

2.10.1 Purification by Ammonium Sulphate precipitation

Hybridoma cell lines producing anti-CD8α and anti-CD8β mAb (YTS156, YTS169) were kindly provided by the Gallimore laboratory, Cardiff, UK. Hybridomas were cultured in 250 ml cell culture flasks in complete medium and the supernatant harvested when cells reached 90% density. 1L of medium was collected from each clone. 2L of 100% ammonium sulphate solution was prepared by adding 707 g/L solid ammonium sulphate (Sigma) to 2L dH20 and stirring continuously. 1L of hybridoma supernatant was centrifuged at 10000 xg for 30 minutes at 4°C to remove large aggregates. The supernatant was placed into a beaker of 4 times it's volume and continuously stirred. 33.3 ml saturated ammonium sulphate was added per 100 ml supernatant, dropwise through a 19G hypodermic needle attached to a 50 ml syringe. The sample was incubated overnight at 4°C with continuous stirring. The sample was centrifuged at 10000 xg, for 30 minutes at 4°C. The supernatant was removed and saved. Antibody was harvested from the pellet by resuspending the pellet in PBS at 1/5 of the starting volume, avoiding generating bubbles. The protein concentration was determined using a BSA Assay Kit (Thermofisher) according to manufacturers' instructions and absorbance was measured by nanodrop. Antibody was aliquoted and stored at -20°C. Protein was analysed using Coomassie staining of an SDS-PAGE gel to determine that each antibody sample had attained the requisite purity. Detailed methods are outlined in Grodzki et al. 2010 (244). To test depleting antibodies, various doses were administered to mice intraperitoneally in PBS as described in Appendix 1, Supplementary Figure S12.

2.10.2 Complement Fixation *In Vitro* to test the efficacy of Depleting antibodies

Rabbit complement was obtained from Cedar Lane Labs (CL311). Spleens from Clone 4 mice were macerated mechanically and passed through a 40 μM cell strainer. Ack lysis buffer (Gibco) was used to lyse red blood cells (1 ml per spleen) and cells were pelleted at 250 xg for 5 minutes. Cells were resuspended in 9 ml complete medium, and 900 μl of suspension was placed into FACS tubes (Corning). 100 μl 10x complement stock was added on top of cells in complete medium along with 2 μg per tube of commercial antiCD8mAb or the combination of two in-house prepared anti-CD8 depleting antibodies (Table 2). Hybridoma supernatant and the supernatant extracted part way through ammonium sulphate precipitation were also added at equivalent concentration to determine that the in-house antibody was produced by the

hybridoma cell line and was not lost during the precipitation steps. Tubes were incubated for 1 hour at 37°C and stained by flow cytometry to determine the percentage of CD8+ T cells remaining. An anti-Vβ8.1 antibody was utilised to detect CD8+ T cells from Clone 4 mice in case the depleting antibody blocked fluorescent antibody binding to CD8 molecules.

2.10.3 *In vivo* testing of Depleting Antibodies

Depleting antibodies were administered as described in section 2.1.1.2 and blood samples were stained to quantify the number of CD8+ T cells as described in Appendix 1, Supplementary Figure S12.

2.11 Immunohistochemistry

Tumours were harvested and cut in half with a scalpel. Half of the tumour was used for cytotoxicity assays. The other half was placed in 2.35 ml RPMI on ice. Within 1 hour of harvest, tumours were snap-frozen in OCT compound (Tissue Tek), on a square of cork, in an isopentane bath, hovering above Liquid Nitrogen. Tumours were sectioned into 5 μM sections and mounted on slides. On day one of staining, acetone was cooled to -20°C. Slides were allowed to air dry for 10 –20 min before being fixed in acetone for 10 min on ice. Slides were dried again then washed 3x in PBS. Slides were dried in the area around the section and a border marked using a hydrophobic pen (ImmEdge). Sections were blocked with 2.5% horse serum (Vector) for 30 min then washed 3x in PBS. Sections were incubated with Primary antibodies or Isotype Controls in 1% BSA/PBS (Sigma-Aldrich) overnight at 4°C or room temperature for 1h (Table 2). On day 2 of staining, secondary antibodies were centrifuged at 14700 xg for 10 min at 4°C. Meanwhile slides were washed 3x with PBS. Slides were incubated with secondary antibody solution prepared in 1% BSA/PBS for 30-60mins at room temperature. Slides were washed 3x in PBS, with the second wash being performed in a shaker for 10 minutes. Hoechst stain (Thermofisher) was applied for 10 mins, and 3x PBS washes were performed. Slides were fixed in 1% PFA for 10 min then washed 2x in PBS, 1x in Glycine (0.3 M)(Fisher Chemical) for 10 min and 1 final wash in PBS. Coverslip was mounted in prolong gold antifade reagent and slides were left to cure at room temperature for 24 hours and images were acquired using a mark and find experiment on a STED Confocal microscope system. Images were analysed using ImageJ (Fiji).

2.12 Data Analysis and Statistics

2.12.1 Power Calculations

The Power of *in vivo* experiments was designed to reach >80%. Experimental group size was determined using the equation:

n = (2/(standardized difference$^{2)}$) x cp,power

n = Sample size per group determined using the formula

d = Standardized difference = ***Measurable difference in tumour volume / Standard Deviation*** (estimated as 1215 mm^3/983.5 mm^3 = 1.23 from previous experiments)

cp,power = constant for p<0.01 and power at 80% defined using standard Altman's Nomogram = 11.7

Therefore, we employed n = 14 mice per group over several experiments. For disease experiments the group size depends on the incidence of disease in the model. We favour a stepped approach in which an initial small experiment allows us to estimate the necessary size of further experiments to give a total >80% chance of demonstrating significance.

2.12.2 Statistical Comparisons

Samples were compared using independent sample t-tests for two sample comparisons. To determine the effect of one or more independent variables on one dependent variable across >2 groups, One way and Two-way ANOVA were used (SPSS statistics). To investigate the effect of one or two independent variables on >1 dependent variable, One-way and Two-way MANOVA were used. Tukey's post-hoc test was used for multiple comparisons unless Holm-Sidak was required to give greater power as determined by consultation with a statistician (Prof. Alan Hedges, personal communication). In some experiments, ANCOVA or MANCOVA was performed, as indicated, to incorporate a covariate (245). Where proportions were compared, Proportional z test or Fisher's exact Boschloo were used as indicated. SPSS statistics and Prism were used to execute analyses.

2.12.3 Analyses of *In Vivo* Tumour Growth and Survival

Variability:

For repeat experiments, tumour cells were passaged the same number of times before injection, and exact numbers were injected using consistent methods. Current work in our lab is focussed on optimising the conditions for tumour cell injection to achieve standard growth.

Experiments using Single Agent treatment of RencaHA tumours

When single immunotherapy was administered, tumour growth was unidirectional and tumours did not shrink, therefore repeated measures ANOVA was utilised to compare growth curves. Kaplan–Meier analysis was used to compare survival (Mantel Cox, Log rank), since there were only two outcomes in the study, survival or death. Mice were censored if tumours were < MATS or if culled for reasons other than tumour size (such as ulceration). Mice bearing tumours > MATS were culled and recorded as dead.

Experiments using combined treatment with Adoptive T cell transfer, TIM3 blockade and A2aR blockade

Cohorts of 14 mice per group were injected to achieve 4-6 tumours per group of uniform size (3-5 mm diameter) between 12-14 days after injection. In some experiments, some mice in the group were treated starting at d12, and some starting at d14 to ensure that sufficient mice could be included in the analysis. Staggering the start of treatment was necessary since few tumours grew at the same rate, and ethically and technically it was not possible to use a larger number of animals. All growth curves are shown from day 12 to allow for comparisons of growth from first treatment.

Multivariate Analysis of Covariance (MANCOVA) was performed to determine the effect of various parameters which could confound the analysis of growth and survival, such as experimental repeat, time until first treatment and volume at first treatment. MANCOVA showed that for the above analyses, it was necessary to exclude mice in which tumours attained starting volume after day 14. Starting treatment later than day 14 after injection was shown to have a significantly negative effect on progression free survival and chance of remission when compared with treating earlier, regardless of the size of tumours at commencement. Therefore,

most mice treated > day 14 were 'Non-responders' to treatment as defined in Chapter 4 (Figure 29).

Although these mice were excluded from growth and survival analysis, mice treated > day 14 were used as Non-responders for flow cytometric staining experiments in Chapter 7 (Figure 57). The results generated using flow cytometric analysis of these Non-responders did not differ significantly to those obtained using Non-responders treated before day 14 (comparison performed using one-way ANOVA of arcsine sqrt transformed data).

Tumour growth was compared using R values (246-249). For early stage tumours, an exponential model was fitted. R value (units of R = 1/time)was calculated using:

R = c(dc/dt)

Where:

θg = 2.76 x 10^5

Renca tumour cell = 17-25 μM diameter in vitro = 3.61 nm^3 volume using modified elliptical formula. Therefore 2.76 x 10^5 Renca cells make up 1 mm^3 of tumour.

dt =8h

Each cell divides 3 times every 24 hours

dc = difference in cell number

= (**θg** x final volume in mm^3) – (**θg** x starting volume in mm^3)

c = number of cells at start

= (**θg** x starting volume in mm^3)

To account for growth over the whole triphasic growth curve, final volume/initial volume is used because an exponential model cannot be applied to tumour growth greater than 1 week. Progression free survival was calculated using Cox's regression with covariates (SPSS). Hazard ratio of relapse was calculated using SPSS statistics.

Depletion Experiments to Assess Relapse

Thy1.1+ or CD8+ cells were depleted as described in section 2.1.1.2. The relapse produced by depletion was shown to be reliably due to depletion and not to spontaneous relapse, because it occurred in 6/6 mice after depletion. Mice were required to spend 6-10 days in remission before depletion was performed. Based on an average of relapse times from previous experiments, the maximum percentage of tumours that would be expected to relapse spontaneously after 6 days in remission would be 30% and the chance of this occurring at exactly d28-30 is 33%. Therefore, in only 9% of mice would relapse occur by chance rather than by depletion, which is less than 1 out of the 6 mice studied.

2.12.4 Analysis of Flow Cytometric Data

Flow cytometric data were analysed using FlowJo™ (Treestar). Gating was performed using Fluorescence Minus One control samples. Boolean gating tool was used to determine all possible combinations of expression of certain markers. Combination expression was converted into pie charts using Microsoft Excel or Pestle™ followed by Spice™. Percentage expression of co-inhibitory receptors as determined by flow cytometry were arcsine square root transformed prior to analysis. Tumour volume was log10 transformed. The gating strategy used for flow cytometric data are shown in Appendix 2.

2.12.5 Principal Component Analysis

Principal component analysis (PCA) was performed using RStudio to analyse the combination expression of 6 markers as determined by flow cytometry, and tumour volume. Tumours with a growth rate >1 standard deviation from the mean were excluded from comparisons. After transformation, each value (x) within the expression data and volume data were standardised (x*) to give a mean (m) of 0 and a standard deviation (SD) of 1 using the formula $x^* = (x-m)/sd$. PCA was then performed using R studio and the packages '*FactoMineR*' and *'Factoextra'*. Principal components (PC) 1-5 were selected for inclusion based on eigenvalues >1. Cos2 values were used to confirm the quality of representation of each variable within 2-dimensional factor maps and were calculated as the square of the variable's co-ordinates. The contribution of variables to PCs 1-4 was calculated using the formula (var.cos2 * 100) / (total cos2 PC) to produce P values.

Table 2 - Antibodies used in Experiments

Surface Marker	Clone	Fluorophore	Application	Manufacturer	Dilution
CD8a	53-6.7	FITC	FC	BD Bioscience	1/100
CD8b	53-6.7	PeCy7	FC	Biolegend	1/200
CD4	CKI1.5	AF700	FC	Biolegend	1/100
CD39	24DMSI	PerCP-Cy5.5	FC	eBioscience	1/100
CD73	T111.8	BV605	FC	Biolegend	1/100
TIM3	B8.2C1.2	PE	FC	Biolegend	1/100
TIGIT	1G9	APC	FC	Biolegend	1/100
LAG3	C9B7W	Pe-Cy7	FC	eBioscience	1/200
PD1	29F.1A12	BV785	FC	Biolegend	1/200
TCRb	H57-597	AF647	FC	Biolegend	1/200
CD62L	MEL-14	PE	FC	Biolegend	1/100
CD44	IM7	PerCP-Cy5.5	FC	Biolegend	1/100
CD69	H1.2F3	BV605	FC	BD Bioscience	1/100
CD103a	2E7	PE-Dazzle	FC	Biolegend	1/50
Thy1.1	OX7	FITC	FC	BD Bioscience	1/100
Thy1.1	OX7	PerCP-Cy5.5	FC	Biolegend	1/100
TIM3	RMT-23	BV605	FC	Biolegend	1/100
Ceacam-1	CC1	APC	FC	Biolegend	1/100
IL-2	JE56-5H4	BV711	FC	Biolegend	1/40
IFNγ	XMG1.2	PeDazzle	FC	Biolegend	1/200
IL-10	JES5-16E3	PE	FC	BD Bioscience	1/20
Galectin-9	RG9-35	BV421	FC	BD Bioscience	1/100
ICAM-1 (CD54)	YN1/1.7.4	FITC	FC	Biolegend	1/100
Total Lck	MOL171	PE	FC, IF	BD Bioscience	1/5
Lck p505	4/Lck-505	AF605	FC, IF	BD Phosflow	1/5
Lck p418	K48-37	AF488	FC, IF	BD Phosflow	1/5
PKCθ	T538	na	IF	CST	1/50 (*in situ* stain)
LAT	Polyclonal	na	IF	CST	1/100 (*in situ* stain)
PLAT	Y.191	na	IF	CST	1/50 (*in situ* stain)
Goat Anti-Rabbit AF488	H+L	AF488	IF (2°)	Life Technologies	1:1000

Goat Anti-Rabbit AF405	H+L	AF405	IF (2°)	Life Technologies	1:1000
Anti-IL-10	1B1.3A	na	*In vitro* blockade	BioXcell In Vivo mAb	15 μg/ml
Isotype for anti-IL-10	HRPN	na	*In vitro* blockade	BioXcell In Vivo mAb	15 μg /ml
Anti-TIM3	RMT.23	na	*In vitro/in vivo* blockade	BioXcell In Vivo mAb	20 μg /g *in vivo* (100 μg/mouse) 10 μg /ml *in vitro*
Isotype for Anti-TIM3	Rat IgG2a, 2A3	na	*In vivo/ in vitro* blockade	BioXcell In Vivo mAb	20 μg/g *in vivo* (100 μg /mouse) 10 μg /ml *in vitro*
Anti-PD-1	RMP1-14	na	*In vitro* blockade	BioXcell In Vivo mAb	*In vitro* 10 μg /ml
Isotype for Anti-PD-1	Rat IgG2a, 2A3	na	*In vitro* blockade	BioXcell In Vivo mAb	*In vitro* 10 μg /ml
Anti-CD8b	53-5.8	na	*In vivo* depletion	BioXcell In Vivo mAb	20 μg /g (100 μg /mouse)
Anti-Thy1.1	19E12	na	*In vivo* depletion	BioXcell In Vivo mAb	50 μg/g (250 μg /mouse)
Anti-CD3	145-2C11	na	*In vitro* priming	BioXcell In Vivo mAb	10 μg /ml
Anti-CD28	37.51	na	*In vitro* priming	BioXcell In Vivo mAb	1 μg /ml
FcBlock	2.4G2	na	Blockade of Fc Receptors	BD Biosciences	1/50 (1/500 for 2° IF)
CD8a	53-6.7	na	IHC (1°)	Biolegend	1:500
Isotype for CD8a IHC	Rat IgG2a, k	na	IHC	Biolegend	1:500
Donkey anti-rat IgG AF594	H+L	AF594	IHC (2°)	Thermofisher	1:2000
Anti-Foxp3	FJK-16s	na	IHC (1°)	Thermofisher	1:100
CD90.1 (Thy1.1)	OX-7	FITC	IHC (1°)	BD Bioscience	1:100
Isotype for CD90.1 IHC	Mouse IgG1 k	FITC	IHC	BD Bioscience	1:100

Chapter 3 Do Endogenous CD8+ TILs suppress Adoptively Transferred TILs?

3.1 Introduction

Studies using the murine RencaHA tumour model have shown that when *in vitro* primed Thy1.1+ Clone 4 CTL are adoptively transferred into RencaHA tumour-bearing mice, Clone 4 TILs recovered from the tumour are unable to directly lyse tumour cell targets *ex vivo*. These findings suggest that a loss of cytotoxic function amongst Clone 4 TILs occurs within the RencaHA TME (76, 77). If RencaHA tumours are grown in RAG-/- mice, there are elevated numbers of IFNγ producing Clone 4 TILs within the tumour when compared with conventional mice with a normal lymphocyte repertoire (40). This finding suggests that lymphocytes within the TME may exert a suppressive effect on adoptively transferred Clone 4 TILs. The most likely candidate cells to exert such suppression are endogenous CD4+ Tregs, as it has been shown that that they suppress the proliferation of naïve CD8+ T cells *ex vivo* in an A2a adenosine-receptor dependent manner (154). However, the endogenous Thy1.2+ CD8+ TIL population could also suppress Clone 4 TILs, and their phenotype has not yet been characterised.

In acute immune responses, populations of CD8+ effector T cells produce either IL-2, IFNγ or both IL-2 and IFNγ together. As the immune response wanes, IL-10 producing CD8+ T cells dampen inflammatory responses in their environment (92, 250). These IL-10-producing CD8+ T cells are found at high numbers within tumours and can represent either a transient suppressed phenotype or a more stable CD8+ Treg fate (151, 251). Therefore, in RencaHA tumour bearing mice, endogenous Thy1.2+ CD8+ TILs could also inhibit adoptively transferred Clone 4 TILs in an IL-10 dependent manner. To investigate this hypothesis, the following experimental approaches were utilised to compare (i) Clone 4 T cells primed *in vitro* using K^dHA peptide (Clone 4 CTL) (ii) Adoptively transferred Thy1.1+ Clone 4 TILs and (iii) Endogenous Thy1.2+ CD8+ TILs.

1. Intracellular staining of to assess the production of cytokines by TILs.
2. Flow cytometric assessment of co-inhibitory receptor expression amongst TILs.
3. Microscope based cytotoxicity assays to assess direct lysis of tumour-target cells by TILs *ex vivo.*

3.2 Results

3.2.1 Are Clone 4 TILs and Endogenous TILs suppressed by exposure to the tumour microenvironment?

3.2.1.1 Clone 4 TILs exhibit reduced lysis of tumour cell targets when compared with Clone 4 CTL

Previous studies in our laboratory used a Widefield microscope system to image killing of a monolayer of fluorescent RencaHA tumour cells by HA-specific Clone 4 cytotoxic T lymphocytes (CTL) and TILs (76, 77). The Widefield killing assay indicated that the rate of cytolysis of tumour cell targets by TILs was reduced when compared with *in vitro* primed Clone 4 CTL (10% kill/hour CTL, 4% kill/hour TILs) (76, 77). However, there are limitations to the use of Widefield killing assays in that only three conditions can be analysed simultaneously, and the Widefield microscope lacks full temperature and humidity control (76, 77). To increase the throughput and allow microscopy within a cell culture incubator, the assay was adapted using the Incucyte Zoom™ live cell imaging system (Supplementary Figure S1) (252). Data produced using the Incucyte showed that Clone 4 CTL were able to lyse tumour cell targets at around twice the rate of Clone 4 TILs (10.5% kill/hour CTL, 5.2 % kill/hour TILs), which is consistent with the results obtained using the Widefield system (Figure 18). These data support previous findings, that the cytolytic ability of Clone 4 TILs is suppressed by exposure to the TME (77).

Figure 18 - Clone 4 TILs have reduced ability to kill tumour cell targets when compared with in vitro primed Clone 4 CTL

Equivalent numbers of Clone 4 CTL and TILs were seeded onto a monolayer of K^dHA peptide-pulsed $Renca^{mCherry}WT$ tumour target cells (which appear red in colour) at an E:T ratio of 3:2. Unpulsed $Renca^{mCherry}WT$ cells were used as controls. Analysis of red fluorescent target cell area over time indicated killing of target cells by Clone 4 CTL and TILs. (A) Representative target area over time is shown from 1 of 4 separate experiments. Each point shows average area over 4 wells. Gradients were compared using Pearson correlation (f test) $p < 0.0001$****. (B) % target cell area per hour was calculated. N = 4 experiments (16 wells). Each point shows one experiment (4 pooled wells) conditions from the same experimental replicate are paired for comparison using t-test (p = 0.031*). (C) Representative images illustrating detection of $Renca^{MCherry}WT$ target cells by a blue outline mask detecting red object area.

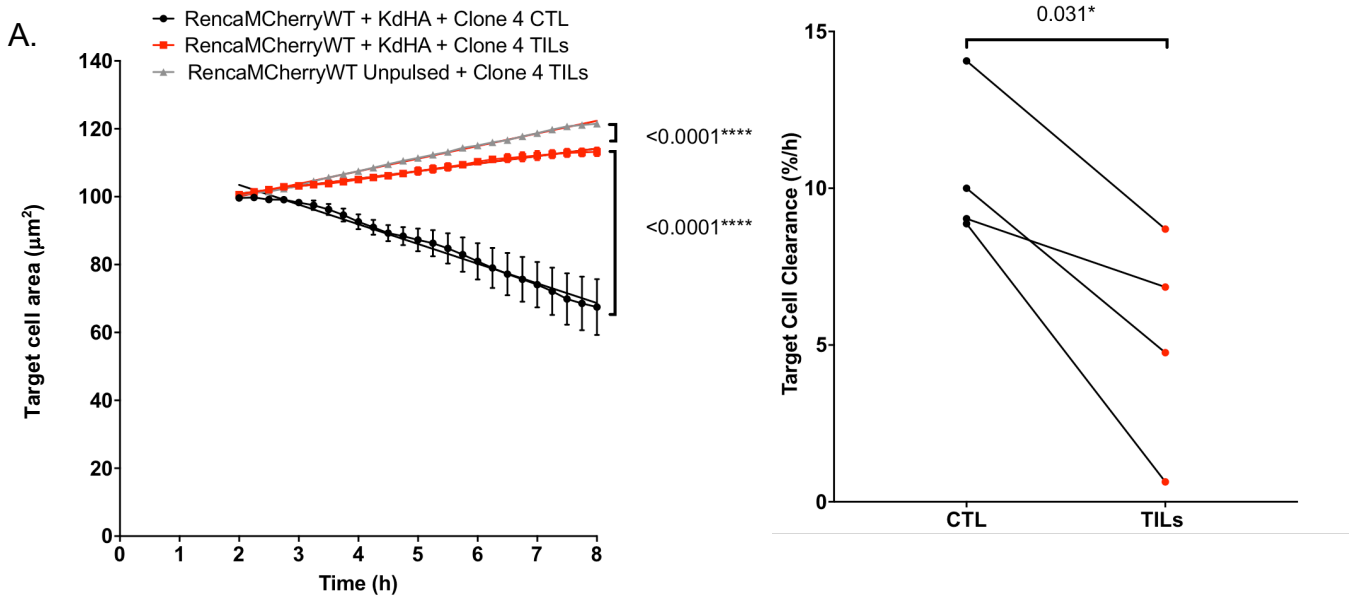

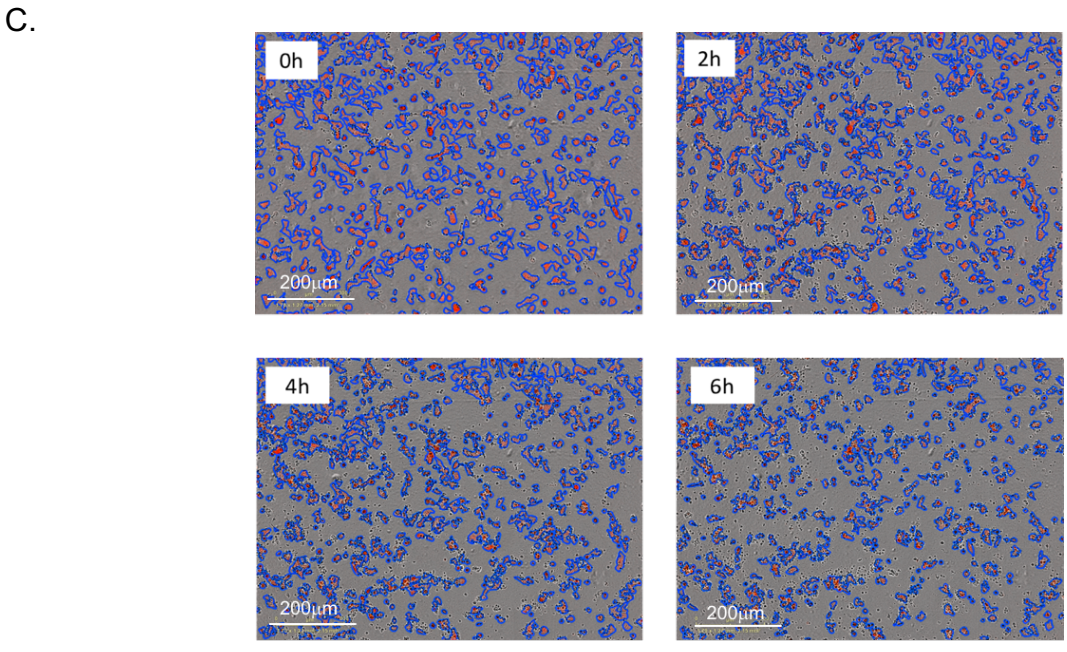

3.2.1.2 Clone 4 TILs and Endogenous TILs produce IL-10

We hypothesised that IL-10 production by endogenous Thy1.2+ CD8+ TILs could suppress effector function amongst Thy1.1+ Clone 4 TILs within the TME. As such, the production of the effector cytokines IL-2 and IFNγ, and the suppressive cytokine IL-10 were quantified amongst Clone 4 CTL, Clone 4 TILs and Endogenous CD8+ TILs stimulated with PMA/Ionomycin (92, 253, 254). Flow cytometric data were analysed using SPICE™ software to assess the various combinations of cytokines expressed by CTL and TILs (92). Blue and yellow segments indicate IL-2 or IFNγ producing effector cells, whereas other segments represent cells which produced IL-10 or produced none of the cytokines tested (92). TILs producing none of the assayed cytokines could be either naïve or suppressed but are unlikely to represent effectors (92).

Prior to stimulation with PMA/Ionomycin 12% of *in vitro* primed Clone 4 CTL were positive for both IL-2 and IFNγ, with the rest of the CTL population being positive for IL-2 alone and 3% of cells falling into other categories. After stimulation, 63% of CTL expressed IL-2/IFNγ concurrently, and only 8% produced IL-10 or none of the cytokines tested. Before PMA/Ionomycin, 38% of Thy1.1+ Clone 4 TILs expressed no cytokines, or combinations including IL-10, however, this dropped to 24% after stimulation. 52% of Clone 4 TILs produced both IL-2 and IFNγ after stimulation, indicating that Clone 4 TILs retained the potential to respond to PMA/ionomycin (Figure 19).

Interestingly, the administration of ATT Clone 4 T cells to tumour-bearing mice influenced the phenotype of the host's Thy1.2+ endogenous CD8+ TILs. Over 50% of endogenous TILs produced IL-10 or none of the cytokines tested before PMA/ionomycin, whether or not ATT was administered to the tumour. However, after stimulation, only 14% of endogenous TILs produced both IL-2 and IFNγ, but 25% of endogenous TILs from ATT tumours produced both effector cytokines. Therefore, based upon cytokine expression it appears that although the cytotoxic ability of Clone 4 TILs is suppressed, they do exert pro-inflammatory effects within the tumour microenvironment (Figure 19).

Figure 19 – A greater percentage of Endogenous TILs produce IL-10 when compared with Clone 4 TILs or CTL

Groups of RencaHA tumour-bearing BALB/c mice were either given ATT of Clone 4 CTL or left untreated. Populations of Clone 4 CTL, Clone 4 TILs, Endogenous CD8+ TILs from mice which received ATT, or Endogenous TILs from mice with no ATT were stained for intracellular cytokines straight after harvesting (pre) or after 4h of incubation with PMA, Ionomycin and Brefeldin-A (post). (A) Flow cytometric analyses are shown as pie charts in which segments indicate the percentage of cells expressing specific cytokine combinations, and pie arcs indicate which cytokines these are. Graphs represent average of 4 experiments comprising 2-4 pooled tumours. (B) Representative flow cytometric data from (i) Clone-4 CTL (ii) Clone 4 TILs (iii) Endogenous CD8+ TILs from mice with no ATT are shown from 1 experiment

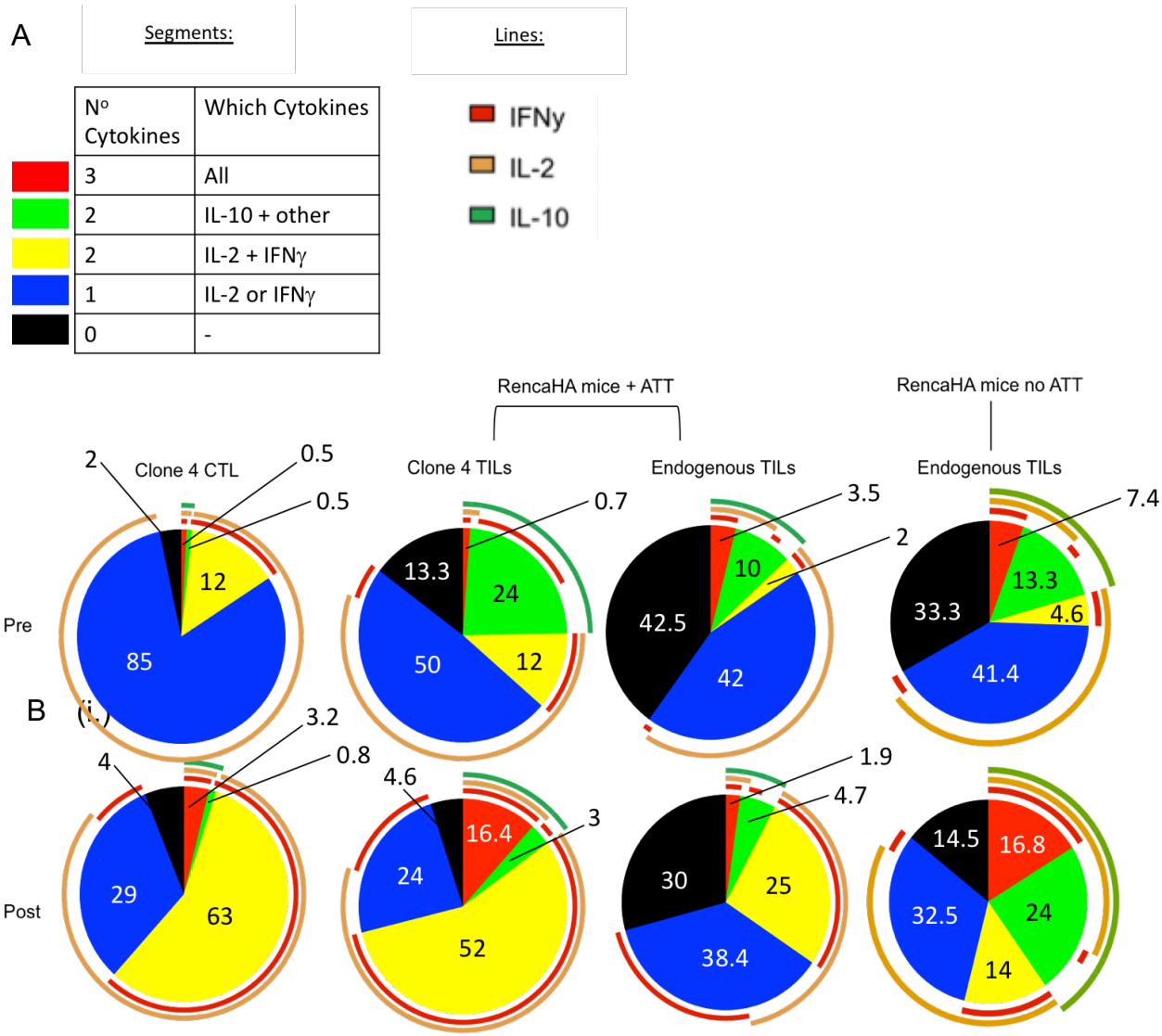

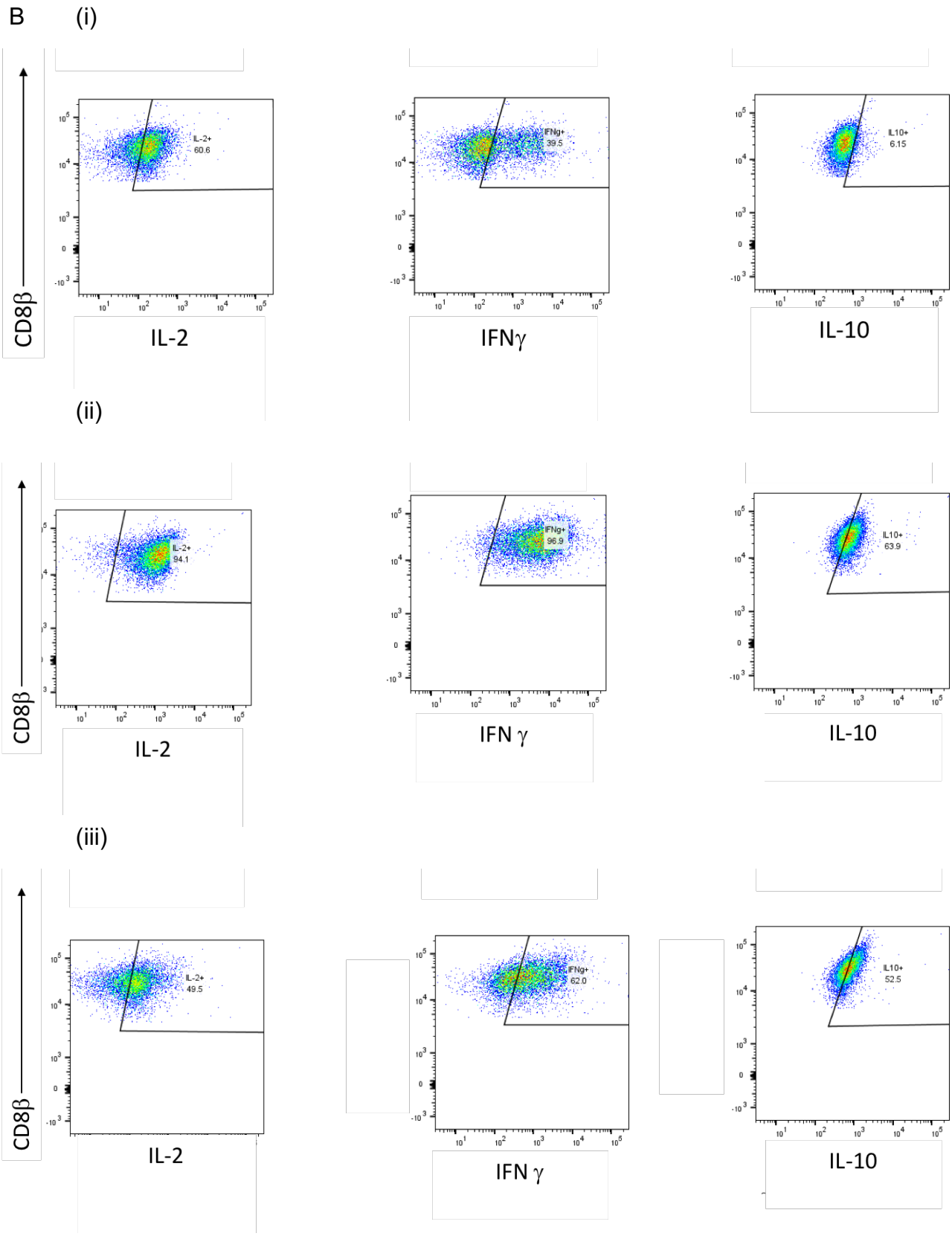
B
(i)
CD8β
IL-2+
60.6
IL-2
IFNg+
39.5
IFNγ
IL10+
6.15
IL-10
(ii)
CD8β
IL-2+
94.1
IL-2
IFNg+
96.9
IFN γ
IL10+
63.9
IL-10
(iii)
CD8β
IL-2+
49.5
IL-2
IFNg+
62.0
IFN γ
IL10+
52.5
IL-10

3.2.1.3 Clone 4 TILs and Endogenous TILs express combinations of CIRs which are characteristic of a Suppressed Genotype

Recent studies by Kuchroo et al. divide CD8+ TILs from B16F10 mouse melanoma into either effector cells or tumour-suppressed cells based upon their profile of CIR expression. Whereas single PD-1 expression is associated with an activated genotype, co-expression of combinations of CIRs is characteristic of cells with a tumour-suppressed genotype (115, 116, 121, 122, 138). Analyses of IL-2, IFNγ and IL-10 production by populations of endogenous and Clone 4 CD8+ TILs from RencaHA tumour-bearing mice suggested that they are suppressed by the tumour. To test this hypothesis, the percentage expression of PD-1, TIM3 and Ceacam-1, a TIM3-ligand, amongst CTL and TILs was determined using flow cytometry.

The data showed that amongst *in vitro* cultured Clone 4 CTL, less than 10% of cells expressed both TIM3 and PD-1, indicating that few Clone 4 CTL had a CIR expression profile characteristic of a suppressed genotype. Expression of PD-1 alone by the majority of CTL suggests that they are effectors. Around half of CTL expressed none of the CIRs tested and these cells could be effectors or naïve cells. Importantly, the pattern of CIR expression amongst CTL did not alter greatly after PMA/ionomycin stimulation (Figure 20).

In contrast, around half of Clone 4 TILs expressed TIM3 and PD-1 in combination, suggesting that they are suppressed cells. Interestingly, 40% of Clone 4 TILs expressed PD-1 and Ceacam-1 in combination and 12% of Clone 4 TILs expressed PD-1 alone suggesting that they are effectors. Endogenous TILs differed from Clone 4 TILs in that a greater proportion expressed none of the CIRs assayed. 31% expressed PD-1 alone, suggesting that they are effectors, and 43% of endogenous TILs expressed TIM3 alongside PD-1, indicating that they are suppressed. Only 6% of endogenous TILs expressed Ceacam-1 alongside PD-1 therefore Ceacam-1 expression is more prevalent amongst Clone 4 TILs than amongst endogenous TILs. However, the functional impact of Ceacam-1 and PD-1 co-expression is unknown. Taken together these data therefore show that, *in vitro* primed CTL have a CIR expression profile of effector cells whereas TILs express CIRs characteristic of tumour-suppressed CD8+ T cells (Figure 20).

Figure 20 – Clone 4 TILs and Endogenous TILs express combinations of CIRs which are characteristic of a Suppressed Genotype

Groups of RencaHA tumour-bearing BALB/c mice were given ATT of Clone 4 CTL. Populations of Clone 4 CTL, Clone 4 TILs and Endogenous CD8+ TILs were stained for co-inhibitory receptor expression straight after harvesting (pre) or after 4h of incubation with PMA, Ionomycin and Brefeldin-A (post). (A) Flow cytometric analyses are shown as pie charts in which segments indicate the percentage of cells expressing specific cytokine combinations, and pie arcs indicate which cytokines these are. Graphs represent average of 4 experiments comprising 2-4 pooled tumours. (B) Representative flow cytometric data from (i) Clone-4 CTL (ii) Clone 4 TILs (iii) Endogenous CD8+ TILs from mice with no ATT are shown from 1 experiment.

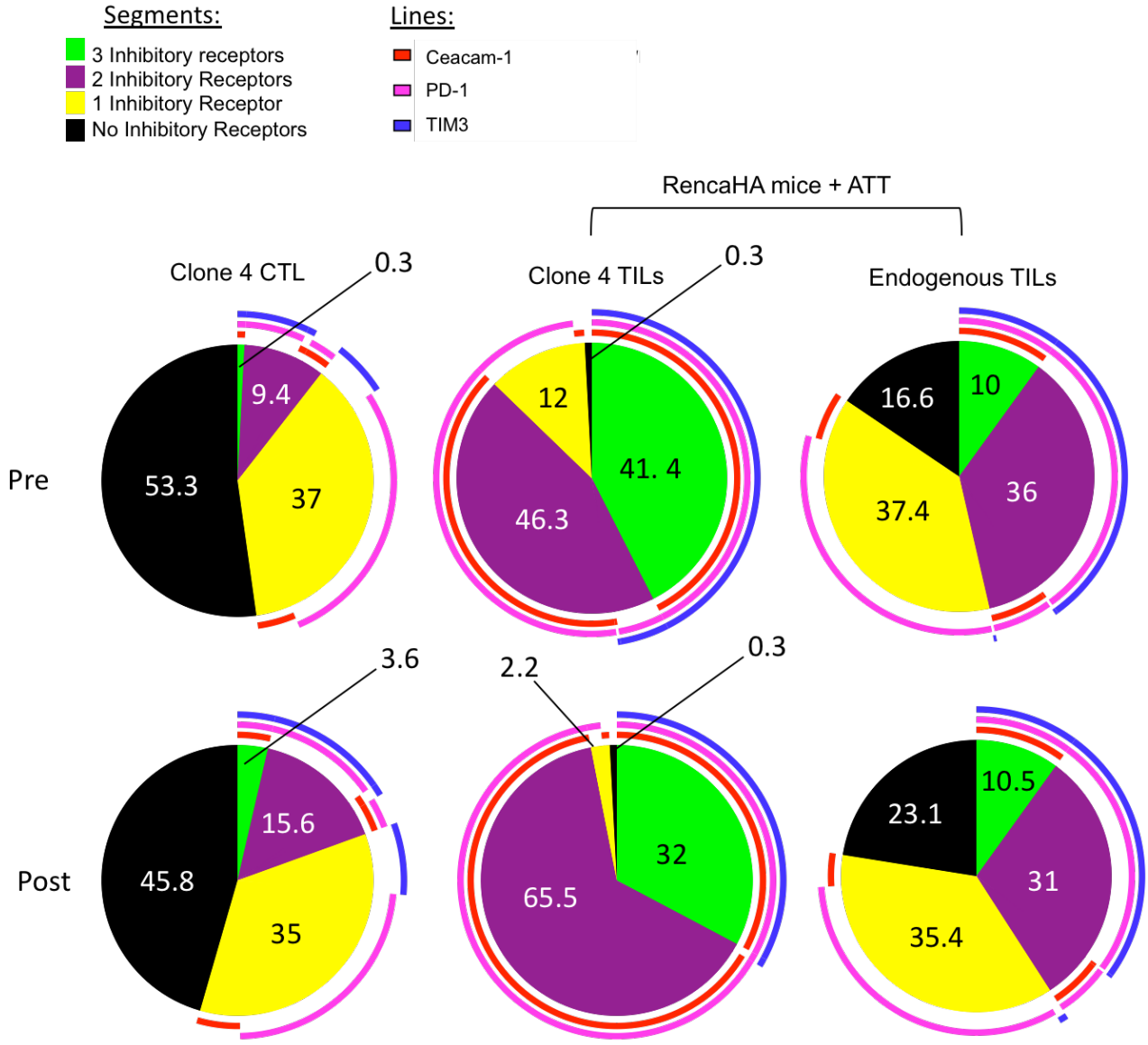

B (i)

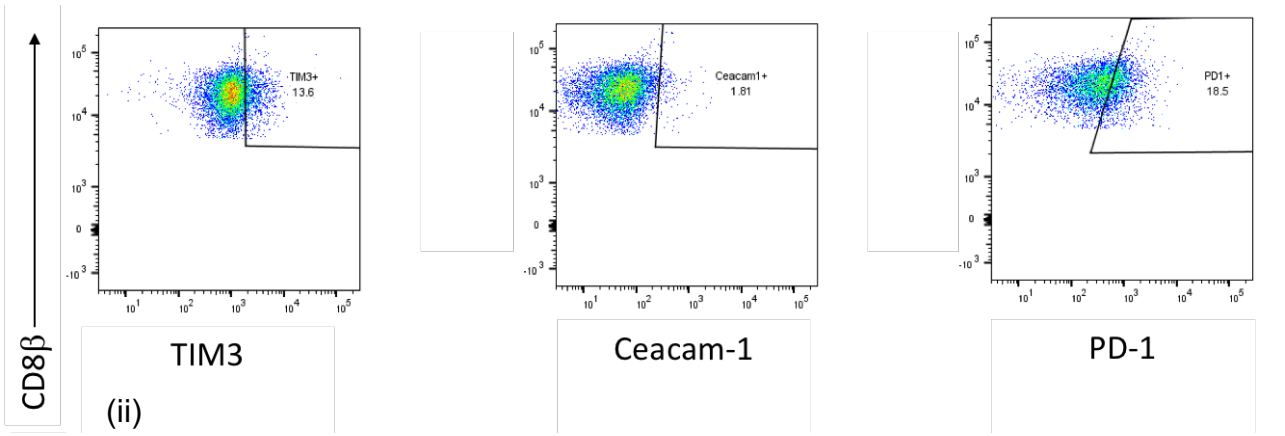
CD8β
TIM3+
13.6
TIM3
Ceacam1+
1.81
Ceacam-1
PD1+
18.5
PD-1

(ii)

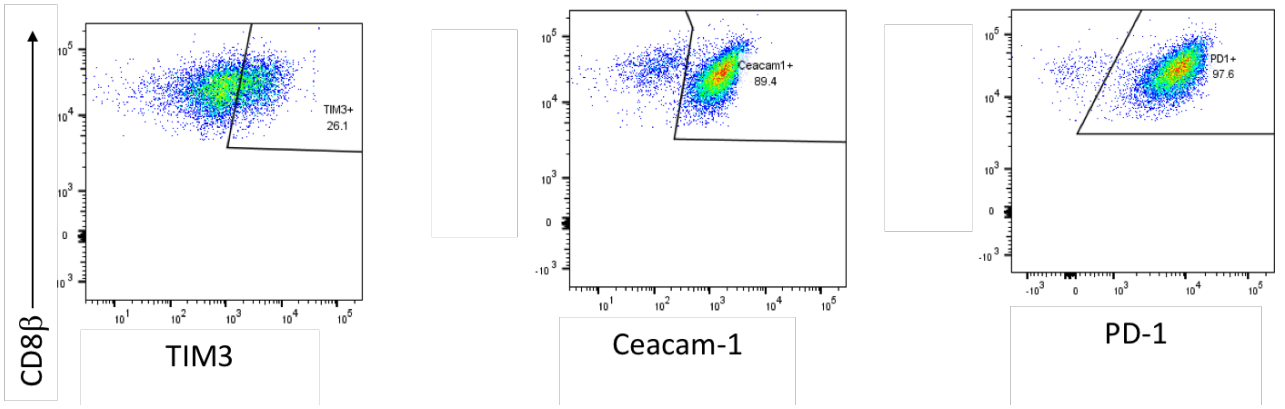
CD8β
TIM3+
26.1
TIM3
Ceacam1+
89.4
Ceacam-1
PD1+
97.6
PD-1

(iii)

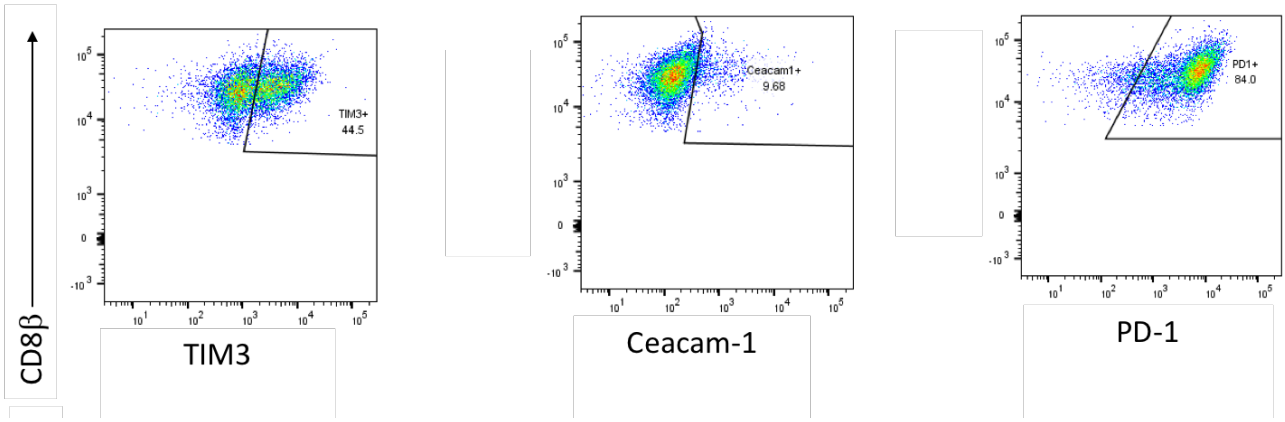
CD8β
TIM3+
44.5
TIM3
Ceacam1+
9.68
Ceacam-1
PD1+
84.0
PD-1

3.2.2 How is IL-10 production regulated within CD8+ TILs?

3.2.2.1 Overexpression of the transcription factor NFIL3 promotes TIM3 and IL-10 expression in Clone 4 CD8+ T cells

Studies have shown that amongst *in vitro* primed CD4+ Th1 cells, a complex of transcription factors including NFIL3 and ETS1 co-promotes transcription of both IL-10 and TIM3. The same transcription factor complex also represses IL-2 production (135, 137). We hypothesized that IL-10 production and TIM3 expression could also be co-controlled by NFIL3 in CD8+ T cells (135, 137). To determine if this was indeed the case, *in vitro* primed Clone 4 cells were transduced with a vector encoding the GFP-tagged NFIL3 protein (241). FACS sorting of GFP-high cells enabled the generation of a population of cells which overexpressed NFIL3 when compared with endogenous levels (Figure 21A) (47). Flow cytometric analyses were used to quantify cytokine production and co-inhibitory expression by NFIL3 overexpressing Clone 4 T cells.

The data showed that the percentage of Clone 4 CTL expressing IL-10 and TIM3 was significantly elevated after overexpression of NFIL3. Fewer NFIL3 overexpressing cells produced IL-2 when compared with control cells, and the MFI of IL-2 was also reduced. NFIL3 overexpression did not significantly affect the expression of other CIRs or cytokines tested. To determine whether or not expression of TIM3 could also influence IL-10 production, $TIM3^{GFP}$ was then overexpressed amongst CD8+ T cells. More TIM3 overexpressing cells produced IL-10 when compared with controls, however overexpression of TIM3 did not significantly affect IL-2, IFNγ, Ceacam-1 or PD-1 expression (Figure 21 B & C).

Figure 21 - Forced overexpression of NFIL3 is associated with elevated IL-10 production by Clone 4 CD8+ T cells

Clone 4 CTL were transduced with $TIM3^{GFP}$ or $NFIL3^{GFP}$. (A) TIM3 or NFIL3 overexpressing cells were FACS sorted. Gates for endogenous levels and overexpression of $TIM3^{GFP}$ are shown. CTL were then treated with PMA, Ionomycin and Brefeldin-A for 4 hours before being stained for extracellular markers, fixed, permeabilised and stained for intracellular cytokines. Data was analysed using flow cytometry. (B) shows % expression and (C) shows MFI of IL-2, Ceacam-1, IL-10, TIM3, PD-1 and IFNγ calculated as mean +/- SEM and compared using paired t-test adjusted for multiple comparisons. Significant P-values are indicated, all other comparisons were none significant. N= 3 experiments.

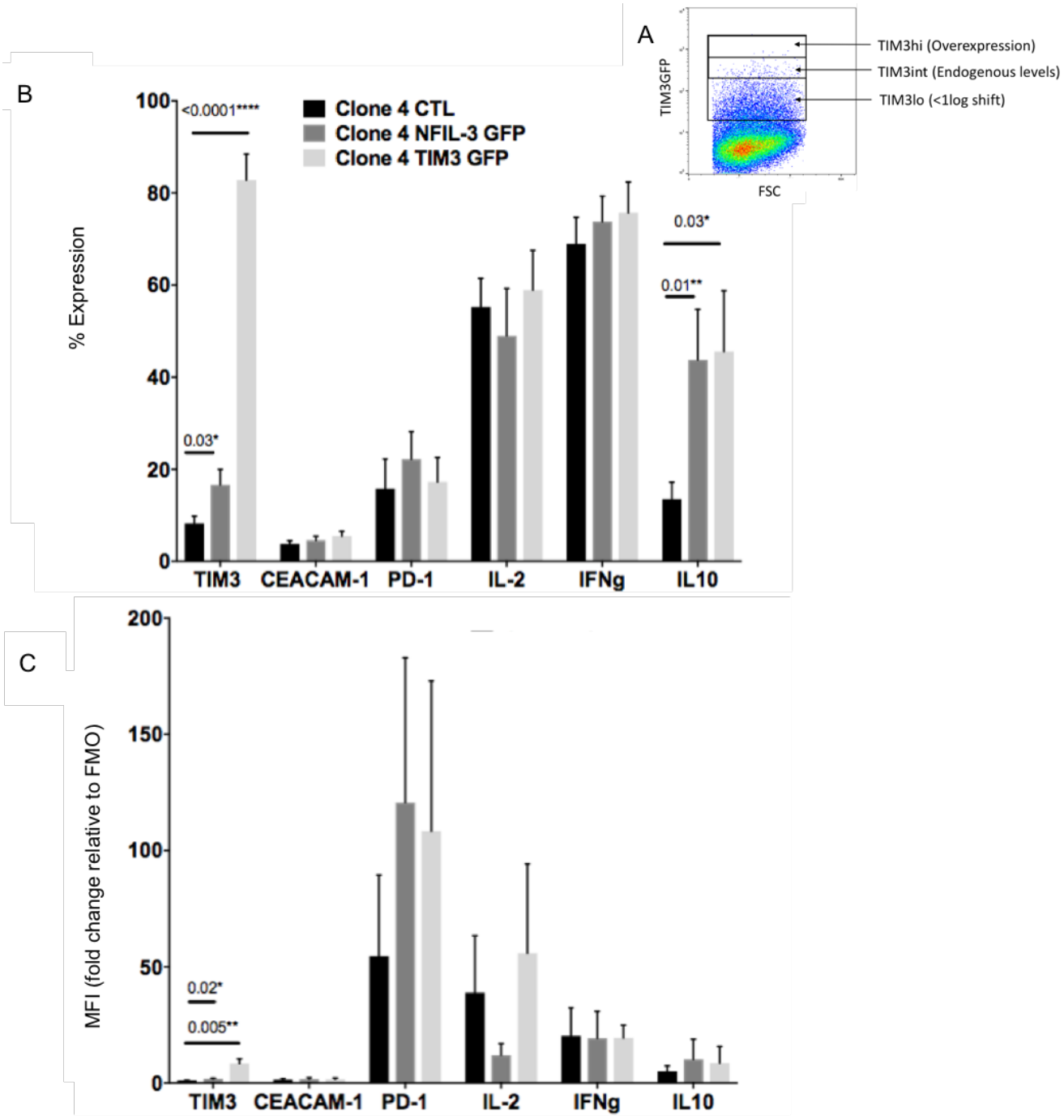

3.2.2.2 Do TIM3+ TILs produce more IL-10 than TIM3- TILs?

The above data indicated that *in vitro*, TIM3 and IL-10 production are co-controlled in CD8+ T cells (135, 137). Therefore, we hypothesised that more TIM3+ TILs would express IL-10 than TIM3- TILs. TIM3 expression and cytokine production was compared between Thy1.2+ endogenous CD8+ TILs and Thy1.1+ Clone 4 TILs by re-analysis of flow cytometric data from Figure 19. Before PMA/ionomycin treatment, more TIM3+ TILs expressed IL-10 than TIM3- TILs, and a greater proportion of IFNγ producers was also found amongst TIM3+ cells when compared with TIM3- populations. In addition, the percentage of IL-10 expressing cells increased amongst endogenous TIM3+ TILs after PMA/Ionomycin, indicating that they are suppressed, however this did not occur amongst endogenous TILs from tumours which received ATT, once again suggesting that the presence of Clone 4 TILs gave rise to fewer IL-10+ endogenous TILs within the RencaHA TME (Figure 22).

3.2.2.3 In vivo blockade of TIM3 reduces IL-10 production amongst CD8+ TILs

These findings suggested that TIM3 and IL-10 are co-regulated amongst populations of CD8+ TILs. Therefore, we postulated that blockade of TIM3 signalling could reduce IL-10 production. To investigate this possibility, tumour bearing mice were treated with anti-TIM3mAb, in the absence of Clone 4 ATT. Treatment with anti-TIM3mAb led to a reduction in tumour growth between 12 and 26 days however this was not significant. On the other hand, there were significantly fewer IL-10 producing cells amongst endogenous CD8+ TILs from anti-TIM3mAb treated mice when compared with isotype controls (Figure 23). These data further suggest that TIM3 expression within the tumour is associated with IL-10 production amongst CD8+ TILs.

Figure 22 - A greater percentage of TIM3+ TILs produce IL-10 when compared with TIM3- TILs

Groups of RencaHA tumour-bearing BALB/c mice were either given ATT of Clone 4 CTL or left untreated. Populations of Clone 4 CTL, Clone 4 TILs, Endogenous CD8+ TILs from mice which received ATT, or Endogenous TILs from mice with no ATT were stained for intracellular cytokines straight after harvesting (pre) or after 4h of incubation with PMA, Ionomycin and Brefeldin-A (post). A) Flow cytometric analyses are shown as pie charts in which segments indicate the percentage of cells expressing specific cytokine combinations, and pie arcs indicate which cytokines these are. Graphs represent average of 4 experiments comprising 2-4 pooled tumours.

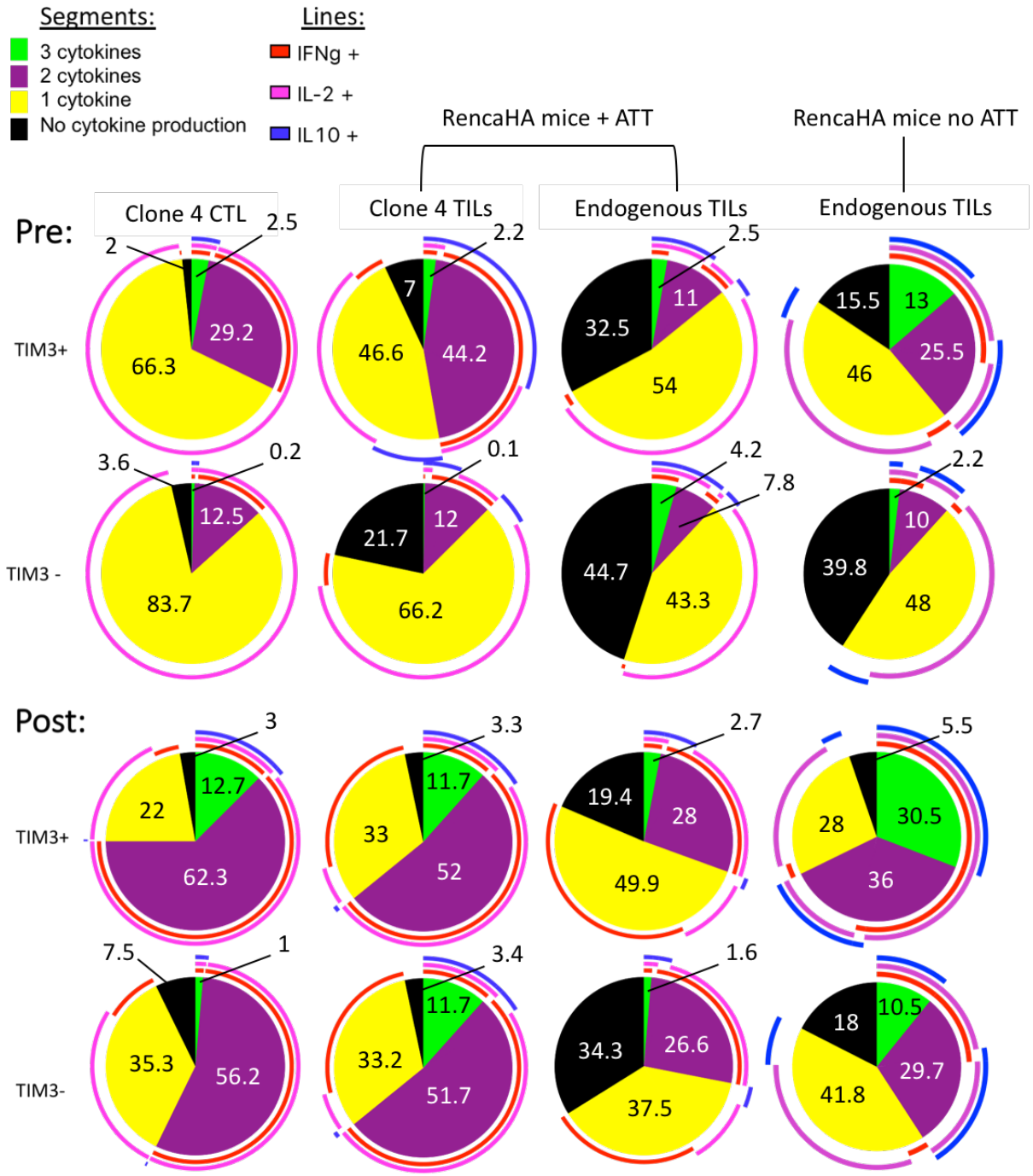

Figure 23 - In vivo treatment with anti-TIM3mAb is associated with reduced IL-10 production amongst CD8+ TILs

Groups of RencaHA tumour-bearing BALB/c mice were treated anti-TIM3mAb (100µg/mouse) or isotype control in the absence of any adoptive T cell transfer. (A) Plot of tumour growth over time, each point represents one mouse at that timepoint with mean shown as a line. Data were compared using repeated measures ANOVA. (B) CD8+ TILs were treated with PMA, Ionomycin and Brefeldin-A for 4h and stained for IL-10 expression. Data was acquired using flow cytometry. % expression of IL-10 was compared using paired t-test p=0.03*. N= 6 treated tumours and N = 3 control tumours over 2 experiments.

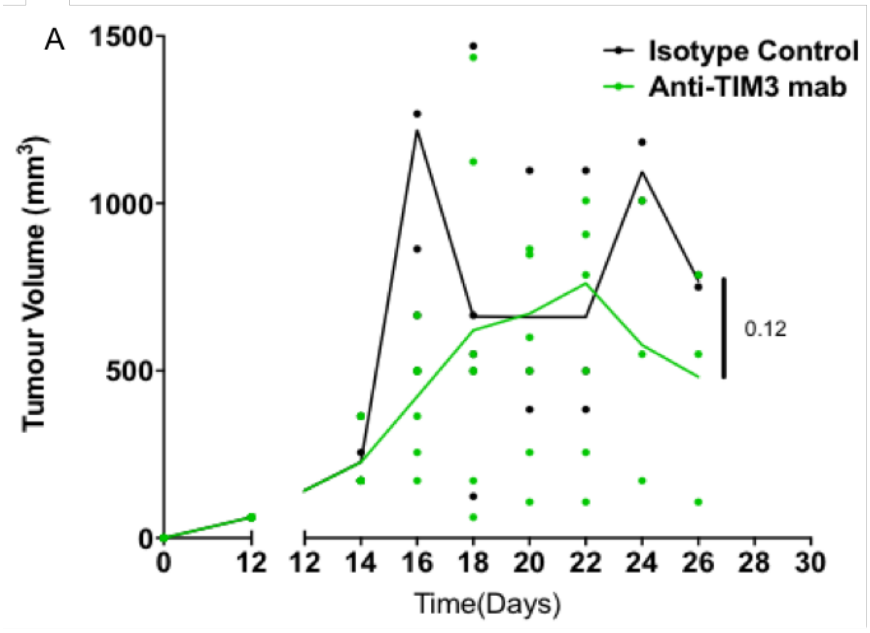

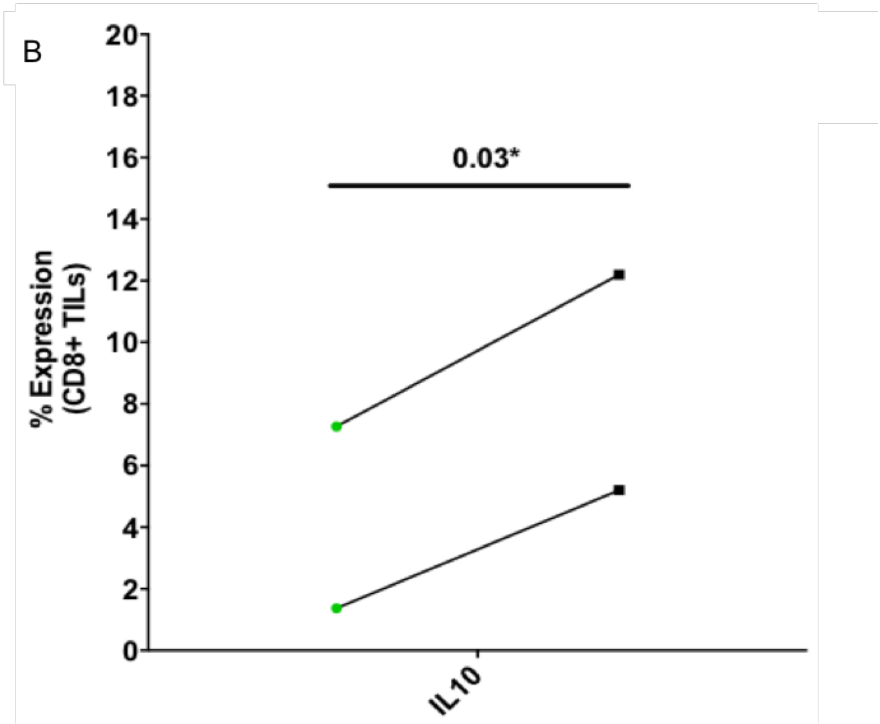

3.2.3 Does production of IL-10 by endogenous TILs suppress Clone 4 T cells *ex vivo*?

As Thy1.2+ CD8+ Endogenous TILs stained positively for IL-10, it was decided to determine if these TILs could suppress naïve Clone 4 T cells, by producing IL-10. As such, *ex vivo* suppression assays were performed by setting up co-cultures of Thy1.2+ CD8+ endogenous TILs with naïve Clone 4 T cells. Assays were performed at a 2:1 TILs: CTL ratio, in the presence or absence of Anti-IL-10R blocking mAb (Figure 24 A & B).[1] The results show that addition of CD8+ TILs was sufficient to suppress naïve CD8+ T cell proliferation *ex vivo* (p=0.02*). However, proliferation was not restored by the addition of anti-IL-10R mAb, suggesting that suppression of Clone 4 T cells by endogenous TILs was not IL-10R dependent.

The fact that blockade of IL-10Rs did not mitigate suppression of naive Clone 4 CTL by CD8+ TILs, meant that other mechanisms of CD8+ TIL mediated suppression could be operating. Previous findings in the RencaHA model showed that endogenous CD4+ TILs suppress naïve Clone 4 T cell proliferation *ex vivo* in an adenosine dependent manner (Introduction 1.7.4.3). Other studies suggest that endogenous CD8+ TILs can also express the adenosine producing enzymes CD39 and CD73 (238). Therefore, we hypothesised that endogenous CD8+ TILs in the RencaHA model may also be able to produce adenosine, and suppress naïve Clone 4 T cell proliferation via A2aRs.

To address this hypothesis, flow cytometric analyses were used to show that in RencaHA tumours, CD8+ TILs do express the adenosine producing enzymes CD39 and CD73 (Figure 25)(154). To determine whether CD8+ TILs suppressed naïve Clone 4 T cell priming via adenosine, co-cultures of CD8+ endogenous TILs and naïve Clone 4 T cells were set up in the presence of the A2a Adenosine Receptor antagonist ZM241385. However, A2aR-Antagonist did not protect naïve cells from suppression (Figure 24 A & B). Interestingly, the addition of both anti-IL-10R mAb and A2aR-Antagonist did produce a synergistic improvement in naive Clone

[1] Adding TILs to naïve Clone 4 cells could produce suppression because the presence of greater numbers of cells in the well causes competition. To eliminate the possibility that suppression occurred due to competition rather than IL-10 signalling, additional control wells were set up. In these wells, an equivalent ratio of unstained effectors were added to celltrace violet stained naïve cells. The presence of additional numbers of cells in the well did not produce a significant reduction in naïve cell proliferation.

4 T cell proliferation over either agent alone, however this improvement was not significant (Figure 24 A & B).

These data therefore show that endogenous CD8+ TILs can suppress the proliferation of naïve CD8+ T cells *in vitro*, and that CD8+ TIL-mediated suppression could only be antagonized by blocking both IL-10R and A2a adenosine receptors concurrently. Although co-blockade of A2aRs and IL-10Rs requires repeat analysis, this combination only partially prevented suppression due to endogenous CD8+ TILs, therefore TILs could also suppress effector CD8+ T cells by other methods.

Figure 24 - Endogenous CD8+ TILs suppress naive Clone 4 T cells ex vivo

Purified naïve Clone 4 CD8+ T cells were labelled with Celltrace Violet (CTV) and co-cultured with K^dHA peptide-pulsed irradiated APCs in the presence of endogenous Thy1.2+ CD8+ TILs at a ratio of 2:1 or 5:1. Anti-IL10 mAb, A2aR-antagonist or isotype control were added where indicated. (A) Representative CTV data showing proliferation of Clone 4 T cells is shown. Red line indicates divisions 3 and 4 of the CTV labelled population. (B) The percentage of CTL which completed 2 or 3 divisions was calculated. Data are shown as mean +/- SEM. Samples were compared using One-way ANOVA. Each bar is representative of 3 separate experiments where error bars are shown, or 1 experiment where no error bars are shown, each comprising 6 pooled tumours, utilising duplicate or triplicate wells per condition.

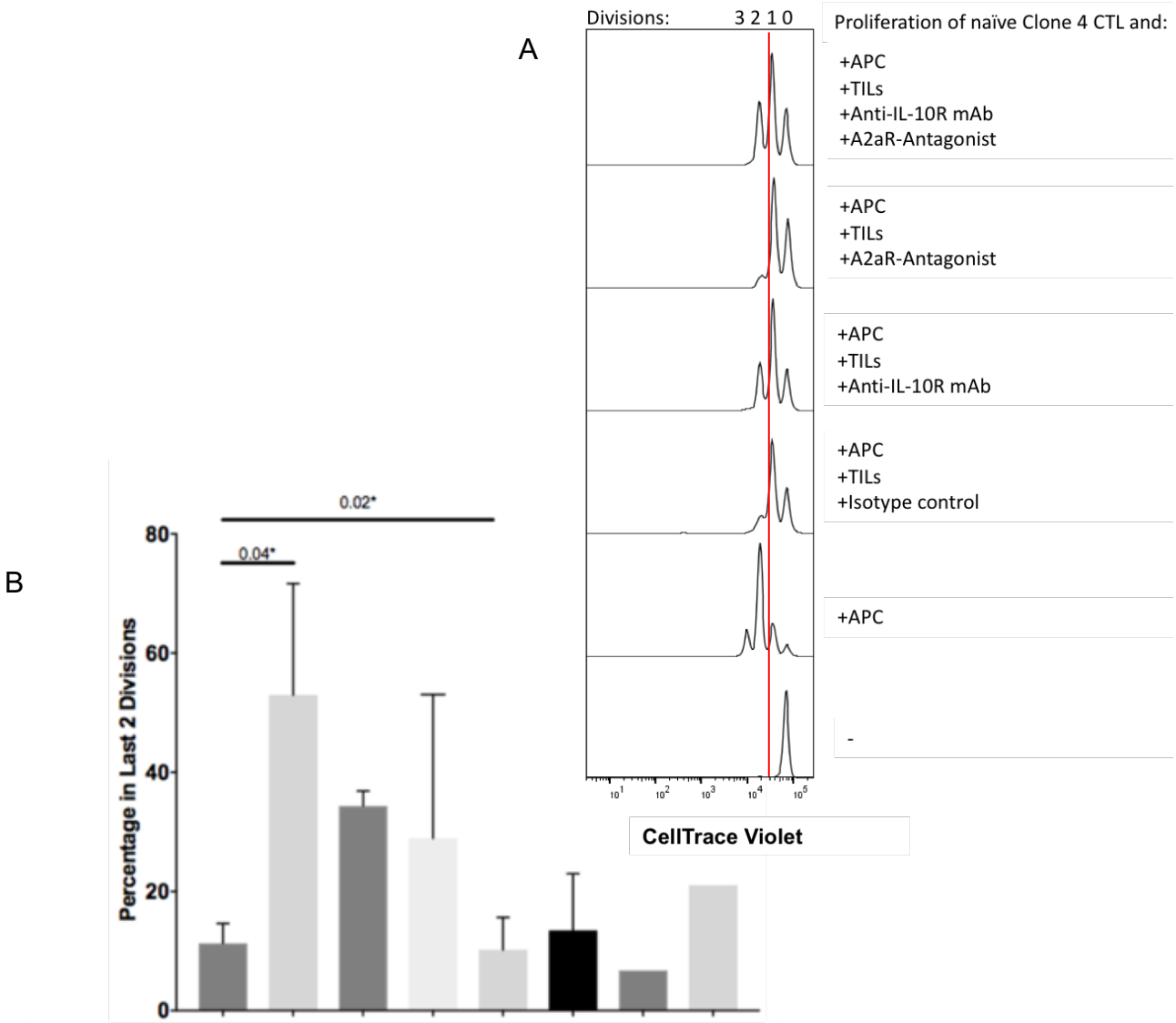

CTL	x	x	x	x	x	x	x	x
Antigen Presenting Cells		x	x	x	x	x	x	x
Additional Unstained CTL			x					
CD8+ TILs					x	x	x	x
Isotype Control					x			
Anti-IL10mAb				x		x		x
AR-Antagonist							x	x

Figure 25 - Thy1.2+ CD8+ Endogenous TILs express CD39 and CD73

Thy1.2+ CD8+ TILs harvested from RencaHA tumour bearing mice were stained using anti-fluorochrome-conjugated CD39 and anti-CD73 mAbs and analysed using flow cytometry. CD39 and CD73 expression were compared using MANOVA of arcsine-square root transformed data. $p < 0.0001$**** CD39 TILs vs TDLN. P= 0.082 CD73. N = 26 tumours over 12 experiments and 3 TDLN over 3 experiments. Data are displayed as mean +/- SEM.

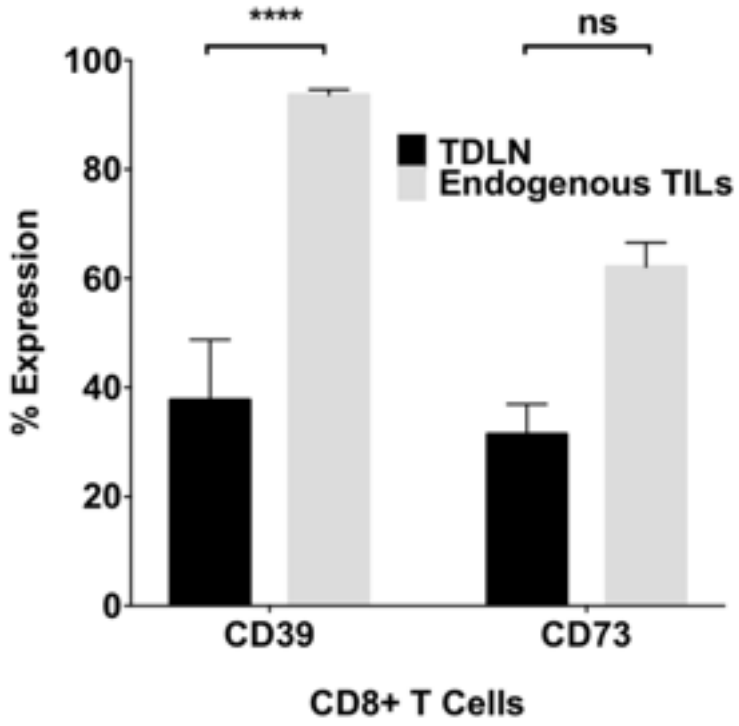

3.3 Discussion

3.3.1 TIM3 expression is associated with IL-10 production amongst Endogenous CD8+ TILs

Experiments were carried out in order to test the hypothesis that Thy1.2+ endogenous CD8+ TILs could produce IL-10 in order to suppress Clone 4 T cells. In so doing, it would be possible to tell whether or not IL-10R signalling is a pathway that could be targeted therapeutically to improve the effector function of Clone 4 TILs within the RencaHA TME. To investigate this hypothesis, the cytokine profiles of populations of Thy1.1+ Clone 4 TILs and Thy1.2+ endogenous CD8+ TILs were used to differentiate between effector TILs, producing combinations of IL-2 and IFNγ, or tumour-suppressed TILs, producing IL-10.

Previous experiments suggested that Thy1.1+ ATT Clone 4 TILs lose cytotoxic effector function within the TME, because although they attempt to kill tumour-cell targets *ex vivo*, this killing does not succeed. Imaging experiments have shown that failed killing occurs because the Clone 4 TIL immune synapse is morphologically unstable when compared with immune synapses formed by Clone 4 CTL (76, 77). However, intracellular staining showed that although some Clone 4 TILs produced IL-10, many responded to stimulation with PMA/Ionomycin by producing IL-2 and IFNγ, suggesting that despite their inability to kill, Clone 4 TILs have the potential to produce effector cytokines. The instability of the Clone 4 TIL immune synapse could explain why Clone 4 TILs, with the potential to behave as effectors when the TCR is bypassed by PMA/Ionomycin, cannot kill when interacting with tumour target cells. Improving the stability of the Clone 4 TIL immune synapse could therefore restore effector function amongst Clone 4 TILs (77).

Amongst Thy1.2+ Endogenous TILs there was a greater proportion of IL-10 producing cells compared with Clone 4 TILs and this did not alter with PMA/ionomycin stimulation. However, in the presence of ATT Clone 4 TILs, a greater number of endogenous CD8+ TILs expressed IL-2 and IFNγ after PMA/Ionomycin. This finding suggests that ATT Clone 4 TILs may condition the TME, inducing a greater proportion of endogenous CD8+ TILs to become effectors and reducing the proportion of IL-10 producing endogenous TILs. This could be due to the fact that although the killing function of Clone 4 TILs is impaired, they still produce some IFNγ which could improve DC maturation, CD4+ Th1 and CD8+ T cell function as well as inducing

macrophages to assume a Type-1 phenotype. Flow cytometric analysis to assess phenotypic markers such as FOXP3 expression (indicating CD4+ Tregs) or CD80/86 (indicating DC maturation) could be used to profile the phenotype of other intratumoural immune cells in the presence and absence of Clone 4 ATT, in order to test this hypothesis. Conditioning of the TME by adoptively transferred cells may therefore explain the partial therapeutic benefit observed after ATT therapy in some clinical scenarios (232, 255). The proportion of endogenous CD8+ TILs which produced none of the cytokines tested also increased in the presence of ATT. The pro-inflammatory environment generated by Clone 4 ATT could induce endogenous TILs which are not producing cytokines to undergo tolerance or death (95).

As endogenous CD8+ TILs are a source of immunosuppressive IL-10 within the TME, targeting IL-10 production by CD8+ T cells may be of therapeutic benefit to cancer patients. Therefore, we aimed to determine how IL-10 production is regulated in CD8+ TILs, which could allow IL-10 production to be blocked therapeutically (135, 137). To assess whether the transcription factor NFIL3 controlled IL-10 and TIM3 expression amongst CD8+ T cells, Clone 4 T cells were primed *in vitro* and transduced to overexpress NFIL3. It was clear that NFIL3 expression promoted both TIM3 and IL-10 production and repressed IL-2 production. Interestingly, preliminary overexpression of NFIL3 amongst CD4+ T cells was associated with reduced IL-2 and elevated IL-10 production, however it was not associated with alterations in TIM3 expression amongst CD4+ T cells in our system, which contradicted published work (Supplementary Figure S2)(135, 137).

Overexpressing $TIM3^{GFP}$, in the absence of NFIL3 overexpression, was sufficient to increase IL-10 production amongst CD8+ T cells. These findings suggest that elevated expression of TIM3 gives rise to upregulation of IL-10 via several possible mechanisms which could depend on whether TIM3 was engaged by any ligand in our system. It is known that expression of TIM3 without ligand engagement can upregulate the TCR pathway because TIM3 sequesters active Lck at the site of TCR signal initiation. When engaged by inhibitory ligands such as Ceacam-1 or Galectin-9, TIM3 then encourages release of the Lck reservoir which is bound to a protein, Bat-3, suppressing TCR signalling (Figure 5) (54, 138). Exogenous TIM3-ligand was not provided to deliberately engage overexpressed TIM3 in this experiment, therefore under these conditions, TIM3 could have acted to promote TCR signalling. Inherent negative feedback mechanisms are built into TCR signalling, and increased activation of the calcium-calmodulin-dependent Kinase

II (CaMKII) pathway, which causes ETS1 and NFIL3 to upregulate TIM3 and IL-10 expression, is one of these mechanisms (19)(54, 55). As such, forced overexpression of TIM3 without inhibitory ligands could promote TCR signalling and initiate IL-10 production through negative feedback mechanisms.

Alternatively, TIM3 could have been engaged by ligands in cell culture (256). Ceacam-1 is expressed at low levels amongst Clone 4 CTL in *in vitro* cultures and this could engage TIM3 (Figure 20). Furthermore, phosphatidylserine produced from apoptotic cells is also a ligand for TIM3. If TIM3 was engaged by inhibitory ligands, then the mechanism by which it mediates upregulation of IL-10 is not clear. Utilising Renca tumour cells which are transfected to overexpress Galectin-9 is one way in which TIM3 engagement could be ensured, and the effects of engaged and unengaged TIM3 on cytokine expression could be compared.

It was concluded that expression of TIM3 was associated with elevated IL-10 production within CD8+ T cells and this activity may or may not require TIM3-ligand interactions. An association was also observed between TIM3 expression and IL-10 production in *ex vivo* studies, wherein TIM3+ TILs produced more IFNγ and IL-10 than TIM3- TILs. During an acute immune response, CD8+ T cells progress from producing IL-2, to IL-2 and IFNγ, to IFNγ and IL-10, to IL-10 alone (122). Thus, production of IFNγ and IL-10 amongst TIM3+ cells is a cytokine profile which is characteristic of late activation to exhaustion (92, 108).

Finally, to conclusively support the hypothesis that TIM3 signalling is associated with elevated IL-10 production amongst TILs, tumour bearing mice were treated with anti-TIM3mAb. Renca tumour cells and leukocytes within the TME were shown to express the TIM3 ligands Ceacam-1 and Galectin-9, therefore TIM3 could be engaged within RencaHA tumours (Supplementary figure S3). A lower percentage of TILs from mice treated with anti-TIM3mAb produced IL-10, when compared with isotype controls. Although blockade of TIM3 and reduced IL-10 production was not associated with a significant reduction in tumour growth in this experiment, mice were only sampled until day 26. Future analyses should address the effects of anti-TIM3mAb over at least 30 days to quantify differences in growth between treated and control tumours.

3.3.2 Endogenous TILs express combinations of CIRs which are characteristic of Tumour-Suppressed CD8+ T cells

Genotype clustering of TILs has shown that effector TILs express PD-1 only, whereas TILs with a tumour-suppressed genotype express PD-1 in combination with TIM3, TIGIT, LAG3 and IL-10 (115, 116, 121, 122). Cytokine production suggested that TILs in the RencaHA model are tumour-suppressed, so combinations of CIR expression were compared with confirm this hypothesis. Clone 4 and endogenous CD8+ TILs were more likely to express CIRs in combination, whereas *in vitro* primed cells tended to express single CIRs. The percentages of suppressed cells expressing PD-1 and TIM3 together is similar between Clone 4 TILs and endogenous TILs. However, the fact that a greater proportion of endogenous CD8+ TILs expressed none of the CIRs tested (and in earlier experiments produced none of the cytokines assayed) when compared with Clone 4 TILs suggests that more endogenous TILs are either naïve or tolerant. Therefore, the total proportion of effector cells is greater amongst ATT Thy1.1+ Clone 4 TILs.

Flow cytometric analyses also showed that most of the TIM3-negative Clone 4 TILs co-expressed Ceacam-1 and PD-1. Inhibitory signalling through TIM3 may rely on co-expression with Ceacam-1 (138). The fact that a high proportion of Clone 4 TILs produce effector cytokines after stimulation, and that most Clone 4 TILs are Ceacam-1+PD-1+ would suggest that PD-1 and Ceacam-1 can be co-expressed without causing suppression, as long as TIM3 is not present. However, further work is required to investigate the role of Ceacam-1 in the absence of TIM3 (54, 138). For example, Ceacam-1^{GFP} could be overexpressed amongst Clone 4 CTL, and their cytokine profile assessed using flow cytometric analyses to determine whether Ceacam-1+ cells are able to produce effector cytokines such as IL-2 and IFNγ.

Few endogenous CD8+ TILs expressed Ceacam-1. We considered that Ceacam-1 expression could therefore be related to TCR affinity, since Clone 4 TILs respond to tumour expressed HA with uniformly high affinity, whereas endogenous TILs have a mixed affinity TCR repertoire. However, priming of Clone 4 cells *in vitro* using K^dHA peptide did not upregulate Ceacam-1. Therefore, high-affinity TCR interaction alone is not sufficient to mediate upregulation of Ceacam-1 and exposure to the tumour microenvironment is also required.

3.3.3 Endogenous CD8+ TILs suppress naïve Clone 4 T cells *ex vivo,* but not through IL-10R signalling

Significant suppression of naïve Clone 4 T cell proliferation occurred when CD8+ TILs were added to cell culture. Although the addition of IL-10R blockade improved proliferation of Clone 4 T cells in the presence of CD8+ TILs, this improvement was not significant. Interestingly, the presence of anti-IL-10RmAb alone in cultures of naïve Clone 4 T cells was able to suppress proliferation when TILs were not present. Such contradicting results have also been reported by several groups, suggesting that IL-10R signalling acts in a context dependent manner. Although IL-10 is classically considered to be immunosuppressive, it may support naïve T cell growth and expansion in the absence of other suppressive pathways (143, 250). Therefore, anti-IL-10R mAb alone suppressed naïve Clone 4 T cell proliferation, whereas anti-IL-10R mAb in the presence of endogenous CD8+ TILs helped to restore it.

Since IL-10 blockade only produced a very modest improvement in T cell proliferation, we considered other CD8+ TIL-derived factors which could suppress Clone 4 T cells. Previous work has shown that CD4+ TILs from the RencaHA model express CD39 and CD73, and we demonstrated that endogenous CD8+ TILs also express these adenosine producing enzymes. Therefore, we attempted to alleviate CD8+ TIL-mediated suppression using A2a adenosine receptor blockade. However, A2aR antagonism did not restore naïve Clone 4 T cell proliferation in the presence of endogenous CD8+ TILs. Nonetheless, the presence of A2aR blockade and anti-IL-10R mAb together synergistically restored naïve Clone 4 T cell proliferation in the presence of TILs. Use of both A2aR blockade and anti-IL-10mAb together was only performed once since a conservative approach to the use of animals was taken, and other experiments were prioritised.

Further work is now needed to determine the mechanism by which CD8+ TILs suppress naïve Clone 4 T cell populations. Use of ^{3}H-Thymidine incorporation to assess proliferation would enable more sensitive and fully quantitative detection of suppression, whereas Celltrace violet incorporation can only measure a limited number of divisions. Recent data suggests that IL-10 producing CD8+ T regulatory cells suppress in a TGFβ dependent and contact-dependent manner, therefore blocking TGFβ could also restore naïve Clone 4 CTL proliferation in the presence of CD8+ TILs (257).

Chapter 4 Does *in vivo* blockade of A2a Adenosine Receptors reduce the growth of RencaHA tumours?

4.1 Introduction

There are many factors within the RencaHA TME which could suppress adoptively transferred Clone 4 TILs, reducing their effector potential (218, 219, 258, 259). RencaHA tumour-infiltrating CD4+ Tregs do not produce Treg-associated factors such as TGF-β and IL-10 therefore adenosine appears to important for Treg-mediated suppression in RencaHA tumours (154, 227). Between 89% and 98% of RencaHA tumour-infiltrating CD4+FOXP3+ Tregs express the adenosine producing enzymes CD39 and CD73, and these CD4+ Tregs suppress naïve Clone 4 T cell proliferation *ex vivo* in an A2a adenosine receptor dependent manner (154, 260). Analysis of endogenous CD8+ TILs from RencaHA tumour-bearing mice shows that although 52% produce IL-10, their ability to suppress naïve Clone 4 T cells *ex vivo* was only partially IL-10R dependent, and partially depended on A2aRs.

To investigate the role of adenosine in suppressing adoptively transferred Clone 4 TIL effector function, and their ability to control RencaHA tumour growth *in vivo*, mice were treated systemically with A2aR-Antagonist and the following parameters assessed: (i) tumour growth, (ii) overall response rate, (iii) survival and (iv) co-inhibitory receptor expression amongst populations of TILs.

4.2 Results

4.2.1 Does Blockade of A2a Adenosine Receptors improve the ability of CD8+ TILs to control RencaHA Tumour Growth *in vivo*?

4.2.1.1 Treatment with A2aR-Antagonist is associated with reduced RencaHA tumour growth

To test the hypothesis that Adenosine Receptor signalling is a crucially important pathway which suppresses anti-tumour immunity within the RencaHA model; tumour bearing mice were treated *in vivo* with A2a Adenosine Receptor antagonist (ATT of Clone 4 T cells was not administered in this experiment; Figure 26A). A2aR-blockade produced a significant reduction in tumour growth over 30 days. Importantly, survival was significantly extended amongst A2aR-Antagonist treated mice when compared with vehicle treated controls. However, although blocking A2aRs in our model halted tumour growth at around 10mm diameter, complete

tumour regression was not observed (Figure 26B). This finding suggested that mechanisms of immune escape could be operating to limit the efficacy of A2aR blockade in the RencaHA model.

4.2.1.2 Expression of Single Co-Inhibitory Receptors amongst TILs is not significantly altered by A2aR blockade

Several studies have shown that when one immunomodulatory pathway is blocked by immunotherapy, other immunosuppressive pathways are initiated within tumours. For example, NK cells are known to upregulate Co-inhibitory receptors (CIRs) when IL-12 is administered as immunotherapy (201, 261). Therefore, we hypothesised that endogenous CD8+ TILs could upregulate CIRs when RencaHA tumour-bearing mice are treated with A2aR antagonist (191, 238). CIR signalling could thus inhibit CD8+ TILs, reducing the efficacy of A2aR blockade. To test this hypothesis, CD4+ and CD8+ TILs from A2aR-Antagonist treated and untreated tumour-bearing mice (Figure 26) were analysed using flow cytometry to assess their levels of expression of the CIRs TIM3, TIGIT, LAG3 and PD-1. Expression of the adenosine producing enzymes CD39 and CD73 was also quantified, because another mechanism of immune escape could be that adenosine production is augmented in response to adenosine receptor blockade (Figure 27).

Flow cytometric analyses revealed that CD39 expression was reduced amongst CD8+ TILs from mice given A2aR-Antagonist, suggesting that A2a adenosine receptor blockade does not drive further adenosine production by CD8+ TILs (Figure 27 A & C). There was a significant reduction in the MFI of TIGIT amongst CD4+ TILs from mice given A2aR-Antagonist when compared with controls. A2aR blockade was also associated with a significant reduction in the percentage of CD39 expressing CD4+ TILs (Figure 27 B & C). As both CD39 and TIGIT are known to be markers of CD4+Tregs, these findings suggested that the numbers of CD4+ Tregs within RencaHA tumours could be reduced by A2aR-blockade (81, 262, 263). There were no other significant differences in the percentage expression or MFI of CIRs between tumour-bearing mice given A2aR-Antagonist, and controls when expression of each CIR was analysed individually.

The growth rate of tumours was included as a covariate in this analysis because previous experiments indicated that tumour volume and the time of sampling (both encapsulated in the growth rate variable) could influence CIR expression and confound the comparison between treated and control tumours (77).

Figure 26- Treatment with A2a Adenosine Receptor Antagonist reduces Tumour Growth Rates and improves Survival amongst RencaHA tumour-bearing mice

BALB/c mice were injected s.c. with 1 x 10^6 RencaHA tumour cells at day 0. When tumours reached 5 mm diameter in one direction (day 12-14), mice were randomly grouped, and the specific A2aR-Antagonist ZM241385 was administered by i.p injection to one group. Control mice received vehicle only. From day 12 after tumour injection, tumour growth was monitored and further treatment was administered every other day. Mice were culled when tumours reached maximum allowable tumour size (MATS), or at 30 days. (A) Tumour growth was compared using linear mixed model to perform repeated measures ANOVA (p = 0.010**). N =26 treated mice and 20 control mice over 4 experiments. (B) Log Rank (Mantel-Cox) test was used for statistical comparison of survival (p<0.0001****).

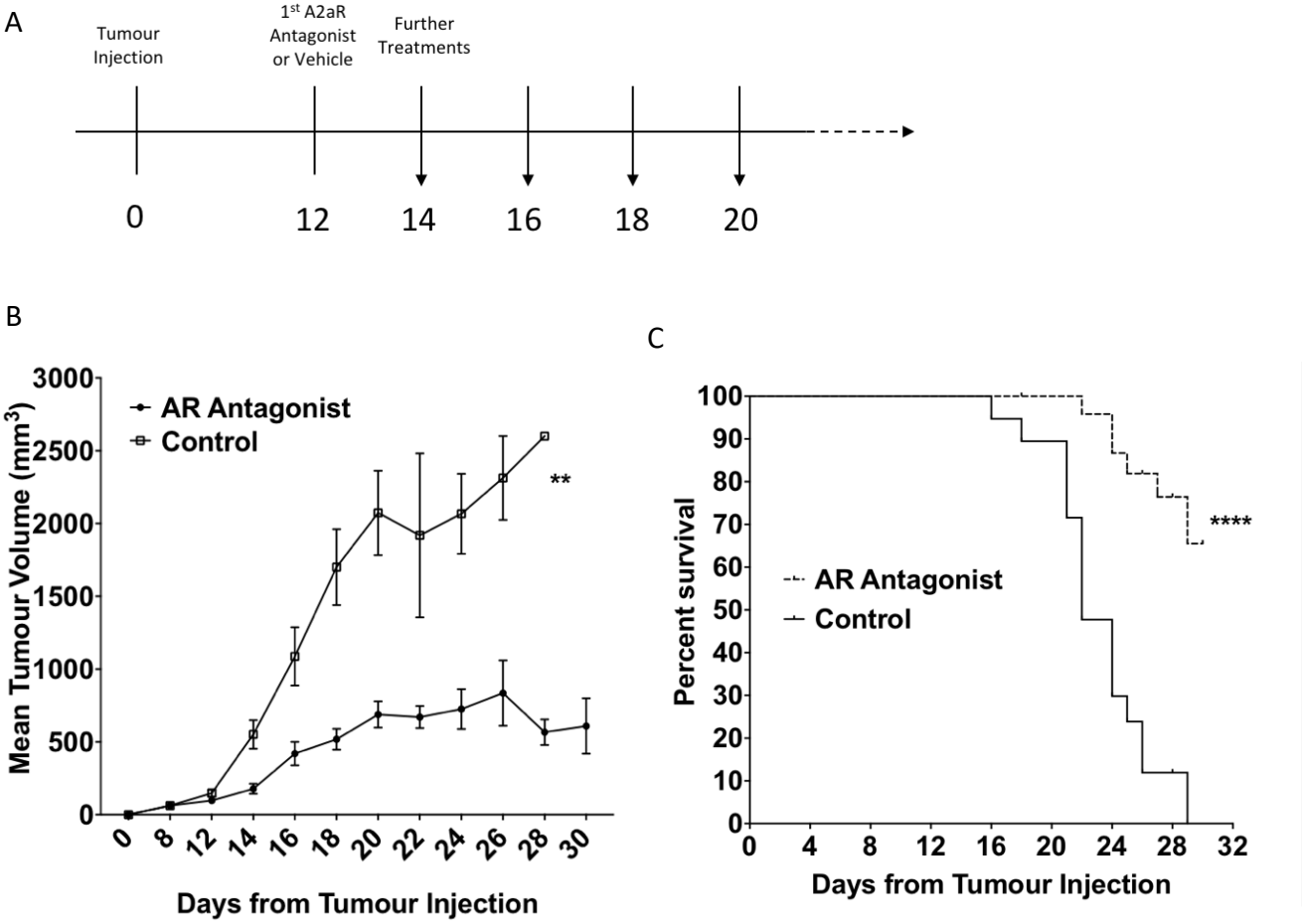

Figure 27 – Flow Cytometric Analysis comparing single Co-Inhibitory Receptor expression between TILs from A2aR-Antagonist-Treated and Control Tumours

RencaHA tumour bearing mice were treated with either A2aR-Antagonist, vehicle or no treatment. CD45+ cells were harvested from tumours and stained using antibodies for CD8, CD4, CD39, CD73, TIM3, TIGIT, LAG3 and PD-1. Samples were analysed using flow cytometry. N=14 treated and 29 control tumours stained over 16 experiments. Samples were compared using multivariate ANOVA, and percentage values were Arcsine-sqrt transformed before analysis. P values for significant comparisons are shown, all other P values were not significant. (A) % expression of CIRs amongst CD8+ TILs, (B) % expression CIRs amongst CD4+ TILs, (C) MFI of CIRs amongst CD8+ TILs and CD4+ TILs. Scales are adjusted for each marker because the MFI with respect to the FMO control varies considerably. (C) Representative flow cytometry data are shown from (i) A2aR-Antagonist treated and (ii) vehicle treated mice.

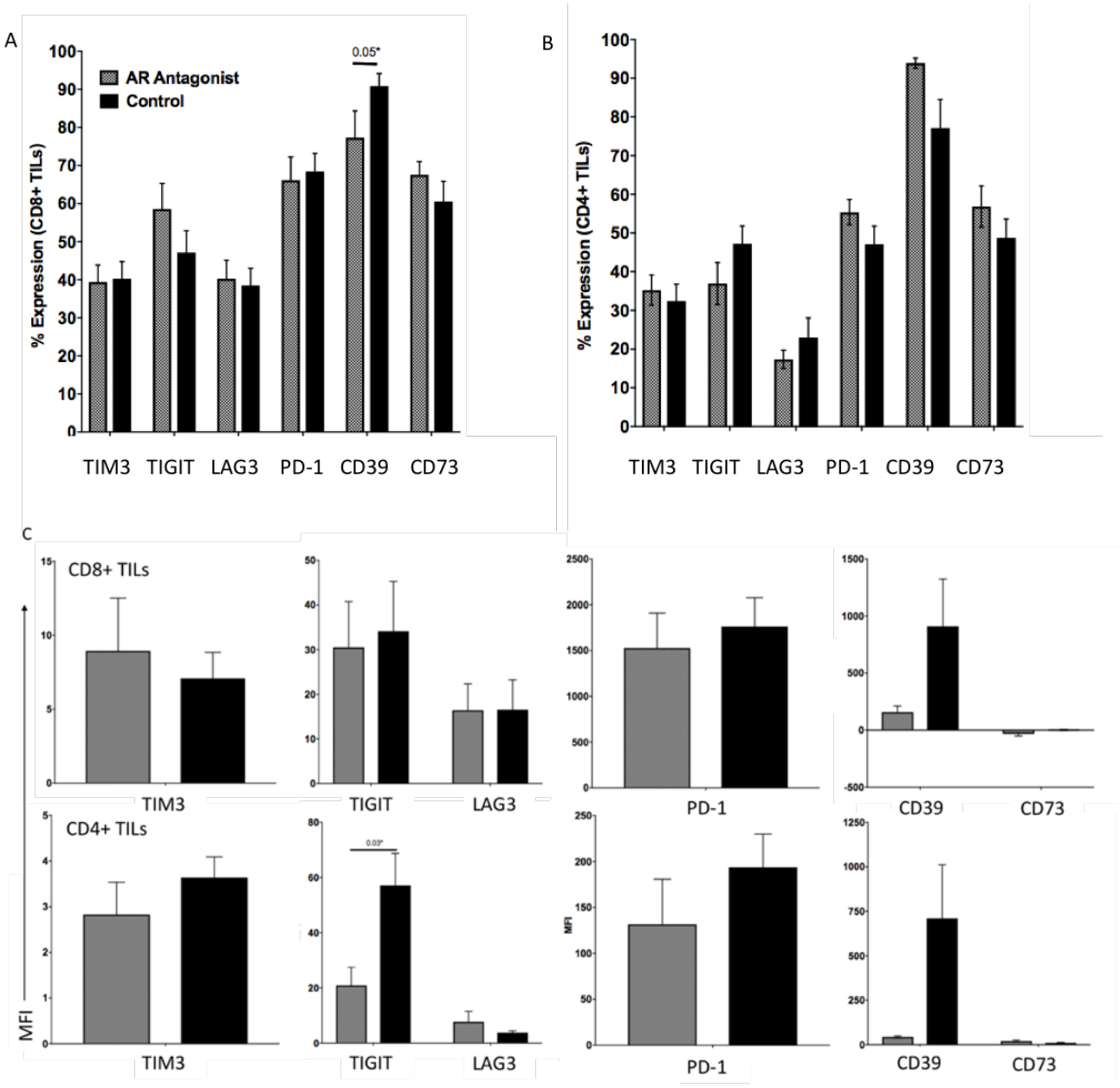

C (i)

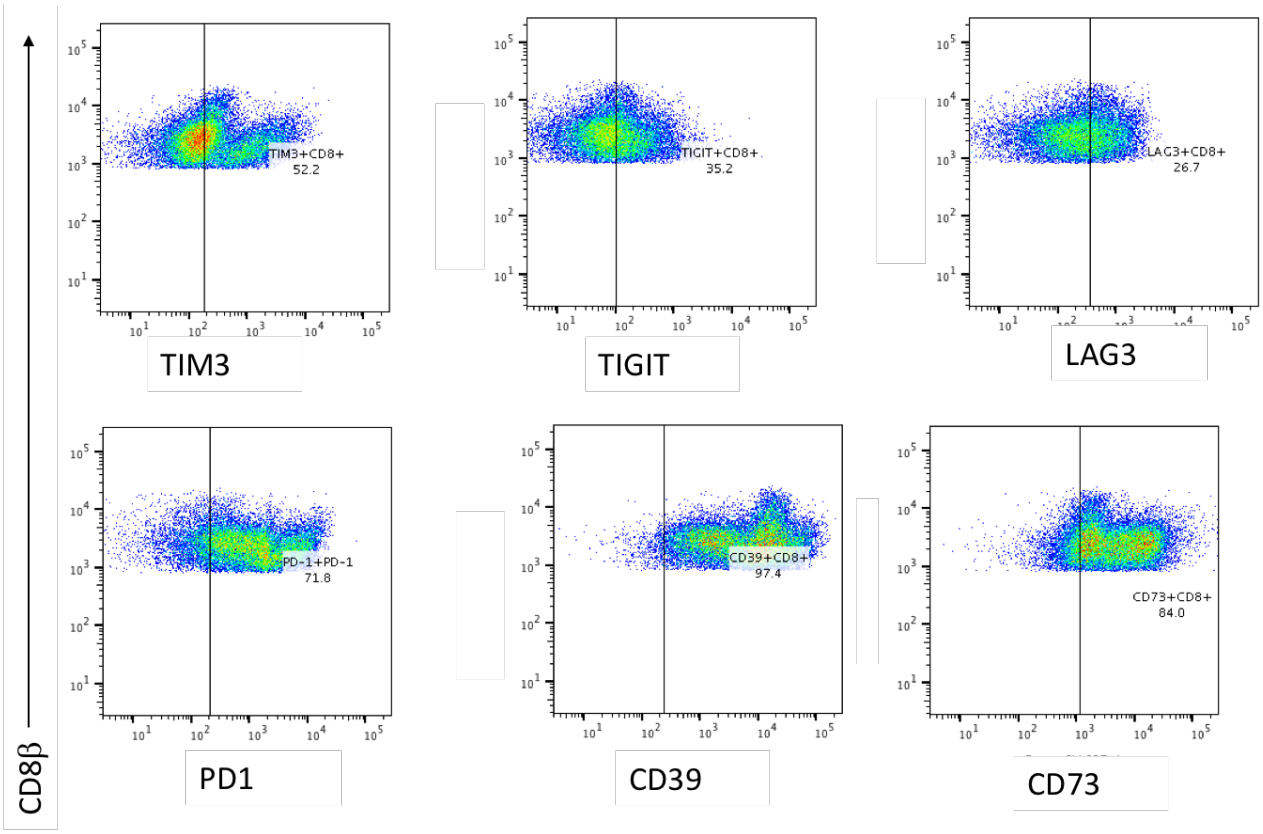
CD8β
TIM3+CD8+
52.2
TIM3
TIGIT+CD8+
35.2
TIGIT
LAG3+CD8+
26.7
LAG3
PD-1+PD-1
71.8
PD1
CD39+CD8+
97.4
CD39
CD73+CD8+
84.0
CD73

(ii)

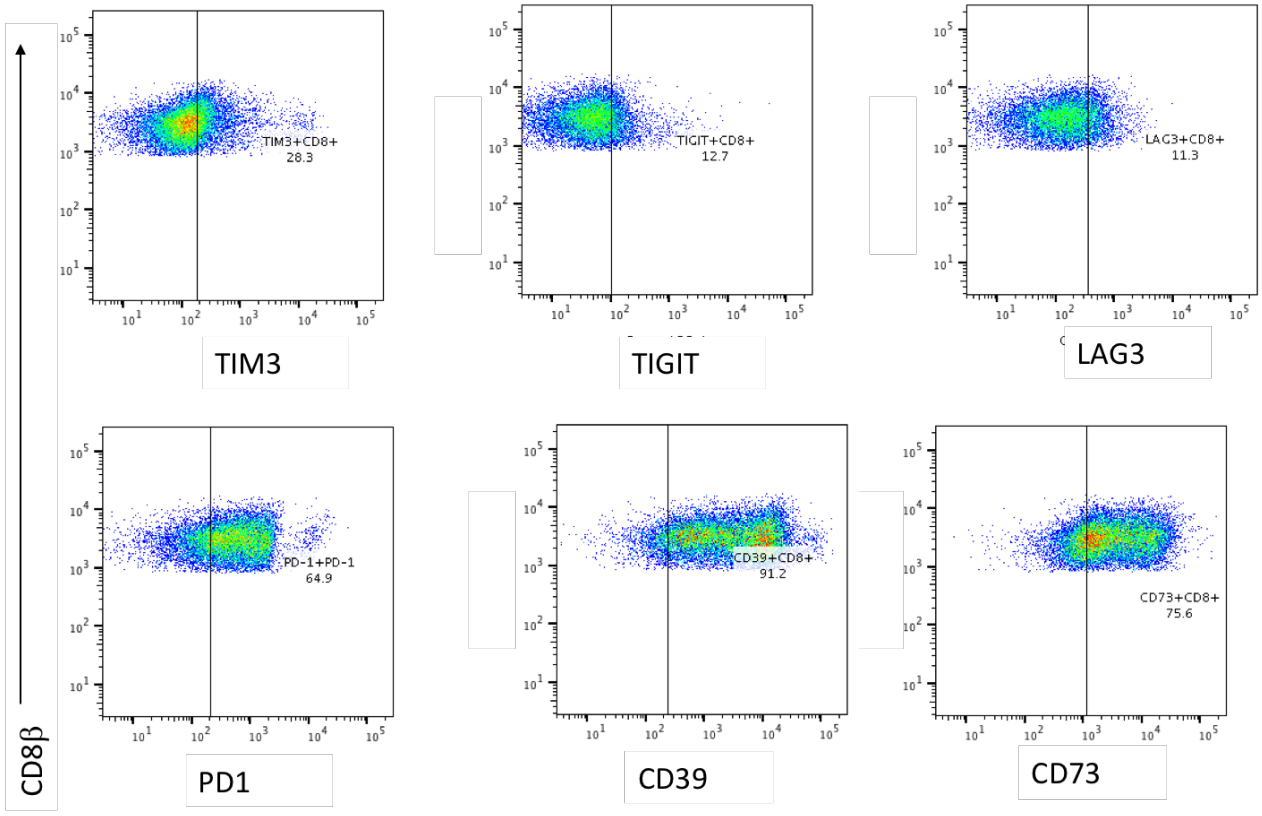
CD8β
TIM3+CD8+
28.3
TIM3
TIGIT+CD8+
12.7
TIGIT
LAG3+CD8+
11.3
LAG3
PD-1+PD-1
64.9
PD1
CD39+CD8+
91.2
CD39
CD73+CD8+
75.6
CD73

4.2.1.3 Treatment with A2aR -antagonist is associated with elevated expression of TIM3 amongst CD8+ TILs

Percentage expression and MFI of CIRs amongst endogenous CD4 and CD8+ TILs did not vary significantly between A2aR-Antagonist-treated and control tumours when each marker was analysed individually. However, recent studies suggest that expression of several CIRs concurrently is required to indicate that CD8+ TILs have a tumour-suppressed genotype (121, 122, 135). Therefore, Principal Component Analysis (PCA) was used to determine if the combinations of CIRs expressed by TILs was altered after A2aR blockade. PCA is a method for assessing the variation within a population of individuals (points) generated by variables (arrows) such as combinations of CIR expression. The expression of TIM3, TIGIT, LAG3, PD-1, CD39 and CD73 was calculated from flow cytometric data and a total of 152 combinations of these CIRs were analysed across 43 individual tumours. Tumour volume was also included in the analysis, making 153 variables in total. Data are transformed such that individuals (i.e. tumour-bearing mice) are spread or clustered along linear axes known as Principal Components (PC). Numbered arrows indicate the variables which are different between individuals, causing this spread or clustering. Different permutations are generated along PCs, until 100% of the variation within the data set has been accounted for. In this analysis, a cut off of 20 variables was determined because only 20 variables made greater than average contributions to the PCA. The first PC (PC1) generated by the analysis accounts for the greatest proportion of variation within the data, in this instance 24.7%. Subsequent PCs account for progressively less variation. In this analysis, the first 4 PC were analysed because other PC had low eigenvalues, meaning that they did not display important differences between individuals. Individuals can be visualised by treatment condition, but the analysis is unable to take into account what group they fall into, therefore PCA is non-hypothesis driven.

When arrows were assessed to determine which variables caused groups of tumours to cluster, it was first noted that the volume arrow associated positively with PC2. When control tumours[2] (red dots) were stratified by their volume (Supplementary Figure S4A), PC2 was shown to split them into two groups with large red tumours clustered at the positive end of the PC2 axis, and

[2] Both vehicle treated tumours and completely untreated tumours were used as controls in PCA, because it was shown that they did not cluster significantly differently.

small red tumours at the negative end (Figure 28A). Therefore, PC2 produced spread between tumours of different volumes.

A limited number of other variables besides volume were also associated with the groups of large and small control tumours (red dots) found on PC2. Variables directed at the negative end, where small tumours clustered, were combinations of CIR expression. Conversely, variables directed at the positive end, where large tumours were located, comprised expression of CD39 and CD73 (adenosine producing enzymes). Therefore, small control tumours appeared to depend on TIM3, PD-1 and TIGIT for immunosuppression, whereas large tumours depended more on adenosine producing enzymes (Figure 28A).

The straightforward clustering of small and large tumours at opposite ends of PC2 was not observed amongst A2aR-Antagonist treated individuals (turquoise triangles). A2aR-Antagonist treated tumours correlated positively with PC1 as well as PC2, therefore they fall to the right of the plot. This is shown by the large symbols (red dot and turquoise triangle) which indicate the position of an average treated and control tumour relative to PC1 (Figure 28A).

PC1 therefore illustrated separation between treatment groups rather than volumes. Treated tumours (turquoise triangles) are found to the right of PC1 whereas all but two control tumours (red dots) are found to the left. The variable arrows which point to the right of PC1, where treated tumours cluster, include many combinations of CIRs which comprise TIM3 expression amongst CD8+ TILs ($p<0.001$) (Supplementary Figure S4B). This finding suggests that increased expression of TIM3 by CD8+ TILs is a key variable which differentiates A2aR-Antagonist-treated from control individuals. Negatively correlated with PC1, and therefore treatment, is a lack of any CIR expression amongst CD8+ T cells ($p< 0.001$)(Figure 28A). Overall, the variables that caused separation between A2aR-blocked tumours and control tumours represented combinations of CIRs, in particular combinations that included TIM3.

Together, the clustering of tumours along PC2 suggested that the immunosuppressive mechanisms operating within small, untreated tumours depend upon CIRs, whereas larger untreated tumours express adenosine producing enzymes. When tumours are treated with A2aR-Antagonist, this switch to adenosine-mediated suppression appears to be prevented, and PC1 shows that tumours from A2aR treated-mice continue to be associated with CIR

expression, especially expression of TIM3, even as they grow larger. Therefore, the data suggest that A2aR-Antagonist treated tumours are more dependent on TIM3 expression for immunosuppression, because adenosine mediated immunosuppression has been blocked. In support of this conclusion, the percentage of CD8+TIM3+ TILs was plotted against size, and TIM3 expression amongst CD8+TILs from A2aR-Antagonist-treated tumours was shown to be elevated in tumours of smaller sizes when compared with control tumours (Figure 28B)[3]. Overall, PCA led us to hypothesise that blocking both A2aR signalling and TIM3 could be required to prevent tumours from escaping the anti-tumour immune response within A2aR-Antagonist treated individuals.

[3] Some volume data had to be imputed for this validation analysis, therefore it remains only a validation of PCA inferences, and PCA represents the most robust data.

Figure 28 - Principal Component Analysis comparing combination CIR expression between A2aR-Antagonist-treated and Control tumours

RencaHA tumour bearing mice were treated with A2aR-Antagonist (turquoise triangle) or vehicle/no treatment (red circle). CD45+ cells were extracted from tumours and stained using antibodies for CD8, CD4, CD39, CD73, TIM3, TIGIT, LAG3 and PD-1. % Expression of all possible combinations of the above markers was quantified using flow cytometry. (A) Each combination of the above eight markers represents one of 154 variables entered into Principal Component Analysis (PCA), along with tumour volume as the final variable. Each triangle or circle represents an individual tumour bearing mouse. Large symbols represent the average position of a treated and control individual along PC1. Direction of the clustering of A2aR blocked tumours on a biplot of PC1 and PC2 is shown by a green arrow. The top 20 of the 154 variables contributing to PC1 and PC2 are shown as arrows labelled numerically. A key detailing the combinations of markers represented by these numbers is shown in (Supplementary Figure S4). The variable representing CD8+ T cells expressing TIM3 in combination with any other marker is shown circled in red, and contributes positively to PC1 ($p<0.0001$****). (B) % expression of TIM3 amongst tumours of different volumes.

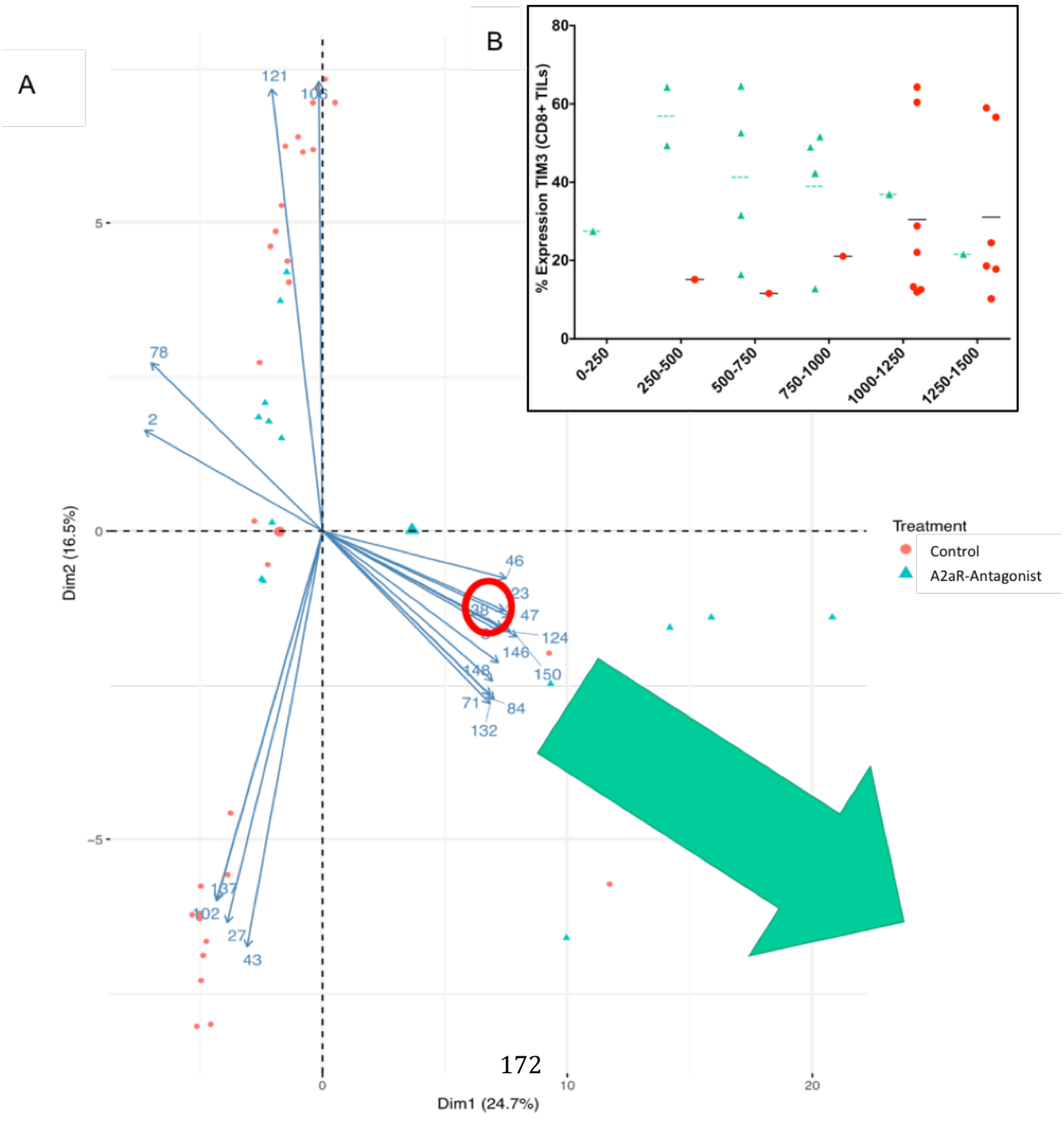

4.2.2 Does treatment with adjunct anti-TIM3mAb improve the control of RencaHA Tumour Growth that is mediated by A2aR blockade?

The PCA suggests that upregulation of CIR combinations which include TIM3 occurs amongst CD8+ TILs from mice treated with A2aR-Antagonist. Thus, to test whether blocking both TIM3 and A2aR signalling could improve immune-mediated control of RencaHA tumour growth, mice bearing RencaHA tumours were treated with combinations of A2aR-Antagonist and anti-TIM3mAb. Adoptive transfer of Clone 4 T cells (ATT) was also given in this experiment since the ultimate aim of these analyses was to determine whether blocking factors within the TME could prevent the suppression of ATT Clone 4 TILs by the tumour, making ATT a more useful option for immunotherapy. The combinations of therapy administered are indicated in Table 3 and the treatment regimen is illustrated in Figure 29. Despite variation in the size of tumour growth between experiments, tumours treated with ATT and combinations of A2aR-Antagonist and anti-TIM3mAb followed a similar growth pattern in each of four separate experiments (Supplementary Figure S5). Tumour growth was divided into 3 phases for analysis: Phase 1 was defined as initial tumour growth from day 12 to days 16-18; in Phase 2, a proportion of tumours regressed from day 16-24, followed by relapse of a percentage of these regressed tumours at day 24; in Phase 3, tumours either remained in remission, or relapsed continued to grow to attain maximum allowable tumour size (MATS) between day 24 and 50 (Figure 29). Each of the three phases of tumour growth was compared between treatment groups.

Table 3 - Combinations of Immunotherapy Administered

Treatment Group	ATT CL4 Cells	A2aR-Antagonist	Anti-TIM3mAb
A	x		
B	x	x	
C	x	x	x
D	x		x

Figure 29 - Treatment of RencaHA tumour-bearing mice with ATT, A2aR-Antagonist and Anti-TIM3mAb results in three Phases of Tumour Growth

Groups of RencaHA tumour-bearing BALB/c mice were given ATT of Clone 4 T cells on two occasions and treated (Tx) with A2aR-Antagonist, anti-TIM3mAb, or vehicle + isotype as control, as shown. A triphasic growth curve was produced. In Phase 1, tumours grew. In Phase 2 and 3 tumours regressed and then either remained regressed until the end of the experiment (Responders) or relapsed (Non-responders). Some Responders were rechallenged with tumour cells. Tumour growth is displayed as mean tumour volumes + SEM, N = 48 mice over 4 experiments with at least 6 mice per group[4].

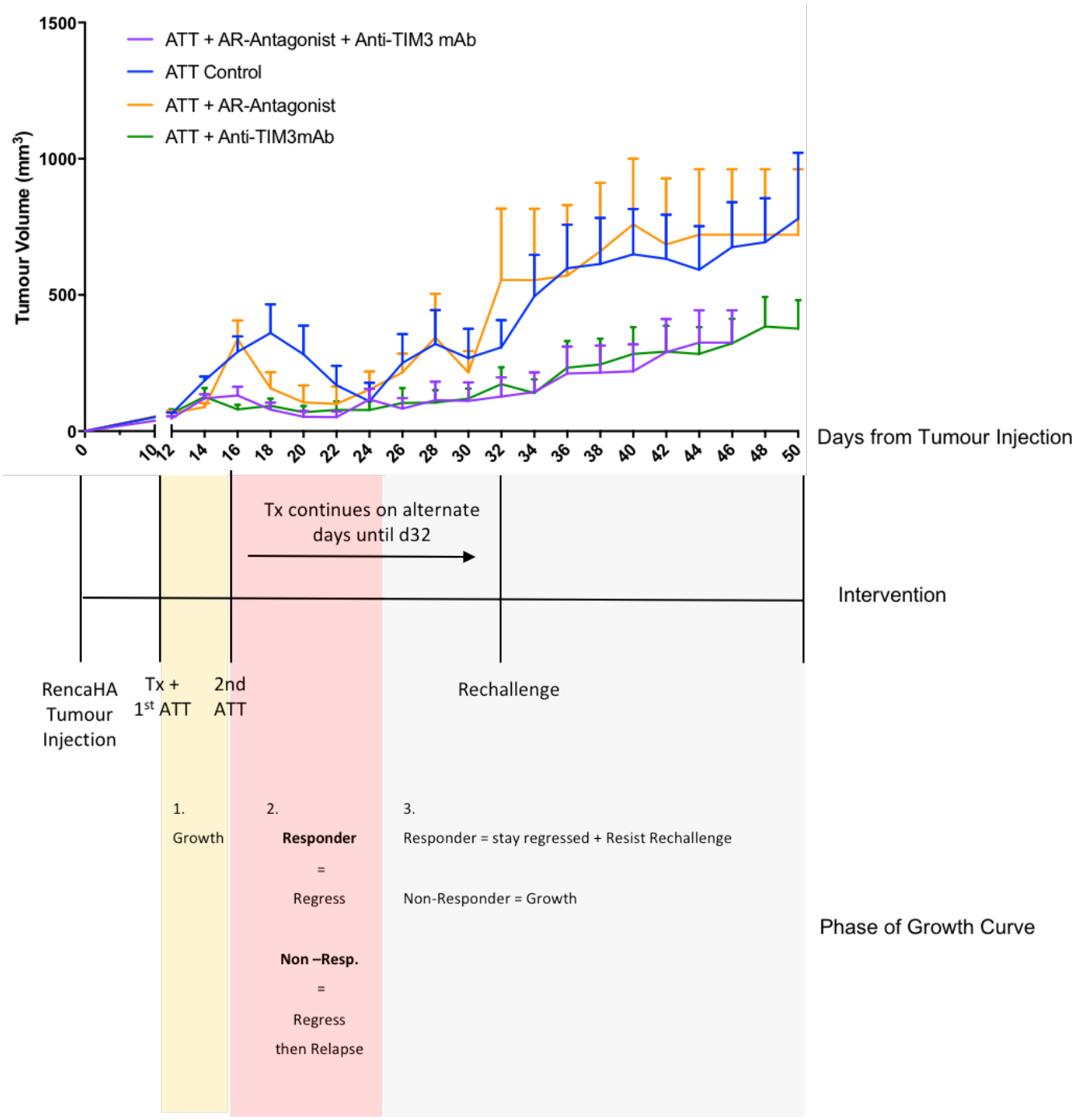

[4] Group D treatment was only included in 2 out of four experimental replicates.

Figure 30 - Comparison of Tumour Growth and Survival between mice treated with combinations of A2aR-Antagonist and Anti-TIM3mAb

Groups of RencaHA tumour-bearing BALB/c mice were given ATT of Clone 4 T cells on two occasions and treated with A2aR-Antagonist, anti-TIM3mAb, or vehicle + isotype as control, as shown. (i) R values to show growth rate between 0-16 days were compared using independent two sample t-test. (ii) Proportion of tumours which responded and proportion of responders which relapsed were compared using Fisher's exact Boschloo test. (iii) Progression free survival (PFS) analysed using Cox Proportional Hazards Regression analysis. Predictive treatments were C (p=0.033*) or D (p=0.005**). Treatments A and B did not significantly predict PFS (p=0.067, p=0.089). (iv) Ratio of Final volume/First volume was compared using independent two sample t-test. N = 48 mice over 4 experiments with at least 6 mice per group.

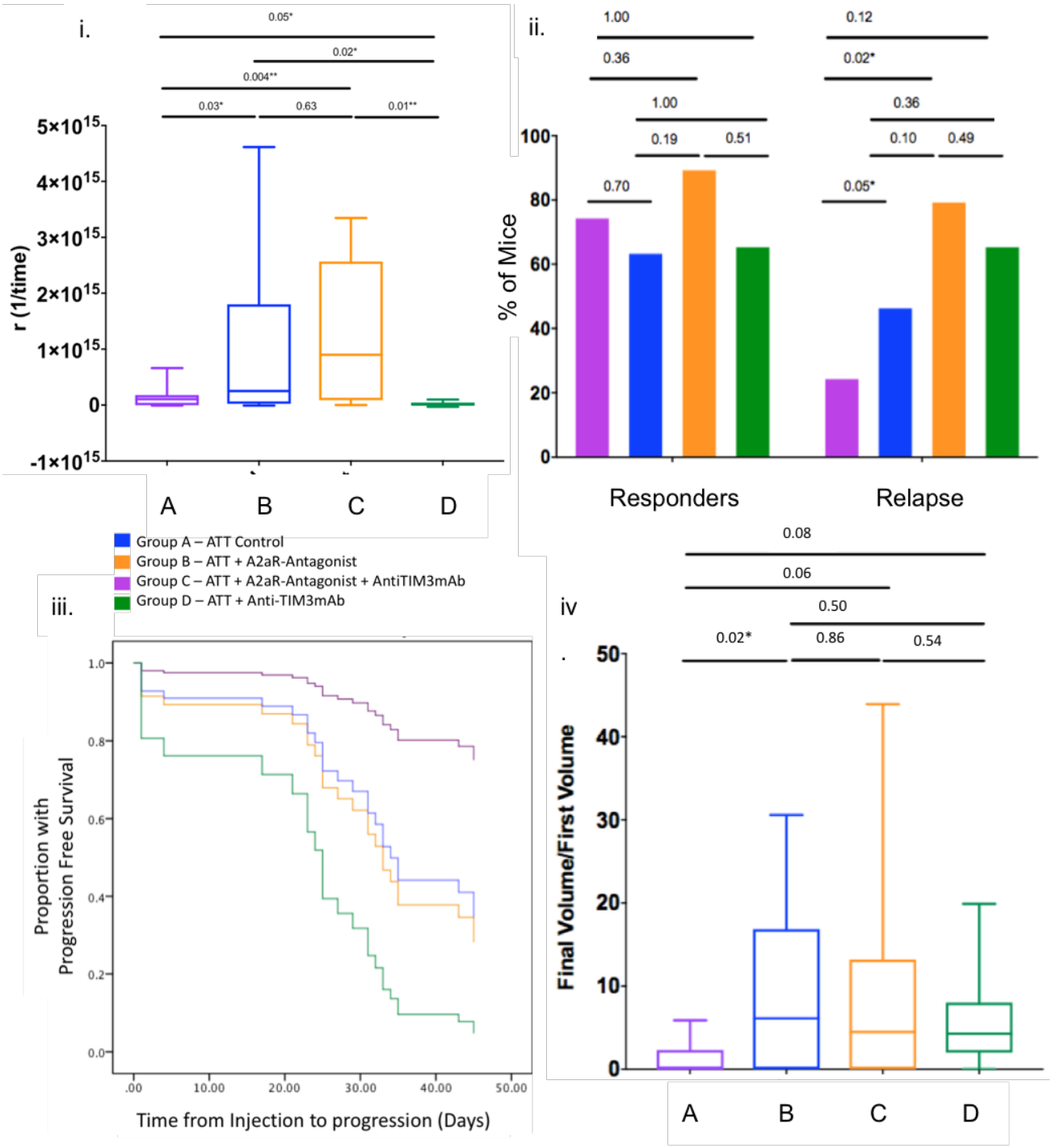

4.2.2.1 Phase 1- Initial Tumour Growth

In Phase 1 of tumour growth, tumours in all treatment groups A-D grew from day 12. Tumour volume peaked at day 14-18, after which tumours then regressed (Figure 29). The magnitude of tumour growth up to the start of regression (d12-16) was quantified by calculating R-values (Methods Section 2.12.3)(Figure 30i). R-values illustrated that tumours from Group D mice (ATT + anti-TIM3mAb) grew the slowest of all groups during this time[5]. Tumours from Group C mice (ATT + AR-Antagonist + anti-TIM3mAb) grew significantly slower than those from control Group A mice (ATT alone) or Group B mice (ATT + AR-antagonist). Thus, the data show that tumours grew significantly slower if anti-TIM3mAb was included in the therapeutic regimen.

4.2.2.2 Phase 2- Regression and Relapse

The main goal of any anti-cancer therapy is to achieve tumour regression and increase the longevity of remission amongst patients (119). Therefore, experiments were carried out in order to determine whether or not blockade of A2aRs and TIM3 was effective in achieving these outcomes. Firstly, the proportion of mice experiencing regression was quantified. In Phase 2 of tumour growth (days 20-26), regression was defined as reduction in tumour volume to below the volume at the start of treatment (Figure 29). Mice in which tumours regressed were termed 'Responders' and the proportion of Responder mice was compared between groups. In Group A 11/17 mice responded to treatment. The response rate was greater in Group B mice (9/10 responders) but not in Group D mice (4/6 responders) when compared with Group A controls. Amongst Group C mice, 9/12 tumours completely regressed. Therefore, Groups B and C, in which mice received combinations of treatment involving A2aR blockade, exhibited the highest percentages of responders out of all treatment groups. However, differences in the proportions of responders were not significant (Figure 30ii).

Following tumour regression, some mice experienced Relapse, which was defined as regrowth of the tumour to attain a volume exceeding the volume at the start of treatment. Relapse was

[5] A stepped approach to experimental design resulted in Group D being added only in the final two experimental repeats. However, final calculations included all four experimental repeats because statistical results did not alter if only the final two experiments were included.

found to occur at any timepoint from day 24 (Figure 29). To determine whether or not treatment with A2aR-Antagonist + anti-TIM3mAb would prevent relapse, the proportion of mice in which relapse occurred was compared between treatment groups. Group C mice (ATT + AR-Antagonist+ anti-TIM3mAb) had significantly lower relapse rates (3/12 individuals) than Group A or B mice (8/17 and 8/10 mice respectively). The percentage of mice with tumour relapse was also reduced in Group C when compared with Group D (3/12 vs. 4/6 individuals), although not significantly. Therefore, treatment with ATT, anti-TIM3mAb and A2aR-Antagonist appears to give rise to a reduction in the percentage of mice with relapsing tumour growth when compared with other groups (Figure 30ii).

Another key aim of cancer therapy is to try to extend the time before relapse occurs. Thus, Progression Free Survival (PFS) was used to quantify the time before relapse (i.e. remission) amongst tumour-bearing mice. This period of PFS was defined as the time between the initial injection of tumour cells, and the tumour reaching a volume which exceeded the starting volume. Cox Proportional Hazards Regression analysis was used to compare PFS between mice (Figure 30iii). PFS was included as the dependent variable, and the analysis was set up to determine whether the treatments carried out within Groups A-D significantly affected PFS. Experimental replicate, time from injection to first treatment, and tumour volume at first treatment (13.5 – 62.5 mm^3) were all included in the initial analysis as covariates, because these factors could confound the analysis of whether the Treatment Group variable affected PFS.

Interestingly, the analyses revealed that none of the other covariates affected PFS, and the only variable that significantly predicted PFS was the Treatment Group. Treatment of tumour bearing mice with A2aR-Antagonist and anti-TIM3mAb (Group C, p=0.033*) or anti-TIM3mAb alone (Group D, p = 0.005**) significantly influenced PFS. Whereas, administering ATT alone (Group A, p=0.067) or with A2aR-Antagonist (Group B p=0.089) did not significantly predict PFS.

Whilst the above P values indicate that the different treatment regimens significantly affect PFS, P values do not indicate the direction of this effect i.e. whether progression (relapse) will occur more quickly or more slowly in the presence of the different treatments. Therefore, a survival curve was produced to indicate the duration of PFS (Figure 30iii). To statistically quantify

whether one treatment group was more likely to relapse sooner than the others, the Hazard Ratio (HR) of tumour relapse was determined by comparing each intervention to the HR of Group C double treated mice. A positive HR indicated that tumour progression was more likely at any time during follow-up when compared with the double treated Group C (Table 4).

Table 4 - Hazard Ratios of Progression after Immunotherapy

Group	Treatment	Hazard Ratio vs Group C	Confidence Interval
A	ATT	3.702	0.819, 16.743
B	ATT + A2aR-Antagonist	4.404	0.899, 21.573
C	ATT + A2aR-Antagonist + Anti-TIM3mAb	na	na
D	ATT + Anti-TIM3mAb	10.608	2.072, 54.324

In Group D mice, receipt of anti-TIM3-mAb + ATT significantly increased the hazard of progression when compared with Group C mice, the significance of this HR is indicated because the confidence interval of the HR does not contain unity (they do not lie either side of the value 1.0). In Group A, receipt of ATT, or in Group B receipt of ATT + A2aR-Antagonist alone, made progression more likely when compared with Group C mice. However, the overall influence of treatments A and B on PFS was not significant because the HR confidence intervals contain unity. Therefore, the chance of relapse was lowest, and PFS extended, amongst Group C mice which received ATT, A2aR-Antagonist and anti-TIM3mAb, whereas Group D mice (anti-TIM3mAb +ATT) were the most likely to relapse. These data therefore support the idea that when two axes of immunosuppression, such as A2aRs and TIM3, are targeted together, immune escape is less likely than when either axis is targeted alone.

4.2.2.3 Phase 3 -Tumour Re-growth and Final Volume

To compare the effects of treatment on long term tumour growth, the average final tumour volume in each group (at time of culling for each mouse) was calculated as a ratio of the final: initial tumour volume (246, 248). Amongst Group C mice, treatment with A2aR-Antagonist and anti-TIM3mAb produced a significantly reduced final: initial tumour volume ratio when compared with Group A control mice. There were no other significant differences in final tumour volume (Figure 30iv). This finding suggests that if tumours relapse in mice treated with both A2aR-Antagonist and anti-TIM3mAb, their growth after relapse is restrained when compared with control mice.

4.2.3 Does treatment with A2aR-Antagonist +/- anti-TIM3mAb produce Anti-tumour Immune Memory?

When tumours completely regress following immunotherapy, protection against relapse can be mediated by anti-tumour immune memory cells, which can destroy any minimal residual disease (MRD)(226-228, 264). To test whether or not Responder mice could mount anti-tumour immune memory responses, tumour-free mice were rechallenged with a further injection of 1 x 10^6 RencaHA tumour cells between day 32 and 34. Rechallenge did not give rise to any tumours over 20 days, suggesting that in Responder mice anti-tumour immune memory had been established (Data not shown).

4.3 Discussion

Several studies have determined that engagement of A2a adenosine receptors expressed on CD8+ TILs can inhibit the ability of CD8+ TILs to kill tumour cells *in vivo* (140, 182-184, 195, 224, 265). Therefore, it was postulated that therapeutic blockade of A2a adenosine receptors could improve the effector function of both Clone 4 and endogenous CD8+ TILs within RencaHA tumours, which could in turn allow them to control tumour growth.

To evaluate this hypothesis, A2a adenosine receptor antagonist was administered systemically to mice bearing RencaHA tumours. ATT Clone 4 T cells were not administered in this experiment, to enable the effects of A2aR blockade to be observed in the absence of other immunotherapies. A2aR antagonism resulted in partial control of tumour growth, however, tumours did not completely regress. Since blockade of one immunosuppressive pathway can select for the upregulation of others, PCA was used to determine if the expression of combinations of certain CIRs were upregulated after treatment with A2aR-Antagonist. (139, 191, 194, 261). Notably, the expression of combinations of CIRs involving TIM3 were increased amongst CD8+ TILs taken from A2aR-Antagonist treated, versus control tumours. Anti-TIM3mAb, was therefore used alongside ATT as adjunct immunotherapy.

Although PD-1 and TIGIT expression was also elevated amongst CD8+ TILs taken from A2aR-Antagonist treated when compared with vehicle/untreated control tumours, TIM3 blockade was chosen as therapy because, as with adenosine, the expression of TIM3 is highly tumour specific and occurs only at low levels in body sites outside of the tumour(188, 190, 266). Blocking TIM3 and A2aRs as an immunotherapeutic combination should therefore be advantageous because neither agent is likely to produce off-target effects if blocked (103, 120, 132, 134). Furthermore, blocking TIM3 with monoclonal antibodies has proved to be an effective adjunct to other cancer immunotherapies, including anti-PD-1 blockade, where it has been shown to rescue control of tumour growth amongst mice which relapse after initial therapy (103).

To determine if control of tumour growth was better when TIM3 and A2aRs were blocked simultaneously, various *in vivo* blockade experiments were performed. RencaHA tumour-bearing mice were given combinations of A2aR-Antagonist and anti-TIM3mAb. ATT Clone 4 cells were also given, as the ultimate aim of these analyses was to improve the function of both

ATT and endogenous CD8+ TILs within the TME. The pattern of tumour growth in treated mice was divided into three phases for analysis: Phase 1, initial growth; Phase 2, regression and relapse; and Phase 3, final volume.

Different parameters of therapeutic benefit were measured at different stages of tumour growth. Although anti-TIM3mAb treatment was most effective at slowing initial tumour growth, this treatment regimen produced the greatest risk of relapse. Importantly, the addition of A2aR-blockade was required to prevent Relapse. Other studies also suggest that anti-TIM3mAb is more effective as an adjunct therapy than a single agent (103). Blocking A2aRs together with TIM3 in the presence of ATT increased the percentage of Responder mice experiencing regression, reduced the Hazard Ratio of relapse, and also produced the lowest final: initial tumour volume ratio amongst relapsed tumours when compared with other groups. Therefore, taking all parameters into account, utilising A2aR-Antagonist and anti-TIM3mAb concurrently produced the best control of RencaHA tumours across the entire disease progression.

Despite the fact that 48 mice were analysed over four experiments, giving this experiment statistical power of >80%, there were some limitations to the findings. Chiefly, to include four treatment groups in each of the individual experiments would have required injecting larger cohorts of mice with tumour cells, violating the 3Rs criteria for this project. Instead, a stepped approach was employed, whereby the treatment of specific interest (i.e. the efficacy of A2aR-Antagonist and anti-TIM3mAb versus A2aR-antagonist alone) was included in all four experimental repeats, and anti-TIM3mAb alone (Group D) was included only in the final two repeats, when the results indicated that the effect of this treatment on the various parameters measured could also be of interest. To determine whether each experiment should be analysed separately, because Group D was only included in two out of four experiments, statistics comparing all of the outcomes tested were performed using individual experimental replicates and with all experimental data together. These two approaches did not produce significantly different results therefore the all mice were analysed as one cohort. One other limitation was that power calculations to determine mouse group size were based on detecting a measurable difference in tumour size, but not on comparing the proportion of tumours which completely regressed or relapsed. Greater numbers of mice per group could therefore be required to compare response and relapse with increased statistical significance. Nonetheless, the fact that

significant differences occurred in these parameters, despite the fact that the experiment was underpowered to detect them, suggests that the effect of the various treatment regimens on response and relapse was statistically very robust.

Several studies suggest that the ability to resist relapse and rechallenge in mouse tumour models is predictive of the ability of immunotherapy to prevent cancer recurrence amongst human patients (224, 226, 267). Prevention of relapse could be related to anti-tumour immune memory, because the duration of remission in some mice extended beyond 30 days, which is the time taken for sufficient immune memory cells to expand and become functional (12, 45, 93). Anti-tumour immune memory was shown to be established amongst Responder mice in which tumours were completely eradicated, because following further injections of tumour there was no tumour re-growth. Injection of the same batch of cells into immunologically naïve mice at the same time as other mice were rechallenged did result in measurable tumours, indicating that the tumour cells used for rechallenge were functional (data not shown). The effect of treatment with A2aR-Antagonist and anti-TIM3mAb on the development of anti-tumour immune memory, is determined using experiments in Chapter 7.

TIM3 and A2a Adenosine receptor signalling pathways represent attractive immunotherapeutic targets because they are specifically upregulated in the TME and are seen only at low levels in normal tissues (103, 116, 191, 268). Therefore blocking A2aRs and TIM3 is less likely to produce immune-related toxicity when compared with other therapies which block molecules, such as CTLA-4, that expressed body-wide and are crucial for normal immune tolerance (221). Additionally, CD73 expression is a useful biomarker which indicates potential responders to anti-adenosine therapy, meaning that selecting patients to receive A2aR blockade could be more straightforward when compared with other cancer immunotherapies, such as anti-CTLA-4 and anti-PD-1 mAbs, for which biomarkers of response are lacking (181, 183, 184, 238). Additionally, currently available A2aR-Antagonists are orally deliverable, making their use more convenient for clinicians and patients when compared with mAbs which must be delivered intravenously (227).

Chapter 5 Blockade of A2a Adenosine Receptors and TIM3 produces improved infiltration and function of CD8+ TILs within RencaHA Tumours

5.1 Introduction

The cytotoxic effector function of CD8+ TILs is important in controlling tumour-growth through direct lysis of tumour cells (68, 231). Experiments detailed in Chapter 4 showed that tumour growth is reduced amongst RencaHA tumour-bearing mice treated with ATT of tumour-specific Clone 4 T cells plus A2aR-Antagonist and anti-TIM3mAb. Therefore, we hypothesised that A2aR-Antagonist and anti-TIM3mAb acted to improve the function of adoptively transferred Clone 4 T cells within RencaHA tumours. Characterisation of Clone 4 TILs has revealed that they lose cytotoxic function after exposure to the RencaHA TME. To determine whether Clone 4 TIL function could be restored in the presence of A2aR and TIM3 blockade, the following experiments were performed:

1. Microscope-based cytotoxicity assays to quantify killing of tumour cell targets by Clone 4 TILs *ex vivo*.

2. Quantification of co-inhibitory receptor (CIR) expression amongst TILs using flow cytometry.

3. Live cell imaging to quantify actin clearance from the cSMAC to form a peripheral ring, during immune synapse formation (cell coupling) between Clone 4 TILs and Renca tumour cell targets.

4. Quantification of immune synapse stability within Clone 4 TILs/Renca tumour couples.

5.2 Results

5.2.1 Does blockade of A2a Adenosine Receptors and TIM3 improve the cytotoxic function of Clone 4 TILs?

5.2.1.1 In vivo blockade of A2aRs and TIM3 improves ex vivo killing of tumour-cell targets by Clone 4 TILs

To determine whether *in vivo* blockade of A2aR and TIM3 signalling improved the cytotoxic effector function of Clone 4 TILs *ex vivo*, Clone 4 TILs were harvested from RencaHA tumour-bearing mice treated with A2aR-Antagonist and anti-TIM3mAb. Cytotoxicity of adoptively transferred Clone 4 TILs was then quantified using a microscope-based killing assay[6]. The data showed that the rate of *ex vivo* killing of tumour cell targets by Clone 4 TILs harvested from mice treated with A2aR-Antagonist + anti-TIM3mAb was significantly greater than Clone 4 TILs harvested from control tumours (Figure 31 A & B). This suggested that blockade of A2aRs and TIM3 had alleviated suppression of Clone 4 TILs.

5.2.1.2 Blockade of TIM3 alone did not improve the ex vivo cytotoxic ability of Clone 4 TILs

Several studies have shown that engagement of some CIRs such as PD-1 can suppress CD8+ T cells over days within the tumour, whereas others, such as CTLA-4, disrupt TCR interactions at the immune synapse at the time of killing (76, 119). It is not known whether TIM3 interacts with its ligand over several days, or acutely, to limit killing by CD8+ TILs. To determine whether blockade of TIM3 acted acutely at the time of killing to restore Clone 4 TIL cytotoxic effector activity, Clone 4 TILs were harvested and treated with blocking anti-TIM3mAb for one hour prior to cytotoxicity assays. Short term incubation with anti-TIM3mAb would prevent acute interactions between TIM3 and target cells. However, no significant improvement in killing occurred after acute treatment with blocking anti-TIM3mAb (Figure 32). To investigate the effect of TIM3 signalling over several days in the tumour, killing by Clone 4 TILs was quantified after single treatment with anti-TIM3mAb over ten days *in vivo*. However, anti-TIM3mAb did not improve cytotoxicity amongst Clone 4 TILs when administered as a single agent. To

[6] Data presented in Chapter 2 showed that tumour regression induced by this treatment regimen began at day 16, so harvest was performed at this time point, whilst there was still sufficient tumour tissue from which to harvest TILs.

determine whether or not A2aR blockade was effective without blockade of TIM3, single treatment with A2aR-Antagonist was also administered. However, treatment with only A2aR-Antagonist did not improve killing of tumour cell targets by Clone 4 TILs either. Therefore, cytotoxicity assays using anti-TIM3mAb or A2aR-Antagonist alone were not repeated in order to reduce animal usage (Supplementary Figure S6). These data showed that blockade of A2aRs and TIM3 together was required to improve the cytotoxic effector function of Clone 4 TILs.

Figure 31 - Treatment with Anti-TIM3mAb and A2aR-Antagonist improves the ability of Clone 4 TILs to directly lyse tumour cells ex vivo

RencaHA tumour-bearing BALB/c mice were treated with A2aR Antagonist and anti-TIM3mAb administered from day 12. ATT of Clone 4 T cells was given on day 12 (arrow), Clone 4 TILs were harvested on day 16 and placed in microscope-based cytotoxicity assays. (A) Tumour growth is shown from two separate experiments. (B) Killing of K^dHA-pulsed $Renca^{mCherry}$ tumour cells in the presence of Clone 4 TILs was calculated at an E:T ratio of 3:2. Each point = 1 tumour, N= 2 experiments. Size-matched tumours analysed on the same day are paired for comparison using t-test.

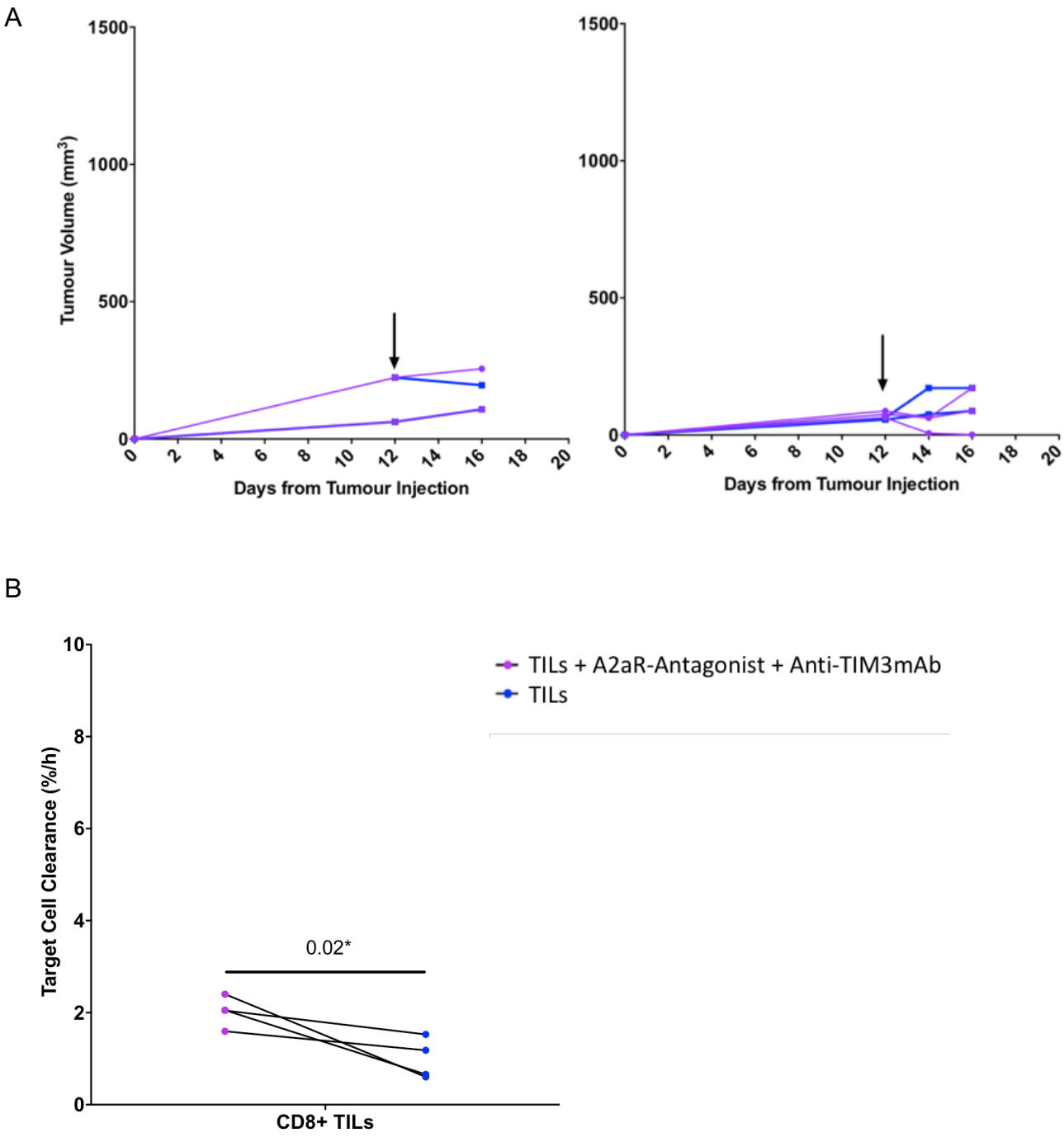

Figure 32 - Ex vivo blockade with Anti-TIM3mAb does not improve cytotoxicity amongst Clone 4 TILs

RencaHA tumour-bearing BALB/c mice were given ATT of Clone 4 T cells. Clone 4 TILs were harvested and incubated with blocking anti-TIM3mAb at a concentration of 10 μg/ml for 1 hour at 37 degrees before being placed in cytotoxicity assays. Killing of K^dHA-pulsed $RencaHA^{mCherry}$ tumour cells in the presence of Clone 4 TILs was calculated at an E:T ratio of 3:2. Each point = 1 tumour, N= 6 tumours per condition over 3 experiments. Size-matched tumours analysed on the same day are paired for comparison using t-test (p=0.3 ns).

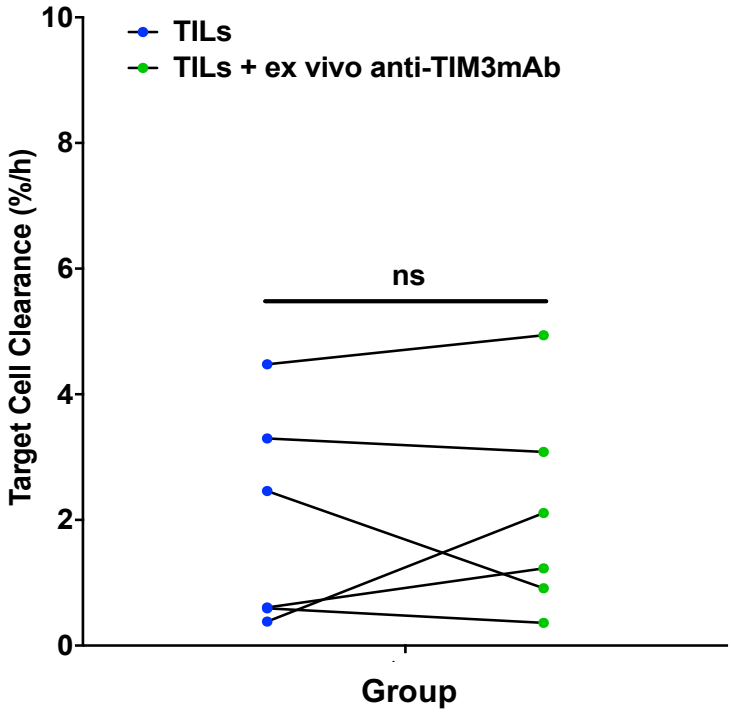

5.2.1.3 Treatment with A2aR-Antagonist and anti-TIM3mAb reduces the levels of TIM3 and PD-1 expression amongst TILs

The levels of cytotoxicity exerted by CD8+ T cells is one measure of their effector function or suppression. An indirect measurement of CD8+ T cell suppression is their surface expression of combinations of CIRs. Amongst CD8+ TILs in a murine melanoma model, co-expression of both TIM3 and PD-1 was associated with a suppressed genotype, whilst cells expressing PD-1 only without TIM3 were shown to have the genotype of effector CD8+ T cells (120, 121, 269). Therefore, to determine whether treatment with A2aR-Antagonist and anti-TIM3mAb was able to influence the genotype of CD8+ TILs, flow cytometry was used to compare CIR expression (120-122).

Analyses showed that there was an increase in TIM3+PD1+ CD8+ T cells amongst TILs from mice which received only A2aR-Antagonist + ATT, compared with control mice receiving ATT alone (Figure 33A). Although this result was not significant, it did further support the hypothesis that blockade of A2aRs promoted upregulation of TIM3 amongst CD8+TILs within RencaHA tumours (Chapter 4, Figure 28). When tumour-bearing mice were treated with both A2aR-Antagonist and anti-TIM3mAb, the percentage of TIM3+PD1+ CD8+ TILs was significantly lower than TIM3+PD-1+ TILs from control mice, suggesting that blocking both A2aRs and TIM3 resulted in significantly fewer suppressed TILs. Interestingly, A2aR-Antagonist + anti-TIM3mAb treated mice also expressed greater numbers of single PD-1+ TILs, which have been shown to possess an effector genotype, than other groups (120-122). There were no significant differences in the MFIs of TIM3 and PD-1 (Figure 33B & C).

Figure 33 – The percentage of TIM3+PD-1+ TILs is reduced amongst Clone 4 TILs from tumours treated with A2aR Antagonist and Anti-TIM3mAb

RencaHA tumour-bearing BALB/c mice received ATT of Clone 4 T cells and treated with combinations of A2aR Antagonist and anti-TIM3mAb. All CD8+ TILs were harvested and stained with antibodies to quantify levels of expression of PD-1 and TIM3 using flow cytometry. (A) Percentage expression of markers was compared using MANOVA of arcsine sqrt transformed data. Each point = 1 tumour, N = 3 experiments in total. Tumours analysed on the same day are paired for comparison. (B and C) Fold change in the MFI of each marker when compared to the Fluorescence minus one (FMO) control from that day of analysis were compared using One-way ANOVA. P-values are shown. Each point = 1 tumour, N = 3 experiments in total.

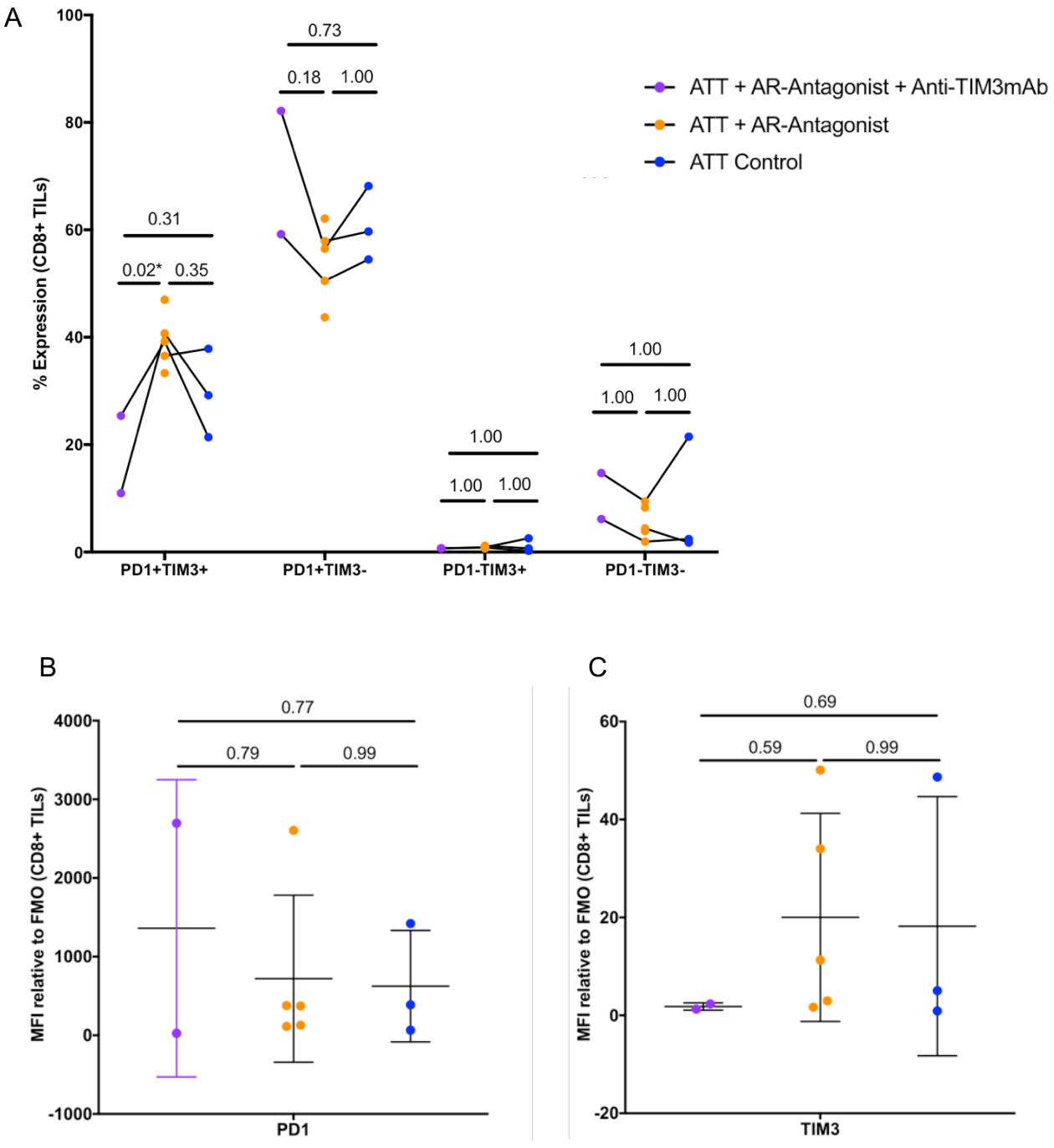

5.2.2 How does treatment with A2aR-Antagonist and anti-TIM3mAb affect Actin regulation during Immune Synapse formation by Adoptively Transferred Clone 4 TILs?

5.2.2.1 Two Models of Actin Regulation to Facilitate T cell killing

Several studies including our own have found that that peripheral actin may be required for multiple aspects of immune synapse formation, also known as cell coupling. One hypothesis states that the peripheral actin ring must be maintained for the duration of the immune synapse to ensure that T cell-Target cell contact is stable. This is termed the Actin Maintenance model. An alternative theory is that although central actin must be effectively cleared to form a ring, allowing cytotoxic granules to move through the cSMAC area, this ring does not need to be complete or stable for long periods. This second model is referred to as the Actin Clearance model (Introduction - Figure 6) (47, 48, 73, 76, 77). *Ex vivo* experiments were carried out to determine how both actin maintenance and actin clearance amongst TILs was affected when RencaHA tumour-bearing mice were treated with A2aR-Antagonist and anti-TIM3mAb.

5.2.2.2 The Actin-Maintenance Model: treatment with A2aR and TIM3 blockade improves Peripheral Actin Ring Maintenance and Immune Synapse Stability

F-tractin is a green fluorescent molecule which labels F-actin structures without affecting actin assembly (270). The location of actin at the immune synapse can be determined by analysing F-tractin accumulation using confocal microscopy (76). Recent studies in our laboratory have shown that activated Clone 4 CTL localise F-tractin from the centre to the periphery of the immune synapse upon target cell contact and maintain a peripheral ring for 180s during killing. Conversely, Clone 4 TILs fail to maintain a peripheral actin ring after exposure to the TME. The observation that, amongst TILs, immune synapse stability and cytotoxicity is also deficient supports the Actin Maintenance model which suggests that poor actin ring maintenance results in unstable immune synapses resulting in unsuccessful target cell killing (76). These recent studies also showed that systemic blockade of PD-1 improved both killing and actin clearance by Clone 4 TILs, suggesting that immunotherapy can modulate actin regulation (76, 77).

Experiments were carried out in which actin localisation was assessed to determine whether A2aR and TIM3 blockade also improved actin ring maintenance and immune synapse stability amongst Clone 4 TILs. To this end, Clone 4 T cells were first transduced with a vector containing the gene for F-tractin, before being adoptively transferred into RencaHA tumours. F-tractin-expressing Clone 4 TILs were harvested from tumour-bearing mice treated with combinations

of A2aR-Antagonist and anti-TIM3mAb, and the formation of immune synapses between TILs and Renca tumour target cells was assessed *ex vivo*. Clone 4 TIL-target cell couples were imaged using confocal microscopy over 420s for each condition, to determine the pattern of accumulation of F-tractin at 20s intervals during immune synapse formation (47). To quantify peripheral actin maintenance, the proportion of cell couples which exhibited peripheral actin at each timepoint was assessed. Growth curves of the tumours used in assays were plotted to show that treatment with A2aR-Antagonist with or without TIM3mAb was producing tumour regression at the time of assay.

Amongst *in vitro* primed Clone 4 CTL, F-tractin forms a peripheral ring within 20s, and is maintained in >80% of cell couples until 180s. >60% of couples maintain a peripheral actin ring until 420s, representing stable ring formation. Within TILs, the percentage of cell couples which accumulate peripheral F-tractin is reduced from 80% to 40% between 0 and 120s (p=0.005** at 120s). Furthermore, the peripheral F-tractin ring declines quickly amongst TILs, with <20% of TILs maintaining peripheral actin beyond 180s (p>0.0001**** vs controls; Figure 34A & D)(76, 77).

Administering specific A2aR-Antagonist to tumour-bearing mice resulted in an increase in the percentage of Clone 4 TIL couples which formed a peripheral F-tractin ring between -20 and 40s (50% to 60%; Figure 34A & D). Additionally, at later timepoints, a significantly higher percentage of TILs from A2aR-Antagonist treated mice maintained a peripheral actin ring when compared with control TILs (p= 0.01** at 420s; Figure 34 A & D).

Treating tumour-bearing mice with A2aR-Antagonist plus anti-TIM3mAb did not significantly alter the percentage of couples accumulating F-tractin at the pSMAC when compared with mice treated with only A2aR-blockade. However, accumulation of peripheral actin was improved in A2aR-Antagonist plus anti-TIM3mAb- treated mice relative to control TILs (p= 0.02* 180s; Figure 34 A & D). Although treating tumour-bearing mice with A2aR-Antagonist with and without anti-TIM3mAb resulted in an increased percentage of TIL couples which maintained peripheral actin when compared with controls, this percentage remained significantly lower than CTL at most timepoints, suggesting that a partial restoration of peripheral actin occurred (Figure 34 A & D).

Figure 34 –Treatment with A2aR-Antagonist + Anti-TIM3mAb improves Peripheral Actin maintenance at the immune synapse of Clone 4 TILs

Groups of RencaHA tumour-bearing BALB/c mice were given ATT of Clone 4 T cells and treated with combinations of A2aR-Antagonist and anti-TIM3mAb. Clone 4 TILs were harvested and immune synapse formation between TILs or *in vitro* primed Clone 4 CTL and K^dHA-pulsed Renca tumour cell targets was imaged *ex vivo* using confocal microscopy. Analyses to quantify accumulation of f-tractin were performed in >30 cell couples per condition, across 2-4 experiments. (A) The percentage of couples which expressed a peripheral actin ring was quantified. (B & C) Growth curves of the tumours used for analyses are shown with representative controls if injected in the same experiment. Arrows indicate the timing of ATT. (D) Percentage of couples with peripheral F-tractin accumulation was compared between conditions using proportional z-test. Darker cells indicate smaller p-values.[7] (E) Computer modelling was used to illustrate the average location of accumulation F-tractin within CTL and TILs by pooling all images in each data set. Accumulation is shown using a pseudocolour scale with lighter colours representing more F-tractin.

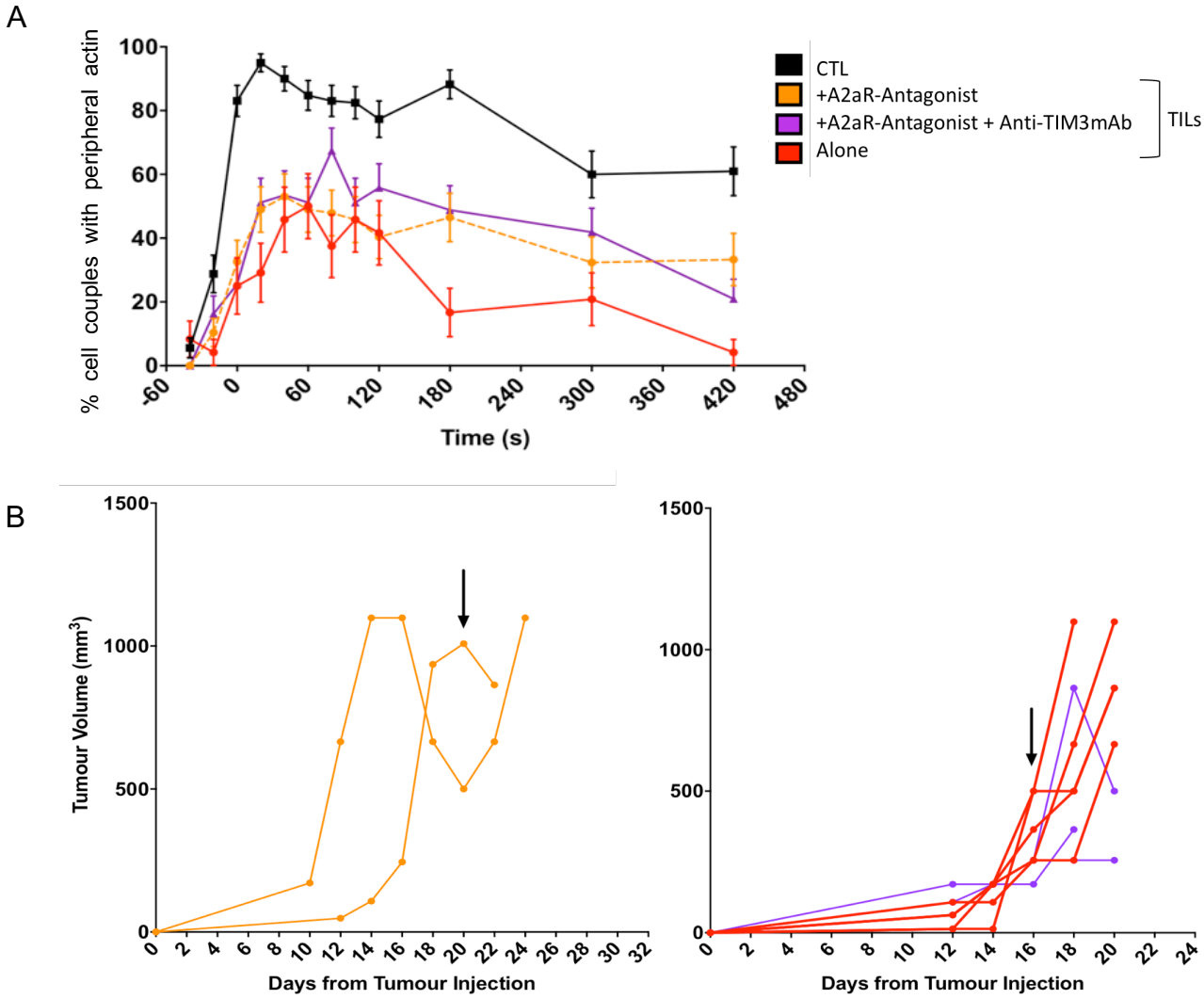

[7] Data for control CTL and control TILs were generated by Rachel Ambler as a reference data set for the Wuelfing lab and re-analysed by GE, to compare different TIL conditions in a blinded manner.

D

Time	-40	-20	0	20	40	60	80	100	120	180	300	420
TILs vs TILs +AR-Antagonist	0.005	0.64	0.69	0.17	0.74	0.74	0.55	0.80	0.72	0.03	0.45	0.01
	*	ns	ns	ns	ns	ns	ns	ns	ns	*	ns	**
TILs vs TILs + AR-Antagonist +Anti-TIM3mAb	0.01	0.30	0.84	0.14	0.76	0.86	0.04	0.88	0.38	0.02	0.14	0.14
	**	ns	ns	ns	ns	ns	*	ns	ns	*	ns	ns
TILs + AR-Antagonist vs TILs + Anti-TIM3mAb + AR-Antagonist	na	0.63	0.35	0.99	0.83	0.99	0.10	0.77	0.20	0.98	0.46	0.12
	na	ns	ns	ns	ns	ns	ns	ns	ns	ns	ns	ns
CTL vs TILs + AR-Antagonist	0.02	0.01	<0.0001	<0.0001	<0.001	<0.0001	<0.0001	<0.0001	<0.0001	<0.0001	0.004	0.005
	*	**	****	****	****	****	****	****	****	****	***	***
CTL vs TILs + AR-Antagonist +Anti-TIM3mAb	0.03	0.08	<0.0001	<0.0001	<0.0001	<0.0001	0.03	0.0003	0.01	<0.0001	0.06	<0.0001
	*	*	****	****	****	****	*	***	**	****	ns	****
CTL vs TILs	0.96	0.01	<0.0001	<0.0001	<0.0001	0.0003	<0.0001	0.0003	0.001	<0.0001	0.001	<0.0001
	ns	**	****	****	****	***	****	***	***	****	***	****

E

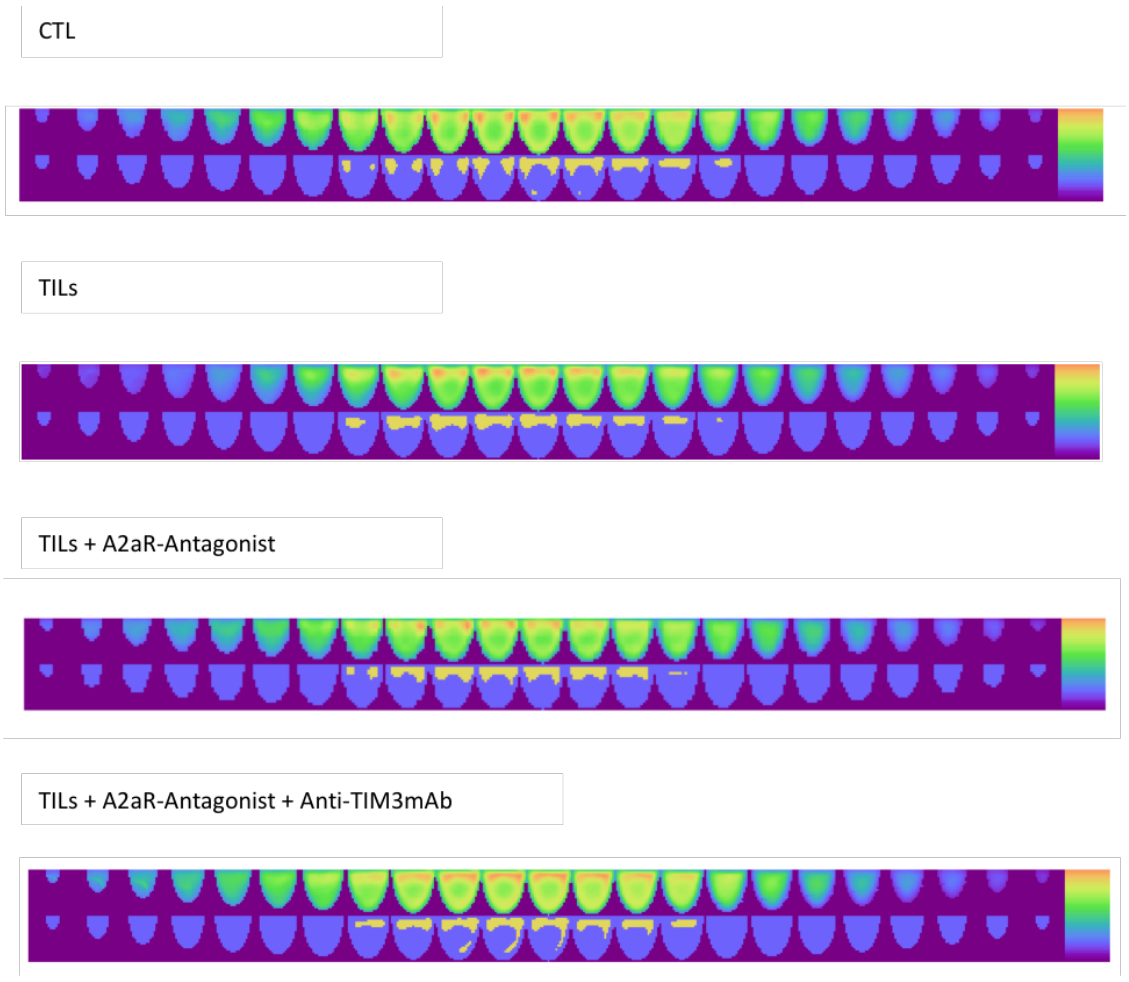

The functional effect of impaired peripheral actin ring maintenance is thought to be reduced immune synapse stability resulting in failed target-cell killing. As peripheral actin ring maintenance was improved amongst TILs harvested from mice which received A2aR-Antagonist with and without anti-TIM3mAb, we hypothesised that immune synapse stability would also be improved amongst these Clone 4 TIL populations when compared with TILs from control mice (76, 77). Immune synapse stability was quantified based upon the morphology of cell couples formed between Clone 4 TILs and RencaHA targets. Couples with poor actin ring maintenance exhibit two morphological characteristics of low immune synapse stability (76, 77). Off-Interface Lamellae (Off-L) are actin-mediated projections which extend from the Clone 4 T cell. However Off-L differ from functional projections which are directed at the immune synapse to ensure its stability, because they are directed away from the target cell. Earlier timepoints of Off-L formation indicate lower immune synapse stability within a cell couple (Figure 35A). A second measure of immune synapse stability in the T cell-target cell couple, is the percentage of cell couples which translocate more than one interface distance away from the initial site of immune synapse formation (Figure 35C).

Ex vivo analyses of TILs from A2aR-Antagonist-treated mice show that both Off-L formation and translocation is reduced, indicating that A2aR-antagonist treated TILs form more stable immune synapses when compared with control TILs. Survival without Off-L and translocation are both restored further towards control levels if both A2aR-Antagonist and anti-TIM3mAb are used to treat tumour bearing mice (Figure 35A-D). These data suggest that double treatment of tumour bearing mice with A2aR-Antagonist and anti-TIM3mAb improved the *ex vivo* stability of immune synapses between TILs and tumour cell targets. Immune synapse stability correlates with longer maintenance of peripheral actin rings by TILs from treated tumours.

Figure 35 – Treatment with A2aR-Antagonist and Anti-TIM3mAb improves Morphological parameters of Immune Synapse Stability amongst Clone 4 TILs

Groups of RencaHA tumour-bearing BALB/c mice were given ATT of Clone 4 T cells and treated with combinations of A2aR-Antagonist and anti-TIM3mAb. Measures of immune synapse stability were quantified using confocal imaging of immune synapse formation between *in vitro* primed Clone 4 CTL or harvested Clone 4 TILs, and K^dHA pulsed Renca tumour cell targets *ex vivo*. Formation of Off-Interface Lamellae (Off-L, membrane projections which are directed away from the immune synapse) was quantified. (Ai) Representative images are shown from a single experiment. The interface of the immune synapse is illustrated in red before off-L formation (Aii) one off-L is shown circled in blue. (B) Survival until formation of first Off-L was compared between conditions using Kaplein-Mayer survival analysis (Log Rank). (C) Translocation is shown as one CTL (red) moves >1 interface diameter from the initial location of the immune synapse (green) between (i) early and (ii) late timepoints. (D) Translocation was compared using One-way ANOVA. P values are indicated. N >30 cell couples per condition over 2-4 experiments.[8]

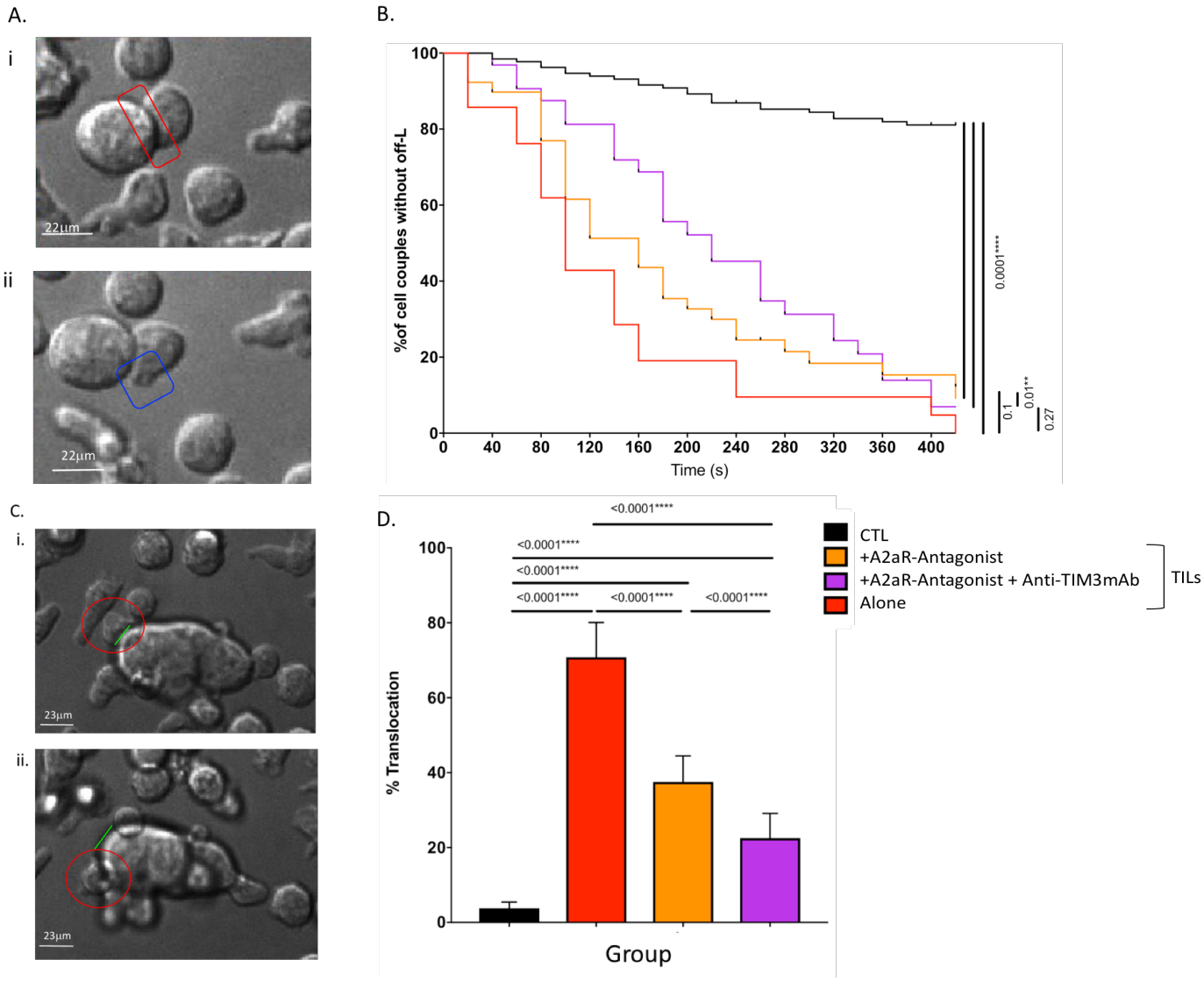

[8] Data for control TILs were generated by Rachel Ambler and re-analysed by GE to enable data sets to be compared blinded.

5.2.2.3 The Actin Clearance Model: treatment with A2aR and TIM3 blockade improves Actin Clearance from the cSMAC

The second model, explaining how actin regulation is linked to the delivery of cytolytic granules by CD8+ T cells, is the Actin Clearance model. The Actin Clearance model suggests that the purpose of peripheral actin ring formation is not immune synapse stability, but rather clearance of actin so that cytotoxic granules can pass through the cSMAC (71). In this model, provided actin clearance is achieved, the actin does not need to form a complete and stable peripheral ring. Therefore, any actin pattern which does not cover the cSMAC would be permissive to killing. According to the Actin Clearance model, Clone 4 TILs from A2aR and TIM3 blocked tumours should clear actin more efficiently from the cSMAC when compared with controls because they have better *ex vivo* cytotoxic ability. To compare actin clearance between Clone 4 TILs from A2aR-antagonist and anti-TIM3mAb-treated and control tumour-bearing mice, the existing data were re-analysed so that couples expressing either peripheral or asymmetric actin were categorised as having 'Permissive' actin patterning which did not cover the cSMAC. Diffuse, Lamellal or Central patterns, which cover the cSMAC, were defined as 'Obstructive' actin (Introduction Figure 3 & Figure 6) (47, 71, 76, 77).

Obstructive actin was significantly elevated amongst TILs when compared with CTL at 0-420s. Treatment of tumour bearing mice with A2aR-Antagonist and anti-TIM3mAb resulted in a reduction in the percentage of TILs expressing obstructive actin between 0 and 60s when compared with control TILs. Treatment of mice with A2aR-Antagonist alone reduced obstructive actin to a lesser degree. These reductions were not statistically significant.

At later timepoints, between 60-120s, A2aR-Antagonist plus anti-TIM3mAb treated mice exhibited lower obstructive actin when compared with TILs from control mice, but TILs from mice that received single A2aR-Antagonist treatment did not exhibit significantly different patterning than TILs from control mice. Although TILs from mice treated with A2aR-Antagonist plus anti-TIM3mAb exhibited obstructive actin that was lower than control TILs, it remained significantly higher than CTL at all timepoints except 80s and 300s (Figure 36 A & C). Therefore, treatment with A2aR-Antagonist and anti-TIM3mAb resulted in a partial reduction in TIL couples with obstructive actin.

Permissive actin was elevated amongst Clone 4 TILs harvested from A2aR-Antagonist treated mice at all timepoints when compared with TILs from control mice. Treatment of mice with A2aR-Antagonist and anti-TIM3mAb also produced elevated numbers of TILs exhibiting permissive actin patterning when compared with control TILs. However, the increase in permissive actin which resulted from treatment with A2aR-Antagonist with and without anti-TIM3mAb was not significant when compared with TILs, and permissive actin remained significantly lower than CTL at all timepoints in both treated conditions, meaning that peripheral actin was only partially elevated by treatment with A2aR-antagonist and anti-TIM3mAb (Figure 36 B & D).

Figure 36 – Treatment with A2aR-Antagonist and Anti-TIM3mAb reduces Obstructive actin patterning and elevates Permissive actin patterning amongst Clone 4 TILs

Groups of RencaHA tumour-bearing BALB/c mice were given ATT of Clone 4 T cells and treated with combinations of A2aR-Antagonist and anti-TIM3mAb. Clone 4 TILs were harvested and immune synapse formation between TILs or *in vitro* primed Clone 4 CTL and K^dHA-pulsed Renca tumour cell targets was imaged *ex vivo* using confocal microscopy. Analyses of the accumulation of f-tractin were performed in >30 cell couples per condition, across 2-4 experiments. The percentage of couples which expressed (A & C) obstructive and (B & D) permissive actin patterns as defined in Figure 6 were quantified and compared using proportional z test (tabulated), darker cells indicate smaller p-values[9].

A

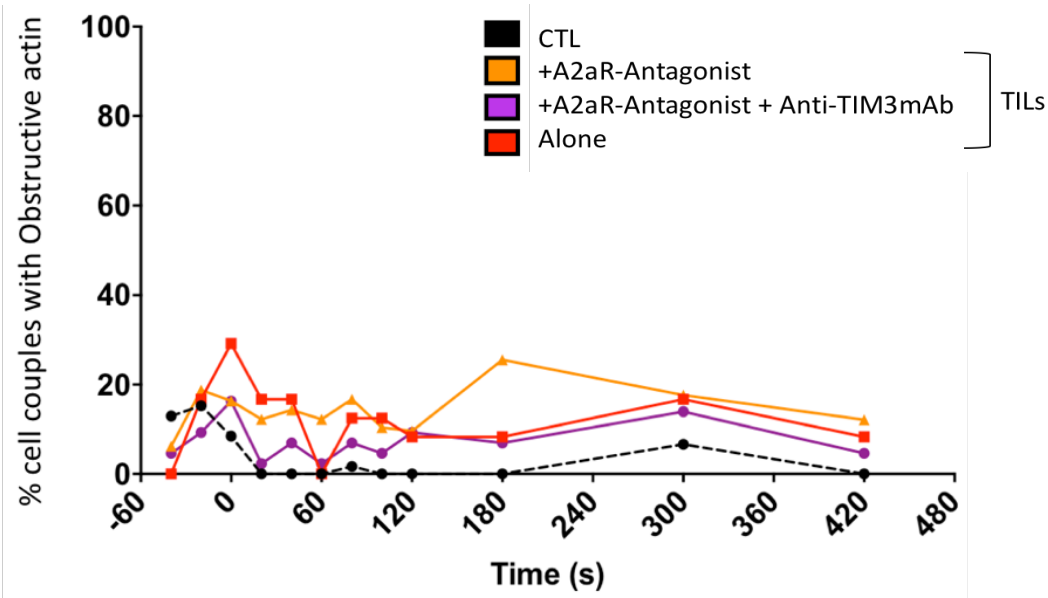

B

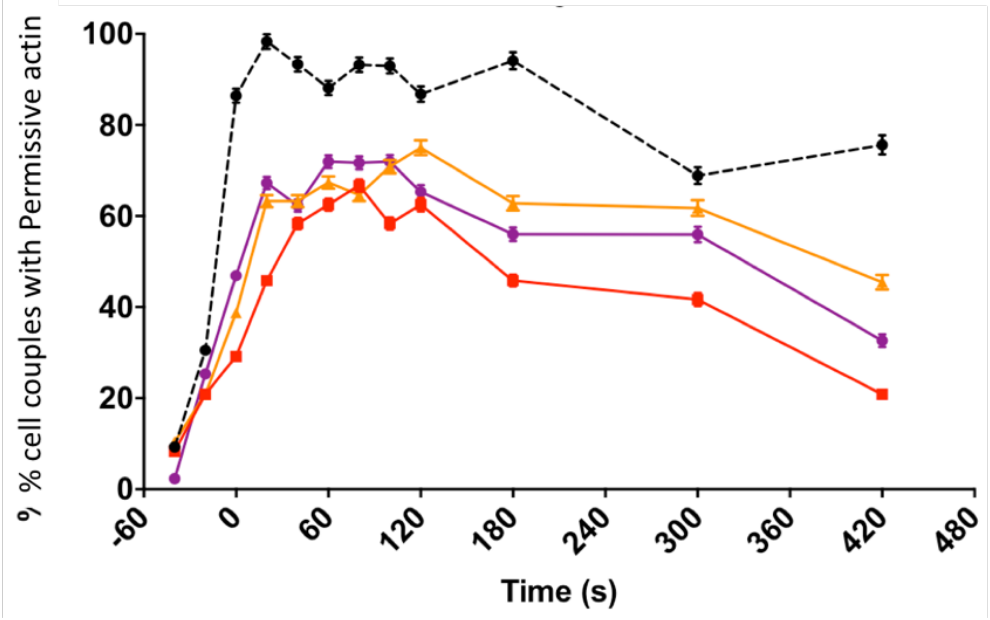

[9] Data for control CTL and control TILs were generated by Rachel Ambler as a reference data set for the Wuelfing lab and re-analysed by GE to allow blinded comparisons

C

Time	-40	-20	0	20	40	60	80	100	120	180	300	420
TILs vs TILs +AR-Antagonist	0.06	0.59	0.33	0.88	0.93	0.03	0.42	0.90	0.54	0.04	0.66	0.37
	ns	ns	ns	ns	ns	*	ns	ns	ns	*	ns	ns
TILs vs TILs + AR-Antagonist +Anti-TIM3mAb	0.07	0.62	0.35	0.10	0.41	0.10	0.75	0.50	0.56	0.78	0.95	0.94
	ns	ns	ns	ns	ns	ns	ns	ns	ns	ns	ns	ns
TILs + AR-Antagonist vs TILs + Anti-TIM3mAb + AR-Antagonist	0.90	0.32	0.78	0.16	0.43	0.16	0.27	0.52	0.76	0.04	0.84	0.37
	ns	ns	ns	ns	ns	ns	ns	ns	ns	*	ns	ns
CTL vs TILs + AR-Antagonist	0.41	0.45	0.12	0.001	0.001	0.001	0.002	0.003	0.01	0.0003	0.05	0.01
	ns	ns	ns	***	***	***	**	**	**	***	*	**
CTL vs TILs + AR-Antagonist +Anti-TIM3mAb	0.29	0.55	0.13	0.03	0.01	0.03	0.06	0.02	0.01	0.01	0.14	0.03
	ns	ns	ns	*	**	*	ns	*	**	**	ns	*
CTL vs TILs	0.16	0.62	0.01	0.0001	0.0001	0.09	0.01	0.001	0.004	0.004	0.08	0.01
	ns	ns	**	****	****	ns	**	***	**	**	ns	**

D

Time	-40	-20	0	20	40	60	80	100	120	180	300	420
TILs vs TILs +AR-Antagonist	0.48	0.76	0.29	0.10	0.51	0.50	0.93	0.18	0.16	0.10	0.16	0.02
	ns	ns	ns	ns	ns	ns	ns	ns	ns	ns	ns	*
TILs vs TILs + AR-Antagonist +Anti-TIM3mAb	0.60	0.48	0.10	0.05	0.56	0.28	0.48	0.16	0.62	0.30	0.17	0.20
	ns	ns	ns	*	ns	ns	ns	ns	ns	ns	ns	ns
TILs + AR-Antagonist vs TILs + Anti-TIM3mAb + AR-Antagonist	0.26	0.45	0.32	0.53	0.90	0.48	0.34	0.73	0.43	0.65	0.73	0.30
	ns	ns	ns	ns	ns	ns	ns	ns	ns	ns	ns	ns
CTL vs TILs + AR-Antagonist	0.60	0.36	0.0001	<0.0001	0.003	0.02	0.0005	0.006	0.2	0.0003	0.61	0.01
	ns	ns	****	****	***	**	***	**	ns	***	ns	**
CTL vs TILs + AR-Antagonist +Anti-TIM3mAb	0.32	0.72	<0.0001	<0.0001	0.0001	0.07	0.02	0.02	0.02	<0.0001	0.30	0.0002
	ns	ns	****	****	****	*	*	*	*	****	ns	***
CTL vs TILs	0.76	0.53	<0.0001	<0.0001	0.0004	0.02	0.02	0.001	0.03	<0.0001	0.05	<0.0001
	ns	ns	****	****	***	*	*	***	**	****	*	****

5.2.3 Blockade of A2aRs and TIM3 improves the number of CD8+ TILs and reduces the number of FOXP3+ Tregs within RencaHA tumours

We hypothesised that the improved control of tumour growth observed when A2aRs and TIM3 were blocked *in vivo*, was linked to the partial improvement in cytotoxic function and peripheral actin ring formation that was observed amongst Clone 4 TILs *ex vivo*. To test whether there was also improved infiltration of TILs into the TME as a result of A2aR and TIM3 blockade, sections of tumours were stained using antibodies specific to CD8, FOXP3 (an indicative marker of Tregs), and Thy1.1.

Immunohistochemical analyses showed that the number of cells expressing FOXP3, an indicative marker of Treg cells, was reduced significantly in the peripheral areas of tumours treated with A2aR-antagonist and anti-TIM3mAb, although not reduced in the central areas of these same tumours when compared with tumours from control mice (Figure 37A). Further examination revealed that although the number of Clone 4 TILs in the periphery of tumours was elevated amongst A2aR-Antagonist + anti-TIM3mAb treated mice when compared with control mice, this was not significant. Endogenous Thy1.2+ CD8+ TIL infiltration was elevated in both the central and peripheral regions of A2aR-antagonist and anti-TIM3mAb treated tumours however this was not significant (Figure 37B). Overall, the number of CD8+ TILs was elevated in the periphery and the centre of tumours treated with A2aR-Antagonist and anti-TIM3mAb when compared with control tumours. In central regions this finding appeared to be mediated by increased infiltration of endogenous CD8+ TILs and not by increased infiltration of Clone 4 TILs. The number of FOXP3+ cells was reduced in the periphery of A2aR-Antagonist and Anti-TIM3mAb treated tumours when compared with controls.

Figure 37 - Blockade of A2aRs and TIM3 is associated with increased infiltration of CD8+ TILs and reduced numbers of FOXP3+ Tregs within RencaHA tumours

RencaHA tumour-bearing BALB/c mice were given ATT of Clone 4 T cells and treated with combinations of A2aR-Antagonist and anti-TIM3mAb. Size-matched tumours from treated and control mice were sectioned and immunohistochemical staining was performed using antibodies specific to CD8b, Thy1.1 and FOXP3. Sections were fixed and imaged using confocal microscopy. 10 peripheral and 10 central areas were examined across sections of each tumour to quantify the numbers of (A+B) total CD8+ TILs and FOXP3+ cells or (C+D) Endogenous Thy1.2+CD8+ TILs and Thy1.1+ Clone4 TILs. N= 2 control tumours and 3 treated tumours analysed over two experiments[10]. Size matched tumours fixed on the same day are paired for analysis using t-test. P-values are shown.

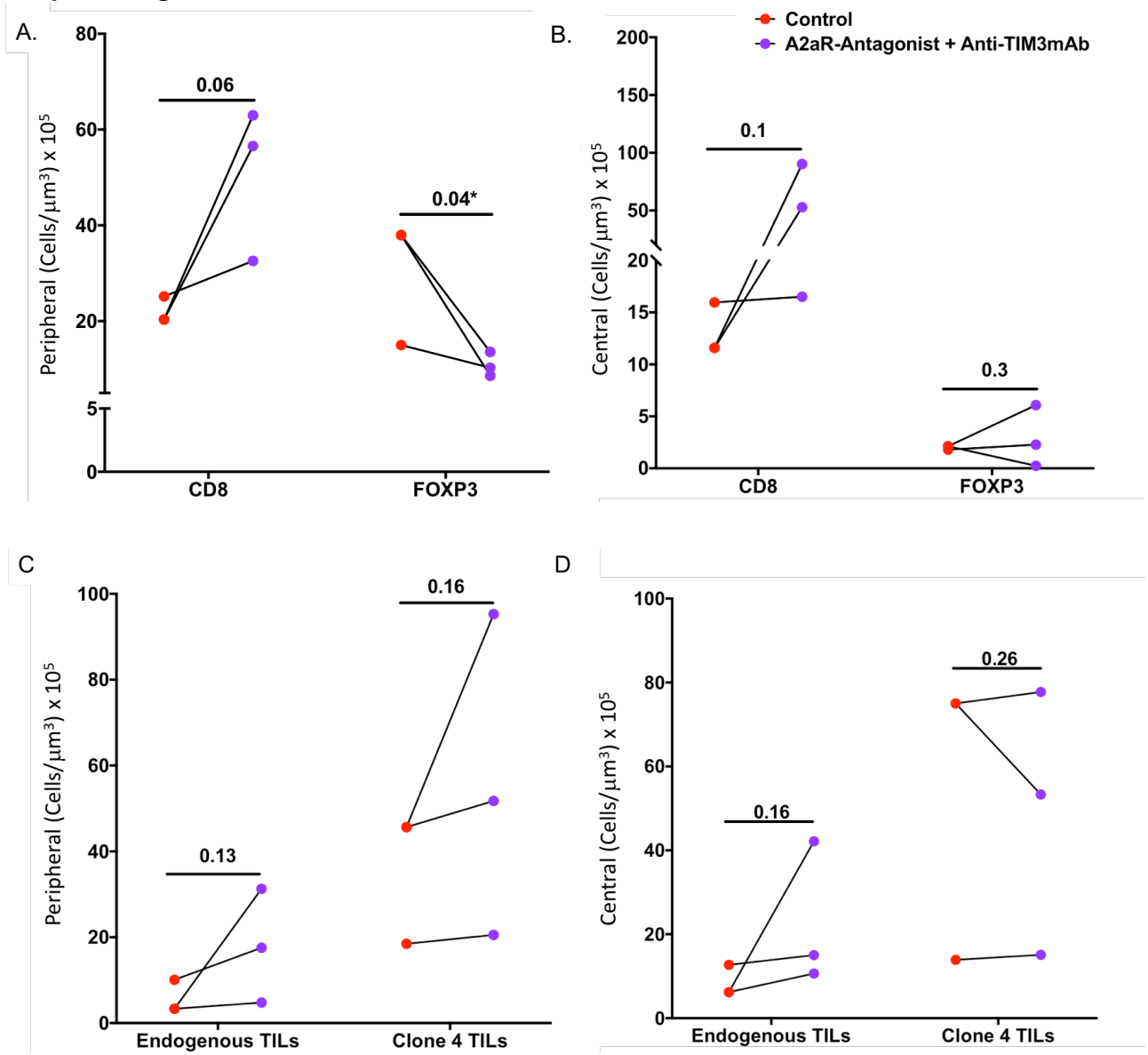

[10] Tumours were grown and harvested by GE and stained by Carissa Wong, a student in the Wuelfing lab. Image analysis was performed by GE.

5.3 Discussion

5.3.1 Treatment of Tumour-bearing mice with A2aR-Antagonist + anti-TIM3mAb restored the ex vivo killing ability of Clone 4 TILs

Microscope-based killing assays were utilised in order to test whether or not treatment with A2aR-Antagonist and anti-TIM3mAb could improve the cytotoxic effector function of Clone 4 TILs within the RencaHA TME. Previous experiments using this type of assay revealed that it was possible to detect restoration of *ex vivo* effector function amongst Clone 4 TILs from mice that received Anti-PD-1 mAb therapy, confirming the efficacy of this type of assay in quantifying changes in Clone 4 TIL function induced by immunotherapy.

Assays were performed, in order to compare the *ex vivo* cytotoxicity exerted by Clone 4 TILs from A2aR-Antagonist and anti-TIM3mAb treated mice, with TILs from control mice. Treatment was administered using the same protocol which produced complete tumour regression (as detailed in Chapter 4). TILs were harvested 16 days after tumour injection, to ensure that there was sufficient tumour mass from which to extract them. The data clearly showed that when A2aR and TIM3 blockade was administered to RencaHA tumour-bearing mice, tumour growth was controlled and TILs were found to exert better cytotoxicity when compared with controls.

We postulated that TIM3 signalling could suppress the cytotoxic effector function of Clone 4 TILs acutely at the time of killing, or over hours to days within the TME. Thus, to determine if *ex vivo* blockade of TIM3 at the time of assay would improve the ability of Clone 4 TILs to kill target cells, anti-TIM3mAb was added to TILs for one hour before cytotoxicity assays. However, adding anti-TIM3mAb to TILs *ex vivo* produced no improvement in cytotoxicity by TILs. This finding agrees with previous data, showing that anti-PD-1 mAb does not improve the cytotoxic function of Clone 4 TILs when added acutely *ex vivo,* despite the fact that *in vivo* blockade or knockdown of PD-1 did improve killing amongst TILs (Supplementary Figure S7) (76, 77). Therefore, the effects of TIM3 and PD-1 expression on Clone 4 TIL killing most likely develop over days in the tumour, rather than involving an acute interaction between TIM3 on TILs and ligands on tumour-target cells acutely at the time of killing.

An alternative explanation for the finding that acute blockade of TIM3 at the time of killing did

not improve cytotoxicity, is that in order to exert its inhibitory effects on TCR signalling, TIM3 must be engaged by its ligands Ceacam-1 or Galectin-9 (54, 120, 134). Although Renca tumour cells do express these TIM3 ligands, their expression is elevated amongst Renca cells harvested from tumours and analysed *ex vivo* when compared with *in vitro* cultured Renca tumour cells (Supplementary Figure S3). Therefore the *in vitro* cultured Renca tumour cell targets used in cytotoxicity assays may not express Ceacam-1 and Galectin-9 at high enough levels to cause acute suppression of Clone 4 TILs via TIM3 engagement. In future experiments, Renca tumour target cells could be transfected to overexpress Ceacam-1 or Galectin-9, and then these cells could be used as targets in cytotoxicity assays. This would ensure that TIM3 expressed on Clone 4 TILs is engaged by Renca target cells at the time of killing, and this interaction could then be blocked with anti-TIM3mAb to determine the effects of acute TIM3 engagement on the cytotoxic effector function of Clone 4 TILs (54, 271).

To quantify the effects of long-term TIM3 engagement within the TME, preliminary data were acquired, in which killing by Clone 4 TILs was compared between mice treated with only anti-TIM3mAb and only A2aR-Antagonist *in vivo*. Neither single agent restored the *ex vivo* killing of tumour target cells by Clone 4 TILs when compared with controls.

5.3.2 Treatment of Tumour-bearing mice with A2aR-Antagonist + anti-TIM3mAb reduced the percentage of TIM3+PD-1+ CD8+ TILs

To determine whether treatment with A2aR-Antagonist and anti-TIM3mAb reduced the proportion of CD8+ TILs with a suppressed genotype, flow cytometry was used to assess TIM3 and PD-1 co-expression. Mice treated with both A2aR and TIM3 antagonism exhibited a lower percentage of TIM3+PD-1+ cells and a lower TIM3 MFI when compared with controls or single treated mice, indicating that double treatment produces fewer suppressed CD8+ TILs. An important limitation of this assay is that therapeutic anti-TIM3mAb could block binding of the fluorescent anti-TIM3mAb, such that TIM3 positive cells could not be detected amongst TILs from mice which received double blockade. However, this is an unlikely scenario, since the blocking antibody was administered 48h before staining, and several studies suggest that it detaches from the TIM3 receptor within this time (103). Even if quantification of TIM3 was limited by binding of the anti-TIM3 blocking antibody, its binding would still render the TIM3 molecule unavailable for signalling. Therefore, cells bound with blocking anti-TIM3mAb could be considered to be functionally TIM3 negative, as they cannot signal through TIM3, and this

would be reflected in their inability to bind to the fluorescent anti-TIM3mAb.

5.3.3 Treatment with A2aR-Antagonist + anti-TIM3mAb improves two parameters of Actin Regulation

A further indicator of TIL effector function is their ability to formulate and maintain an actin ring at the periphery of the immune synapse. There are two models to explain the importance of the peripheral actin ring. In the Actin Maintenance model, the longevity of the peripheral ring determines the stability of contacts between CD8+ T cells and APCs. Clone 4 TILs exhibit shortened peripheral ring maintenance and impaired parameters of immune synapse stability when compared with Clone 4 CTL. By blocking PD-1 systemically in tumour bearing mice, we have previously restored the longevity of peripheral actin ring maintenance during a 420s imaging period, indicating that immunotherapy can manipulate actin regulation and immune synapse stability (76, 77).

Treatment of tumour-bearing mice with A2aR-Antagonist produced improved peripheral actin ring maintenance amongst Clone 4 TILs when compared with TILs from control mice. Dual blockade of A2aRs and TIM3 improved the *ex vivo* maintenance of the peripheral actin ring still further amongst TILs, but this improvement was not significantly different to that produced by A2aR-Antagonist alone. In both instances, restoration of peripheral actin amongst TILs was partial when compared with control CTL. Although the improvement in peripheral actin accumulation was relatively modest, improvements in immune synapse stability, which reflect the functional effects of actin ring maintenance, were significant. Importantly, the use of anti-TIM3mAb and A2aR-blockade together produced synergistic benefit to immune synapse stability.

The Actin Clearance model suggests that movement of actin away from the centre of the interface is required to allow cytotoxic granules to pass through at the cSMAC. In this model, the longevity of maintenance of the peripheral ring is less important than a clearance of actin at the central interface (71). To compare actin clearance amongst TILs from mice treated with A2aR-Antagonist and Anti-TIM3mAb and TILs from control mice, data were re-analysed to quantify ‘Permissive’ actin patterns which allow granule release, and ‘Obstructive’ actin patterns which prevent granule release.

A2aR blockade gave rise to TILs which displayed reduced obstructive actin between 0-60s, and this was reduced still further amongst TILs treated with A2aR-Antagonist and adjunct anti-TIM3mAb. Other studies have shown that 0-60s is a key timepoint during which granules pass through the cSMAC, therefore although the levels of obstructive actin amongst TILs from mice which received A2aR-antagonist plus anti-TIM3mAb were only partially reduced when compared with control TILs, this reduction occurred at key timepoints, suggesting that there may be synergistic benefit gained from blocking both A2aRs and TIM3 to permit granule release by Clone 4 TILs (48, 71).

It may be possible to discern which actin patterning model correlates best with the timing of successful cytotoxic granule delivery by Clone 4 CTL and TILs, by visualising the delivery of lytic hits to Renca tumour cell targets. To achieve this, Renca tumour targets were transfected with GCAMP6s, a calcium sensor which fluoresces green after the lytic hit occurs, causing calcium influx into the target cell (71). However, Renca tumour cells were found to perform spontaneous calcium flux when not in-contact with CTL, indicating that the Renca cell line cannot be used as targets to assess lytic hit delivery by Clone 4 T cells (Data not shown). Further work will be aimed at optimising a different HA-expressing target cell population for this purpose (260).

5.3.4 Blockade of A2aRs and TIM3 results in improved numbers of CD8+ TILs and reduced numbers of FOXP3+ Tregs within the RencaHA TME

The ex vivo assays that were carried out to quantify cytotoxicity, CIR expression and actin regulation by Clone 4 TILs revealed that treatment of tumour-bearing mice with A2aR and TIM3 blockade resulted in improved cytotoxic effector function amongst CD8+ TILs. However, we hypothesised that synergy between improved CD8+ TIL function and greater infiltrating numbers of CD8+ TILs could explain the durable control of tumour growth that is observed in mice after A2aR and TIM3 blockade. Adenosine signalling is known to affect infiltration of TILs in models of mouse melanoma, whereby blockade of A2b receptors is associated with an increase in the percentage of CD8+ TILs within the TME (272). Histological sections of size-matched RencaHA tumours from mice given ATT of Clone 4 T cells alone (Control) or with A2aR-Antagonist plus anti-TIM3mAb were assessed using immunohistochemistry. These analyses revealed that the only significant difference between treated and control tumours was a reduction in the number of FOXP3+ TILs within tumours from treated mice. This finding

suggests that engagement of A2aRs and TIM3 either affects Treg development or recruitment and infiltration into RencaHA tumours. In addition, infiltration of both endogenous CD8+ TILs and Clone 4 TILs was elevated, leading to an increase in the overall numbers of CD8+ TILs within A2aR-antagonist and anti-TIM3mAb treated tumours. An increase in the ratio of CD8+TILs to FOXP3+ Tregs has been associated with a positive prognosis in several tumour models (119).

Since A2aRs and TIM3 are expressed on multiple immune cell types other than CD8+ T cells, it is likely that systemic blockade of these pathways provokes a generalised increase in pro-inflammatory signalling within the TME. This could cause multiple immune cell types to release chemoattractant signals which attract CD8+ T cells. Such pro-inflammatory mediators could result in the reversal of CD4+ Tregs back to a Th1 phenotype, which could account for the reduction in FOXP3+ Tregs within A2aR-Antagonist and anti-TIM3mAb treated tumours. Blockade of A2aRs could also improve tumour infiltration of CD8+ TILs directly, because the A2aR elevates PKA activity which, by inhibiting RhoA, could influence lymphocyte polarity and the migratory abilities of CD8+ T cells (179, 192, 205). Furthermore, endothelial cells express adenosine receptors, and blockade of CD73 on endothelia has been shown to facilitate endothelial activation and upregulation of adhesion molecules which promote lymphocyte transmigration (273-275). Analyses to determine the mechanism by which adenosine and TIM3 signalling affects infiltration are the focus of other work within our laboratory.

Overall, the combination of A2aR-Antagonist plus anti-TIM3mAb was shown to improve several measures of effector function amongst adoptively transferred Clone 4 TILs as well as endogenous CD8+ TILs. Therefore, this combination of immunotherapy targets both infiltration and function within the TME, to improve control of tumour growth by CD8+ TILs in the RencaHA model.

Chapter 6 Does engagement of A2a Adenosine Receptors and TIM3 expressed on Clone 4 T cells directly affect their Function in vitro?

6.1 Introduction

Several studies have shown that engagement of A2aRs and TIM3 expressed on CD8+ T cells directly suppresses their cytotoxic effector function. Knockdown of A2aRs improved effector cytokine production amongst adoptively transferred CAR-T cells in a model of primary melanoma (194, 201). Furthermore, TIM3 knockdown directly affects cytokine production by CD8+ T cells in a model of LCMV (256).

Data presented in Chapter 5 suggested that systemic delivery of A2aR-Antagonist and anti-TIM3mAb to RencaHA tumour-bearing mice resulted in restoration of *ex vivo* actin regulation and cytotoxic function amongst adoptively transferred Clone 4 TILs. It is possible that blockade was acting directly on Clone 4 TILs to improve their cytotoxic effector function. Alternatively, the function of Clone 4 TILs could have been improved indirectly, through the pro-inflammatory effects of blocking A2aRs and TIM3 on innate immune cells and Treg populations within the TME.

However, we hypothesised that engagement of A2aRs and TIM3 on Clone 4 T cells would result in direct inhibition of their cytotoxic effector function *in vitro* and *in vivo* (201, 276). To test this hypothesis, *in vitro* assays were devised wherein Adenosine Receptor and TIM3 signalling were initiated amongst Clone 4 T cells in culture, and the following measures of cytotoxic effector function were assessed:

a. Killing ability of Clone 4 CTL
b. Expression of Co-Inhibitory Receptors by Clone 4 CTL
c. Actin regulation at the immune synapse of Clone 4 CTL

In section 6.2.1, the effects of A2aR signalling on the above parameters are examined, and similarly in section 6.2.2 the effect of TIM3 engagement is considered. Finally, section 6.2.3 assesses how engagement of both A2aRs and TIM3 could synergise to inhibit TCR signalling at the level of Lck within Clone 4 CTL.

6.2 Results

6.2.1 Do Adenosine Receptor agonists suppress Clone 4 T cells primed *in vitro*?

6.2.1.1 Treatment with Adenosine Receptor agonists inhibits proliferation of Clone 4 T cells

One measure of suppression of TCR signalling by immunosuppressive receptor engagement is the proliferation of CD8+ T cells in response to TCR stimulation. To determine whether engagement of adenosine receptors directly suppresses TCR signalling amongst Clone 4 T cells *in vitro*, proliferation in response to anti-CD3/28 mAbs was quantified by loss of Celltrace Violet fluorescence in the presence of various adenosine receptor agonists[11].

The data showed that as adenosine is unstable in cell culture, high concentrations of 1.25 mM adenosine were required to suppress the number of highly divided cells within the population (Figure 38 A & B). However, poor cell viability is associated with this high concentration so for further experiments, the pan-adenosine receptor agonist 5-N-Ethylcarboxamidoadenosine (NECA) was utilised. (277-279). Addition of 1 μM or 10 μM NECA at time zero was sufficient to suppress the total proportion of divided Clone 4 cells, as well as the percentage of cells reaching the 5th and 6th divisions of the population (Figure 38C). At these concentrations of NECA, no reduction in cell viability was observed when compared with vehicle-treated control Clone 4 T cells (data not shown). Proliferation of Clone 4 T cells in the presence of NECA was partially restored to control levels by the addition of A2aR-Antagonist (Figure 38C). In experiments in which NECA was added at 24h, 10 μM concentrations were required to suppress the percentage of Clone 4 T cells which had undergone 5 or 6 divisions (Figure 38D). However, proliferation was restored by the addition of A2aR-Antagonist in the presence of 10 μM NECA at 24h. Therefore, these data suggested that addition of the pan-adenosine receptor agonist, NECA, to *in vitro* cell culture results in suppression of Clone 4 T cell proliferation, however, none of the above findings were significant.

It appeared that adding NECA to Clone 4 T cells at various time points and in different

[11] In this chapter, two methods of priming were used. Anti-CD3/28mAb were used for assays of proliferation and co-inhibitory receptor expression. K^{d}HA peptide priming (as used in other chapters) was employed for all other experiments. For consistency with other chapters, *in vitro* primed Clone 4 T cells are only referred to as "CTL" if K^{d}HA peptide priming was used.

concentrations could produce dose-dependent suppression of Clone 4 T cell proliferation. However, Celltrace Violet can only detect a limited number of population divisions, whereas ^{3}H-Thymidine incorporation is fully quantitative. Therefore, to test this hypothesis, ^{3}H-Thymidine assays were used to quantify the proliferation of Clone 4 T cells primed with anti-CD3/28mAb in the presence of various concentrations of NECA.

First, NECA was added to Clone 4 T cells at time zero and cells harvested at 24, 48 and 72h. The results clearly showed that at 24h, cells had not yet proliferated sufficiently to detect any differences between conditions. At 48h, a dose dependent reduction in proliferation of Clone 4 T cells was induced by NECA when compared with vehicle treated Clone 4 T cells. When Clone 4 cells were harvested at 72h, the addition of 1 μM NECA resulted in a significant reduction in Clone 4 cell proliferation when compared with vehicle-treated controls (p=0.01**) and interestingly, 1 μM NECA produced more suppression of proliferation than 10 μM. These findings suggested that lower concentrations of NECA could produce more profound suppression of Clone 4 T cell proliferation than higher concentrations in some contexts. When 100 μM NECA was added to Clone 4 T cells at 0h and cells harvested at 72h, proliferation was significantly suppressed when compared with 1 μM NECA, however cell viability was also reduced in the presence of 100 μM NECA (Figure 39). Therefore, when NECA was added at time zero, 1 μM concentrations produced the greatest suppression of Clone 4 T cell proliferation whilst maintaining Clone 4 T cell viability.

When NECA was added to Clone 4 T cells after 24h in culture, concentrations of 1 μM NECA did not result in suppression of proliferation unless cells were harvested at 72h, suggesting that Clone 4 T cells were required to spend at least 48h in the presence of NECA to be suppressed. In support of this, adding NECA at to Clone 4 cells after 48h in culture, and harvesting at 72h, did not suppress proliferation (Figure 39).

Finally, when 1 μM and 20 μM NECA were added to Clone 4 T cells at time zero in the presence of the specific A2aR-Antagonist ZM241385, and cells were then harvested at 72h, the suppression of Clone 4 T cell proliferation achieved by both concentrations of NECA was successfully eradicated by A2aR-Antagonist. However, these findings were not found to be significant (p = 0.056)(Figure 40).

In summary, the data generated using Celltrace Violet and ^{3}H-Thymidine-based proliferation assays indicate that concentrations as low as 1 μM NECA are sufficient to suppress CD8+ T cell proliferation during *in vitro* culture, however, at least 48h in the presence of NECA is required for suppression to occur. Although NECA is a pan-adenosine receptor agonist, it appears to have a predominantly suppressive effect on CD8+ T cells stimulated by anti-CD3/28 mAb, and suppression can be partly prevented by specifically antagonising inhibitory type-A2a adenosine receptors.

Figure 38 - 5-N-Ethylcarboxamidoadenosine suppresses the proliferation of naïve Clone 4 T cells in vitro as quantified by Flow Cytometry

Clone 4 T cells were primed using Anti-CD3/28mAb and treated with combinations of Adenosine, NECA, the A2aR-Antagonist ZM241385 or DMSO (vehicle). Cells were stained with Celltrace Violet and proliferation control was fixed at 0h to show the fluorescence of naïve cells. N= 5 experiments. (A) Example celltrace violet gating wherein cells were gated on total divided cells and cells that had undergone 5 and 6 population divisions after 72h in culture. (B) Adenosine was added at 0h (p= 0.97 overall MANOVA, p = ns multiple comparisons). (C) NECA was added at 0h (p=0.02* MANOVA, p = ns multiple comparisons). (D) NECA was added at 24h (p = 0.71 overall MANOVA, p = ns multiple comparisons).

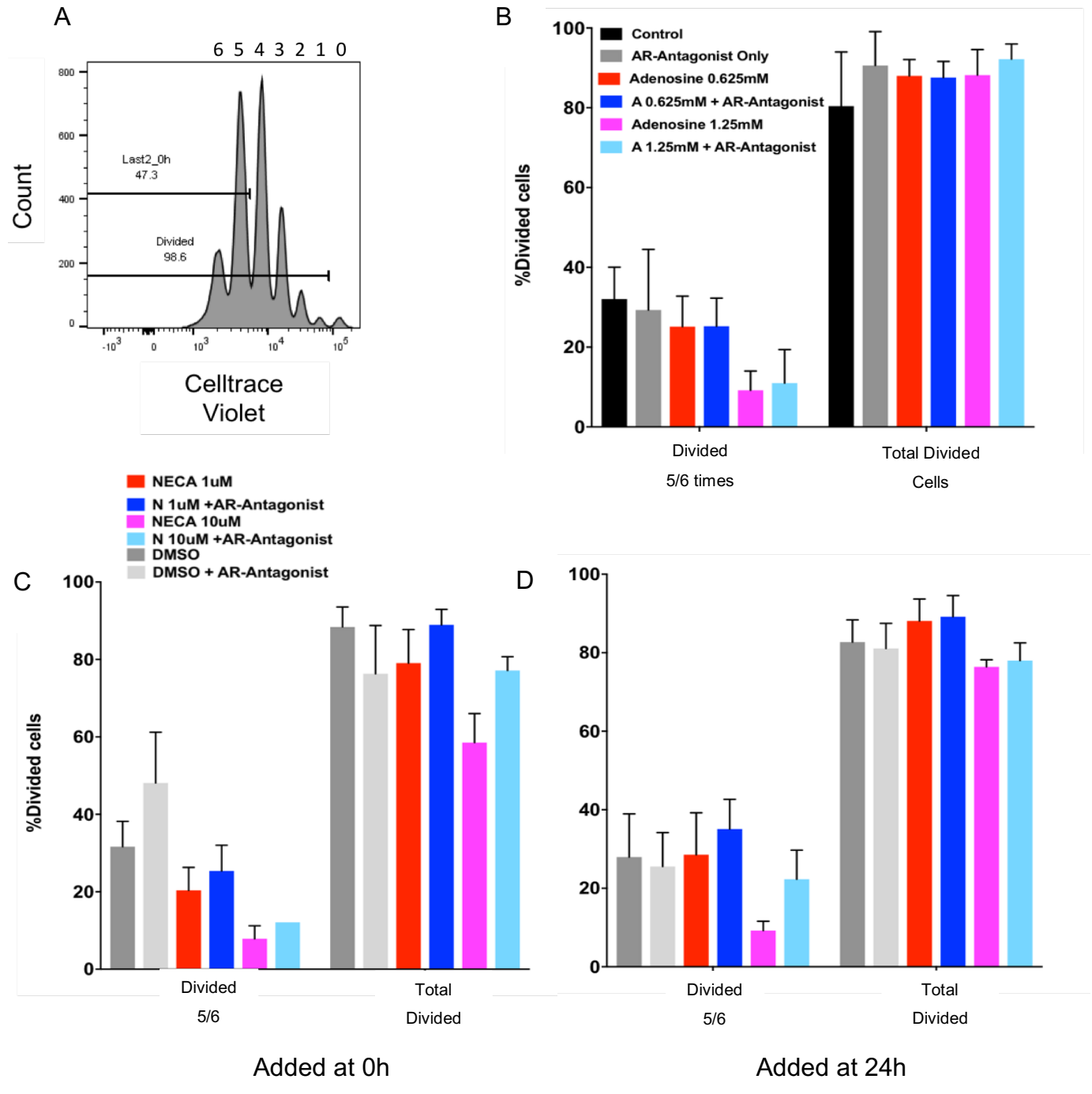

Figure 39 - 5-N-ethylcarboxamidoadenosine suppresses the proliferation of naïve Clone 4 T cells in vitro as quantified by ^{3}H-Thymidine incorporation

Clone 4 T cells were primed using Anti-CD3/28mAb. NECA or DMSO (vehicle) were added to cultures at various times and different concentrations as indicated. ^{3}H-thymidine was added for the final 8h of incubation. Proliferation (cpm) quantified by ^{3}H-thymidine incorporation is shown. One-way ANOVA was used to compare all conditions. Significant p-values are shown, all other comparisons were non-significant. Each column represents mean +/- SEM of 6 replicate wells over 2 separate experiments.

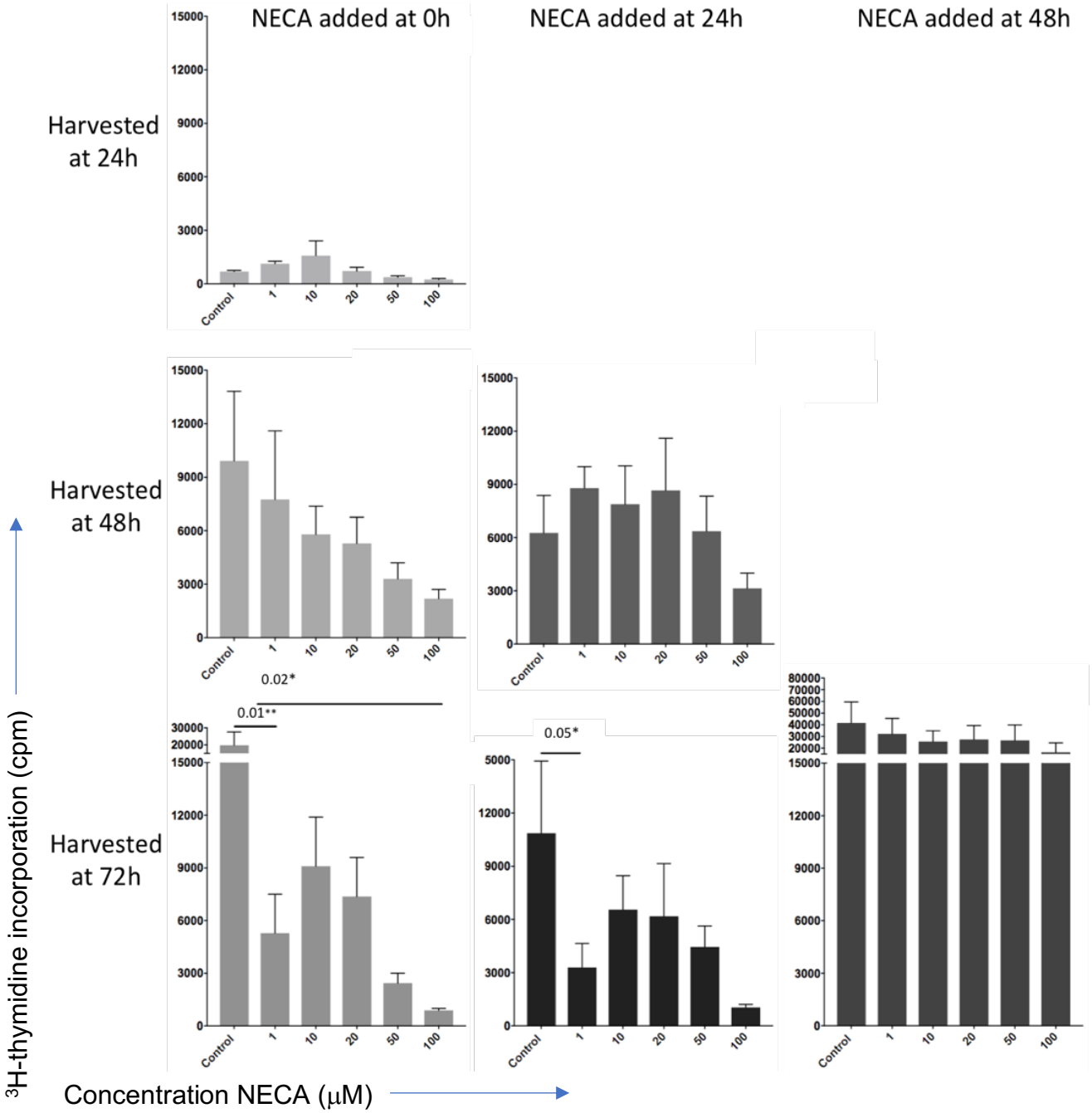

Figure 40 - Suppression of Clone 4 T cell proliferation in the presence of 5-N-ethylcarboxamidoadenosine and A2aR-Antagonist

Clone 4 T cells were primed using Anti-CD3/28mAb. 1 μM or 20 μM NECA +/- 1.25 μM A2aR-Antagonist (ZM241385) was added at 0h. ^{3}H-thymidine was added for the last 8h of cell culture. Proliferation was quantified by ^{3}H-thymidine incorporation (cpm) and compared using Two-way ANOVA (p=0.056 overall, p=ns multiple comparisons).

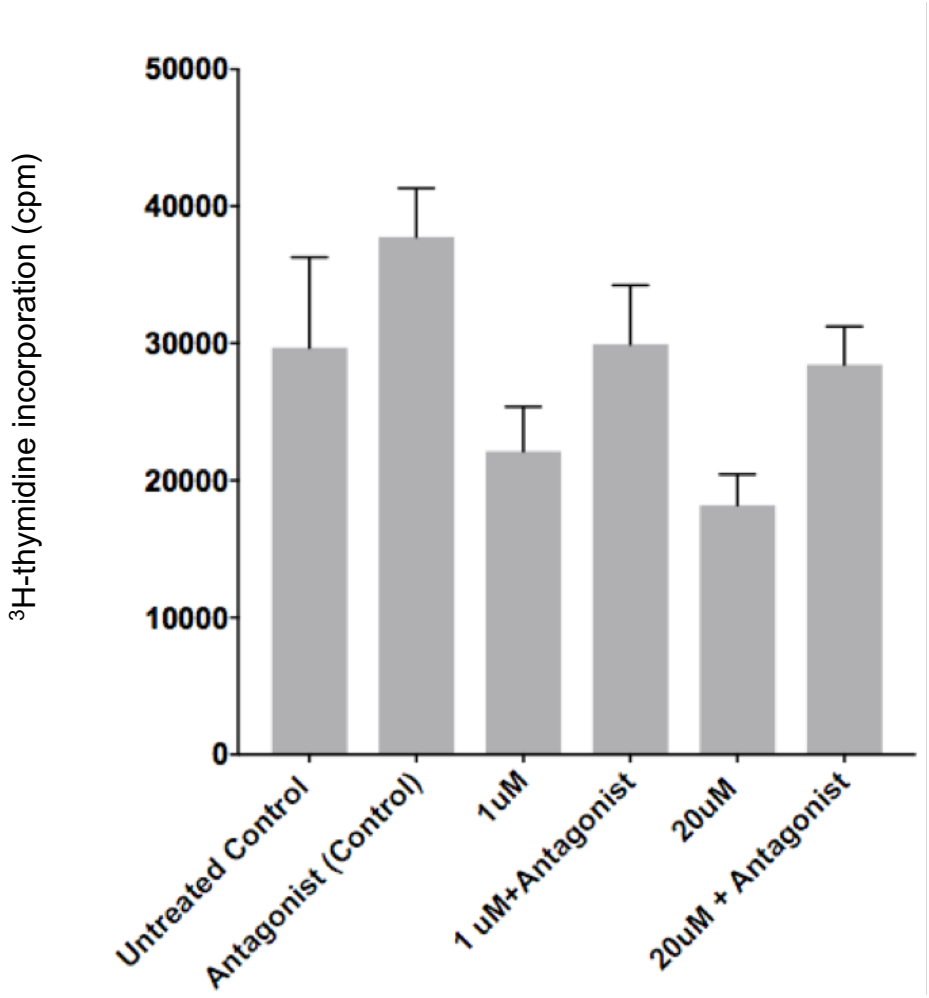

6.2.1.2 Treatment with Adenosine Receptor agonists does not significantly alter Co-Inhibitory Receptor Expression amongst in vitro primed Clone 4 T cells

A2a adenosine receptors are G-protein-coupled receptors which result in elevated cAMP within T cells. Increases in intracellular cAMP have been associated with IL-27 production which can signal in an autocrine manner to promote co-inhibitory receptor (CIR) expression amongst CD8+ T cells (121, 144, 202). We therefore hypothesised that the suppression of proliferation amongst Clone 4 T cells, which was observed in the presence of NECA, could be mediated by upregulation of CIRs at the surface of Clone 4 T cells.

To test this hypothesis, flow cytometry was used to quantify CIR expression amongst Clone 4 T cells primed using anti-CD3/28mAb in the presence of NECA +/- A2aR-Antagonist. The addition of 1 μM NECA at time zero or at 24h did not produce significant alterations in the percentage of Clone 4 T cells expressing TIM3, TIGIT, LAG3 or PD1, when each marker was assessed individually (Figure 41 A & B). Therefore, we chose to assess different combinations of CIR expression (121, 122, 280). Figure 41C shows that the changes which were induced by NECA in an A2aR dependent manner were as follows:

- An increase in the proportion of cells expressing none of the CIRs tested (cf. 2% control, 11% NECA, 1% NECA + A2aR-Antagonist)
- A reduction in the percentage of cells expressing TIGIT, LAG3 and PD-1 together (cf. 50% control, 44% NECA, 58.3% A2aR-Antagonist + NECA)
- An increase in the percentage of cells expressing LAG3 and PD-1 (cf. 19.4% control, 27.7% NECA, 20% NECA + A2aR-Antagonist).

These data suggest that following activation in culture, Clone 4 T cells express co-inhibitory receptors, and that the balance of expression of combinations of CIRs is somewhat affected by A2aR signalling but not significantly.

Figure 41 - 5-N-Ethylcarboxamidoadenosine does not significantly alter co-inhibitory receptor expression amongst CD8+ T cells in vitro

Clone 4 T cells were primed using anti-CD3/28mAb. 1 μM NECA and 1.25 μM specific A2aR-Antagonist ZM241385 were added in DMSO (vehicle) at: (A) 0h or (B) 24h. Cells were cultured for 72h before being harvested and stained with a panel of antibodies specific to CD8, CD3, and TIM3, TIGIT, LAG3 and PD-1. Single (A & B) and combination (C) expression was compared using MANOVA of asin-sqrt transformed data. No comparisons were significant. Percentage of cells expressing combinations of CIRs is indicated numerically on pie chart segments. Unlabelled segments contain <1% of cells. Data shown is mean of N= 3 experiments.

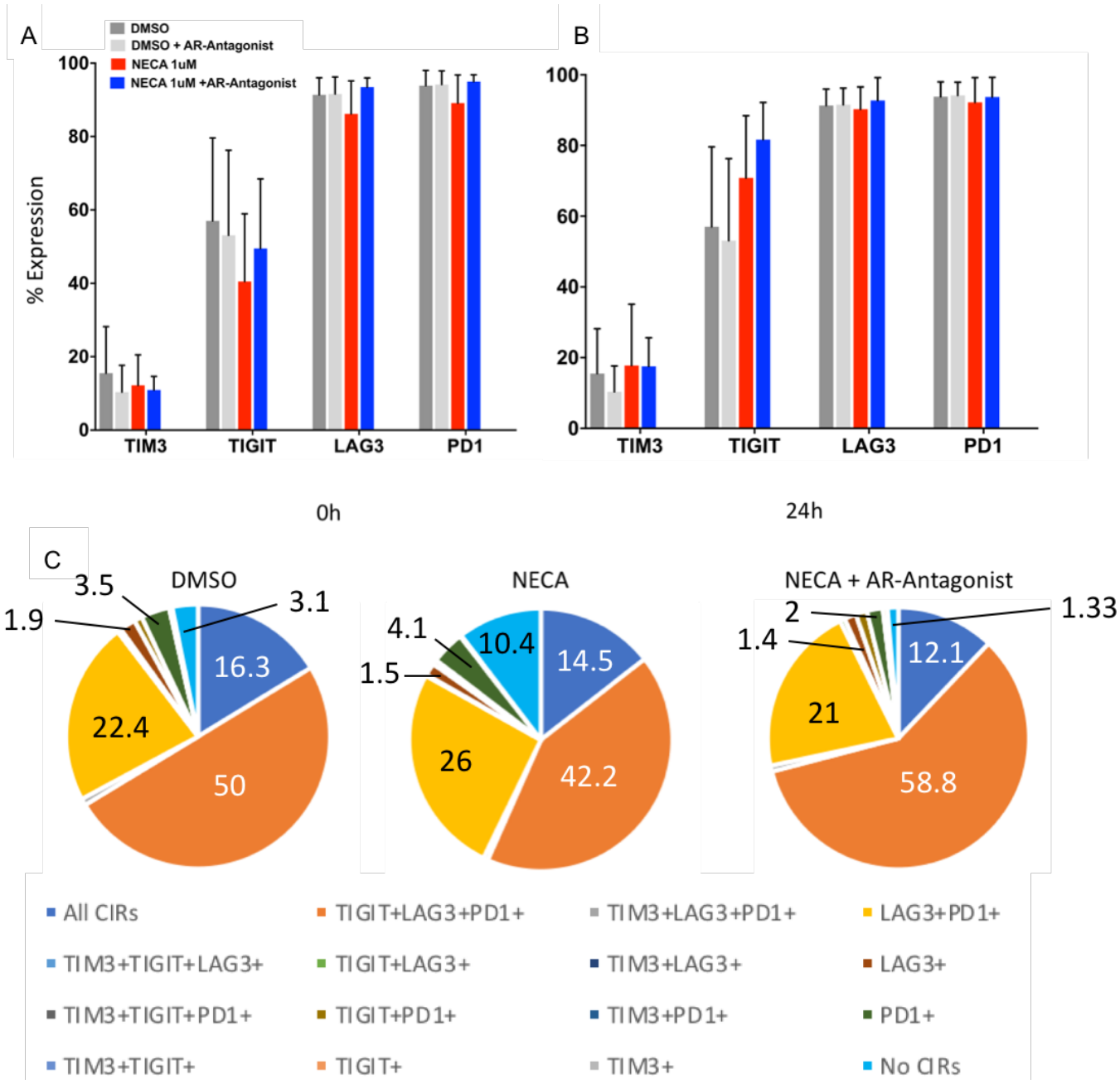

6.2.1.3 Treatment with Adenosine Receptor Agonists does not impair the killing ability of in vitro primed Clone 4 CTL

As the presence of NECA suppressed proliferation of Clone 4 T cells, we hypothesised that A2aR signalling also directly inhibits the cytotoxic effector function of Clone 4 CTL. In support of this hypothesis, data presented in Chapter 5 showed that systemic blockade of A2aRs and TIM3 amongst RencaHA tumour-bearing mice improved the *ex vivo* cytotoxic ability of Clone 4 TILs. To determine if engagement of adenosine receptors by NECA resulted in suppression of killing by *in vitro* primed Clone 4 CTL, microscope-based cytotoxicity assays were performed[12]. The results showed that direct killing of tumour-target cells by *in vitro* primed Clone 4 CTL was unaffected by treatment with 1 μM or 10 μM NECA. Interestingly, the presence of NECA led to enhanced killing, which was elevated still further by the addition of A2aR-Antagonist (Figure 42B & C).

Previous studies in the laboratory have shown that Clone 4 CTL primed *in vitro* express both inhibitory (A2a and A2b) and stimulatory (A1 and A3) adenosine receptor subtypes (Fatemah Basingab, unpublished)(260). Therefore, the pan-adenosine receptor agonist NECA may not suppress the cytotoxic function of *in vitro* primed Clone 4 CTL because it has the capacity to act on both stimulatory as well as inhibitory adenosine receptor subtypes. However, the predominant adenosine receptor subtype expressed in tumours is the inhibitory A2a receptor. This finding suggests that factors found within the TME could promote the upregulation of inhibitory A2a adenosine receptors but not the other AR subtypes (181-184, 194, 195).

The immunosuppressive small molecules PGE_2 and TGFβ, are known to be expressed within immunosuppressive tumour microenvironments. Therefore, we postulated that the addition of these other immunosuppressive factors may increase A2a adenosine receptor expression by Clone 4 CTL relative to other adenosine receptor subtypes, making Clone 4 CTL more susceptible to the suppressive effects of NECA. However, cytotoxicity exerted by Clone 4 CTL

[12] For these experiments, instead of using anti-CD3/28mAb stimulation, Clone 4 CTL were primed using K^dHA peptide and cultured in IL-2 for 5 days. This cell culture protocol allows for the transduction of GFP-tagged signalling intermediates into CTL, therefore it was utilised because imaging of signalling proteins was performed in parallel with cytotoxicity assays.

was not suppressed in the presence of NECA, PGE_2 and TGFβ together (Figure 42D). To further determine whether specific agonism of A2aRs could suppress Clone 4 CTL cytotoxicity, the A2aR-Antagonist CGS2680 was added to culture (281). Although the addition of CGS2680 to culture did result in inhibition of killing by Clone 4 CTL, which was reversed by A2aR blockade, this effect was not significant (Figure 42E).

Another reason that the cytotoxic effector function of Clone 4 CTL was unaffected by agonism of adenosine receptors *in vitro* could be because IL-2 supplementation was added to the cell cultures. IL-2 has been shown to restore the cytotoxic effector function of tumour-suppressed CD8+ TILs in other studies, and it is thought that IL-2 achieves this by lowering the threshold for TCR signal transduction (51). Therefore, to determine whether or not culturing Clone 4 CTL in the presence of NECA but in the absence of IL-2 would result in greater suppression of cytotoxic function, IL-2 was omitted from cell culture. However, this resulted in a decrease in both the overall cell viability and cytotoxicity amongst control Clone 4 CTL in the absence of IL-2 (Figure 42F). As such, viable Clone 4 T cell culture protocols which do not involve IL-2 supplementation should be developed for future experiments.

Figure 42 – Adding Immunosuppressive small molecules to Clone 4 CTL in vitro does not suppress their cytotoxic ability

Clone 4 CTL were primed *in vitro* using K^dHA peptide stimulation and cultured in IL-2 medium unless indicated otherwise. Various immunosuppressive factors or DMSO vehicle were added to cell culture as indicated. Killing of K^dHA-pulsed $RencaHA^{mCherry}$ tumour cells in the presence of Clone CTL was calculated at an E:T ratio of 3:2. Samples were compared using t-test if <2 conditions are compared, and One-way ANOVA if >2 conditions are compared. P-values are indicated. Each point = average value from 4 wells in 1 experimental repeat, conditions analysed in the same repeat are paired.

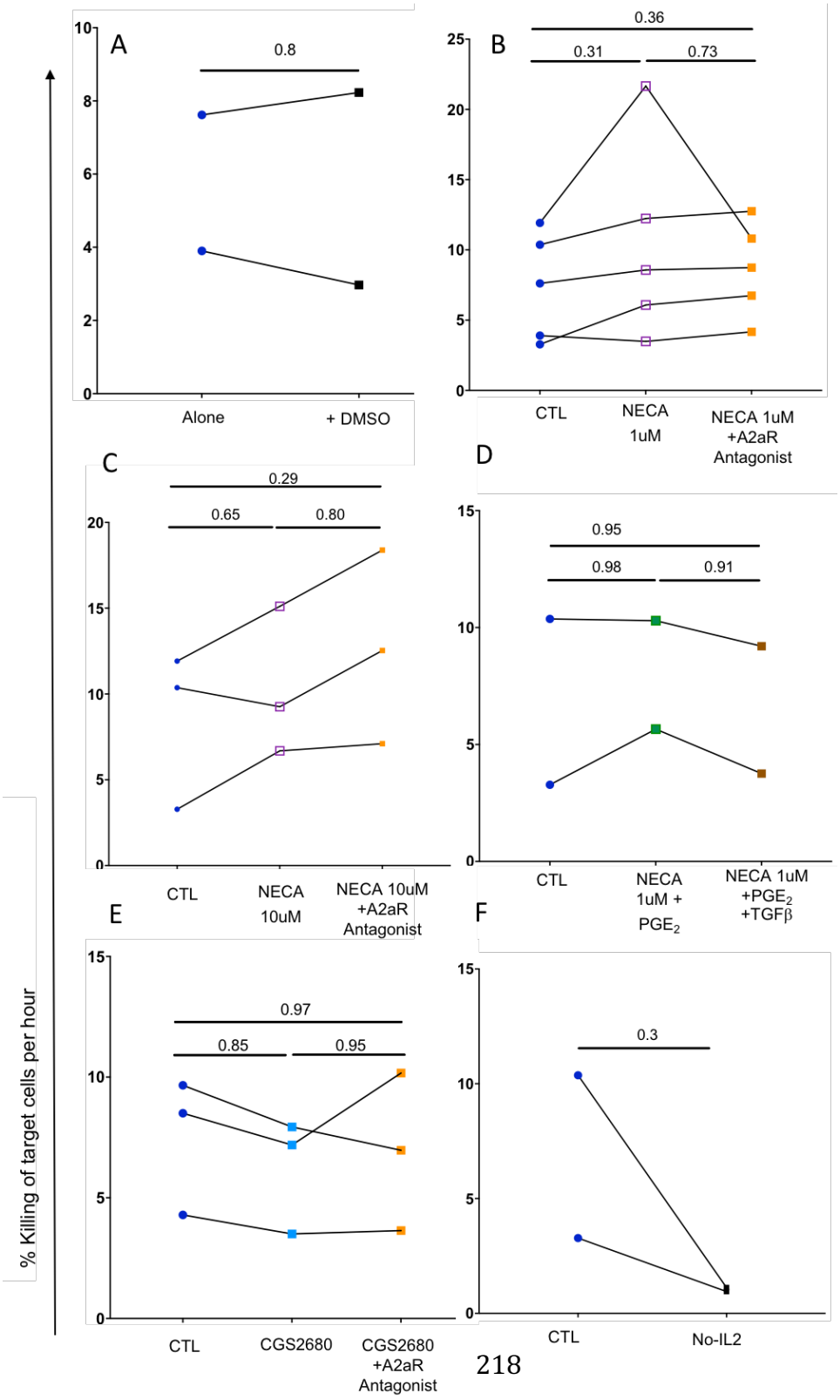

6.2.1.4 Treatment with Adenosine Receptor Agonists impairs both Peripheral Actin ring Maintenance and Actin Clearance at the cSMAC of immune synapses formed by Clone 4 CTL

Another measure of Clone 4 CTL effector function is their ability to mobilise actin after TCR engagement. Data presented in Chapter 5 considered two models of actin regulation, the 'Actin Maintenance Model' and the 'Actin Clearance Model' which postulate different requirements for actin behaviour at the CTL immune synapse in order to permit the delivery of cytolytic granules to target cells (Introduction, Figure 43). The Actin Maintenance model suggests that formation and maintenance of a peripheral actin ring is required to achieve stable immune synapses between CTL and target cells. The Actin Clearance model suggests that the stability of the immune synapse is less important than clearance of actin from the cSMAC to permit cytotoxic granule release. Both actin ring maintenance and actin clearance from the cSMAC were improved amongst Clone 4 TILs from RencaHA tumour-bearing mice which had received systemic A2aR blockade. Therefore, we hypothesised that direct engagement of A2a adenosine receptors on Clone 4 CTL by NECA could inhibit actin ring maintenance and actin clearance at the immune synapse. Live cell imaging approaches were employed to test this hypothesis by quantifying the percentage of cell couples accumulating F-tractin at the immune synapse in different patterns (as shown in Introduction, Figure 6 and Chapter 5 Figures 34, 35 and 36).

The Actin Maintenance Model: Addition of NECA to Clone 4 CTL in culture impairs peripheral actin ring maintenance and immune synapse stability

To test whether the requirements of the Actin Maintenance Model were disrupted by engagement of adenosine receptors expressed on Clone 4 CTL, peripheral actin ring maintenance and immune synapse stability were quantified during immune synapse formation between Clone 4 CTL and Renca tumour target cells.

First, experiments were carried out to compare two measures of immune synapse stability, Off-interface Lamellae (Off-L) and translocation, between NECA-treated Clone 4 CTL and untreated control CTL. Both of these parameters are quantified based upon the morphology of cell couples formed between Clone 4 TILs and RencaHA targets, imaged using confocal microscopy. Off-L are functionless actin-mediated projections directed away from the immune synapse and translocation is the movement of Clone 4 CTL away from the site of immune synapse formation relative to the target cell. (Chapter 5, Figure 36).

Earlier times of Off-L formation are indicative of immune synapse instability, hence Off-L formation was compared using a Mantel-Cox survival analysis. In control CTL, 77% of couples do not form any Off-L within the coupling period, indicating stable contact with target cells. The percentage of CTL couples surviving without Off-L was significantly reduced amongst both concentrations of NECA-treated cells ($p < 0.0001$****). Adding A2aR-Antagonist to Clone 4 CTL in the presence of NECA resulted in a significant improvement in the time of survival before Off-L ($p<0.0001$****), however survival amongst CTL in the presence of both NECA and A2aR-Antagonist remained lower than amongst untreated CTL ($p<0.0001$****)(Figure 43A). These findings suggested that Clone 4 CTL cultured in the presence of NECA exhibited more unstable immune synapses when compared with untreated control CTL, because their immune synapse survives for s shorter time before Off-L formation occurs.

As discussed, the presence of other immunosuppressive pathways such as PGE_2 could render Clone 4 CTL more susceptible to the suppressive effects of NECA, by causing them to express higher levels of immunosuppressive A2aRs relative to immunostimulatory A1 and A3 adenosine receptors (1, 14-18). Therefore Off-L formation was quantified when PGE_2 was added to Clone 4 CTL. Adding PGE_2 to culture, either alone or with NECA, resulted in earlier Off-L formation by CTL, although survival without off L in the presence of both NECA and PGE_2 was not significantly lower than NECA treatment alone (Figure 43A; $p=0.4$). These results suggest that adding either NECA or PGE_2 to cultures of Clone 4 CTL inhibits the stability of immune synapses formed by Clone 4 CTL, but that adding both NECA and PGE_2 together does not have an additive effect.

Translocation of Clone 4 CTL away from the original site of immune synapse formation is another measure of immune synapse instability. Treatment of Clone 4 CTL with either 1 μM or 10 μM NECA resulted in increased translocation amongst Clone CTL couples when compared with untreated CTL ($p<0.0001$****). Levels of translocation were successfully restored to control levels when both NECA and A2aR-Antagonist were added to cultures of Clone 4 CTL. Treatment of Clone 4 CTL with PGE_2 also increased levels of translocation amongst CTL couples when compared with untreated CTL ($p<0.0001$****). However addition of PGE_2 to Clone 4 CTL in culture did not result in a significant increase in translocation when compared with adding 10 μM NECA ($p= 0.43$); nor did combined treatment with NECA and PGE_2 produce more translocation than NECA 10 μM alone ($p>0.99$) (Figure 43B). These data therefore suggest that

treatment of Clone 4 CTL with NECA *in vitro* suppresses immune synapse stability, because a greater percentage of CTL translocate over the surface of the APC in the presence of NECA when compared with untreated control CTL. The presence of PGE_2 also results in increased translocation amongst Clone 4 CTL, but treating CTL with both NECA and PGE_2 does not produce a synergistic increase in translocation by CTL.

Figure 43 –5-N-Ethylcarboxamidoadenosine significantly reduces the stability of immune synapses formed between Clone 4 CTL and Renca tumour cell targets

Clone 4 CTL were primed *in vitro* and treated with NECA, A2aR-Antagonist and PGE_2 as indicated. Immune synapse formation between Clone 4 CTL and K^dHA-pulsed Renca tumour cell targets was imaged using confocal microscopy. (A) Shows survival until formation of first Off-L was compared between conditions using a Kaplein-Mayer survival analysis (Log Rank). Significant comparisons are shown, all other comparisons were not significant. (B) Shows the percentage of cell couples in which translocation occurs was compared using One Way ANOVA. All comparisons were significant (p< 0.0001****) unless indicated. N>30 cell couples per condition over 2-4 experiments[13].

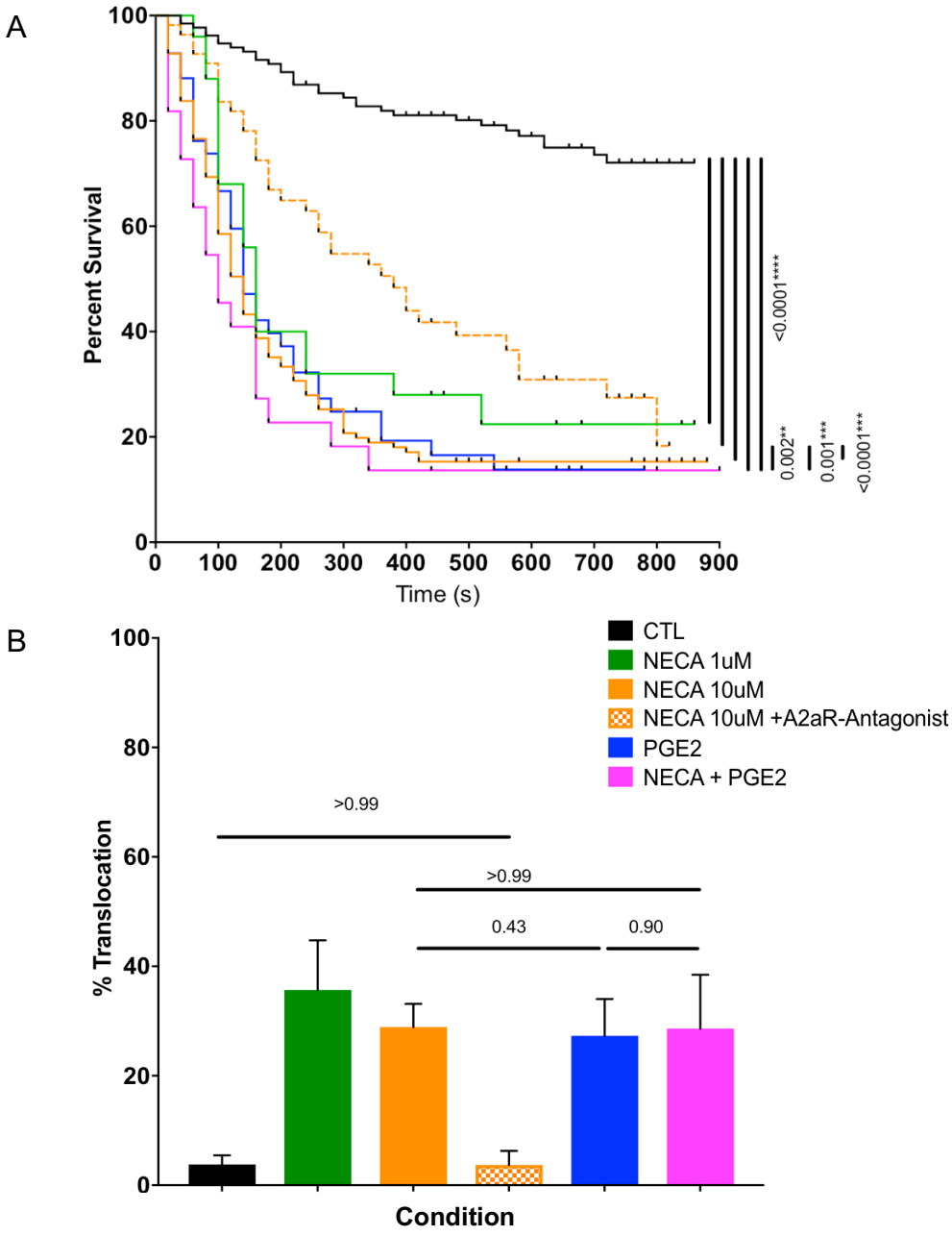

[13] Data from untreated CTL was provided by Rachel Ambler as a reference data set for the Wuelfing lab and re-analysed by GE.

Immune synapse stability amongst *in vitro* primed Clone 4 CTL was reduced when NECA was added to cell culture. The Actin Maintenance model suggests that low immune synapse stability is associated with a poorly maintained actin ring at the pSMAC of the CTL immune synapse. Therefore, we hypothesised that NECA-treated Clone 4 CTL could also fail to maintain a peripheral actin ring at the immune synapse. Live cell imaging was used to determine the percentage of *in vitro* primed NECA-treated Clone 4 CTL with accumulation of peripheral F-tractin at the immune synapse.

At early timepoints, between 0-40s from immune synapse formation, treatment with NECA led to a reduction in peripheral F-tractin accumulation by Clone 4 CTL, in a dose dependent manner, when compared with untreated CTL. Therefore between 0-40s of immune synapse formation, peripheral actin localisation amongst 1 μM and 10 μM NECA-treated Clone 4 CTL was suppressed to levels as low as that shown amongst TILs (Figure 44A & B; p=0.39).

At later timepoints, after 180s, NECA treatment also resulted in a dose-dependent reduction in the percentage of CTL which maintained a peripheral actin ring at the IS, when compared with untreated control CTL ($p<0.0001$**** 180s). Thus, the number of NECA-treated CTL which maintained a peripheral actin ring at such later timepoints was not significantly higher than TILs (Figure 44 A & B; p=0.06 at 180s).

The addition of A2aR-Antagonist to cell culture in the presence of 10 μM NECA resulted in a significant improvement in the percentage of CTL forming a peripheral actin ring between 0-60s when compared with CTL treated with 10 μM NECA alone ($p<0.001$***). However, after 180s, peripheral actin ring maintenance amongst Clone 4 CTL treated with 10 μM NECA plus A2aR-Antagonist was not significantly improved when compared to CTL treated with NECA alone (Figure 44A & B). Thus, the results clearly show that culturing Clone 4 CTL in the presence of NECA causes a significant reduction in their ability to form a peripheral actin ring at early timepoints after immune synapse formation, and an inability to maintain that actin ring across later timepoints. The addition of specific A2aR-Antagonist improved, but could not completely restore the peripheral actin ring maintenance amongst Clone 4 CTL exposed to 10 μM NECA *in vitro*.

Figure 44 –5-N-Ethylcarboxamidoadenosine reduces the percentage of Clone 4 CTL which maintain a Peripheral Actin Ring at the Immune Synapse

Clone 4 CTL were primed *in vitro* and transduced with F-tractin. Cells were treated with NECA, A2aR-Antagonist (ZM) and PGE_2 as indicated or ATT into RencaHA tumour-bearing mice to generate TILs. Cells were harvested and immune synapse formation between TILs or *in vitro* primed CTL and K^dHA-pulsed Renca tumour cell targets was imaged *ex vivo* using confocal microscopy. Analyses of the accumulation of f-tractin were performed in >30 cell couples per condition, across 2-4 experiments. (A) The percentage of couples which expressed a peripheral actin ring was quantified. (B) The percentage of couples with peripheral f-tractin accumulation was compared between conditions using proportional z-test. Darker cells indicate smaller p-values.[14] (C) Computer modelling was used to illustrate the average location of accumulation F-tractin within CTL by pooling all images in each data set. Representative images of accumulation are shown using a pseudocolour scale with lighter colours representing more F-tractin.

A.

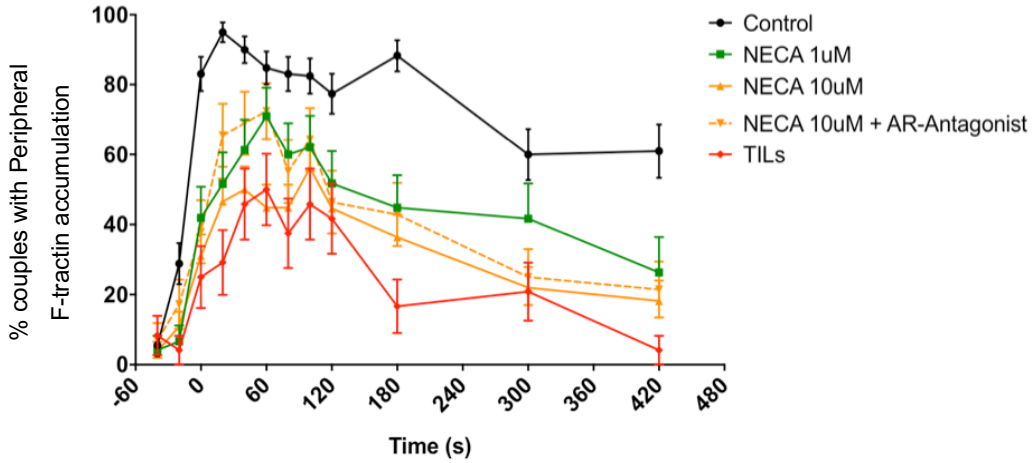

B.

Time	-40	-20	0	20	40	60	80	100	120	180	300	420
CTL vs NECA 1uM	0.76	0.03	0.0002	<0.0001	0.003	0.2	0.03	0.07	0.03	<0.0001	0.23	0.03
	ns	*	***	****	**	ns	*	ns	*	****	ns	*
CTL vs NECA 10uM	0.97	0.03	<0.0001	<0.0001	<0.0001	<0.0001	<0.0001	0.004	0.001	<0.0001	<0.0001	<0.0001
	ns	*	****	****	****	****	****	**	***	****	****	****
NECA 10uM vs NECA 1uM	0.57	0.30	0.42	0.82	0.43	0.03	0.26	0.76	0.70	0.60	0.14	0.69
	ns	ns	ns	ns	ns	*	ns	ns	ns	ns	ns	ns
CTL vs NECA 10uM + ZM	0.47	0.36	<0.0001	0.0007	0.03	0.3	0.01	0.11	0.01	<0.0001	0.001	0.003
	ns	ns	****	***	*	ns	**	ns	**	****	****	***
NECA10uM vs NECA10uM + ZM	0.25	0.25	0.37	0.06	0.06	0.01	0.26	0.34	0.70	0.42	0.56	0.52
	ns	ns	ns	ns	ns	**	ns	ns	ns	ns	ns	ns
CTL vs TILs	0.33	0.03	<0.0001	<0.0001	<0.0001	0.0003	<0.0001	0.002	0.005	<0.0001	0.004	<0.0001
	ns	*	****	****	****	***	****	**	**	****	**	****
TILs vs NECA 1uM	0.23	0.84	0.31	0.16	0.39	0.19	0.17	0.37	0.65	0.06	0.21	0.10
	ns	ns	ns	ns	ns	ns	ns	ns	ns	ns	ns	ns
TILs vs NECA 10uM	0.17	0.58	0.78	0.22	0.92	0.50	0.72	0.55	1.00	0.14	0.85	0.21
	ns	ns	ns	ns	ns	ns	ns	ns	ns	ns	ns	ns
TILs vs NECA 10uM + ZM	0.47	0.28	0.48	0.02	0.16	0.16	0.31	0.30	0.95	0.08	0.98	0.16
	ns	ns	ns	*	ns	ns	ns	ns	ns	ns	ns	ns

[14] Data for control CTL was generated by Rachel Ambler as a reference data set for the Wuelfing lab and re-analysed by GE.

C.

CTL

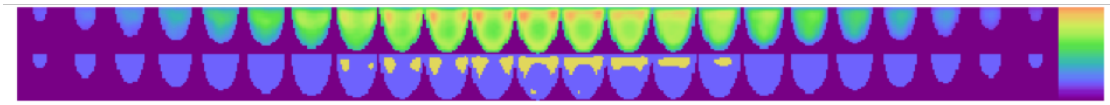

NECA 10uM

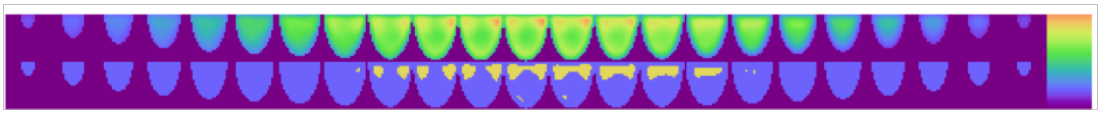

NECA 10uM + AR-Antagonist

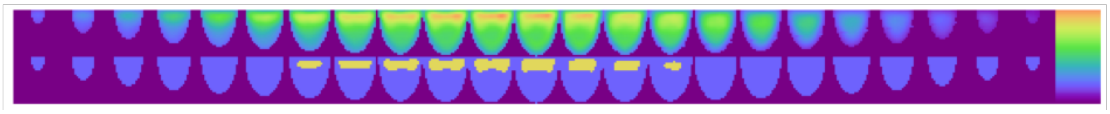

Impaired Peripheral Cofilin localisation is associated with impaired Peripheral Actin ring formation at the immune synapse

Assembly of peripheral actin at the immune synapse is regulated by cofilin. As the addition of NECA to cultures of Clone 4 CTL *in vitro*, affected their ability to form a peripheral actin ring, at the immune synapse, we therefore hypothesised that the correct accumulation of cofilin at the immune synapse could also be altered by the addition of NECA to Clone 4 CTL. To test this hypothesis, the localisation of cofilin^{GFP} in a peripheral pattern was quantified during immune synapse formation by CTL, using live cell imaging. In untreated control Clone 4 CTL, peripheral cofilin accumulation occurred in two phases: (i) initial elevation of peripheral cofilin, and (ii) cofilin decline from 60s onwards. The early increase in peripheral cofilin could be required at the pSMAC, because cofilin generates new barbed ends for polymerisation of F-actin. However, peripheral cofilin decline is then necessary to ensure peripheral actin ring maintenance after 60s, since the peripheral actin ring would be constantly broken down by cofilin if it remained at the pSMAC (76, 77).

The results show that amongst TILs, the percentage of cell couples with early cofilin accumulation is comparable to CTL between 0-40s ($p=0.51$). However, from 40s onwards, peripheral cofilin accumulation fails to decline amongst TIL couples and the number of TILs with peripheral cofilin accumulation remains significantly higher than amongst untreated CTL (Figure 45A & B; $p<0.0001$****). Therefore, the main difference which was observed between Clone 4 CTL and Clone 4 TILs is a failure of peripheral cofilin levels to decline at late timepoints. This finding suggests that within TILs, cofilin may continue disassembling actin at the pSMAC, resulting in poor peripheral actin-ring maintenance and immune synapse instability (Figure 45A & B)(76).

When peripheral cofilin accumulation was quantified amongst NECA-treated CTL, significantly fewer NECA-treated Clone 4 CTL couples accumulated peripheral cofilin when compared with untreated CTL or TILs between 0-40s ($p<0.0001$****). Therefore, the results showed that the initial peak of peripheral cofilin accumulation amongst CTL appeared to be attenuated by NECA treatment. After 40s, the percentage of cell couples accumulating cofilin peripherally reached lower levels amongst NECA-treated CTL when compared with TILs but not when compared with CTL (Figure 45A & B). Therefore, the data showed that decline of peripheral cofilin accumulation occurred better amongst NECA-treated CTL when compared with TILs.

The addition of specific A2aR-Antagonist to cell culture, in the presence of 10 μM NECA, restored the ability of Clone 4 CTL to accumulate peripheral cofilin between 0-40s, such that the percentage of NECA plus A2aR-Antagonist-treated CTL which accumulated peripheral cofilin was not significantly lower than untreated control CTL between 0-40s (p=0.52). At later timepoints, after 40s from immune synapse formation, peripheral cofilin accumulation remained significantly higher amongst cells treated with NECA plus A2aR-Antagonist when compared with untreated control CTL but it was significantly lower when compared to TILs (p= 0.006**, p+ 0.003** respectively). Overall the data suggest that amongst untreated Clone 4 CTL, peripheral cofilin accumulation peaks at 20-40s and then declines. In TILs the peak of cofilin accumulation is intact but the decline is attenuated. Amongst NECA-treated CTL the cofilin peak is lacking, therefore the decline cannot be assessed fully because there is little peripheral cofilin accumulation to begin with. However, the levels of decline appear to be intermediate, with peripheral cofilin accumulation remaining higher than CTL, but lower than TILs. Treatment with A2aR-Antagonist in the presence of NECA results in restoration of the peak of peripheral cofilin accumulation amongst Clone 4 CTL when compared with controls but the decline is unaffected.

PGE_2 is another immunosuppressive mediator found within RencaHA tumours. The expression of A2aRs amongst CD8+ TILs has been shown to be elevated when compared to CD8+ CTL primed *in vitro*, because factors within the TME cause A2aRs to be upregulated (140, 184, 238). Therefore, we hypothesised that the presence of PGE_2 could potentially increase the expression of A2aRs amongst CTL, making them more susceptible to suppression by NECA. However, the addition of PGE_2 did not produce an additive suppression of initial cofilin accumulation when compared with NECA alone (Figure 45A). This finding is in concordance with previous data which indicates that adding both PGE_2 and NECA to Clone 4 CTL does not synergistically inhibit cytotoxicity, peripheral actin ring formation or immune synapse stability.

Figure 45 - 5-N-Ethylcarboxamidoadenosine reduces the percentage of Clone 4 CTL accumulating Peripheral Cofilin at the immune synapse

Clone 4 CTL were primed *in vitro* and transduced with cofilin. Cells were treated with NECA, A2aR-Antagonist and PGE_2, or ATT into RencaHA tumour-bearing mice to generate TILs. Cells were harvested and immune synapse formation between TILs or CTL and K^dHA-pulsed Renca tumour cell targets was imaged *ex vivo* using confocal microscopy. Analyses of the accumulation of cofilin were performed in >30 cell couples per condition, across 2-4 experiments. (A) The percentage of couples which expressed Peripheral cofilin was quantified. (B) Percentage of couples expressing peripheral cofilin was compared between conditions using proportional z-test. Darker cells indicate smaller p-values.[15]

A

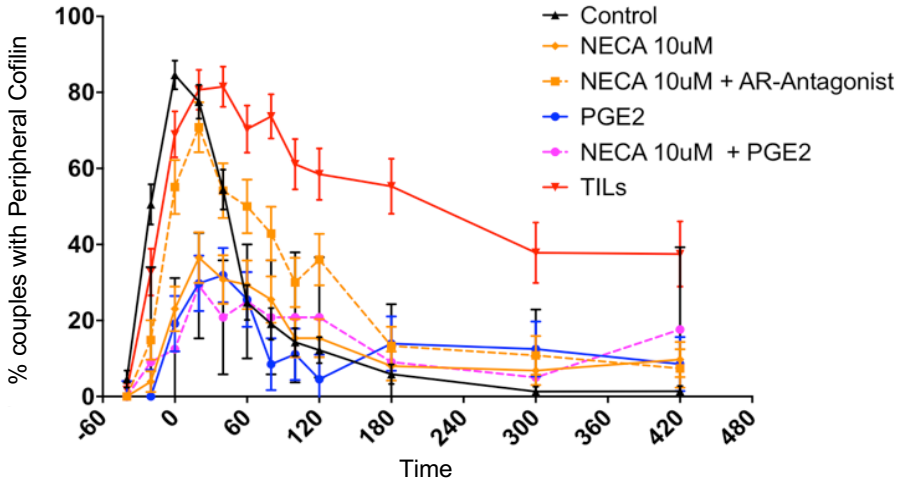

B

Time	-40	-20	0	20	40	60	80	100	120	180	300	420
CTL vs NECA 10uM	0.32	<0.0001	<0.0001	<0.0001	0.01	0.42	0.27	0.67	0.43	0.40	0.03	0.01
	ns	****	****	****	**	ns	ns	ns	ns	ns	*	**
CTL vs NECA 10uM +AR-Antagonist	0.32	<0.0001	0.0003	0.51	0.88	0.001	0.001	0.01	0.0004	0.07	0.006	0.03
	ns	****	***	ns	ns	***	***	**	***	ns	**	*
CTL vs PGE_2	0.39	<0.0001	<0.0001	<0.0001	0.02	0.75	0.17	0.81	0.27	0.06	0.003	0.06
		****	****	****	*	ns	ns	ns	ns	ns	**	ns
CTL vs NECA 10uM + PGE2	0.70	0.001	<0.0001	<0.0001	0.007	0.77	0.63	0.27	0.16	0.30	0.06	0.0004
		**	****	****	**	ns	ns	ns	ns	ns	ns	***
NECA 10uM vs NECA 10uM + AR-antagonist	<0.0001	0.13	0.002	0.001	0.03	0.06	0.10	0.13	0.03	0.61	0.81	0.44
	****	ns	**	***	*	ns	ns	ns	*	ns	ns	ns
NECA 10uM vs NECA + PGE_2	na	0.15	0.44	0.71	0.53	0.90	0.88	0.36	0.36	0.54	0.78	0.20
	na	ns	ns	ns	ns	ns	ns	ns	ns	ns	ns	ns
CTL vs TILs	0.64	0.05	0.04	0.51	0.001	<0.0001	<0.0001	<0.0001	<0.0001	<0.0001	<0.0001	<0.0001
	ns	*	*	ns	***	****	****	****	****	****	****	****
TILs vs NECA 10uM	0.05	<0.0001	<0.0001	<0.0001	<0.0001	<0.0001	<0.0001	<0.0001	<0.0001	<0.0001	0.0002	0.002
	*	****	****	****	****	****	****	****	****	****	***	**
TILs vs NECA 10uM + AR-Antagonist	0.05	0.02	0.09	0.16	0.001	0.02	0.001	0.001	0.01	<0.0001	0.003	0.003
	*	*	ns	ns	***	**	***	***	**	****	**	**

[15] Data for control CTL was generated by Rachel Ambler as a reference data set for the Wuelfing lab and re-analysed by GE.

In summary, NECA-treated CTL exhibit attenuated peripheral actin ring maintenance at timepoints after 180s from immune synapse formation, and this phenotype is also observed amongst TILs. However, the peripheral accumulation of cofilin at the immune synapse between 0-40s is much lower amongst NECA-treated CTL when compared with TILs. Quantification of Off-L and translocation amongst NECA-treated CTL couples indicates that the disturbances in F-tractin and cofilin induced by NECA treatment are associated with significantly reduced immune synapse stability when compared with untreated CTL. Although, amongst cells cultured with NECA plus A2aR-Antagonist, the phenotype of F-tractin, cofilin and Off-interface lamellae was partially restored to resemble untreated CTL, immune synapse stability as measured by translocation was completely restored.

The Actin Clearance Model: Addition of NECA to cell culture impairs Actin clearance from the cSMAC of in vitro primed Clone 4 CTL

CTL which were treated with NECA exhibited suppressed actin regulation according to the Actin Maintenance model (Figure 43, Figure 44, Figure 45). However, CTL were able to kill tumour target cells after NECA treatment (Figure 42). Thus, perturbation of actin as described by the Actin Maintenance model is not always associated with a loss of cytotoxic ability. We therefore hypothesised that the Actin Clearance model could perhaps better explain the relationship between actin and killing in CTL, than the Actin Maintenance model could. The Actin Clearance model states that even if the peripheral actin ring is poorly maintained, as long as actin is not covering the cSMAC, granule release and killing by CTL can proceed. Therefore, we hypothesised that actin clearance from the cSMAC would be intact amongst NECA-treated Clone 4 CTL, because they are able to kill tumour cell targets (71).

To quantify actin clearance amongst NECA-treated Clone 4 CTL, imaging data from Figure 44 were re-analysed as follows:

- The percentage of cell couples exhibiting central, lamellal and diffuse actin patterns at each timepoint were combined to determine the proportion of couples with 'Obstructive' patterning, these patterns involve actin covering the interface, which could prevent cytotoxic granule release.
- The proportion of couples with peripheral or asymmetric patterning was combined to generate the number of couples with 'Permissive' actin, these patterns involve clearance of actin from the cSMAC, which should allow cytotoxic granules to pass through (Introduction, Figure 6) (71).

The data showed that when 1 μM or 10 μM NECA-treated Clone 4 CTL were compared with untreated control Clone 4 CTL, obstructive actin patterning was significantly elevated, at both early (20-40s), and late (100-180s) timepoints (p=0.006** p=0.003** respectively). Treatment with NECA 10 μM plus A2aR-Antagonist did not lower obstructive actin, and actually significantly exacerbated obstructive actin patterning amongst CTL when compared with treatment using 10 μM NECA alone (p=0.002** at time zero). However, between 300-420s, obstructive actin patterning amongst NECA plus A2aR-Antagonist-treated cells had reduced such that obstructive patterning did not significantly exceed the levels of untreated control CTL (p = 0.62). Interestingly, at all timepoints, obstructive actin amongst TILs was not significantly higher or lower than Clone 4 CTL treated with NECA and A2aR-Antagonist (Figure 46 A & C). Therefore, the results suggest that obstructive actin patterning at the immune synapse of Clone 4 CTL was elevated in the presence of NECA, but that this effect was only A2aR-dependent at timepoints after 300s from immune synapse formation.

Treatment with NECA resulted in a dose-dependent reduction in permissive actin patterning amongst NECA-treated Clone 4 CTL when compared with Control CTL at all timepoints. The most significant reduction in permissive patterning occurred between 0-40s (p < 0.0001****). Treatment with 10 μM NECA plus A2aR-Antagonist resulted in significantly elevated permissive actin at 40-60s when compared with 10 μM NECA alone (p=0.05*). Permissive actin accumulation amongst TILs was not significantly different to 10 μM NECA-treated CTL at any timepoint (Figure 46 B & D). These findings therefore suggest that NECA could exert a suppressive effect on permissive actin accumulation by Clone 4 CTL between 0-60s, and that this effect is A2aR dependent.

Overall, NECA treatment perturbed both actin clearance at the cSMAC and actin maintenance at the pSMAC but it did not inhibit killing by Clone 4 CTL. Therefore, neither the Actin Clearance Model nor the Actin Maintenance Model fully explain the link between actin localisation at the immune synapse and Clone 4 CTL killing ability. Further studies are required to determine the actin patterns that are linked to cytotoxicity in Clone 4 CTL (Section 6.3.5).

Figure 46 - 5-N-Ethylcarboxamidoadenosine increases Obstructive Actin and reduces Permissive patterning amongst Clone 4 CTL

Clone 4 CTL were primed *in vitro* and transduced with cofilin. Cells were treated with NECA, A2aR-Antagonist and PGE_2, or ATT into RencaHA tumour-bearing mice to generate TILs. Cells were harvested and immune synapse formation between TILs or CTL and K^dHA-pulsed Renca tumour cell targets was imaged *ex vivo* using confocal microscopy. Analyses of the accumulation of f-tractin was performed in >30 cell couples per condition, across 2-4 experiments. The percentage of couples which expressed: (A) obstructive and (B) permissive actin patterns were quantified as described in Figure 6 and the proportions of cells expressing these patterns were compared using proportional z test, darker cells indicate smaller p-values (C: Obstructive and D: Permissive)[16].

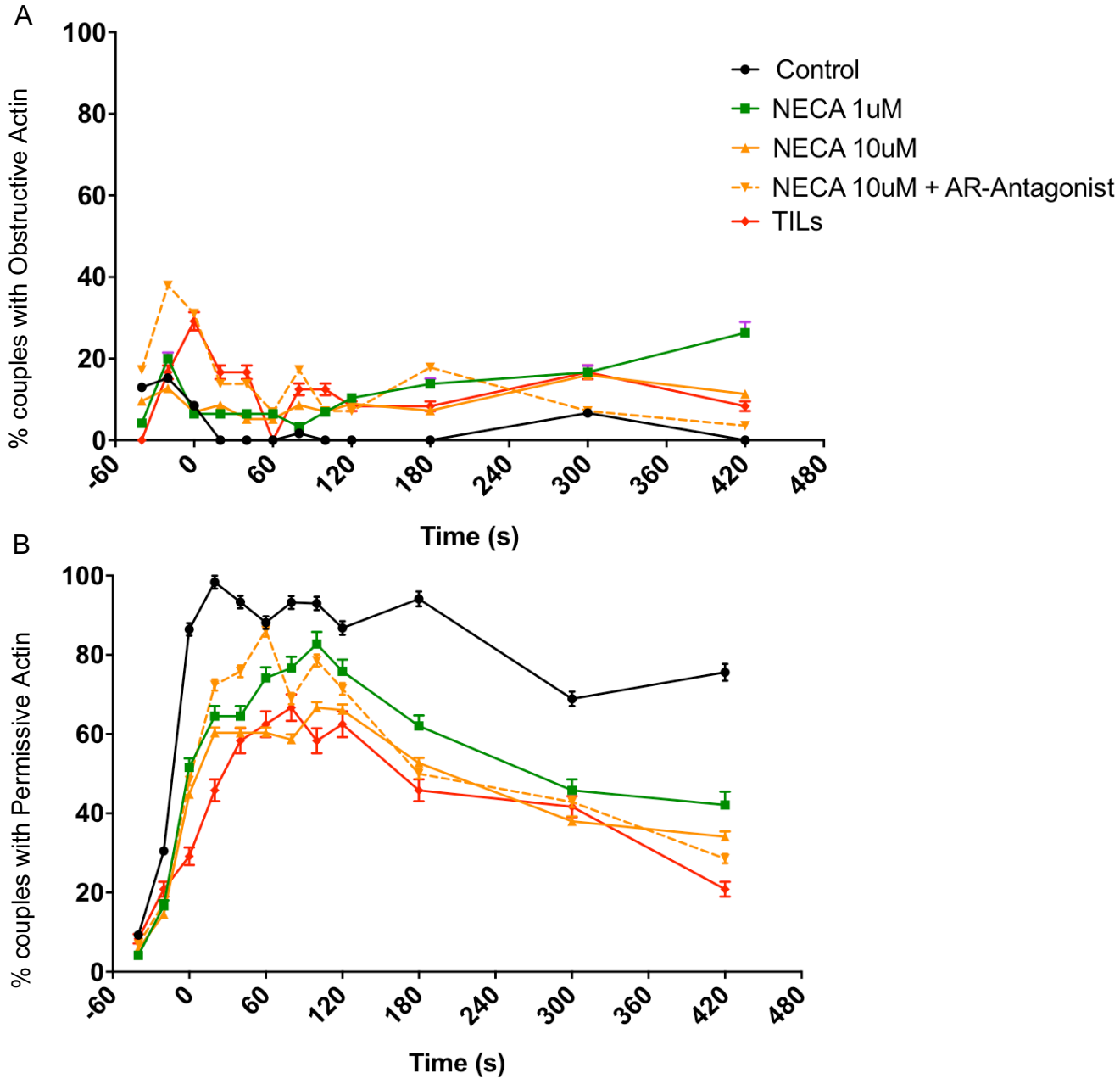

[16] Data for control CTL and control TILs were generated by Rachel Ambler as a reference data set for the Wuelfing lab and re-analysed by GE to allow blinded comparisons

C

Time	-40	-20	0	20	40	60	80	100	120	180	300	420
CTL vs NECA 1uM	0.44	0.40	0.94	0.006	0.006	0.006	0.21	0.01	0.003	0.001	0.08	<0.0001
	ns	ns	ns	**	**	**	ns	**	**	***	ns	****
CTL vs NECA 10uM	0.81	0.91	1.00	0.01	0.01	0.02	0.03	0.01	0.01	0.01	0.1	0.01
	ns	ns	ns	**	**	*	*	**	**	**	ns	**
NECA 10uM vs NECA 1uM	0.20	0.56	0.60	0.43	0.81	0.81	0.17	0.64	0.86	0.56	0.79	0.26
	ns	ns	ns	ns	ns	ns	ns	ns	ns	ns	ns	ns
CTL vs NECA 10uM + ZM	0.37	0.003	0.001	0.001	0.001	0.01	0.001	0.01	0.01	0.0001	0.62	0.04
	ns	**	***	***	***	**	***	**	**	****	ns	*
NECA10uM vs NECA10uM + ZM	0.39	0.004	0.002	0.55	0.20	1.00	0.27	0.73	0.49	0.17	0.09	0.07
	ns	**	**	ns	ns	ns	ns	ns	ns	ns	ns	ns
CTL vs TILs	0.16	0.62	0.01	0.0001	0.0001	na	0.01	0.001	0.004	0.004	0.08	0.01
	ns	ns	**	****	****	na	**	***	**	**	ns	**
NECA10uM vs TILs	0.28	0.41	0.002	0.15	0.03	0.62	0.34	0.22	0.73	0.53	0.68	0.98
	ns	ns	**	ns	*	ns	ns	ns	ns	ns	ns	ns
NECA10uM + ZM vs TILs	0.07	0.10	0.92	0.50	0.50	0.45	0.84	0.23	0.52	0.45	0.09	0.16
	ns	ns	ns	ns	ns	ns	ns	ns	ns	ns	ns	ns

D

Time	-40	-20	0	20	40	60	80	100	120	180	300	420
CTL vs NECA 1uM	0.73	0.24	0.001	<0.0001	0.001	0.16	0.06	0.27	0.34	0.001	0.11	0.03
0.03	ns	ns	***	****	***	ns	ns	ns	ns	***	ns	*
CTL vs NECA 10uM	0.75	0.07	0.0001	<0.0001	0.0005	0.001	0.0003	0.001	0.02	0.0001	0.05	0.0002
	ns	ns	****	****	***	***	***	***	*	****	*	***
NECA 10uM vs NECA 1uM	0.40	0.96	0.70	0.88	0.88	0.28	0.15	0.19	0.50	0.56	0.70	0.75
	ns	ns	ns	ns	ns	ns	ns	ns	ns	ns	ns	ns
CTL vs NECA 10uM + ZM	0.93	0.15	<0.0001	0.0002	0.02	0.97	0.002	0.05	0.08	<0.0001	0.02	<0.0001
	ns	ns	****	***	*	ns	**	*	ns	****	*	****
NECA10uM vs NECA10uM + ZM	0.52	0.52	0.58	0.12	0.05	0.001	0.18	0.10	0.42	0.92	0.48	0.74
	ns	ns	ns	ns	*	***	ns	ns	ns	ns	ns	ns
CTL vs TILs	0.77	0.53	<0.0001	<0.0001	0.0004	0.02	0.01	0.001	0.03	<0.0001	0.05	<0.0001
	ns	ns	****	****	***	*	**	***	*	****	*	****
NECA10uM vs TILs	0.36	0.31	0.29	0.34	0.94	0.67	0.35	0.65	0.96	0.75	0.58	0.39
	ns	ns	ns	ns	ns	ns	ns	ns	ns	ns	ns	ns
NECA10uM + ZM vs TILs	0.49	0.49	0.18	0.04	0.19	0.03	0.95	0.11	0.60	0.92	0.88	0.68
	ns	ns	ns	*	ns	*	ns	ns	ns	ns	ns	ns

6.2.2 Does direct engagement of TIM3 suppress Clone 4 T cell function in vitro?

6.2.2.1 Generation of a Chimeric TIM3 Inhibitory Receptor

Based on *in vivo* A2aR and TIM3 blockade experiments described in Chapter 5, we hypothesised that direct engagement of A2aRs and TIM3 would suppress CTL effector function amongst Clone 4 T cells primed *in vitro*. After determining the effect of A2aR engagement on CTL effector functions such as cytotoxicity, CIR expression and actin regulation, experiments were set up in order to determine whether TIM3 signalling also suppressed the cytotoxic effector function of Clone 4 CTL.

Several experimental approaches were used to enable TIM3 signalling to be engaged and halted on demand within cultures of Clone 4 CTL. Firstly, knockdown of TIM3 was attempted amongst primary Clone 4 CTL, however two different techniques of siRNA delivery were unsuccessful (Data not shown). Therefore, TIM3 overexpression was performed by transduction of Clone 4 CTL with $TIM3^{GFP}$. However, overexpression did not guarantee that the TIM3 receptor was engaged by any ligand in cell culture (Chapter 3, Figure 21).

To better control signalling through TIM3, a 'Chimeric Inhibitory Receptor' (ChIR) was generated based on Chimeric Antigen Receptors used in T cell immunotherapy (218, 259, 282, 283). To generate ChIR TIM3, the extracellular domain of the human CD2 (hCD2) receptor was cloned onto a transmembrane linker, attached to the intracellular signalling tail of TIM3. This construct was named 'hCD2TIM3' (Figure 47A & B). Engagement of the hCD2 domain initiates signalling through the TIM3 cytoplasmic tail. As there are no murine ligands to hCD2, TIM3 signalling would only occur if human CD58 (hCD58) was added to cell culture; thus, Renca tumour cells transfected with hCD58 were utilised for this purpose (Timse Raj, unpublished) (284). In this manner, signalling through hCD2TIM3 could be tightly controlled (Figure 47C).

Figure 47 - Chimeric TIM3 Receptor Signalling

(A) Structure of the hCD2TIM3 vector and the hCD2TIM3+Ig vector. (B) Schematic to illustrate the design of the chimeric inhibitory receptor and its predicted localisation in relation to the cell surface membrane. Binding of endogenous Ceacam-1 occurs at the optional Ig domain. (C) Schematic to illustrating control of signalling through hCD2TIM3 in cell culture. When RencaHA tumour cells are included in cell culture, Clone 4 TCRs engage with HA, bringing CTL into proximity with Renca tumour cells. In addition (i) when RencaHACD58 tumour cells are added to cell culture the hCD2TIM3 expressed by the Clone 4 cell is engaged by hCD58 expressed by the Renca cell. Engagement of the CD2 domain of hCD2TIM3 initiates signalling through the TIM3 cytoplasmic tail; (ii) when RencaHA tumour cells are added to culture, there is no hCD58 ligand, therefore hCD2TIM3 is not engaged and no signalling occurs through the TIM3 cytoplasmic tail.

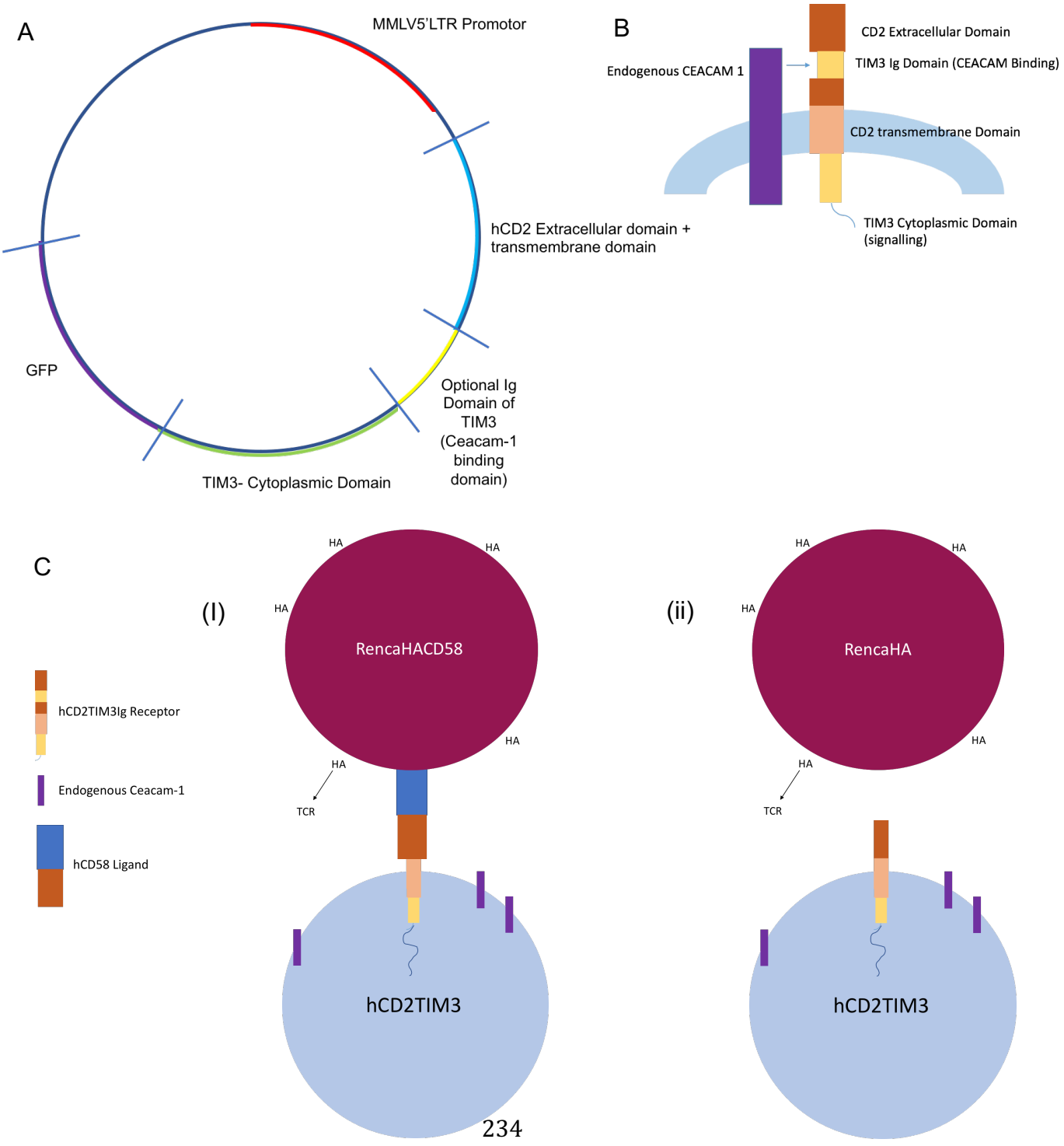

As well as acting as a signal initiator, the fact that hCD2 is a cell surface membrane protein forces the chimeric TIM3 construct to localise to the cell surface, thus allowing the construct to be engaged by external ligands. To test the success of the hCD2 domain in ensuring membrane localisation of the chimeric TIM3 construct, Total Internal Reflection (TIRF) microscopy, was used, because TIRF is able to detect the presence of objects within 20nM of the cell surface membrane (Figure 48A). hCD2TIM3^{GFP} was available for signalling at the cell surface membrane, and it inserted in the same punctate pattern seen with unmodified TIM3^{GFP}. This punctate pattern appears to represent vesicular insertion, since CIRs are stored in vesicles before being expressed at the cell surface upon TCR engagement (134, 138).

Clone 4 CTL expressing hCD2TIM3 were cultured with either RencaHACD58 cells, which should signal through hCD2 or RencaHA cells as neutral controls. There was no significant difference in CTL killing ability when hCD2TIM3 was engaged versus not engaged, as determined by microscope-based cytotoxicity assays. Therefore, signalling through hCD2TIM3 did not affect Clone 4 CTL function (data not shown). However, several other studies have shown that TIM3 may not exert its inhibitory function without binding to Ceacam-1 in *cis* (54, 116, 138).

6.2.2.2 Generation of a Chimeric TIM3 receptor with the ability to bind Ceacam-1 in cis

In case the close proximity of Ceacam-1 was required to allow inhibitory signalling through the TIM3 cytoplasmic tail, the hCD2TIM3 construct was modified, giving it the ability to bind to Ceacam-1 in *cis*. To achieve Ceacam-1 recruitment, the Immunoglobulin (Ig) domain of TIM3 (which is the Ceacam-1 binding site of the TIM3 molecule), was added to hCD2TIM3 (Figure 47A & B). The resulting construct was named 'hCD2TIM3Ig'. We hypothesised that the Ig domain in hCD2TIM3Ig would enable this construct to recruit Ceacam-1 to the cell surface, whereas hCD2TIM3 without the Ig domain would not be able to do this. However, when flow cytometry was used to assess surface Ceacam-1 expression, it was comparable between the two constructs (Figure 48B). It was concluded that endogenous expression of Ceacam-1 amongst *in vitro* primed Clone 4 CTL could be too low for the hCD2TIM3Ig to attract any Ceacam-1 at the cell surface. Therefore, Clone 4 CTL were transduced with Ceacam-1^{GFP} to ensure that Ceacam-1 was expressed and available to be recruited by the Ig domain of hCD2TIM3Ig. Flow cytometry data showed that co-transduction of Ceacam-1^{GFP} with hCD2TIM3 increased the surface MFI of Ceacam-1 when compared with transduction of hCD2TIM3Ig alone (Data not shown).

6.2.2.3 Signalling through Chimeric TIM3 and Ceacam-1 does not affect the cytotoxic function of in vitro primed Clone 4 CTL

To determine whether or not signalling through hCD2TIM3Ig suppressed the killing function of Clone 4 CTL, microscope-based cytotoxicity assays were performed. Clone 4 CTL were transduced with various combinations of hCD2TIM3Ig and Ceacam-1^{GFP}, and cultured either with RencaCD58 cells, to engage the hCD2TIM3 receptor during cell culture, or with RencaHA cells as a neutral control. After 5 days of culture, Clone 4 CTL were utilised in cytotoxicity assays. There were no significant differences in the cytotoxic abilities of cells expressing different hCD2TIM3Ig/Ceacam-1^{GFP} construct combinations (Figure 48C). To determine whether signalling through A2aRs, Ceacam-1 and hCD2TIM3Ig together within Clone 4 CTL suppressed their cytotoxic abilities, NECA was added to Clone 4 CTL transduced with both constructs. However, killing of target cells was not inhibited when hCD2TIM3Ig/Ceacam-1 transduced cells were treated with NECA.

Figure 48 - Signalling through a Chimeric Inhibitory TIM3 receptor does not significantly affect the Cytotoxic function of Clone 4 T cells

(A) Clone 4 CTL were transduced with $TIM3^{GFP}$ or $hCD2TIM3^{GFP}$. Cells were allowed to couple to a coverslip coated with Anti-CD3mAb and ICAM-1. Upon cell spreading, GFP signal was observed within 20nm of the cell surface membrane, by TIRF microscopy Early (top) and late (bottom) time points are shown. (B) Clone 4 CTL were transduced with hCD2TIM3 or hCD2TIM3Ig Flow cytometric analyses of Ceacam-1 expression at the surface are shown. (C) Clone 4 CTL were transduced with combinations of hCD2TIM3, hCD2TIM3Ig and Ceacam-1. Cells were cultured in media containing RencaHA cells or RencaCD58 cells +/- NECA as shown (table and schematic). Killing of K^dHA-pulsed $RencaHA^{mCherry}$ tumour cells in the presence of Clone CTL was calculated at an E:T ratio of 3:2. Each point = average of 4 wells in 1 experimental repeat and samples compared within the same repeat were paired. One-way ANOVA was used for statistical comparison p = ns all comparisons.

A

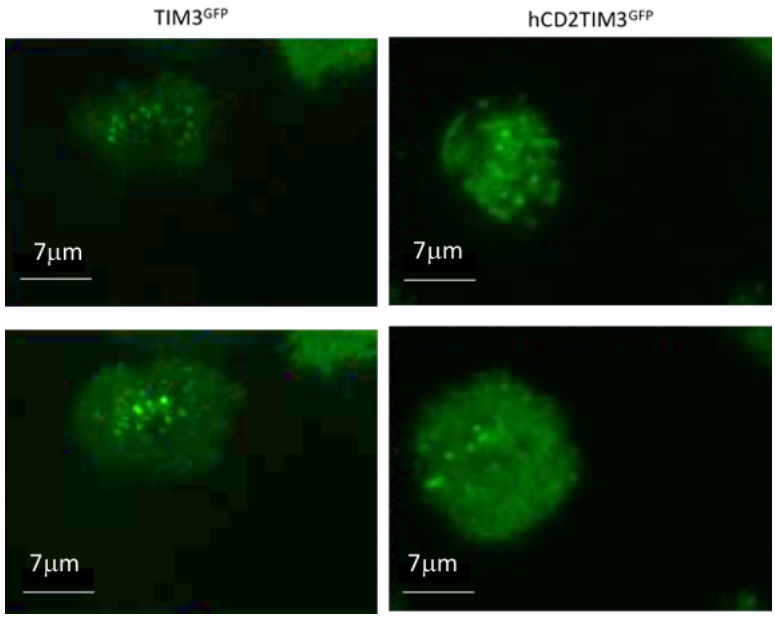

B

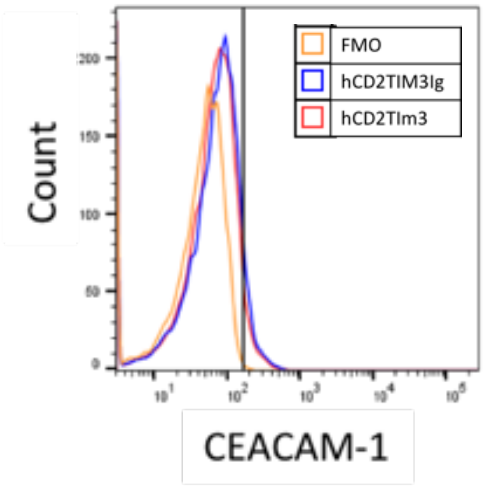

C.

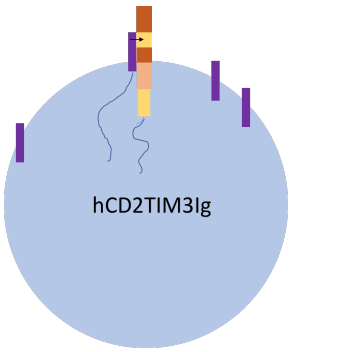

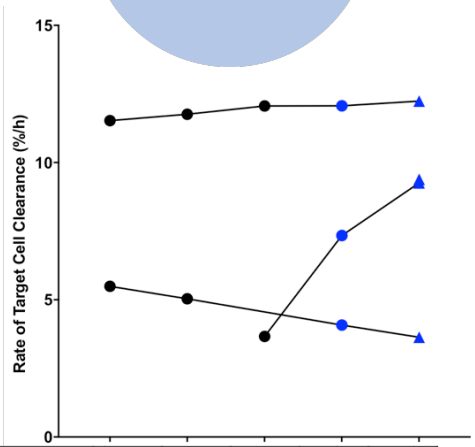

IL-2 Medium	+	+	+	+	+
RencaHA		+		+	
RencaHACD58			+		+
hCD2TIM3Ig				+	+

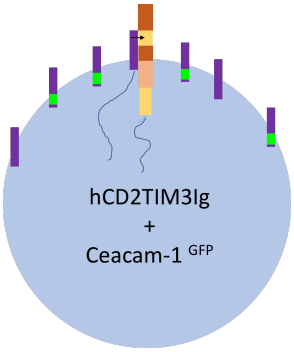

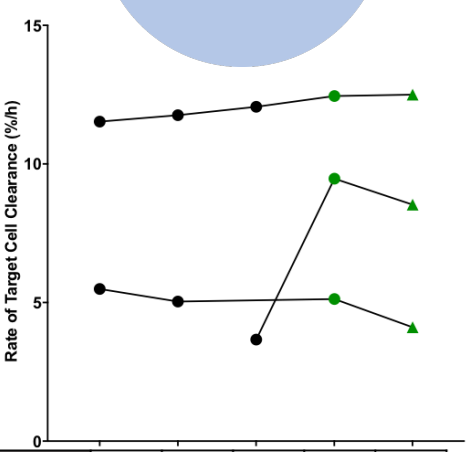

IL-2 Medium	+	+	+	+	+
RencaHA		+		+	
RencaHACD58			+		+
hCD2TIM3Ig				+	+
Ceacam-1^{GFP}				+	+

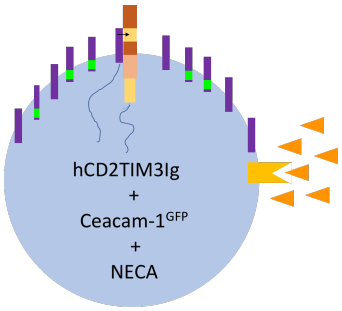

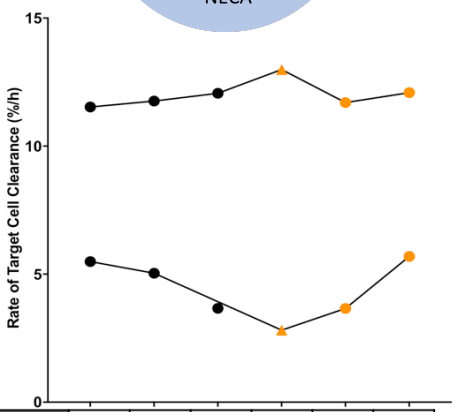

IL-2 Medium	+	+	+	+	+	+
RencaHA		+		+		
RencaHACD58			+		+	+
hCD2TIM3Ig				+	+	+
Ceacam-1^{GFP}				+	+	+
1uM NECA						+

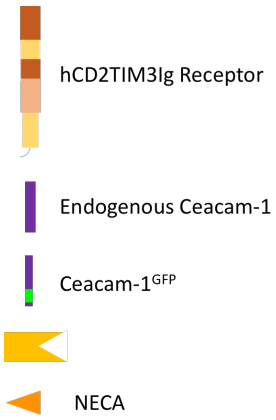

6.2.3 Does signalling through TIM3 and A2aRs synergise to inhibit TCR signalling through Lck?

Data presented in Chapter 5 showed that systemic blockade of A2aRs and TIM3 within tumour bearing mice resulted in improved *ex vivo* cytotoxic effector function amongst Clone 4 TILs. Therefore, it was decided to examine the TCR signalling events that could be inhibited downstream of A2aR and TIM3 engagement in order to suppress Clone 4 CTL. Previous studies have suggested that A2aR engagement could inhibit TCR signalling within Clone 4 CTL by increasing PKA activity, resulting in the addition of inhibitory phosphate groups at Y505 of Lck (205). Whilst A2aR signalling could affect Lck phosphorylation, TIM3 signalling is thought to affect the spatiotemporal localisation of Lck at the immune synapse (54, 55, 285). Several studies suggest that engagement of TIM3 by inhibitory ligands causes the release of Bat-3 from the TIM3 cytoplasmic tail, and Bat-3 takes with it a pool of active Lck. Thus, TIM3 engagement could cause Lck to localise away from the immune synapse (54, 55). Overall, we propose a model whereby engagement of A2aRs and TIM3 could synergise to inhibit TCR signalling at the level of Lck by reducing its activity, and by physically removing Lck from the location of the TCR (Figure 49).

6.2.3.1 NECA treatment does not significantly influence the phosphorylation status of Lck within in vitro primed Clone 4 CTL

To investigate whether engagement of A2aRs could indeed increase the inhibitory phosphorylation of Lck, Clone 4 CTL were cultured *in vitro* with NECA, and the phosphorylation status of Lck was assessed using Phosflow cytometry. Y418 staining is indicative of activating phosphorylation of Lck (53). Although auto-phosphorylation at Y394 causes Lck to assume an open, active confirmation, Y418 is only available to staining when Lck is active, therefore Y418 is an indirect measure of Y394 phosphorylation (53). Y505 staining indicates phosphorylation of the inactivating site of Lck. To confirm that phosflow staining was capable of detecting Lck phosphorylation, a subset of cells was treated with pervanadate, to cause phosphorylation of most tyrosine residues in the cell, before staining. Phosphorylation was detected at both the activating Y418 site and the inhibitory Y505 site within 80% of pervanadate treated cells, indicating that the staining was working. However, there were no significant differences in the expression of active Lck versus inactive Lck amongst NECA-treated cells when compared with controls. Interestingly, the MFI of total Lck was elevated amongst cells treated with NECA 10

μM + A2aR-Antagonist, or 50 μM NECA. The functional significance of this finding is unknown (Figure 50).

6.2.3.2 The Spatiotemporal localisation of Lck cannot be determined amongst in vitro primed Clone 4 CTL using Confocal Microscopy

To determine if engagement of TIM3 mediates re-localisation of active Lck away from the immune synapse, *in situ* antibody staining was used to identify the localisation of Lck during immune synapse formation. Staining of intracellular actin with Phalloidin^{GFP} (a small molecule which binds to F-actin) was utilised as a control to determine that fixation and permeabilisation of Clone 4 CTL on coverslips was successful (Figure 51A). Clone 4 CTL were labelled with Celltrace Violet prior to coupling, to identify the location of CTL on the Renca cell monolayer. Staining was then performed using the anti-phospho Lck mAb that had been used in previous phosflow cytometry experiments. The images show that there was no specific staining of total Lck, Lck Y505 or Lck Y418 amongst Clone 4 CTL conjugated to Renca tumour cells (Figure 51B). Therefore, *in situ* staining could be too insensitive to detect different phosphorylated forms of Lck.

Figure 49 – Proposed model in which Adenosine and TIM3 synergistically inhibit TCR signalling through Lck

Lck is present within CD8+ T cells in three main phosphorylated forms, and the balance of availability of these phosphotypes affects the potential for successful TCR signalling. Engagement of the A2aR, a G-protein coupled receptor, mediates an increase in intracellular cyclic AMP, increasing the activity of PKA, and subsequently Csk - a tyrosine kinase which adds an inhibitory Y505 phosphorylation to Lck (194, 210, 286). Unless an inhibitory ligand is present, TIM3 cytoplasmic tails are thought to bind to Bat3, which acts as a reservoir for active Lck, thus ensuring the availability of Lck at the immune synapse and promoting TCR signalling potential (54, 55, 138). After TIM3 engagement by Ceacam-1 or Galectin-9,Bat3 detaches from the TIM3 cytoplasmic tail and with it removes a pool of Lck, reducing the potential for TCR signal amplification (54, 138). Therefore, A2aR signalling and TIM3 signalling could synergise to inhibit T cells, via addition of inactivating phosphate groups to Lck (A2aRs) and physical removal of active Lck from the immune synapse (TIM3).

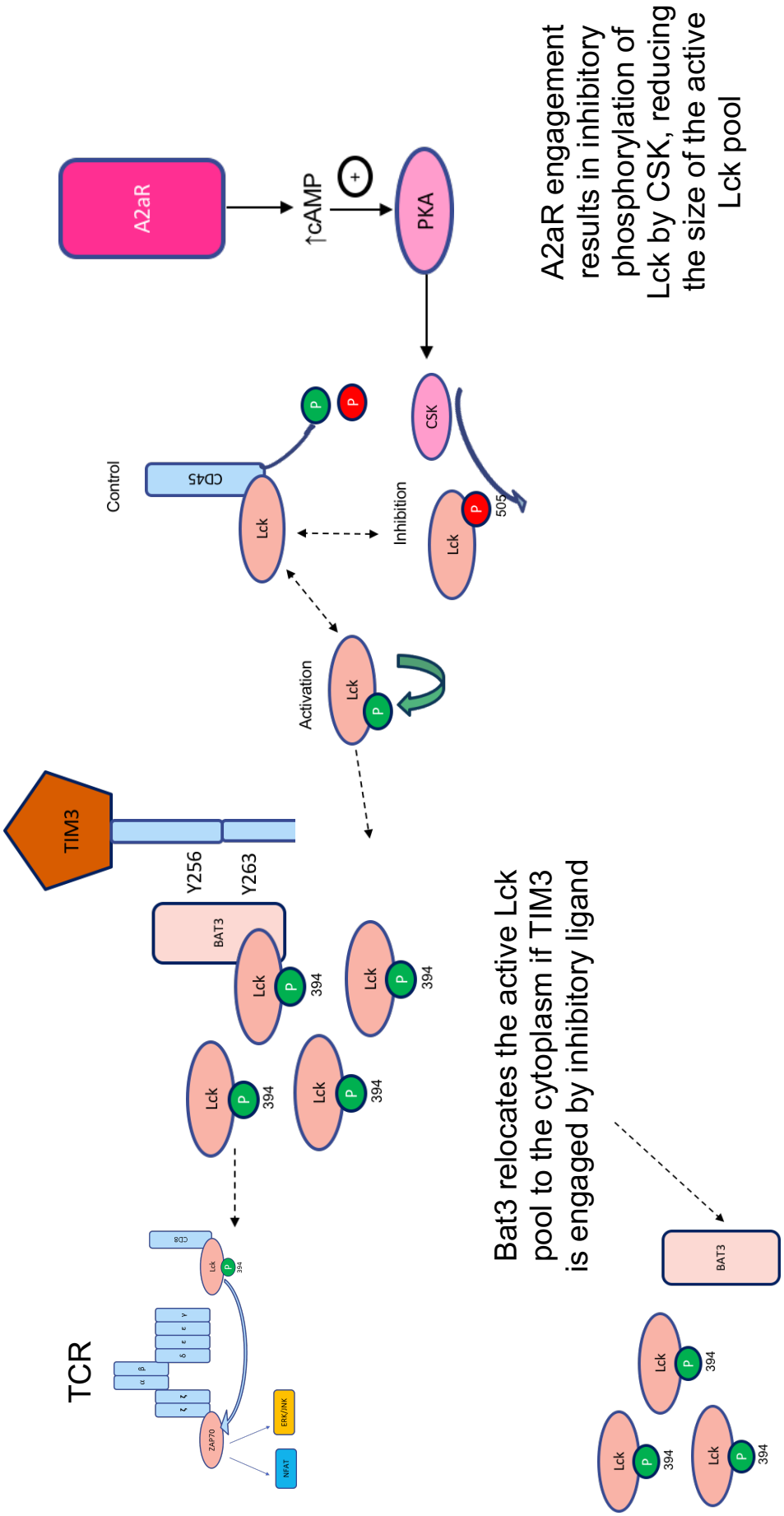
A2aR
↑cAMP
PKA
A2aR engagement results in inhibitory phosphorylation of Lck by CSK, reducing the size of the active Lck pool
CSK
Control
CD45
Lck
Inhibition
505
Activation
TIM3
Y256
Y263
BAT3
394
TCR
ZAP70
ERK/INK
NFAT
Bat3 relocates the active Lck pool to the cytoplasm if TIM3 is engaged by inhibitory ligand

Figure 50 – Treatment with 5-N-Ethylcarboxamidoadenosine (NECA) does not significantly affect the proportion of Lck Phosphotypes present within Clone 4 CTL

Clone 4 CTL were treated for 96h with combinations of NECA and specific A2aR-Antagonist as indicated. A subset of cells was treated with pervanadate, to induce phosphorylation of all tyrosine residues within the cell (positive control). Cells were stained with antibodies specific to total Lck, Lck phosphorylated at Y505 (inactive Lck), or Lck phosphorylated at Y418 (active Lck). Cells were analysed by flow cytometry. N= 3 experiments, mean +/-SEM is shown. (A) Percentage expression of each Lck pool was compared using MANOVA. p> 0.999 all samples except for each condition vs pervanadate treated CTL, where p<0.0001**** as indicated (B) MFI of each Lck pool was compared using MANOVA. No comparisons were significant.

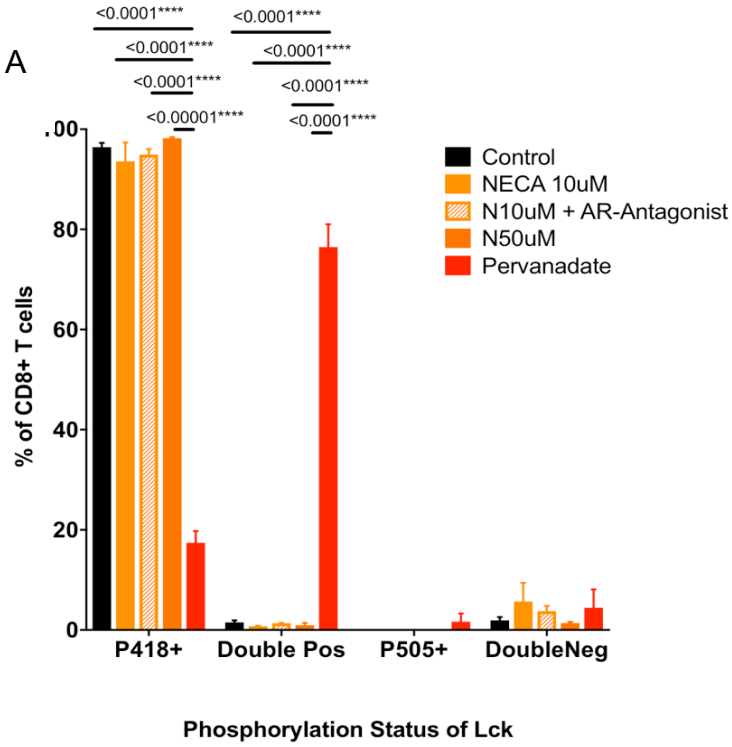

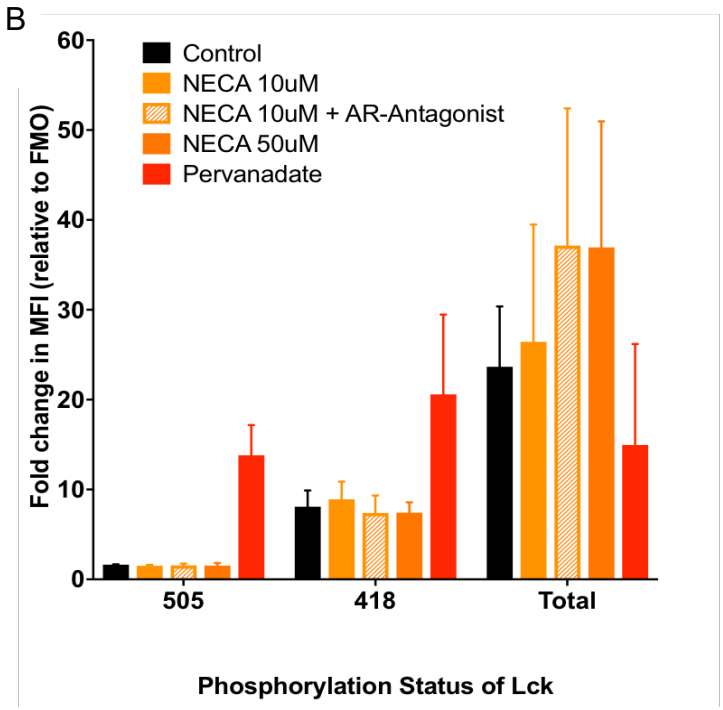

Figure 51 - In situ staining to determine the localisation of Lck during immune synapse formation between Clone 4 CTL and RencaHA targets

Clone 4 CTL were added to a monolayer of K^dHA pulsed Renca tumour cell targets on a coverslip Cells were allowed 4 minutes to form cell couples before being fixed, permeabilised and stained with phalloidin stain or antibodies, Samples were mounted in antifade mountant and analysed using confocal microscopy. (A) Celltrace violet labelled Clone 4 CTL (blue) and intracellular actin stained with phalloidin (green) are shown. (B) Celltrace-violet labelled Clone 4 CTL (blue) were treated with pervanadate to induce phosphorylation of cellular tyrosine residues (positive control) before being allowed to couple with Renca tumour cells. Cells were then stained fluorescent conjugated primary antibodies to (i) total Lck (PE, red) (ii) LckY418 (FITC, green) (iii) LckY505 (AF647, pink). Overlay images are shown. No specific Lck staining was observed in any image[17].

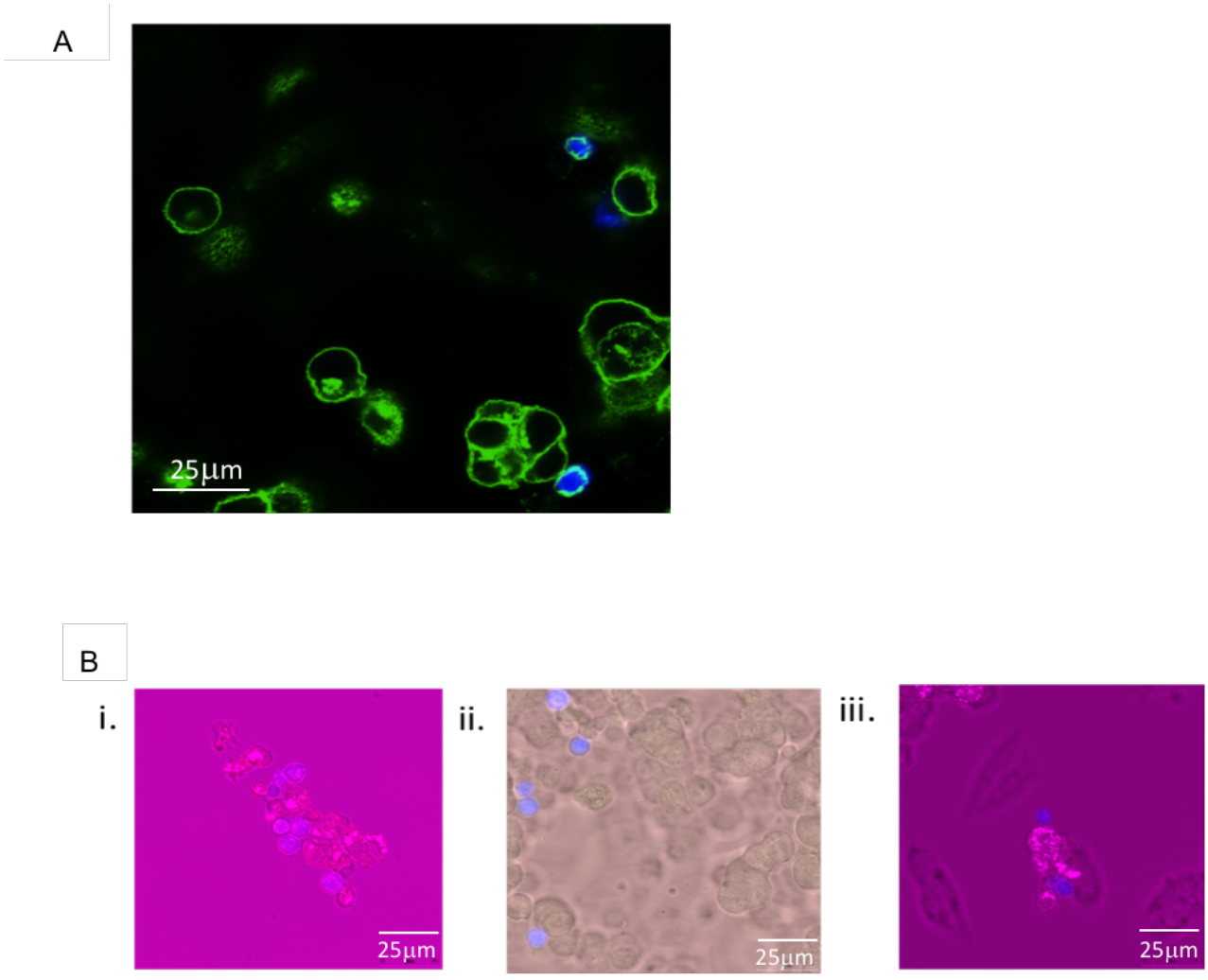

[17] All staining, image acquisition and analysis for this figure was performed together by GE and Clara Kouaku, a student in the Wuelfing lab.

6.3 Discussion

Previous experiments showed that systemic blockade of A2aRs and TIM3 was associated with improved cytotoxic effector function of adoptively transferred Clone 4 TILs when assayed *ex vivo* after recovery from the tumour (287, 288). However, *in vivo* studies do not illustrate whether blockade was acting directly, improving Clone 4 T cell function by blocking A2aRs and TIM3 engagement on their surface, or indirectly, by blocking anti-inflammatory signalling amongst other immune cell populations in the TME. The *in vitro* culture environment lacks the complex mixture of immunoinhibitory and immunostimulatory factors found within the TME, which allows the direct effects of individual pathways to be studied in a reductionist fashion. Therefore, an *in vitro* model was developed to study the functional effects of engagement of TIM3 and A2aRs on Clone 4 CTL in culture.

6.3.1 The addition of Adenosine Receptor Agonists to cell culture suppresses Clone 4 T cell Proliferation and Actin regulation, but does not suppress Cytotoxic function

CD8+ T cell proliferation induced by TCR engagement is one measurement of suppression of TCR signalling by immunoinhibitory receptor engagement. Therefore, it was postulated that adding the pan-adenosine receptor agonist, NECA, to cell culture would result in suppression of proliferation amongst *in vitro* primed Clone 4 T cells. To test this, experiments were carried out in which Clone 4 CTL were primed using Anti-CD3/28mAb stimulation and proliferation was assessed using Celltrace Violet staining and ^{3}H-thymidine incorporation. The results showed that proliferation of naïve Clone 4 T cells was suppressed in the presence of 1 μM NECA.

Various concentrations of NECA were tested, to determine the minimum suppressive concentration which could be used in further assays of Clone 4 CTL function. Anti-CD3/28 mAb stimulation was used for priming in proliferation experiments so that no other cell types would be included in the cell culture. Other immune cells also express adenosine receptors and could be influenced by NECA, which could prevent quantification of the concentration of NECA required to suppress CTL directly. Priming using K^{d}HA peptide, which is the method usually employed by our laboratory, requires APCs in cell culture therefore it was not used for proliferation assays.

Although the experimental aim was to determine the effects of the inhibitory A2a Adenosine Receptor (rather than stimulatory A1 and A3 receptors) on Clone 4 T cell proliferation, a pan-AR agonist (NECA) was utilised to try and emulate Adenosine itself, which agonises all four AR subtypes in the TME. However, the use of a specific A2aR-Antagonist blocked the effects of NECA, indicating that suppression of proliferation by NECA was A2aR dependent. Nonetheless, studies have shown that CD8+ T cells could express a different balance of stimulatory (A1 and A3) versus inhibitory (A2a and A2b) adenosine receptor subtypes in the TME when compared with *in vitro* cultures. Therefore, to fully understand how A2aRs affect Clone 4 CTL, further studies should utilise A2a specific agonists such as CGS2680 in these same proliferation assays.

The use of Adenosine itself, rather than NECA, was attempted. However, concentrations of 1.25 mM Adenosine were required to suppress Clone 4 T cell proliferation because Adenosine is not stable in cell culture. This concentration is 1000 times higher than the amount of NECA required to limit proliferation, and it produced significant cytotoxicity amongst Clone 4 T cells, suggesting that suppression of proliferation by Adenosine was caused by cell death rather than by A2aR dependent signalling (278, 289). Therefore, NECA was used in future proliferation assays.

Interestingly, when using ^{3}H-thymidine to assess proliferation, 10 μM or 20 μM NECA was found to be less suppressive than 1 μM NECA, but suppression then occurred again at 50-100 μM. This finding indicates that there could be an optimum concentration to achieve suppression of Clone 4 T cells by NECA. Studies using synthetic adenosine receptor agonists in neuronal cultures have since noted that AR agonists can behave as antagonists and vice versa depending on the concentration used and the particular cell culture conditions, including the levels of calcium flux occurring within neurones (211, 278, 281, 290, 291). It is likely that the effects of NECA on T cells will also differ depending on their activation state, the method of cell culture utilised, and the concentration added. Therefore both 1 μM and 10 μM NECA were used for ongoing analyses. Adding NECA to Clone 4 T cells did not produce significant suppression unless cells were cultured with NECA for 72h. Therefore, NECA was added at 0h for future experiments, and concentrations of NECA were maintained in culture for at least 72h, before Clone 4 T cell effector functions were quantified.

The suppressive effects of NECA on Clone 4 T cells could be mediated by an increase in Co-

Inhibitory Receptor (CIR) expression. After engagement of PGE_2 receptors, elevated cAMP has been shown to promote IL-27 production through activation of the cAMP response element in T cells (144, 202). In a separate study, autocrine IL-27/IL-27R interactions were shown to promote expression of the CIR gene module in CD8+ T cells, which results in TIM3, TIGIT, LAG3, PD-1 and IL-10 expression (121). Engagement of A2aRs by NECA also causes elevated intracellular cAMP, so we hypothesised that A2aR engagement could lead to autocrine IL-27 signalling and CIR expression amongst Clone 4 T cells. To test this hypothesis, the percentage of Clone 4 CTL expressing TIM3, TIGIT, LAG3 and PD-1 was quantified, but expression of these CIRs did not alter significantly after NECA treatment. Therefore, AR engagement did not directly influence CIR expression amongst Clone 4 T cells primed *in vitro*. IL-27R expression has not been compared between *in vitro* primed CTL and TILs. Much like A2aRs, which are upregulated within immunosuppressive microenvironments such as tumours or necrotic tissue, IL-27Rs might only be expressed at low levels *in vitro* meaning that autocrine IL-27 signalling resulting from A2aR engagement could not occur (1, 14-18). Further studies could aim to quantify IL-27R expression amongst *in vitro* primed Clone 4 CTL and TILs, to determine whether IL-27Rs are available to mediate the effects of cAMP on CIR expression *in vitro*, or whether they are selectively upregulated within the TME.

Cytotoxicity assays were utilised to determine the effect of NECA on Clone 4 CTL effector function. Clone 4 CTL retained their cytotoxic abilities after treatment with NECA, and in fact NECA-treated cells killed better than untreated CTL. Clone 4 CTL treated with both NECA and A2aR-Antagonist killed most efficiently out of all conditions. These findings could suggest that NECA was acting on both stimulatory and inhibitory adenosine receptor subtypes. When A2aR-Antagonist was included in cell culture, only the immunostimulatory A1 and A3 receptor subtypes were available for NECA to bind, explaining why cytotoxicity was increased in the presence of both NECA + A2aR-Antagonist versus untreated cells.

The presence of an immunosuppressive milieu within the tumour has been shown to affect the balance of AR subtypes which are expressed, favouring expression of the inhibitory A2aR over other subtypes (1, 14-18). Therefore, PGE_2 and TGFβ, two factors which are known to be present within the RencaHA TME, were added to cell culture along with NECA. We postulated that the presence of these additional immunosuppressive factors could result in elevated immunosuppressive A2aR expression, making Clone 4 CTL more susceptible to the suppressive

effects of NECA. However, adding these factors did not produce a reduction in Clone 4 T cell cytotoxicity in the presence of NECA. Furthermore, utilising a specific A2aR-agonist (CGS2680) did not suppress killing by CTL either, suggesting that preferential agonism of A1 and A3 receptors was unlikely to be the reason that NECA failed to inhibit cytotoxicity *in vitro*.

Whereas anti-CD3/28mAb priming was used for proliferation assays, cells were primed using K^dHA peptide to assess the effect of NECA on the killing ability of Clone 4 CTL. Peptide-priming was used because cytotoxicity assays were executed in parallel with live cell imaging experiments, which required Clone 4 CTL to be transduced with GFP-tagged signalling intermediates. Our current transduction protocol can only be achieved in peptide-primed cells. However, the rapid cell division generated by K^dHA peptide results in IL-2 depletion within cultures of Clone 4 CTL, therefore IL-2 supplementation is required. IL-2 supplementation can reduce the threshold for TCR signalling amongst CTL, and can allow recovery of suppressed TILs (51, 292). Therefore, the presence of exogenous IL-2 could have prevented immunosuppressive molecules such as NECA and PGE_2 from suppressing CTL effector function. Culture of K^dHA-primed Clone 4 CTL without IL-2 was attempted, however, the cells did not survive over 5 days. In one preliminary experiment, peptide-primed CTL were shown to survive without IL-2 for 3 days, however they were not fully activated or able to kill tumour cell targets (data not shown). Anti-CD3/28 mAb stimulation initiates slower proliferation, therefore this could be used as an alternative to K^dHA peptide priming, to allow Clone 4 T cells to be cultured without IL-2. However, Anti-CD3/28mAb priming methods need to be optimised to produce sufficient proliferation for uptake of GFP-tagged constructs after transduction for live cell imaging experiments.

6.3.2 Adding Adenosine Receptor Agonists to cell culture impairs clearance of Actin from the Central to the Peripheral immune synapse

Another measure of CD8+ T cell function is actin regulation at the immune synapse. Two models have been proposed to explain how actin regulates the delivery of cytotoxic granules by CD8+ T cells. The Actin maintenance model stipulates a requirement for peripheral actin ring maintenance, and this was dysregulated amongst NECA-treated Clone 4 CTL, resulting in morphologically unstable immune synapses. However, NECA-treated CTL were still able to kill Renca tumour cell targets in cytotoxicity assays. Therefore, maintenance of a peripheral actin ring and a stable immune synapse may not be required for target cells to be killed by CTL.

Alternatively, the Actin Clearance model suggests that immune synapse stability is less important, and actin clearance from the cSMAC is fundamental to allow the delivery of lytic granules by CTL (71). NECA-treated cells, which are capable of killing, exhibit permissive and obstructive actin patterning resembling that of TILs, which cannot kill target cells. Therefore, neither the Actin Maintenance nor Actin Clearance models explain how actin distributions relate to CTL killing *in vitro* (71).

PGE_2 was also added to cell culture, to determine the effects of concurrent engagement of multiple pathways, which are found within RencaHA tumours, on Clone 4 T cell immune synapses. The effects of NECA and PGE_2 appeared to be redundant rather than additive, which could be explained, because both molecules suppress CD8+ T cells by engaging G-protein coupled receptors, resulting in elevated cyclic AMP.

6.3.3 Engineering TIM3 signalling amongst Clone 4 T cells cultured *in vitro*

After quantifying the effects of adenosine signalling, experiments were designed to determine whether direct engagement of TIM3 inhibited Clone 4 CTL function. At the start of these studies, the ligand for TIM3 was not well defined, nor was its signalling mechanism. Furthermore, the quantity of surface expression of TIM3 was variable between *in vitro* cultures, and TIM3 expression was affected by the method of priming used in preliminary studies (Supplementary Figure S8). To circumvent the problem that TIM3 is not consistently expressed, and that we could not engage TIM3 with any known ligand to confidently ensure inhibitory signalling, generated a chimeric inhibitory receptor (ChIR) was generated. The ChIR comprised the cytoplasmic signalling domain of TIM3 with the extracellular domain of human CD2 (hCD2). This allowed TIM3 signalling to be pulled to the surface membrane by hCD2, and to be initiated when hCD2 was engaged by hCD58-expressing Renca tumour cells.

However, the engagement of hCD2TIM3 failed to inhibit Clone 4 CTL cytotoxicity, and in-fact produced a small improvement in killing of tumour cell targets when compared with controls. Recent studies published during the course of these experiments demonstrated that engagement of TIM3 by either of its inhibitory ligands, Galectin-9 or Ceacam-1, is required for TIM3 to exert an inhibitory function (Figure 49) (54, 138). In the absence of these ligands, TIM3 cytoplasmic tails bind Bat3, a molecule which maintains a reservoir of Lck at the immune

synapse and lowers the threshold for TCR signalling (54). Therefore, it is possible that hCD2TIM3 was functioning, but that it was exerting the stimulatory effect of TIM3 by recruiting Bat3 and Lck to the immune synapse (54). A Ceacam-1 binding immunoglobulin domain was added to the hCD2TIM3 molecule to allow it to pull in Ceacam-1 expressed by Clone 4 CTL. Ceacam-1 can interact with TIM3 on the same cell in *cis*, causing Bat3 to be released from the TIM3 tail, taking with it the reservoir of Lck required for TCR signalling (54, 134, 138). However, *in vitro* primed Clone 4 CTL express low levels of Ceacam-1 at the cell surface, and flow cytometric analyses revealed that insufficient Ceacam-1 was available to be recruited to the membrane by the hCD2TIM3Ig receptor. One approach to resolving this problem would be to transduce Clone 4 CTL with hCD2TIM3Ig and to co-transduce Ceacam-1 at the same time. Although this was attempted, because both constructs were GFP conjugated, TIRF microscopy could not be used to confirm that both constructs colocalised at the cell surface. In future, the use of a Ceacam-$1^{mCherry}$ vector would allow colocalization of hCD2TIM3Ig^{GFP} and Ceacam-$1^{mCherry}$ to be examined using TIRF microscopy.

6.3.4 Signalling through TIM3 and A2aRs could inhibit TCR signal transduction through Lck

TIM3 signalling could affect Lck localisation at the CD8+ T cell immune synapse (54, 138). A2aR signalling could also affect Lck, however A2aRs are thought to influence the phosphorylation of Lck, rather than its localisation. Therefore we proposed a model, whereby TIM3 and A2aRs synergise to inhibit TCR signalling through Lck (Figure 49)(54, 55, 194). To identify evidence in support of this model, we aimed to determine the localisation and phosphorylation of Lck within Clone 4 T cells.

First, the phosphorylation status of Lck amongst NECA treated cells was quantified using phosflow cytometry to determine whether inhibitory Y505 phosphorylation was elevated in the presence of A2aR signalling. There were no alterations in the percentage expression or MFI of different Lck phosphotypes under the influence of NECA. As discussed, the inhibitory effects A2aR agonism by NECA could be overcome, because the presence of IL-2 in cell culture could have a permissive effect on TCR signalling, as shown by other groups (51, 292). In case the presence of IL-2 in culture was affecting detection of phosphorylated Lck, cells were cultured for 72h without IL-2 in the presence of combinations of NECA, the specific A2aR agonist

CGS2680 and PGE_2. Phosphorylated Lck was assessed using phosflow cytometry and proliferation was also quantified using loss of Celltrace Violet fluorescence. Treatment with NECA, CGS2680 or PGE_2 resulted in suppression of Clone 4 cell proliferation, and a reduction in the percentage of cells which expressed Lck phosphorylated at both Y505 and Y418 (Supplementary Figure S9). This experiment indicated that omitting IL-2 from cell culture could allow alterations in Lck phosphorylation to be detected, however the functional significance of a reduction in double-phosphorylated Lck is unclear (53).

To determine the localisation of Lck when TIM3 was engaged, we aimed to utilise the same live cell imaging techniques performed for F-tractin and cofilin localisation. In these experiments, Lck^{GFP} would be transduced into Clone 4 CTL and its localisation imaged during immune synapse formation (Figure 44, Figure 45). However, to engineer TIM3 signalling, transduction with hCD2TIM3Ig and Ceacam-1 constructs would have to be performed as well as transduction with Lck^{GFP} into Clone 4 CTL before live cell imaging. Clone 4 CTL cannot express 3 constructs concurrently (data not shown). Thus, an alternative approach was required to determine Lck localisation in Clone 4 T cells expressing hCD2TIM3Ig and Ceacam-1^{GFP}.

To this end*, in situ* antibody staining of Clone 4 CTL coupled to K^dHA pulsed Renca tumour cell targets was carried out on a cover slip, and cell couples were fixed before analysis. In theory, Lck localisation at the immune synapse would be determined by fluorescent antibody binding, therefore this method could be applied to Clone 4 CTL expressing both hCD2TIM3Ig and Ceacam-1^{GFP}. However, specific Lck staining was not detected.

Live cell imaging of untreated Clone 4 CTL was performed, and it was determined that levels of Lck at the immune synapse were too low for their localisation to be detected using either live or fixed cell microscopy (Supplementary Figure S10). This finding can be explained, because although CD4+ T cells localise large molecular numbers of TCR signalling intermediates to the immune synapse in both the priming and effector interactions between T cell and APC, CD8+ T cells localise many intermediates with much lower magnitude during killing interactions, when compared with priming. Therefore, a more sensitive approach to quantify the localisation of Lck at the immune synapse needs to be developed.

6.3.5 Further Work

Although the localisation of Lck could not be assessed using microscopy, Lck was detectable using flow cytometry. Further experiments will utilise an image-stream flow cytometer, which enables the quantity and subcellular localisation of signalling intermediates to be identified simultaneously, and with great sensitivity, after Phosflow staining.

To more closely model the effects of the tumour microenvironment *in vitro*, our laboratory has recently developed a 3D tumour organoid model, in which Renca tumour cells are grown as spheroids. *In vitro* primed Clone 4 T cells infiltrate the spheroid, producing Spheroid Infiltrating Lymphocytes (SILs) and can be recovered and analysed. Spheroids contain only K^dHA-pulsed Renca tumour cells, with no other cell types normally present within tumours growing *in vivo*, and yet after 24h in the spheroid microenvironment (SME), Clone 4 SILs exhibit 75% of the killing function of control Clone 4 CTL and upregulate the expression of TIM3 and PD-1 concurrently. These findings indicate that exposure to Renca tumour cells alone is sufficient to induce suppression amongst Clone 4 T cells (Silvia Cirillo, unpublished)(76). The SME is an ideal platform with which to dissect the effects of individual elements of the TME on Clone 4 CTL function, because the basic spheroid model is composed of only tumour cells and Clone 4 SILs, whereas the *in vivo* tumour microenvironment contains many immunosuppressive cells and molecules operating at once. Renca tumour cells do not express CD39/73 and therefore they do not have the capacity to produce adenosine. The A2aR agonist CGS2680, and A2aR-Antagonist ZM241385 could therefore be added to spheroids to determine if A2aR signalling increases the existing suppression of cytotoxicity which spheroids exert upon SILs.

Additionally, the effects of TIM3 on Clone 4 T cell cytotoxic effector function could be determined using the RencaHA spheroid system. $TIM3^{GFP}$ can be overexpressed amongst Clone 4 T cells and these cells used for spheroid infiltration. Renca tumour cells could also be transfected with Ceacam-1 or Galectin-9 to ensure that spheroids express TIM3 ligands. Furthermore, hCD2TIM3Ig expressing Clone 4 T cells could be transferred into spheroids expressing hCD58, to determine the effect of ChIR TIM3 engagement within the context of a suppressive microenvironment.

Chapter 7 Adoptively Transferred and Endogenous CD8+ T cells prevent tumour re-growth through Anti-Tumour Immune Memory

7.1 - Introduction

A major advantage of tumour-specific immunotherapy is that it supports the development of anti-tumour immune memory T cells. Memory CD8+ T cells are able to rapidly respond to secondary tumour antigen, and can therefore prevent regrowth of minimal residual disease (MRD). MRD describes microscopic populations of cancer cells that remain after macroscopic tumour lesions have been eradicated. It is now accepted that MRD is an important mediator of relapse in solid and in haematological tumours, and it can lead to tumour re-growth at the original site, or to dissemination and metastatic re-occurrence (293, 294). The development of reliable anti-cancer immune memory is difficult to study in human patients. However, it can be examined in pre-clinical models by rechallenging mice with further injections of tumour cells (226, 227, 264).

Different memory T cell subsets have distinct surface marker profiles, gene expression signatures, and functional abilities (Table 5)(12, 295).

Table 5 - Properties of different subsets of Memory T cells

Cell Type	Murine Surface Markers	Anatomical Location	Functional properties
CD8+ T Effector Memory (TEM)	$CD62L^{low}$, CD44+, CD69-, CD103a-	Sites of antigen > 2° lymphoid tissues	Rapid effector killing ability, eventual senescence or death
CD8+ T Central Memory (TCM)	$CD62L^{high}$, CD44+, CD69-, CD103a-	2° lymphoid tissues > sites of antigen but recirculate	Migration, self renewal
CD8+ Tissue Resident Memory (TRM)	$CD62L^{low}$, CD44+, CD69+, CD103a+	Resident at sites of antigen	Accelerated pathogen control and activation of innate immunity

Which subsets of immune cells produce an advantage in anti-cancer immune memory remains an important question. Characterisation of the specific memory T cell subsets that prevent relapse within murine tumour models could allow T cells to be diverted to achieve a specific memory phenotype before being administered as part of adoptive transfer therapies which aim to prevent relapse in human cancer patients (230, 296). However studies disagree about whether CD8+ T cells which possess a T Central memory (TCM) phenotype or a T Effector Memory (TEM) phenotype are the most effective at preventing cancer re-occurrence (230,

296). Furthermore, whether or not adoptively transferred T cells can differentiate to form the part of the memory repertoire has not been established (218). Therefore, current studies do not provide sufficient information to allow T cell memory to be manipulated therapeutically in cancer patients; thus there is a need to identify the exact memory T cell subsets which prevent cancer relapse.

Data presented in Chapter 4 (Figure 29) showed that tumour regression occurred in RencaHA tumour-bearing mice given ATT of Clone 4 T cells and combinations of A2aR-Antagonist and anti-TIM3mAb. In a proportion of mice, tumours did not relapse after regression and mice were able to resist rechallenge with further injections of tumour cells, these mice were termed 'Responders'. In some mice, tumours did relapse, and these mice were termed 'Non-Responders'. It was hypothesised that by comparing populations of memory T cells present in the tissues of Responder and Non-Responder mice, it would be possible to identify which memory subsets are present within tumour-bearing mice that resist tumour relapse.

Memory T cell subsets were also compared between mice receiving different treatment regimens as shown in Table 6. As systemic blockade of A2aRs and TIM3 has been shown to restore the *ex vivo* cytotoxic effector function of Clone 4 TILs, it was postulated that treatment with A2aR-Antagonist and anti-TIM3mAb would also support memory T cell formation. Therefore, A2aR-antagonist and anti-TIM3mAb-treated mice could possess greater numbers of memory T cells in the secondary lymphoid tissues when compared with vehicle-treated control mice (12, 45).

Table 6 - Combinations of Immunotherapy Administered to mice bearing RencaHA tumours

Treatment Group	ATT CL4 Cells	AR-Antagonist	Anti-TIM3mAb
A	x		
B	x	x	
C	x	x	x
D	x		x

To determine which memory T cell subsets could prevent relapse of RencaHA tumours, the following experimental approaches were utilised (Figure 52):

1. Flow cytometric analyses were used to quantify the proportion of CD8+ T cells with Effector, TEM, TCM and Naive phenotypes in the spleen and TDLN of tumour bearing mice. The proportions of each cell type were compared between:

    a. **Responders** (in which tumours regressed and did not relapse) and **Non-responders** (in which tumours regressed and then relapsed).

    b. Treatment groups **A, B, C** and **D**, comprising combinations of ATT, A2aR-Antagonist and anti-TIM3mAb.

2. Depletion experiments, utilising specific mAbs to determine whether memory T cells derived from adoptively transferred Clone 4 TILs, or from the host's endogenous CD8+ TIL population, play the greatest role in preventing tumour re-growth.

Figure 52 – Experiments to determine the importance of memory T cell subsets in preventing relapse amongst RencaHA tumour-bearing mice

RencaHA tumour-bearing BALB/c mice were given ATT of Clone 4 T cells and treated as follows: Group A - Vehicle and Isotype control; Group B - A2aR-Antagonist; Group C - A2aR-Antagonist + anti-TIM3mAb; and Group D- anti-TIM3mAb. Tumours in all groups regressed between 16 and 24 days from tumour injection. Some of these tumours remained regressed, these mice were termed 'Responders' (R). In some mice, tumours relapsed, and these mice were termed, 'Non-responders' (NR). (1) Spleens, TDLN and tumours were harvested from R and NR mice between 42 and 56 days, to assess the presence of different subsets of memory CD8+ T cells. A subset of mice received secondary antigen challenge by immunisation with influenza virus A/PR/8/H1N1, six days before flow cytometric staining. (2) Some R mice were treated with depleting mAbs to eradicate either all CD8+ T cell memory populations, or only Thy1.1+ Clone 4 memory populations.

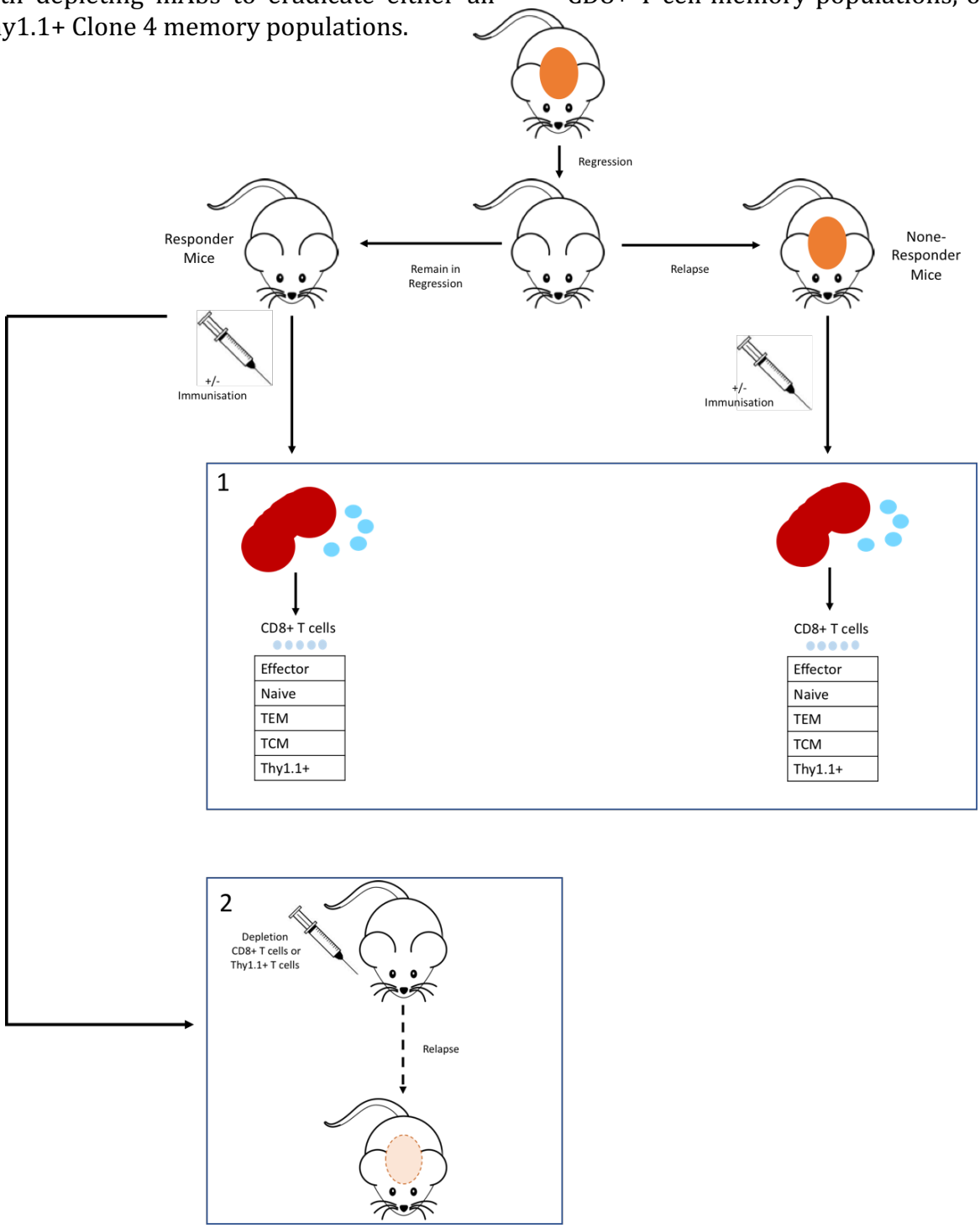

7.2 Results

7.2.1 In the RencaHA model, are Anti-Tumour Immune Memory cells derived from adoptively transferred Thy1.1+ Clone 4 TILs, or Thy1.2+ endogenous CD8+ TILs?

7.2.1.1 Thy1.1+ Clone 4 T cells cannot be isolated from the Spleen or TDLN of RencaHA tumour-bearing mice 42-56 days after tumour regression

Several studies have suggested that adoptive transfer of memory T cells could be used as immunotherapy to prevent relapse in cancer patients. However, it is not known whether or not T cells can form part of the memory repertoire after ATT. In fact, studies have shown that clones of T cells which respond to tumour-antigen with high affinity are less likely to differentiate into memory T cells than those which respond with low affinity (12, 45). Therefore, it was postulated that within the RencaHA model, endogenous CD8+ TILs could differentiate into immune memory cells, whereas ATT Clone 4 TILs with a TCR which responds to HA antigen with very high affinity, would be less likely to differentiate into memory T cell populations.

To determine if endogenous or Clone 4 CD8+ TILs developed into memory T cells within RencaHA tumour-bearing mice, the proportion of T cells expressing the Thy1.1 lineage marker was quantified amongst total CD8+ T cells within the spleens and tumour draining lymph nodes (TDLN) 42-56 days after tumour injection (Figure 52). The 42-56 day timeframe was selected because memory T cell populations establish >30 days from primary antigen challenge (297, 298). Mice were sampled from treatment groups A-D and were stratified into Responders and Non-Responders for analyses. In the Non-Responder cohort, tumour tissue was analysed alongside spleens and TDLN, however this could not be performed in Responders since their tumours had completely regressed in these mice.

The results showed that Thy1.1+ Clone 4 T cells could not be identified within the spleen or TDLN of either Responders or Non-responders using flow cytometry. This suggested that the numbers of memory Clone 4 T cells in secondary lymphoid tissues was too low to be detected (Figure 53). However, Thy1.1+ Clone 4 TILs were isolated from the tumours of Non-responders in Group C (ATT, anti-TIM3mAb + A2aR-Antagonist) and Group D (ATT + AntiTIM3mAb). There were no Thy1.1+ cells present in tumours from other treatment groups. These data suggest that persistance of Thy1.1+ Clone 4 TILs in tumour tissue was improved in mice which received

anti-TIM3mAb as part of the treatment regimen when compared with mice that did not (Figure 53).

7.2.1.2 Thy1.1+ Clone 4 T cells cannot be isolated from the Spleen or TDLN of RencaHA tumour-bearing mice after immunisation with Influenza A/PR/8

Typically, antigen-specific memory T cells decrease in number around 30 days after the waning of specific antigen therefore it was possible that the numbers of Clone 4 memory T cells in the secondary lymphoid tissues were too low to be quantified using flow cytometry (12, 45, 295, 299). The Clone 4 TCR responds specifically to the HA peptide from influenza A/PR8/H1N1. Therefore, to expand Clone 4 memory T cell numbers within the secondary lymphoid tissues of RencaHA tumour-bearing mice, mice were immunised with live influenza PR8 virus prior to quantification of the numbers of Thy1.1+ cells present within the secondary lymphoid tissues using flow cytometry[18].

The data showed that following immunisation, Thy1.1+ cells could not be identified in the spleen or TDLN of any treatment group (Figure 54). However, Thy1.1+ cells were isolated from the tumours of Non-responders of mice in all treatment groups except Group B (A2aR-Antagonist alone) after immunisation. As before, Group C and D mice possessed the greatest numbers of Thy1.1+ Clone 4 TILs. These data supported findings from pre-immunisation, suggesting that treatment with anti-TIM3mAb favoured the persistance of Thy1.1+ TILs within the TME (300). Interestingly, whereas Thy1.1+ cells were not present within the TME of Group A (Control, ATT only) mice prior to immunisation, Thy1.1+ cells could be isolated from the tumours of Group A mice after immunisation (Figure 54).

Overall, these experiments suggested that at 42-56 days from tumour injection, Thy1.1+ memory T cells could not be identified within the secondary lymphoid tissues of RencaHA tumour-bearing mice using flow cytometric analyses. Thy1.1+ TILs were detectable in the tumour tissue of mice which received treatment regimens including anti-TIM3mAb (Groups C and D), however immunisation was required to expand Thy1.1+ TILs to detectable numbers in the tumours of mice from Group A, which received ATT alone.

[18] Using influenza injection to achieve *in vivo* expansion of adoptively transferred Clone 4 T cells was validated using transfer of naïve Clone 4 T cells into non-tumour bearing BALB/c mice (Supplementary Figure S11).

Figure 53 - Thy1.1+ Clone 4 memory T cells were identified within the tumour, but not the Secondary Lymphoid Tissues, of RencaHA tumour-bearing mice

RencaHA tumour-bearing BALB/c mice were given 2 doses of ATT Clone 4 T cells and treated as follows: Group A - Vehicle and Isotype control; Group B - A2aR-Antagonist; Group C - A2aR-Antagonist + anti-TIM3mAb; Group D- anti-TIM3mAb. 42-56 days after tumour injection, CD8+ T cells were harvested from Spleens, Tumour Draining Lymph Nodes (TDLN) and Tumours, and the percentage of Thy1.1+ cells was quantified using flow cytometry. Clone 4 splenocytes were used as an antibody control. Representative flow cytometric data are shown, N =12 mice over 7 experiments.

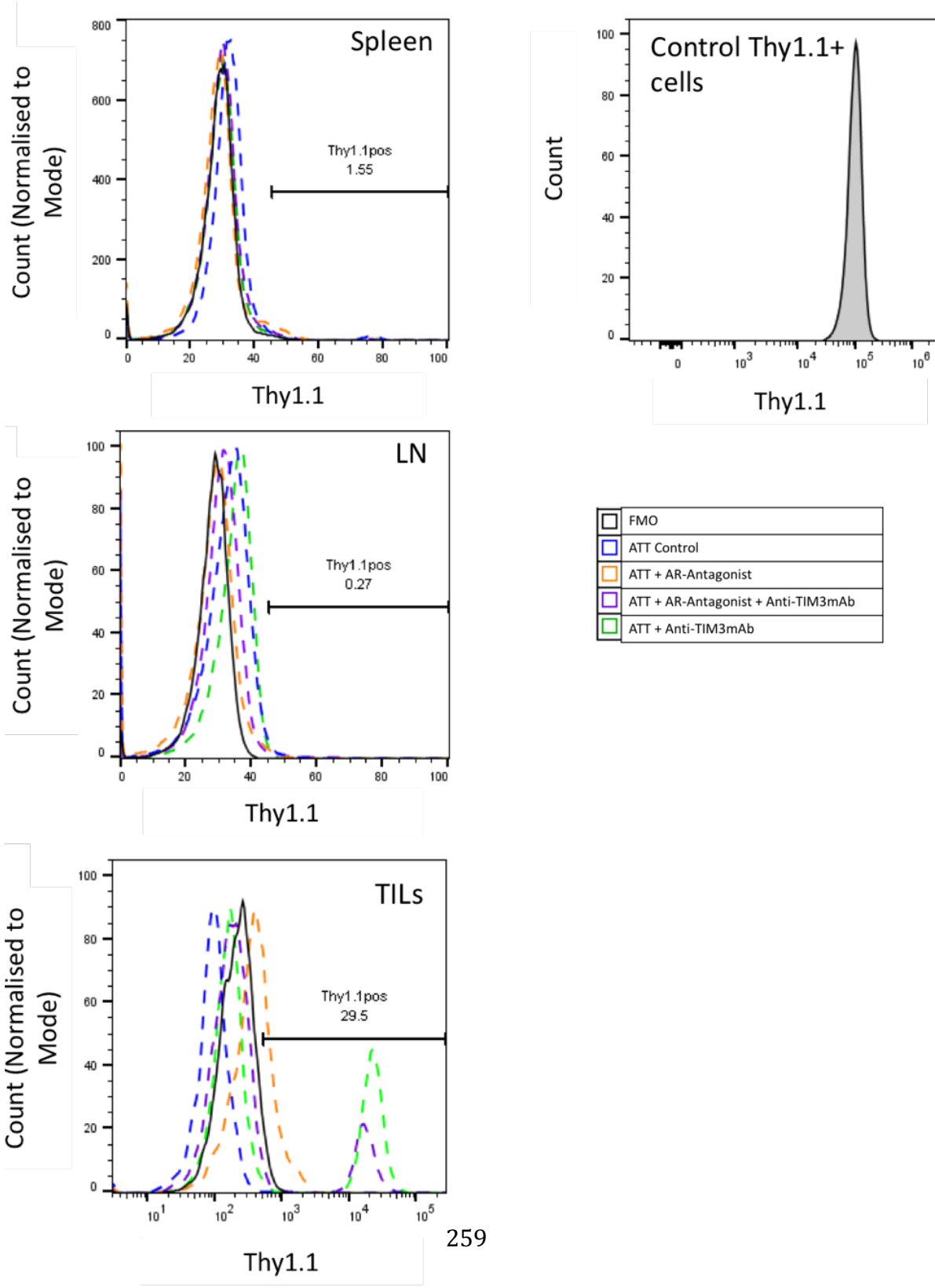

Figure 54 - Immunisation with Influenza A/PR/8 did not induce expansion of Thy1.1+ Clone 4 memory T cells within RencaHA tumour bearing mice

RencaHA tumour-bearing BALB/c mice were given 2 doses of ATT Clone 4 T cells and treated as follows: Group A - Vehicle and Isotype control; Group B - A2aR-Antagonist; Group C - A2aR-Antagonist + anti-TIM3mAb; Group D- anti-TIM3mAb. 42-56 days after tumour injection, mice were immunised with influenza A/PR/8/H1N1. CD8+ T cells were harvested from Spleens, Tumour Draining Lymph Nodes (TDLN) and Tumours, and the percentage of Thy1.1+ cells was quantified using flow cytometry. Clone 4 splenocytes were used as an antibody control. Representative flow cytometric data are shown. N = 11 mice over 7 experiments.

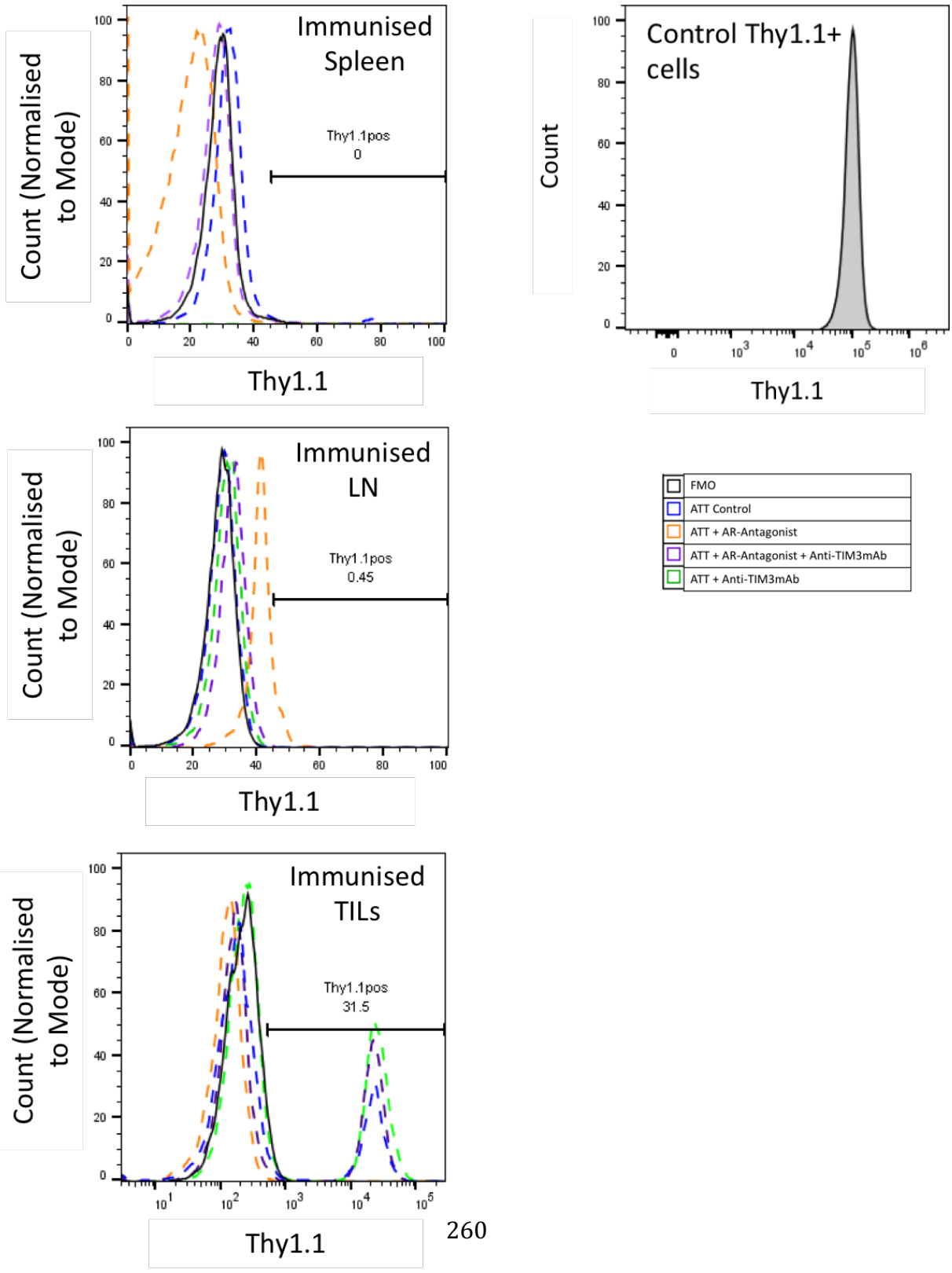

7.2.1.3 Thy1.1+ Clone 4 T Cells cannot be expanded from the Spleens of tumour bearing mice in ex vivo culture

Flow cytometric analyses suggested that Thy1.1+ Clone 4 T cell populations were either absent from within the secondary lymphoid tissues of tumour bearing mice, or that their numbers were below the limit of detection. To determine if Clone 4 memory T cells could be expanded *ex vivo* using specific antigen, splenocytes were harvested and placed in culture with K^dHA peptide and IL-2 medium, as this culture protocol reliably induces expansion of naïve Thy1.1+ Clone 4 CD8+ T cells from Clone 4 spleen preparations (76). Cells were stained at Day 8 to identify Thy1.1+ populations, however, Clone 4 T cells could not be expanded *ex vivo* from the spleens of tumour-bearing mice (Figure 55).

7.2.1.4 Depletion of Thy1.1+ Clone 4 T cells permits Tumour Relapse amongst mice which experienced complete tumour regression

Clone 4 memory T cells could not be detected in the secondary lymphoid tissues of RencaHA tumour bearing mice using flow cytometry. Therefore, depletion experiments were utilised to further determine whether or not memory T cells derived from ATT Clone 4 TILs were required to prevent relapse of RencaHA tumours *in vivo,* (Figure 52). Responder mice were selected, in which tumours were undergoing a period of regression. The data showed that amongst a subset of mice that were treated with anti-Thy1.1 depleting mAb, depletion of Thy1.1+ Clone 4 T cells resulted in tumour relapse. Therefore, it appears that the presence of a pool of memory T cells derived from Thy1.1+ Clone 4 TILs is essential to prevent regrowth of RencaHA tumours (Figure 56A).

It was hypothesised that endogenous CD8+ TILs could also form part of the memory T cell pool, and that the regrowth of RencaHA tumours would occur more rapidly if both Clone 4 memory and endogenous memory CD8+ T cells were depleted simultaneously, rather than depletion of Clone 4 subsets alone. To test this hypothesis, mice were depleted of all CD8+ T cells, and the speed of tumour re-growth was determined by R-values. The results showed that tumour regrowth occurred more rapidly in mice when all CD8+ T cells were depleted when compared to mice in which only Clone 4 T cells were depleted (Figure 56A & B). These data suggest that relapse of RencaHA tumours is prevented in mice by memory T cells derived from both the tumour bearing host's endogenous CD8+ TIL population and ATT Clone 4 TILs.

Figure 55 - Thy1.1+ Clone 4 memory T cells cannot be expanded ex vivo from the spleen of Tumour-bearing mice

RencaHA tumour-bearing BALB/c mice were given 2 doses of ATT Clone 4 T cells and treated as follows: Group A - Vehicle and Isotype control; Group B - A2aR-Antagonist; Group C - A2aR-Antagonist + anti-TIM3mAb. Splenocytes were harvested and incubated with K^dHA peptide for 5 days after which fresh Thy1.2+/+ splenocytes and peptide were added for 3 days before flow cytometric analyses. Data shows quantification of Thy1.1+ cells using flow cytometry, representative of 7 mice over 2 experiments.

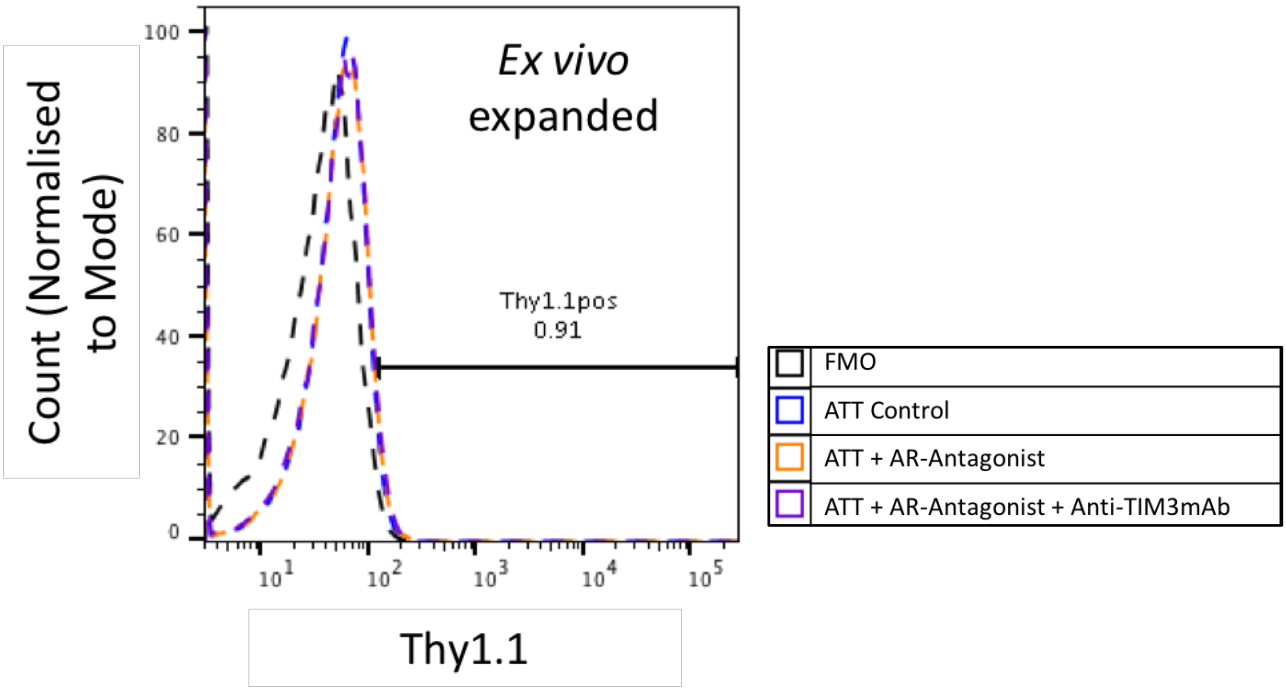

Figure 56 - Depletion of Thy1.1+ Clone 4 T cells results in relapse of RencaHA tumours

RencaHA tumour-bearing BALB/c mice were given 2 doses of ATT Clone 4 T cells and treated as follows: Group A - Vehicle and Isotype control; Group B - A2aR-Antagonist; Group C - A2aR-Antagonist + anti-TIM3mAb. (A) Growth curves are shown from mice which had experienced complete and durable tumour remission (Responders). Each line represents one individual mouse. After tumours regressed, depletion of all CD8+ T cells (filled circles) or Thy1.1+/+ CD8+ T cells (open circles) was performed using depleting mAb at the time indicated by the arrow. (B) R values (1/time) were calculated to indicate the growth rate of each tumour between 30-38 days. N = 5 mice over 1 experiment, each bar represents one mouse, therefore statistical comparisons could not be performed.

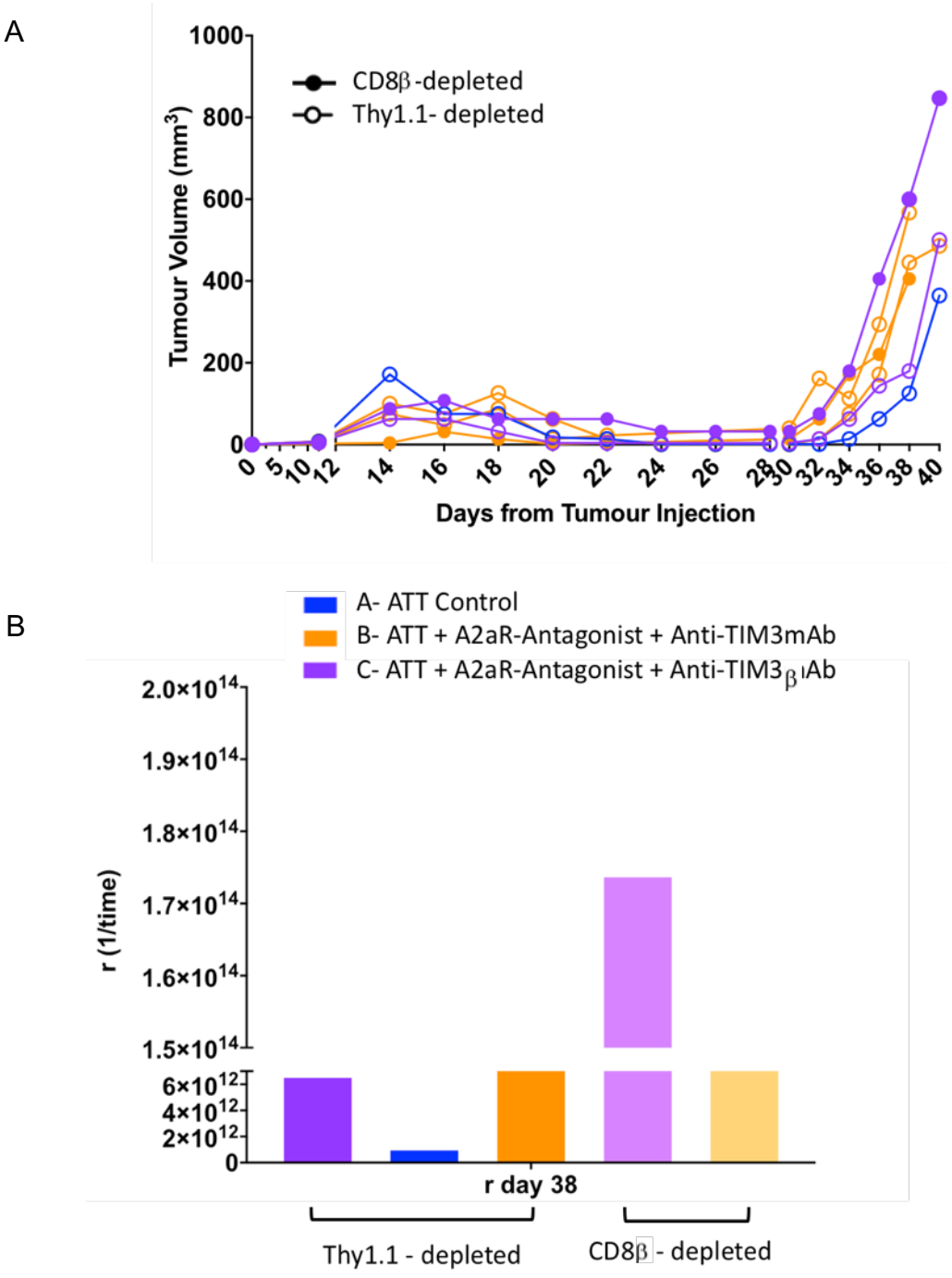

7.2.2 Does the balance of TEM and TCM cells vary between mice in which RencaHA tumours relapse, and those in which RencaHA tumours do not relapse?

7.2.2.1 Responder mice possess elevated numbers of T Effector Memory cells in the Spleen and TDLN when compared with Non-responders

Depletion experiments using mAb suggested that the activity of CD8+ memory T cells prevents relapse of RencaHA tumours *in vivo*. However, there are several studies which disagree about whether CD8+ TEM or TCM subsets play the greatest role in preventing tumour relapse. Thus identification of the memory T cell subsets which work towards preventing relapse could help to develop a more effective type of adoptive T cell transfer therapy utilising such subsets with the aim of preventing regrowth of MRD (230, 296, 301).

Experiments were carried out to determine which memory T cell subsets were associated with a reduced risk of relapse in the RencaHA tumour setting. To this end, the proportion of activated, naïve, TEM and TCM CD8+ T cells within the secondary lymphoid tissues was compared between of Responder mice (in which relapse did not occur) and Non-responder mice (in which relapse did occur)(Figure 52). Data presented in Chapter 4 showed that the hazard ratio (i.e. the statistical likelihood) of relapse was influenced by treatment with different regimens comprising A2aR-Antagonist and anti-TIM3mAb. Therefore, the balance of memory T cell subsets was also compared across different treatment groups, in case specific memory T cell subsets were present in the secondary lymphoid tissues of mice in those treatment groups with the lowest hazard ratio of relapse (Figure 57).

If the various treatment regimens are ignored, then Responder mice possessed more TEM cells in the spleen and TDLN than Non-Responders (Figure 57 i & iii)[19]. Immunisation with influenza A/PR/8 was then performed to determine if specific memory T cell subsets expanded after secondary challenge with live influenza. The data show that after immunisation, the number of TEM cells was reduced within the spleen and TDLN of Responders, but the proportion of TEM

[19] There was only one individual in the Group D responder category, however to generate more would have necessitated repeating the entire experiment, resulting in the use of more animals, which would fail to satisfy the 3Rs criteria for this project.

cells within the secondary lymphoid tissues of Non-responders did not change when compared with pre-immunisation (Figure 57 ii & iv).

When different treatment groups were compared, the proportions of the various different memory T cell subsets did not differ significantly between treatment groups, except that Group D mice (ATT + anti-TIM3mAb) possessed lower numbers of TEM cells in the spleen and TDLN than mice from other groups both before and after immunisation (Figure 57).

Figure 57 –TEM cells are more numerous in the secondary lymphoid tissues of RencaHA tumour-bearing mice which do not experience Relapse

RencaHA tumour-bearing BALB/c mice were given 2 doses of ATT Clone 4 T cells and treated as follows: Group A - Vehicle and Isotype control; Group B - A2aR-Antagonist; Group C - A2aR-Antagonist + anti-TIM3mAb; Group D- anti-TIM3mAb. (i & ii) show data from spleens and (iii & iv) show data from Tumour Draining Lymph Nodes (TDLN). CD8+T cells were extracted from mice which had experienced complete and durable tumour remission (Responders - R), or mice in which tumours which experienced relapse (Non-responders - NR). A subset of mice was immunised with influenza A/PR/8/H1N1 as indicated. Cells were stained with antibodies against CD62L, CD69 and CD44. Pie charts show proportion of TEM, TCM, naïve and effector cells. N = 23 mice analysed over 7 experiments. Proportion of cells in each segment was compared between R and NR within each treatment group using MANOVA, p=values are tabulated.

i. Spleen

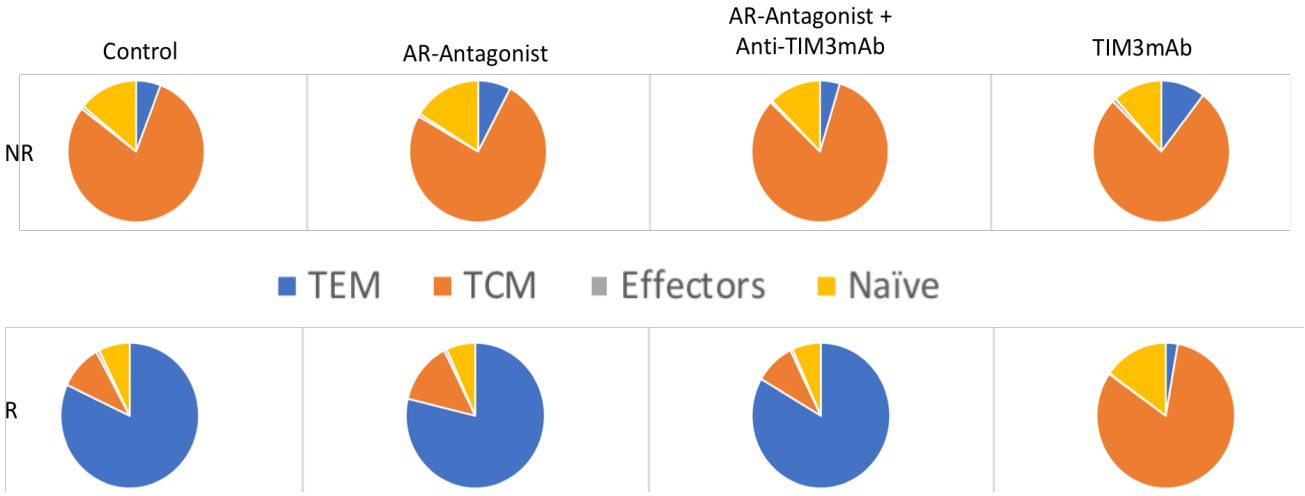

	Control ATT	AR-Antagonist	AR-Antagonist + Anti-TIM3mAb	Anti-TIM3mAb
TEM	0.017*	0.009*	0.001****	0.45
TCM	0.006**	0.028*	0.0001***	0.47
Naïve	0.10	0.14	0.20	0.48
Effector	0.10	0.81	0.67	0.39

ii. – Spleen (Immunised)

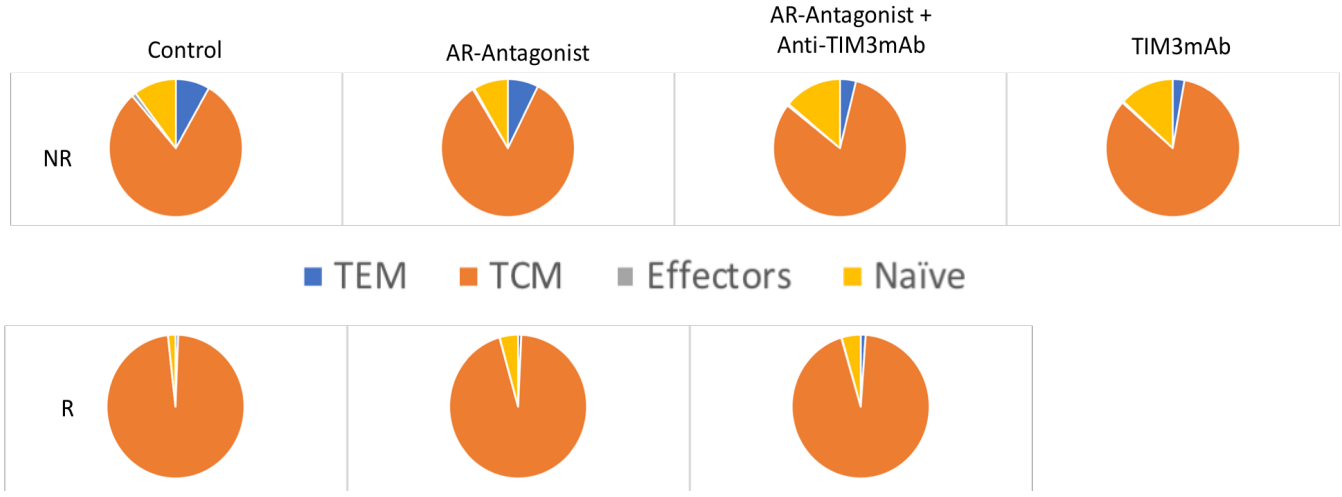

	Control ATT	AR-Antagonist	AR-Antagonist + Anti-TIM3mAb	Anti-TIM3mAb
TEM	0.29	0.07	0.40	
TCM	0.17	0.10	0.004**	
Naïve	0.17	0.08	0.51	
Effector		0.81	0.67	

iii – TDLN

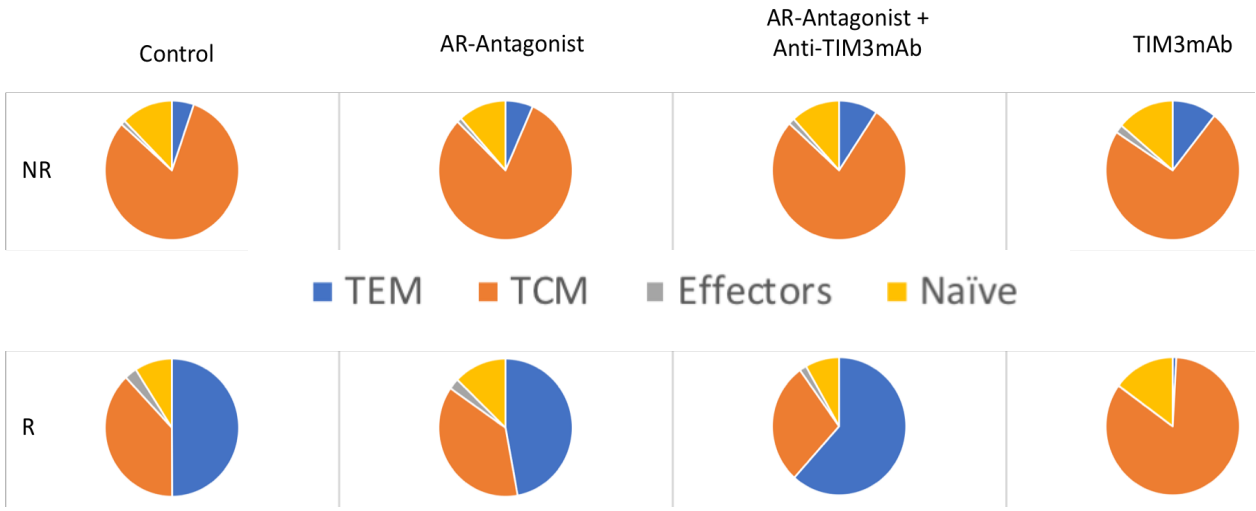

	Control ATT	AR-Antagonist	AR-Antagonist + Anti-TIM3mAb	Anti-TIM3mAb
TEM	0.04*	0.007**	0.02*	0.19
TCM	0.26	0.42	0.13	0.23
Naïve	0.33	0.29	0.89	0.004**
Effector	0.92	0.60	0.43	0.76

iv – TDLN (Immunised)

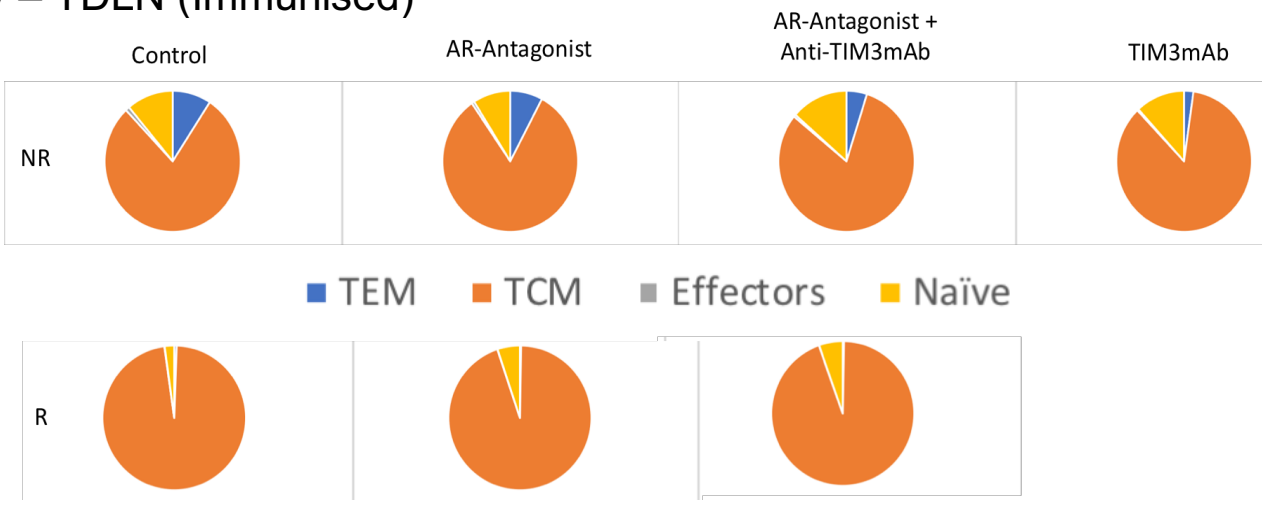

	Control ATT	AR-Antagonist	AR-Antagonist + Anti-TIM3mAb	Anti-TIM3mAb
TEM	0.41	0.19	0.03*	
TCM	0.31	0.09	0.09	
Naïve	0.66	0.42	0.04*	
Effector	0.23	0.08	0.16	

7.2.4 Does A2aR and anti-TIM3mAb engagement affect the TCR signalling required to generate a memory T cell response?

7.2.4.1 Spatiotemporal localisation of PKCθ at the immune synapse is not altered by Adenosine Receptor signalling

Data presented in Chapter 4 shows that in RencaHA tumour-bearing mice treated systemically with A2aR-antagonist and anti-TIM3mAb, their tumours were statistically less likely to relapse when compared to vehicle-treated control mice. This finding clearly suggests that blockade of A2a and TIM3 receptors potentiates CD8+ memory T cell development (299). Several groups have determined that failure of PI3k and PKCθ to localise to the immune synapse, or NF-kB to localise to the nucleus, in clones of CD8+ T cells during primary immune responses, is associated with reduced expansion of these same CD8+ T cell clones as memory T cells (299, 302, 303). Therefore, we hypothesised that A2aR and TIM3 signalling could inhibit the ability of PI3k, NF-kB, and PKCθ to localise to the Clone 4 CTL immune synapse.

Live cell imaging was therefore utilised to assess the patterns of accumulation of NF-kB^{GFP}, PI3k^{GFP} (the SH2-interSH2-SH2 domain as shown in Roybal et al. 2009) and PKCθ^{GFP} during immune synapse formation between Clone 4 CTL and Renca tumour cell targets (47). Patterns of accumulation were characterised as described previously (Introduction, Figure 3). However, the levels of NF-kB^{GFP} and PI3K^{GFP} which accumulated at the immune synapse formed by *in vitro* primed Clone 4 CTL were too low to be detected using live cell imaging approaches (Data not shown). Therefore, only the localisation of PKCθ could be quantified.

To identify whether or not adenosine receptor engagement inhibited the ability of PKCθ^{GFP} to localise to the immune synapse, Clone 4 CTL were cultured in the presence of the pan-adenosine receptor agonist NECA. NECA-treated CTL were then imaged during cell-couple formation with Renca tumour cell targets. Several studies have shown that PKCθ localises to the central area of immune synapse to exert its signal transduction, therefore central patterns of PKCθ accumulation were compared between NECA-treated CTL and untreated CTL (47). Overall, the data showed that an initial peak of central PKCθ accumulation occurred at the CTL immune synapse. This peak was delayed but greater in magnitude amongst NECA-treated CTL when compared with untreated Clone 4 CTL. Therefore, adenosine receptor signalling does appear to affect PKCθ localisation at the immune synapse, but rather than being inhibited by

NECA, central PKCθ accumulation is promoted by adenosine receptor engagement, although this finding was not significant (Figure 58).

7.2.4.2 Development of an Assay to assess spatiotemporal localisation of PKCθ amongst TILs

As the localisation of PKCθ was affected by adenosine receptor signalling *in vitro*, it was concluded that systemic blockade of A2aRs *in vivo* could affect the localisation of PKCθ amongst Clone 4 TILs, and this could improve the potential for TILs to form anti-tumour immune memory cells. Experiments to determine if this is the case could involve adoptive transfer of $PKC\theta^{GFP}$-expressing Clone 4 CTL into tumour-bearing mice receiving systemic blockade of A2aRs. $PKC\theta^{GFP}$-expressing Clone 4 TILs could then be recovered, and the localisation of PKCθ at the immune synapse could be quantified amongst TILs using live cell imaging *ex vivo*. However, Clone 4 T cell populations do not take up the $PKC\theta^{GFP}$ construct efficiently during transduction. Therefore, transduction produces inadequate numbers of $PKC\theta^{GFP}$ expressing Clone 4 CTL to be administered in adoptive T cell transfer, and live cell imaging could not be used to assess the spatiotemporal localisation of PKCθ amongst TILs *ex vivo*.

An alternative method of assessing PKCθ localisation, would be to utilise untransduced TILs and to fix them during cell coupling formation with Renca tumour cell targets. *In situ* antibody staining on a coverslip could then be used to identify the location of PKCθ at the immune synapse. However, the activating phosphorylation of Threonine 538 of PKCθ could not be identified amongst TILs using this method with currently available antibodies (Figure 59).

Figure 58 - Central localisation of PKCθ at the immune synapse is elevated amongst Clone 4 CTL cultured in the presence of 5-N-ethylcarboxamidoadenosine

In vitro primed Clone 4 CTL were transduced with $PKC\theta^{GFP}$. A subset of cells was cultured in media containing 10 μM NECA. Immune synapse formation between CTL and K^dHA-pulsed Renca tumour cell targets was imaged *ex vivo* using confocal microscopy. Analysis of the central pattern of accumulation of PKCθ was performed in >30 cell couples per condition, across 2-4 experiments and compared between conditions using proportional z-test (tabulated).

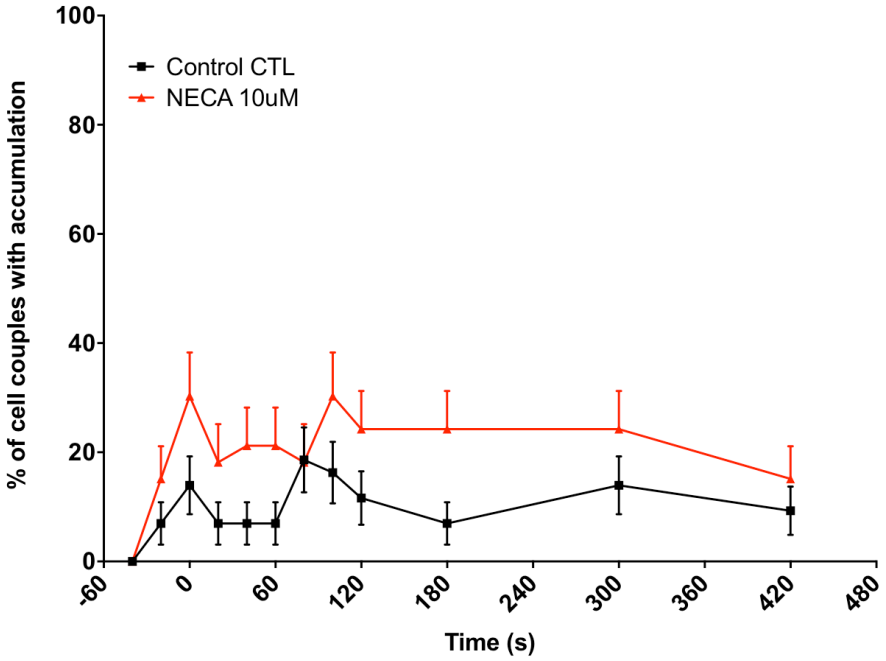

Time	-40	-20	0	20	40	60	80	100	120	180	300	420
CTL vs NECA 10uM	na	0.98	0.70	0.39	0.49	0.49	0.25	0.62	0.55	0.59	0.50	0.29
	ns	ns	ns	ns	ns	ns	ns	ns	ns	ns	ns	ns

Figure 59 - In situ staining cannot detect PKCθ localisation at the immune synapse of CD8+ TILs

CD8+ TILs were harvested from RencaHA tumour-bearing mice and labelled with CFSE (green). TILs were added to K^dHA pulsed Renca tumour cell targets on a coverslip. Cells were allowed 4 minutes to form cell couples before being fixed, permeabilised and stained with primary anti-PKCθ Thr538, and secondary anti rabbit AF405. Slides were mounted in antifade mountant prior to analysis using confocal microscopy[20]. No specific staining of PKCθ was identified in the images (blue on green).

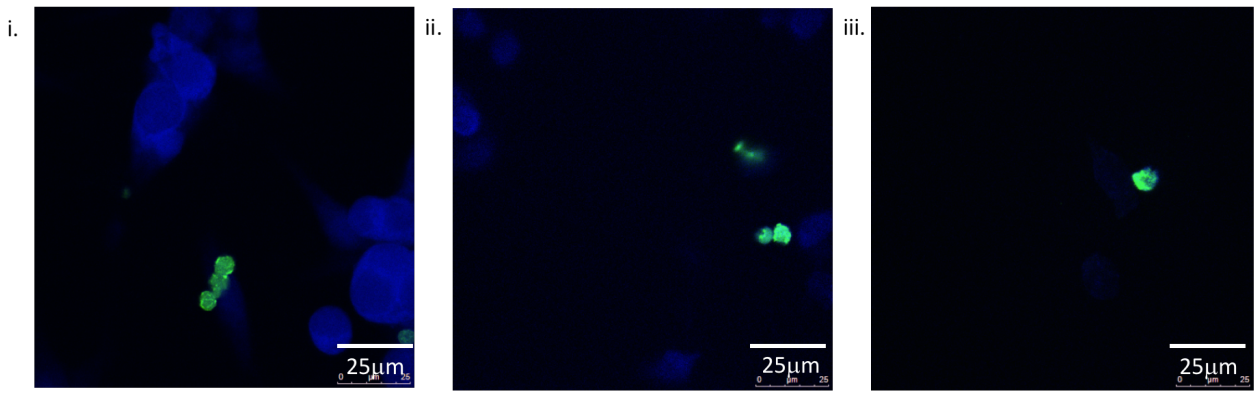

[20] For these experiments, GE was assisted by Clara Kouaku, a project student in the Wuelfing lab.

7.3 Discussion

A key aim of cancer immunotherapy is to generate anti-tumour immune memory within cancer patients. CD8+ T cell memory is thought to prevent tumour relapse through the destruction of cancer cells, preventing the recrudescence of MRD and also the formation of new lesions (226, 227, 264). RencaHA tumour-bearing mice given ATT of Clone 4 T cells plus combinations of A2aR-Antagonist and anti-TIM3mAb fell into two distinct categories:

- Responders, in which tumours regressed and did not relapse
- Non-Responders, in which tumours relapsed.

Populations of CD8+ memory T cells were quantified in the secondary lymphoid tissues of Responder and Non-responder mice, to determine if the presence of specific subsets of memory cells within Responder mice was associated with their ability to resist tumour relapse.

7.3.1 Both adoptively transferred Thy1.1+ Clone 4 TILs and Thy1.2+ Endogenous CD8+ TILs give rise to Memory T cells which prevent tumour relapse

Adoptive T cell Transfer (ATT) Therapies have shown great promise in enabling patients to eradicate existing tumour lesions. However, the ability of ATT cells to form anti-tumour immune memory populations is not clear (218, 259). In fact, T cells used for ATT typically respond to tumour antigen with high affinity, and studies have shown that T cell clones with lower TCR affinities may have greater potential to form memory T cells in response to secondary antigen challenge (12, 45).

Amongst RencaHA tumour-bearing mice given 2 separate rounds of ATT of Clone 4 T cells with combinations of A2aR-Antagonist and anti-TIM3mAb, some mice experienced complete and sustained tumour regression (Responders). Responder mice were able to resist rechallenge with further injections of tumour cells, suggesting that they possessed anti-tumour immune memory (226, 228, 264). As Thy1.1+ ATT Clone 4 T cells respond to HA antigen with such high affinity, we hypothesised that they would not differentiate into memory T cells, and that immune memory to RencaHA tumours would be mediated by the host's endogenous Thy1.2+ CD8+ T cells instead. Staining and depletion experiments were carried out, to determine whether memory cells derived from Clone 4 TILs or endogenous CD8+ TILs were present in the

secondary lymphoid tissues of RencaHA tumour-bearing mice. When spleens and TDLN were examined using flow cytometry, memory T cells derived from the ATT Clone 4 population were not identified. Previous studies using other murine models suggest that 30 days after antigen challenge, less than 2% of adoptively transferred cells remain as memory cells (297, 299). Therefore, in case ATT Clone 4 memory cells were not numerous enough to be detected using flow cytometry, immunisation with Influenza A/PR/8 was performed, with the aim of inducing the expansion of Clone 4 memory T cells. However, no Thy1.1+ cells could be isolated from either the spleens or the TDLN after immunisation. This suggests that Clone 4 memory T cells are either present in very low numbers, or are not involved in preventing RencaHA tumour relapse amongst Responder mice.

Since Clone 4 memory T cell expansion could not be induced *in vivo* using immunisation*, ex vivo* expansion was attempted. Spleens were harvested from Responder mice and stimulated with K^dHA peptide in cell culture. However, no Thy1.1+ Clone 4 T cells were detected at the end of the culture period. A limitation of this approach is that exposure of antigen-experienced Clone 4 T cells to strong antigenic stimulus (K^dHA peptide) with repeated stimulation for 8 days *ex vivo* could have caused antigen induced cell death to occur. One preliminary experiment was carried out, involving a shorter duration of cell culture (72h), with only one addition of peptide. However, no Thy1.1+ cells were isolated from this culture either (data not shown). Microscopic analyses showed that the density of activated cells in the splenocyte culture was greatest at 24h, which suggests that this would have been the optimal time to stain for Thy1.1+ T cells, however, we chose not to repeat this experiment, in order to conserve mice for use in other depletion experiments.

As an alternative strategy to determine if memory T cells derived from Clone 4 TILs were required to prevent tumour relapse, depletion of Thy1.1+ cells in Responder mice was performed after tumour regression. Tumours relapsed after depletion, indicating that memory cells derived from Clone 4 TILs were actively preventing relapse. Tumour relapse occurred faster if endogenous CD8+ memory T cells were depleted as well as Clone 4 populations. This finding suggests that populations of both endogenous CD8+ TILs and adoptively transferred Clone 4 TILs gave rise to memory cells, which prevent relapse by controlling re-growth of tumour cells in the RencaHA model.

Despite the fact that depletion clearly produced relapse, there were some limitations with the interpretation of this data, as low numbers of mice were used, meaning that the speed of relapse could not be statistically compared between Thy1.1-depleted and pan-CD8-depleted mice. Therefore, these depletion analyses should be repeated. A second combination of anti-CD8 depleting antibodies was generated in-house from hybridoma cultures, however this reagent was not used for these analyses, as commercially purchased antibodies produced more reliable results during optimisation experiments (Supplementary Figure S12).

The way in which the effector functions of both Clone 4 and endogenous CD8+ memory T cell populations combine to prevent relapse is not known. In the presence of Clone 4 TILs, a greater proportion of endogenous CD8+ TILs produce effector cytokines, and fewer produce IL-10 when compared with endogenous TILs harvested from tumour-bearing mice which did not receive tumours without ATT of Clone 4 T cells (Chapter 3, Figure 19). The fact that endogenous CD8+ TILs function better as cytotoxic effectors in the presence of Clone 4 TILs could make endogenous TILs less likely to proceed to exhaustion, and more likely to develop into memory cells as their terminal fate (12, 45).

7.3.2 Elevated numbers of CD8+TEM cells are found in the secondary lymphoid tissues of mice with a reduced risk of tumour Relapse

Regardless of their clonal origin, CD8+ memory T cells fall into two main subsets, TCM or TEM cells. It is not clear whether or not the presence of elevated numbers of either subset is associated with prevention of tumour relapse. TCM cells may be advantageous because they can home-to and persist within secondary lymphoid tissues, enabling them to propagate further priming of naïve cells to join the memory response. However, TEM cells have more immediate killing ability than TCM populations (230, 301, 304). It has been suggested that if one subset is found to prevent tumour relapse more effectively, CD8+ T cells could be diverted using cytokines to acquire specific memory phenotypes before use in ATT therapies, aiming to prevent relapse in cancer patients (230, 301, 304).

We postulated that by identifying differences in the memory T cell subsets present within Responder mice (in which tumours did not relapse) and Non-responder mice (in which tumours relapsed) we could determine whether TEM or TCM cells are more important for the prevention of tumour relapse. To achieve this, CD8+ T cells residing in the spleen and TDLN

between 42-56 days after tumour injection were stratified into Naïve, Effector, TEM and TCM cell populations using flow cytometric analyses. Samples from the skin at the site of tumour regression were also stained using CD103a, with the aim of quantifying tissue resident memory (TRM) cells. However, processing of the epidermis and dermis of the dorsal neck did not provide sufficient CD8+ T cells to quantify TRM cells using flow cytometry, so CD103a was omitted from further analyses (Supplementary Figure S13).

The data showed that Responder mice possessed a greater proportion of TEM cells in both the spleen and the TDLN when compared with Non-Responders. One explanation for this finding could be that Non-Responder mice still possess a macroscopic tumour. Therefore, their TEM cells could be responding to tumour antigen in the periphery rather than residing in the secondary lymphoid tissues. This would not occur in Responders because they don't have remaining tumour tissue.

However, Responder mice in Group D (ATT + anti-TIM3mAb), which did not have tumour tissue, also had low numbers of TEM cells in the spleen, at a level which resembled Non-responders. Group D mice had the highest risk of relapse of any treatment group. This led us to suggest that the presence of TEM cells in the spleen was different between Responders and Non-responders because it was associated with relapse potential, and not because Non-responders still had tumour lesions. The fact that Groups A and B (in which intermediate hazard ratios of relapse were scored) expressed intermediate levels of TEM cells, and Group C mice (in which the lowest hazard ratio of relapse was scored) possessed the highest number of TEM cells, supported this hypothesis.

It is not known whether or not TEM cells are mechanistically protective against relapse. Since TEM cells possess both effective killing ability and the ability to develop into self-renewing TCM populations, these cells possess advantageous qualities of both cell types, which could explain their association with a reduced hazard ratio of tumour relapse within the RencaHA model (305). Alternatively, after the first immune memory response, repeated secondary and tertiary exposures to antigen generate predominantly TEM cells. Therefore, the presence of TEM cells could simply indicate that Responder mice effectively mount secondary and tertiary immune memory responses each time MRD recrudesces, whereas None responders do not. Nevertheless, the data suggest that the percentage of TEM cells present in secondary lymphoid

tissues could be used as a biomarker of relapse potential. Lymph node biopsies are routinely sampled in cancer patients therefore further studies utilising human tissue could be used to assess whether there is a correlation between TEM cells and relapse in human cancers (117, 221).

7.3.3 A loss of CD8+TEM cells from the secondary lymphoid tissues after immunisation, is associated with a reduced risk of tumour Relapse

Following immunisation with influenza virus A/PR/8, the number of TEM cells within the spleen and TDLN of Responders reduced dramatically, whereas in Non-Responders, TEM cell numbers remained the same. In Responders, the fact that immunisation with HA antigen induced a loss of TEM cells could indicate that they diverted to a TCM phenotype. Alternatively, the TEM pool within responders could have mobilised from the lymphoid tissues to the peripheral site of influenza antigen. The latter explanation is more likely, since studies suggest that TEM cells involved in repeated memory responses will rapidly exit lymph nodes for peripheral tissues upon antigen exposure. Furthermore, TEM cells do not become TCM cells if specific antigen is still present (12).

Therefore, our findings suggest that TEM cells in Responder mice may effectively migrate out of secondary lymphoid tissues in response to immunisation with HA from PR8 virus, which is the model-tumour antigen expressed by RencaHA tumour cells. In Non-responder mice, the percentage of TEM cells in the spleen and TDLN remained constant after immunisation, which could suggest that migration of memory T cells is inhibited amongst Non-responders. Studies using LCMV indicate that the formation and migration of CD44+ memory T cells is inhibited in the presence of chronic viral antigen. Thus, the continued presence of tumour antigen in Non-responder mice could impair their ability to generate and mobilise TEM cells (114). For future experiments, a two photon microscopy approach could enable the ability of tumour-specific TEM cells to mobilise and infiltrate various tissues to be determined within RencaHA tumour-bearing mice (12, 305).

A further interesting observation from the above experiments is that anti-tumour immune memory appears to be HA-specific in the RencaHA model. Depletion experiments show the importance of HA-specific Thy1.1+ Clone 4 T cells in preventing relapse, and immunisation with influenza A/PR/8 expressing HA antigen produces detectable alterations in the TEM/TCM

balance within the spleen and TDLN, even though most of these memory cells are derived from endogenous CD8+ TILs. Therefore, these data suggest that in models of ATT, the host's mixed repertoire of endogenous cells gain the ability to form memory responses to the antigen targeted by ATT populations.

7.3.4 Blockade of A2aRs and TIM3 is associated with a reduced risk of relapse, how could signalling through A2aRs and TIM3 suppress T cell memory?

RencaHA tumour-bearing mice which received anti-TIM3mAb and A2aR-Antagonist alongside ATT had the lowest likelihood of relapse of any treatment group as measured by hazard ratios (Chapter 4, Figure 30). This finding suggests that the development of memory T cells which are required to prevent relapse, such as a TEM population with efficient migratory abilities, could be favoured by treatment with A2aR-Antagonist and anti-TIM3mAb.

Our previous data suggests that infiltration of CD8+ T cells into RencaHA tumours can directly be enhanced by blocking TIM3 and A2aRs (Chapter 5, Figure 37). A2aR engagement could inhibit Rho GTPases required for migration, and suppress endothelial activation, explaining this finding. The ability of TEM cells to migrate from the secondary lymphoid tissues to the site of influenza injection could be influenced by A2aRs in the same way. The effects of TIM3 engagement on T cell migratory pathways have not been studied however, TIM3 could affect the propensity of clones of CD8+ TILs to differentiate into T effector memory cells. One study has indicated that TIM3 signalling directly promotes short lived effector cell fates amongst CD8+ T cells, and inhibits memory formation during LCMV infection (256).

To determine whether A2aR and TIM3 engagement directly inhibited memory T cell differentiation by suppressing TCR signalling, live cell imaging was used to quantify the percentage of Clone 4 CTL in which PKCθ localised to the centre of the immune synapse during target cell killing. We hypothesised that central localisation of PKCθ would be suppressed in the presence of the adenosine receptor agonist NECA, however NECA treatment was associated with an increase in the percentage of cell couples expressing central PKCθ. Previously, cytotoxicity assays have demonstrated that NECA enhances the cytotoxic ability of Clone 4 CTL *in vitro* (Chapter 6, Figure 42), therefore enhancement of central PKCθ localisation correlates with enhanced killing ability amongst Clone 4 CTL. NECA could have this stimulatory effect on CTL, because it agonises stimulatory A1 and A3 adenosine receptor subtypes expressed on T

cells as well as immunosuppressive A2a and A2b receptors. Future studies could utilise CGS2680, a specific A2aR agonist to assess the effect of specifically engaging inhibitory A2aRs on PKCθ localisation within Clone 4 CTL immune synapses.

7.3.5 Further Work

The development of an improved assay to assess the effects of A2aR and TIM3 engagement on PKCθ localisation could involve the use of the RencaHA spheroid system (Chapter 6, 6.3.5). PKCθ^{GFP}-expressing Clone 4 CTL could be allowed to infiltrate spheroids, and live cell imaging of SILs could be used to determine the localisation of PKCθ^{GFP} when Clone 4 SILs form immune synapses after recovery from the spheroid. This experiment would determine whether exposure to a microenvironment of RencaHA cells, with no other factors in the organoid, affects PKCθ localisation and therefore memory potential. A2aR signalling could be manipulated within the spheroid using the A2aR agonist CGS2680. Additionally, overexpression of TIM3^{GFP} could be engineered amongst by transduction of Clone 4 CTL prior to spheroid infiltration. The RencaHA tumour cells used to make spheroids could be transfected with Ceacam-1 or Galectin-9 to ensure that TIM3 was engaged within the spheroid. These experiments may allow us to determine whether engagement of TIM3 and A2aRs causes suppression of memory TCR signalling within the spheroid microenvironment.

Priming events are important in determining T cell fates including memory, therefore the localisation of PI3K, NFκB and PKCθ should be also be examined during priming of naïve Clone 4 T cells at the TDLN. The use of live cell imaging assays only assesses the localisation of signalling intermediates during killing interactions exerted by primed cells. However, one method to quantify TCR signalling events during priming could involve transfer of naïve (rather than primed) Thy1.1+ Clone 4 T cells into tumour bearing mice. Immunohistochemistry could then be used to determine the localisation of PI3K, NFκB and PKCθ during immune synapse formation by naïve Clone 4 T cells undergoing priming at the TDLN.

Chapter 8 Discussion

8.1 New Approaches to Cancer Immunotherapy

In recent years, there has been a huge increase in interest in the field of cancer immunotherapy (102, 119, 306). Some of the most successful immunotherapeutic treatments harness the ability of CD8+ T cells to bind to and directly lyse cancer cells. CD8+ Tumour Infiltrating Lymphocytes (TILs) are frequently inhibited when immunosuppressive receptors on their surface are engaged by ligands within the tumour microenvironment (TME). Blockade of such pathways can restore the ability of CD8+ TILs to kill tumour cells *in vivo* (68, 307-310). Amongst therapies which block inhibitory receptors within the tumour, CTLA-4 and PD-1 co-inhibitory receptor (CIR) blockade has shown great promise, improving the overall anti-tumour immune response and controlling tumour growth amongst clinical patients with melanoma, NSCLC and haematological cancers. However, many other cancers do not respond well to these therapies (117, 119).

Two emerging concepts have helped to identify the reason that CTLA-4 and PD-1 blockade are not universally applicable to all cancer types. Firstly, the 'Cancer Immunity Cycle' was defined, identifying 7 crucial stages in the anti-tumour immune response. If any of these stages are inhibited, cancers can escape immune destruction (174). Although the result of the Cancer Immunity Cycle is tumour killing by CD8+ T cells, the stages which precede this involve interactions between multiple immune cell types and the TME (51, 174). Briefly, crucial stages in the Cancer Immunity Cycle include:

- Cancer cells are lysed or damaged to release antigens which are taken up and presented by DC.
- There must be sufficient damage signalling for DC to mature within the TME, enabling them to prime CD4+ and CD8+T cells at the TDLN.
- Lymphocytes infiltrate the tumour to become TILs.
- There must be a sufficiently pro-inflammatory milieu in the tumour to ensure that CD4+ TILs remain as T helper cells and are not induced to acquire Treg characteristics.
- CD8+ TILs must retain their cytotoxic effector function and not become tumour suppressed by pathways within the TME (119, 311, 312).

Different stages of the Cancer Immunity Cycle are inhibited in different tumour types. CTLA-4 and PD-1 blockade target the latter stages of this cycle, improving the function of CD8+ T cells which have infiltrated the tumour, and inhibiting Treg development and function. However, this combination of blocking mAb does not target tumour infiltration or the steps which precede it in the Cancer Immunity Cycle (Figure 60). Therefore, novel immunotherapeutic combinations must be developed in order to improve immune activity at multiple other stages of the Cancer Immunity Cycle.

Figure 60 - The Cancer Immunity Cycle

The Cancer Immunity Cycle describes the events which are required for effective anti-tumour immunity. These events are known as a cycle, because Step 7, tumour killing by immune cells, releases antigen and damage signals to promote Step 1 in the cycle, amplifying the response further (174). Steps 1, 2 and 3 involve the expression and release of tumour antigens, uptake of these antigens by dendritic cells (DC), and DC maturation and presentation of antigen to prime anti-tumour CD8+ T cells at the tumour draining lymph node (TDLN). Steps 4 and 5 involve the traffic of CD8+ T cells to tumours, and tumour-infiltration. Step 6 is the recognition and killing of tumours by primed CD8+ T cells. Thus there are three key levels at which CD8+ T cell-mediated anti-cancer immunity is inhibited, priming, infiltration and killing (174). Depending on the tumour type, different stages of the cycle are inhibited, and immunotherapy should aim to define and target the areas of weakness in the cancer immunity cycle for each individual tumour (119, 174).

Figure taken from 'The Cancer Immunity Cycle. Chen and Mellman. 2013'(174).

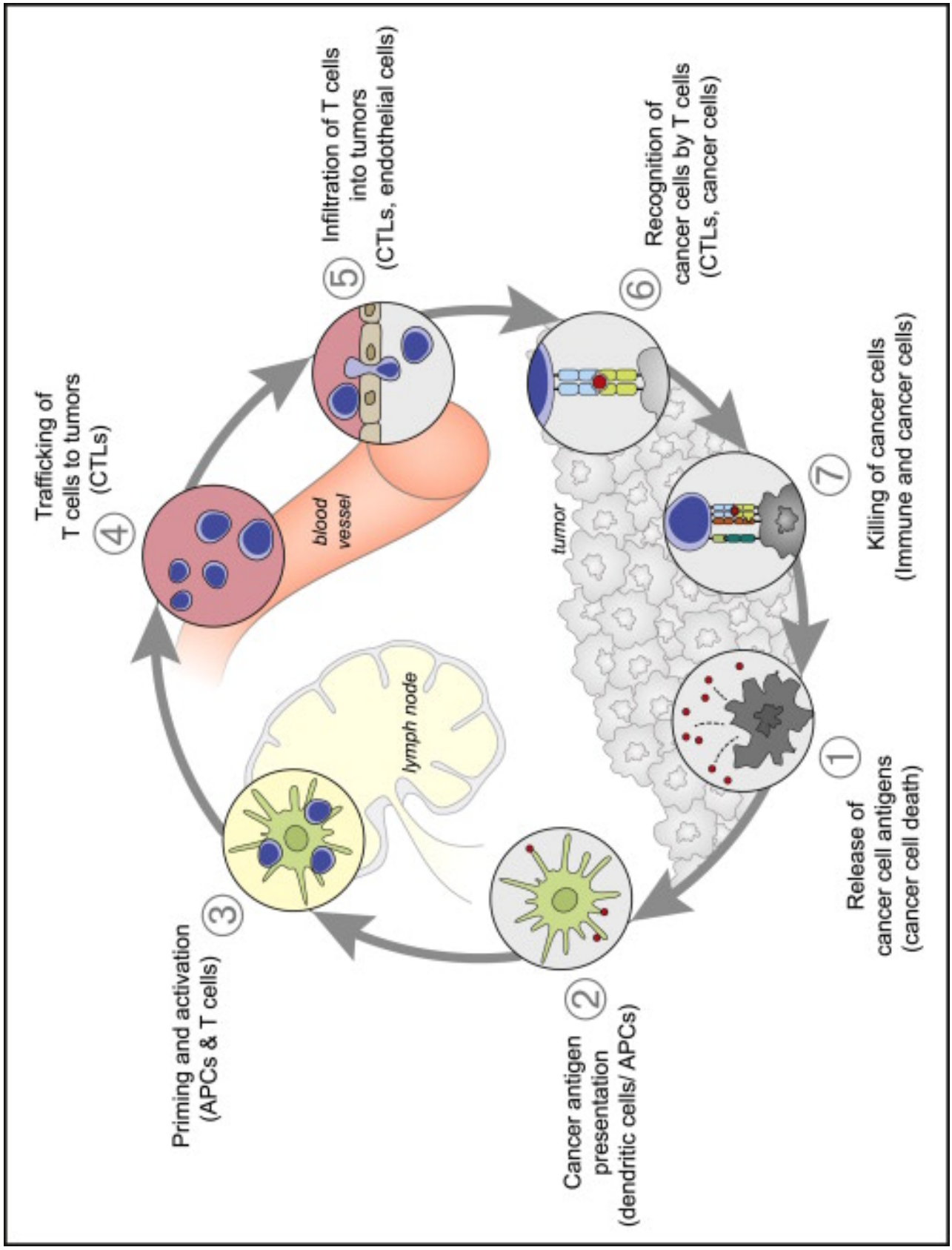
1
Release of
cancer cell antigens
(cancer cell death)
2
Cancer antigen
presentation
(dendritic cells/ APCs)
3
Priming and activation
(APCs & T cells)
4
Trafficking of
T cells to tumors
(CTLs)
5
Infiltration of T cells
into tumors
(CTLs, endothelial cells)
6
Recognition of
cancer cells by T cells
(CTLs, cancer cells)
7
Killing of cancer cells
(Immune and cancer cells)
blood
vessel
lymph node
tumor

As well as the Cancer Immunity Cycle, a novel system of classifying cancers by their 'immunoscore' has been developed (Figure 61) (102, 119). Immunoscores classify cancer types according to their CD8+ T cell infiltrate, and according to which immunoinhibitory pathways are active within that tumour. Therefore, the immunoscore can be used to predict which stages of the Cancer Immunity Cycle will be suppressed within that cancer type (119, 174).

The first immunoscore category is 'Hot' tumours, in which priming and infiltration of CD8+ TILs is successful, but the anti-tumour activity of CD8+TILs is inhibited by CIR expression, especially that of CTLA-4 and PD-1. Expression of more than two CIRs in combination is less common in hot tumours (102, 117, 119). Therefore, only the latter stages of the Cancer Immunity Cycle are inhibited in Hot tumours, and they often respond well to blockade of CTLA-4 and PD-1. Melanoma is an example of a hot tumour (102, 117, 119).

However, in 'Cold' tumours, tumour-specific CD8+ T cells are not primed and do not infiltrate the tumour (102, 119). This may occur because cancers downregulate surface antigens required for the anti-tumour immune response, or because cancer cell death as a source of antigen is occurring at low levels (102, 119, 312). Combining targeted therapy with immunotherapy can be an effective strategy to engender cancer cell death as a source of antigen, for example, the use of Focal Adhesion Kinase (FAK) inhibitors has been shown to increase pancreatic cancer cell apoptosis (312). After treatment with FAK inhibitors, some pancreatic tumours, which have traditionally been categorised as Cold tumours refractory to CIR blockade, become responsive to anti-PD-1 immunotherapy. Thus, the killing of cancer cells to generate antigen for priming of anti-tumour CD8+ T cells must often be achieved before CIR blockade can be effective in cold tumours (102, 119, 312).

Most tumours fall into two intermediate categories of immunoscore known as Altered-Immunosuppressed or Altered-Excluded (119). There is often much overlap between tumours in these categories and many cancers are found to possess characteristics of both intermediate immunoscores (102, 119, 306). In these categories, cancer cells typically express tumour-specific or tumour-associated antigens, and CD8+ TIL priming and infiltration do occur. However, the processes of priming and infiltration are inhibited by the presence of immunosuppressive factors within the TME (102, 119, 174, 308). Hypoxia, small molecules such as Adenosine and PGE_2, immunosuppressive cell types such as MDSC and Tregs, and

multiple inhibitory cytokines such as IL-10 and TGF-β all synergise to inhibit processes such as DC maturation, antigen presentation and lymphocyte migration (44, 311, 313). Commonly, infiltration of TILs is only partial, reaching only the peripheral regions of the tumour mass, and any CD8+ TILs which do successfully infiltrate the tumour are quickly suppressed by the same immunosuppressive pathways listed above, and also by CTLA-4 and PD-1 expression in combination with multiple other CIRs such as TIM3, LAG3, and TIGIT (Figure 61)(68, 102, 119).

The combined study of both tumour immunoscores and the Cancer Immunity Cycle therefore indicates that combinations of immunotherapy which improves both T cell priming and infiltration, as well as the targeting of inhibitory factors within the TME other than CTLA-4 and PD-1, are required so that Cold, Altered-immunosuppressed or Altered-Excluded tumours can be treated with equal efficacy to Hot tumours.

Figure 61 - Tumour Immunoscores

Cancers are categorised by the quality and quantity of their immune infiltrate, and the immunosuppressive pathways that are present, in order to generate an immunoscore (119).

Hot tumours possess large numbers of CD8+ TILs, which are predominantly suppressed by Co-Inhibitory Receptor (CIR/checkpoint) expression. Hence these tumours respond well to CIR blockade for immunotherapy.

Cold tumours lack an immune infiltrate, and priming and trafficking of CD8+ Cytotoxic T cells into tumours must be promoted by immunotherapy.

Altered-Excluded and Altered-Immunosuppressed immunoscores are assigned to tumours which have CD8+TILs (here, labelled CT cells). However, in Excluded and Immunosuppressed tumours, a complex combination of immunosuppressive (IM) immune cells and soluble factors synergise with co-inhibitory receptor expression to suppress CD8+ TIL cytotoxic function. Hence improving the priming and infiltration of CD8+ TILs into Immunosuppressed or Excluded tumours is beneficial, to change the quality of the infiltrate towards an inflammatory, anti-tumour type (119). Excluded tumours are differentiated from immunosuppressed tumours, because they have fewer CD8+ TILs ,

Figures taken from ‘Approaches to treat immune hot, altered and cold tumours with combination immunotherapies. Galon and Bruni. 2019 (119).

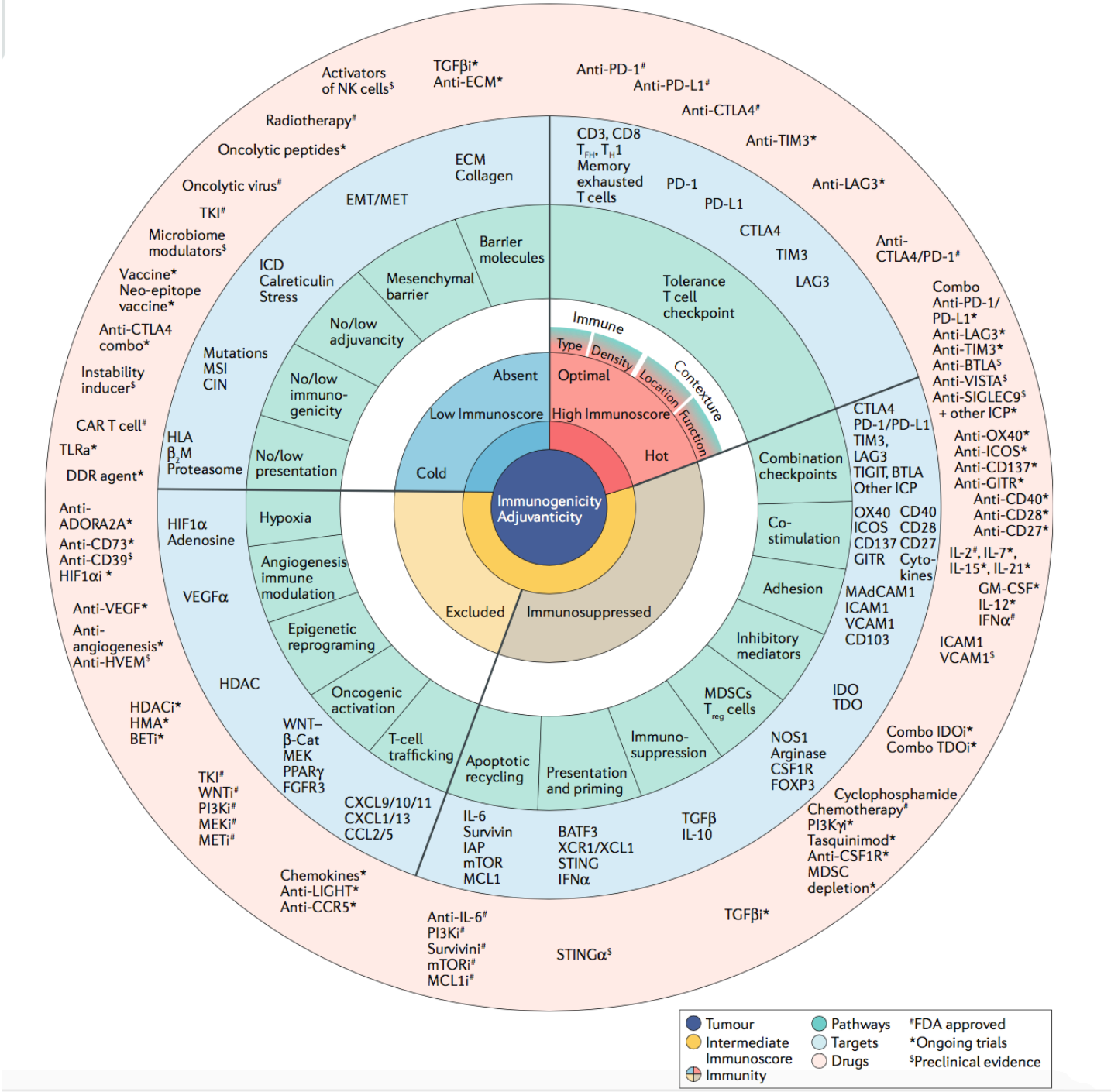
Activators of NK cells$
TGFβi* Anti-ECM*
Anti-PD-1# Anti-PD-L1#
Anti-CTLA4#
Anti-TIM3*
Anti-LAG3*
Anti-CTLA4/PD-1#
Radiotherapy#
Oncolytic peptides*
Oncolytic virus#
TKI#
Microbiome modulators$
Vaccine* Neo-epitope vaccine*
Anti-CTLA4 combo*
Instability inducer$
CAR T cell#
TLRa*
DDR agent*
Anti-ADORA2A*
Anti-CD73*
Anti-CD39$
HIF1αi *
Anti-VEGF*
Anti-angiogenesis*
Anti-HVEM$
HDACi* HMA* BETi*
TKI# WNTi# PI3Ki# MEKi# METi#
Chemokines* Anti-LIGHT* Anti-CCR5*
Anti-IL-6# PI3Ki# Survivini# mTORi# MCL1i#
STINGα$
TGFβi*
Combo Anti-PD-1/ PD-L1* Anti-LAG3* Anti-TIM3* Anti-BTLA$ Anti-VISTA$ Anti-SIGLEC9$ + other ICP*
Anti-OX40* Anti-ICOS* Anti-CD137* Anti-GITR*
Anti-CD40* Anti-CD28* Anti-CD27*
IL-2#, IL-7*, IL-15*, IL-21*
GM-CSF* IL-12* IFNα#
ICAM1 VCAM1$
Combo IDOi* Combo TDOi*
Cyclophosphamide Chemotherapy# PI3Kγi* Tasquinimod* Anti-CSF1R* MDSC depletion*
ECM Collagen
EMT/MET
ICD Calreticulin Stress
Mutations MSI CIN
HLA β2M Proteasome
HIF1α Adenosine
VEGFα
HDAC
WNT–β-Cat MEK PPARγ FGFR3
CXCL9/10/11 CXCL1/13 CCL2/5
IL-6 Survivin IAP mTOR MCL1
BATF3 XCR1/XCL1 STING IFNα
TGFβ IL-10
NOS1 Arginase CSF1R FOXP3
IDO TDO
MAdCAM1 ICAM1 VCAM1 CD103
CD3, CD8 TFH, TH1 Memory exhausted T cells
PD-1
PD-L1
CTLA4
TIM3
LAG3
CTLA4 PD-1/PD-L1 TIM3, LAG3 TIGIT, BTLA Other ICP
OX40 CD40 ICOS CD28 CD137 CD27 GITR Cyto-kines
Barrier molecules
Mesenchymal barrier
No/low adjuvancity
No/low immuno-genicity
No/low presentation
Tolerance T cell checkpoint
Combination checkpoints
Co-stimulation
Adhesion
Inhibitory mediators
MDSCs Treg cells
Immuno-suppression
Presentation and priming
Apoptotic recycling
T-cell trafficking
Oncogenic activation
Epigenetic reprograming
Angiogenesis immune modulation
Hypoxia
Immune
Type
Density
Location
Contexture
Function
Absent
Optimal
Low Immunoscore
High Immunoscore
Cold
Hot
Immunogenicity Adjuvanticity
Excluded
Immunosuppressed
Tumour
Intermediate Immunoscore
Immunity
Pathways
Targets
Drugs
#FDA approved
*Ongoing trials
$Preclinical evidence

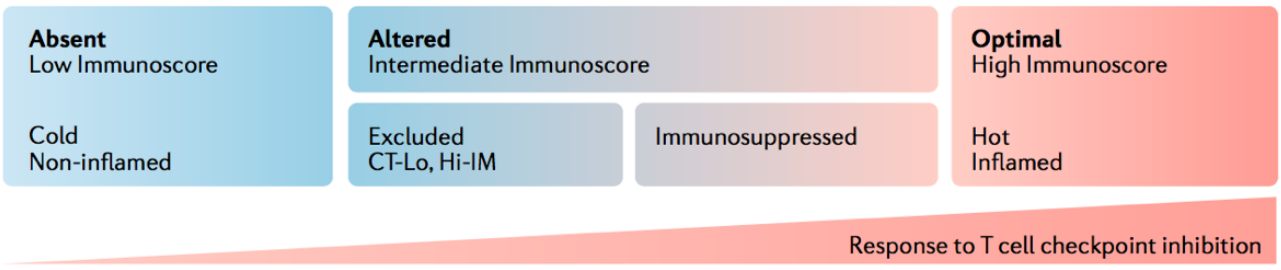
Absent
Low Immunoscore
Cold
Non-inflamed
Altered
Intermediate Immunoscore
Excluded
CT-Lo, Hi-IM
Immunosuppressed
Optimal
High Immunoscore
Hot
Inflamed
Response to T cell checkpoint inhibition

8.2 Immunosuppression in the RencaHA model

The aim of this study was to develop combinations of immunotherapy that would be effective in tumours in which the activity of CD8+ TILs is suppressed by other factors besides CTLA-4 and PD-1 engagement. Previous studies indicate that the following immunosuppressive factors are found within RencaHA tumours:

- Expression of the adenosine producing enzymes CD39 and CD73.
- Soluble mediators such as TGFβ and PGE_2.
- Expression of combinations of other CIRs amongst TILs, besides CTLA-4 and PD-1.
- The presence of MDSCs and CD4+ Tregs (44, 76, 77, 154, 260).

Thus, it was concluded that RencaHA tumours have characteristics of both Altered-Excluded, and Altered-Immunosuppressed immunoscores, and that the RencaHA model could be a useful model within which to develop therapies for these tumour types (119).

Currently, studies suggest that Anti-CTLA-4 and Anti-PD-1 mAbs are most effective in the treatment of Hot tumours, and that they only improve CD8+ TIL effector function within the TME, without improving CD8+ TIL priming or infiltration. Therefore developing immunotherapy which potentiates multiple other aspects of the Cancer Immunity Cycle is required for the treatment of common cancers; such as those of the breast, pancreas and colon; which have been shown to have Immunosuppressed, Excluded or Cold immunoscores (119, 314).

Another limitation of current anti-cancer immunotherapies is immune-mediated toxicity. Autoimmune adverse effects occur in around half of patients receiving anti-PD-1 and anti-CTLA-4 mAbs, because CTLA-4 and PD-1 are found on immune cells outside the tumour. Both molecules are important in maintaining peripheral tolerance to self-antigen as part of normal homeostasis, and toxicities such as cutaneous inflammation and colitis can result from CTLA-4 and PD-1 blockade. Incidences of such toxicity can be potentially fatal, and often necessitate the discontinuation of immunotherapy (117, 224, 226, 227, 264). Therefore, developing immunotherapies which target pathways that are selectively upregulated within the TME and not expressed body-wide, was a key aim of this research.

8.3 A2a Adenosine-Receptors as a Target for Immunotherapy in RencaHA tumours

There are multiple signalling axes in operation within RencaHA tumours, which are known to be potently immunosuppressive, and which could be blocked for immunotherapy (119). Previous studies showed that CD4+Tregs and MDSC within the RencaHA TME express the adenosine producing enzymes CD39 and CD73, and that RencaHA tumour-infiltrating CD4+ Tregs suppressed naïve CD8+ T cells *ex vivo* in an A2a adenosine receptor (A2aR) dependent manner (154). Other studies suggested that blocking immunosuppressive A2aRs or adenosine production via CD73 *in vivo,* produces control of tumour growth in several murine tumour models (182, 183, 191, 201, 238). Therefore, adenosine signalling was selected as a target for immunotherapy in RencaHA tumours. Furthermore, several studies have shown that adenosine is expressed at levels up to 100x higher within tumours when compared with peripheral body sites, even those undergoing inflammation or necrosis (196, 315). Therefore, we hypothesised that blocking A2aRs would relieve immunosuppression within RencaHA tumours without causing systemic adverse effects (196, 238, 315).

Having identified A2a Adenosine Receptors as an important immune inhibitory receptor which could be targeted therapeutically, A2aR-Antagonist was administered systemically to RencaHA tumour bearing mice, to determine whether blocking A2aRs was indeed effective in controlling tumour growth (119). Blockade of A2a Adenosine Receptors produced partial control of RencaHA tumour growth, causing tumour size to plateau at 10mm diameter, but complete tumour regression did not occur. This finding aligns with current clinical trial data, in which A2aR antagonists have been found to produce only partial responses or stable disease in other tumour models, but they do not give rise to complete tumour elimination (224, 226-228, 264). Nonetheless, these results were encouraging, as previous attempts to control tumour growth *in vivo* using Adoptive T Cell transfer, Anti-PD-1mAb or tumour vaccines had not achieved a plateau of tumour growth in the RencaHA model (44, 68, 76, 316).

8.4 Improving the response of RencaHA tumours to A2aR-Antagonist

It was postulated that immune escape mechanisms could limit the efficacy of A2aR blockade. Several studies suggest that the benefit of A2aR-antagonist occurs because A2aR signalling exerts a direct inhibitory effect on CD8+ TILs which, when relieved, allows them to kill tumours

(200, 201). A2aRs are expressed on multiple immune cell types, but in several mouse tumour models when CD8+ T cells are depleted there is no benefit from A2aR blockade, confirming that the blockade worked on CD8+ TILs. Furthermore, knockdown of A2aRs on adoptively transferred CAR CD8+ T cells produced the same effect as pharmacological A2aR antagonism, also suggesting that CD8+ T cells are required for the anti-tumour response to A2aR blockade (201, 276).

Therefore, we hypothesised that A2aR blockade only produced stable disease, and not tumour regression, because another immunosuppressive pathway was restraining the cytotoxic effector function of CD8+ TILs in our model, allowing RencaHA tumours to escape immune control. Other studies have also shown that when immunotherapy is used to alleviate one axis of suppression within the TME, the upregulation of other immunosuppressive pathways occurs. For example, intratumoural NK cells were shown to upregulate combinations of CIRs in the presence of IL-12 immunotherapy (261). In addition, tumour specific CTL cultured with MC38 tumour cells *in vitro* were shown to upregulate A2a adenosine receptors in the presence of Anti-PD-1mAb but not in the presence of isotype control (317). Therefore, to determine whether blockade of A2aRs led to the upregulation of other suppressive pathways in the RencaHA tumour model, combinations of expression of various CIRs by CD8+ TILs was quantified using flow cytometry.

Principal Component Analyses of flow cytometric data indicated that expression of the CIR TIM3, was elevated amongst CD8+ TILs from A2aR blocked tumours when compared with vehicle-treated control tumours. These findings suggested that when A2aRs were antagonised within RencaHA tumours, CD8+ TIL function was instead inhibited by TIM3 signalling. Indeed, RencaHA tumour cells were shown to express the TIM3 ligands Ceacam-1 and Galectin-9 when analysed *ex vivo*, so TIM3 engagement by inhibitory ligands can occur within RencaHA tumours. Therefore, we hypothesised that TIM3 blockade could synergise with A2aR blockade to improve CD8+ TIL effector function within the TME. Although the percentage expression of PD-1 and TIGIT was also elevated amongst TILs from RencaHA tumours which received A2aR-Antagonist, these two CIRs are known to be involved in peripheral tolerance, so they were not targeted for therapy (117, 120). TIM3, has been shown to be overexpressed amongst TILs when compared with PBMC, therefore blockade of TIM3 is less likely to be associated with autoimmune toxicity than blockade of PD-1 or TIGIT (188, 190).

8.5 Adoptive T cell Transfer as Immunotherapy for RencaHA Tumours

In blocking TIM3 and A2aRs in combination, we identified an immunotherapeutic strategy which targets two axes of immunosuppression found within Altered-Excluded/Immunosuppressed tumours, and which is unlikely to be associated with autoimmune side effects. We postulated that blockade of these molecules would improve the cytotoxic effector function of CD8+ TILs within the TME.

However, Priming of CD8+ T cells by DCs can also be a limiting step in the Cancer Immunity Cycle amongst excluded/immunosuppressed tumours (134, 238),(154). In human immunotherapy, ATT of engineered or CAR-T cells is one way to ensure the presence of primed CD8+ T cells specific to tumour antigen within patients. Such therapies effectively bypass the early stages of the Cancer Immunity Cycle, which require priming of anti-tumour CD8+ TILs within the host (174, 218, 219, 259, 283, 318, 319). However, the use of ATT has only shown real promise in haematological malignancies, because the cytotoxic function of ATT CD8+ TILs is inhibited by engagement of immunosuppressive pathways within the TME. Therefore, there is new emphasis on using ATT, which ensures priming of CD8+ TILs, concurrently with immunotherapies which block immunosuppressive pathways to restore the cytotoxic effector function of ATT TILs within the TME (201, 217, 259).

The RencaHA model utilises HA as a model tumour-specific antigen, so that ATT of TCR-transgenic HA-specific Clone 4 CD8+ T cells can be used to replicate human T cell transfer therapies. We hypothesised that combining both A2aR-Antagonist and anti-TIM3mAb therapy with ATT of Thy1.1+ Clone 4 T cells would preserve the cytotoxic effector function of Clone 4 TILs after infiltration into the RencaHA TME (119). Therefore, immunotherapy comprising A2aR-Antagonist, anti-TIM3mAb and ATT could control RencaHA tumour growth, by targeting multiple aspects of the Cancer Immunity Cycle.

8.6 Treating RencaHA tumours with ATT, A2aR-Antagonist and anti-TIM3mAb restored immune function at multiple stages of the Cancer-Immunity Cycle

8.6.1 Improving Killing of Tumour Cells by CD8+ TILs

Administration of two doses of ATT Clone 4 T cells was sufficient to eradicate tumours in a proportion of RencaHA tumour-bearing mice treated with ATT alone, however eradication was

more rapid if A2aR antagonism was utilised alongside ATT, and even more rapid, if anti-TIM3mAb was added to the regime. As tumours regressed fastest in the presence of both ATT, anti-TIM3mAb and A2aR blockade, we hypothesised that the direct cytotoxic function of ATT Clone 4 TILs was improved when A2aRs and TIM3 were antagonised.

To test this hypothesis, ATT Clone 4 TILs were harvested from RencaHA tumours treated with A2aR-antagonist and anti-TIM3mAb, and cytotoxicity assays were performed to quantify their ability to kill tumour cell targets *ex vivo*. Clone 4 TILs from A2aR-antagonist and anti-TIM3mAb-treated tumours demonstrated improved killing when compared with TILs from untreated tumours, however their killing ability remained lower than Clone 4 CTL primed *in vitro*. Therefore, only a partial restoration of killing ability was achieved (201).

However, as well as an increase in killing ability, the data also showed an improvement in the stability of immune synapses formed by Clone 4 TILs from A2aR-Antagonist and anti-TIM3mAb treated tumours, when compared with TILs from untreated tumours, and immune synapse stability was restored to the levels observed amongst *in vitro* primed Clone 4 CTL (48, 71, 76). We have previously shown that blockade of PD-1 in RencaHA tumours can also improve morphological measures of immune synapse stability amongst TILs, therefore immunotherapy is known to modulate this process. Together tumour growth data and *ex vivo* analyses support the hypothesis that ATT Clone 4 TILs are able to form more stable immune synapses in the presence of A2aR and TIM3 blockade, and that this results in better killing of tumour cells and therefore better control of tumour growth when compared with ATT alone.

8.6.2 Improved priming of Endogenous CD8+ TILs

The dramatic tumour regression produced by A2aR-antagonist and anti-TIM3mAb was unlikely to occur with only a partial restoration of cytotoxicity amongst Clone 4 TILs, suggesting that A2aR and TIM3 blockade could exert other beneficial effects besides directly improving tumour killing by Clone 4 TILs. The data showed that when ATT Clone 4 TILs are present in the RencaHA TME, a greater proportion of the host's endogenous CD8+ TILs produce IL-2 and IFNγ, and fewer produce IL-10. Therefore, ATT Clone 4 TILs exert a pro-inflammatory influence on other cell types within the TME, as well as directly lysing tumour cells.

Recent studies demonstrate that A2aR -/- CAR T cells exhibited improved IFNγ and TNFα production after recovery from the TME of a lung cancer model, when compared with CAR T cells which expressed A2aRs (201). Furthermore, the improved IFNγ and TNFα production by CAR T cells in this ATT model resulted in improved priming of endogenous CD8+ T cells from the tumour bearing host, generating more CD44+ CD8+TILs (201).

Hence, as well as directly improving the killing function of ATT cells, administering A2aR antagonist and anti-TIM3mAb may also improve the ability of Clone 4 TILs to produce effector cytokines such as IFNγ. Further work could use intracellular cytokine staining to compare IFNγ production by Clone 4 TILs in the presence and absence of A2aR and TIM3 blockade. IFNγ derived from ATT Clone 4 TILs could facilitate DC maturation, which would favour successful priming of endogenous anti-tumour CD8+ TILs at the TDLN. Furthermore, killing of tumour cells by ATT Clone 4 TILs could produce DAMP signalling to further promote DC maturation, and could also produce tumour-antigen for cross-presentation by DCs (174). Further studies could use flow cytometry to quantify the proportion of CD44+ endogenous CD8+ TILs and the numbers of mDC (expressing CD80/86) within RencaHA tumours treated with combinations of ATT, A2aR-Antagonist and anti-TIM3mAb. This would determine whether or not blockade of A2aRs and TIM3 does indeed improve priming of endogenous CD8+ TILs. Depletion experiments using specific mAb could be utilised to establish whether an improvement in priming of endogenous TILs depended on IFNγ produced by ATT Clone 4 TILs.

8.6.3 Improving the number of CD8+ TILs and reducing the number of T Regulatory cells within the TME

Immunohistochemistry data demonstrated that RencaHA tumours treated with A2aR-Antagonist and anti-TIM3mAb possessed a greater number of peripheral and central CD8+ TILs per unit area, and lower numbers of peripheral FOXP3+ Treg cells, when compared with control tumours. Therefore, blockade of A2aRs and TIM3 appears to result in CD8+ TIL infiltration, and to prevent either Treg development or ingress into RencaHA tumours. Increased infiltration of CD8+ TILs may occur because A2aR blockade directly causes the endothelium itself to become more active however, although adenosine signalling is known to downregulate the expression of adhesion molecules by endothelia, the role of A2aRs in this process is not clear (320-322). Alternatively, engagement of A2aRs is thought to inhibit RhoA signalling amongst lymphocytes,

which is required for them to migrate from the TDLN into the TME (320-322). The effect of TIM3 on infiltration is not well understood, however in later experiments, the ability of T Effector Memory cells to leave the secondary lymphoid tissues was improved amongst mice from treatment groups comprising A2aR-Antagonist and anti-TIM3mAb when compared with mice receiving anti-TIM3mAb alone. This finding could suggest that of the two agents in the treatment regimen, A2aR-antagonist benefits lymphocyte migration, whereas Anti-TIM3mAb benefits cytotoxic effector function within the TME. The effects of A2aRs and TIM3 on infiltration of lymphocytes into the TME is now the focus of experiments by another member of the laboratory, and will be studied using two-photon microscopy.

As well as improving priming of endogenous CD8+ TILs by DCs, increased production of IFNγ by ATT Clone 4 T cells in the presence of A2aR-Antagonist and anti-TIM3mAb could encourage multiple other populations of immune cells to produce chemotactic molecules which attract CD8+ T cells. Additionally, IFNγ promotes T helper rather than Treg fates amongst CD4+ TILs. Further experiments could use depletion of Thy1.1+ Clone 4 T cells to determine whether IFNγ production by ATT Clone 4 populations is required to reduce the numbers of CD4+ Tregs within the RencaHA TME in the presence of A2aR and TIM3 blockade (201).

8.6.4 Generation of Anti-Tumour Immune Memory

One key aim of cancer immunotherapy is to generate populations of anti-tumour immune memory cells which could be activated to eradicate minimal residual disease in cancer patients (230, 323). Amongst RencaHA tumour-bearing mice treated with combinations of ATT, A2aR-antagonist and anti-TIM3mAb, some mice experienced sustained tumour regression (Responders), whereas tumours relapsed in another population of mice (Non-responders). We hypothesised that Responder mice mounted better anti-tumour immune memory responses than Non-responders, thus preventing relapse. Furthermore, relapse potential was affected by treatment. Relapse occurred in a greater proportion of control or single treated mice when compared with cohorts that received both A2aR-antagonist and anti-TIM3mAb, suggesting that A2aR and TIM3 blockade potentiated anti-tumour immune memory.

Amongst Responder mice which resisted relapse, there was a greater proportion of T effector memory (TEM) cells within the spleen and TDLN. Furthermore, after immunisation with

influenza A/PR8 was used to provide secondary challenge with HA antigen, TEM cells appeared to mobilise out of the secondary lymphoid tissues of Responder mice however this did not occur amongst Non-responders. Therefore, a functional and mobile secondary TEM response was associated with resistance to relapse in the RencaHA model. Depletion experiments using specific mAbs indicated that memory cells derived from both adoptively transferred Clone 4 TILs and the host's endogenous CD8+ TIL repertoire were actively functioning to prevent relapse.

To determine how A2aRs and anti-TIM3mAb could influence the potential of endogenous or Clone 4 CD8+ TILs to acquire a memory fate, live cell imaging was used to determine the localisation of TCR signalling intermediates, which have been associated with memory development, during immune synapse formation (230, 299, 324). Clone 4 T cells cultured in the presence of the pan adenosine receptor agonist, NECA, exhibited elevated central localisation of PKCθ at the immune synapse, however further live cell imaging experiments are required to determine whether the localisation of PKCθ amongst TILs *in vivo* is affected by A2aR or TIM3 engagement.

8.6.5 Overall benefits of using ATT, A2aR-Antagonist and anti-TIM3mAb as Combination Immunotherapy

Overall, the data provide compelling pre-clinical evidence that targeting A2aRs and TIM3 concurrently with cell-based therapies can produce durable tumour regression in the RencaHA model. Tumour regression is faster, lasts longer, and occurs in more individuals when anti-TIM3mAb and A2aR-Antagonist are administered with ATT, when compared with ATT alone. Targeting A2aRs and TIM3 could be beneficial in many cancer types, because this regimen appears to act on multiple stages of the cancer-immunity cycle. Further studies in our lab will determine the intracellular signalling mechanisms by which A2aR and TIM3 blockade benefit priming, infiltration, effector function and memory formation amongst adoptively transferred and endogenous CD8+ TILs in the RencaHA model.

Furthermore, we perceived no evidence of autoimmune toxicity amongst mice treated with A2aR and TIM3-blockade, and published data suggests that off-target effects are rare when A2aR-antagonist or anti-TIM3mAb are administered to individuals (116, 120, 181, 183, 184, 325). Levels of adenosine within the tumour are up to 100-fold higher than those detected

during inflammation (191, 194, 268). Similarly, TIM3 expression is 30-fold higher amongst tumour infiltrating lymphocytes (TILs) than amongst PBMC taken from the same individual (188). The fact that upregulation of Adenosine production and TIM3 expression occurs specifically within tumour microenvironments, means that blocking these two pathways is less likely to be associated with immune related adverse events than when targeting other immune checkpoints, which are expressed body-wide. Indeed, A2aR agonists have already passed Phase 1 trials for use in Parkinson's disease, and their use as a single agent in cancer is currently undergoing Phase II trials (224, 228).

8.7 Further Work

8.7.1 Determine the signalling which occurs within Clone 4 T cells after A2aR and TIM3 engagement

In vitro and *ex vivo* analyses were used to begin to dissect the signalling pathways which are altered amongst Clone 4 CTL or TILs under the influence of A2aR and TIM3 signalling. However, since beginning this work, new studies have given rise to the following hypotheses which will be assessed using established techniques in our laboratory.

8.7.1.1 Does Lck represent a common downstream effector molecule for many immunosuppressive pathways which inhibit CD8+ TILs within the RencaHA TME?

The findings in this study led us to propose a model whereby signalling pathways downstream of A2aRs and TIM3 synergise to inhibit CD8+ T cell effector function. Engagement of A2aRs, PGE_2 and TIM3 could theoretically converge to regulate CD8+ TCR signalling at the level of Lck (Figure 62). Adenosine binding to the A2aR, or engagement of EP receptors by PGE_2, both result in elevated cyclic AMP within T cells which activates PKA. This could theoretically produce increased activity of the PKA/Csk axis leading to inhibitory phosphorylation of Lck by addition of a phosphate group to Y505 (194, 326, 327). TIM3 binding to Galectin-9 or Ceacam-1 is known to cause release of Bat3, which could carry Lck away from the immune synapse (54, 134, 138). Therefore, the combined effect of TIM3 moving Lck away from the immune synapse, and A2aR engagement resulting in inhibitory phosphorylation of the small amount of Lck that remains, could cause more potent inhibition of Lck signalling when A2aRs and TIM3 are engaged together, compared with either pathway alone.

To determine whether the above pathways operate within CD8+ T cells, Lck phosphorylation was assessed using Phosflow cytometric analyses, and Lck localisation was quantified using live cell imaging. However, the location of phosphorylated Lck could not be reliably determined. In future, the analyses of Clone 4 CTL-target cell couples could be executed using an Imagestream™ flow cytometer. This instrument would allow both the location and the phosphorylation status of Lck to be determined simultaneously, after staining with phosflow antibodies.

Applying this technique to analyse Lck phosphorylation and localisation within TILs and *in vitro* cultures would allow us to determine whether A2aR and TIM3 signalling, as well as other pathways such as PGE_2 and PD-1 engagement, regulate Lck at the CD8+ T cell immune synapse. If Lck represents one molecule which co-ordinates the effects of several upstream immunosuppressive pathways, ensuring the function of Lck within CD8+ TILs could prevent them from being suppressed by several axes of immunosuppression within the tumour, representing a new and effective option for cancer-immunotherapy. However, since Lck is expressed in T cells body-wide, manipulation of Lck could cause autoimmune toxicity. One potential approach to immunotherapy could be to utilise T cells with engineered Lck in adoptive T cell transfer, ensuring that the TCR of such T cells is specific to tumour antigen.

Figure 62 – Proposed model in which signalling though A2aRs and TIM3 inhibits TCR signalling through Lck

Lck is present within CD8+ T cells in three main phosphorylated forms, and the balance of availability of these phosphotypes affects the potential for successful TCR signalling. Engagement of the A2aR, a G-protein coupled receptor, mediates an increase in intracellular cyclic AMP, increasing the activity of PKA, and subsequently Csk - a tyrosine kinase which adds an inhibitory Y505 phosphorylation to Lck (194, 210, 286). Unless an inhibitory ligand is present, TIM3 cytoplasmic tails are thought to bind to Bat3, which acts as a reservoir for active Lck, thus ensuring the availability of Lck at the immune synapse and promoting TCR signalling potential (54, 55, 138). After TIM3 engagement by Ceacam-1 or Galectin-9, Bat3 detaches from the TIM3 cytoplasmic tail and with it removes a pool of Lck, reducing the potential for TCR signal amplification (54, 138). Therefore, A2aR signalling and TIM3 signalling could synergise to inhibit T cells, via addition of inactivating phosphate groups to Lck (A2aRs) and physical removal of active Lck from the immune synapse (TIM3).

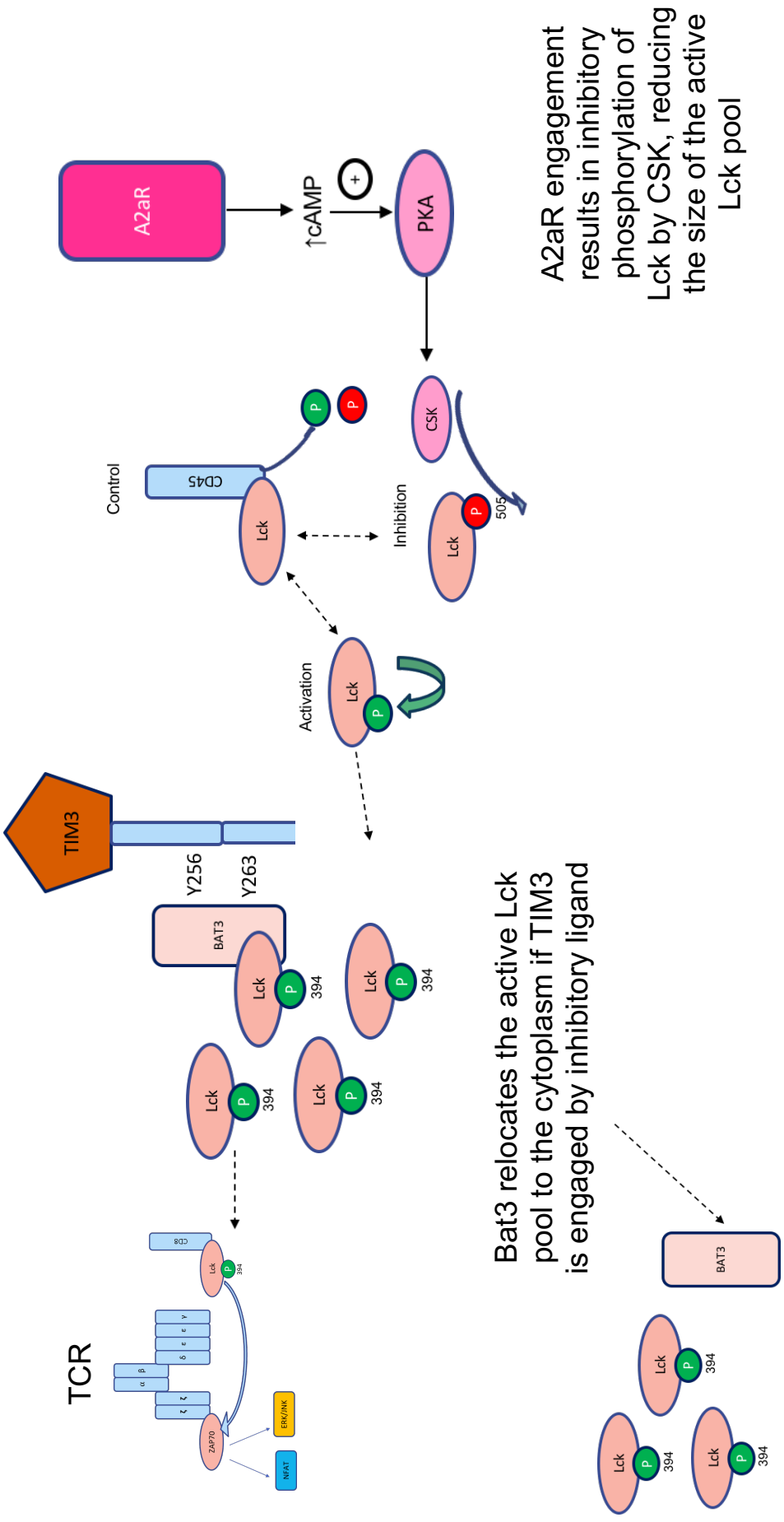
A2aR
↑cAMP
PKA
A2aR engagement results in inhibitory phosphorylation of Lck by CSK, reducing the size of the active Lck pool
Control
CD45
Lck
Inhibition
CSK
Lck
505
Activation
Lck
TIM3
Y256
Y263
BAT3
Lck
394
Lck
394
Lck
394
Lck
394
TCR
CD8
Lck
394
ZAP70
ERK/JNK
NFAT
Bat3 relocates the active Lck pool to the cytoplasm if TIM3 is engaged by inhibitory ligand
BAT3
Lck
394
Lck
394

8.7.1.2 Does engagement of the A2aR affect CD8+ T cell migration or immune synapse formation through RhoA and CDC42?

Published studies suggest that A2aR signalling through the cAMP/PKA axis results in inhibition of Rho A and CDC42 signalling in leukocytes during cell-cell adhesion (179, 328). However, the effect of A2aR engagement on these molecules during lymphocyte migration and immune synapse formation has not been examined. Transfecting Clone 4 T cells with RhoA-GFP or CDC42-GFP would allow the localisation of these GFP-conjugated molecules to be compared during immune synapse formation by CTL and TILs using live cell imaging. If the spatiotemporal localisation of Rho-A and CDC42 is inhibited by exposure to the TME, treatment with A2aR-Antagonist may restore the ability of TILs to localise these molecules correctly. The activation status of Rho GTPases is also crucial in their regulation, and this could be assessed using phosflow staining or phostag™ western blotting. Example methods for these techniques are discussed in Nika et al. 2010 and Ambler et al. 2017 (53, 77). These experiments could provide new insights about the effects of A2aR signalling on actin regulators within CD8+ TILs during infiltration and killing. Furthermore, *in vitro* assays of cell migration could be used to determine whether CD8+ T cell transmigration across blood vessel endothelia is impaired when A2aRs are engaged. The incucyte microscope could be used to perform cell migration assays using existing manufacturer's protocols (329).

8.7.1.3 Does A2aR signalling induce IL-27-mediated upregulation of co-inhibitory receptors in CD8+ T cells?

A recent study has established IL-27 as a master controller of CIR gene expression in CD8+ T cells (121). Elevated cAMP has been shown to promote IL-27 transcription through the transcription factor CREB (150, 208). A2aR signalling is known to result in elevated cAMP within T cells, however a conclusive link between cAMP derived from A2aR engagement, and IL-27 release with subsequent CIR expression has not been shown (Figure 63)(121, 135, 137, 210, 330). Recently, an association between A2aR signalling and elevated CIR expression amongst CD8+ T cells was reported, with one study finding that blockade of A2aRs *in vivo* was associated with reduced CIR expression amongst CD8+ TILs (121). However, the study did not determine the mechanism by which A2aR engagement could result in CIR upregulation.

Figure 63 – Inhibition of T cell functions downstream of A2aR engagement

The immunoinhibitory A2a Adenosine Receptor is a G-protein coupled receptor. Ligation of this receptor by adenosine induces elevation of cyclic AMP at the T cell membrane (191). cAMP has been associated with multiple signalling events in T cells.

Firstly, cAMP recruits and activates Protein kinase A (PKA), which activates Csk. Csk is known to add the inhibitory Y505 phosphorylation to Lck, inhibiting TCR signalling, however the effects of A2aR engagement on Lck phosphotype have not been conclusively demonstrated (204, 209, 210).

PKA also inhibits the actin regulators RhoA and CDC42, which could interfere with T cell migration, polarisation and MTOC translocation to the immune synapse (205).

Finally, elevated cAMP is associated with the activation of the CREB transcription factor, which promotes IL-27 expression (205). Autocrine and paracrine IL-27 signalling produces expression of the co-inhibitory receptor gene module within T cells, causing the expression of multiple co-inhibitory receptors and IL-10 to be upregulated concurrently. Again, a complete pathway from A2aR signalling to IL-27 production remains to be demonstrated (121).

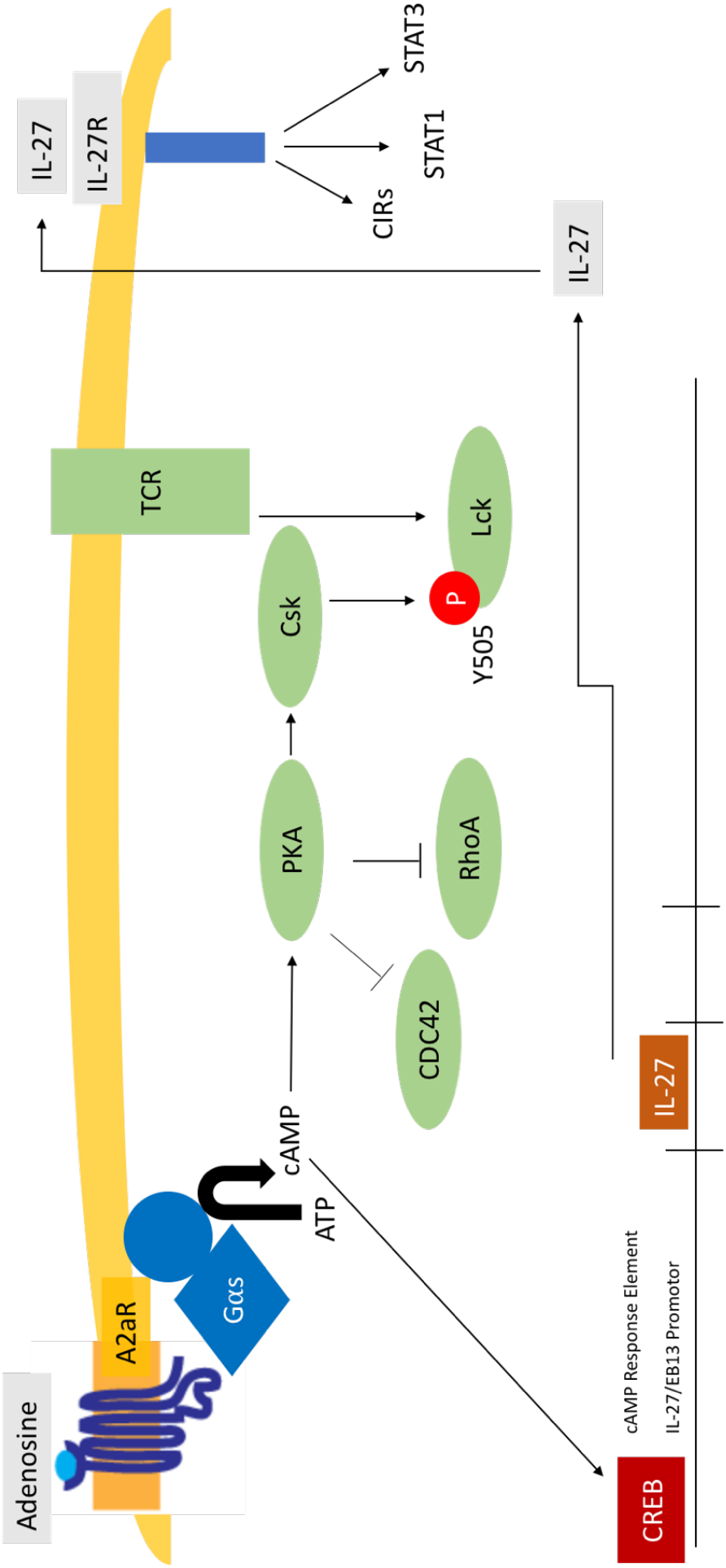
IL-27
IL-27R
STAT3
STAT1
CIRs
IL-27
TCR
Lck
Csk
P
Y505
PKA
RhoA
CDC42
cAMP
ATP
Gαs
A2aR
Adenosine
IL-27
cAMP Response Element
IL-27/EB13 Promotor
CREB

The observation that CIR expression amongst TILs was reduced in A2aR-blocked tumours contradicts our principal component analysis data, which suggests that blockade of A2aRs *in vivo* is associated with elevated CIR expression amongst TILs in the RencaHA model. Our findings could be explained because the RencaHA TME is thought to be rich in PGE_2. Therefore, the reduction in cAMP which results from disabling A2aR signalling could be compensated for by high levels of cAMP production downstream of EP2 receptor engagement within RencaHA tumours. Use of RencaT3 tumours which overproduce PGE_2 could determine whether elevated PGE_2 production compensates for adenosine receptor blockade by upregulating cAMP in the absence of A2aR signalling (44).

In future, *in vitro* assays could also be used to assess the effect of A2aR signalling on IL-27 release and CIR expression amongst CTL in culture. We assessed CIR expression amongst Clone 4 CTL after NECA treatment using flow cytometry and did not determine a significant effect of NECA on CIR expression. However, NECA is a pan-adenosine receptor agonist, so future studies should repeat this assay using CGS2680, a specific A2aR agonist, to fully determine the effect of the A2aR on CIR expression. Furthermore, we have not determined IL-27 production in the presence of A2aR agonists, and this could be achieved using ELISA.

Recent studies have shown that IL-27 mediates upregulation of combinations of CIRs which are characteristically observed only in the immunosuppressive TME (121). Therefore, the downstream effects of IL-27 signalling are most frequently observed in the context of an immunosuppressive niche, and not *in vitro*. IL-27 receptor expression may only be induced in the presence of tumour-derived factors, and IL-27R expression may represent one level of control that determines the propensity of T cells to upregulate different combinations of CIRs in different contexts (121, 135, 137). Flow cytometry could be used to compare IL-27R expression between CTL and TILs to investigate this hypothesis.

8.8 Translation of Combination Immunotherapy to the Clinic

Further studies are required before translation of our immunotherapeutic approach could be achieved in human patients. Firstly, human tissue samples should be analysed to confirm the presence of the adenosine producing enzymes CD39 and CD73, as well as the four subtypes of Adenosine Receptors and TIM3. Many of these studies have already been performed in a range

of cancers, suggesting that A2aRs and TIM3 are widely expressed in human tumours that respond poorly to anti-CTLA-4 and anti-PD-1 immunotherapy, such as breast, ovarian and pancreatic cancer (103, 116, 132, 134, 140, 182-184, 195, 201, 265, 266). Another member of the lab is currently assessing the presence of the above pathways in human tissue samples from melanoma patients

Secondly, the utility of ATT, A2aR-Antagonist and anti-TIM3mAb in controlling the growth of different tumour types should be assessed. Our lab is currently optimising a CT-26^{HA} colon cancer model and a 4-T1^{HA} breast cancer model in order to achieve this. Additionally, before translation, the testing of anti-cancer drugs in patient-derived xenograft models is often used. The use of xenograft models can determine whether the tumour regression observed in murine tumours after receipt of a new anti-cancer therapy, also occurs when the model tumour tissue is derived from human patients (314, 331). However, a key limitation of using this strategy to determine the efficacy of immunotherapy is that xenograft models involve the injection of tumour cells derived from human cancer patients into immunodeficient mice so that mice do not reject the human tissue (314, 331). Therefore, immunomodulatory drugs cannot be assessed in this context. The generation of xenograft models in which mice are subsequently implanted with populations of human immune cells, to test the humanised immune response to cancer, is currently the focus of several studies (314). When these models become widely available, they could represent an ideal translational step towards establishing the efficacy of A2aR-Antagonist, ATT and anti-TIM3mAb in human patients.

Finally, in addition to efficacy data, the safety profile of A2aR Antagonists and anti-TIM3mAb must be established. A2aR-antagonists are already used in clinical trials as single agents to treat cancer, and they have proven to be safe, having previously been licensed for use in Parkinson's disease. The ability of A2aR-antagonists to cross the blood brain barrier could make them uniquely useful in brain tumours, since most immunotherapies take the form of mAb which penetrate poorly into the central nervous system (224, 226, 228). Further studies are required to determine the safety profile of anti-TIM3 blocking mAb, although several are currently in early trials in combination with Anti-PD-1 mAb (119).

8.9 Concluding Remarks

Cancer immunotherapy shows enormous promise, especially in the treatment of melanoma. However, the recent definitions of Tumour Immunoscore and the Cancer Immunity Cycle have led us to look beyond CTLA-4 and PD-1 blockade to achieve immune control of other cancer types. Combining cell-based therapies with modulation of the tumour microenvironment is an effective way to manipulate several stages of the Cancer Immunity Cycle, ensuring that the priming, infiltration and function of tumour-specific CD8+ T cells proceeds effectively. The result of this is CD8+ TIL-mediated destruction of tumour cells, and increased immunogenicity within the TME. We devised a combination of therapies which should target multiple stages of the Cancer Immunity Cycle, showing that blockade of A2a Adenosine Receptors alongside antagonism of TIM3 synergises with Adoptive T cell Transfer to mediate complete and durable tumour regression. Our current data suggests that this multi-pronged approach could provide benefit for multiple cancer types, without significant toxicity, meaning that its translation to the clinic should be considered.

Chapter 9 References

1. Janeway C. Immunobiology : the immune system in health and disease. 6th ed. ed. New York ; London: Garland Science; 2005.
2. Chaplin DD. Overview of the immune response. J Allergy Clin Immunol. 2010;125(2 Suppl 2):S3-23.
3. Janeway CA, Jr. How the immune system protects the host from infection. Microbes Infect. 2001;3(13):1167-71.
4. Bonilla FA, Oettgen HC. Adaptive immunity. J Allergy Clin Immunol. 2010;125(2 Suppl 2):S33-40.
5. Parkin J, Cohen B. An overview of the immune system. Lancet. 2001;357(9270):1777-89.
6. Gajewski TF, Schreiber H, Fu YX. Innate and adaptive immune cells in the tumor microenvironment. Nat Immunol. 2013;14(10):1014-22.
7. Corrales L, Matson V, Flood B, Spranger S, Gajewski TF. Innate immune signaling and regulation in cancer immunotherapy. Cell Res. 2017;27(1):96-108.
8. Spits H, Cupedo T. Innate lymphoid cells: emerging insights in development, lineage relationships, and function. Annu Rev Immunol. 2012;30:647-75.
9. Alberts B. Molecular biology of the cell. 5th ed. ed. New York: Garland Science ; [London : Taylor & Francis, distributor]; 2008.
10. Wraith DC. Lecture Notes for Final Year Undergraduates: Antigen Presentation. 2011.
11. Borde M, Barrington RA, Heissmeyer V, Carroll MC, Rao A. Transcriptional basis of lymphocyte tolerance. Immunological Reviews. 2006;210:105-19.
12. Kaech SM, Wherry EJ. Heterogeneity and cell-fate decisions in effector and memory CD8+ T cell differentiation during viral infection. Immunity. 2007;27(3):393-405.
13. LeBien TW, Tedder TF. B lymphocytes: how they develop and function. Blood. 2008;112(5):1570-80.
14. Muramatsu M, Kinoshita K, Fagarasan S, Yamada S, Shinkai Y, Honjo T. Pillars Article: Class Switch Recombination and Hypermutation Require Activation-Induced Cytidine Deaminase (AID), a Potential RNA Editing Enzyme. Cell. 2000. 102: 553-563. J Immunol. 2018;201(9):2530-40.
15. Muramatsu M, Kinoshita K, Fagarasan S, Yamada S, Shinkai Y, Honjo T. Class switch recombination and hypermutation require activation-induced cytidine deaminase (AID), a potential RNA editing enzyme. Cell. 2000;102(5):553-63.
16. Boyd SD, Joshi SA. High-Throughput DNA Sequencing Analysis of Antibody Repertoires. Microbiol Spectr. 2014;2(5).
17. Carrithers MD, Visintin I, Kang SJ, Janeway CA, Jr. Differential adhesion molecule requirements for immune surveillance and inflammatory recruitment. Brain. 2000;123 (Pt 6):1092-101.
18. Vasilevko V, Ghochikyan A, Holterman MJ, Agadjanyan MG. CD80 (B7-1) and CD86 (B7-2) are functionally equivalent in the initiation and maintenance of CD4+ T-cell proliferation after activation with suboptimal doses of PHA. DNA Cell Biol. 2002;21(3):137-49.
19. Abdul-Majeed S, Moloney BC, Nauli SM. Mechanisms regulating cilia growth and cilia function in endothelial cells. Cellular and molecular life sciences : CMLS. 2012;69(1):165-73.
20. Alt FWe, Honjo Te, Radbruch Ae, Reth Me. Molecular biology of B cells. Second edition / edited by Frederick W. Alt, Tasuku Honjo, Andreas Radbruch, Michael Reth. ed.
21. Neefjes J, Jongsma ML, Paul P, Bakke O. Towards a systems understanding of MHC class I and MHC class II antigen presentation. Nat Rev Immunol. 2011;11(12):823-36.

22. Guermonprez P, Saveanu L, Kleijmeer M, Davoust J, Van Endert P, Amigorena S. ER-phagosome fusion defines an MHC class I cross-presentation compartment in dendritic cells. Nature. 2003;425(6956):397-402.
23. Segura E, Amigorena S. Cross-Presentation in Mouse and Human Dendritic Cells. Adv Immunol. 2015;127:1-31.
24. Rocca A, Opolski A, Samaan A, Frangoulis B, Degos L, Pla M. Localization of the conformational alteration of MHC molecules induced by the association of mouse class I heavy chain with a xenogeneic beta 2-microglobulin. Mol Immunol. 1992;29(4):481-7.
25. Sollid LM, Jabri B. Triggers and drivers of autoimmunity: lessons from coeliac disease. Nat Rev Immunol. 2013;13(4):294-302.
26. Segura E, Amigorena S. Cross-presentation by human dendritic cell subsets. Immunol Lett. 2014;158(1-2):73-8.
27. Berkers CR, de Jong A, Schuurman KG, Linnemann C, Meiring HD, Janssen L, et al. Definition of Proteasomal Peptide Splicing Rules for High-Efficiency Spliced Peptide Presentation by MHC Class I Molecules. J Immunol. 2015;195(9):4085-95.
28. Romieu-Mourez R, Francois M, Boivin MN, Stagg J, Galipeau J. Regulation of MHC class II expression and antigen processing in murine and human mesenchymal stromal cells by IFN-gamma, TGF-beta, and cell density. J Immunol. 2007;179(3):1549-58.
29. Cresswell P. Invariant chain structure and MHC class II function. Cell. 1996;84(4):505-7.
30. Amigorena S, Webster P, Drake J, Newcomb J, Cresswell P, Mellman I. Invariant chain cleavage and peptide loading in major histocompatibility complex class II vesicles. J Exp Med. 1995;181(5):1729-41.
31. Liu X, Zhan Z, Li D, Xu L, Ma F, Zhang P, et al. Intracellular MHC class II molecules promote TLR-triggered innate immune responses by maintaining activation of the kinase Btk. Nat Immunol. 2011;12(5):416-24.
32. Raulet DH. Missing self recognition and self tolerance of natural killer (NK) cells. Semin Immunol. 2006;18(3):145-50.
33. Takahama Y. Journey through the thymus: stromal guides for T-cell development and selection. Nat Rev Immunol. 2006;6(2):127-35.
34. Divya.K.Shah. T cell development in thymus: British Society for Immunology; 2018 [Available from: https://www.immunology.org/public-information/bitesized-immunology/immune-development/t-cell-development-in-thymus.
35. Krangel MS. Mechanics of T cell receptor gene rearrangement. Curr Opin Immunol. 2009;21(2):133-9.
36. Olaru A, Petrie HT, Livak F. Beyond the 12/23 rule of VDJ recombination independent of the Rag proteins. J Immunol. 2005;174(10):6220-6.
37. Prinz I, Silva-Santos B, Pennington DJ. Functional development of gammadelta T cells. Eur J Immunol. 2013;43(8):1988-94.
38. Hayday AC, Eberl, M. . Gamma Delta T cells British Society for Immunology; 2019 [Available from: https://www.immunology.org/public-information/bitesized-immunology/cells/gamma-delta-%CE%B3%CE%B4-t-cells.
39. Gogoi D, Chiplunkar SV. Targeting gamma delta T cells for cancer immunotherapy: bench to bedside. Indian J Med Res. 2013;138(5):755-61.
40. Janicki CN, Jenkinson SR, Williams NA, Morgan DJ. Loss of CTL function among high-avidity tumor-specific CD8+ T cells following tumor infiltration. Cancer Res. 2008;68(8):2993-3000.
41. Morgan DJ. Control of Anti-Tumour CD8+ T cell Responses Anticancer Res. 2008;28(5C):3413.

42. Raveney B, Morgan DJ. Dynamic control of self-specific CD8+ T cell responses via a combination of signals mediated by dendritic cells. J Immunol. 2007;179(5):2870-9.
43. Dockree T, Holland CJ, Clement M, Ladell K, McLaren JE, van den Berg HA, et al. CD8(+) T-cell specificity is compromised at a defined MHCI/CD8 affinity threshold. Immunol Cell Biol. 2017;95(1):68-76.
44. Basingab FS, Ahmadi M, Morgan DJ. IFNgamma-Dependent Interactions between ICAM-1 and LFA-1 Counteract Prostaglandin E2-Mediated Inhibition of Antitumor CTL Responses. Cancer Immunol Res. 2016;4(5):1-12.
45. Kaech SM, Cui W. Transcriptional control of effector and memory CD8+ T cell differentiation. Nat Rev Immunol. 2012;12(11):749-61.
46. Huse M. The T-cell-receptor signaling network. J Cell Sci. 2009;122(Pt 9):1269-73.
47. Singleton KL, Roybal KT, Sun Y, Fu G, Gascoigne NR, van Oers NS, et al. Spatiotemporal patterning during T cell activation is highly diverse. Sci Signal. 2009;2(65):ra15.
48. Griffiths GM, Tsun A, Stinchcombe JC. The immunological synapse: a focal point for endocytosis and exocytosis. Journal of Cell Biology. 2010;189(3):397-406.
49. Brownlie RJ, Zamoyska R. T cell receptor signalling networks: branched, diversified and bounded. Nat Rev Immunol. 2013;13(4):257-69.
50. Williams NA. TCR Signalling. Lecture Notes provided to Final Year Undergraduate Students. University of Bristol2011.
51. Radoja S, Saio M, Schaer D, Koneru M, Vukmanovic S, Frey AB. CD8(+) tumor-infiltrating T cells are deficient in perforin-mediated cytolytic activity due to defective microtubule-organizing center mobilization and lytic granule exocytosis. Journal of Immunology. 2001;167(9):5042-51.
52. Akbay EA, Koyama S, Carretero J, Altabef A, Tchaicha JH, Christensen CL, et al. Activation of the PD-1 pathway contributes to immune escape in EGFR-driven lung tumors. Cancer Discov. 2013;3(12):1355-63.
53. Nika K, Soldani C, Salek M, Paster W, Gray A, Etzensperger R, et al. Constitutively active Lck kinase in T cells drives antigen receptor signal transduction. Immunity. 2010;32(6):766-77.
54. Rangachari M, Zhu C, Sakuishi K, Xiao S, Karman J, Chen A, et al. Bat3 promotes T cell responses and autoimmunity by repressing Tim-3-mediated cell death and exhaustion. Nat Med. 2012;18(9):1394-400.
55. Zhu C, Anderson AC, Schubart A, Xiong H, Imitola J, Khoury SJ, et al. The Tim-3 ligand galectin-9 negatively regulates T helper type 1 immunity. Nat Immunol. 2005;6(12):1245-52.
56. Gagnon E, Connolly A, Dobbins J, Wucherpfennig KW. Studying Dynamic Plasma Membrane Binding of TCR-CD3 Chains During Immunological Synapse Formation Using Donor-Quenching FRET and FLIM-FRET. Methods Mol Biol. 2017;1584:259-89.
57. Gaud G, Lesourne R, Love PE. Regulatory mechanisms in T cell receptor signalling. Nat Rev Immunol. 2018;18(8):485-97.
58. Davis SJ, van der Merwe PA. The kinetic-segregation model: TCR triggering and beyond. Nat Immunol. 2006;7(8):803-9.
59. Danielle J. Clark LEM, Clémentine Massoué, Lidiya Mykhaylechko, Xiongtao Ruan, Kentner L. Singleton, Minna Du, Alan J. Hedges, Pamela L. Schwartzberg, Robert F. Murphy, Christoph Wülfing. Transient μm scale protein accumulation at the center of the T cell antigen presenting cell interface drives efficient IL-2 secretion. bioRxiv. 2019.
60. Zhang W, Samelson LE. The role of membrane-associated adaptors in T cell receptor signalling. Semin Immunol. 2000;12(1):35-41.
61. Singleton KL, Gosh M, Dandekar RD, Au-Yeung BB, Ksionda O, Tybulewicz VL, et al. Itk controls the spatiotemporal organization of T cell activation. Sci Signal. 2011;4(193):ra66.

62. Fu G, Chen Y, Schuman J, Wang D, Wen R. Phospholipase Cgamma2 plays a role in TCR signal transduction and T cell selection. J Immunol. 2012;189(5):2326-32.
63. Wulfing C, Rabinowitz JD, Beeson C, Sjaastad MD, McConnell HM, Davis MM. Kinetics and extent of T cell activation as measured with the calcium signal. J Exp Med. 1997;185(10):1815-25.
64. Laguette N, Sobhian B, Casartelli N, Ringeard M, Chable-Bessia C, Segeral E, et al. SAMHD1 is the dendritic- and myeloid-cell-specific HIV-1 restriction factor counteracted by Vpx. Nature. 2011;474(7353):654-U132.
65. Vang T, Torgersen KM, Sundvold V, Saxena M, Levy FO, Skalhegg BS, et al. Activation of the COOH-terminal Src kinase (Csk) by cAMP-dependent protein kinase inhibits signaling through the T cell receptor. J Exp Med. 2001;193(4):497-507.
66. Romio M, Reinbeck B, Bongardt S, Huls S, Burghoff S, Schrader J. Extracellular purine metabolism and signaling of CD73-derived adenosine in murine Treg and Teff cells. Am J Physiol Cell Physiol. 2011;301(2):C530-9.
67. Morgan D. CTL Effector Mechanisms. University of Bristol; 2011.
68. Janicki CN, Jenkinson SR, Williams NA, Morgan DJ. Loss of CTL function among high-avidity tumor-specific CD8(+) T cells following tumor infiltration. Cancer Res. 2008;68(8):2993-3000.
69. Dustin ML, Long EO. Cytotoxic immunological synapses. Immunol Rev. 2010;235(1):24-34.
70. Ortega-Carrion A, Vicente-Manzanares M. Concerning immune synapses: a spatiotemporal timeline. F1000Res. 2016;5.
71. Ritter AT, Kapnick SM, Murugesan S, Schwartzberg PL, Griffiths GM, Lippincott-Schwartz J. Cortical actin recovery at the immunological synapse leads to termination of lytic granule secretion in cytotoxic T lymphocytes. Proc Natl Acad Sci U S A. 2017;114(32):E6585-E94.
72. Stinchcombe JC, Griffiths GM. Secretory mechanisms in cell-mediated cytotoxicity. Annual Review of Cell and Developmental Biology. 2007;23:495-517.
73. Stinchcombe JC, Salio M, Cerundolo V, Pende D, Arico M, Griffiths GM. Centriole polarisation to the immunological synapse directs secretion from cytolytic cells of both the innate and adaptive immune systems. Bmc Biology. 2011;9.
74. Jenkins MR, Griffiths GM. The synapse and cytolytic machinery of cytotoxic T cells. Current Opinion in Immunology. 2010;22(3):308-13.
75. Azimzadeh J, Bornens M. Structure and duplication of the centrosome. Journal of Cell Science. 2007;120(13):2139-42.
76. Ambler RJ, Edmunds, G.L, Toti, G, Morgan, D.J, Wuelfing, C. . PD-1 suppresses the maintenance of cell couples between cytotoxic T cells and tumor target cells within the tumor. bioRxiv. 2018;443788.
77. Ambler RJ. Impaired Polarisation of CD8+ T Lymphocytes is regulated by PD-1: University of Bristol; 2017.
78. Brown ACN, Oddos S, Dobbie IM, Alakoskela J-M, Parton RM, Eissmann P, et al. Remodelling of Cortical Actin Where Lytic Granules Dock at Natural Killer Cell Immune Synapses Revealed by Super-Resolution Microscopy. Plos Biology. 2011;9(9).
79. Sallusto F. Heterogeneity of Human CD4(+) T Cells Against Microbes. Annu Rev Immunol. 2016;34:317-34.
80. Gregori S, Bacchetta R, Passerini L, Levings MK, Roncarolo MG. Isolation, expansion, and characterization of human natural and adaptive regulatory T cells. Methods Mol Biol. 2007;380:83-105.

81. Hall BM, Verma ND, Tran GT, Hodgkinson SJ. Distinct regulatory CD4+T cell subsets; differences between naive and antigen specific T regulatory cells. Curr Opin Immunol. 2011;23(5):641-7.
82. Curotto de Lafaille MA, Lafaille JJ. Natural and adaptive foxp3+ regulatory T cells: more of the same or a division of labor? Immunity. 2009;30(5):626-35.
83. DuPage M, Bluestone JA. Harnessing the plasticity of CD4(+) T cells to treat immune-mediated disease. Nat Rev Immunol. 2016;16(3):149-63.
84. Adachi K, Davis MM. T-cell receptor ligation induces distinct signaling pathways in naive vs. antigen-experienced T cells. Proc Natl Acad Sci U S A. 2011;108(4):1549-54.
85. Burton BR, Britton GJ, Fang H, Verhagen J, Smithers B, Sabatos-Peyton CA, et al. Sequential transcriptional changes dictate safe and effective antigen-specific immunotherapy. Nat Commun. 2014;5:4741.
86. Mucida D, Park Y, Kim G, Turovskaya O, Scott I, Kronenberg M, et al. Reciprocal TH17 and regulatory T cell differentiation mediated by retinoic acid. Science. 2007;317(5835):256-60.
87. Chen W, Jin W, Hardegen N, Lei KJ, Li L, Marinos N, et al. Conversion of peripheral CD4+CD25- naive T cells to CD4+CD25+ regulatory T cells by TGF-beta induction of transcription factor Foxp3. J Exp Med. 2003;198(12):1875-86.
88. Zhong H, Liu Y, Xu Z, Liang P, Yang H, Zhang X, et al. TGF-beta-Induced CD8(+)CD103(+) Regulatory T Cells Show Potent Therapeutic Effect on Chronic Graft-versus-Host Disease Lupus by Suppressing B Cells. Front Immunol. 2018;9:35.
89. Allan SE, Broady R, Gregori S, Himmel ME, Locke N, Roncarolo MG, et al. CD4+ T-regulatory cells: toward therapy for human diseases. Immunol Rev. 2008;223:391-421.
90. Zeng H, Zhang R, Jin B, Chen L. Type 1 regulatory T cells: a new mechanism of peripheral immune tolerance. Cell Mol Immunol. 2015;12(5):566-71.
91. Weiner HL. Induction and mechanism of action of transforming growth factor-beta-secreting Th3 regulatory cells. Immunol Rev. 2001;182:207-14.
92. Tran TTP, Eichholz K, Amelio P, Moyer C, Nemerow GR, Perreau M, et al. Humoral immune response to adenovirus induce tolerogenic bystander dendritic cells that promote generation of regulatory T cells. PLoS Pathog. 2018;14(8):e1007127.
93. Wherry EJ, Ha SJ, Kaech SM, Haining WN, Sarkar S, Kalia V, et al. Molecular signature of CD8+ T cell exhaustion during chronic viral infection. Immunity. 2007;27(4):670-84.
94. Schietinger A, Greenberg PD. Tolerance and exhaustion: defining mechanisms of T cell dysfunction. Trends Immunol. 2014;35(2):51-60.
95. Wherry EJ, Kurachi M. Molecular and cellular insights into T cell exhaustion. Nat Rev Immunol. 2015;15(8):486-99.
96. Chang JT, Wherry EJ, Goldrath AW. Molecular regulation of effector and memory T cell differentiation. Nat Immunol. 2014;15(12):1104-15.
97. Morgan DJ, Kurts C, Kreuwel HTC, Holst KL, Heath WR, Sherman LA. Ontogeny of T cell tolerance to peripherally expressed antigens. Proceedings of the National Academy of Sciences of the United States of America. 1999;96(7):3854-8.
98. Chen JH, Perry CJ, Tsui YC, Staron MM, Parish IA, Dominguez CX, et al. Prostaglandin E2 and programmed cell death 1 signaling coordinately impair CTL function and survival during chronic viral infection. Nat Med. 2015;21(4):327-34.
99. Tallerico R, Todaro M, Di Franco S, Maccalli C, Garofalo C, Sottile R, et al. Human NK cells selective targeting of colon cancer-initiating cells: a role for natural cytotoxicity receptors and MHC class I molecules. J Immunol. 2013;190(5):2381-90.
100. Sallusto F, Lanzavecchia A. Heterogeneity of CD4+ memory T cells: functional modules for tailored immunity. Eur J Immunol. 2009;39(8):2076-82.

101. Kotturi MF, Swann JA, Peters B, Arlehamn CL, Sidney J, Kolla RV, et al. Human CD8(+) and CD4(+) T cell memory to lymphocytic choriomeningitis virus infection. J Virol. 2011;85(22):11770-80.
102. Galluzzi L, Vacchelli E, Bravo-San Pedro JM, Buque A, Senovilla L, Baracco EE, et al. Classification of current anticancer immunotherapies. Oncotarget. 2014;5(24):12472-508.
103. Sakuishi K, Apetoh L, Sullivan JM, Blazar BR, Kuchroo VK, Anderson AC. Targeting Tim-3 and PD-1 pathways to reverse T cell exhaustion and restore anti-tumor immunity. J Exp Med. 2010;207(10):2187-94.
104. Mothe BR, Stewart BS, Oseroff C, Bui HH, Stogiera S, Garcia Z, et al. Chronic lymphocytic choriomeningitis virus infection actively down-regulates CD4+ T cell responses directed against a broad range of epitopes. J Immunol. 2007;179(2):1058-67.
105. Darrah PA, Hegde ST, Patel DT, Lindsay RW, Chen L, Roederer M, et al. IL-10 production differentially influences the magnitude, quality, and protective capacity of Th1 responses depending on the vaccine platform. J Exp Med. 2010;207(7):1421-33.
106. Rehr M, Cahenzli J, Haas A, Price DA, Gostick E, Huber M, et al. Emergence of polyfunctional CD8+ T cells after prolonged suppression of human immunodeficiency virus replication by antiretroviral therapy. J Virol. 2008;82(7):3391-404.
107. Crawford A, Angelosanto JM, Kao C, Doering TA, Odorizzi PM, Barnett BE, et al. Molecular and transcriptional basis of CD4(+) T cell dysfunction during chronic infection. Immunity. 2014;40(2):289-302.
108. Pauken KE, Wherry EJ. Overcoming T cell exhaustion in infection and cancer. Trends Immunol. 2015;36(4):265-76.
109. Zinselmeyer BH, Heydari S, Sacristan C, Nayak D, Cammer M, Herz J, et al. PD-1 promotes immune exhaustion by inducing antiviral T cell motility paralysis. J Exp Med. 2013;210(4):757-74.
110. Crespo J, Sun H, Welling TH, Tian Z, Zou W. T cell anergy, exhaustion, senescence, and stemness in the tumor microenvironment. Curr Opin Immunol. 2013;25(2):214-21.
111. Zhou S, Ou R, Huang L, Price GE, Moskophidis D. Differential tissue-specific regulation of antiviral CD8+ T-cell immune responses during chronic viral infection. J Virol. 2004;78(7):3578-600.
112. Turnis ME, Andrews LP, Vignali DA. Inhibitory receptors as targets for cancer immunotherapy. Eur J Immunol. 2015;45(7):1892-905.
113. Kurktschiev PD, Raziorrouh B, Schraut W, Backmund M, Wachtler M, Wendtner CM, et al. Dysfunctional CD8+ T cells in hepatitis B and C are characterized by a lack of antigen-specific T-bet induction. J Exp Med. 2014;211(10):2047-59.
114. Bucks CM, Norton JA, Boesteanu AC, Mueller YM, Katsikis PD. Chronic antigen stimulation alone is sufficient to drive CD8+ T cell exhaustion. J Immunol. 2009;182(11):6697-708.
115. Qing Zhou MEM, Rachelle G. Veenstra, Brenda J. Weigel, Mitsuomi Hirashima, David H. Munn, William J. Murphy, Miyuki Azuma, Ana C. Anderson, Vijay K. Kuchroo and Bruce R. Blazar. Coexpression of Tim-3 and PD-1 identifies a CD8 T-cell exhaustion phenotype in mice with disseminated acute myelogenous leukemia. Blood. 2011;117(17):4501-10.
116. Anderson AC. Tim-3: an emerging target in the cancer immunotherapy landscape. Cancer Immunol Res. 2014;2(5):393-8.
117. Hodi FS, Chiarion-Sileni V, Gonzalez R, Grob JJ, Rutkowski P, Cowey CL, et al. Nivolumab plus ipilimumab or nivolumab alone versus ipilimumab alone in advanced melanoma (CheckMate 067): 4-year outcomes of a multicentre, randomised, phase 3 trial. Lancet Oncol. 2018;19(11):1480-92.

118. Garidou L, Heydari S, Gossa S, McGavern DB. Therapeutic blockade of transforming growth factor beta fails to promote clearance of a persistent viral infection. J Virol. 2012;86(13):7060-71.
119. Galon J, Bruni D. Approaches to treat immune hot, altered and cold tumours with combination immunotherapies. Nat Rev Drug Discov. 2019.
120. Anderson AC, Joller N, Kuchroo VK. Lag-3, Tim-3, and TIGIT: Co-inhibitory Receptors with Specialized Functions in Immune Regulation. Immunity. 2016;44(5):989-1004.
121. Chihara N, Madi A, Kondo T, Zhang H, Acharya N, Singer M, et al. Induction and transcriptional regulation of the co-inhibitory gene module in T cells. Nature. 2018;558(7710):454-9.
122. Singer M, Wang C, Cong L, Marjanovic ND, Kowalczyk MS, Zhang H, et al. A Distinct Gene Module for Dysfunction Uncoupled from Activation in Tumor-Infiltrating T Cells. Cell. 2017;171(5):1221-3.
123. Murakami N, Riella LV. Co-inhibitory pathways and their importance in immune regulation. Transplantation. 2014;98(1):3-14.
124. Buchbinder EI, Desai A. CTLA-4 and PD-1 Pathways: Similarities, Differences, and Implications of Their Inhibition. Am J Clin Oncol. 2016;39(1):98-106.
125. Manieri NA, Chiang EY, Grogan JL. TIGIT: A Key Inhibitor of the Cancer Immunity Cycle. Trends Immunol. 2017;38(1):20-8.
126. Wang J, Sanmamed MF, Datar I, Su TT, Ji L, Sun J, et al. Fibrinogen-like Protein 1 Is a Major Immune Inhibitory Ligand of LAG-3. Cell. 2019;176(1-2):334-47 e12.
127. Ocana-Guzman R, Torre-Bouscoulet L, Sada-Ovalle I. TIM-3 Regulates Distinct Functions in Macrophages. Front Immunol. 2016;7:229.
128. Monney L, Sabatos CA, Gaglia JL, Ryu A, Waldner H, Chernova T, et al. Th1-specific cell surface protein Tim-3 regulates macrophage activation and severity of an autoimmune disease. Nature. 2002;415(6871):536-41.
129. Gorman JV, Colgan JD. Regulation of T cell responses by the receptor molecule Tim-3. Immunol Res. 2014;59(1-3):56-65.
130. Dixon KO, Das M, Kuchroo VK. Human disease mutations highlight the inhibitory function of TIM-3. Nat Genet. 2018;50(12):1640-1.
131. Cheng G, Li M, Wu J, Ji M, Fang C, Shi H, et al. Expression of Tim-3 in gastric cancer tissue and its relationship with prognosis. International Journal of Clinical and Experimental Pathology. 2015;8(8):9452-7.
132. Zhu C, Anderson AC, Kuchroo VK. TIM-3 and its regulatory role in immune responses. Curr Top Microbiol Immunol. 2011;350:1-15.
133. Li Y, Zhang J, Zhang D, Hong X, Tao Y, Wang S, et al. Tim-3 signaling in peripheral NK cells promotes maternal-fetal immune tolerance and alleviates pregnancy loss. Sci Signal. 2017;10(498).
134. Das M, Zhu C, Kuchroo VK. Tim-3 and its role in regulating anti-tumor immunity. Immunol Rev. 2017;276(1):97-111.
135. Zhu C, Sakuishi K, Xiao S, Sun Z, Zaghouani S, Gu G, et al. An IL-27/NFIL3 signalling axis drives Tim-3 and IL-10 expression and T-cell dysfunction. Nat Commun. 2015;6:6072.
136. <Immunotherapy for Melanoma (Skin Cancer) - CRI.pdf>.
137. Zhu C, Gu G, Zhang H, Xiao S, Wang C, Xiong H, et al. NFIL3 and Ets1 co-regulate a cluster of genes, including Tim-3, that is associated with T cell tolerance. The Journal of Immunology. 2016;196(1 Supplement):58.1-.1.
138. Huang YH, Zhu C, Kondo Y, Anderson AC, Gandhi A, Russell A, et al. CEACAM1 regulates TIM-3-mediated tolerance and exhaustion. Nature. 2015;517(7534):386-90.

139. Antonioli L, Blandizzi C, Pacher P, Hasko G. Immunity, inflammation and cancer: a leading role for adenosine. Nat Rev Cancer. 2013;13(12):842-57.
140. Di Virgilio F. Purines, purinergic receptors, and cancer. Cancer Res. 2012;72(21):5441-7.
141. Benci JL, Xu B, Qiu Y, Wu TJ, Dada H, Twyman-Saint Victor C, et al. Tumor Interferon Signaling Regulates a Multigenic Resistance Program to Immune Checkpoint Blockade. Cell. 2016;167(6):1540-54 e12.
142. Clement M, Marsden M, Stacey MA, Abdul-Karim J, Gimeno Brias S, Costa Bento D, et al. Cytomegalovirus-Specific IL-10-Producing CD4+ T Cells Are Governed by Type-I IFN-Induced IL-27 and Promote Virus Persistence. PLoS Pathog. 2016;12(12):e1006050.
143. Mumm JB, Emmerich J, Zhang X, Chan I, Wu L, Mauze S, et al. IL-10 elicits IFNgamma-dependent tumor immune surveillance. Cancer Cell. 2011;20(6):781-96.
144. Eigler A, Siegmund B, Emmerich U, Baumann KH, Hartmann G, Endres S. Anti-inflammatory activities of cAMP-elevating agents: enhancement of IL-10 synthesis and concurrent suppression of TNF production. J Leukoc Biol. 1998;63(1):101-7.
145. Nagaraj S, Gabrilovich DI. Myeloid-derived suppressor cells in human cancer. Cancer J. 2010;16(4):348-53.
146. Li Z, Zhang LJ, Zhang HR, Tian GF, Tian J, Mao XL, et al. Tumor-derived transforming growth factor-beta is critical for tumor progression and evasion from immune surveillance. Asian Pac J Cancer Prev. 2014;15(13):5181-6.
147. Lu L, Yu Y, Li G, Pu L, Zhang F, Zheng S, et al. CD8(+)CD103(+) regulatory T cells in spontaneous tolerance of liver allografts. Int Immunopharmacol. 2009;9(5):546-8.
148. Morgan DJ, Kreuwel HT, Sherman LA. Antigen concentration and precursor frequency determine the rate of CD8+ T cell tolerance to peripherally expressed antigens. J Immunol. 1999;163(2):723-7.
149. Fujinami RS, von Herrath MG, Christen U, Whitton JL. Molecular mimicry, bystander activation, or viral persistence: infections and autoimmune disease. Clin Microbiol Rev. 2006;19(1):80-94.
150. Liu L, Cao Z, Chen J, Li R, Cao Y, Zhu C, et al. Influenza A virus induces interleukin-27 through cyclooxygenase-2 and protein kinase A signaling. J Biol Chem. 2012;287(15):11899-910.
151. Aandahl EM, Torgersen KM, Tasken K. CD8+ regulatory T cells-A distinct T-cell lineage or a transient T-cell phenotype? Hum Immunol. 2008;69(11):696-9.
152. Schmidt A, Oberle N, Krammer PH. Molecular mechanisms of treg-mediated T cell suppression. Front Immunol. 2012;3:51.
153. Carroll MW, Matthews DA, Hiscox JA, Elmore MJ, Pollakis G, Rambaut A, et al. Temporal and spatial analysis of the 2014-2015 Ebola virus outbreak in West Africa. Nature. 2015;524(7563):97-101.
154. Al Yafei Z. Tumour-specific CTLs: What does it take to wake them up? : University of Bristol; 2012.
155. Hanahan D, Weinberg RA. Hallmarks of cancer: the next generation. Cell. 2011;144(5):646-74.
156. Hanahan D, Weinberg RA. The hallmarks of cancer. Cell. 2000;100(1):57-70.
157. Williams AB, Schumacher B. p53 in the DNA-Damage-Repair Process. Cold Spring Harb Perspect Med. 2016;6(5).
158. Gossage L, Eisen T, Maher ER. VHL, the story of a tumour suppressor gene. Nat Rev Cancer. 2015;15(1):55-64.
159. A bucket full of science, the hallmarks of cancer 2019 [Available from: https://abucketfullofscience.wordpress.com/2017/01/.

160. Vega SL, Liu E, Arvind V, Bushman J, Sung HJ, Becker ML, et al. High-content image informatics of the structural nuclear protein NuMA parses trajectories for stem/progenitor cell lineages and oncogenic transformation. Exp Cell Res. 2017;351(1):11-23.
161. Baserga R, Peruzzi F, Reiss K. The IGF-1 receptor in cancer biology. Int J Cancer. 2003;107(6):873-7.
162. McKian KP, Haluska P. Cixutumumab. Expert Opin Investig Drugs. 2009;18(7):1025-33.
163. Gurevich DB, Severn CE, Twomey C, Greenhough A, Cash J, Toye AM, et al. Live imaging of wound angiogenesis reveals macrophage orchestrated vessel sprouting and regression. EMBO J. 2018;37(13).
164. Wang Y, Shi J, Chai K, Ying X, Zhou BP. The Role of Snail in EMT and Tumorigenesis. Curr Cancer Drug Targets. 2013;13(9):963-72.
165. De Palma M, Hanahan D. The biology of personalized cancer medicine: facing individual complexities underlying hallmark capabilities. Mol Oncol. 2012;6(2):111-27.
166. Hatfield SM, Kjaergaard J, Lukashev D, Belikoff B, Schreiber TH, Sethumadhavan S, et al. Systemic oxygenation weakens the hypoxia and hypoxia inducible factor 1alpha-dependent and extracellular adenosine-mediated tumor protection. J Mol Med (Berl). 2014;92(12):1283-92.
167. Wong ALA, Bellot GL, Hirpara JL, Pervaiz S. Understanding the Cancer Stem Cell Phenotype: A Step Forward in the Therapeutic Management of Cancer. Biochem Pharmacol. 2019.
168. Sanchez-Vega F, Mina M, Armenia J, Chatila WK, Luna A, La KC, et al. Oncogenic Signaling Pathways in The Cancer Genome Atlas. Cell. 2018;173(2):321-37 e10.
169. Smyth MJ, Dunn GP, Schreiber RD. Cancer immunosurveillance and immunoediting: the roles of immunity in suppressing tumor development and shaping tumor immunogenicity. Adv Immunol. 2006;90:1-50.
170. Boon T, Coulie PG, Van den Eynde B. Tumor antigens recognized by T cells. Immunol Today. 1997;18(6):267-8.
171. Mittal D, Gubin MM, Schreiber RD, Smyth MJ. New insights into cancer immunoediting and its three component phases--elimination, equilibrium and escape. Curr Opin Immunol. 2014;27:16-25.
172. O'Donnell JS, Teng MWL, Smyth MJ. Cancer immunoediting and resistance to T cell-based immunotherapy. Nat Rev Clin Oncol. 2018.
173. Schreiber RD, Old LJ, Smyth MJ. Cancer immunoediting: integrating immunity's roles in cancer suppression and promotion. Science. 2011;331(6024):1565-70.
174. Chen DS, Mellman I. Oncology meets immunology: the cancer-immunity cycle. Immunity. 2013;39(1):1-10.
175. Smyth MJ, Ngiow SF, Ribas A, Teng MW. Combination cancer immunotherapies tailored to the tumour microenvironment. Nat Rev Clin Oncol. 2016;13(3):143-58.
176. Coulie PG, Van den Eynde BJ, van der Bruggen P, Boon T. Tumour antigens recognized by T lymphocytes: at the core of cancer immunotherapy. Nat Rev Cancer. 2014;14(2):135-46.
177. Yarchoan M, Johnson BA, 3rd, Lutz ER, Laheru DA, Jaffee EM. Targeting neoantigens to augment antitumour immunity. Nat Rev Cancer. 2017;17(9):569.
178. Melero I, Rouzaut A, Motz GT, Coukos G. T-cell and NK-cell infiltration into solid tumors: a key limiting factor for efficacious cancer immunotherapy. Cancer Discov. 2014;4(5):522-6.
179. Laudanna C, Campbell JJ, Butcher EC. Elevation of intracellular cAMP inhibits RhoA activation and integrin-dependent leukocyte adhesion induced by chemoattractants. J Biol Chem. 1997;272(39):24141-4.
180. Colbeck EJ, Jones E, Hindley JP, Smart K, Schulz R, Browne M, et al. Treg Depletion Licenses T Cell-Driven HEV Neogenesis and Promotes Tumor Destruction. Cancer Immunol Res. 2017;5(11):1005-15.

181. Stagg J, Smyth MJ. Extracellular adenosine triphosphate and adenosine in cancer. Oncogene. 2010;29(39):5346-58.
182. Ohta A. A Metabolic Immune Checkpoint: Adenosine in Tumor Microenvironment. Front Immunol. 2016;7:109.
183. Sitkovsky M, Lukashev D, Deaglio S, Dwyer K, Robson SC, Ohta A. Adenosine A2A receptor antagonists: blockade of adenosinergic effects and T regulatory cells. Br J Pharmacol. 2008;153 Suppl 1:S457-64.
184. Young A, Mittal D, Stagg J, Smyth MJ. Targeting cancer-derived adenosine: new therapeutic approaches. Cancer Discov. 2014;4(8):879-88.
185. Gabrilovich DI, Nagaraj S. Myeloid-derived suppressor cells as regulators of the immune system. Nat Rev Immunol. 2009;9(3):162-74.
186. Lin EY, Pollard JW. Macrophages: modulators of breast cancer progression. Novartis Found Symp. 2004;256:158-68; discussion 68-72, 259-69.
187. Yang L, Zhang Y. Tumor-associated macrophages: from basic research to clinical application. J Hematol Oncol. 2017;10(1):58.
188. Gao X, Zhu Y, Li G, Huang H, Zhang G, Wang F, et al. TIM-3 expression characterizes regulatory T cells in tumor tissues and is associated with lung cancer progression. PLoS One. 2012;7(2):e30676.
189. Yang ZZ, Grote DM, Ziesmer SC, Niki T, Hirashima M, Novak AJ, et al. IL-12 upregulates TIM-3 expression and induces T cell exhaustion in patients with follicular B cell non-Hodgkin lymphoma. J Clin Invest. 2012;122(4):1271-82.
190. Gupta S, Thornley TB, Gao W, Larocca R, Turka LA, Kuchroo VK, et al. Allograft rejection is restrained by short-lived TIM-3+PD-1+Foxp3+ Tregs. J Clin Invest. 2012;122(7):2395-404.
191. Leone RD, Lo YC, Powell JD. A2aR antagonists: Next generation checkpoint blockade for cancer immunotherapy. Comput Struct Biotechnol J. 2015;13:265-72.
192. Brudvik KW, Tasken K. Modulation of T cell immune functions by the prostaglandin E(2) - cAMP pathway in chronic inflammatory states. Br J Pharmacol. 2012;166(2):411-9.
193. Nakanishi M, Rosenberg DW. Multifaceted roles of PGE2 in inflammation and cancer. Semin Immunopathol. 2013;35(2):123-37.
194. Cekic C, Linden J. Adenosine A2A receptors intrinsically regulate CD8+ T cells in the tumor microenvironment. Cancer Res. 2014;74(24):7239-49.
195. Leone RD, Emens LA. Targeting adenosine for cancer immunotherapy. J Immunother Cancer. 2018;6(1):57.
196. Blay J, White TD, Hoskin DW. The extracellular fluid of solid carcinomas contains immunosuppressive concentrations of adenosine. Cancer Res. 1997;57(13):2602-5.
197. Chouker A, Thiel M, Lukashev D, Ward JM, Kaufmann I, Apasov S, et al. Critical role of hypoxia and A2A adenosine receptors in liver tissue-protecting physiological anti-inflammatory pathway. Mol Med. 2008;14(3-4):116-23.
198. Liu M, Du K, Fu Z, Zhang S, Wu X. Hypoxia-inducible factor 1-alpha up-regulates the expression of phospholipase D2 in colon cancer cells under hypoxic conditions. Med Oncol. 2015;32(1):394.
199. Lukashev D, Ohta A, Sitkovsky M. Targeting hypoxia--A(2A) adenosine receptor-mediated mechanisms of tissue protection. Drug Discov Today. 2004;9(9):403-9.
200. Allard B, Beavis PA, Darcy PK, Stagg J. Immunosuppressive activities of adenosine in cancer. Curr Opin Pharmacol. 2016;29:7-16.
201. Beavis PA, Henderson MA, Giuffrida L, Mills JK, Sek K, Cross RS, et al. Targeting the adenosine 2A receptor enhances chimeric antigen receptor T cell efficacy. J Clin Invest. 2017;127(3):929-41.

202. Tasken K, Aandahl EM. Localized effects of cAMP mediated by distinct routes of protein kinase A. Physiol Rev. 2004;84(1):137-67.
203. Vang T, Abrahamsen H, Myklebust S, Horejsi V, Tasken K. Combined spatial and enzymatic regulation of Csk by cAMP and protein kinase a inhibits T cell receptor signaling. J Biol Chem. 2003;278(20):17597-600.
204. Yaqub S, Abrahamsen H, Zimmerman B, Kholod N, Torgersen KM, Mustelin T, et al. Activation of C-terminal Src kinase (Csk) by phosphorylation at serine-364 depends on the Csk-Src homology 3 domain. Biochem J. 2003;372(Pt 1):271-8.
205. Mosenden R, Tasken K. Cyclic AMP-mediated immune regulation--overview of mechanisms of action in T cells. Cell Signal. 2011;23(6):1009-16.
206. Hodge RG, Ridley AJ. Regulating Rho GTPases and their regulators. Nat Rev Mol Cell Biol. 2016;17(8):496-510.
207. Saoudi A, Kassem S, Dejean A, Gaud G. Rho-GTPases as key regulators of T lymphocyte biology. Small GTPases. 2014;5.
208. Torgersen KM, Vang T, Abrahamsen H, Yaqub S, Tasken K. Molecular mechanisms for protein kinase A-mediated modulation of immune function. Cell Signal. 2002;14(1):1-9.
209. Tasken K, Ruppelt A. Negative regulation of T-cell receptor activation by the cAMP-PKA-Csk signalling pathway in T-cell lipid rafts. Front Biosci. 2006;11:2929-39.
210. Wehbi VL, Tasken K. Molecular Mechanisms for cAMP-Mediated Immunoregulation in T cells - Role of Anchored Protein Kinase A Signaling Units. Front Immunol. 2016;7:222.
211. Bonaventura J, Navarro G, Casado-Anguera V, Azdad K, Rea W, Moreno E, et al. Allosteric interactions between agonists and antagonists within the adenosine A2A receptor-dopamine D2 receptor heterotetramer. Proc Natl Acad Sci U S A. 2015;112(27):E3609-18.
212. Ferre S, Bonaventura J, Zhu W, Hatcher-Solis C, Taura J, Quiroz C, et al. Essential Control of the Function of the Striatopallidal Neuron by Pre-coupled Complexes of Adenosine A2A-Dopamine D2 Receptor Heterotetramers and Adenylyl Cyclase. Front Pharmacol. 2018;9:243.
213. Sawyers C. Targeted cancer therapy. Nature. 2004;432(7015):294-7.
214. Azam F, Mehta S, Harris AL. Mechanisms of resistance to antiangiogenesis therapy. Eur J Cancer. 2010;46(8):1323-32.
215. Kasuga K. Comprehensive analysis of MHC ligands in clinical material by immunoaffinity-mass spectrometry. Methods Mol Biol. 2013;1023:203-18.
216. Sallets A, Robinson S, Kardosh A, Levy R. Enhancing immunotherapy of STING agonist for lymphoma in preclinical models. Blood Adv. 2018;2(17):2230-41.
217. Gilham DE, Anderson J, Bridgeman JS, Hawkins RE, Exley MA, Stauss H, et al. Adoptive T-cell therapy for cancer in the United kingdom: a review of activity for the British Society of Gene and Cell Therapy annual meeting 2015. Hum Gene Ther. 2015;26(5):276-85.
218. Rosenberg SA, Restifo NP. Adoptive cell transfer as personalized immunotherapy for human cancer. Science. 2015;348(6230):62-8.
219. Mehta GU, Malekzadeh P, Shelton T, White DE, Butman JA, Yang JC, et al. Outcomes of Adoptive Cell Transfer With Tumor-infiltrating Lymphocytes for Metastatic Melanoma Patients With and Without Brain Metastases. J Immunother. 2018;41(5):241-7.
220. Lukashev M, LePage D, Wilson C, Bailly V, Garber E, Lukashin A, et al. Targeting the lymphotoxin-beta receptor with agonist antibodies as a potential cancer therapy. Cancer Res. 2006;66(19):9617-24.
221. Weber JS, D'Angelo SP, Minor D, Hodi FS, Gutzmer R, Neyns B, et al. Nivolumab versus chemotherapy in patients with advanced melanoma who progressed after anti-CTLA-4 treatment (CheckMate 037): a randomised, controlled, open-label, phase 3 trial. Lancet Oncol. 2015;16(4):375-84.

222. Weber JS, Gibney G, Sullivan RJ, Sosman JA, Slingluff CL, Jr., Lawrence DP, et al. Sequential administration of nivolumab and ipilimumab with a planned switch in patients with advanced melanoma (CheckMate 064): an open-label, randomised, phase 2 trial. Lancet Oncol. 2016;17(7):943-55.
223. Godkin.A WC, Gallimore.A, Williams,A. . Targeting LAG3+ T cells for Cancer Immunotherapy. MRC; 2017.
224. Leone RD, Sun IM, Oh MH, Sun IH, Wen J, Englert J, et al. Inhibition of the adenosine A2a receptor modulates expression of T cell coinhibitory receptors and improves effector function for enhanced checkpoint blockade and ACT in murine cancer models. Cancer Immunol Immunother. 2018.
225. Sitkovsky MV. T regulatory cells: hypoxia-adenosinergic suppression and re-direction of the immune response. Trends Immunol. 2009;30(3):102-8.
226. Leone RD, Englert JM, Cheng C-H, Wen J, Oh M-H, Sun I-H, et al. Abstract 4364: Adenosine A2a receptor blockade as a means of enhancing immune checkpoint inhibition and adoptive T-cell therapy. Cancer Res. 2016;76:4364-.
227. Willingham S, Hotson A, Ho P, Choy C, Laport G, McCaffery I, et al. Abstract PR04: CPI-444: A potent and selective inhibitor of A2AR induces antitumor responses alone and in combination with anti-PD-L1 in preclinical and clinical studies. Cancer Immunology Research. 2016;4:PR04-PR.
228. Willingham SB, Ho PY, Hotson A, Hill C, Piccione EC, Hsieh J, et al. A2AR Antagonism with CPI-444 Induces Antitumor Responses and Augments Efficacy to Anti-PD-(L)1 and Anti-CTLA-4 in Preclinical Models. Cancer Immunol Res. 2018;6(10):1136-49.
229. Schadendorf D, Larkin J, Wolchok J, Hodi FS, Chiarion-Sileni V, Gonzalez R, et al. Health-related quality of life results from the phase III CheckMate 067 study. Eur J Cancer. 2017;82:80-91.
230. Enamorado M, Iborra S, Priego E, Cueto FJ, Quintana JA, Martinez-Cano S, et al. Enhanced anti-tumour immunity requires the interplay between resident and circulating memory CD8(+) T cells. Nat Commun. 2017;8:16073.
231. Ali HR, Provenzano E, Dawson SJ, Blows FM, Liu B, Shah M, et al. Association between CD8+ T-cell infiltration and breast cancer survival in 12,439 patients. Ann Oncol. 2014;25(8):1536-43.
232. Owens GL, Price MJ, Cheadle EJ, Hawkins RE, Gilham DE, Edmondson RJ. Ex vivo expanded tumour-infiltrating lymphocytes from ovarian cancer patients release anti-tumour cytokines in response to autologous primary ovarian cancer cells. Cancer Immunol Immunother. 2018;67(10):1519-31.
233. Murphy GP, Hrushesky WJ. A murine renal cell carcinoma. J Natl Cancer Inst. 1973;50(4):1013-25.
234. Youn JI, Nagaraj S, Collazo M, Gabrilovich DI. Subsets of myeloid-derived suppressor cells in tumor-bearing mice. J Immunol. 2008;181(8):5791-802.
235. Sueiro Ballasteros L. Analyses of tumour-mediated suppression of CD8+ cytotoxic T lymphocytes function: University of Bristol; 2015.
236. Hilchey SP, Kobie JJ, Cochran MR, Secor-Socha S, Wang JC, Hyrien O, et al. Human follicular lymphoma CD39+-infiltrating T cells contribute to adenosine-mediated T cell hyporesponsiveness. J Immunol. 2009;183(10):6157-66.
237. Vijayan D, Young A, Teng MWL, Smyth MJ. Targeting immunosuppressive adenosine in cancer. Nat Rev Cancer. 2017;17(12):765.
238. Young A, Ngiow Shin F, Barkauskas Deborah S, Sult E, Hay C, Blake Stephen J, et al. Co-inhibition of CD73 and A2AR Adenosine Signaling Improves Anti-tumor Immune Responses. Cancer Cell. 2016;30(3):391-403.

239. Morgan DJ, Liblau R, Scott B, Fleck S, McDevitt HO, Sarvetnick N, et al. CD8(+) T cell-mediated spontaneous diabetes in neonatal mice. J Immunol. 1996;157(3):978-83.
240. Chan ESL, Montesinos MC, Fernandez P, Desai A, Delano DL, Yee H, et al. Adenosine A(2A) receptors play a role in the pathogenesis of hepatic cirrhosis. British Journal of Pharmacology. 2006;148(8):1144-55.
241. Nolan. Phoenix helper-free retrovirus producer lines: Stanford University2018 [Available from: https://web.stanford.edu/group/nolan/_OldWebsite/retroviral_systems/phx.html.
242. Roybal KT, Mace EM, Mantell JM, Verkade P, Orange JS, Wulfing C. Early Signaling in Primary T Cells Activated by Antigen Presenting Cells Is Associated with a Deep and Transient Lamellal Actin Network. PLoS One. 2015;10(8):e0133299.
243. Facility WB. TIRF Mircoscopy Technical Specifications Bristol UK: University of Bristol; 2019 [Available from: http://www.bristol.ac.uk/wolfson-bioimaging/equipment/light-microscopy/total-internal-reflection-fluorescence-microscopy-/.
244. Grodzki AC, Berenstein E. Antibody purification: ammonium sulfate fractionation or gel filtration. Methods Mol Biol. 2010;588:15-26.
245. Laerd Statistics. Statistical tutorials and software guides. 2015 [Available from: Retrieved from https://statistics.laerd.com/.
246. Enderling H, Chaplain MA, Anderson AR, Vaidya JS. A mathematical model of breast cancer development, local treatment and recurrence. J Theor Biol. 2007;246(2):245-59.
247. Enderling H, Chaplain MA. Mathematical modeling of tumor growth and treatment. Curr Pharm Des. 2014;20(30):4934-40.
248. Loizides C, Iacovides D, Hadjiandreou MM, Rizki G, Achilleos A, Strati K, et al. Model-Based Tumor Growth Dynamics and Therapy Response in a Mouse Model of De Novo Carcinogenesis. PLoS One. 2015;10(12):e0143840.
249. D S. Case studies in ecology and Evolution. [Lecture Notes]. In press 2010.
250. Couper KN, Blount DG, Riley EM. IL-10: the master regulator of immunity to infection. J Immunol. 2008;180(9):5771-7.
251. Hu Z, Zhang W, Usherwood EJ. Regulatory CD8+ T cells associated with erosion of immune surveillance in persistent virus infection suppress in vitro and have a reversible proliferative defect. J Immunol. 2013;191(1):312-22.
252. Stewart H, Bartlett C, Ross-Thriepland D, Shaw J, Griffin S, Harris M. A novel method for the measurement of hepatitis C virus infectious titres using the IncuCyte ZOOM and its application to antiviral screening. J Virol Methods. 2015;218:59-65.
253. Ng TH, Britton GJ, Hill EV, Verhagen J, Burton BR, Wraith DC. Regulation of adaptive immunity; the role of interleukin-10. Front Immunol. 2013;4:129.
254. Mitchell RE, Hassan M, Burton BR, Britton G, Hill EV, Verhagen J, et al. IL-4 enhances IL-10 production in Th1 cells: implications for Th1 and Th2 regulation. Sci Rep. 2017;7(1):11315.
255. Rosenberg SA, Dudley ME. Cancer regression in patients with metastatic melanoma after the transfer of autologous antitumor lymphocytes. Proc Natl Acad Sci U S A. 2004;101 Suppl 2:14639-45.
256. Avery L, Filderman J, Szymczak-Workman AL, Kane LP. Tim-3 co-stimulation promotes short-lived effector T cells, restricts memory precursors, and is dispensable for T cell exhaustion. Proc Natl Acad Sci U S A. 2018;115(10):2455-60.
257. Chen H, Chen Y, Liu H, Que Y, Zhang X, Zheng F. Integrated Expression Profiles Analysis Reveals Correlations Between the IL-33/ST2 Axis and CD8(+) T Cells, Regulatory T Cells, and Myeloid-Derived Suppressor Cells in Soft Tissue Sarcoma. Front Immunol. 2018;9:1179.
258. Hawkins RE, Gilham DE, Debets R, Eshhar Z, Taylor N, Abken H, et al. Development of adoptive cell therapy for cancer: a clinical perspective. Hum Gene Ther. 2010;21(6):665-72.

259. Rosenberg SA. Cell transfer immunotherapy for metastatic solid cancer--what clinicians need to know. Nat Rev Clin Oncol. 2011;8(10):577-85.
260. Basingab FS. Disabling Factors mediating CD8+ tumour infiltrating lymphocyte Dysfunction. Bristol, UK: University of Bristol; 2016.
261. Ohs I, Ducimetiere L, Marinho J, Kulig P, Becher B, Tugues S. Restoration of Natural Killer Cell Antimetastatic Activity by IL12 and Checkpoint Blockade. Cancer Res. 2017;77(24):7059-71.
262. Gregori S, Bacchetta R, Hauben E, Battaglia M, Roncarolo MG. Regulatory T cells: prospective for clinical application in hematopoietic stem cell transplantation. Curr Opin Hematol. 2005;12(6):451-6.
263. Zhang L, Bertucci AM, Ramsey-Goldman R, Burt RK, Datta SK. Regulatory T cell (Treg) subsets return in patients with refractory lupus following stem cell transplantation, and TGF-beta-producing CD8+ Treg cells are associated with immunological remission of lupus. J Immunol. 2009;183(10):6346-58.
264. Willingham S, Ho P, Leone R, Piccione E, Choy C, Hotson A, et al. Abstract 2337: The adenosine A2A receptor antagonist CPI-444 blocks adenosine-mediated T-cell suppression and exhibits antitumor activity alone and in combination with anti-PD-1 and anti-PD-L1. Cancer Res. 2016;76:2337-.
265. Allard D, Turcotte M, Stagg J. Targeting A2 adenosine receptors in cancer. Immunol Cell Biol. 2017;95(4):333-9.
266. Zhuang X, Zhang X, Xia X, Zhang C, Liang X, Gao L, et al. Ectopic expression of TIM-3 in lung cancers: a potential independent prognostic factor for patients with NSCLC. Am J Clin Pathol. 2012;137(6):978-85.
267. Krabbendam L, Nagasawa M, Spits H, Bal SM. Isolation of Human Innate Lymphoid Cells. Curr Protoc Immunol. 2018:e55.
268. Koyama S, Akbay EA, Li YY, Herter-Sprie GS, Buczkowski KA, Richards WG, et al. Adaptive resistance to therapeutic PD-1 blockade is associated with upregulation of alternative immune checkpoints. Nat Commun. 2016;7:10501.
269. Singer M, Wang C, Cong L, Marjanovic ND, Kowalczyk MS, Zhang H, et al. A Distinct Gene Module for Dysfunction Uncoupled from Activation in Tumor-Infiltrating T Cells. Cell. 2016;166(6):1500-11 e9.
270. Spracklen AJ, Fagan TN, Lovander KE, Tootle TL. The pros and cons of common actin labeling tools for visualizing actin dynamics during Drosophila oogenesis. Dev Biol. 2014;393(2):209-26.
271. Saresella M, Piancone F, Marventano I, La Rosa F, Tortorella P, Caputo D, et al. A role for the TIM-3/GAL-9/BAT3 pathway in determining the clinical phenotype of multiple sclerosis. FASEB J. 2014;28(11):5000-9.
272. Iannone R, Miele L, Maiolino P, Pinto A, Morello S. Blockade of A2b adenosine receptor reduces tumor growth and immune suppression mediated by myeloid-derived suppressor cells in a mouse model of melanoma. Neoplasia. 2013;15(12):1400-9.
273. Cernuda-Morollon E, Ridley AJ. Rho GTPases and leukocyte adhesion receptor expression and function in endothelial cells. Circ Res. 2006;98(6):757-67.
274. Infante E, Ridley AJ. Roles of Rho GTPases in leucocyte and leukaemia cell transendothelial migration. Philos Trans R Soc Lond B Biol Sci. 2013;368(1629):20130013.
275. Millan J, Williams L, Ridley AJ. An in vitro model to study the role of endothelial rho GTPases during leukocyte transendothelial migration. Methods Enzymol. 2006;406:643-55.
276. Kjaergaard J, Hatfield S, Jones G, Ohta A, Sitkovsky M. A2A Adenosine Receptor Gene Deletion or Synthetic A2A Antagonist Liberate Tumor-Reactive CD8(+) T Cells from Tumor-Induced Immunosuppression. J Immunol. 2018;201(2):782-91.

277. Ohta A, Kjaergaard J, Sharma S, Mohsin M, Goel N, Madasu M, et al. In vitro induction of T cells that are resistant to A2 adenosine receptor-mediated immunosuppression. Br J Pharmacol. 2009;156(2):297-306.
278. Jacobson KA, Kim YC, King BF. In search of selective P2 receptor ligands: interaction of dihydropyridine derivatives at recombinant rat P2X(2) receptors. J Auton Nerv Syst. 2000;81(1-3):152-7.
279. Ryzhov S, Novitskiy SV, Carbone DP, Biaggioni I, Zaynagetdinov R, Goldstein AE, et al. Host A2B Adenosine Receptors Promote Carcinoma Growth. Neoplasia. 2008;10(9):987-95.
280. Kandage D. Modulating Anti-Tumour Specific CD8+ T cell responses: University of Bristol; 2018.
281. Jeon SJ, Rhee SY, Ryu JH, Cheong JH, Kwon K, Yang SI, et al. Activation of adenosine A2A receptor up-regulates BDNF expression in rat primary cortical neurons. Neurochem Res. 2011;36(12):2259-69.
282. Bridgeman JS, Hawkins RE, Hombach AA, Abken H, Gilham DE. Building better chimeric antigen receptors for adoptive T cell therapy. Curr Gene Ther. 2010;10(2):77-90.
283. Bridgeman JS, Ladell K, Sheard VE, Miners K, Hawkins RE, Price DA, et al. CD3zeta-based chimeric antigen receptors mediate T cell activation via cis- and trans-signalling mechanisms: implications for optimization of receptor structure for adoptive cell therapy. Clin Exp Immunol. 2014;175(2):258-67.
284. Kato K, Koyanagi M, Okada H, Takanashi T, Wong YW, Williams AF, et al. CD48 is a counter-receptor for mouse CD2 and is involved in T cell activation. J Exp Med. 1992;176(5):1241-9.
285. Manu Rangachari, 10 Chen Zhu,1,10 Kaori Sakuishi,1 Sheng Xiao,1 Jozsef Karman,1,9 Andrew Chen,1 Mathieu Angin,2 Andrew Wakeham,3 Edward A Greenfield,4 Raymond A Sobel,5 Hitoshi Okada,3,6,7 Peter J McKinnon,8 Tak W Mak,3 Marylyn M Addo,2 Ana C Anderson,1 and Vijay K Kuchroo1. Bat3 Protects T cell Responses by Repressing Tim-3-Mediated Exhaustion and Death. Nat Med Author manuscript; available in PMC 2013 Sep 1
Published in final edited form as:
Nat Med 2012 Sep; 18(9): 1394–1400
doi: 101038/nm2871. 2012.
286. Ruppelt A, Mosenden R, Gronholm M, Aandahl EM, Tobin D, Carlson CR, et al. Inhibition of T cell activation by cyclic adenosine 5'-monophosphate requires lipid raft targeting of protein kinase A type I by the A-kinase anchoring protein ezrin. J Immunol. 2007;179(8):5159-68.
287. Gruener NH, Lechner F, Jung MC, Diepolder H, Gerlach T, Lauer G, et al. Sustained dysfunction of antiviral CD8+ T lymphocytes after infection with hepatitis C virus. J Virol. 2001;75(12):5550-8.
288. Antonia SJ, Mirza N, Fricke I, Chiappori A, Thompson P, Williams N, et al. Combination of p53 cancer vaccine with chemotherapy in patients with extensive stage small cell lung cancer. Clin Cancer Res. 2006;12(3 Pt 1):878-87.
289. Ohta A, Madasu M, Subramanian M, Kini R, Jones G, Chouker A, et al. Hypoxia-induced and A2A adenosine receptor-independent T-cell suppression is short lived and easily reversible. Int Immunol. 2014;26(2):83-91.
290. Brown SG, Townsend-Nicholson A, Jacobson KA, Burnstock G, King BF. Heteromultimeric P2X(1/2) receptors show a novel sensitivity to extracellular pH. J Pharmacol Exp Ther. 2002;300(2):673-80.
291. Jacobson KA, Muller CE. Medicinal chemistry of adenosine, P2Y and P2X receptors. Neuropharmacology. 2016;104:31-49.

292. Au-Yeung BB, Smith GA, Mueller JL, Heyn CS, Jaszczak RG, Weiss A, et al. IL-2 Modulates the TCR Signaling Threshold for CD8 but Not CD4 T Cell Proliferation on a Single-Cell Level. J Immunol. 2017;198(6):2445-56.
293. Pantel K, Alix-Panabieres C. Liquid biopsy and minimal residual disease - latest advances and implications for cure. Nat Rev Clin Oncol. 2019.
294. Pantel K, Alix-Panabieres C. Tumour microenvironment: informing on minimal residual disease in solid tumours. Nat Rev Clin Oncol. 2017;14(6):325-6.
295. Rosenblum MD, Way SS, Abbas AK. Regulatory T cell memory. Nat Rev Immunol. 2016;16(2):90-101.
296. Chin CS, Miller CH, Graham L, Parviz M, Zacur S, Patel B, et al. Bryostatin 1/ionomycin (B/I) ex vivo stimulation preferentially activates L-selectinlow tumor-sensitized lymphocytes. Int Immunol. 2004;16(9):1283-94.
297. Wherry EJ, Barber DL, Kaech SM, Blattman JN, Ahmed R. Antigen-independent memory CD8 T cells do not develop during chronic viral infection. Proc Natl Acad Sci U S A. 2004;101(45):16004-9.
298. Muller V, Alix-Panabieres C, Pantel K. Insights into minimal residual disease in cancer patients: implications for anti-cancer therapies. Eur J Cancer. 2010;46(7):1189-97.
299. Teixeiro E, Daniels MA, Hamilton SE, Schrum AG, Bragado R, Jameson SC, et al. Different T cell receptor signals determine CD8+ memory versus effector development. Science. 2009;323(5913):502-5.
300. Jenkinson SR, Williams NA, Morgan DJ. The Role of Intercellular Adhesion Molecule-1/LFA-1 Interactions in the Generation of Tumor-Specific CD8+ T Cell Responses. The Journal of Immunology. 2005;174(6):3401-7.
301. Chin CS, Graham LJ, Hamad GG, George KR, Bear HD. Bryostatin/ionomycin-activated T cells mediate regression of established tumors. J Surg Res. 2001;98(2):108-15.
302. Yasuda T, Wirtz T, Zhang B, Wunderlich T, Schmidt-Supprian M, Sommermann T, et al. Studying Epstein-Barr virus pathologies and immune surveillance by reconstructing EBV infection in mice. Cold Spring Harb Symp Quant Biol. 2013;78:259-63.
303. Hettmann T, Opferman JT, Leiden JM, Ashton-Rickardt PG. A critical role for NF-kappaB transcription factors in the development of CD8+ memory-phenotype T cells. Immunol Lett. 2003;85(3):297-300.
304. Yang ZZ, Grote DM, Ziesmer SC, Manske MK, Witzig TE, Novak AJ, et al. Soluble IL-2Ralpha facilitates IL-2-mediated immune responses and predicts reduced survival in follicular B-cell non-Hodgkin lymphoma. Blood. 2011;118(10):2809-20.
305. Schwendemann J, Choi C, Schirrmacher V, Beckhove P. Dynamic differentiation of activated human peripheral blood CD8+ and CD4+ effector memory T cells. J Immunol. 2005;175(3):1433-9.
306. Teng MW, Galon J, Fridman WH, Smyth MJ. From mice to humans: developments in cancer immunoediting. J Clin Invest. 2015;125(9):3338-46.
307. Bu M, Shen Y, Seeger WL, An S, Qi R, Sanderson JA, et al. Ovarian carcinoma-infiltrating regulatory T cells were more potent suppressors of CD8+ T cell inflammation than their peripheral counterparts, a function dependent on TIM3 expression. Tumor Biology. 2016;37(3):3949-56.
308. Liu F, Lang R, Zhao J, Zhang X, Pringle GA, Fan Y, et al. CD8(+) cytotoxic T cell and FOXP3(+) regulatory T cell infiltration in relation to breast cancer survival and molecular subtypes. Breast Cancer Res Treat. 2011;130(2):645-55.
309. Rosenberg SA, Yang JC, Robbins PF, Wunderlich JR, Hwu P, Sherry RM, et al. Cell transfer therapy for cancer: lessons from sequential treatments of a patient with metastatic melanoma. J Immunother. 2003;26(5):385-93.

310. Waickman AT, Alme A, Senaldi L, Zarek PE, Horton M, Powell JD. Enhancement of tumor immunotherapy by deletion of the A2A adenosine receptor. Cancer Immunol Immunother. 2012;61(6):917-26.
311. Chiba S, Baghdadi M, Akiba H, Yoshiyama H, Kinoshita I, Dosaka-Akita H, et al. Tumor-infiltrating DCs suppress nucleic acid-mediated innate immune responses through interactions between the receptor TIM-3 and the alarmin HMGB1. Nat Immunol. 2012;13(9):832-42.
312. Symeonides SN, Anderton SM, Serrels A. FAK-inhibition opens the door to checkpoint immunotherapy in Pancreatic Cancer. J Immunother Cancer. 2017;5:17.
313. Fu J, Kanne DB, Leong M, Glickman LH, McWhirter SM, Lemmens E, et al. STING agonist formulated cancer vaccines can cure established tumors resistant to PD-1 blockade. Sci Transl Med. 2015;7(283):283ra52.
314. Choi Y, Lee S, Kim K, Kim SH, Chung YJ, Lee C. Studying cancer immunotherapy using patient-derived xenografts (PDXs) in humanized mice. Exp Mol Med. 2018;50(8):99.
315. Vaupel P, Mayer A. Can respiratory hyperoxia mitigate adenosine-driven suppression of antitumor immunity? Ann Transl Med. 2015;3(19):292.
316. Ondondo B, Faulkner L, Williams NA, Morgan AJ, Morgan DJ. The B subunit of Escherichia coli enterotoxin helps control the in vivo growth of solid tumors expressing the Epstein-Barr virus latent membrane protein 2A. Cancer Med. 2015;4(3):457-71.
317. Beavis PA, Milenkovski N, Henderson MA, John LB, Allard B, Loi S, et al. Adenosine Receptor 2A Blockade Increases the Efficacy of Anti-PD-1 through Enhanced Antitumor T-cell Responses. Cancer Immunol Res. 2015;3(5):506-17.
318. Boni A, Muranski P, Cassard L, Wrzesinski C, Paulos CM, Palmer DC, et al. Adoptive transfer of allogeneic tumor-specific T cells mediates effective regression of large tumors across major histocompatibility barriers. Blood. 2008;112(12):4746-54.
319. Chhabra A. TCR-engineered, customized, antitumor T cells for cancer immunotherapy: advantages and limitations. TheScientificWorldJournal. 2011;11:121-9.
320. Allard B, Pommey S, Smyth MJ, Stagg J. Targeting CD73 enhances the antitumor activity of anti-PD-1 and anti-CTLA-4 mAbs. Clin Cancer Res. 2013;19(20):5626-35.
321. Wang L, Fan J, Thompson LF, Zhang Y, Shin T, Curiel TJ, et al. CD73 has distinct roles in nonhematopoietic and hematopoietic cells to promote tumor growth in mice. J Clin Invest. 2011;121(6):2371-82.
322. Takedachi M, Qu D, Ebisuno Y, Oohara H, Joachims ML, McGee ST, et al. CD73-generated adenosine restricts lymphocyte migration into draining lymph nodes. J Immunol. 2008;180(9):6288-96.
323. Beckhove P, Feuerer M, Dolenc M, Schuetz F, Choi C, Sommerfeldt N, et al. Specifically activated memory T cell subsets from cancer patients recognize and reject xenotransplanted autologous tumors. J Clin Invest. 2004;114(1):67-76.
324. Knudson KM, Pritzl CJ, Saxena V, Altman A, Daniels MA, Teixeiro E. NFkappaB-Pim-1-Eomesodermin axis is critical for maintaining CD8 T-cell memory quality. Proc Natl Acad Sci U S A. 2017;114(9):E1659-E67.
325. Ohta A, Sitkovsky M. Extracellular adenosine-mediated modulation of regulatory T cells. Front Immunol. 2014;5:304.
326. Yaqub S, Tasken K. Role for the cAMP-protein kinase A signaling pathway in suppression of antitumor immune responses by regulatory T cells. Crit Rev Oncog. 2008;14(1):57-77.
327. Tasken K, Stokka AJ. The molecular machinery for cAMP-dependent immunomodulation in T-cells. Biochem Soc Trans. 2006;34(Pt 4):476-9.
328. Ridley AJ. Rho GTPases and actin dynamics in membrane protrusions and vesicle trafficking. Trends Cell Biol. 2006;16(10):522-9.

329. Salomon C, Yee S, Scholz-Romero K, Kobayashi M, Vaswani K, Kvaskoff D, et al. Extravillous trophoblast cells-derived exosomes promote vascular smooth muscle cell migration. Front Pharmacol. 2014;5:175.
330. Zeddou M, Greimers R, de Valensart N, Nayjib B, Tasken K, Boniver J, et al. Prostaglandin E2 induces the expression of functional inhibitory CD94/NKG2A receptors in human CD8+ T lymphocytes by a cAMP-dependent protein kinase A type I pathway. Biochem Pharmacol. 2005;70(5):714-24.
331. Jung J. Human tumor xenograft models for preclinical assessment of anticancer drug development. Toxicol Res. 2014;30(1):1-5.

Chapter 10 Appendices

10.1 Table of Supplementary Figures

Appendix 1

Appendix 2

10.2 Appendix 1 – Supplementary Information

10.2.1 Supplementary Information for Chapter 3

10.2.1.1 Optimisation of a Cytotoxicity Assay using the Incucyte™ Live Cell Imaging Platform

To overcome the limitations of a microscopic cytotoxicity assay using a Widefield microscope, the Incucyte™ microscopy system was used. Clone 4 CTL were placed on top of a monolayer of KdHA-pulsed Renca tumour cells, and tumour cell apoptosis was quantified using the shrinkage of Renca cell area.

In early assays, a green Caspase 3/7 activated fluorogenic dye was used such that tumour cells undergoing apoptosis within the incucyte would fluoresce green (Molecular Probes). However, the dye was membrane permeable, meaning that Clone 4 CTL which underwent apoptosis when attempting to kill tumour cells, also fluoresced green (Figure S1A,B). Apoptotic fragments of Renca tumour cells could not easily be distinguished from apoptotic CTL as both objects have similar size. Therefore, the number or area of apoptotic Renca tumour cells could not be determined.

To enable green CTL fluorescence to be distinguished from green tumour cell fluorescence, Renca tumour target cells were stained with a red nuclear stain prior to analysis (Bacmam Nuclite™, Essen Bioscience). Objects with both green and red fluorescence could therefore be identified as apoptotic tumour cells. However, because the Renca cell cytoplasm spreads as they bind to the imaging plate, and then fragments break off during apoptosis, a nuclear stain did not accurately indicate the full Renca cell area (Figure S1C).

To overcome this problem, Renca cells were transfected with a vector encoding the mCherry gene, such that they produced red fluorescence over the entire cytoplasmic area (Lorena Sueiro-Ballasteros, unpublished). This allowed a reduction in red object area to be used to quantify Renca cell killing by CTL, without the need for caspase-activated fluorescence (Figure S1D,E). Hence, an effective microscopic killing assay was developed.

Figure S1- Development of a Microscopic Cytotoxicity Assay using the Incucyte Microscope

Clone 4 CTL were plated onto a monolayer of KdHA pulsed Renca tumour target cells and imaged using the Incucyte Zoom™ live cell analysis system. (A) Renca cells were incubated with red Bacmam nuclite dye for 1 hour, prior to plating in medium containing a Caspase 3/7 activated green fluorogenic dye. Renca cell nuclei (red objects) and apoptotic objects (green) are shown. (B) Same image as in (A) but with green object mask applied showing detection of both apoptotic tumour cells and apoptotic CTL as green. (C) Renca cells stained with Bacmam nuclite dye lack red staining within the cytoplasm, meaning that cytoplasmic fragments cannot be accurately detected. (D) RencaWT cells were transfected with plasmids expressing mCherry (Renca^{mCherry}WT) and were pulsed with KdHA peptide and plated at various densities as indicated. A density of 10-15 x 10^3 cells/well, prepared 4 hours before analysis provided optimum confluence to assess tumour cell killing over the following 10 hours, since tumour cells had space to expand, but the starting confluence was also sufficient for contraction to be assessed. (E) Using mCherry expressing Renca cells allows the red object area mask (blue outline) to detect the entire cytoplasmic area of plated tumour cells during tumour cell killing.

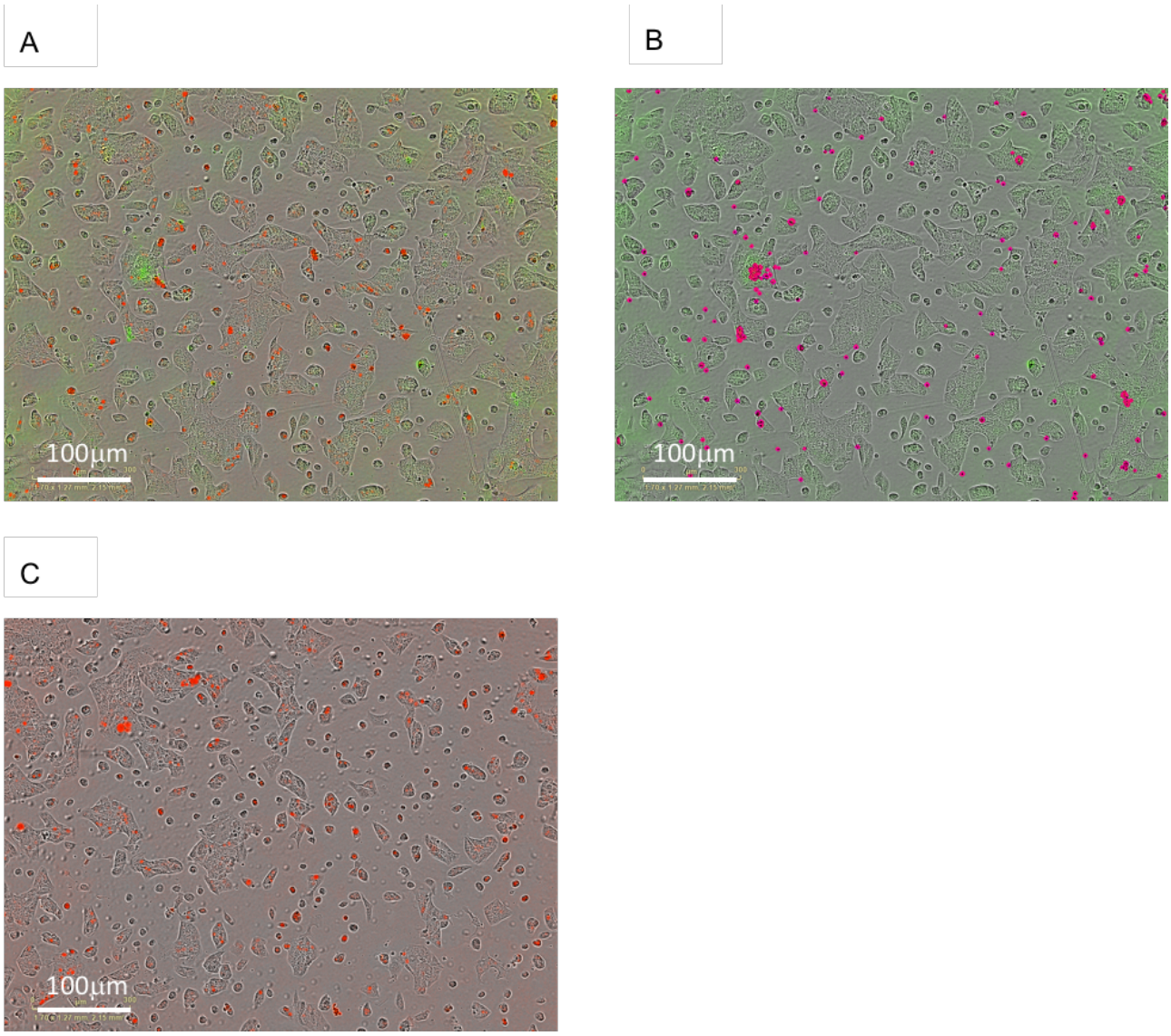

D

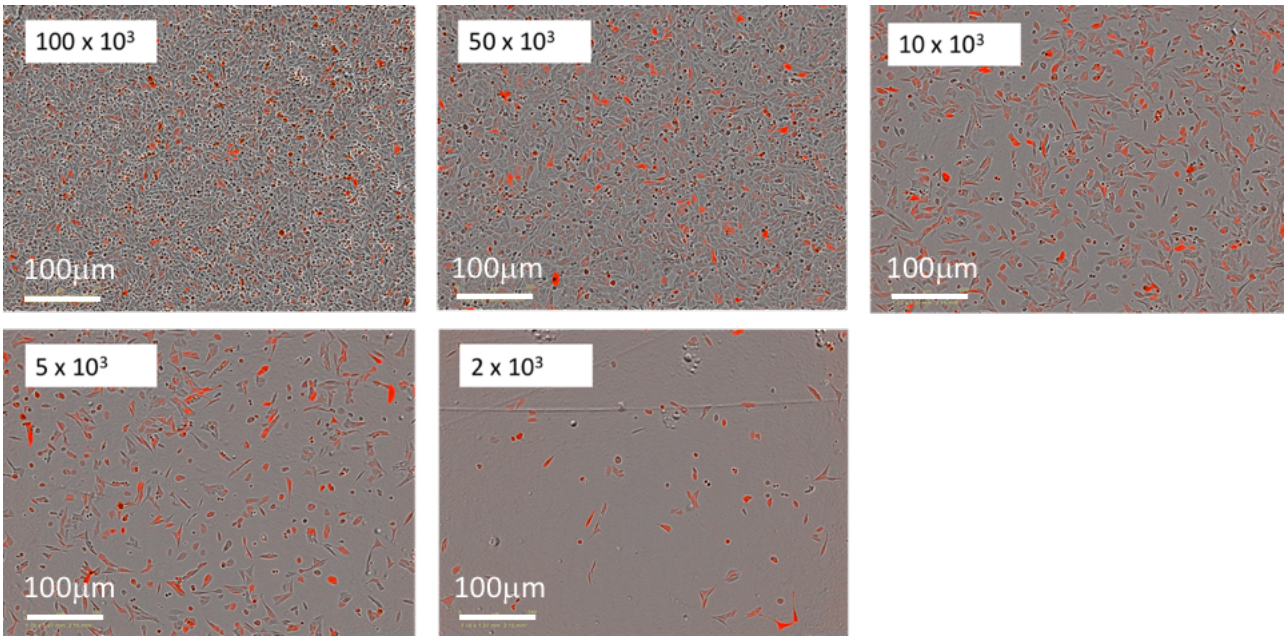
100 x 10³
100µm
50 x 10³
100µm
10 x 10³
100µm
5 x 10³
100µm
2 x 10³
100µm

E

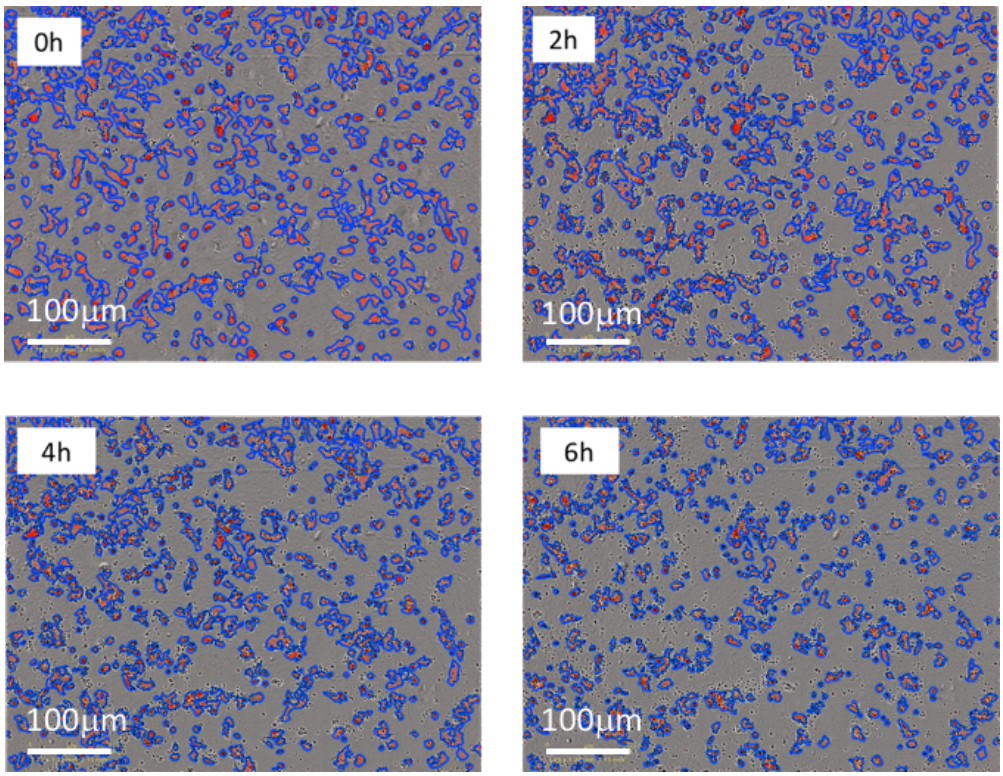
0h
100µm
2h
100µm
4h
100µm
6h
100µm

Figure S2 - Overexpression of NFIL3 is associated with elevated IL-10 production amongst CD4+ T cells

5CC7 TCR transgenic CD4+ T cells were primed *in vitro* using MCC peptide and transduced with $TIM3^{GFP}$ or $NFIL3^{GFP}$. Cells were sorted using FACS to establish populations of cells which overexpressed TIM3 or NFIL3 and cells were treated with PMA, Ionomycin and Brefeldin-A for 4 hours prior to staining using antibodies for IL-2, Ceacam-1, IL-10, TIM3, PD-1 and IFNγ. Data was analysed using flow cytometry.(A) % expression and (B)MFI of markers is shown. Statistics were not performed on one experimental repeat.

A.

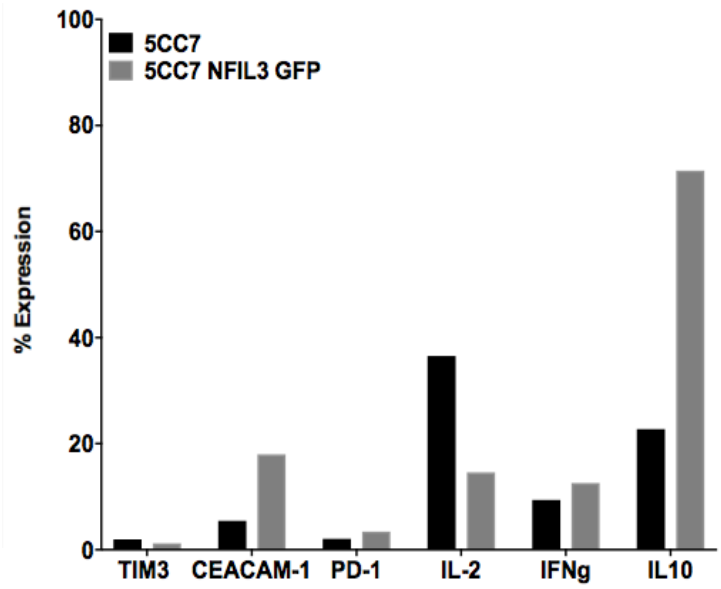

B.

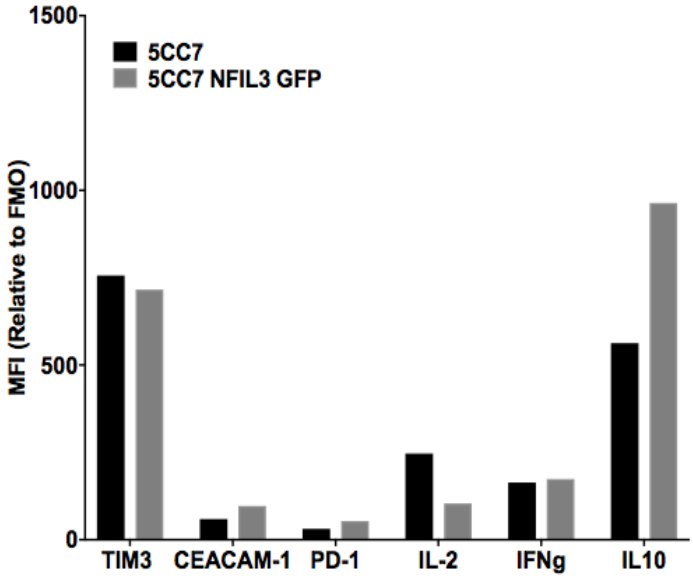

Figure S3 - Analysis of Ceacam-1 and Galectin-9 Expression amongst Tumour cells and Leukocytes from RencaHA tumours

Renca^{MCherry}HA tumours were harvested from BALB/c mice and digested using enzymes. Tumour cells were stained using antibodies specific to CD45, ICAM-1, Galectin-9 and Ceacam-1 and analysed using flow cytometry. (A) The sample was gated to select live, mCherry+ populations. Live cells were divided into CD45+ immune cells and CD45- tumour cells and ICAM-1, Ceacam-1 and Galectin-9 expression was quantified. (B) MFI is shown for leukocytes and tumour cells from two tumours and *in vitro* cultured tumour cells and (C) % expression is shown for *ex vivo* tumour samples.

A

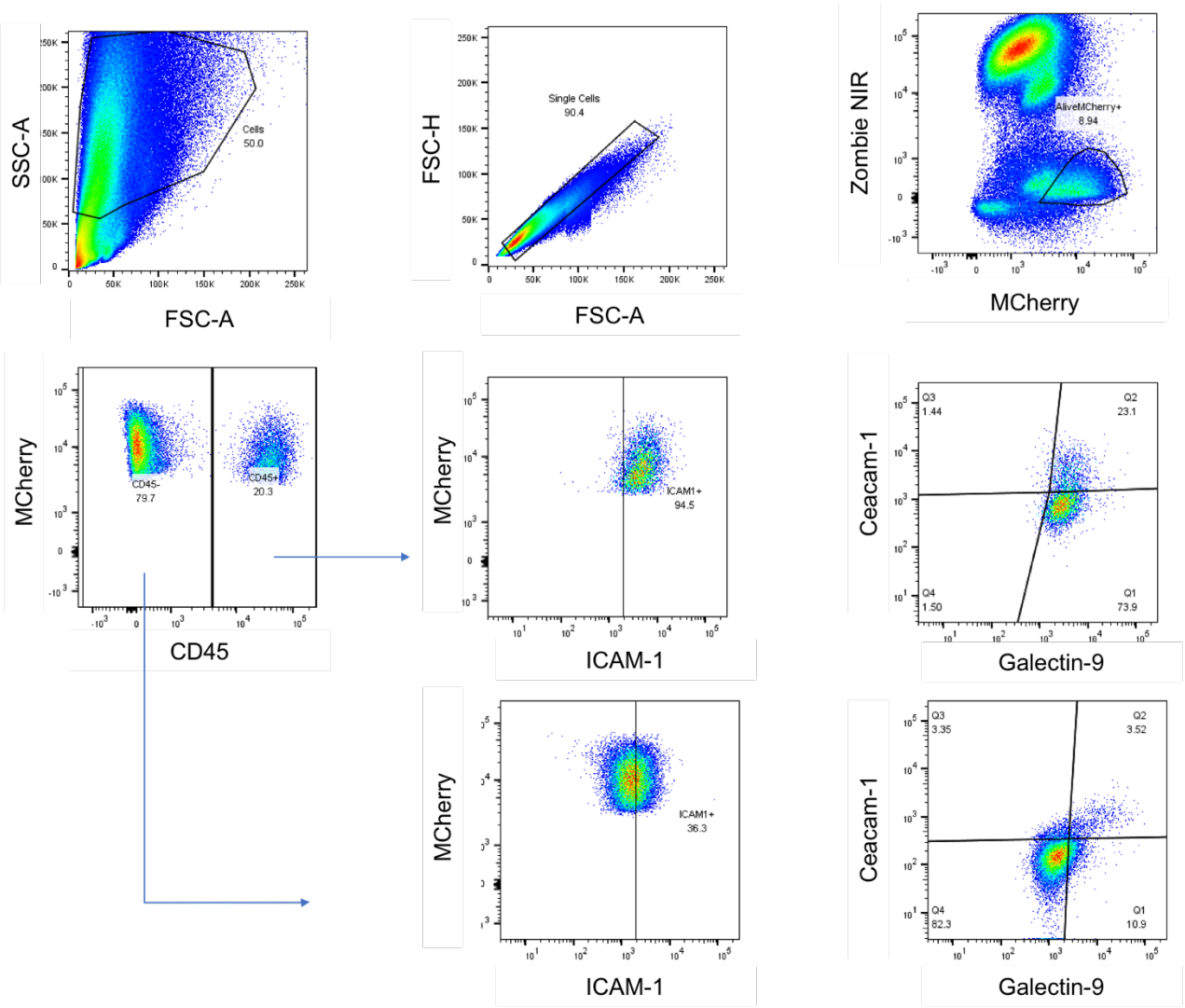

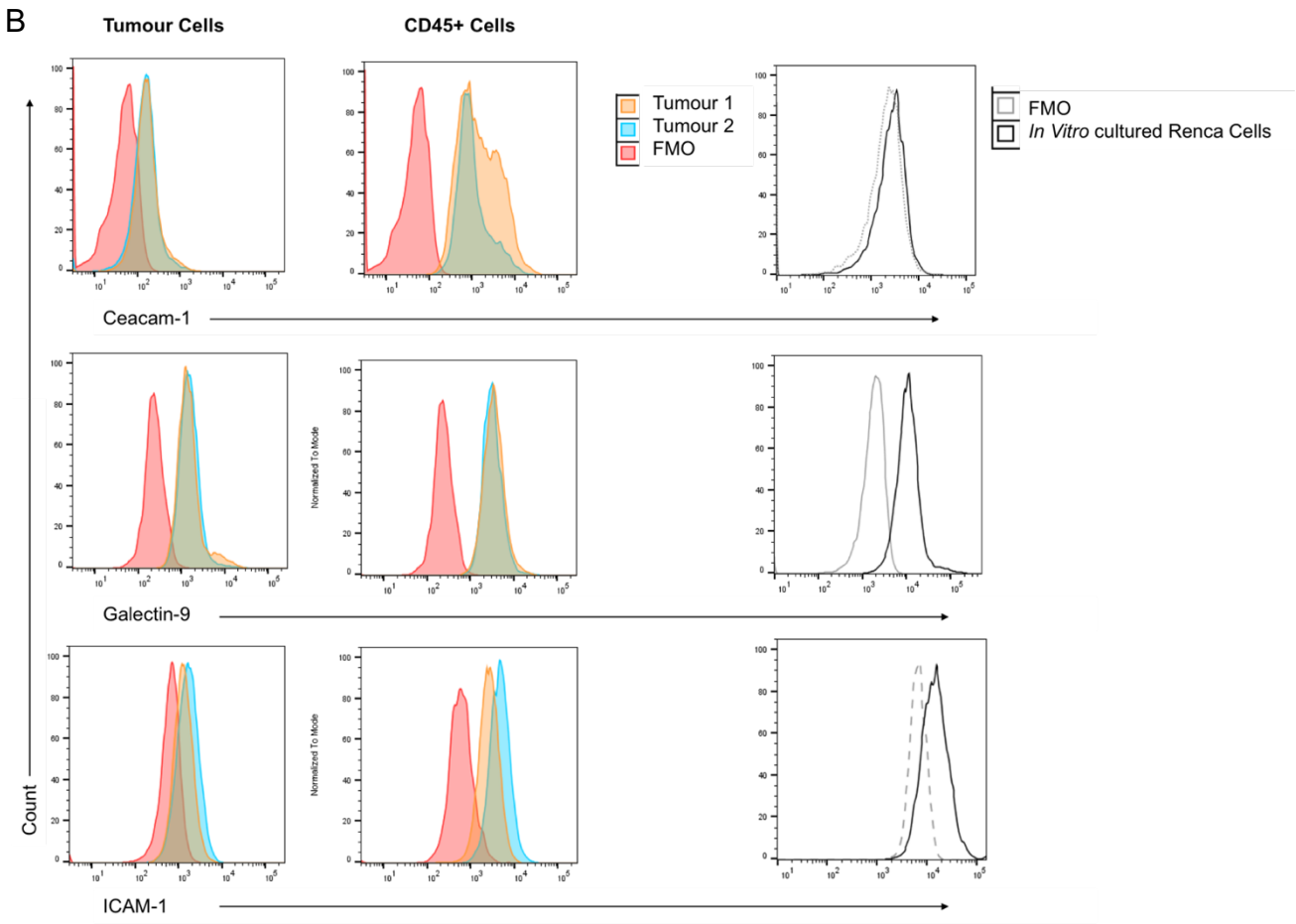
B
Tumour Cells
CD45+ Cells
Tumour 1
Tumour 2
FMO
FMO
In Vitro cultured Renca Cells
Ceacam-1
Galectin-9
ICAM-1
Count
Normalized To Mode

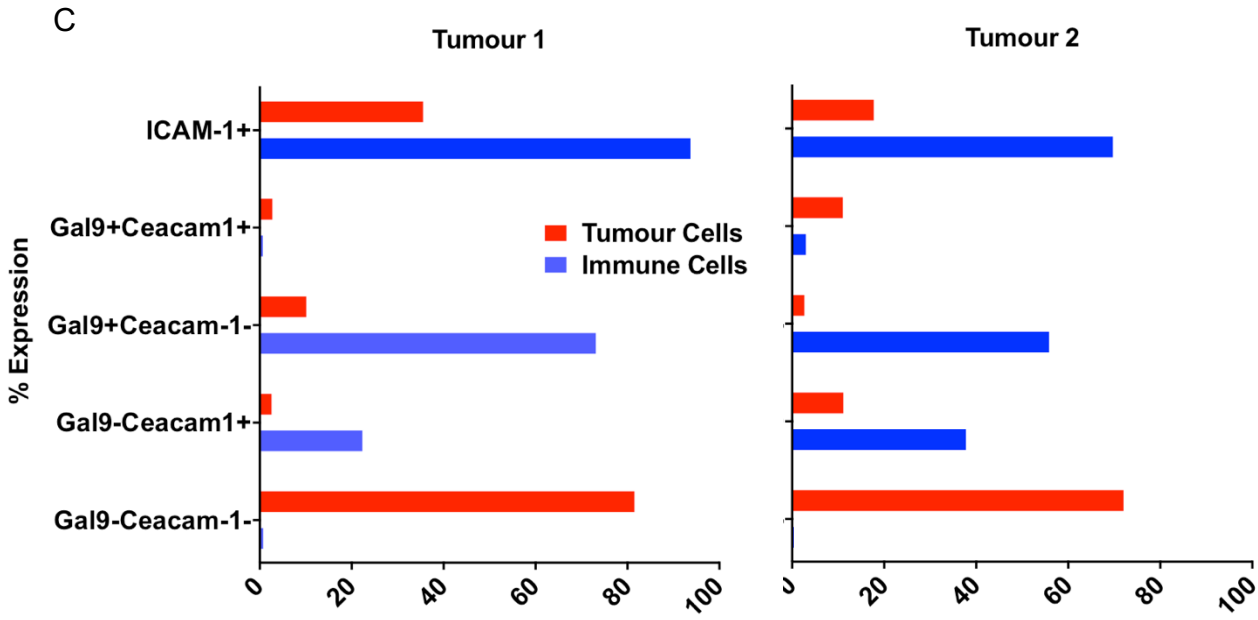
C
Tumour 1
Tumour 2
ICAM-1+
Gal9+Ceacam1+
Gal9+Ceacam-1-
Gal9-Ceacam1+
Gal9-Ceacam-1-
Tumour Cells
Immune Cells
% Expression
0
20
40
60
80
100

10.2.2 Supplementary Information for Chapter 4

Figure S4 - Principal Component Analysis of CIR expression- Individuals stratified by Tumour Volume

Groups of RencaHA tumour bearing BALB/c mice were treated with A2aR-Antagonist or vehicle/no treatment (control). Mice were not given ATT of Clone 4 T cells. CD45+ TILs were harvested from tumours and stained using antibodies for CD8, CD4, CD39, CD73, TIM3, TIGIT, LAG3 and PD-1. % Expression of all combinations of the above markers was quantified using flow cytometry. Each combination represents one of 154 variables entered into Principal Component Analysis (PCA), along with tumour volume. (A) Each dot represents an individual tumour bearing mouse and its volume is shown on a biplot of PC1 and PC2. The variables contributing to PC1 and PC2 are shown as arrows. (B) A key detailing the combinations of markers represented by the numbered arrows from the biplot in Figure 28, Chapter 4.

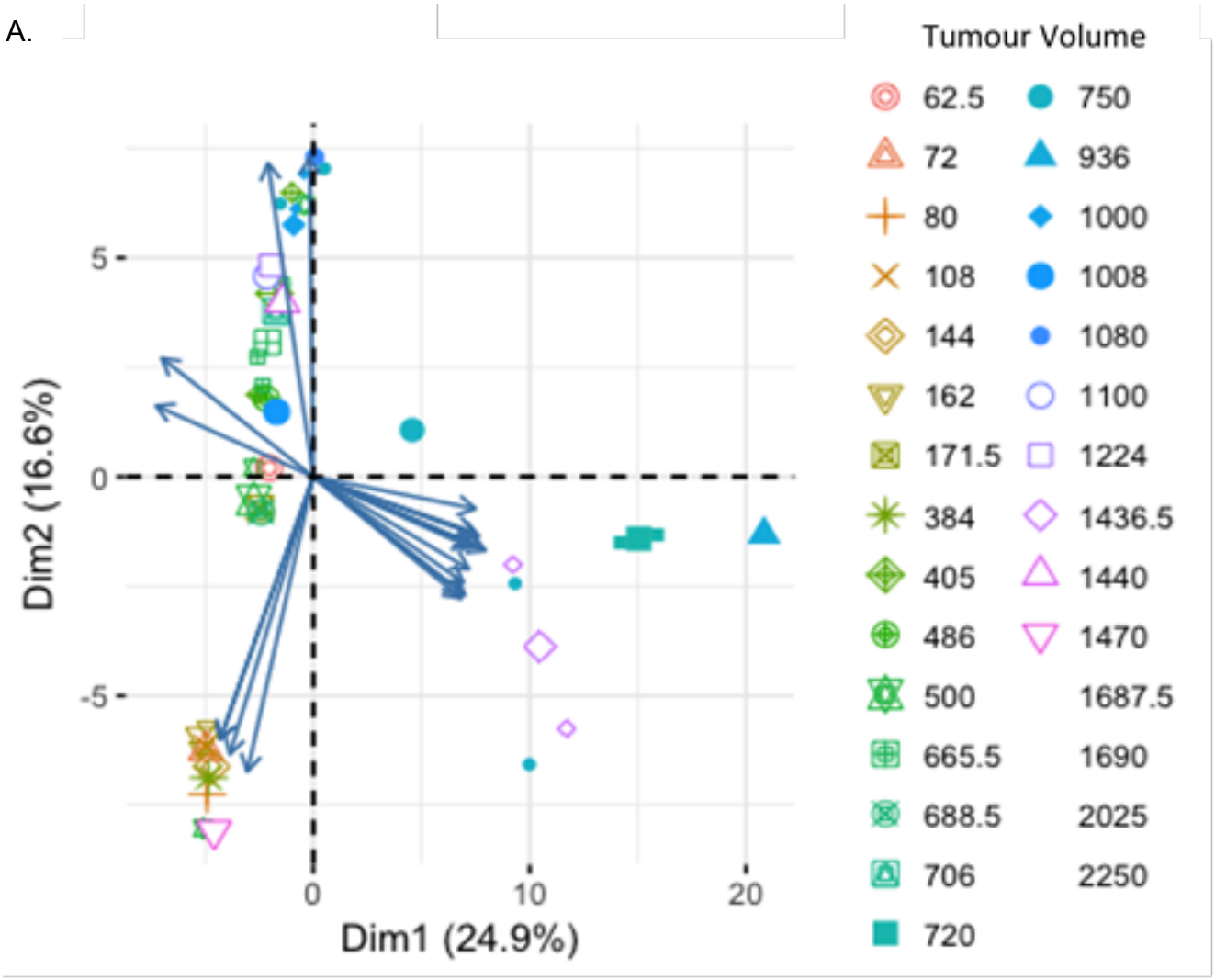

B.

	PC1 Positive			PC1 Negative			PC2 Positive			PC 2 Negative		
Associated Individuals	AR-Antagonist Treated (ZM)			Control			Large Tumours			Small Tumours		
Contributing Variables	Cell Type	Variable Number	Variable Name	Cell Type	Variable Number	Variable Name	Cell Type	Variable Number	Variable Name	Cell Type	Variable Number	Variable Name
	CD8+	8.	TIM3 with any other	n/a	2.	Volume	n/a	2.	Volume	CD8+	27.	CD39, CD73, TIGIT, TIM3
		46.	CD39 only	CD8+	78.	No CIRs	CD4+	106.	CD39, CD73		43.	CD39, TIGIT, TIM3
		47.	All except CD39					121.	CD39, TIM3	CD4+	102.	CD39, CD73, PD-1
		71.	PD1, TIGIT, TIM3								137.	CD73, TIM3
	CD4+	84.	TIM3 with any other									
		123.	All except CD39									
		124.	All except CD39 and TIM3									
		138.	CD73 only									
		132.	CD73, PD1, TIGIT									
		146.	LAG3 only									
		148.	PD1, TIGIT									
		150.	PD1 only									
		151.	TIGIT, TIM3									
		152.	TIM3 only									

Figure S5 – Tumour Growth from Individual Experiments in which RencaHA-bearing mice were treated with in vivo blockade of A2aRs and TIM3

RencaHA tumour-bearing BALB/c mice were treated with combinations of A2aR-Antagonist and Anti-TIM3mAb as indicated and given 2 doses of ATT Clone 4 T cells on days 12 and 16. Growth curves are shown from each of 4 experimental replicates. N= 6 mice per group in each experiment.

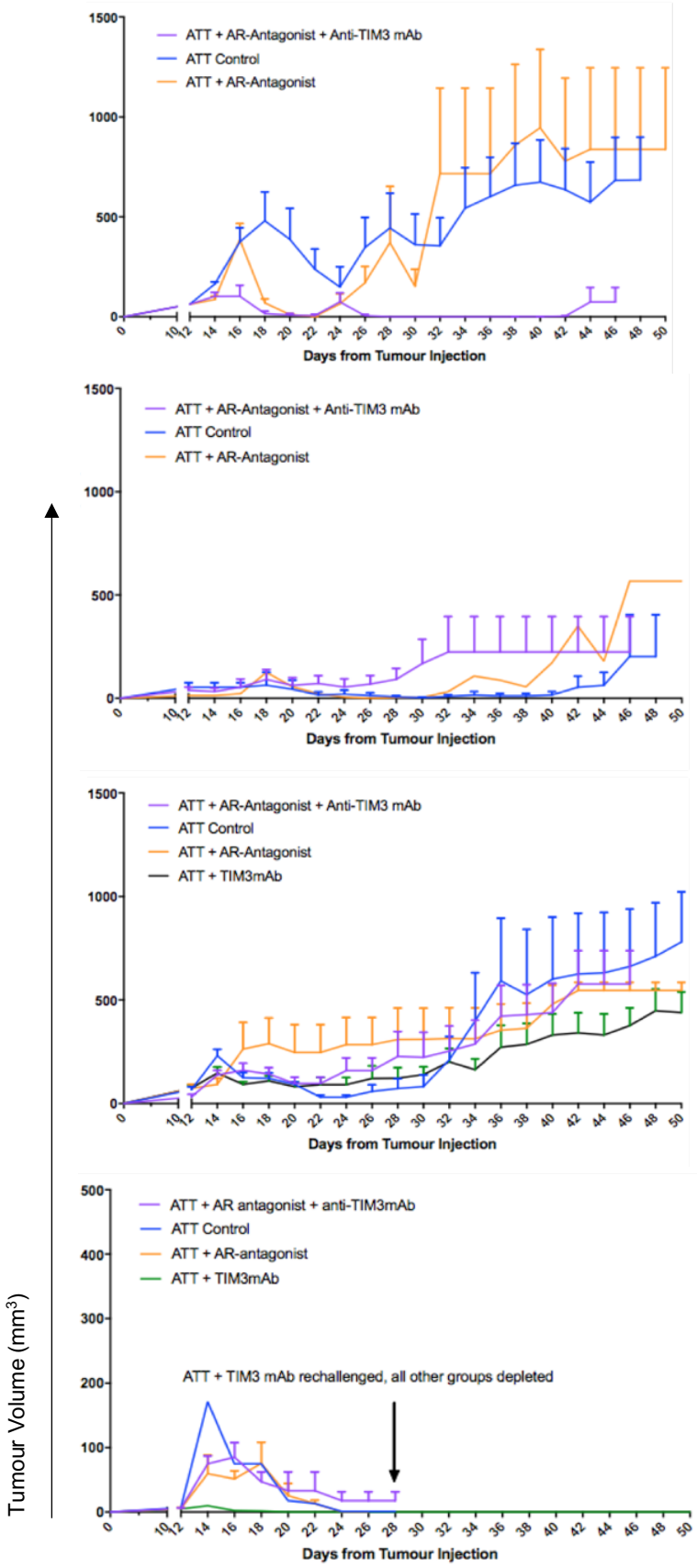

10.2.3 Supplementary Information for Chapter 5

Figure S6 - Treatment of RencaHA Tumour bearing mice with either A2aR-Antagonist or Anti-TIM3mAb does not improve ex vivo cytotoxicity of Clone 4 TILs

RencaHA tumour-bearing BALB/c mice were treated with A2aR-Antagonist (A, N=1 tumour per condition) or Anti-TIM3mAb (B N= 3 pooled tumours per condition) and given ATT of Clone 4 T cells. Clone 4 TILs were harvested and killing of a monolayer of KdHA-pulsed RencaHA^{mCherry} tumour cells in the presence of Clone 4 TILs was calculated at an E:T ratio of 3:2. Statistics could not be performed on one experimental repeat.

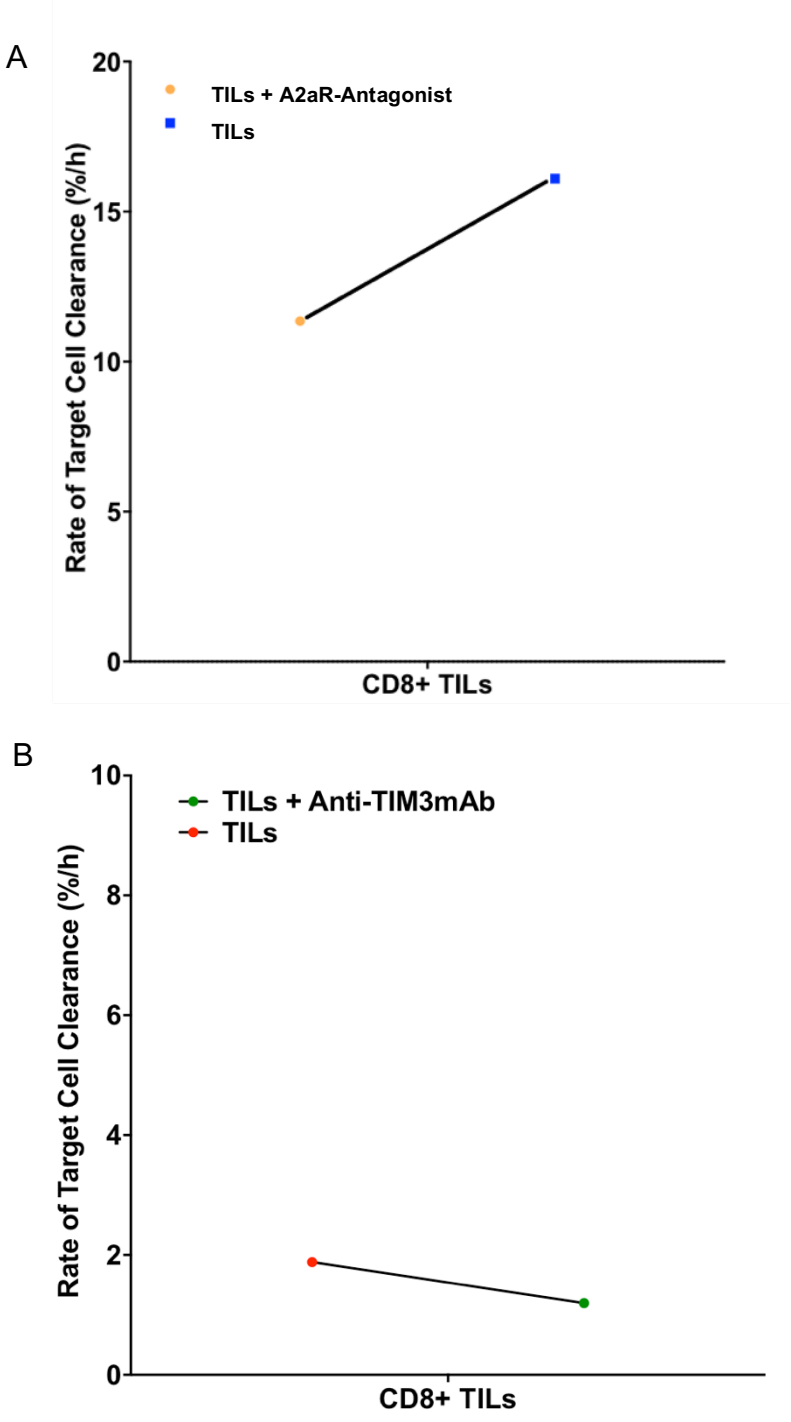

Figure S7 - In vivo but not ex vivo blockade of PD-1 amongst Clone 4 TILs improves Cytotoxicity and Peripheral Actin ring Maintenance

Clone 4 CTL were primed *in vitro.* RencaHA or RencaHA$^{PDL1-/-}$ tumour bearing BALB/c mice were given Clone 4 ATT and treated with either anti-PD-1 mAb or isotype control. Clone 4 TILs were harvested and (A) patterns of F-tractin accumulation were quantified during immune synapse formation using confocal imaging or (C) TILs were harvested and placed in a microscopic cytotoxicity assay. Alternatively, RencaHA tumour-bearing mice were given Clone 4 ATT in the absence of systemic treatment and (B) CTL and TILs were harvested and incubated with Anti-PD-1mAb for 1h before confocal imaging. Patterns of F-tractin accumulation are shown (D) CTL and TILs were placed in microscopic cytotoxicity assays. Some cells were incubated with Anti-PD-1mAb for 1h before imaging. Target cells were either RencaHA, RencaHA$^{PD\text{-}L1\ GFP}$ (PD-1 overexpression) or RencaHA $^{PDL-/-}$ as indicated[21].

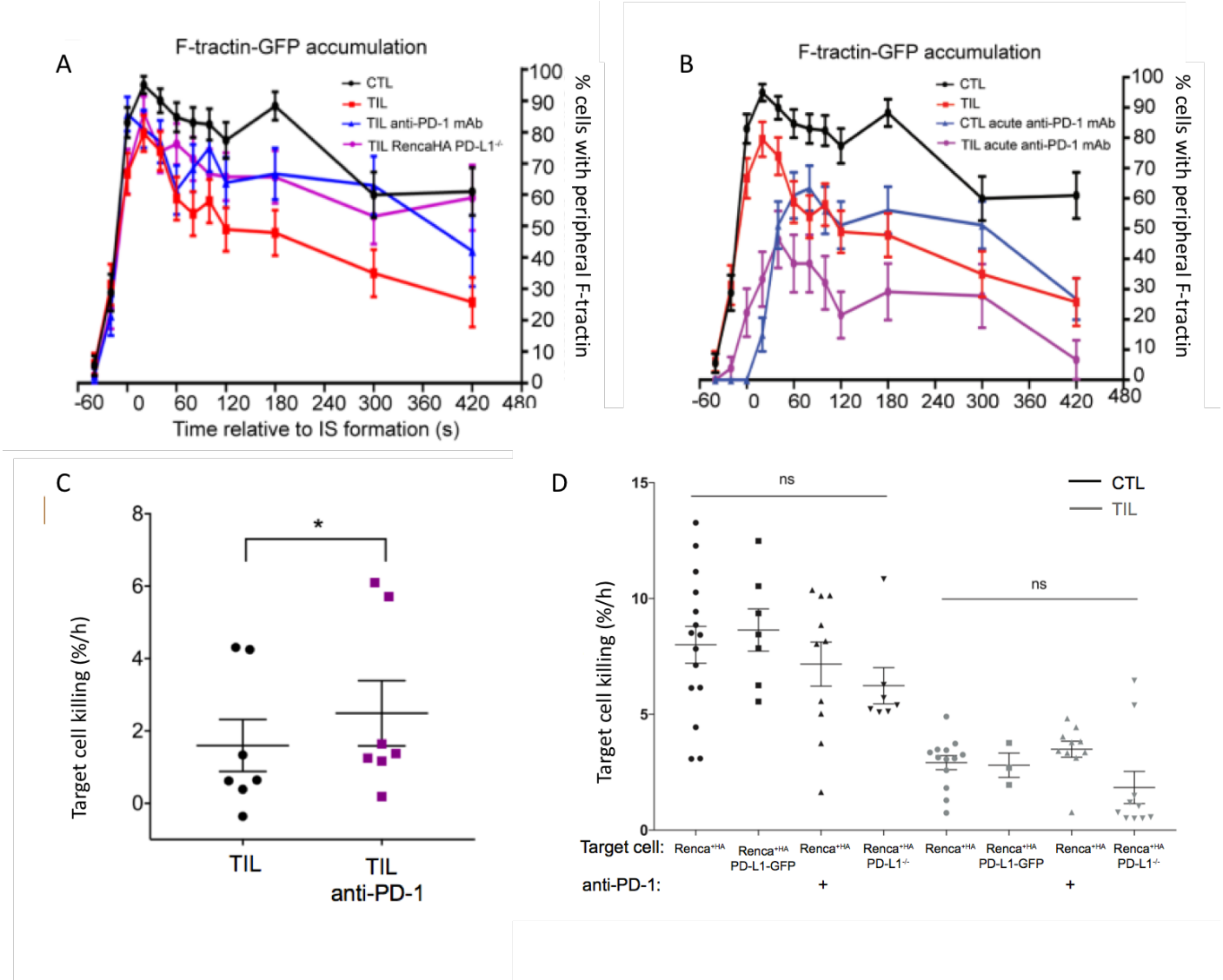

[21] Figures from Science Signalling publication "PD-1 suppresses the maintenance of cell couples between cytotoxic T cells and tumor target cells within the tumor" Rachel Ambler, Grace L. Edmunds, Guilia Toti, David J. Morgan, Christoph Wuelfing. GE Generated figures B and D. RA generated Figures A and C.

10.2.4 Supplementary Information for Chapter 6

Figure S8 - TIM3 expression was compared between Clone 4 T cells primed using Anti-CD3/28mAb or KdHA peptide

Naive Clone 4 T cells were extracted from macerated spleen. The spleen preparation was divided into two and Clone 4 T cells were either purified using MACS and primed *in vitro* by anti-CD3/28 mAb stimulation; or macerated murine spleen was placed in culture and KdHA peptide was used to prime Clone 4 T cells. Surface expression of TIM3 was quantified daily using fluorescent antibody staining and flow cytometric analysis. Percentage expression is shown as mean +/- SEM. N = 2 experiments with 1 mouse per experiment. Samples compared using One-way ANOVA.

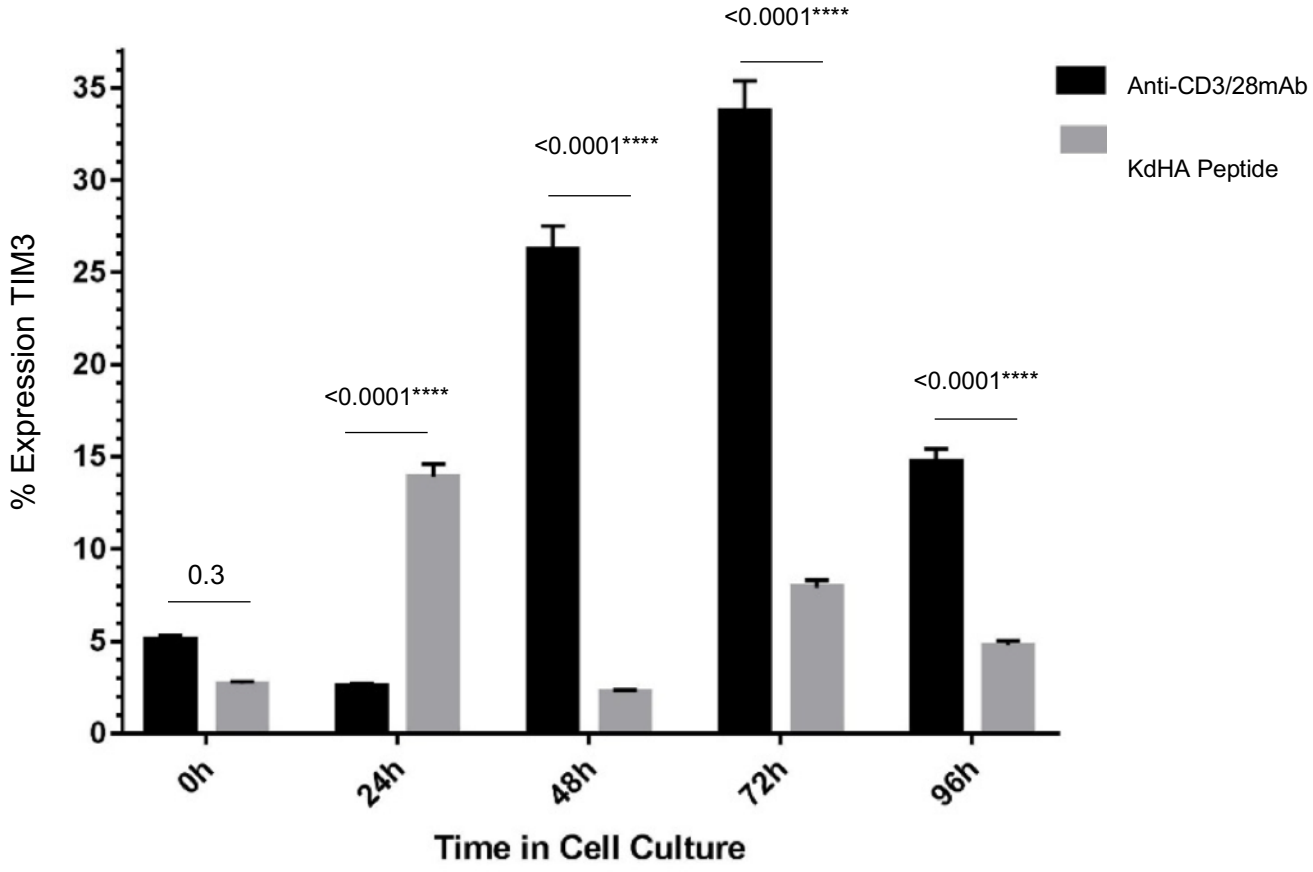

Figure S9 - Omitting IL-2 from cell culture allows alterations in Lck phosphorylation to be detected

Clone 4 CTL were stained with Celltrace violet and cultured for 72h in complete medium without IL-2. Various treatments were added after 24h in culture, as indicated. Cells were harvested at 72h and stained with antibodies specific to total Lck, Lck phosphorylated at Tyrosine 505 (inactive Lck), or Lck phosphorylated at Tyrosine 418 (active Lck)(2). Data was analysed by flow cytometry. N=1 experiment therefore no statistics were performed. Proliferation was calculated by quantifying the number of cells which divided in relation to a celltrace violet proliferation control, and those which reached the last 2 divisions of the population. (A) Cells treated with 1 μM PGE_2 +/- 1 μM of the PGE_2 EP2 receptor antagonist TG4-155. (B) Cells treated with 1 μM or 10 μM NECA +/- 1.25 μM A2a adenosine receptor antagonist ZM241385. (C) Cells treated with 1 μM CGS2680 +/- 1.25 μM A2a adenosine receptor antagonist ZM241385.

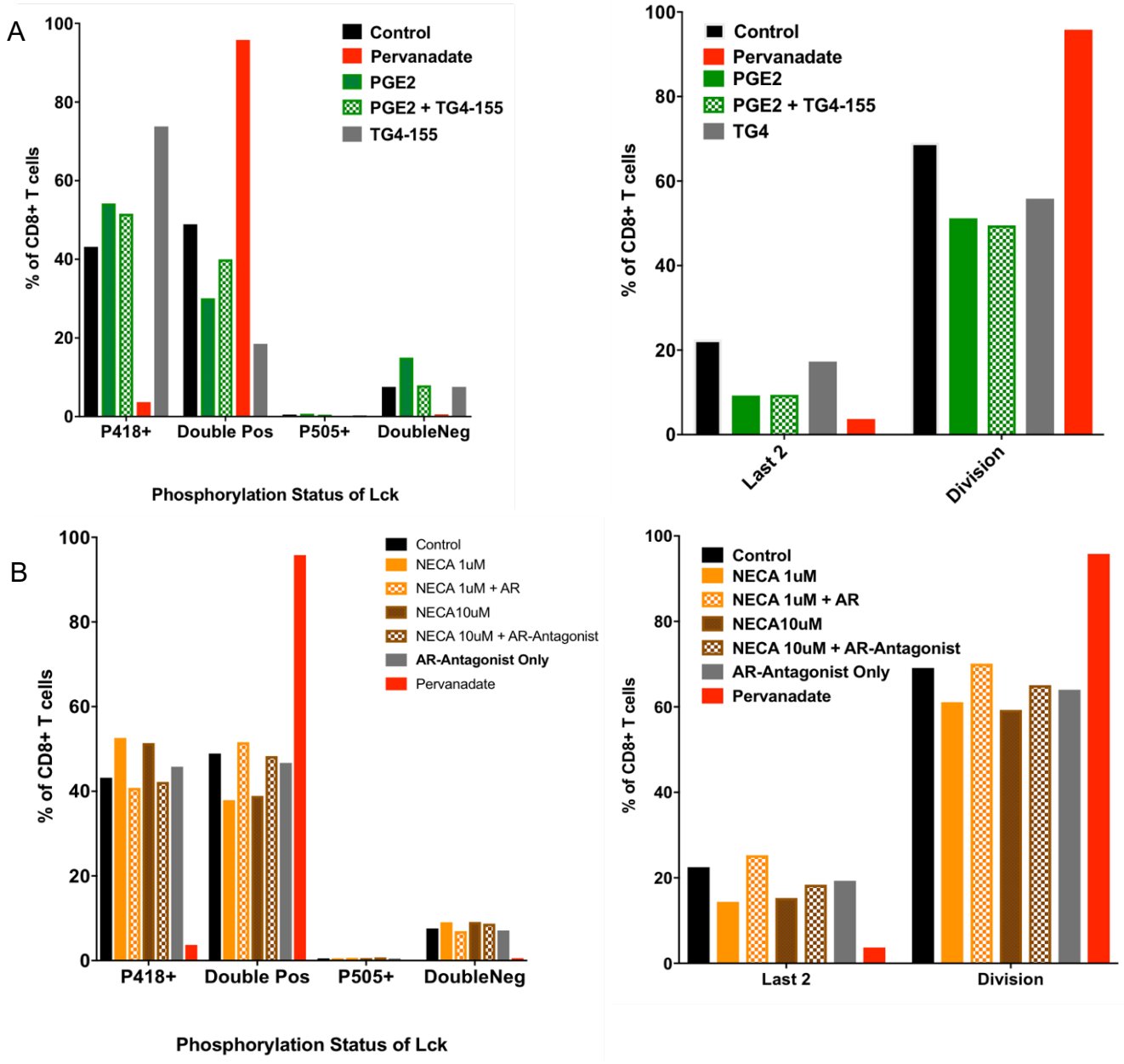

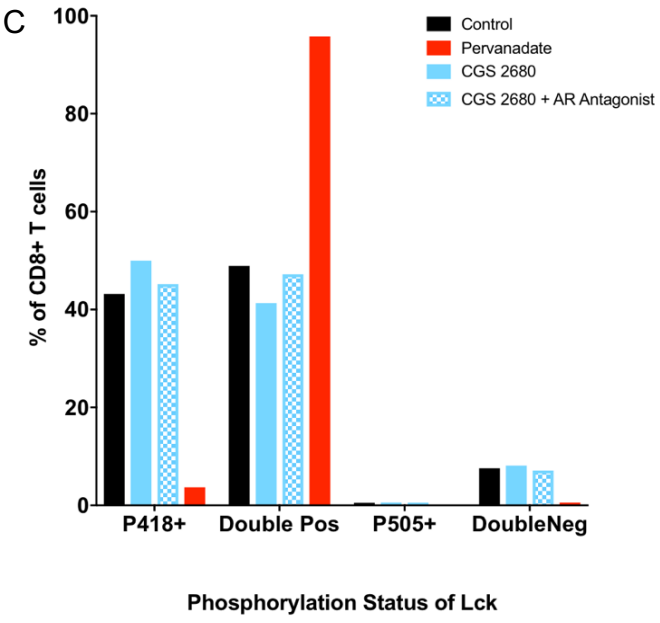
C
100
80
60
40
20
0
% of CD8+ T cells
Control
Pervanadate
CGS 2680
CGS 2680 + AR Antagonist
P418+
Double Pos
P505+
DoubleNeg
Phosphorylation Status of Lck

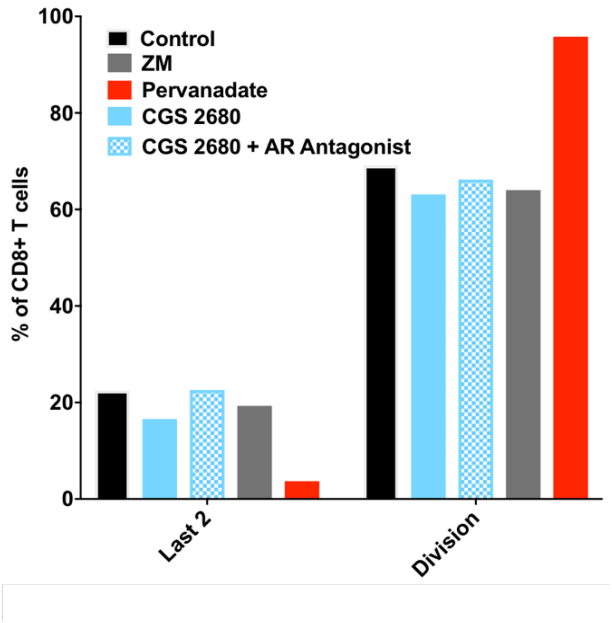
100
80
60
40
20
0
% of CD8+ T cells
Control
ZM
Pervanadate
CGS 2680
CGS 2680 + AR Antagonist
Last 2
Division

Figure S10 - Lck does not localise strongly to the immune synapses formed between Clone 4 CTL and Renca tumour cells

Clone 4 CTL were transduced with Lck^{GFP} and allowed to couple to KdHA-pulsed Renca tumour cell targets. Immune synapse formation (cell coupling) was imaged every 15s over 46 timepoints using spinning disc confocal microscopy. N = 30 couples. (A) Analysis of the accumulation of Lck^{GFP} is shown. (Bi) Representative DIC image indicating 3 cell couples with immune synapse location outlined in red. (Bii) Pseudocolour image to indicate the localisation of Lck GFP, showing that Lck does not localise to the site of the immune synapse in any cell couple, when compared to cytoplasmic brightness[22].

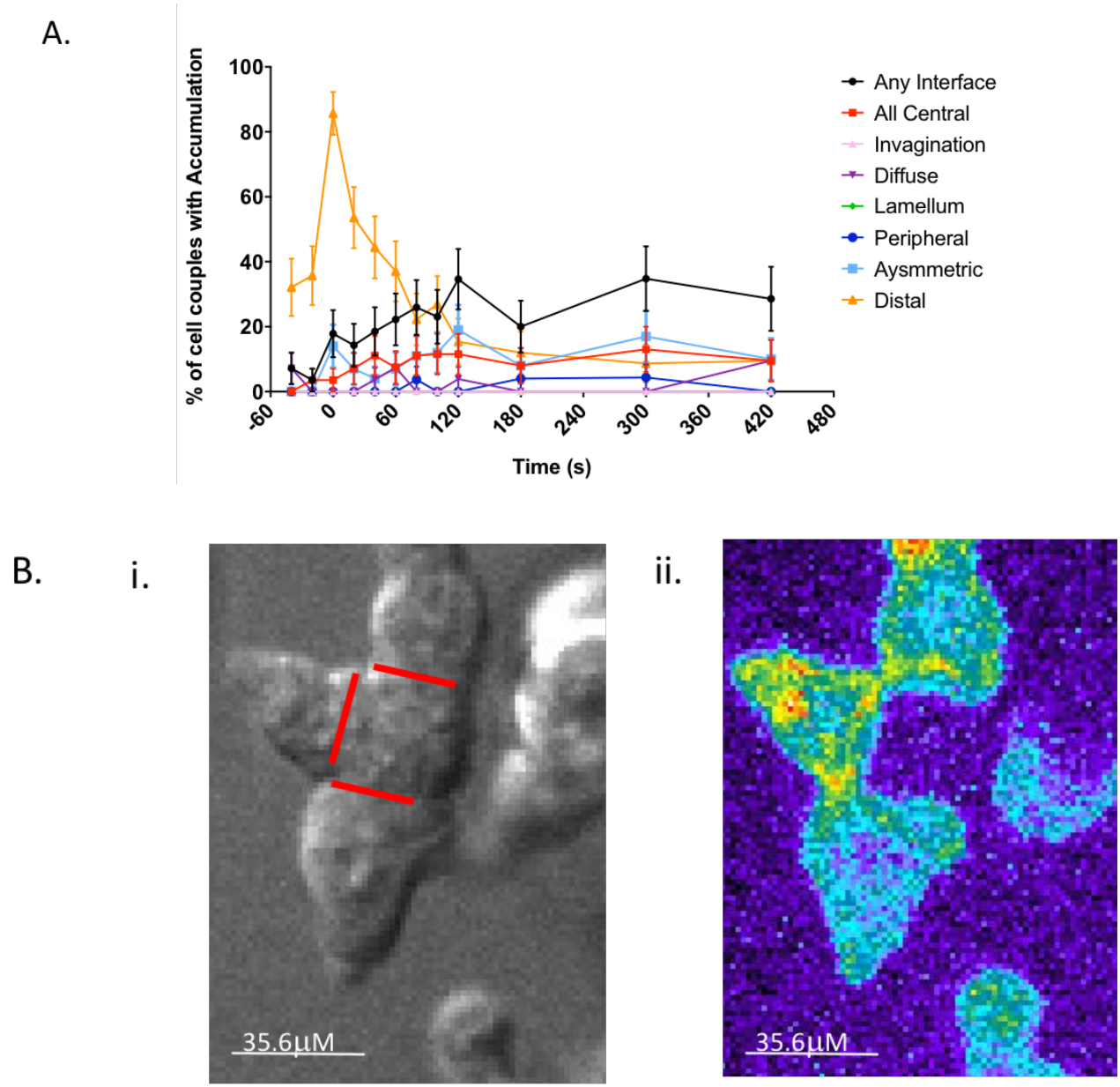

[22] Cells and images were generated by Rachel Ambler, data were analysed by GE.

10.2.5 Supplementary Information for Chapter 7

Figure S11 - Injection of BALB/c mice with Influenza A/PR/8 induces priming of naive adoptively transferred Clone 4 CD8+ T cells in vivo

Thy1.2+ BALB/c Mice were injected concurrently with Influenza A/PR/8 (intraperitoneal) and naïve, Celltrace Violet-labelled Thy1.1+ Clone 4 T cells (intravenous). After 4 days, Clone 4 T cells were extracted from the spleen and lymph nodes using FACS sorting. Loss of celltrace violet fluorescence was quantified using flow cytometry, showing that proliferation of Clone 4 T cells was induced *in vivo* by the HA antigen of influenza.

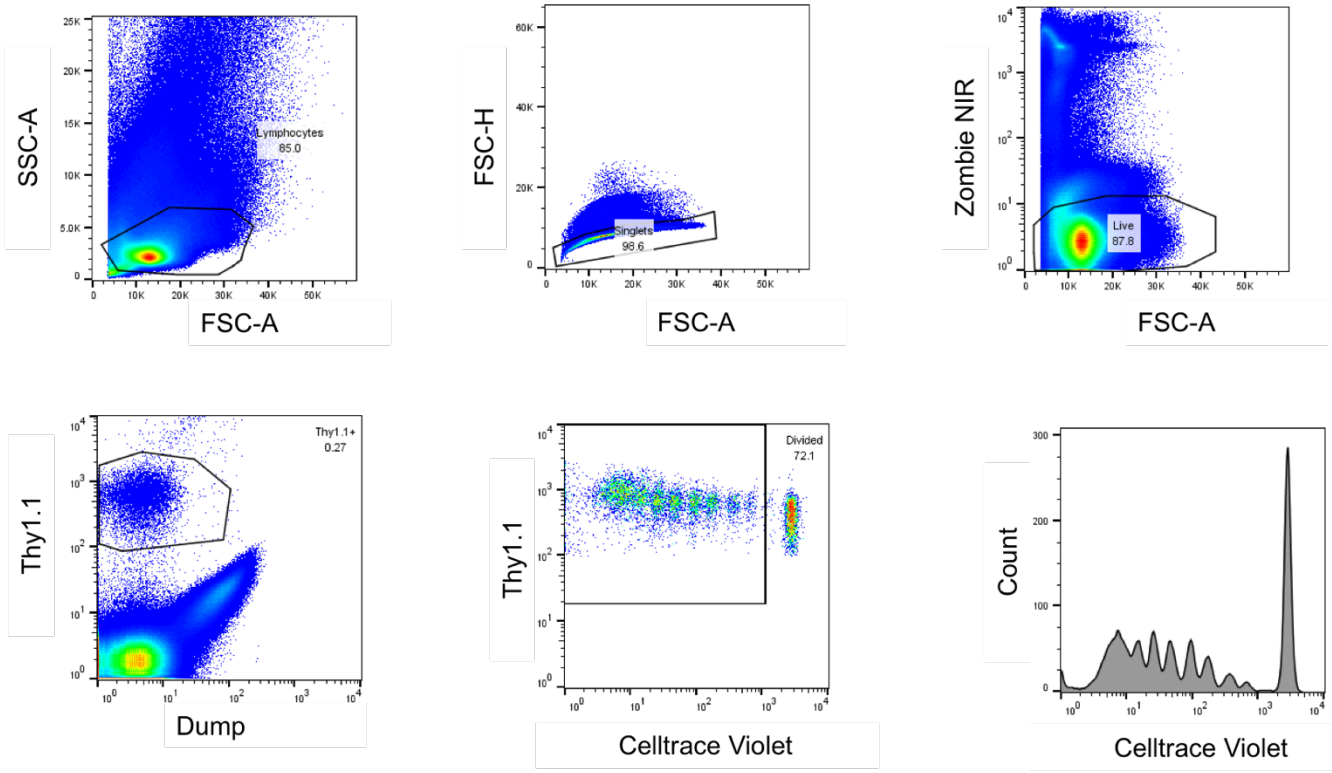

Figure S12 – Testing the efficacy of Anti-CD8 depleting Antibodies generated from hybridoma supernatant versus commercial Anti-CD8 Antibody

In order to perform experiments in which all CD8+ T cells were depleted, or populations of Thy1.1+ Clone 4 T cells were selectively depleted within tumour-bearing BALB/c mice, monoclonal antibodies were tested to determine dose and efficacy. Commercial Anti-CD8b antibody (InVivoMAb Clone 53-5.8) was purchased from BioXcell. In-house Anti-CD8α and CD8β depleting antibodies, to be used in combination, were generated from hybridoma cell lines (Clones YTS156 and YTS169). (A) Preparations of commercial and in-house-prepared antibodies were added to *in vitro* primed Clone 4 CTL and incubated with and without purified rabbit complement. Number of CD8+ T cells was quantified using flow cytometry. At the dose used *in vitro*, commercial antibody depleted CD8+ T cells more efficiently than in-house prepared antibodies. (B) Dose regimen used to administer antibodies to BALB/c mice *in vivo* and flow cytometric analysis of blood samples from treated mice to quantify CD8+ T cells. Commercial antibody achieved depletion of CD8+ T cells *in vivo* more efficiently than in-house prepared antibody, therefore commercial antibody was used in future experiments.

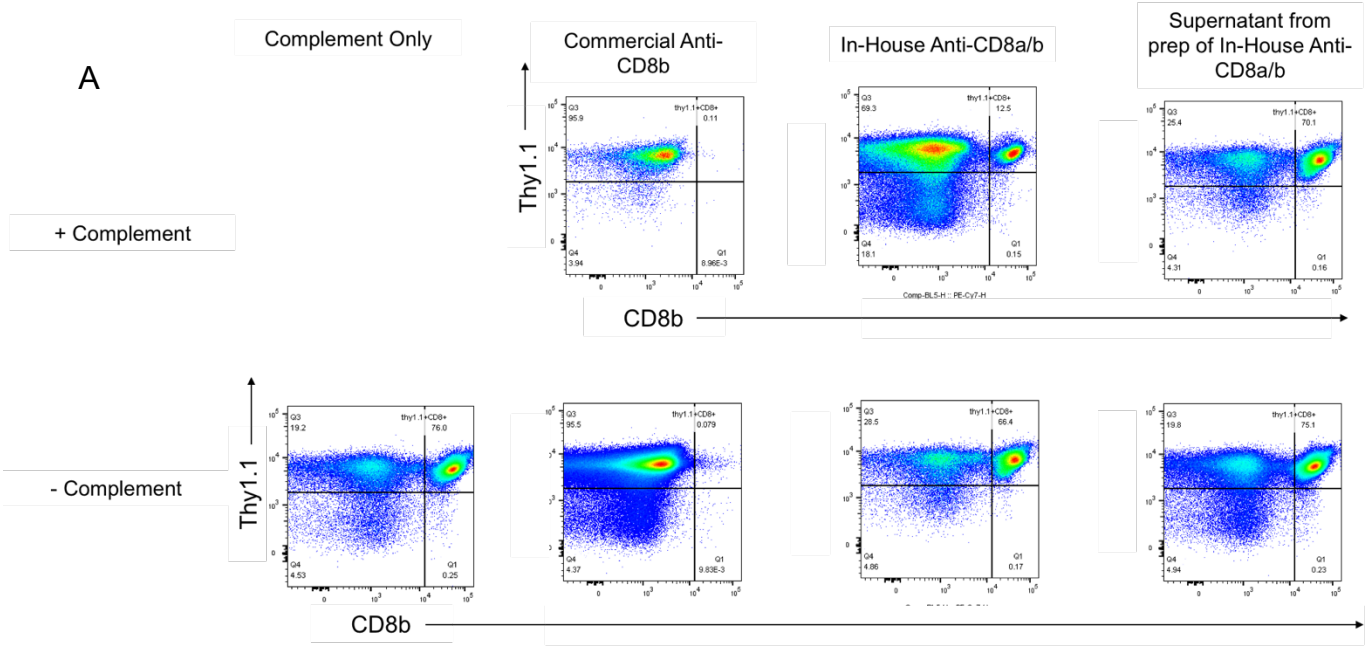

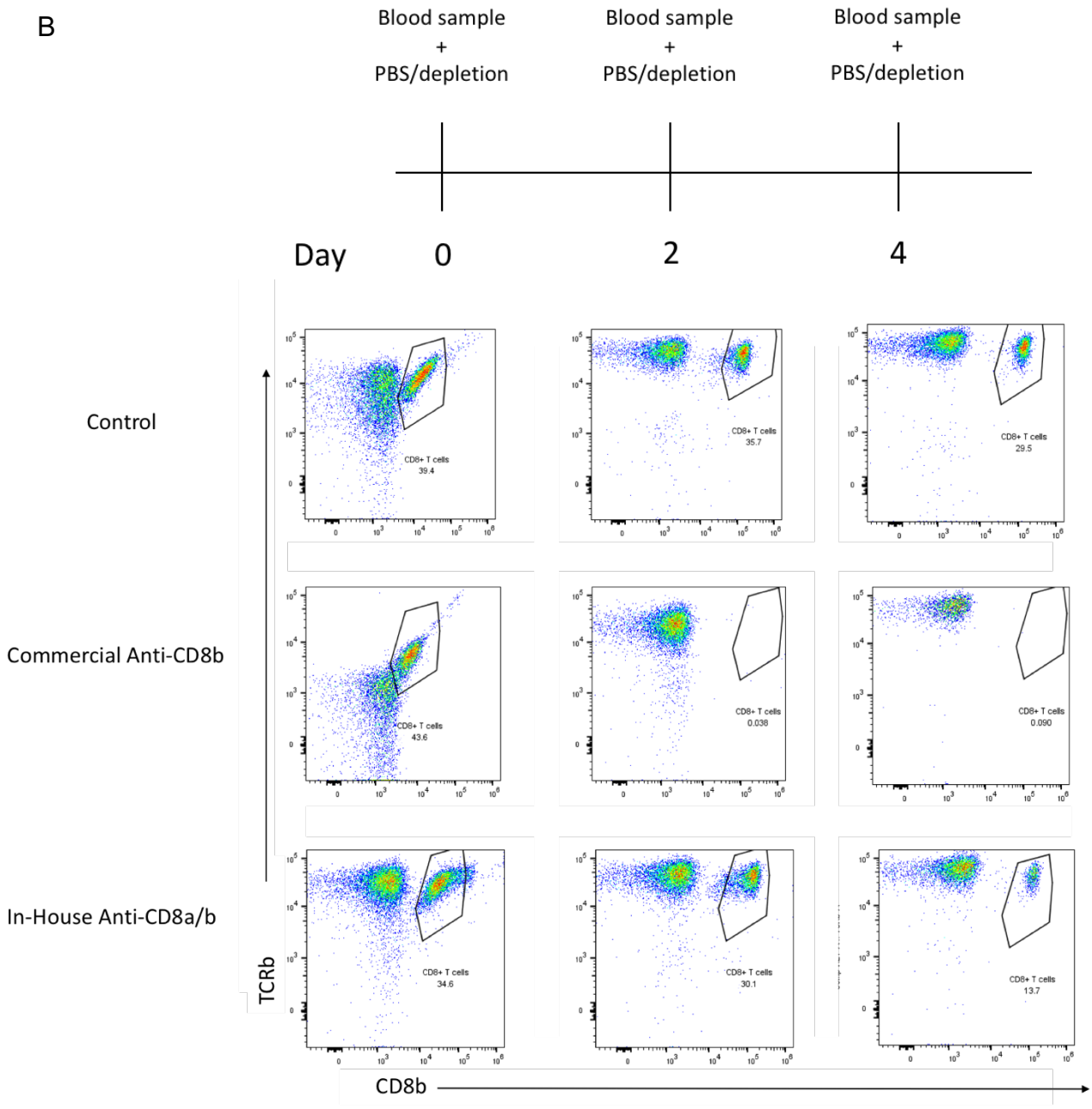
B
Blood sample + PBS/depletion
Blood sample + PBS/depletion
Blood sample + PBS/depletion
Day
0
2
4
Control
Commercial Anti-CD8b
In-House Anti-CD8a/b
CD8+ T cells 39.4
CD8+ T cells 35.7
CD8+ T cells 29.5
CD8+ T cells 43.6
CD8+ T cells 0.038
CD8+ T cells 0.090
CD8+ T cells 34.6
CD8+ T cells 30.1
CD8+ T cells 13.7
TCRb
CD8b

Figure S13 - Flow cytometric analysis of skin preparations from Tumour-bearing mice to identify CD8+ T cells

Punch biopsies were sampled from the dorsal neck skin of mice in which RencaHA tumours had grown and then regressed. Skin preparations were digested, and the dermis separated from the epidermis. After macerating to form a single cell suspension, cells were stained with antibodies specific to CD8b, TCRb, CD103a, CD44, CD69 and CD62L. TCRγδ staining was used as a positive extraction control, since TCRγδ cells should always be present in skin preparations. Flow cytometric gating from two experiments is shown. In the first experiment, extraction of T cells failed, however in the second one T cells could be identified. The numbers of cells isolated from dorsal neck skin were very small, therefore mice could not be compared with accuracy, so this technique was not used for further analyses.

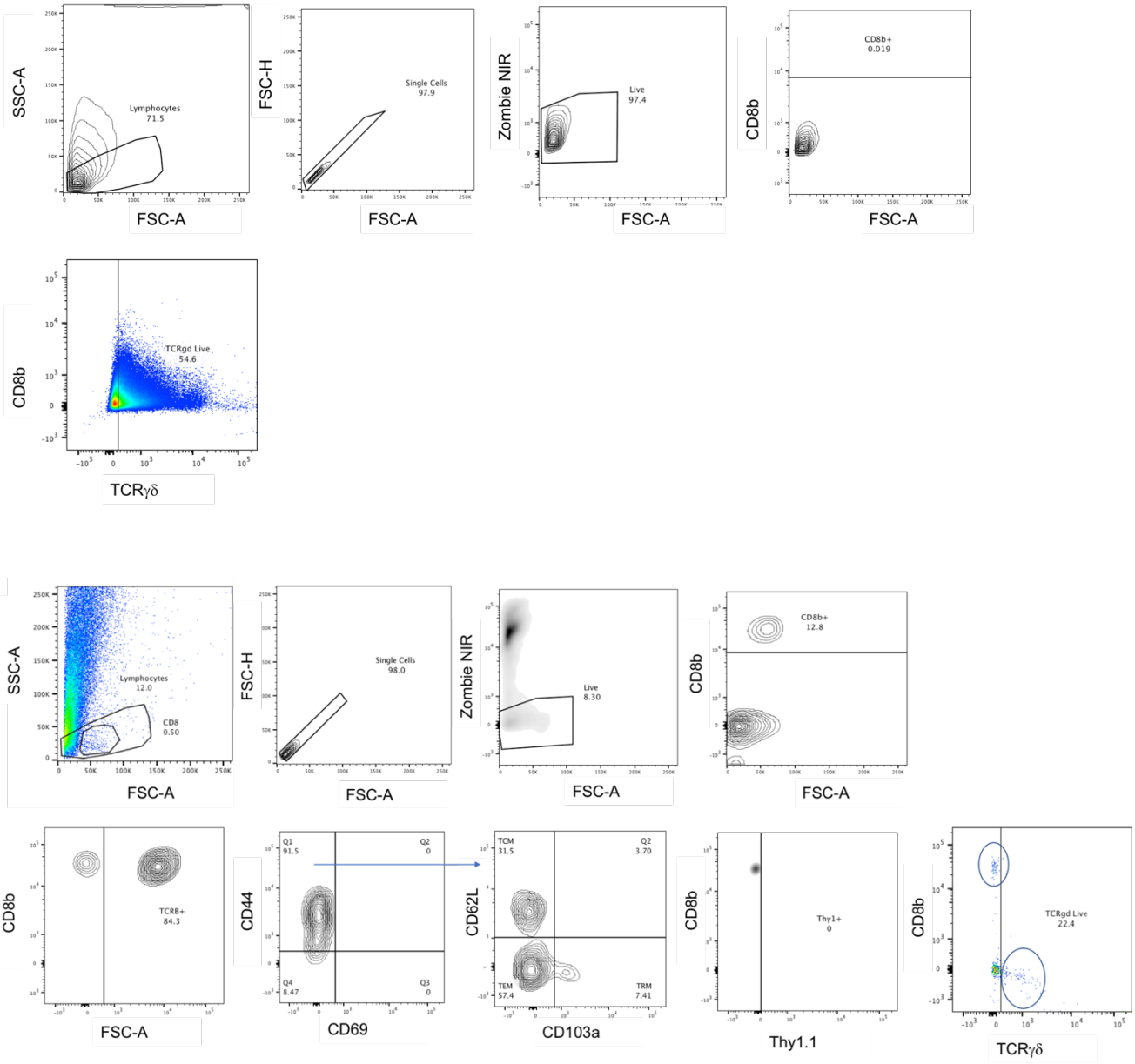

10.3 Appendix 2- Flow Cytometric Gating and Optimisation Data

Figure S14 - Clone 4 CD8+ T cells are naive immediately after extraction from Clone 4 spleens

The expression of CD44, CD69 and CD62L by naïve Clone 4 CD8+ T cells was quantified using flow cytometry. Samples were stained immediately after MACS purification from murine spleen (A,C), and after 72h in culture with anti-CD3/28 mAb stimulation (B,D), indicating that <2% of Clone 4 cells display activation markers at the time of harvesting.

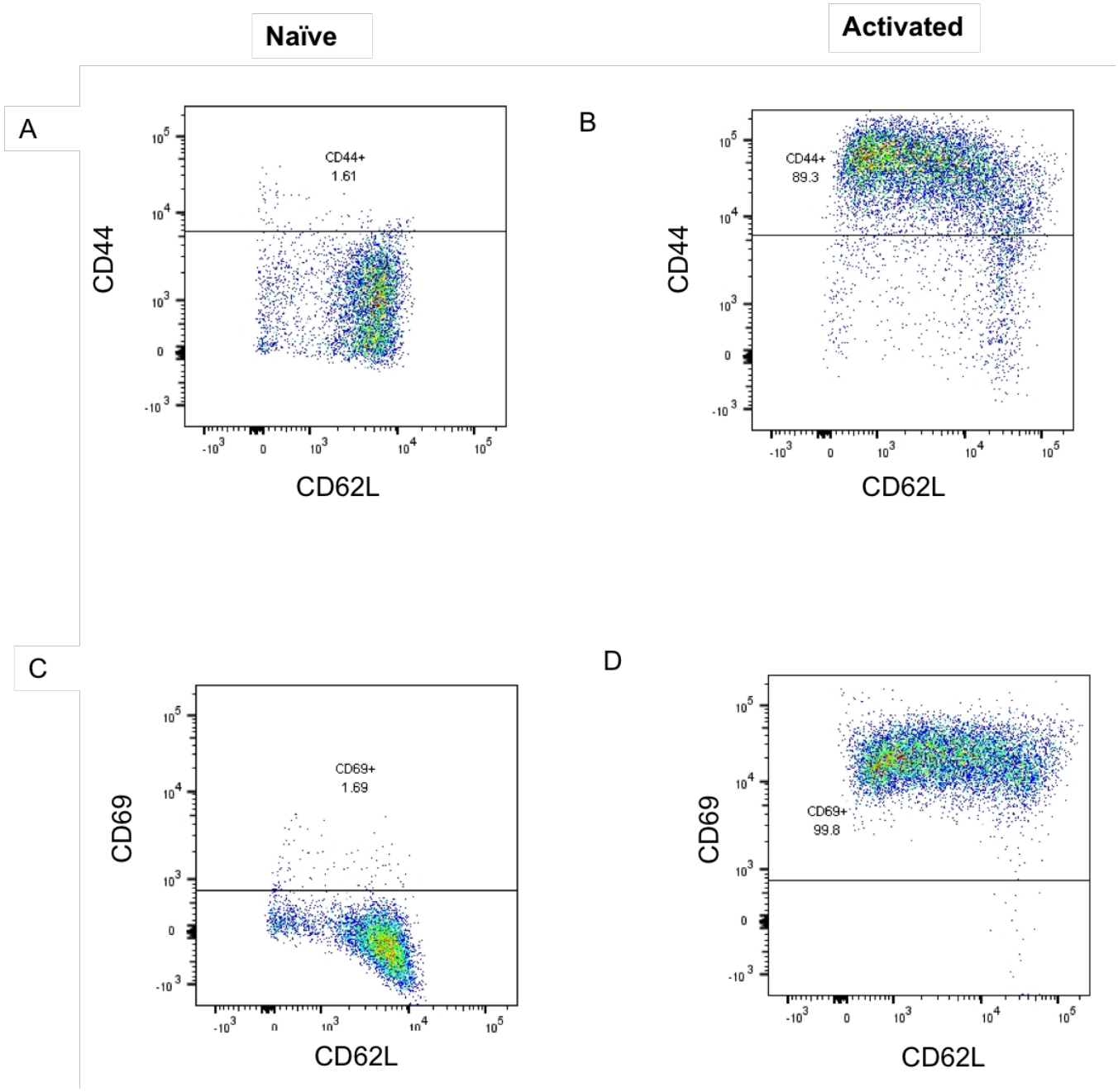

Figure S15 - MACS purification of CD8+ T cells from the spleens of Clone 4 mice

Splenocytes from Clone 4 mice were stained with antibodies specific to CD8b and TCR Vβ8.1, to identify CD8+ Clone 4 T cells. After purification using Magnetic Activated cell Sorting (MACS), 93% of cells in the single cell suspension are CD8+ Clone 4 T cells.

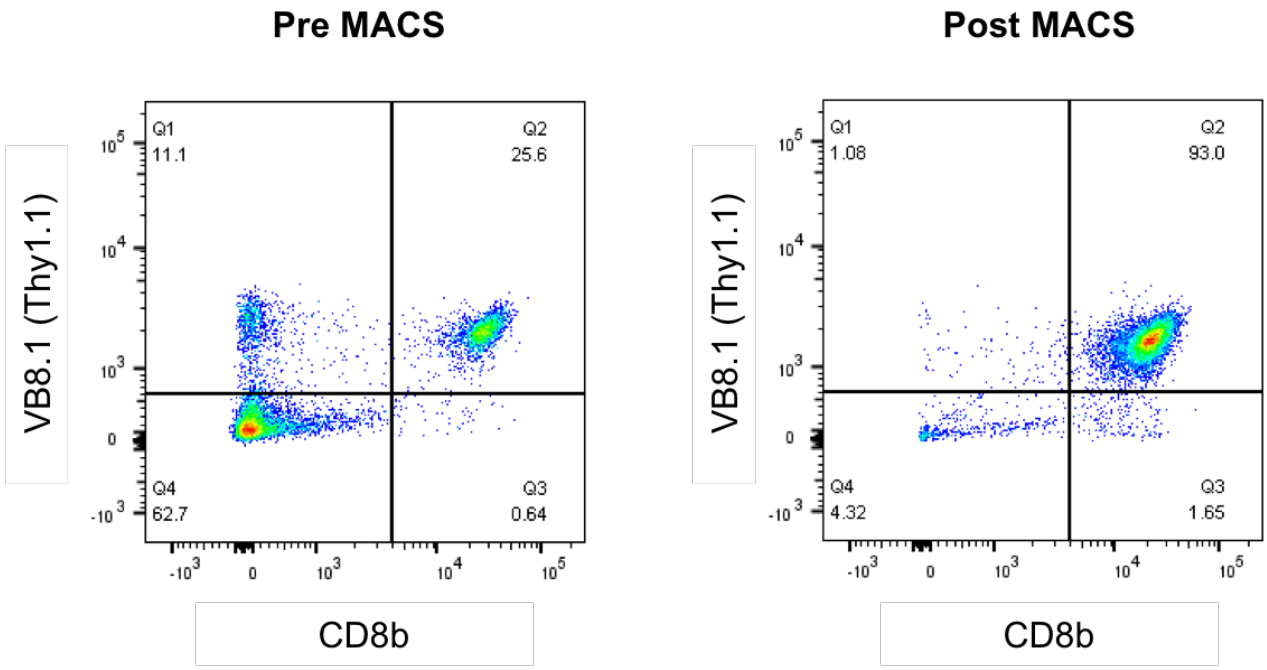

Figure S16- Flow Cytometric Gating for Staining of Intracellular Cytokines

Clone 4 CTL were primed *in vitro,* or TILs were harvested from RencaHA tumour-bearing mice. Cells were sorted using FACS and stained with Zombie-NIR to identify live cells and antibodies specific to CD8, TIM3, PD-1 and Ceacam-1. Cells were then fixed, permeabilised and stained with antibodies specific to IL-2, IFNγ and IL-10. A subset of cells was incubated for 4 hours with PMA/Ionomycin and Brefeldin-A before staining. Samples were analysed using flow cytometry. Cells were gated to quantify the above markers using Fluorescence Minus One (FMO) samples.

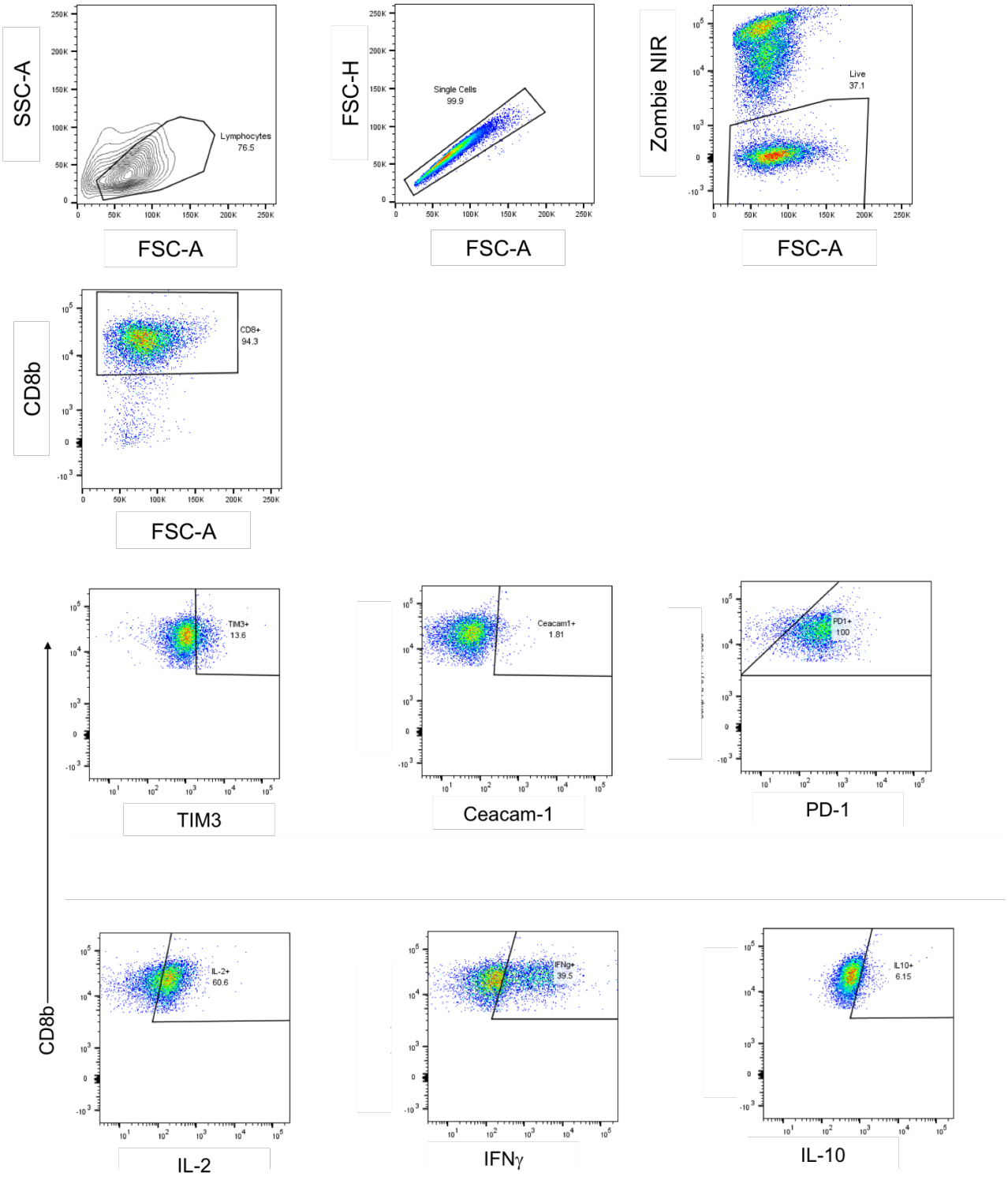

Figure S17 - Flow cytometric Gating for In Vitro Suppression Assays

Naive Clone 4 T cells were stained with Celltrace violet and 1 x 10^5 cells were plated in each well of a 96 well plate. Cells were cultured for 72h in the presence of KdHA pulsed antigen presenting cells +/- CD8+ TILs extracted from RencaHA tumours. Cells were stained with ZombieNIR to identify live cells and antibodies specific to CD8 and TCR Vβ8.1 to identify Clone 4 T cells. The number of cells in the last 2 divisions was quantified amongst the Celltrace violet-labelled population.

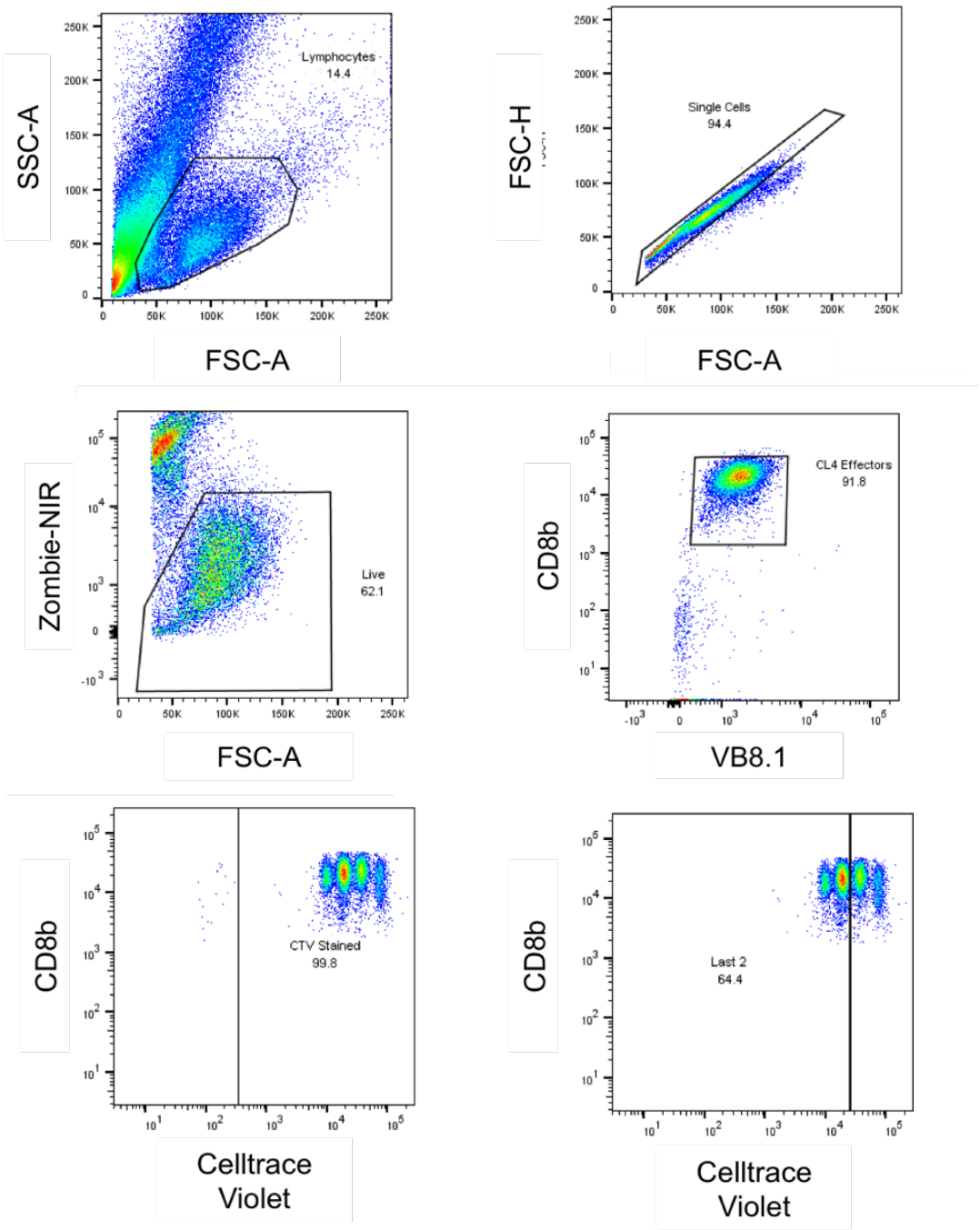

Figure S18 - Flow cytometric gating to quantify CIR expression amongst TILs

Endogenous CD8+ TILs were harvested from RencaHA tumour bearing mice given A2aR-Antagonist or vehicle. Cells were stained with Zombie Aqua to identify live cells and antibodies specific to CD8, CD4, TIM3, TIGIT, LAG3, PD-1, CD39 and CD73. Expression of the above markers was quantified by gating using FMO samples.

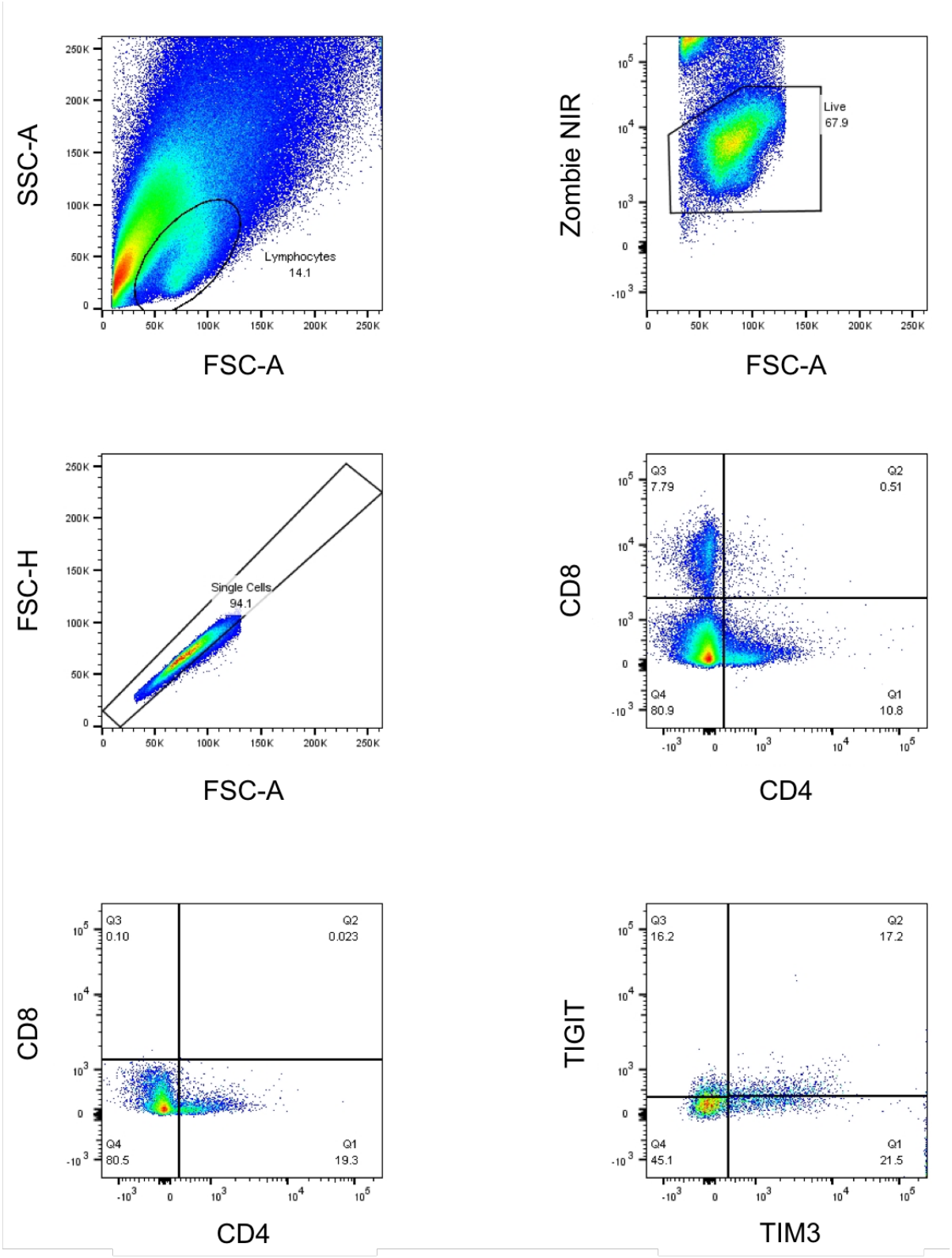

Figure S19 - Flow cytometric gating to quantify CIR expression and proliferation amongst Clone 4 CTL treated with NECA

Clone 4 CTL were Celltrace Violet labelled before being primed *in vitro* in the presence of NECA +/- A2aR-Antagonist. Cells were stained with antibodies specific to TIM3, TIGIT, LAG3 and PD-1. A fixed sample of CTV labelled naïve cells was used to determine the position of undivided cells. Gates to quantify co-inhibitory receptor expression were generated using FMO samples.

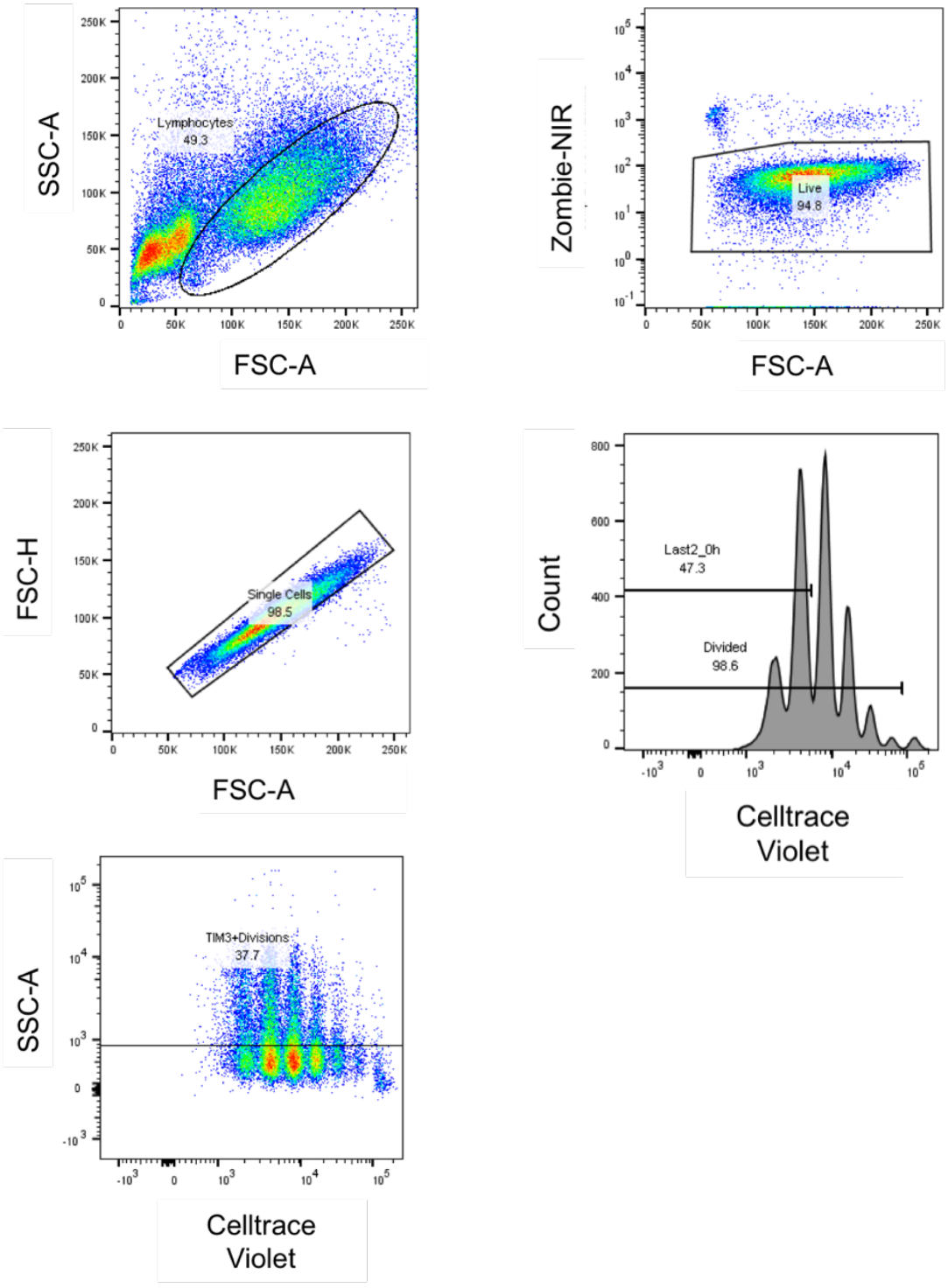

Figure S20 - Flow Cytometric Gating to quantify Ceacam-1 expression amongst Clone 4 CTL transduced with hCD2TIM3 constructs

Clone 4 CTL were transduced with hCD2TIM3 or hCD2TIM3Ig and stained with ZombieNIR and antibodies specific to CD8, CD3, TIM3 and Ceacam-1. Gates to quantify expression of Ceacam-1 and TIM3 were generated using FMO samples.

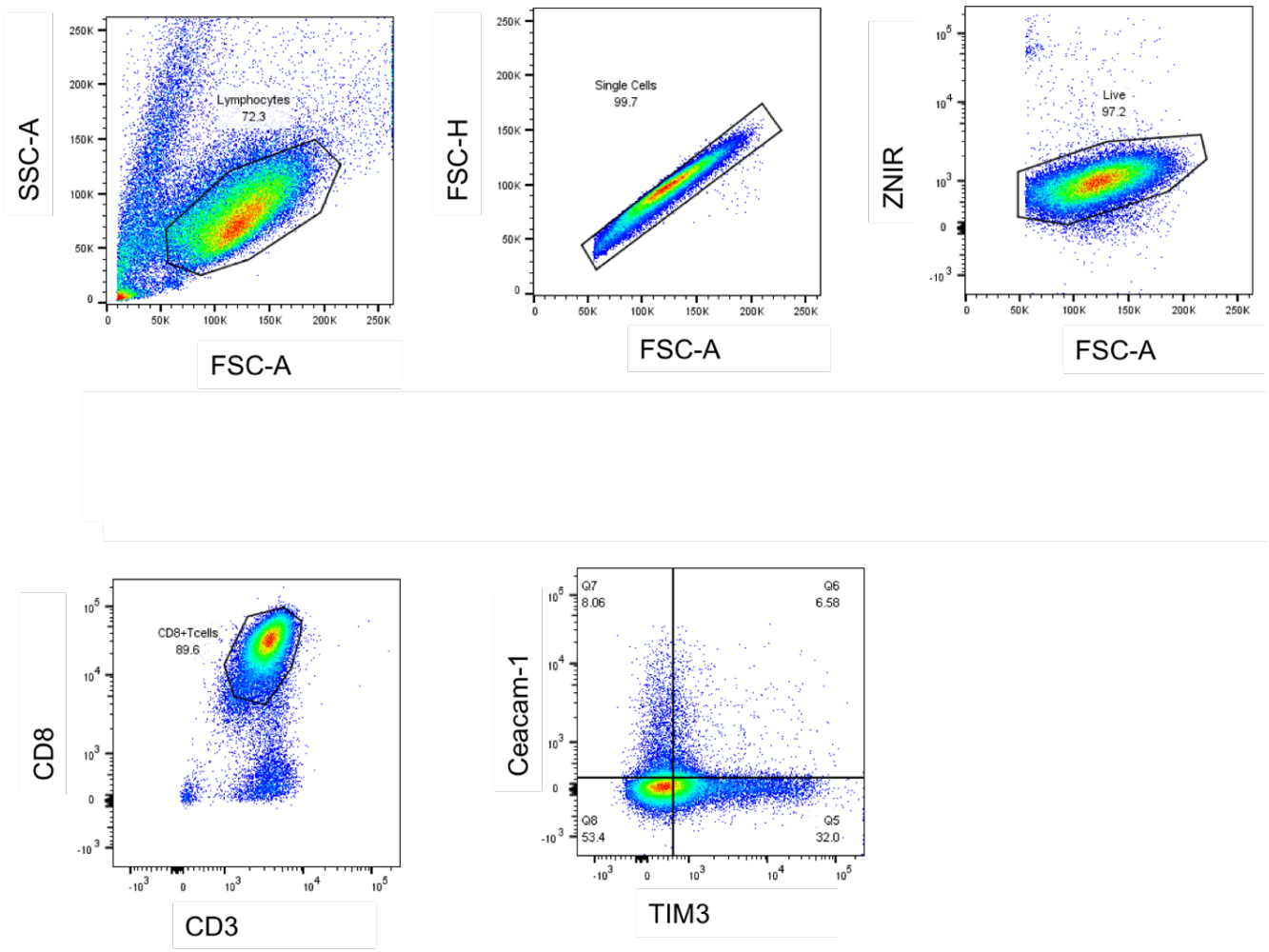

Figure S21 - Flow cytometric gating to quantify Phosphorylation of Lck

Clone 4 CTL were stained with ZombieNIR to identify live cells, and antibody specific to CD8b. Cells were then fixed in Phosflow cytofix buffer and permeabilised using phosflow perm buffer II before being stained with antibodies specific to Lck PY505, Lck PY418 and total Lck. Cells were analysed using flow cytometry. Gates to quantify the expression of markers were generated using FMO samples.

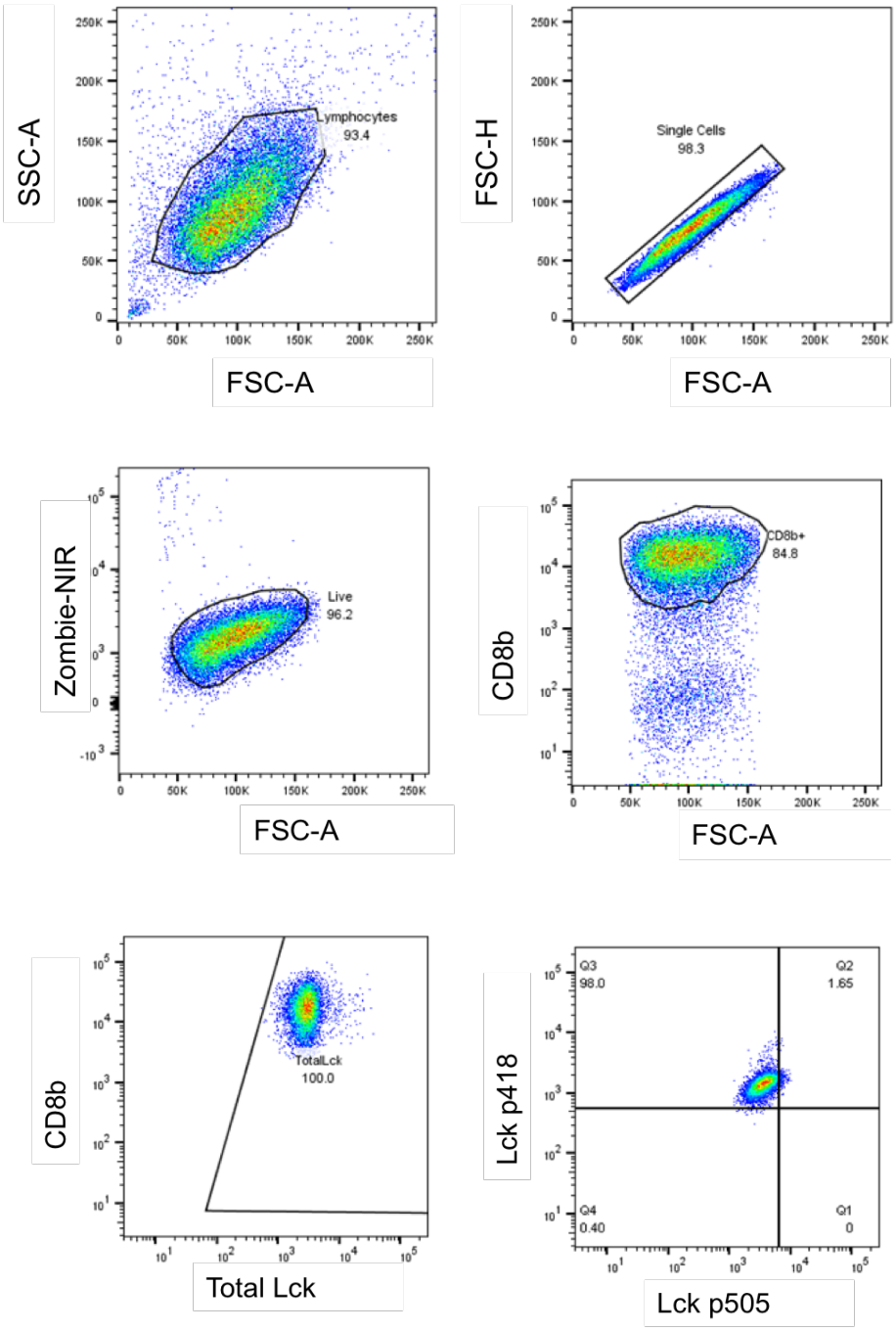

Figure S22 - Flow cytometric gating to identify Memory T cell populations

Spleens and TDLN were harvested from RencaHA tumour bearing mice. Samples were stained with ZombieNIR to identify live cells, and antibodies specific to CD8, TCRβ, CD44, CD69, CD62L and CD103a. Data were gated using FMO samples to quantify expression of these markers.